frontiers | Research Topics

Endocrinology of obesity, aging and stress

Edited by
Yuko Maejima, Kenju Shimomura and
Heidi de Wet

Published in
Frontiers in Endocrinology

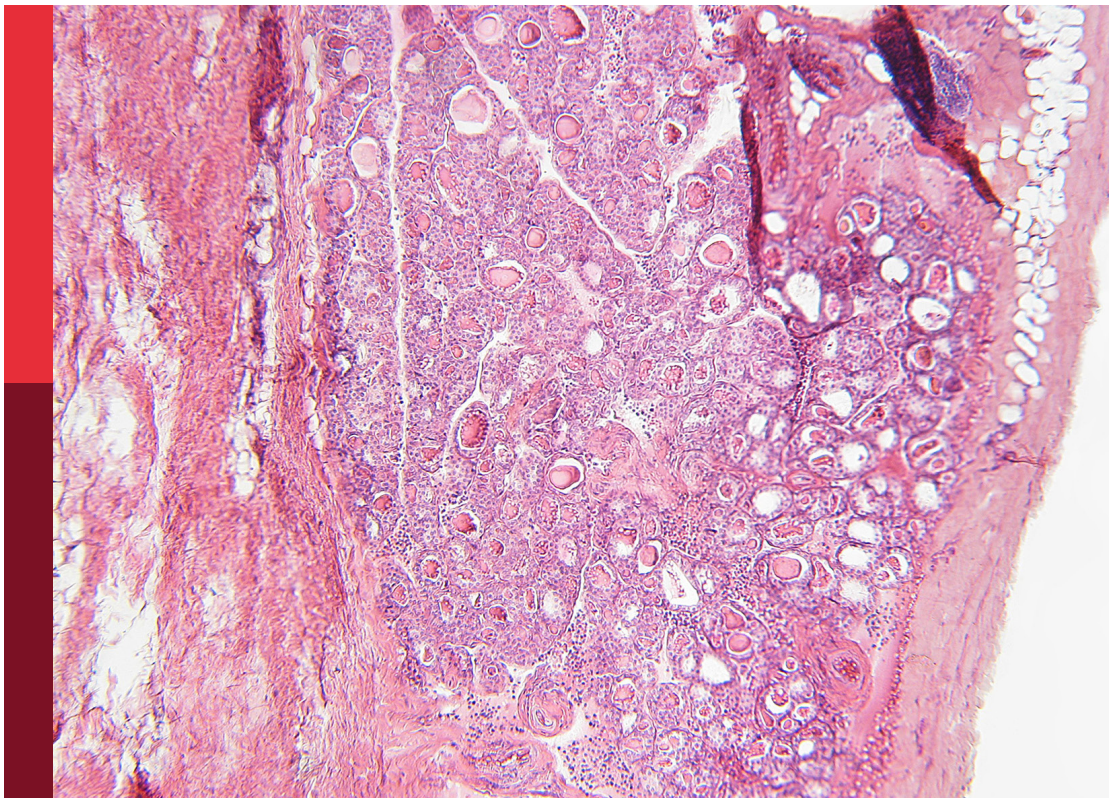

ISSN 1664-8714
ISBN 978-2-8325-6223-9
DOI 10.3389/978-2-8325-6223-9

About Frontiers

Frontiers is more than just an open access publisher of scholarly articles: it is a pioneering approach to the world of academia, radically improving the way scholarly research is managed. The grand vision of Frontiers is a world where all people have an equal opportunity to seek, share and generate knowledge. Frontiers provides immediate and permanent online open access to all its publications, but this alone is not enough to realize our grand goals.

Frontiers journal series

The Frontiers journal series is a multi-tier and interdisciplinary set of open-access, online journals, promising a paradigm shift from the current review, selection and dissemination processes in academic publishing. All Frontiers journals are driven by researchers for researchers; therefore, they constitute a service to the scholarly community. At the same time, the *Frontiers journal series* operates on a revolutionary invention, the tiered publishing system, initially addressing specific communities of scholars, and gradually climbing up to broader public understanding, thus serving the interests of the lay society, too.

Dedication to quality

Each Frontiers article is a landmark of the highest quality, thanks to genuinely collaborative interactions between authors and review editors, who include some of the world's best academicians. Research must be certified by peers before entering a stream of knowledge that may eventually reach the public - and shape society; therefore, Frontiers only applies the most rigorous and unbiased reviews. Frontiers revolutionizes research publishing by freely delivering the most outstanding research, evaluated with no bias from both the academic and social point of view. By applying the most advanced information technologies, Frontiers is catapulting scholarly publishing into a new generation.

What are Frontiers Research Topics?

Frontiers Research Topics are very popular trademarks of the *Frontiers journals series*: they are collections of at least ten articles, all centered on a particular subject. With their unique mix of varied contributions from Original Research to Review Articles, Frontiers Research Topics unify the most influential researchers, the latest key findings and historical advances in a hot research area.

Find out more on how to host your own Frontiers Research Topic or contribute to one as an author by contacting the Frontiers editorial office: frontiersin.org/about/contact

Endocrinology of obesity, aging and stress

Topic editors

Yuko Maejima — Fukushima Medical University, Japan

Kenju Shimomura — Fukushima Medical University, Japan

Heidi de Wet — University of Oxford, United Kingdom

Citation

Maejima, Y., Shimomura, K., de Wet, H., eds. (2025). *Endocrinology of obesity, aging and stress*. Lausanne: Frontiers Media SA. doi: 10.3389/978-2-8325-6223-9

Table of contents

frontiers | Frontiers in Endocrinology

TYPE Editorial
PUBLISHED 27 March 2025
DOI 10.3389/fendo.2025.1587811

OPEN ACCESS

EDITED AND REVIEWED BY
James Harper,
Sam Houston State University, United States

*CORRESPONDENCE
Kenju Shimomura
shimomur@fmu.ac.jp

RECEIVED 05 March 2025
ACCEPTED 11 March 2025
PUBLISHED 27 March 2025

CITATION
Maejima Y, Shimomura K and de Wet H (2025) Editorial: Endocrinology of obesity, aging and stress.
Front. Endocrinol. 16:1587811.
doi: 10.3389/fendo.2025.1587811

Editorial: Endocrinology of obesity, aging and stress

Yuko Maejima[1], Kenju Shimomura[1]* and Heidi de Wet[2]

[1]Department of Bioregulation and Pharmacological Medicine, Fukushima Medical University, Fukushima, Japan, [2]Department of Physiology, Anatomy and Genetics, University of Oxford, Oxford, United Kingdom

KEYWORDS

aging, obesity, stress, endocrinology, metabolism

Editorial on the Research Topic
Endocrinology of obesity, aging and stress

The intricate relationship between the endocrine system, obesity, aging, and stress has become a focal point in contemporary research. This Research Topic, "*Endocrinology of obesity, aging, and stress*," gathers pivotal studies that collectively enhance our understanding of these interrelated physiological systems. By examining the fields of hormonal, metabolic, and psychological systems, these contributions offer a comprehensive and integrated view of the factors influencing health and disease in the context of obesity, aging, and stress.

Various studies within this Research Topic have illuminated the significant roles of body composition and metabolic health in aging processes, highlighting how certain body indices can serve as predictors of important anti-aging markers. This perspective is further enriched by research into the regulatory mechanisms of body composition, emphasizing the therapeutic potential of targeting specific genetic markers and metabolic pathways to manage health. Global research trends on aging associated with periodontal health over the last two decades reveal significant technical advancements, providing a rich backdrop for future research directions in this field. The exploration of psychological factors also proves crucial, as emotional and social support systems are shown to significantly impact glycemic control, particularly in patients managing chronic conditions such as diabetes over a lifetime. These studies highlight that the mental health aspect of dealing with long-term conditions needs as much attention as the management of the physiological pathologies associated with chronic disease.

Mechanisms underlying weight regulation have been another critical area of focus. Investigations into hormonal influences reveal that processes beyond traditional sympathetic innervation contribute to the regulation of body weight and adiposity, underscoring the complexity of endocrine interactions. Moreover, novel therapeutic agents have been identified that may offer new avenues for obesity treatment, acting on specific hormonal receptors to reduce energy intake and promote weight loss. Additionally, comprehensive assessments of body composition beyond BMI are emphasized for evaluating health risks, particularly in the context of obesity-related mortality. The predictive value of obesity and lipid-related indices in the onset of type 2 diabetes underscores the importance of regular monitoring and early intervention to mitigate health risks.

The relationship between metabolic health and cognitive function, particularly in aging populations, is another vital aspect explored in this Research Topic. Findings suggest a clear link between metabolic indices and cognitive performance, highlighting the importance of maintaining metabolic health to preserve cognitive abilities in older adults. Early detection and intervention strategies based on advanced metabolic profiling techniques offer promising pathways to mitigate risks associated with muscle deterioration and cognitive decline.

Gender-specific responses to stress and therapeutic interventions are also addressed, with research indicating that aromatherapy and other non-pharmacological treatments may have differing effects based on sex. This highlights the necessity for personalized approaches in stress management and therapeutic applications. Reproductive health factors, such as age at first birth and menopause, are shown to influence the risk of ovarian cysts, offering insights into the long-term impacts of reproductive milestones.

Clinical interventions for degenerative diseases muscle degeneration and cervical disc degenerative diseases are also examined, providing guidance on optimal surgical approaches to improve patient outcomes.

The long-term outcomes and potential complications of surgical treatments for benign prostatic hyperplasia, as well as the significant impact of abdominal obesity on mortality rates in specific populations, highlight the need for targeted interventions to improve survival rates and patient care.

In conclusion, the articles featured in this Research Topic collectively advance our understanding of the endocrine, metabolic, and psychological factors influencing obesity, aging, and stress. By integrating diverse research methodologies and interdisciplinary approaches, these studies provide a robust foundation for future exploration and innovation in health promotion and disease prevention strategies.

Author contributions

YM: Writing – original draft, Writing – review & editing. KS: Writing – original draft. HW: Writing – original draft, Writing – review & editing.

Conflict of interest

The authors declare that the research was conducted in the absence of any commercial or financial relationships that could be construed as a potential conflict of interest.

Generative AI statement

The author(s) declare that no Generative AI was used in the creation of this manuscript.

Publisher's note

frontiers | Frontiers in Endocrinology

TYPE Original Research
PUBLISHED 26 October 2023
DOI 10.3389/fendo.2023.1287834

OPEN ACCESS

EDITED BY
Heidi de Wet,
University of Oxford, United Kingdom

REVIEWED BY
Jonathan Samuel Chávez-Iñiguez,
University of Guadalajara, Mexico
Abraham Wall-Medrano,
Universidad Autónoma de Ciudad Juárez, Mexico

*CORRESPONDENCE
Yang Luo
luoy@bjsjth.cn

RECEIVED 02 September 2023
ACCEPTED 16 October 2023
PUBLISHED 26 October 2023

CITATION
Shi Z, Guo Y, Ye P and Luo Y (2023) Abdominal obesity in Chinese patients undergoing hemodialysis and its association with all-cause mortality. *Front. Endocrinol.* 14:1287834. doi: 10.3389/fendo.2023.1287834

Abdominal obesity in Chinese patients undergoing hemodialysis and its association with all-cause mortality

Zhihua Shi[1], Yidan Guo[1], Pengpeng Ye[2] and Yang Luo[1]*

[1]Division of Nephrology, Beijing Shijitan Hospital, Capital Medical University, Beijing, China, [2]Division of Injury Prevention and Mental Health, National Center for Chronic and Non-communicable Disease Control and Prevention, Chinese Center for Disease Control and Prevention, Beijing, China

Introduction: Obesity in patients undergoing hemodialysis is common. However, there is limited information on the relationship between obesity types defined by the combined body mass index (BMI) and waist circumference (WC) classification criteria and all-cause mortality in Chinese hemodialysis patients. Our objective was to determine the association between obesity types and all-cause mortality in hemodialysis patients.

Methods: We conducted a prospective cohort study including patients from 11 hemodialysis centers in Beijing. According to the World Health Organization's standards, patients were classified into 2 categories with WC and 4 categories with BMI and then followed up for 1 year. Kaplan–Meier survival analysis was used to compare the difference in the cumulative survival rate in different BMI and WC groups. A multivariate Cox regression analysis was used to determine the association between different types of obesity and all-cause mortality.

Results: A total of 613 patients were enrolled, the mean age was 63.8 ± 7.1 years old, and 42.1% were women. Based on the baseline BMI, there were 303 (49.4%) patients with normal weight, 227 (37.0%) with overweight, 37(6.0%) with obesity, and 46 (7.5%) with underweight. Based on the baseline WC, 346 (56.4%) patients had abdominal obesity. During a median follow-up of 52 weeks, 69 deaths occurred. Kaplan–Meier plots demonstrated a significant association of BMI categories (log-rank $\chi 2$ = 18.574, p<0.001) and WC categories (log-rank $\chi 2$ = 5.698, p=0.017) with all-cause death. With normal BMI and non-abdominal obesity as a reference, multivariate Cox regression analysis results showed that obesity (HR 5.36, 95% CI, 2.09-13.76, p<0.001), underweight (HR, 5.29, 95% CI, 2.32-12.07, p<0.001), normal weight combined with abdominal obesity (HR 2.61, 95% CI, 1.20-5.66, p=0.016), and overweight combined with abdominal obesity (HR 1.79, 95% CI, 1.03-3.73, p=0.031, respectively) were significantly associated with higher risks of all-cause mortality.

Conclusion: Our study indicated that abdominal obesity is common and associated with all-cause mortality among Chinese hemodialysis patients.

KEYWORDS

abdominal obesity cohort study, hemodialysis, waist circumference, body mass index, all-cause mortality

Introduction

Obesity has reached epidemic proportions worldwide, and concerns about its influence on adverse outcomes have kept rising in the last decades (1, 2). In the general population, increased body mass index (BMI) has been shown to be an independent risk factor for all-cause mortality (3, 4). Compared with that in the general population, the results regarding this association in patients undergoing hemodialysis were different, a recent meta-analysis showed that BMI-defined obesity in hemodialysis patients was actually associated with reduced all-cause mortality, challenging the paradigm that obesity is related to increased mortality in the general population, and this inconsistent result was also called the "obesity paradox" (5). However, such a significantly different association in hemodialysis patients should not be simply explained as increased BMI is a protective factor, some studies in hemodialysis patients couldn't validate this conclusion because of the existence of obese sarcopenia or protein-energy malnutrition (6).

Previous data showed that the use of BMI as a measurement of obesity has an important limitation because it does not discriminate abdominal from gluteofemoral fat (5, 7). To find more incremental risk information beyond the measurement of BMI alone among the obesity population, waist circumference (WC) measurement was introduced to assess abdominal obesity in various studies from different ethnic populations, and increased WC was also proved to be an independent risk factor of all-cause mortality even among normal-weight or overweight individuals in the general populations and peritoneal dialysis patients, however, there is still no information about the combination use of BMI and WC in the prediction of adverse outcomes among Chinese hemodialysis patients (8–11).

Compared with that in the general populations, the information about the characteristics of obesity and its influence on clinical adverse outcomes among elder hemodialysis patients is scarce, most previous studies about the relationship between obesity and mortality in hemodialysis patients were conducted with the measurement of BMI (12, 13),. There was still limited information about the association between abdominal obesity and all-cause mortality by combining measurements of BMI and WC in older hemodialysis patients in China. Therefore, we determined to investigate the characteristics of obesity and explore the association between abdominal obesity and all-cause mortality in a prospective cohort study of Chinese older patients undergoing hemodialysis.

Materials and methods

Ethics declaration and participants

The study protocol was approved by the Institutional Ethical Review Board of Beijing Shijitan Hospital, Capital Medical University (Approval No. SJT2016-18). We also performed the STROBE checklist for cohorts (supplementary STROBE checklist). All participants provided written informed consent for this study by themselves or their legal guardians. The patients' identification numbers were anonymized to protect individuals' privacy.

The data used in this study were obtained from a prospective cohort study: the cognitive impairment in Chinese hemodialysis patients (Registered in ClinicalTrials.gov, ID: NCT03251573). The cohort included 613 patients between the ages of 50 and 83 years from 11 hemodialysis centers in Beijing between April and June 2017, diagnosed with end-stage renal disease, treated with maintenance hemodialysis for a minimum of 3 months, and followed up for 1 year for the outcome of all-cause mortality (14). The inclusion criteria were as follows (1): age ≥50 years (2), end-stage renal disease with maintained hemodialysis treatment for a minimum of 3 months, and (3) willing to join the study and provide written informed consent. The exclusion criteria were as follows (1): estimation of a life expectancy of six months or less according to the nephrologists, and (2) planned kidney transplantation within 6 months of baseline.

Participants' baseline characteristics were obtained from patient's medical charts at the time of enrollment, including demographics (age, sex), lifestyle characteristics (smoking and alcohol intake), medical history (diabetes, hypertension, stroke, and coronary heart disease [CHD]) and laboratory variables (hemoglobin, albumin, total cholesterol, triglyceride, serum creatinine, blood urea nitroge, calcium, phosphate, intact parathyroid hormone [iPTH] and C reactive protein [CRP]). The single-pool Kt/V was calculated from the pre-and post-dialysis serum urea nitrogen levels as we applied in the previous study (15). Baseline CHD was defined as a history of recognized myocardial infarction, angina, and prior coronary angioplasty or bypass procedures.

Definition of BMI and WC

In our study, we used BMI and WC measured at baseline as the indexes of obesity. All of the patients had received maintenance hemodialysis for at least 3 months to avoid the influence of fluid overload at the initial stage of the hemodialysis that would distort BMI and WC measurements. The anthropometric data (height, weight, and waist circumference) were measured after a dialysis session to avoid inaccurate that may be caused by fluid overload before dialysis. BMI was calculated as weight in kilograms divided by height in meters squared. Training personnel measured WC in centimeters using the smallest circumference between the lower ribs and iliac crests. In order to make the obesity-related data comparable with other ethnic groups, we applied the classification of World Health Organization guidelines, we defined normal weight as a BMI of 18.5~24 kg/m^2, overweight as a BMI of 24~30 kg/m^2, obesity as a BMI ≥30 kg/m^2, and underweight as a BMI<18.5 kg/m^2. Abdominal obesity was defined as a waist circumference with sex-specific criteria (WC ≥90cm in men and ≥80cm in women) (4, 16).

Study outcomes and follow-up

The primary outcome of this study was all-cause mortality. The incidence of all-cause mortality for each participant was evaluated between June 30, 2017, and June 30, 2018. Survival time was defined as the time elapsed from initial study enrollment until the occurrence of an outcome event, kidney transplantation, and the end of the follow-up period. We obtained the survival status of the patients through periodic medical chart monitoring and contacting each patient's dialysis unit.

Statistical analyses

Variables are presented as mean with SD or median with interquartile range (IQR) or number (proportion) where appropriate. Baseline characteristics were compared by using the Chi-square test for categorical variables and t or Wilcoxon rank sum tests, as appropriate, for continuous variables. Restricted cubic splines were used to evaluate for nonlinear relationships between baseline BMI or WC measures and outcomes. Kaplan–Meier curves for all-cause mortality based on BMI and WC were constructed, and the log-rank test was used to compare the inter-group differences. Multivariable Cox proportional hazards regression analyses were conducted to quantify the risk of all-cause death associated with baseline BMI or WC.

We also performed a sensitivity analysis to validate the stability of our study findings. Because the patients in each BMI group may differ by WC, we further stratified the participants of each BMI group into abdominal obesity and non-abdominal obesity groups, and generated the analysis of the joint associations of BMI and WC status with all-cause mortality, with the subgroup having normal BMI and non-abdominal obesity considered as reference, adjusting for baseline covariates.

Statistical significance was set at a value of $p<0.05$. All analyses were performed with SPSS version 21.0 statistical software (SPSS Inc, Chicago, IL, USA) and JMP Pro 13.2 statistical software (SAS Institute Inc.)

Results

Basic characteristics of the participants

We finally included 613 patients in this cohort study (Figure 1). The mean age was 63.82 ± 7.14 years, and 42.1% were women. The median hemodialysis vintage was 57 months,

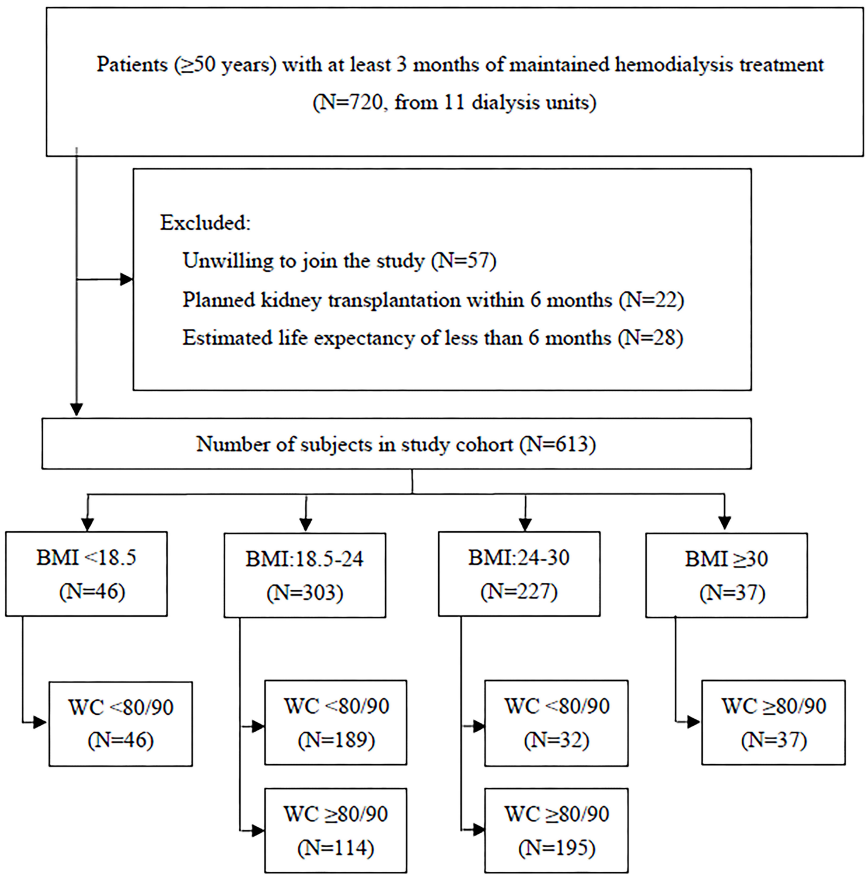

FIGURE 1
Flowchat of cohort creation.

10.3389/fendo.2023.1287834

and the average dialysis treatment session length was 3.81 ± 0.27 h. each time, three times a week. The baseline characteristics of participants are displayed in Table 1. The male patients tended to have lower proportions of CHD history, abdominal obesity, shorter hemodialysis vintage, and higher level of serum creatinine and blood urea nitroge. (p<0.05).

Based on the baseline BMI, there were 303 (49.4%) patients with normal weight, 227 (37.0%) with overweight, 37(6.0%) with obesity, and 46 (7.5%) with underweight. Based on the baseline WC, there were 346 (56.4%) patients with abdominal obesity and 267 (43.6%) with non-abdominal obesity. The number of patients with abdominal obesity was 0 (0%) in the underweight group, 114 (37.6%) in the normal weight group, 195 (85.9%) in the overweight group, and 37 (100.0%) in the obesity group, respectively. None of the underweight patients had abdominal obesity, and all the patients in the obesity group were abdominal obesity patients. The distribution of the obesity status of the patients is shown in Figure 2.

TABLE 1 Baseline characteristics of the participants.

Characteristic	Total (N = 613)	Males (N=355)	Females (N=258)	p-value
Demographics				
Age, years	63.82 ± 7.14	63.86 ± 7.51	63.37 ± 8.14	0.444
Smoking history, n (%)	270(44.0)	150(42.3)	120(46.5)	0.294
Alcohol intake, n (%)	261(42.6)	147(41.4)	114(44.2)	0.492
Comorbidity				
Hypertension, n (%)	545(88.9)	311(87.6)	234(90.7)	0.229
Diabetes, n (%)	231(37.7)	131(36.9)	100(38.8)	0.639
Stroke, n (%)	101(16.5)	55(15.5)	46(17.8)	0.441
CHD, n (%)	194(31.6)	95(26.8)	99(38.4)	0.002
Dialysis vintage, month	57 (24–101)	54.00(21.00-91.00)	63.00 (30.00-110.50)	0.022
Single-pool Kt/V	1.29 ± 0.18	1.30 ± 0.18	1.27 ± 0.17	0.108
BMI (range), kg/m^2	23.03(21.00-26.10)	23.00 (21.26-25.95)	23.27 (20.75-26.57)	0.638
BMI (status), n (%)				**0.461**
< 18.5 kg/m^2	46(7.5)	29(8.2)	17(6.6)	
18.5–24 kg/m^2	303(49.4)	180(50.7)	123(47.7)	
24–30 kg/m^2	227(37.0)	124(34.9)	103(39.9)	
≥ 30 kg/m^2	37(6.0)	22(6.2)	15(5.8)	
WC (range), cm	87.00(78.00-94.00)	86.00 (78.00-94.00)	87.00 (78.00-96.00)	0.320
Abdominal obesity, n (%)	346(56.4)	188(53.0)	158(61.2)	0.041
Laboratory data				
Hb, g/L	111.16 ± 14.53	111.09 ± 14.86	111.24 ± 14.08	0.896
Alb, g/L	39.73 ± 3.25	39.61 ± 3.18	39.90 ± 3.35	0.286
TC, mmol/L	4.25 ± 1.28	4.21 ± 0.94	4.30 ± 1.63	0.380
TG, mmol/L	2.09 ± 1.46	2.03 ± 1.30	2.19 ± 1.64	0.178
Scr, ummol/L	832.50(620.30-1006.70)	906.80(682.20-1075.70)	733.00(533.00-898.10)	<0.001
BUN, mmol/L	22.32(17.99-26.68)	23.35(19.60-27.83)	21.02(15.49-25.44)	<0.001
Calcium, mmol/L	2.24 ± 0.24	2.25 ± 0.25	2.23 ± 0.24	0.308
Phosphate, mmol/L	1.72 ± 0.65	1.71 ± 0.60	1.72 ± 0.71	0.848
iPTH, pg/mL	187.60(103.50-358.15)	176.20(99.70-332.70)	223.45(111.47-376.13)	0.093
CRP, mg/L	2.75(1.41-6.02)	2.72(1.33-4.88)	2.82(1.50-8.05)	0.080

Data were presented as mean ± SD or median (interquartile range) for continuous variables and number (%) for categorical variables. CHD, coronary heart disease; MoCA, Montreal Cognitive Assessment; Kt/V, an indicator for evaluating dialysis adequacy; BMI, body mass index; WC, waist circumference; Hb, hemoglobin; ALB, albumin; TC, total cholesterol; TG, triglyceride; Scr, serum creatinine; BUN, blood urea nitrogen; iPTH, intact parathyroid hormone; CRP, C-reactive protein.

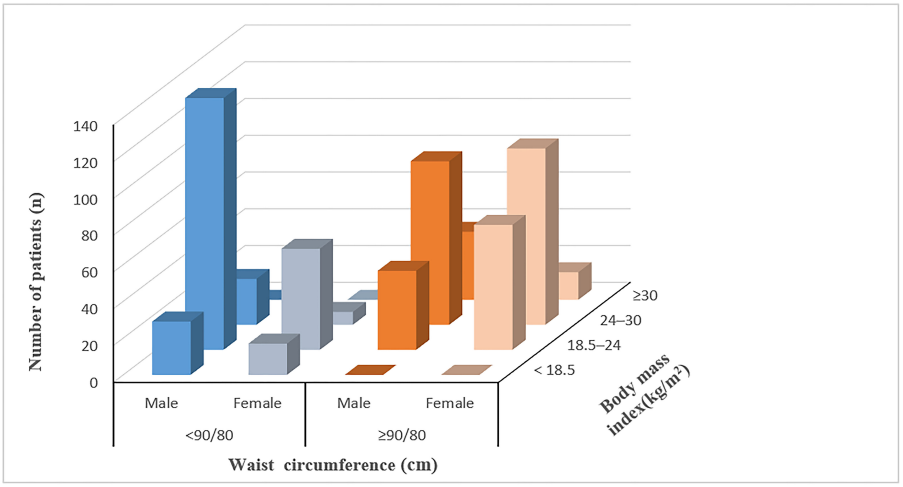

FIGURE 2
Distribution of patients according to the combination categories of BMI and WC.

Association of BMI and WC with the risk of all-cause mortality

After a median follow-up of 52 weeks, all-cause death occurred in 69 patients. (). Kaplan-Meier plots showed the association between BMI categories (log-rank χ^2 = 18.574, p<0.001) and WC categories (log-rank χ^2 = 5.698, p=0.017) and all-cause death, respectively. (Figures 3A, B).

Restricted cubic splines showed the nonlinear relationships between BMI and WC and the hazard ratios for all-cause mortality. (Figures 4A, B). Figure 4A showed a U-shaped relationship between BMI and mortality, with the lowest BMI integer value of 25 kg/m^2. Both the increase and decrease in BMI were associated with an increasing trend of death risk. Figure 4B shows the relationship between WC and mortality, with a hazard ratio <1.0 for WC<85cm and a hazard ratio >1.0 for WC>85cm.

Results of univariable and multivariable Cox proportional hazard analyses were summarized in Table 2. Using the normal weight group as a reference, multivariate Cox regression analysis showed that the risk of all-cause death tended to increase in the obesity group (HR 2.50, 95% CI, 1.12-5.59, p=0.026) and the underweight group (HR 3.49, 95% CI, 1.75-6.99, p<0.001), but not in the overweight group (HR 1.10, 95% CI, 0.62-1.93, p=0.758); and using the non-abdominal obesity group as a reference, the risk of all-cause death was increased in the abdominal obesity group (HR 1.80, 95% CI, 1.06-3.05, p=0.029).

The sensitive analysis showed the association between abdominal obesity status and all-cause mortality in different ranges of BMI. We used the group of patients with normal BMI and non-abdominal obesity as a reference, multivariate Cox regression analysis results showed that obesity (HR 5.36, 95% CI, 2.09-13.76, p<0.001) and underweight (HR, 5.29, 95% CI, 2.32-

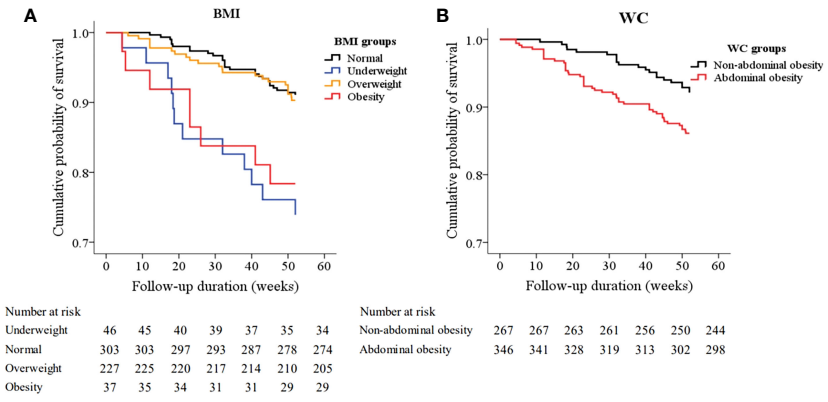

FIGURE 3
Kaplan–Meier survival curves for all-cause mortality based on body mass index (BMI) **(A)** and waist circumference (WC) **(B)**. The pairwise comparison showed that there were significant differences between the underweight group (log-rank χ^2 = 13.571, P<0.001) and the obesity group (log-rank χ^2 = 6.664 P=0.010) and the normal BMI group respectively, but there is no significant difference between the overweight group (log-rank χ^2 = 0.102 P=0.750) and the normal BMI group. (Figure 3A), and there was a significant difference between the abdominal obesity group and the non-abdominal obesity group (log-rank χ^2 = 5.698, P=0.017). (Figure 3B).

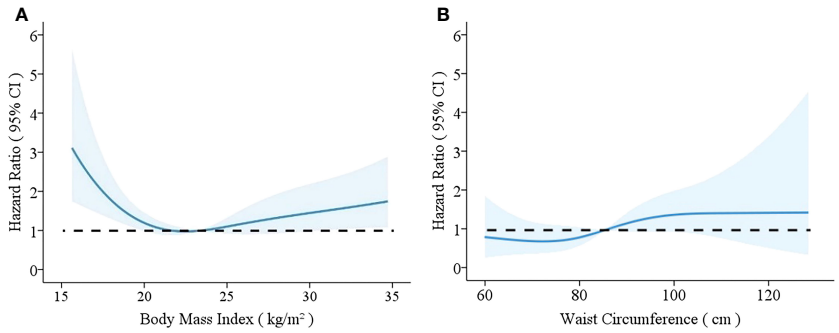

FIGURE 4
Relationships between body mass index (BMI) **(A)** and waist circumference (WC) **(B)** and mortality rates with 95% confidence intervals for hemodialysis patients. Hazard ratios for mortality depending on BMI **(A)** and WC **(B)** were modeled by separate restricted cubic splines Cox regression model analyses. The models were adjusted for age, sex, smoking, alcohol drinking, medical history of hypertension, diabetes, stroke, and CHD, dialysis vintage, Kt/V, hemoglobin, serum levels of albumin, total cholesterol, triglycerides, calcium, phosphate, intact parathyroid hormone, and C-reactive protein.

12.07, $p<0.001$) were still significantly associated with higher risks of all-cause mortality. In addition, for normal weight and overweight patients, the risks of all-cause mortality were also significantly increased in patients combined with abdominal obesity (HR 2.61, 95% CI, 1.20-5.66, $p=0.016$ and HR 1.79, 95% CI, 1.03-3.73, $p=0.031$, respectively), but not in patients with non-abdominal obesity (HR 0.89, 95% CI, 0.11-6.93, $p=0.907$). (Table 3).

Discussion

In this cohort study of hemodialysis patients, we found that both underweight and obese patients defined by BMI had a significantly increased all-cause mortality compared with the patients with normal weight, while the overweight patients did not exhibit such kind of association with death. In addition, our data showed that participants with abdominal obesity defined by WC also had an increased risk of all-cause mortality compared with non-abdominal obesity counterparts even after adjusted with some potential mediators, notably, this association was observed in the patients with a wide range of BMI, even in the patients with BMI defined normal or overweight. Our data delineated the characteristics of obesity in Chinese older hemodialysis patients and provided evidence about the association between abdominal obesity and all-cause mortality in different BMI ranges.

Currently, obesity has been regarded as a kind of chronic disease, and obesity-related issues in patients with chronic kidney disease also cause great attention (9, 10). In 2002, the prevalence of obesity in the U.S. Renal Data System was 29% (17). Data from some European countries showed that the proportion of obese patients on dialysis was less than in the U.S., ranging from 10% to 12% (18). In China, the latest national survey showed that the prevalence was 34.3% for overweight and 16.4% for obesity in the general population from 2015 to 2019, and the study also found that there is a trend that Chinese people with obesity tend to have abdominal obesity (apple-shaped) rather than gluteofemoral obesity (pear-shaped) (19). In our study, the proportion of overweight was 37% and obesity was 6% defined by BMI; we also

TABLE 2 The association between BMI and WC status and all-cause mortality.

Groups	Death rate n/N (%)	Unadjusted Model		Multivariate Model 1		Multivariate Model 2	
		HR (95% CI)	*p*-Value	HR (95% CI)	*p*-Value	HR (95% CI)	*p*-Value
BMI status, kg/m^2							
< 18.5	12/46(26.1)	3.32 (1.68-6.56)	<0.001	3.56 (1.79-7.08)	<0.001	3.49 (1.75-6.99)	<0.001
18.5–24	27/303(8.9)	1.00 (reference)		1.00 (reference)		1.00 (reference)	
24–30	22/227(9.7)	1.096(0.62-1.92)	0.750	1.025(0.58-1.80)	0.932	1.01(0.62-1.93)	0.758
≥ 30	8/37(21.6)	2.70 (1.23-5.94)	0.014	2.75 (1.24-6.14)	0.013	2.50 (1.12-5.59)	0.026
WC status, cm							
< 80/90	21/267(7.9)	1.00 (reference)		1.00 (reference)		1.00 (reference)	
≥ 80/90	48/346(13.9)	1.85(1.11-3.09)	0.019	1.75(1.04-2.92)	0.034	1.80 (1.06-3.05)	0.029

HR, hazard ratio; CI, confidence interval; BMI, body mass index; WC, waist circumference.
Unadjusted and multivariable-adjusted HRs were analyzed by the Cox proportional hazards risk model with all-cause death. Multivariable-adjusted model 1 was adjusted for age, sex, smoking, alcohol drinking, and comorbidities of hypertension, diabetes, stroke, and CHD. Multivariable-adjusted model 2 was adjusted for model 1 plus dialysis vintage, Kt/V, hemoglobin, serum levels of albumin, total cholesterol, triglycerides, calcium, phosphate, intact parathyroid hormone, and C-reactive protein.

TABLE 3 Associations of abdominal obesity and all-cause mortality in different ranges of BMI.

Group		Death rate n/N (%)	Unadjusted Model		Multivariate Model 1		Multivariate Model 2	
BMI, kg/m^2	WC, cm		HR (95% CI)	*p*-Value	HR (95% CI)	*p*-Value	HR (95% CI)	*p*-Value
< 18.5	<80/90	12/46(26.1)	5.28(2.33-11.96)	<0.001	5.49(2.41-12.49)	<0.001	5.29(2.32-12.07)	<0.001
	≥80/90	–	–	–	–	–	–	–
18.5–24	<80/90	11/189(5.8)	1.00(reference)		1.00(reference)		1.00(reference)	
	≥80/90	16/114(14.0)	2.67(1.28-5.74)	0.012	2.53(1.17-5.47)	0.018	2.61(1.20-5.66)	0.016
24–30	<80/90	1/32(3.1)	0.54(0.07-4.16)	0.551	0.66(0.09-5.13)	0.692	0.89(0.11-6.93)	0.907
	≥80/90	21/195(10.8)	1.95(1.01-4.04)	0.023	1.72(1.02-4.05)	0.036	1.79(1.03-3.73)	0.031
≥30	<80/90	–	–	–	–	–	–	–
	≥80/90	8/37(21.6)	4.29(1.72-10.66)	0.002	4.36(1.73-11.02)	0.002	5.36(2.09-13.76)	<0.001

HR, hazard ratio; CI, confidence interval; BMI, body mass index; WC, waist circumference.
Unadjusted and multivariable-adjusted HRs were analyzed by the Cox proportional hazards risk model with all-cause death. Multivariable-adjusted model 1 was adjusted for age, sex, smoking, alcohol drinking, and comorbidities of hypertension, diabetes, stroke, and CHD. Multivariable-adjusted model 2 was adjusted for model 1 plus dialysis vintage, Kt/V, hemoglobin, serum levels of albumin, total cholesterol, triglycerides, calcium, phosphate, intact parathyroid hormone, and C-reactive protein.

noticed that the total abdominal obesity had reached 56.4%. Notably, all of the obese patients defined by increased BMI in our study also had abdominal obesity, and abdominal obesity even existed in the normal weight and overweight groups defined by BMI, that is to say, the main feature of obesity in this group of elder patients undergoing hemodialysis was abdominal obesity, these results also mirrored the differences between the general population and patients undergoing hemodialysis in China. Although most of the current understanding of the negative influence of excess body fat on health was built up on the basis of the data on general obesity, which was defined by increased BMI (13, 16, 20), evidence is emerging that BMI is an imperfect metric for obesity, and WC appears to be a better indicator of this disease than BMI (21–23). A pooled analysis included 650000 white adults from the Mayo Clinic indicated that abdominal obesity defined by increased WC was positively associated with higher all-cause mortality at all levels of BMI from 20 to 50 kg/m^2 (24). These data provide evidence that abdominal obesity is an independent risk factor for all-cause mortality in community individuals, based on such related information, we used WC to evaluate the status of abdominal obesity on the basis of BMI classification, and this is also the first report about the features of obesity among Chinese elder hemodialysis patients.

Another major concern is the relationship between obesity and adverse outcomes in hemodialysis patients. Maleeka (5) made a meta-analysis that included 852162 patients undergoing hemodialysis in 65 cohorts, the results showed that a 1 kg/m^2 increase in BMI was associated with a 3 and 4% reduction in all-cause and cardiovascular mortality in patients on hemodialysis, the results seemed to indicate that being obese is protective against all-cause and cardiovascular mortality. However, some studies didn't show this "obesity paradox". Ellen (25) found a U-shaped association between obesity measured by BMI and all-cause mortality after 7 years of follow-up in a group of hemodialysis patients who were younger than 65 years old. Like the limitation in the general population, using BMI in the evaluation of obesity in dialysis patients also couldn't reflect the real situation of abdominal fat deposition (23). By applying both BMI and WC measurements, our results showed that abdominal obesity existed in individuals with a wide range of BMI, even in the patients with BMI defined as normal or overweight, this result was in accordance with the results from the cohort study from Korean, they included the data of 18,699 adult hemodialysis patients who were followed up for 4 years and for whom BMI and WC information were available, participants with the highest WC had a higher risk of mortality, these data in Asian hemodialysis population reflected the important in monitoring the WC among hemodialysis patients (26).

As abdominal obesity was the marker of visceral fat accumulation, previous studies indicated that it was more strongly associated with multiple chronic diseases than gluteofemoral obesity (27, 28). This overlapped classification of obesity between BMI and WC measurements in our study might partially explain the reason why we didn't see the "obesity paradox" in these participants, at the same time, our data also indicated that visceral fat accumulation played an important role in deciding the relationship of obesity and all-cause mortality, it seems necessary to use BMI and WC at the same time in evaluating the obesity status in hemodialysis patients, this combining metrics of overall body size with BMI and local fat accumulation with WC seems to be particularly important in predicting the clinical outcomes in patients undergoing hemodialysis.

Our study has various strengths. We used standardized data from a prospective cohort of participants undergoing hemodialysis from 11 centers, all participants had relatively stable states with proper dry weight at the enrollment, which significantly reduced the influence of fluid overload on the evaluation of obesity. Furthermore, both BMI and WC applied in our study are simple and reliable metrics for different types of obesity, which provide an accurate classification of obesity status in our study. Nevertheless, several limitations should be recognized, including a relatively small sample size and short time of follow-up, the representative of the enrolled patients was only restricted within Beijing which may lead

to selection bias, and some larger cohorts are needed to delineate the characteristics of obesity in patients undergoing hemodialysis in China. In addition, spectroscopic bioimpedance has not yet been used in this study, and it is crucial in determining the distribution of fat and muscle mass. The results of this study suggested that patients undergoing hemodialysis might improve life expectancy by proper weight control to the recommended levels, and both BMI and WC measurements are important metrics in identifying obesity status which should be used simultaneously in the obesity-related evaluation.

Conclusions

In conclusion, our findings indicate that abdominal obesity is common and associated with all-cause mortality among middle-aged and older age Chinese patients undergoing hemodialysis. The obese patients defined by increased BMI also have abdominal obesity, which reflects that visceral fat deposition is a key feature among this group of patients, it might be necessary to make a combined measurement of BMI and WC while evaluating of obesity status in these patients.

Data availability statement

The raw data supporting the conclusions of this article will be made available by the authors, without undue reservation.

Ethics statement

The studies involving humans were approved by Beijing Shijitan Hospital ethics committee. The studies were conducted in accordance with the local legislation and institutional requirements. The participants provided their written informed consent to participate in this study.

Author contributions

ZS: Writing - original draft. YG: Data curation, Writing - review & editing. PY: Data curation, Methodology, Software, Conceptualization, Writing - original draft. YL: Conceptualization, Supervision, Writing - original draft.

Funding

The author(s) declare financial support was received for the research, authorship, and/or publication of this article. This project was supported by a grant from the Beijing Municipal Science & Technology Commission (No. Z161100002616005) and The Capital's Funds for Health Improvement and Research (2022–2–2081). The funders had no role in the study design, data collection, data analysis, decision to publish, and preparation of the manuscript.

Acknowledgments

The authors would like to thank the doctors and nurses in the dialysis centers at 11 hospitals in Beijing for their support and collaboration in this research. We also acknowledged the important contribution of the staff and patients at the 11 units; without their cooperation, the study would not have been successful.

Conflict of interest

The authors declare that the research was conducted in the absence of any commercial or financial relationships that could be construed as a potential conflict of interest.

Publisher's note

Supplementary material

The Supplementary Material for this article can be found online at: https://www.frontiersin.org/articles/10.3389/fendo.2023.1287834/full#supplementary-material

References

1. Jaacks LM, Vandevijvere S, Pan A, McGowan CJ, Wallace C, Imamura F, et al. The obesity transition: stages of the global epidemic. *Lancet Diabetes Endocrinol* (2019) 7:231–40. doi: 10.1016/S2213-8587(19)30026-9

2. Health TLP. Tackling obesity seriously: the time has come. *Lancet Public Health* (2018) 3:e153. doi: 10.1016/S2468-2667(18)30053-7

3. Williams M, Lee M, Alfadhel M, Kerr AJ. Obesity and all-cause mortality following acute coronary syndrome (ANZACS-QI 53). *Heart Lung Circ* (2021) 30:1854–62. doi: 10.1016/j.hlc.2021.04.014

4. Flegal KM, Kit BK, Orpana H, Graubard BI. Association of all-cause mortality with overweight and obesity using standard body mass index categories: a systematic review and meta-analysis. *JAMA*. (2013) 309:71–82. doi: 10.1001/jama.2012.113905

5. Ladhani M, Craig JC, Irving M, Clayton PA, Wong G. Obesity and the risk of cardiovascular and all-cause mortality in chronic kidney disease: a systematic review and meta-analysis. *Nephrol Dial Transplant.* (2017) 32:439–49. doi: 10.1093/ndt/gfw075

6. Hall YN, Xu P, Chertow GM. Relationship of body size and mortality among US Asians and Pacific Islanders on dialysis. *Ethn Dis* (2011) 21:40–6.

7. Postorino M, Marino C, Tripepi G, Zoccali C. Abdominal obesity and all-cause and cardiovascular mortality in end-stage renal disease. *J Am Coll Cardiol* (2009) 53:1265–72. doi: 10.1016/j.jacc.2008.12.040

8. Pujilestari CU, Nyström L, Norberg M, Ng N. Waist circumference and all-cause mortality among older adults in rural Indonesia. *Int J Environ Res Public Health* (2019) 16:116. doi: 10.3390/ijerph16010116

9. Chen Y, Yang Y, Jiang H, Liang X, Wang Y, Lu W. Associations of BMI and waist circumference with all-cause mortality: A 22-year cohort study. *Obesity.* (2019) 27:662–9. doi: 10.1002/oby.22423

10. Seidell JC. Waist circumference and waist/hip ratio in relation to all-cause mortality, cancer and sleep apnea. *Eur J Clin Nutr* (2010) 64:35–41. doi: 10.1038/ejcn.2009.71

11. Castro A, Bazanelli AP, Nerbass FB, Cuppari L, Kamimura MA. Waist circumference as a predictor of mortality in peritoneal dialysis patients: a follow-up study of 48 months. *Br J Nutr* (2017) 117:1299–303. doi: 10.1017/S0007114517001179

12. Lowrie EG, Li Z, Ofsthun N, Lazarus JM. Body size, dialysis dose and death risk relationships among hemodialysis patients. *Kidney Int* (2002) 62:1891–7. doi: 10.1046/j.1523-1755.2002.00642.x

13. Kalantar-Zadeh K, Kopple JD, Kilpatrick RD, McAllister CJ, Shinaberger CS, Gjertson DW, et al. Association of morbid obesity and weight change over time with cardiovascular survival in hemodialysis population. *Am J Kidney Dis* (2005) 46:489–500. doi: 10.1053/j.ajkd.2005.05.020

14. Luo Y, Murray AM, Guo YD, Tian R, Ye PP, Li X, et al. Cognitive impairment and associated risk factors in older adult hemodialysis patients: a cross-sectional survey. *Sci Rep* (2020) 10:12542. doi: 10.1038/s41598-020-69482-1

15. Guo Y, Tian R, Ye P, Luo Y. Frailty in older patients undergoing hemodialysis and its association with all-cause mortality: A prospective cohort study. *Clin Interv Aging*. (2022) 17:265–75. doi: 10.2147/CIA.S357582

16. Safaei M, Sundararajan EA, Driss M, Boulila W, Shapi'i A. A systematic literature review on obesity: Understanding the causes & consequences of obesity and reviewing various machine learning approaches used to predict obesity. *Comput Biol Med* (2021) 136:104754. doi: 10.1016/j.compbiomed.2021.104754

17. Kramer HJ, Saranathan A, Luke A, Durazo-Arvizu RA, Guichan C, Hou S, et al. Increasing body mass index and obesity in the incident ESRD population. *J Am Soc Nephrol.* (2006) 17:1453–9. doi: 10.1681/ASN.2005111241

18. Bossola M, Giungi S, Tazza L, Luciani G. Is there any survival advantage of obesity in Southern European haemodialysis patients. *Nephrol Dial Transplant.* (2010) 25:318–9. doi: 10.1093/ndt/gfp543

19. Pan XF, Wang L, Pan A. Epidemiology and determinants of obesity in China. *Lancet Diabetes Endocrinol* (2021) 9:373–92. doi: 10.1016/S2213-8587(21)00045-0

20. Bouchard CBMI. fat mass, abdominal adiposity and visceral fat: where is the 'beef'. *Int J Obes (Lond).* (2007) 31:1552–3. doi: 10.1038/sj.ijo.0803653

21. Rothman KJ. BMI-related errors in the measurement of obesity. *Int J Obes (Lond).* (2008) 32 Suppl 3:S56–9. doi: 10.1038/ijo.2008.87

22. Nimptsch K, Konigorski S, Pischon T. Diagnosis of obesity and use of obesity biomarkers in science and clinical medicine. *Metabolism.* (2019) 92:61–70. doi: 10.1016/j.metabol.2018.12.006

23. Goh VH, Tain CF, Tong TY, Mok HP, Wong MT. Are BMI and other anthropometric measures appropriate as indices for obesity? A study in an Asian population. *J Lipid Res* (2004) 45:1892–8. doi: 10.1194/jlr.M400159-JLR200

24. Cerhan JR, Moore SC, Jacobs EJ, Kitahara CM, Rosenberg PS, Adami HO, et al. A pooled analysis of waist circumference and mortality in 650,000 adults. *Mayo Clin Proc* (2014) 89:335–45. doi: 10.1016/j.mayocp.2013.11.011

25. Hoogeveen EK, Halbesma N, Rothman KJ, Stijnen T, van Dijk S, Dekker FW, et al. Obesity and mortality risk among younger dialysis patients. *Clin J Am Soc Nephrol.* (2012) 7:280–8. doi: 10.2215/CJN.05700611

26. Kim CS, Han KD, Choi HS, Bae EH, Ma SK, Kim SW. Association of body mass index and waist circumference with all-cause mortality in hemodialysis patients. *J Clin Med* (2020) 9:1289. doi: 10.3390/jcm9051289

27. Ibrahim MM. Subcutaneous and visceral adipose tissue: structural and functional differences. *Obes Rev* (2010) 11:11–8. doi: 10.1111/j.1467-789X.2009.00623.x

28. Karpe F, Pinnick KE. Biology of upper-body and lower-body adipose tissue–link to whole-body phenotypes. *Nat Rev Endocrinol* (2015) 11:90–100. doi: 10.1038/nrendo.2014.185

frontiers | Frontiers in Endocrinology

TYPE Systematic Review
PUBLISHED 09 November 2023
DOI 10.3389/fendo.2023.1287212

OPEN ACCESS

EDITED BY
Kenju Shimomura,
Fukushima Medical University, Japan

REVIEWED BY
Jens Djurhuus,
Aarhus University, Denmark
Biagio Barone,
Azienda Ospedaliera di Caserta, Italy

*CORRESPONDENCE
Weijun Qin
qinwj@fmmu.edu.cn

†These authors have contributed equally to this work

RECEIVED 01 September 2023
ACCEPTED 03 October 2023
PUBLISHED 09 November 2023

CITATION
He W, Ding T, Niu Z, Hao C, Li C, Xu Z, Jing Y and Qin W (2023) Reoperation after surgical treatment for benign prostatic hyperplasia: a systematic review. *Front. Endocrinol.* 14:1287212. doi: 10.3389/fendo.2023.1287212

Reoperation after surgical treatment for benign prostatic hyperplasia: a systematic review

Weixiang He[1†], Ting Ding[2†], Zhiping Niu[3†], Chunlin Hao[1], Chengbin Li[1], Zhicheng Xu[1], Yuming Jing[1] and Weijun Qin[1*]

[1]Department of Urology, Xijing Hospital, The Fourth Military Medical University, Xi'an, China, [2]Department of Clinical Laboratory Medicine, Xijing Hospital, The Fourth Military Medical University, Xi'an, China, [3]Department of Environmental Health, School of Public Health, Fudan University, Shanghai, China

Context: Surgical treatment is important for male lower urinary tract symptom (LUTS) management, but there are few reviews of the risks of reoperation.

Objective: To systematically evaluate the current evidence regarding the reoperation rates of surgical treatment for LUTS in accordance with current recommendations and guidelines.

Evidence acquisition: Eligible studies published up to July 2023, were searched for in the PubMed® (National Library of Medicine, Bethesda, MD, USA), Embase® (Elsevier, Amsterdam, the Netherlands), and Web of Science™ (Clarivate™, Philadelphia, PA, USA) databases. STATA® (StataCorp LP, College Station, TX, USA) software was used to conduct the meta-analysis. Random-effects models were used to calculate the pooled incidences (PIs) of reoperation and the 95% confidence intervals (CIs).

Evidence synthesis: A total of 119 studies with 130,106 patients were included. The reoperation rate of transurethral resection of the prostate (TURP) at 1, 2, 3, and 5 years was 4.0%, 5.0%, 6.0%, and 7.7%, respectively. The reoperation rate of plasma kinetic loop resection of the prostate (PKRP) at 1, 2, 3, and 5 years was 3.5%, 3.6%, 5.7%, and 6.6%, respectively. The reoperation rate of holmium laser enucleation of the prostate (HoLEP) at 1, 2, 3, and 5 years was 2.4%, 3.3%, 5.4%, and 6.6%, respectively. The reoperation rate of photoselective vaporization of the prostate (PVP) at 1, 2, 3, and 5 years was 3.3%, 4.1%, 6.7%, and 7.1%, respectively. The reoperation rate of surgery with AquaBeam® at 1, 2, 3, and 5 years was 2.6%, 3.1%, 3.0%, and 4.1%, respectively. The reoperation rate of prostatic artery embolization (PAE) at 1, 2, 3, and 5 years was 12.2%, 20.0%, 26.4%, and 23.8%, respectively. The reoperation rate of transurethral microwave thermotherapy (TUMT) at 1, 2, 3, and 5 years was 9.9%, 19.9%, 23.3%, and 31.2%, respectively. The reoperation rate of transurethral incision of the prostate (TUIP) at 5 years was 13.4%. The reoperation rate of open prostatectomy (OP) at 1 and 5 years was 1.3% and 4.4%, respectively. The reoperation rate of thulium laser enucleation of the prostate (ThuLEP) at 1, 2, and 5 years was 3.7%, 7.7%, and 8.4%, respectively.

Conclusion: Our results summarized the reoperation rates of 10 surgical procedures over follow-up durations of 1, 2, 3, and 5 years, which could provide reference for urologists and LUTS patients.

Systematic review registration: https://www.crd.york.ac.uk/PROSPERO, identifier CRD42023445780.

KEYWORDS

benign prostate hyperplasia, lower urinary tract symptoms, surgery, retreatment, reoperation

Introduction

Lower urinary tract symptoms (LUTSs) related to benign prostatic hyperplasia (BPH) are very common in older men and seriously affect their quality of life (1). Although α1-adrenoceptor antagonists and 5α-reductase inhibitors are first-line drugs with good efficacy, many adverse events such as dizziness, asthenia, postural hypotension, and low libido may occur as a result of treatment with them (1). In addition, there are some patients who have poor drug responsiveness or for whom these drugs are eventually unable to delay disease progress. Therefore, many patients ultimately require surgical intervention (1). According to the current guidelines, indications of the need for surgery include renal insufficiency, refractory urinary retention, recurrent urinary tract infections (UTIs) or gross hematuria, bladder stones, or the patient being refractory to or unwilling to use other therapies (2, 3). Transurethral resection of prostate (TURP) has long been considered the "gold standard" for the surgical management of LUTSs/BPH (4). In recent decades, many new technologies and procedures have been widely used and recommended by clinical guidelines, such as plasma kinetic resection of prostate (PKRP), holmium laser enucleation of the prostate (HoLEP), and photoselective vaporization of the prostate (PVP) (2, 3). Based on the current guidelines, the most suitable type of surgery for a patient depends on their prostate volume (PV), physical condition, and economic situation, and can also even be dependent on the preference of the surgeon and the machines owned by the hospital (2, 3).

Since the physical characteristics of the surgical technique and the anatomy of the prostate vary across patients, some may suffer bladder neck contracture (BNC), urethral stricture, or other complex complications postoperatively, and these may need surgical retreatment (1). In addition, some surgical procedures do not provide patients with satisfactory relief from their symptoms, or do not prevent the reappearance of bladder outlet obstruction over time after surgery, which may also require surgical retreatment. Moreover, some recommended surgical procedures are still under investigation such as surgery with AquaBeam® and prostatic artery embolization (PAE), of which the efficacy, safety, and tolerability still need to be confirmed (3). When selecting an appropriate surgical approach, knowledge of the reoperation rates could be used to predict the cost and management of disease in the years following the operation.

In the past, many studies have reported on the reoperation rate after various kinds of surgery. For patients who had undergone TURP, an Austrian nationwide study reported that the retreatment rate at the 1-year follow-up was 3.7%, and that this increased by approximately 1%–2% with each subsequent year (5, 6). A recent study reported that the rate of secondary surgery for TURP, transurethral incision of prostate (TUIP), and PVP at the 5-year follow-up was 10.3%, 13.6%, and 11.6%, respectively (7). Other procedures such as PAE and transurethral microwave thermotherapy (TUMT) were reported to have a higher risk of retreatment (8, 9). Recently, a systematic review also summarized the pharmacologic and surgical retreatment rates after newer office-based treatments, including water vapor thermal therapy (WVTT), prostatic urethral lift (PUL), and that using a temporarily implanted nitinol device (iTIND) (10). However, there is still a limited number of reviews on the reoperation rate of common surgeries recommended by the guidelines. We therefore conducted an updated systematic review and meta-analysis to summarize the reoperation rates of common surgical treatment for LUTSs/BPH. This review could be important to both BPH/LUTS patients and urologists when they are selecting an appropriate surgical procedure.

Methods

Literature search

This systematic review was conducted in accordance with the Preferred Reporting Items for Systematic Reviews and Meta-Analyses (PRISMA) guidelines (11). The protocol was registered in the International Prospective Register of Systematic Reviews (PROSPERO) database (registration number CRD42023445780).

Studies were searched for in the PubMed® (National Library of Medicine, Bethesda, MD, USA), Embase® (Elsevier, Amsterdam, the Netherlands), and Web of Science™ (Clarivate™, Philadelphia, PA, USA) databases up to July 2023. The primary outcomes were the rates of surgical retreatment during follow-up. The search strategy is provided in the Supplementary Files. The initial screening, which included reading the title and abstract, was performed by the two authors independently (WXH and TD).

Subsequently, the full text of potentially relevant studies was acquired for further confirmation and the data extraction process. Any conflicts that arose between the two authors during article selection and data extraction were resolved through discussion with an arbitrator (ZPN).

Inclusion and exclusion criteria

Articles that met the following criteria were included: (1) those that reported on the surgical retreatment rate of BPH/LUTS patients who had undergone operations in hospitals during the follow-up period; (2) those that were focused only on procedures recommended in the recent guidelines of the Association of University Administrators (AUA) and the European Association of Urology (EAU), including TURP, PKRP, TUIP, open prostatectomy (OP), thulium:yttrium aluminum garnet laser (Tm : YAG), enucleation of the prostate (ThuLEP), HoLEP, PVP, surgery with AquaBeam, PAE, and TUMT; (3) those that reported on a randomized controlled trial (RCT), non-randomized prospective study, or retrospective study; (4) those that were original peer-reviewed human participant research studies; (5) those that were published in English; and (6) those with a follow-up duration of 1, 2, 3, or 5 years. Studies such as reviews, editorials, commentaries, meeting abstracts of unpublished studies, and case reports were excluded. For duplicate publications, the higher-quality study, or the study that had been most recently published was selected.

Data extraction

Data were extracted from eligible studies by the two authors independently (WXH and TD). The extracted data included the first author's surname, publication year, country of research, study design, patient information, follow-up time, and rates of surgical retreatment. The patient information collected included the patient's number, age, prostate volume (PV), International Prostate Symptom Score (IPSS), postvoid residual volume (PVR), and maximum urinary flow rate (Q_{max}). It should be noted that surgical retreatment included both the management of the prostatic obstruction and of postoperative complications such as bladder neck contracture or urethral stricture. For some studies, we calculated the rate for further investigation if authors reported only the number of retreatment patients.

Quality assessment

The risk of bias (RoB) and quality of each eligible study were assessed by two authors independently (WXH and TD). For RCTs, the RoB was assessed, summarized, and then visualized using the Cochrane Collaboration RoB tool embedded in the RevMan (The Cochrane Collaboration, The Nordic Cochrane Centre, Copenhagen, Denmark) software (version 5.4). For single-arm studies, the RoB was assessed in accordance with the EAU guidelines for systematic reviews (12).

Data synthesis

For each surgical type, the baseline characteristics of patients were summarized and then pooled using Microsoft Excel® (Microsoft Corporation, Redmond, WA, USA) software (2016). In addition, the pooled incidences (PIs) and corresponding 95% confidence intervals (CIs) of the surgical retreatment rates were evaluated and stratified by the surgical type and follow-up duration (i.e., 1 year, 2 years, 3 years, and 5 years) using STATA (version 17.0; StataCorp LP, College Station, TX, USA). A random-effects model was used to estimate the pooled incidences.

Results

Study selection and characteristics

The study selection process is presented in the PRISMA flow chart shown in Figure 1. A total of 119 studies met our inclusion criteria. The baseline characteristics of the included studies are presented in Table 1. A total of 130,106 patients were included, of whom 100,295 had undergone TURP, 1,530 had undergone PKRP, 90 had undergone TUIP, 4,621 had undergone OP, 3,956 had undergone HoLEP, 1,584 had undergone ThuLEP, 14,058 had undergone PVP, 217 had undergone surgery with AquaBeam, 1,796 had undergone PAE, and 1,959 had undergone TUMT procedures. Forty-two studies were RCTs, 29 were non-randomized prospective studies, and 48 were retrospective single-arm case series. Forty-nine studies were conducted in Europe, 34 were conducted in Asia, 22 studies were conducted in North America, six studies were conducted in Africa, and two studies were conducted in Oceania. In addition, another six multi-institutional studies were conducted in Europe and North America.

Risk of bias

The quality and RoB assessments are summarized in the Supplementary Files. For the 42 RCT studies, the RoBs of the 32 studies were considered unclear, whereas 47 of the 77 single-arm studies were assessed as having a high RoB.

Baseline patient characteristics

As shown in Table 2, the preoperative characteristics of the patients were summarized and pooled in accordance with the type of procedure. It appeared that the PV, IPSS, and PVR values of patients who had undergone TUIP, OP, or TUMT were different from those of other groups. For patients who had undergone TURP, the average age was 70 years, the average PV was 55 cm^3, the average IPSS was 22, the average PVR was 184 mL, and the average Q_{max} was 8 mL per s. For patients who had undergone PKRP, the average age was 69 years, the average PV was 67 cm^3, the average IPSS was 21, the average PVR was 112 mL, and the average Q_{max} was 7 mL per s. For patients who had undergone TUIP, the average age was 71 years, the average

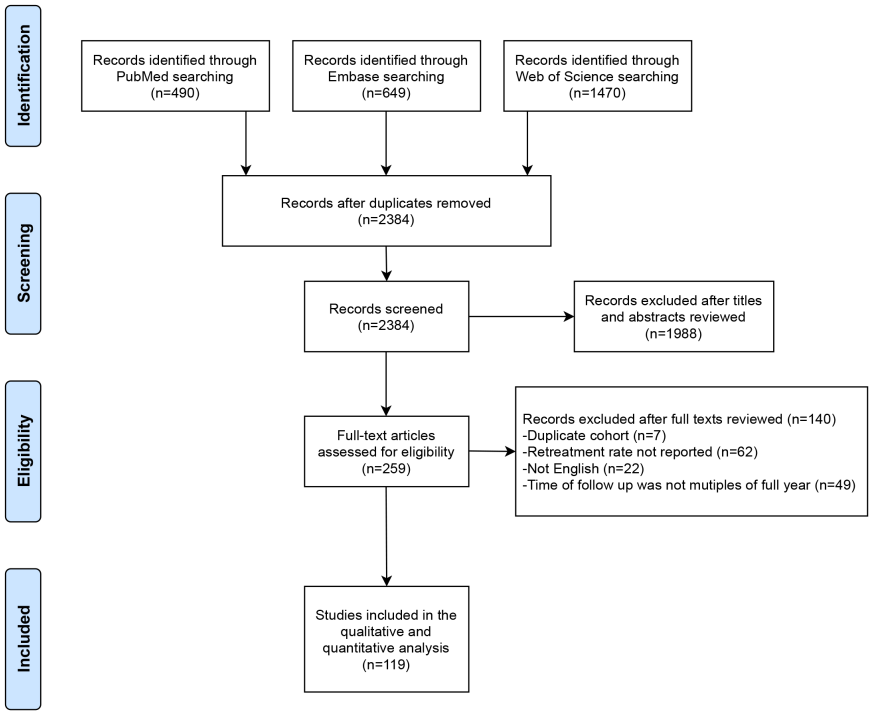

FIGURE 1
Preferred Reporting Items for Systematic Reviews and Meta-Analyses (PRISMA) flow diagram.

PV was 26 cm^3, the average IPSS was 16, the average PVR was 139 mL, and the average Q_{max} was 9 mL per s. For patients who had undergone OP, the average age was 71 years, the average PV was 106 cm^3, the average IPSS was 24, the average PVR was 147 mL, and the average Q_{max} was 6 mL per s. For patients who had undergone HoLEP, the average age was 70 years, the average PV was 79 cm^3, the average IPSS was 21, the average PVR was 186 mL, and the average Q_{max} was 8 mL per s. For patients who had undergone ThuLEP, the average age was 70 years, the average PV was 65 cm^3, the average IPSS was 24, the average PVR was 138 mL, and the average Q_{max} was 7 mL per s. For patients who had undergone PVP, the average age was 72 years, the average PV was 63 cm^3, the average IPSS was 22, the average PVR was 166 mL, and the average Q_{max} was 8 mL per s. For patients who had undergone surgery with AquaBeam, the average age was 67 years, the average PV was 79 cm^3, the average IPSS was 23, the average PVR was 117 mL, and the average Q_{max} was 7 mL per s. For patients who had undergone PAE, the average age was 66 years, the average PV was 86 cm^3, the average IPSS was 22, the average PVR was 124 mL, and the average Q_{max} was 10 mL per s. For patients who had undergone TUMT, the average age was 67 years, the average PV was 48 cm^3, the average IPSS was 21, the average PVR was 76 mL, and the average Q_{max} was 9 mL per s.

Surgical retreatments after different procedures

In Table 3, the surgical retreatment rates of various procedures in different follow-up years are shown. Most of the evidence was derived from studies on TURP, PKRP HoLEP, and PVP, as there were fewer studies on TUIP, OP, ThuLEP, AquaBeam, PAE, and TUMT. For almost every procedure, the risk of surgical retreatment increased over time.

At 1 year, the pooled incidence of surgical retreatment was 4.0% (95% CI 3.0% to 5.1%) for the TURP cohort, 3.5% (95% CI 0.6% to 8.2%) for the PKRP cohort, 1.3% (95% CI 0.3% to 2.8%) for the OP cohort, 2.4% (95% CI 1.1% to 4.1%) for the HoLEP cohort, 3.7% (95% CI 2.2% to 5.5%) for the ThuLEP cohort, 3.3% (95% CI 1.8% to 5.2%) for the PVP cohort, 2.6% (95% CI 0.5% to 7.4%) for the AquaBeam cohort, 12.2% (95% CI 2.4% to 27.8%) for the PAE cohort, and 9.9% (95% CI 7.0% to 13.3%) for the TUMT cohort.

At 2 years, the pooled incidence of surgical retreatment was 5.0% (95% CI 3.5% to 6.6%) for the TURP cohort, 3.6% (95% CI 1.9% to 5.8%) for the PKRP cohort, 3.3% (95% CI 0.1% to 17.2%) for the HoLEP cohort, 7.7% (95% CI 4.4% to 11.8%) for the ThuLEP cohort, 4.1% (95% CI 2.9% to 5.6%) for the PVP cohort, 3.1% (95% CI 1.1% to 6.0%) for the AquaBeam cohort, 20.0% (95% CI 8.9% to 34.1%) for the PAE cohort, and 19.9% (95% CI 15.0% to 25.7%) for the TUMT cohort.

At 3 years, the pooled incidence of surgical retreatment was 6.0% (95% CI 4.4% to 7.7%) for the TURP cohort, 5.7% (95% CI 3.2% to 8.8%) for the PKRP cohort, 5.4% (95% CI 3.7% to 7.2%) for the HoLEP cohort, 6.7% (95% CI 4.3% to 9.5%) for the PVP cohort, 3.0% (95% CI 0.6% to 8.4%) for the AquaBeam cohort, 26.4% (95% CI 18.9% to 35.0%) for the PAE cohort, and 23.3% (95% CI 16.3% to 31.2%) for the TUMT cohort.

At 5 years, the pooled incidence of surgical retreatment was 7.7% (95% CI 5.8% to 9.8%) for the TURP cohort, 6.6% (95% CI

10.3389/fendo.2023.1287212

TABLE 1 Study characteristics.

Study	Patients (*n*)	Therapy	Study design	Setting	Country	FU (mo)
Stephenson 1991 (13)	318	TURP	RS	Database	United States	72
Sidney 1992 (14)	7,771	TURP	RS	Database	United States	96
Matani 1996 (15)	166	TURP	RS	Single center	Germany	60
Jahnson 1998 (16)	42	TURP	RCT	Single center	Sweden	60
Carter 1999 (17)	96	TURP	RCT	Single center	United Kingdom	12
Hammadeh 2000 (18)	52	TURP	RCT	Single center	United Kingdom	36
Schatzl 2000 (19)	28	TURP	NRPS	Single center	Austria	24
Keoghane 2000 (20)	76	TURP	RCT	Single center	United Kingdom	24
Floratos 2001 (21)	73	TURP	RCT	Single center	The Netherlands	36
Tuhkanen 2001 (22)	25	TURP	RCT	Single center	Finland	24
Helke 2001 (23)	93	TURP	NRPS	Single center	Germany	12
Hammadeh 2003 (24)	52	TURP	RCT	Single center	United Kingdom	60
van Melick 2003 (25)	50	TURP	RCT	Single center	The Netherlands	12
Tan 2003 (26)	30	TURP	RCT	Single center	New Zealand	12
Hill 2004 (27)	56	TURP	RCT	Multicenter	United States	60
Madersbacher 2005 (5)	20,671	TURP	RS	Single center	Austria	96
Liu 2005 (28)	32	TURP	RCT	Single center	Taiwan	24
Wilson 2006 (29)	30	TURP	RCT	Single center	New Zealand	24
Ahyai 2007 (30)	100	TURP	RCT	Single center	Germany	36
Tasci 2008 (31)	41	TURP	NRPS	Single center	Türkiye	24
Zhao 2010 (32)	102	TURP	RCT	Single center	China	36
Ou 2010 (33)	35	TURP	RCT	Single center	China	12
Muslumanoglu 2011 (34)	47	TURP	RCT	Single center	Türkiye	12
Xue 2013 (35)	100	TURP	RCT	Single center	China	36
Cui 2013 (36)	49	TURP	RCT	Single center	China	48
Mamoulakis 2013 (37)	149	TURP	RCT	Multicenter	The Netherlands, Germany, Greece, and Italy	36
Stucki 2014 (38)	67	TURP	RCT	Single center	Switzerland	12
Bachmann 2014 (39)	127	TURP	RCT	Multicenter	Austria, Belgium, France, Germany, Italy, the Netherlands, Spain, Switzerland, and the United Kingdom	6
Guo 2015 (40)	68	TURP	NRPS	Multicenter	Switzerland	60
Thomas 2015 (41)	121	TURP	RCT	Multicenter	Austria, Belgium, France, Germany, Italy, the Netherlands, Spain, Switzerland, and the United Kingdom	24
Al-Rawashdah, 2017 (42)	251	TURP	RCT	Single center	Italy	36
Eredics, 2018 (6)	20,388	TURP	RS	Database	Austria	96
Mordasini, 2018 (43)	126	TURP	RCT	Single center	Switzerland	60
Ray 2018 (44)	89	TURP	RS	Database	United Kingdom	12

(Continued)

10.3389/fendo.2023.1287212

TABLE 1 Continued

Study	Patients (*n*)	Therapy	Study design	Setting	Country	FU (mo)
Prudhomme 2019 (45)	34	TURP	RS	Multicenter	France	12
Sagen 2020 (46)	355	TURP	RS	Single center	Sweden	36
Stoddard 2021 (47)	36,040	TURP	NRPS	Database	United States	60
Abt 2021 (48)	51	TURP	RCT	Single center	Switzerland	24
Ofoha 2021 (49)	30	TURP	RS	Single center	Nigeria	12
Gilling 2022 (50)	65	TURP	RCT	Multicenter	United States, Australia, New Zealand, and the United Kingdom	60
Loloi 2022 (51)	304	TURP	RS	Single center	United States	60
Yang 2022 (52)	370	TURP	RS	Single center	China	36
Yang 2023 (53)	320	TURP	RS	Single center	China	36
Raizenne 2023 (54)	11,205	TURP	RS	Database	United States	24
Hu, 2016 (55)	467	PKRP	RS	Single center	China	60
Al-Rawashdah, 2017 (42)	246	PKRP	RCT	Single center	Italy	36
Cheng 2021 (56)	60	PKRP	NRPS	Single center	China	36
Zhu 2012 (57)	132	PKRP	NRPS	Single center	China	36
Li 2017 (58)	44	PKRP	NRPS	Single center	China	36
Elshal 2020 (59)	62	PKRP	RCT	Single center	Egypt	36
Mamoulakis 2013 (37)	146	PKRP	RCT	Multicenter	The Netherlands, Germany, Greece, and Italy	36
Wei 2016 (60)	204	PKRP	RS	Single center	China	24
Peng 2016 (61)	59	PKRP	RCT	Single center	China	12
Yip 2011 (62)	40	PKRP	RCT	Single center	Hong Kong	12
Stucki 2014 (38)	70	PKRP	RCT	Single center	Switzerland	12
Jahnson 1998 (16)	43	TUIP	RCT	Single center	Sweden	60
Elshal 2014 (63)	47	TUIP	RS	Database	Egypt	60
Sidney 1992 (14)	448	OP	RS	Database	United States	96
Eredics 2018 (6)	1,286	OP	RS	Database	Austria	96
Kuntz 2007 (64)	60	OP	RCT	Single center	Germany	60
Madersbacher 2005 (5)	2,452	OP	RS	Single center	Austria	96
Ou 2010 (33)	34	OP	RCT	Single center	China	12
Sofimajidpour 2020 (65)	80	OP	RS	Single center	Iran	12
Ofoha 2021 (49)	29	OP	RS	Single center	Nigeria	12
Varkarakis 2004 (66)	232	OP	NRPS	Single center	Greece	12
Shah 2021 (67)	94	HoLEP	RCT	Single center	India	60
Gilling 2008 (68)	71	HoLEP	NRPS	Single center	New Zealand	60
Whiting 2022 (69)	1,016	HoLEP	NRPS	Single center	United Kingdom	60
Elshal 2012 (70)	978	HoLEP	RS	Single center	Canada	60
Droghetti 2022 (71)	567	HoLEP	RS	Single center	Italy	60
Kuntz 2007 (64)	60	HoLEP	RCT	Single center	Germany	60

(Continued)

TABLE 1 Continued

Study	Patients (*n*)	Therapy	Study design	Setting	Country	FU (mo)
Enikeev 2019 (72)	127	HoLEP	RS	Single center	Russia	60
Elshal 2020 (59)	60	HoLEP	RCT	Single center	Egypt	36
Bhandarkar 2022 (73)	86	HoLEP	RCT	Single center	India	36
Vavassori 2008 (74)	330	HoLEP	NRPS	Single center	Italy	36
Ahyai 2007 (30)	100	HoLEP	RCT	Single center	Germany	36
Wilson 2006 (29)	30	HoLEP	RCT	Single center	New Zealand	24
Prudhomme 2019 (45)	17	HoLEP	RS	Multicenter	France	12
Tan 2003 (75)	30	HoLEP	RCT	Single center	New Zealand	12
Elshal 2014 (63)	50	HoLEP	RCT	Single center	Canada	12
Bae 2011 (76)	309	HoLEP	RS	Single center	Korea	12
Aho 2005 (77)	20	HoLEP	RCT	Single center	New Zealand	12
Neill 2006 (78)	20	HoLEP	RCT	Single center	New Zealand	12
Castellani 2019 (79)	412	ThuLEP	RS	Single center	Italy	12
Gross 2017 (80)	500	ThuVEP	RS	Single center	Germany	60
Tao 2019 (81)	198	ThuVEP	RCT	Single center	China	24
Tao 2017 (82)	248	ThuVEP	RS	Single center	China	24
Becker 2017 (83)	80	ThuVEP	RS	Multicenter	Italy	24
Bach 2011 (84)	90	ThuVEP	NRPS	Single center	Germany	12
Netsch 2012 (85)	56	ThuVEP	NRPS	Single center	Germany	12
Park 2017 (86)	159	PVP	RS	Single center	Korea	60
Law 2021 (87)	3,627	PVP	RS	Multicenter	Canada, France, Germany, Italy, Mexico, Brazil, and Argentina	60
Yamada 2016 (88)	1,154	PVP	RS	Single center	Japan	120
Hai 2009 (89)	321	PVP	RS	Single center	United States	60
Elshal 2014 (63)	144	PVP	RS	Database	Egypt	60
Mordasini 2018 (43)	112	PVP	RCT	Single center	Switzerland	60
Guo 2015 (40)	120	PVP	NRPS	Multicenter	Switzerland	60
Malde 2012 (90)	115	PVP	NRPS	Single center	United Kingdom	60
Ajib 2018 (91)	370	PVP	RS	Single center	Canada	60
Cheng 2021 (56)	60	PVP	RS	Single center	China	36
Kim 2016 (92)	630	PVP	RS	Single center	Korea	36
Te 2006 (93)	139	PVP	NRPS	Single center	United States	36
Tasci 2011 (94)	550	PVP	NRPS	Single center	Türkiye	36
Meskawi 2017 (95)	438	PVP	RS	Multicenter	Canada, United States, and France	36
Xue 2013 (35)	100	PVP	RCT	Single center	China	6
Guo 2015 (40)	56	PVP	NRPS	Single center	Switzerland	36
Malek 2000 (96)	55	PVP	NRPS	Single center	United States	24

(Continued)

10.3389/fendo.2023.1287212

TABLE 1 Continued

Study	Patients (*n*)	Therapy	Study design	Setting	Country	FU (mo)
Hueber 2015 (97)	1,196	PVP	RS	Multicenter	Canada, United States, France, and England	24
Tao 2013 (98)	188	PVP	NRPS	Single center	China	24
Chung 2011 (99)	162	PVP	NRPS	Single center	United States	24
Stone 2016 (100)	70	PVP	NRPS	Single center	United States	24
Liu 2020 (101)	150	PVP	RS	Single center	China	24
Campobasso 2019 (102)	1,031	PVP	RS	Multicenter	Italy	24
Tao 2019 (81)	216	PVP	RCT	Single center	China	24
Chen 2013 (103)	132	PVP	RS	Single center	Taiwan	24
Valdivieso 2016 (104)	440	PVP	RS	Multicenter	Canada, United States, United Kingdom, and France	24
Kim 2010 (105)	169	PVP	NRPS	Single center	Korea	24
Tasci 2008 (31)	40	PVP	NRPS	Single center	Türkiye	24
Ruszat 2006 (106)	183	PVP	NRPS	Single center	Switzerland	24
Ghobrial 2020 (107)	58	PVP	RCT	Single center	Egypt	24
Huet 2019 (108)	100	PVP	NRPS	Single center	France	24
Thomas 2015 (41)	128	PVP	RCT	Multicenter	Austria, Belgium, France, Germany, Italy, the Netherlands, Spain, Switzerland, and the United Kingdom	24
Prudhomme 2019 (45)	9	PVP	RS	Multicenter	France	12
Liu 2022 (109)	77	PVP	RCT	Single center	China	12
Mosli 2013 (110)	103	PVP	NRPS	Single center	Egypt	12
Seki 2008 (111)	161	PVP	NRPS	Single center	Japan	12
Hueber 2012 (112)	250	PVP	RS	Single center	Canada	12
Peng 2016 (61)	61	PVP	RCT	Single center	China	12
Tao 2019 (113)	102	PVP	RCT	Single center	China	12
Tugcu 2007 (114)	100	PVP	RS	Single center	Türkiye	12
Bachmann 2014 (39)	131	PVP	RCT	Multicenter	Austria, Belgium, France, Germany, Italy, the Netherlands, Spain, Switzerland, and the United Kingdom	6
Carter 1999 (17)	95	PVP	RCT	Single center	United Kingdom	12
Pfitzenmaier 2008 (115)	173	PVP	NRPS	Single center	Germany	12
Abolazm 2020 (116)	49	PVP	RCT	Single center	Egypt	12
Bhojani 2023 (117)	101	AquaBeam	NRPS	Multicenter	United States, Canada	60
Gilling 2022 (50)	116	AquaBeam	RCT	Multicenter	United States, Australia, New Zealand, and the United Kingdom	60
Zorn 2022 (118)	101	AquaBeam	RCT	Multicenter	United States and Canada	36
Bilhim 2022 (119)	1,072	PAE	RS	Single center	Portugal	120
Xu 2022 (120)	125	PAE	RS	Single center	China	60

(Continued)

TABLE 1 Continued

Study	Patients (*n*)	Therapy	Study design	Setting	Country	FU (mo)
Abt 2021 (48)	48	PAE	RCT	Single center	Switzerland	24
Raizenne 2023 (54)	335	PAE	RS	Database	United States	24
Ray 2018 (44)	216	PAE	RS	Database	United Kingdom	12
Gravas 2007 (121)	213	TUMT	NRPS	Single center	Greece	60
Francisca 1999 (122)	1,092	TUMT	NRPS	Multicenter	Korea, Sweden, Singapore, Spain, Canada, and the Netherlands	60
Raizenne 2022 (123)	119	TUMT	RS	Database	United States	60
Lau 1998 (124)	106	TUMT	RS	Single center	Singapore	60
Ohigashi 2007 (125)	34	TUMT	NRPS	Single center	Japan	60
Keijzers 1998 (126)	231	TUMT	NRPS	Single center	The Netherlands	60
Tsai 2000 (127)	82	TUMT	RCT	Single center	Taiwan	60
Floratos 2001 (21)	82	TUMT	RCT	Single center	The Netherlands	36

FU (mo), follow-up (months); RCT, randomized controlled trial; NRPS, non-randomized prospective study; RS, retrospective study; TURP, transurethral resection of the prostate (monopolar); PKRP, plasma kinetic resection of prostate; TUIP, transurethral incision of prostate; OP, open prostatectomy; HoLEP, holmium laser enucleation of the prostate; ThuLEP, thulium:yttrium aluminum garnet laser (Tm : YAG) enucleation of the prostate, also including ThuVEP (vapoenucleation); PVP, photoselective vaporization of the prostate; AquaBeam, image-guided robotic waterjet ablation; PAE, prostatic artery embolization; TUMT, transurethral microwave therapy.

4.6% to 9.3%) for the PKRP cohort, 13.4% (95% CI 6.9% to 21.5%) for the TUIP cohort, 4.4% (95% CI 1.5% to 8.7%) for the OP cohort, 6.6% (95% CI 4.2% to 9.5%) for the HoLEP cohort, 8.4% (95% CI 6.1% to 11.2%) for the ThuLEP cohort, 7.1% (95% CI 5.1% to 9.4%) for the PVP cohort, 4.1% (95% CI 1.7% to 7.2%) for the AquaBeam cohort, 23.8% (95% CI 21.4% to 26.3%) for the PAE cohort, and 31.2% (95% CI 25.5% to 37.2%) for the TUMT cohort.

Discussion

This systematic review comprehensively summarized the reoperation rates after surgeries for male LUTS management. We found that the retreatment rates increased over time and differed among procedures. Our results can be used to counsel both the urologists and patients regarding the different therapeutic strategies.

As the gold standard of surgical treatment for BPH/LUTSs, it was reported after a nationwide analysis of 20,671 patients that the surgical retreatment rate of TURP was 3.7% for 1 year and 9.5% for 5 years (5), which was similar to our current result. As the most widely investigated alternative to TURP and PKRP (bipolar TURP) was found to have a comparable efficacy in regard to the long-term follow-up, but was safer during the perioperative period (3). Numerous studies have reported that PKRP exhibited similar rates of surgical retreatment as TURP (3), which was consistent with our results.

TABLE 2 Pooled estimates for baseline confounders.

Treatment	Patients (*n*)	Age (years)	PV (cm^3)	IPSS	PVR (mL)	Q_{max} (mL/s)
TURP	100,295	70	55	22	184	8
PKRP	1,530	69	67	21	112	7
TUIP	90	71	26	16	139	9
OP	4,621	71	106	24	147	6
HoLEP	3,956	70	79	21	186	8
ThuLEP	1,584	70	65	24	138	7
PVP	14,058	72	63	22	166	8
AquaBeam	217	67	79	23	117	7
PAE	1,796	66	86	22	124	10
TUMT	1,959	67	48	21	76	9

PV, prostate volume; IPSS, International Prostate Symptom Score; PVR, postvoid residual volume; Q_{max}, maximum urinary flow rate; TURP, transurethral resection of the prostate (monopolar); PKRP, plasma kinetic resection of prostate; TUIP, transurethral incision of prostate; OP, open prostatectomy; HoLEP, holmium laser enucleation of the prostate; ThuLEP, thulium:yttrium aluminum garnet laser (Tm : YAG) enucleation of the prostate, also including ThuVEP (vapoenucleation); PVP, photoselective vaporization of the prostate; AquaBeam, image-guided robotic waterjet ablation; PAE, prostatic artery embolization; TUMT, transurethral microwave therapy.

10.3389/fendo.2023.1287212

TABLE 3 Surgical retreatment after different operation procedures.

	1 year		2 years		3 years		5 years	
	PI (95% CI)	Studies	PI (95% CI)	Studies	PI (95% CI)	Studies	PI (95% CI)	Studies
Resection								
TURP	4.0% (3.0% to 5.1%)	23	5.0% (3.5% to 6.6%)	14	6.0% (4.4% to 7.7%)	13	7.7% (5.8% to 9.8%)	13
PKRP	3.5% (0.6% to 8.2%)	7	3.6% (1.9% to 5.8%)	3	5.7% (3.2% to 8.8%)	6	6.6% (4.6% to 9.3%)*	1
TUIP	–	0	–	0	–	0	13.4% (6.9% to 21.5%)	2
Enucleation								
OP	1.3% (0.3% to 2.8%)	7	–	0	–	0	4.4% (1.5% to 8.7%)	4
HoLEP	2.4% (1.1% to 4.1%)	8	3.3% (0.1% to 17.2%)*	1	5.4% (3.7% to 7.2%)	5	6.6% (4.2% to 9.5%)	7
ThuLEP	3.7% (2.2% to 5.5%)	3	7.7% (4.4% to 11.8%)	3	–	0	8.4% (6.1% to 11.2%) *	1
Vaporization								
PVP	3.3% (1.8% to 5.2%)	16	4.1% (2.9% to 5.6%)	19	6.7% (4.3% to 9.5%)	9	7.1% (5.1% to 9.4%)	9
Other								
AquaBeam	2.6% (0.5% to 7.4%) *	1	3.1% (1.1% to 6.0%)	2	3.0% (0.6% to 8.4%)*	1	4.1% (1.7% to 7.2%)	2
PAE	12.2% (2.4% to 27.8%)	4	20.0% (8.9% to 34.1%)	3	26.4% (18.9% to 35.0%)*	1	23.8% (21.4% to 26.3%)	2
TUMT	9.9% (7.0% to 13.3%)	2	19.9% (15.0% to 25.7%)*	1	23.3% (16.3% to 31.2%)	3	31.2% (25.5% to 37.2%)	7

*Incidence rates were not pooled as only one article reported the predefined outcome.
PI, pooled incidence; CI, confidence interval; TURP, transurethral resection of the prostate (monopolar); PKRP, plasma kinetic resection of prostate; TUIP, transurethral incision of prostate; OP, open prostatectomy; HoLEP, holmium laser enucleation of the prostate; ThuLEP, thulium:yttrium aluminum garnet laser (Tm : YAG) enucleation of the prostate, also including ThuVEP (vapoenucleation); PVP, photoselective vaporization of the prostate; AquaBeam, image-guided robotic waterjet ablation; PAE, prostatic artery embolization; TUMT, transurethral microwave therapy. "-" means no data.

Moreover, TUIP was recommended for patients with a PV of < 30 mL and those without a middle lobe (2, 3). A meta-analysis of six trials published 13 years ago showed that reoperation was more common after TUIP (18.4%) than it was after TURP (7.2%) (128). The follow-up periods of the six trials included above were different, which may introduce some bias; however, our updated review showed a similar result in that the reoperation rate of TUIP was 13.4% in 5 years, which was higher among these surgical procedures. The higher risk of surgical retreatment associated with TUIP may be due to its method, which involves only incising the bladder outlet without removing prostatic tissue. However, TUIP has been underutilized in the urological community over the years, the reasons for this include concerns related to the limitations of PV as an indicator of the need for surgery and also its long-term efficacy (129). In contrast to TUIP, during OP, the whole prostate is removed, which is recommended for patients with a PV of > 80 mL (2, 3). A nationwide analysis reported that the surgical retreatment rate of OP was 3.0% for 1 year and 6.0% for 5 years (130), which was similar to our result. Although its long-term reoperation rate seems lower than those of the other procedures, OP showed poorer perioperative safety than the other transurethral approaches, and was associated with higher rates of blood transfusions and even death (131, 132). Therefore, OP was less popular than the other minimally invasive surgeries. However, in recent years, prostatectomy with laparoscopy or robot-assisted surgery showed better safety and were also recommended by guidelines (2).

As an alternative to open enucleation, some studies reported that HoLEP has a lower risk of reoperation than TURP or PKRP (59, 133, 134), whereas another reported that there was no difference (135, 136). Indeed, our results suggest that the reoperation rates for HoLEP are similar to (and possibly slightly lower than) those for TURP or PKRP. Enucleation using another laser, ThuLEP has a rate of reoperation that is similar to (and possibly slightly higher than) that of HoLEP, which may be due to them being similar procedures. A recent interesting study from Italy reported that an improved ThuLEP technique successfully preserved the ejaculation function in most patients (137), which suggested its potential in decreasing the reoperation rates.

For vaporization, PVP has been used in clinical settings for many years and there are many related studies that have shown it has a similar efficacy to TURP (2, 3). A previous meta-analysis published by Zhou and colleagues reported that the reoperation rate after PVP was higher than that after TURP (138). However, there were only three related trials included in Zhou's study, and the follow-up durations of these trials were different (138). Our current summarized results, which included 53 trials, reported that the reoperation rates are similar between PVP and TURP. The

difference between the results of these two meta-analyses may be due to the number of articles included.

AquaBeam has come under investigation in recent years and two related trails, WATER and WATER II, reported the reoperation rate associated with it (50, 117, 118). However, there are few studies on this technique and a lack of long-term follow-up data. Although the rate of surgical retreatment appeared to be better than other procedures in our current review, whether or not AquaBeam could be an alternative to traditional procedures still needs a lot of studies and long-term follow-up to be carried out. Previous studies indicate that PAE, another surgical procedure that remains under investigation, has a higher risk of surgical retreatment than that shown in our results (9). Due to the variability of blood supply to the human prostate, non-target embolization may occur, and secondary surgical retreatment is required (139). In addition, it takes time for the prostate to shrink after vessel embolization, and PV will also stop decreasing and begin to increase after a period of time (140). Therefore, both complications and insufficient treatment response may result in a higher risk of reoperation. Overall, the efficacy and reliability of PAE remain undetermined, and further investigations and improvements are still needed. TUMT, one of the earliest technologies used for the treatment of BPH/LUTSs, has been used and studied less in recent years, due to its higher risk of retreatment and the emergence of newer, minimally invasive technologies (2, 8). Our current results confirmed that it has a higher rate of surgical retreatment. In fact, TUMT was not recommended by the latest version of the EAU guidelines, whereas the AUA guidelines still suggest that this is a reasonable approach. However, considering its higher reoperation rate and the newer, minimally invasive technologies, TUMT will likely be displaced within the next several years (2, 141).

There are some limitations or shortcomings in our current analysis and review which must be acknowledged. First, RoB was in some of the studies included through assessment. Second, our review focused only on the reoperation rates at follow-up periods of 1, 2, 3, and 5 years. However, the follow-up duration was different among studies; examples of follow-up periods were 6 months, 4 years, long term (> 5 years), and some did not last for a 'regular' (i.e., a multiple of a year, half a year, or 1 year) length of time. Therefore, our results are limited by the lack of data obtained during these follow-up durations. Third, 10 surgical procedures were included in our current review, of which the indication that recommended by guidelines are different. The baseline characteristics and therapeutic outcomes of patients may also have varied. Meanwhile, the great difference between data retrieved across techniques may also have led to bias. Fourth, the risk of misestimating the reoperation rate must be noted since patients lost to follow-up are common in studies. Finally, the reoperation rates of other surgical approaches excluded in our review while recommended by guidelines were also obtained during the literature search. However, as their surgical methods were outdated, less commonly used, or they were associated with a smaller number of studies, we excluded them from our current review.

In future, studies of higher quality and longer follow-up durations should be included. With the development of surgical approaches and techniques, the reoperation rate data should also be updated every few years. Meanwhile, the reoperation rate should be further refined based on its cause, and studies exploring the reason for reoperation are needed. In addition to the reoperation rate, the cost of surgical management across procedures varies, and sometimes there are even huge differences, which also affects what procedures are available for patients to choose from (142, 143). For example, a recent study reported that robotic-assisted simple prostatectomy (RASP) showed comparable efficacy and safety with a shorter hospitalization than laparoscopic simple prostatectomy (LSP) (144). However, considering the cost and unavailability of robot-assisted surgery, LSP is also a better alternative (144). Therefore, studies that evaluate the cost-effectiveness of these surgical approaches are also needed. Overall, these further investigations may lead to a reduction in the reoperation rate or prevent some common reoperation cases, which may give more information for clinical practitioners, better improve patient quality of life, and reduce medical expenses for patients.

Conclusions

Our results summarized the reoperation rates of 10 surgical procedures over follow-up durations of 1, 2, 3, and 5 years. There was a great difference in the reoperation rate among these procedures. The OP, AquaBeam, PKRP, and HoLEP procedures exhibited a lower reoperation rate, whereas the PAE and TUMT procedures exhibited a higher rate. These data could provide reference for urologists and BPH/LUTS patients.

Data availability statement

The original contributions presented in the study are included in the article/Supplementary Material. Further inquiries can be directed to the corresponding author.

Author contributions

WH: Conceptualization, Formal Analysis, Methodology, Writing – original draft, Writing – review and editing. TD: Conceptualization, Formal Analysis, Methodology, Writing – original draft, Writing – review and editing. ZN: Software, Writing – review and editing. CH: Validation, Writing – review and editing. CL: Validation, Writing – review and editing. ZX: Data curation, Writing – review and editing. YJ: Data curation, Writing – review and editing. WQ: Funding acquisition, Supervision, Writing – review and editing.

Funding

The author(s) declare financial support was received for the research, authorship, and/or publication of this article. This work

was supported by grants from the National Natural Science Foundation of China (No. 81772734).

Acknowledgments

The authors acknowledge all the participants and administrators of this study.

Conflict of interest

The authors declare that the research was conducted in the absence of any commercial or financial relationships that could be construed as a potential conflict of interest.

Publisher's note

All claims expressed in this article are solely those of the authors and do not necessarily represent those of their affiliated organizations, or those of the publisher, the editors and the reviewers. Any product that may be evaluated in this article, or claim that may be made by its manufacturer, is not guaranteed or endorsed by the publisher.

Supplementary material

The Supplementary Material for this article can be found online at: https://www.frontiersin.org/articles/10.3389/fendo.2023.1287212/full#supplementary-material

References

1. Claus G, Roehrborn DWS. *Benign prostatic hyperplasia: etiology, pathophysiology, epidemiology and natural history. TWELFTH ed.* Alan W, Partin RRD, Kavoussi LR, Peters CA, editors. Elsevier: Campbell-Walsh-Wein Urology (2021).

2. Lerner LB, McVary KT, Barry MJ, Bixler BR, Dahm P, Das AK, et al. Management of lower urinary tract symptoms attributed to benign prostatic hyperplasia: AUA GUIDELINE PART II-surgical evaluation and treatment. *J Urol* (2021) 206(4):818–26. doi: 10.1097/JU.0000000000002184

3. Cornu MG JN, Hashim H, Herrmann TRW, Malde S, Netsch C, Rieken M, et al. EAU guidelines on non-neurogenic male lower urinary tract symptoms (LUTS), incl. Benign prostatic obstruction (BPO). *EAU Guidelines* (2023).

4. Rassweiler J, Teber D, Kuntz R, Hofmann R. Complications of transurethral resection of the prostate (TURP) - Incidence, management, and prevention. *Eur Urol* (2006) 50(5):969–79. doi: 10.1016/j.eururo.2005.12.042

5. Madersbacher S, Lackner J, Brossner C, Rohlich M, Stancik I, Willinger M, et al. Reoperation, myocardial infarction and mortality after transurethral and open prostatectomy: A nation-wide, long-term analysis of 23,123 cases. *Eur Urol* (2005) 47(4):499–504. doi: 10.1016/j.eururo.2004.12.010

6. Eredics K, Wachabauer D, Röthlin F, Madersbacher S, Schauer I. Reoperation rates and mortality after transurethral and open prostatectomy in a long-term nationwide analysis: have we improved over a decade? *Urology* (2018) 118:152–7. doi: 10.1016/j.urology.2018.04.032

7. Jain A, Nassour AJ, Khannani H, Wines MP, Chalasani V, Katelaris P, et al. Australian surgical revision rate for benign prostatic obstruction. *BJU Int* (2023) 131 Suppl 4:43–7. doi: 10.1111/bju.16031

8. Franco JV, Jung JH, Imamura M, Borofsky M, Omar MI, Liquitay CME, et al. Minimally invasive treatments for benign prostatic hyperplasia: a Cochrane network meta-analysis. *Bju Int* (2022) 130(2):142–56. doi: 10.1111/bju.15653

9. Jung JH, McCutcheon KA, Borofsky M, Young S, Golzarian J, Kim MH, et al. Prostatic arterial embolization for the treatment of lower urinary tract symptoms in men with benign prostatic hyperplasia. *Cochrane Database Syst Rev* (2022) 3). doi: 10.1002/14651858.CD012867.pub2

10. Baboudjian M, Cornu JN, Gondran-Tellier B, Fourmarier M, Robert G, Peyronnet B, et al. Pharmacologic and surgical retreatment after office-based treatments for benign prostatic hyperplasia: A systematic review. *Eur Urol Focus* (2023). doi: 10.1016/j.euf.2023.03.004

11. Page MJ, McKenzie JE, Bossuyt PM, Boutron I, Hoffmann TC, Mulrow CD, et al. The PRISMA 2020 statement: an updated guideline for reporting systematic reviews. *Bmj* (2021) 372:n71. doi: 10.1136/bmj.n71

12. Knoll T, Omar MI, Maclennan S, Hernández V, Canfield S, Yuan Y, et al. Key steps in conducting systematic reviews for underpinning clinical practice guidelines: methodology of the european association of urology. *Eur Urol* (2018) 73(2):290–300. doi: 10.1136/bmj.n71

13. Stephenson WP, Chute CG, Guess HA, Schwartz S, Lieber M. Incidence and outcome of surgery for benign prostatic hyperplasia among residents of rochester, minnesota - 1980-87 - a population-based study. *Urology* (1991) 38(1):32–42. doi: 10.1136/bmj.n71

14. Sidney S, Quesenberry CP, Sadler MC, Cattolica EV, Lydick EG, Guess HA. Reoperation and mortality after surgical-treatment of benign prostatic hypertrophy in a large prepaid medical-care program. *Med Care* (1992) 30(2):117–25. doi: 10.1136/bmj.n71

15. Matani Y, Mottrie AM, Stockle M, Voges GE, Fichtner J, Hohenfellner R. Transurethral prostatectomy: A long-term follow-up study of 166 patients over 80 years of age. *Eur Urol* (1996) 30(4):414–7. doi: 10.1159/000474208

16. Jahnson S, Dalén M, Gustavsson G, Pedersen J. Transurethral incision versus resection of the prostate for small to medium benign prostatic hyperplasia. *Br J Urol* (1998) 81(2):276–81. doi: 10.1046/j.1464-410x.1998.00535.x

17. Carter A, Sells H, Speakman M, Ewings P, MacDonagh R, O'Boyle P. A prospective randomized controlled trial of hybrid laser treatment or transurethral resection of the prostate, with a 1-year follow-up. *BJU Int* (1999) 83(3):254–9. doi: 10.1046/j.1464-410x.1999.00936.x

18. Hammadeh MY, Madaan S, Singh M, Philp T. A 3-year follow-up of a prospective randomized trial comparing transurethral electrovaporization of the prostate with standard transurethral prostatectomy. *BJU Int* (2000) 86(6):648–51. doi: 10.1046/j.1464-410x.2000.00879.x

19. Schatzl G, Madersbacher S, Djavan B, Lang T, Marberger M. Two-year results of transurethral resection of the prostate versus four 'less invasive' treatment options. *Eur Urol* (2000) 37(6):695–700. doi: 10.1159/000020220

20. Keoghane SR, Lawrence KC, Gray AM, Doll HA, Hancock AM, Turner K, et al. A double-blind randomized controlled trial and economic evaluation of transurethral resection vs contact laser vaporization for benign prostatic enlargement: a 3-year follow-up. *Bju Int* (2000) 85(1):74–8. doi: 10.1046/j.1464-410x.2000.00407.x

21. Floratos DL, Kiemeney LA, Rossi C, Kortmann BB, Debruyne FM, de la Rosette JJ. Long-term followup of randomized transurethral microwave thermotherapy versus transurethral prostatic resection study. *J Urol* (2001) 165(5):1533–8. doi: 10.1016/S0022-5347(05)66343-4

22. Tuhkanen K, Heino A, Ala-Opas M. Two-year follow-up results of a prospective randomized trial comparing hybrid laser prostatectomy with TURP in the treatment of big benign prostates. *Scand J Urol Nephrol* (2001) 35(3):200–4. doi: 10.1080/003655901750291962

23. Helke C, Manseck A, Hakenberg OW, Wirth MP. Is transurethral vaporesection of the prostate better than standard transurethral resection? *Eur Urol* (2001) 39(5):551–7. doi: 10.1159/000052502

24. Hammadeh MY, Madaan S, Hines J, Philp T. 5-year outcome of a prospective randomized trial to compare transurethral electrovaporization of the prostate and standard transurethral resection. *Urology* (2003) 61(6):1166–71. doi: 10.1016/S0090-4295(03)00109-2

25. van Melick HHE, van Venrooij G, Boon TA. Long-term follow-up after transurethral resection of the prostate, contact laser prostatectomy, and electrovaporization. *Urology* (2003) 62(6):1029–34. doi: 10.1016/S0090-4295(03)00769-6

26. Tan AHH, Gilling PJ, Kennett KM, Frampton C, Westenberg AM, Fraundorfer MR. A randomized trial comparing holmium laser enucleation of the prostate with transurethral resection of the prostate for the treatment of bladder outlet obstruction secondary to benign prostatic hyperplasia in large glands (40 to 200 grams). *J Urol* (2003) 170(4):1270–4. doi: 10.1097/01.ju.0000086948.55973.00

27. Hill B, Belville W, Bruskewitz R, Issa M, Perez-Marrero R, Roehrborn C, et al. Transurethral needle ablation versus transurethral resection of the prostate for the treatment of symptomatic benign prostatic hyperplasia: 5-year results of a prospective, randomized, multicenter clinical trial. *J Urol* (2004) 171(6):2336–40. doi: 10.1097/01.ju.0000127761.87421.a0

28. Liu CK, Lee WK, Ko MC, Chiang HS, Wan KS. Transurethral electrovapor resection versus standard transurethral resection treatment for a large prostate: A 2-year follow-up study conducted in Taiwan. *Urol. Internationalis* (2006) 76(2):144–9. doi: 10.1159/000090878

29. Wilson LC, Gilling PJ, Williams A, Kennett KM, Frampton CM, Westenberg AM, et al. A randomised trial comparing holmium laser enucleation versus transurethral resection in the treatment of prostates larger than 40 grams: Results at 2 years. *Eur Urol* (2006) 50(3):569–73. doi: 10.1016/j.eururo.2006.04.002

30. Ahyai SA, Lehrich K, Kuntz RM. Holmium laser enucleation versus transurethral resection of the prostate: 3-year follow-up results of a Randomized clinical trial. *Eur Urol* (2007) 52(5):1456–64. doi: 10.1016/j.eururo.2007.04.053

31. Tasci AI, Tugcu V, Sahin S, Zorluoglu F. Photoselective vaporization of the prostate versus transurethral resection of the prostate for the large prostate: A prospective nonrandomized bicenter trial with 2-year follow-up. *J Endourol* (2008) 22(2):347–53. doi: 10.1089/end.2007.0137

32. Zhao ZG, Zeng GH, Zhong W, Mai ZL, Zeng SH, Tao XT. A prospective, randomised trial comparing plasmakinetic enucleation to standard transurethral resection of the prostate for symptomatic benign prostatic hyperplasia: three-year follow-up results. *Eur Urol* (2010) 58(5):752–8. doi: 10.1016/j.eururo.2010.08.026

33. Ou RB, You M, Tang P, Chen H, Deng XR, Xie KJ. A randomized trial of transvesical prostatectomy versus transurethral resection of the prostate for prostate greater than 80 mL. *Urology* (2010) 76(4):958–61. doi: 10.1016/j.urology.2010.01.079

34. Muslumanoglu AY, Yuruk E, Binbay M, Akman T. Transurethral resection of prostate with plasmakinetic energy: 100 months results of a prospective randomized trial. *Bju Int* (2012) 110(4):546–9. doi: 10.1111/j.1464-410X.2011.10770.x

35. Xue B, Zang Y, Zhang Y, Yang D, Gao J, Sun C, et al. GreenLight HPS 120-W laser vaporization versus transurethral resection of the prostate for treatment of benign prostatic hyperplasia: a prospective randomized trial. *J Xray Sci Technol* (2013) 21 (1):125–32. doi: 10.3233/XST-130359

36. Cui D, Sun F, Zhuo J, Sun X, Han B, Zhao F, et al. A randomized trial comparing thulium laser resection to standard transurethral resection of the prostate for symptomatic benign prostatic hyperplasia: four-year follow-up results. *World J Urol* (2014) 32(3):683–9. doi: 10.1007/s00345-013-1103-6

37. Mamoulakis C, Schulze M, Skolarikos A, Alivizatos G, Scarpa RM, Rassweiler JJ, et al. Midterm results from an international multicentre randomised controlled trial comparing bipolar with monopolar transurethral resection of the prostate. *Eur Urol* (2013) 63(4):667–76. doi: 10.1016/j.eururo.2012.10.003

38. Stucki P, Marini L, Mattei A, Xafis K, Boldini M, Danuser H. Bipolar versus monopolar transurethral resection of the prostate: A prospective randomized trial focusing on bleeding complications. *J Urol* (2015) 193(4):1371–5. doi: 10.1016/j.juro.2014.08.137

39. Bachmann A, Tubaro A, Barber N, d'Ancona F, Muir G, Witzsch U, et al. 180-W XPS greenLight laser vaporisation versus transurethral resection of the prostate for the treatment of benign prostatic obstruction: 6-month safety and efficacy results of a European multicentre randomised trial-the GOLIATH study. *Eur Urol* (2014) 65 (5):931–42. doi: 10.1016/j.eururo.2013.10.040

40. Guo S, Müller G, Lehmann K, Talimi S, Bonkat G, Püschel H, et al. The 80-W KTP GreenLight laser vaporization of the prostate versus transurethral resection of the prostate (TURP): adjusted analysis of 5-year results of a prospective non-randomized bi-center study. *Lasers Med Sci* (2015) 30(3):1147–51. doi: 10.1007/s10103-015-1721-x

41. Thomas JA, Tubaro A, Barber N, d'Ancona F, Muir G, Witzsch U, et al. A multicenter randomized noninferiority trial comparing greenLight-XPS laser vaporization of the prostate and transurethral resection of the prostate for the treatment of benign prostatic obstruction: two-yr outcomes of the GOLIATH study. *Eur Urol* (2016) 69(1):94–102. doi: 10.1016/j.eururo.2015.07.054

42. Al-Rawashdah SF, Pastore AL, Al Salhi Y, Fuschi A, Petrozza V, Maurizi A, et al. Prospective randomized study comparing monopolar with bipolar transurethral resection of prostate in benign prostatic obstruction: 36-month outcomes. *World J Urol* (2017) 35(10):1595–601. doi: 10.1007/s00345-017-2023-7

43. Mordasini L, Di Bona C, Klein J, Mattei A, Wirth GJ, Iselin CE. 80-W greenLight laser vaporization versus transurethral resection of the prostate for treatment of benign prostatic obstruction: 5-year outcomes of a single-center prospective randomized trial. *Urology* (2018) 116:144–9. doi: 10.1016/j.urology.2018.01.037

44. Ray AF, Powell J, Speakman MJ, Longford NT, DasGupta R, Bryant T, et al. Efficacy and safety of prostate artery embolization for benign prostatic hyperplasia: an observational study and propensity-matched comparison with transurethral resection of the prostate (the UK-ROPE study). *Bju Int* (2018) 122(2):270–82. doi: 10.1111/bju.14249

45. Prudhomme T, Marquette T, Pere M, Patard PM, Michiels C, Sallusto F, et al. Benign prostatic hyperplasia endoscopic surgical procedures in kidney transplant recipients: a comparison between HoLEP, GreenLight photoselective vaporization of the prostate and TURP. *J endourology/Endourological Soc* (2019) 34(2):184–91. doi: 10.1089/end.2019.0430

46. Sagen E, Nelzén O, Peeker R. Transurethral resection of the prostate: fate of the non-responders. *Scand J Urol* (2020) 54(5):443–8. doi: 10.1080/21681805.2020.1812712

47. Stoddard MD, Zheng XY, Mao JL, Te A, Sedrakyan A, Chughtai B. Safety and efficacy of outpatient surgical procedures for the treatment of benign prostatic enlargement in New York state and California (2005-2016). *J Urol* (2021) 205 (3):848–54. doi: 10.1097/JU.0000000000001401

48. Abt D, Muellhaupt G, Hechelhammer L, Markart S, Gusewell S, Schmid HP, et al. Prostatic artery embolisation versus transurethral resection of the prostate for benign prostatic hyperplasia: 2-yr outcomes of a randomised, open-label, single-centre trial. *Eur Urol* (2021) 80(1):34–42. doi: 10.1016/j.eururo.2021.02.008

49. Ofoha CG, Raphael JE, Dakum NK, Shu'aibu SI, Akhaine J, Yaki IM. Surgical management of benign prostate hyperplasia in Nigeria: open prostatectomy versus transurethral resection of the prostate. *Pan. Afr Med J* (2021) 39:165. doi: 10.11604/pamj.2021.39.165.24767

50. Gilling PJ, Barber N, Bidair M, Anderson P, Sutton M, Aho T, et al. Five-year outcomes for Aquablation therapy compared to TURP: results from a double-blind, randomized trial in men with LUTS due to BPH. *Can J Urol* (2022) 29(1):10960–8.

51. Loloi J, Wang S, Labagnara K, Plummer M, Douglass L, Watts K, et al. Predictors of reoperation after transurethral resection of the prostate in a diverse, urban academic centre. *J Clin Urol* (2022). doi: 10.1177/20514158221132102

52. Yang BB, Shen BX, Liu WZ, Cheng Y, Shao YP, Qian JH. Medium-term clinical efficacy and complications of plasmakinetic enucleation of the prostate versus transurethral resection of the prostate for benign prostatic hyperplasia. *Urology* (2022) 164:204–10. doi: 10.1016/j.urology.2022.01.013

53. Yang CY, Chen GM, Wu YX, Zhang WJ, Wang J, Chen PP, et al. Clinical efficacy and complications of transurethral resection of the prostate versus plasmakinetic enucleation of the prostate. *Eur J Med Res* (2023) 28(1):83. doi: 10.1186/s40001-023-00989-9

54. Raizenne BL, Zheng X, Oumedjbeur K, Mao J, Zorn KC, Elterman D, et al. Prostatic artery embolization compared to transurethral resection of the prostate and prostatic urethral lift: a real-world population-based study. *World J Urol* (2023) 41 (1):179–88. doi: 10.1007/s00345-022-04218-6

55. Hu YY, Dong XC, Wang GC, Huang JH, Liu M, Peng B. Five-year follow-up study of transurethral plasmakinetic resection of the prostate for benign prostatic hyperplasia. *J Endourol* (2016) 30(1):97–101. doi: 10.1089/end.2015.0506

56. Cheng X, Qin CY, Xu P, Li YJ, Peng M, Wu SQ, et al. Comparison of bipolar plasmakinetic resection of prostate versus photoselective vaporization of prostate by a three year retrospective observational study. *Sci Rep* (2021) 11(1):10142. doi: 10.1038/s41598-021-89623-4

57. Zhu GB, Xie CY, Wang XH, Tang XQ. Bipolar plasmakinetic transurethral resection of prostate in 132 consecutive patients with large gland: three-year follow-up results. *Urology* (2012) 79(2):397–402. doi: 10.1016/j.urology.2011.08.052

58. Li K, Wang DJ, Hu C, Mao YH, Li MY, Jie ST, et al. A Novel Modification of Transurethral Enucleation and Resection of the Prostate in Patients With Prostate Glands Larger than 80 mL: Surgical Procedures and Clinical Outcomes. *Urology* (2018) 113:153–9. doi: 10.1016/j.urology.2017.11.036

59. Elshal AM, Soltan M, El-Tabey NA, Laymon M, Nabeeh A. Randomised trial of bipolar resection vs holmium laser enucleation vs Greenlight laser vapo-enucleation of the prostate for treatment of large benign prostate obstruction: 3-years outcomes. *Bju Int* (2020) 126(6):731–8. doi: 10.1111/bju.15161

60. Wei Y, Xu N, Chen SH, Li XD, Zheng QS, Lin YZ, et al. Bipolar transurethral enucleation and resection of the prostate versus bipolar resection of the prostate for prostates larger than 60gr: A retrospective study at a single academic tertiary care center. *Int Braz J Urol* (2016) 42(4):747–56. doi: 10.1590/S1677-5538.IBJU.2015.0225

61. Peng M, Yi L, Wang YH. Photoselective vaporization of the prostate vs plasmakinetic resection of the prostate: A randomized prospective trial with 12-month follow-up in Mainland China. *Urology* (2016) 87:161–5. doi: 10.1016/j.urology.2014.08.038

62. Yip SK, Chan NH, Chiu P, Lee KW, Ng CF. A randomized controlled trial comparing the efficacy of hybrid bipolar transurethral vaporization and resection of the prostate with bipolar transurethral resection of the prostate. *J Endourol* (2011) 25 (12):1889–94. doi: 10.1089/end.2011.0269

63. Elshal AM, Elkoushy MA, Elmansy HM, Sampalis J, Elhilali MM. Holmium : YAG transurethral incision versus laser photoselective vaporization for benign prostatic hyperplasia in a small prostate. *J Urol* (2014) 191(1):148–54. doi: 10.1016/j.juro.2013.06.113

64. Kuntz RM, Lehrich K, Ahyai SA. Holmium laser enucleation of the prostate versus open prostatectomy for prostates greater than 100 grams: 5-year follow-up results of a randomised clinical trial. *Eur Urol* (2008) 53(1):160–8. doi: 10.1016/j.eururo.2007.08.036

65. Sofimajidpour H, Khoshyar A, Zareie B, Sofimajidpour H, Rasouli MA. Comparison of the effectiveness and safety of transvesical open prostatectomy versus transurethral resection of the prostate in patients with benign prostatic hyperplasia with a prostate weight of 65-40 gram. *Urol J* (2020) 18(3):289–94. doi: 10.22037/uj.v16i7.6342

66. Varkarakis I, Kyriakakis Z, Delis A, Protogerou V, Deliveliotis C. Long-term results of open transvesical prostatectomy from a contemporary series of patients. *Urology* (2004) 64(2):306–10. doi: 10.1016/j.urology.2004.03.033

67. Shah HN, Etafy MH, Katz JE, Garcia Lopez EA, Shah RH. A randomized controlled trial comparing high and medium power settings for holmium laser enucleation of prostate. *World J Urol* (2021) 39(8):3005–11. doi: 10.1007/s00345-020-03535-y

68. Gilling PJ, Aho TF, Frampton CM, King CJ, Fraundorfer MR. Holmium laser enucleation of the prostate: Results at 6 years. *Eur Urol* (2008) 53(4):744–9. doi: 10.1016/j.eururo.2007.04.052

69. Whiting D, Penev B, Guest K, Cynk M. Holmium laser enucleation of the prostate: A single-centre case series of 1000 patients. *J Clin Urol* (2022) 15(5):370–5. doi: 10.1177/20514158211033741

70. Elshal AM, Elmansy HM, Elhilali MM. Feasibility of holmium laser enucleation of the prostate (HoLEP) for recurrent/residual benign prostatic hyperplasia (BPH). *Bju Int* (2012) 110(11C):E845–E50. doi: 10.1111/j.1464-410X.2012.11290.x

71. Droghetti M, Porreca A, Bianchi L, Piazza P, Giampaoli M, Casablanca C, et al. Long-term outcomes of Holmium laser enucleation of prostate and predictive model for symptom recurrence. *Prostate* (2022) 82(2):203–9. doi: 10.1002/pros.24259

72. Enikeev D, Taratkin M, Morozov A, Singla N, Gabdulina S, Tarasov A, et al. Long-term outcomes of holmium laser enucleation of the prostate: A 5-year single-center experience. *J Endourol* (2020) 34(10):1055–63. doi: 10.1089/end.2020.0347

73. Bhandarkar A, Patel D. Comparison of holmium laser enucleation of the prostate with bipolar plasmakinetic enucleation of the prostate: A randomized, prospective controlled trial at midterm follow-up. *J Endourol* (2022) 36(12):1567–74. doi: 10.1089/end.2022.0449

74. Vavassori I, Valenti S, Naspro R, Vismara A, Dell'Acqua V, Manzetti A, et al. Three-year outcome following holmium laser enucleation of the prostate combined with mechanical morcellation in 330 consecutive patients. *Eur Urol* (2008) 53(3):599–606. doi: 10.1016/j.eururo.2007.10.059

75. Tan AHH, Gilling PJ, Kennett KM, Fletcher H, Fraundorfer MR. Long-term results of high-power holmium laser vaporization (ablation) of the prostate. *Bju Int* (2003) 92(7):707–9. doi: 10.1046/j.1464-410x.2003.04474.x

76. Bae J, Choo M, Park JH, Oh JK, Paick JS, Oh SJ. Holmium laser enucleation of prostate for benign prostatic hyperplasia: seoul national university hospital experience. *Int Neurourol J* (2011) 15(1):29–34. doi: 10.5213/inj.2011.15.1.29

77. Aho TF, Gilling PJ, Kennett KM, Westenberg AM, Fraundorfer MR, Frampton CM. Holmium laser bladder neck incision versus holmium enucleation of the prostate as outpatient procedures for prostates less than 40 grams: A randomized trial. *J Urol* (2005) 174(1):210–4. doi: 10.1097/01.ju.0000161610.68204.ee

78. Neill MG, Gilling PJ, Kennett KM, Frampton CM, Westenberg AM, Fraundorfer MR, et al. Randomized trial comparing holmium laser enucleation of prostate with plasmakinetic enucleation of prostate for treatment of benign prostatic hyperplasia. *Urology* (2006) 68(5):1020–4. doi: 10.1016/j.urology.2006.06.021

79. Castellani D, Di Rosa M, Gasparri L, Pucci M, Dellabella M. Thulium laser vapoenucleation of the prostate (ThuVEP) in men at high cardiovascular risk and on antithrombotic therapy: A single-center experience. *J Clin Med* (2020) 9(4):917. doi: 10.3390/jcm9040917

80. Gross AJ, Orywal AK, Becker B, Netsch C. Five-year outcomes of thulium vapoenucleation of the prostate for symptomatic benign prostatic obstruction. *World J Urol* (2017) 35(10):1585–93. doi: 10.1007/s00345-017-2034-4

81. Tao W, Xue B, Sun C, Yang D, Zhang Y, Shan Y. Comparison of vaporization using 120-W GreenLight laser versus 2-micrometer continuous laser for treating benign prostatic hyperplasia: A 24-month follow-up study of a single center. *J Xray Sci Technol* (2019) 27(4):755–64. doi: 10.3233/XST-190507

82. Tao W, Sun CY, Xue BX, Yang DR, Wang MC, Cai CJ, et al. The efficacy and safety of 2-mu m continuous laser in the treatment of high-risk patients with benign prostatic hyperplasia. *Lasers Med Sci* (2017) 32(2):351–6. doi: 10.1007/s10103-016-2122-5

83. Becker B, Buttice S, Magno C, Gross AJ, Netsch C. Thulium vaporesection of the prostate and thulium vapoenucleation of the prostate: A retrospective bicentric matched-paired comparison with 24-month follow-up. *Urol Int* (2018) 100(1):105–11. doi: 10.1159/000484444

84. Bach T, Netsch C, Pohlmann L, Herrmann TRW, Gross AJ. Thulium : YAG vapoenucleation in large volume prostates. *J Urol* (2011) 186(6):2323–7. doi: 10.1016/j.juro.2011.07.073

85. Netsch C, Bach T, Pohlmann L, Herrmann T, Gross AJ. Comparison of 120-200 W 2 mu m Thulium: Yttrium-Aluminum-Garnet Vapoenucleation of the Prostate. *J Endourol* (2012) 26(3):224–9. doi: 10.1089/end.2011.0173

86. Park J, Cho SY, Cho MC, Jeong H, Son H. 5-year long-term efficacy of 120-W GreenLight photoselective vaporization of the prostate for benign prostate hyperplasia. *PloS One* (2017) 12(9):e0184442. doi: 10.1371/journal.pone.0184442

87. Law KW, Tholomier C, Nguyen DD, Sadri I, Couture F, Zakaria AS, et al. Global Greenlight Group: largest international Greenlight experience for benign prostatic hyperplasia to assess efficacy and safety. *World J Urol* (2021) 39(12):4389–95. doi: 10.1007/s00345-021-03688-4

88. Yamada Y, Furusawa J, Sugimura Y, Kuromatsu I. Photoselective vaporization of the prostate: long-term outcomes and safety during 10 years of follow-up. *J Endourol* (2016) 30(12):1306–11. doi: 10.1089/end.2016.0522

89. Hai MA. Photoselective vaporization of prostate: five-year outcomes of entire clinic patient population. *Urology* (2009) 73(4):807–10. doi: 10.1016/j.urology.2008.08.502

90. Malde S, Rajagopalan A, Patel N, Simoes A, Choi W, Shrotri N. Potassium-titanyl-phosphate laser photoselective vaporization for benign prostatic hyperplasia: 5-year follow-up from a district general hospital. *J Endourol* (2012) 26(7):878–83. doi: 10.1089/end.2011.0370

91. Ajib K, Mansour M, Zanaty M, Alnazari M, Hueber PA, Meskawi M, et al. Photoselective vaporization of the prostate with the 180-W XPS-Greenlight laser: Five-year experience of safety, efficiency, and functional outcomes. *Cuaj-Canadian. Urol Assoc J* (2018) 12(7):E318–E24. doi: 10.1016/j.juro.2018.02.2019

92. Kim KS, Choi JB, Bae WJ, Kim SJ, Cho HJ, Hong SH, et al. Risk factors for reoperation after photoselective vaporization of the prostate using a 120 W greenLight high performance system laser for the treatment of benign prostatic hyperplasia. *Photomed Laser Surgery* (2016) 34(3):102–7. doi: 10.1089/pho.2015.4050

93. Te AE, Malloy TR, Stein BS, Ulchaker JC, Nseyo UO, Hais MA. Impact of prostate-specific antigen level and prostate volume as predictors of efficacy in photoselective vaporization prostatectomy: analysis and results of an ongoing prospective multicentre study at 3 years. *Bju Int* (2006) 97(6):1229–33. doi: 10.1111/j.1464-410X.2006.06197.x

94. Tasci AI, Ilbey YO, Luleci H, Cicekler O, Sahin S, Cevik C, et al. 120-W greenLight laser photoselective vaporization of prostate for benign prostatic hyperplasia: midterm outcomes. *Urology* (2011) 78(1):134–40. doi: 10.1016/j.urology.2010.12.085

95. Meskawi M, Hueber PA, Valdivieso R, Bruyere F, Misrai V, Fournier G, et al. Multicenter international experience of 532 nm-laser photo-vaporization with Greenlight XPS in men with large prostates (prostate volume > 100 cc). *World J Urol* (2017) 35(10):1603–9. doi: 10.1007/s00345-017-2007-7

96. Malek RS, Kuntzman RS, Barrett DM. High power potassium-titanyl-phosphate laser vaporization prostatectomy. *J Urol* (2000) 163(6):1730–3. doi: 10.1016/S0022-5347(05)67530-1

97. Hueber PA, Bienz MN, Valdivieso R, Lavigueur-Blouin H, Misrai V, Rutman M, et al. Photoselective vaporization of the prostate for benign prostatic hyperplasia using the 180 watt system: multicenter study of the impact of prostate size on safety and outcomes. *J Urol* (2015) 194(2):462–9. doi: 10.1016/j.juro.2015.03.113

98. Tao W, Xue BX, Zang YC, Sun CY, Yang DR, Zhang YY, et al. The application of 120-W high-performance system GreenLight laser vaporization of the prostate in high-risk patients. *Lasers Med Sci* (2013) 28(4):1151–7. doi: 10.1007/s10103-012-1212-2

99. Chung DE, Wysock JS, Lee RK, Melamed SR, Kaplan SA, Te AE. Outcomes and complications after 532 nm laser prostatectomy in anticoagulated patients with benign prostatic hyperplasia. *J Urol* (2011) 186(3):977–81. doi: 10.1016/j.juro.2011.04.068

100. Stone BV, Chughtai B, Forde JC, Tam AW, Lewicki P, Te AE. Safety and efficacy of greenLight XPS laser vapoenucleation in prostates measuring over 150mL. *J Endourol* (2016) 30(8):906–12. doi: 10.1089/end.2016.0288

101. Liu XL, Yuan F, Xue BX. GreenLight XPS 180-W laser vaporization of prostate in high-risk elderly patients: A single-center experience. *Photobiomodulation Photomed Laser Surgery* (2020) 38(6):380–4. doi: 10.1089/photob.2019.4735

102. Campobasso C, Marchioni M, Greco F, De Nunzio C, Destefanis P, Ricciardulli S, et al. No matter for prostate sizes: Multicentric Italian Green Light photoselective vaporization study. *Eur Urol. Supplements* (2019) 18(9):e3168. doi: 10.1016/S1569-9056(19)33500-6

103. Chen CH, Lin SE, Chiang PH. Outcome of GreenLight HPS laser therapy in surgically high-risk patients. *Lasers Med Sci* (2013) 28(5):1297–303. doi: 10.1007/s10103-012-1234-9

104. Valdivieso R, Meyer CP, Hueber PA, Meskawi M, Alenizi AM, Azizi M, et al. Assessment of energy density usage during 180W lithium triborate laser photoselective vaporization of the prostate for benign prostatic hyperplasia. Is there an optimum amount of kilo-Joules per gram of prostate? *Bju Int* (2016) 118(4):633–40. doi: 10.1111/bju.13479

105. Kim HS, Cho MC, Ku JH, Kim SW, Paick JS. The efficacy and safety of photoselective vaporization of the prostate with a potassium-titanyl-phosphate laser for symptomatic benign prostatic hyperplasia according to prostate size: 2-year surgical outcomes. *Korean J Urol* (2010) 51(5):330–6. doi: 10.4111/kju.2010.51.5.330

106. Ruszat R, Wyler S, Seifert HH, Reich O, Forster T, Sulser T, et al. Photoselective vaporization of the prostate: Subgroup analysis of men with refractory urinary retention. *Eur Urol* (2006) 50(5):1040–9. doi: 10.1016/j.eururo.2006.01.019

107. Ghobrial FK, Shoma A, Elshal AM, Laymon M, El-Tabey N, Nabeeh A, et al. A randomized trial comparing bipolar transurethral vaporization of the prostate with GreenLight laser (xps-180watt) photoselective vaporization of the prostate for treatment of small to moderate benign prostatic obstruction: outcomes after 2 years. *Bju Int* (2020) 125(1):144–52. doi: 10.1111/bju.14926

108. Huet R, Peyronnet B, Khene ZE, Freton L, Verhoest G, Manunta A, et al. Prospective assessment of the sexual function after greenlight endoscopic enucleation and greenlight 180W XPS photoselective vaporization of the prostate. *Urology* (2019) 131:184–9. doi: 10.1016/j.urology.2019.06.020

109. Liu ZC, Chen ZP, Yan DS, Jiang T, Fu J, Zheng J, et al. Photoselective sharp enucleation of the prostate with a front-firing 532-nm laser versus photoselective vaporization of the prostate in the treatment of benign prostatic hyperplasia: a randomised controlled trial with 1-year followup results. *BMC Urol* (2022) 22(1):173. doi: 10.1186/s12894-022-01129-x

110. Mosli HA, Abdel-Meguid TA, Abdulwahhab MH, Al-Sayyad A, Farsi HM, Tayib A. Photoselective vaporization of the prostate using GreenLight 120-W lithium triborate laser to treat symptomatic benign prostatic hyperplasia: A single-centre prospective study. *Cuaj-Canadian. Urol Assoc J* (2013) 7(3-4):E193–E6. doi: 10.1186/s12894-022-01129-x

111. Seki N, Nomura H, Yamaguchi A, Naito S. Effects of photoselective vaporization of the prostate on urodynamics in patients with benign prostatic hyperplasia. *J Urol* (2008) 180(3):1024–8. doi: 10.1186/s12894-022-01129-x

112. Hueber PA, Ben-Zvi T, Liberman D, Bhojani N, Gautam G, Deklaj T, et al. Mid term outcomes of initial 250 case experience with GreenLight 120W-HPS photoselective vaporization prostatectomy for benign prostatic hyperplasia: comparison of prostate volumes < 60 cc, 60 cc-100 cc and > 100 cc. *Can J Urol* (2012) 19(5):6450–8.

113. Tao W, Sun CY, Yang DR, Zang YC, Zhu J, Zhang YY, et al. Application of 180W XPS GreenLight laser vaporization of the prostate for treatment of benign prostatic hyperplasia. *J X-Ray Sci Technol* (2019) 27(6):1121–9. doi: 10.1186/s12894-022-01129-x

114. Tugcu V, Tasci AI, Sahin S, Ordekci Y, Karakas OF, Zorluoglu F. Outcomes of 80 WKTP laser vaporization of the large prostate. *Urol Internationalis* (2007) 79 (4):316–20. doi: 10.1159/000109716

115. Pfitzenmaier J, Gilfrich C, Pritsch M, Herrmann D, Buse S, Haferkamp A, et al. Vaporization of prostates of > or =80 mL using a potassium-titanyl-phosphate laser: midterm-results and comparison with prostates of <80 mL. *BJU Int* (2008) 102(3):322–7. doi: 10.1111/j.1464-410X.2008.07563.x

116. Abolazm AE, El-Hefnawy AS, Laymon M, Shehab-El-Din AB, Elshal AM. Ejaculatory Hood Sparing versus Standard Laser Photoselective Vaporization of the Prostate: Sexual and Urodynamic Assessment through a Double Blinded, Randomized Trial. *J Urol* (2020) 203(4):792–801. doi: 10.1097/JU.0000000000000685

117. Bhojani N, Bidair M, Kramolowsky E, Desai M, Doumanian L, Zorn KC, et al. Aquablation therapy in large prostates (80-150 mL) for lower urinary tract symptoms due to benign prostatic hyperplasia: final WATER II 5-year clinical trial results. *J Urol* (2023) 210(1):143–53. doi: 10.1186/s12894-022-01129-x

118. Zorn KC, Bidair M, Trainer A, Arther A, Kramolowsky E, Desai M, et al. Aquablation therapy in large prostates (80-150 cc) for lower urinary tract symptoms due to benign prostatic hyperplasia: WATER II 3-year trial results. *BJUI Compass* (2022) 3(2):130–8. doi: 10.1186/s12894-022-01129-x

119. Bilhim T, Costa NV, Torres D, Pinheiro LC, Spaepen E. Long-term outcome of prostatic artery embolization for patients with benign prostatic hyperplasia: single-centre retrospective study in 1072 patients over a 10-year period. *Cardiovasc Intervent Radiol* (2022) 45(9):1324–36. doi: 10.1186/s12894-022-01129-x

120. Xu ZW, Zhou CG, Tian W, Shi HB, Liu S. Long-term efficacy and recurrence prediction of prostatic artery embolization for lower urinary tract symptoms secondary to benign prostatic hyperplasia. *Cardiovasc Interventional Radiol* (2022) 45(12):1801–9. doi: 10.1186/s12894-022-01129-x

121. Gravas S, Laguna P, Kiemeney L, de la Rosette J. Durability of 30-minute high-energy transurethral microwave therapy for treatment of benign prostatic hyperplasia: A study of 213 patients with and without urinary retention. *Urology* (2007) 69(5):854–8. doi: 10.1016/j.urology.2007.01.070

122. Francisca EA, Keijzers GB, d'Ancona FC, Debruyne FM, de la Rosette JJ. Lower-energy thermotherapy in the treatment of benign prostatic hyperplasia: long-term follow-up results of a multicenter international study. *World J Urol* (1999) 17 (5):279–84. doi: 10.1007/s003450050146

123. Raizenne BL, Zheng X, Mao J, Zorn KC, Cho A, Elterman D, et al. Real-world data comparing minimally invasive surgeries for benign prostatic hyperplasia. *World J Urol* (2022) 40(5):1185–93. doi: 10.1007/s00345-021-03926-9

124. Lau KO, Li MK, Foo KT. Long-term follow-up of transurethral microwave thermotherapy. *Urology* (1998) 52(5):829–33. doi: 10.1016/S0090-4295(98)00285-4

125. Ohigashi T, Nakamura K, Nakashima J, Baba S, Murai M. Long-term results of three different minimally invasive therapies for lower urinary tract symptoms due to benign prostatic hyperplasia: Comparison at a single institute. *Int J Urol* (2007) 14 (4):326–30. doi: 10.1111/j.1442-2042.2007.01692.x

126. Keijzers GB, Francisca EA, D'Ancona FC, Kiemeney LA, Debruyne FM, de la Rosette JJ. Long-term results of lower energy transurethral microwave thermotherapy. *J Urol* (1998) 159(6):1966–72; discussion 72-3. doi: 10.1016/S0022-5347(01)63211-7

127. Tsai YS, Lin JS, Tong YC, Tzai TS, Yang WH, Chang CC, et al. Transurethral microwave thermotherapy for symptomatic benign prostatic hyperplasia: long-term durability with Prostcare. *Eur Urol* (2001) 39(6):688–92; discussion 93-4. doi: 10.1159/000052528

128. Lourenco T, Shaw M, Fraser C, MacLennan G, N'Dow J, Pickard R. The clinical effectiveness of transurethral incision of the prostate: a systematic review of randomised controlled trials. *World J Urol* (2010) 28(1):23–32. doi: 10.1007/s00345-009-0496-8

129. Hueber PA, Zorn KC. Let's not forget about TUIP: A highly underutilized, minimally-invasive and durable technique for men with <30 g prostates. *Can Urol Assoc J* (2015) 9(7-8):255–6. doi: 10.5489/cuaj.3239

130. Agarwal A, Eryuzlu LN, Cartwright R, Thorlund K, Tammela TL, Guyatt GH, et al. What is the most bothersome lower urinary tract symptom? Individual- and population-level perspectives for both men and women. *Eur Urol* (2014) 65(6):1211–7. doi: 10.1016/j.eururo.2014.01.019

131. Li M, Qiu J, Hou Q, Wang D, Huang W, Hu C, et al. Endoscopic enucleation versus open prostatectomy for treating large benign prostatic hyperplasia: a meta-analysis of randomized controlled trials. *PloS One* (2015) 10(3):e0121265. doi: 10.1371/journal.pone.0121265

132. Lin YC, Wu X, Xu AB, Ren R, Zhou XQ, Wen Y, et al. Transurethral enucleation of the prostate versus transvesical open prostatectomy for large benign prostatic hyperplasia: a systematic review and meta-analysis of randomized controlled trials. *World J Urol* (2016) 34(9):1207–19. doi: 10.1007/s00345-015-1735-9

133. Zhang Y, Yuan P, Ma D, Gao X, Wei C, Liu Z, et al. Efficacy and safety of enucleation vs. resection of prostate for treatment of benign prostatic hyperplasia: a meta-analysis of randomized controlled trials. *Prostate. Cancer Prostatic Dis* (2019) 22 (4):493–508. doi: 10.1016/S0022-5347(01)63211-7

134. Tan A, Liao C, Mo Z, Cao Y. Meta-analysis of holmium laser enucleation versus transurethral resection of the prostate for symptomatic prostatic obstruction. *Br J Surgery* (2007) 94(10):1201–8. doi: 10.1002/bjs.5916

135. Qian XQ, Liu HL, Xu D, Xu L, Huang F, He W, et al. Functional outcomes and complications following B-TURP versus HoLEP for the treatment of benign prostatic hyperplasia: a review of the literature and Meta-analysis. *Aging Male* (2017) 20(3):184–91. doi: 10.1080/13685538.2017.1295436

136. Huang KC, Chow YC, Chen M, Chiu AW. Combination of thulium laser incision and bipolar resection offers higher resection velocity than bipolar resection alone in large prostates. *Urol J* (2019) 16(4):397–402. doi: 10.22037/uj.v0i0.4363

137. Trama F, Lauro GD, Illiano E, Iacono F, Romis L, Mordente S, et al. Ejaculation sparing thulium laser enucleation of the prostate: an observational prospective study. *J Clin Med* (2022) 11(21):6365. doi: 10.3390/jcm11216365

138. Zhou Y, Xue B, Mohammad NA, Chen D, Sun X, Yang J, et al. Greenlight high-performance system (HPS) 120-W laser vaporization versus transurethral resection of the prostate for the treatment of benign prostatic hyperplasia: a meta-analysis of the published results of randomized controlled trials. *Lasers Med Sci* (2016) 31(3):485–95. doi: 10.1007/s10103-016-1895-x

139. Moreira AM, de Assis AM, Carnevale FC, Antunes AA, Srougi M, Cerri GG. A review of adverse events related to prostatic artery embolization for treatment of bladder outlet obstruction due to BPH. *Cardiovasc Intervent Radiol* (2017) 40 (10):1490–500. doi: 10.1007/s00270-017-1765-3

140. Pisco J, Campos Pinheiro L, Bilhim T, Duarte M, Rio Tinto H, Fernandes L, et al. Prostatic arterial embolization for benign prostatic hyperplasia: short- and intermediate-term results. *Radiology* (2013) 266(2):668–77. doi: 10.1148/radiol.12111601

141. Nishiya M, Miller GJ, Lookner DH, Crawford ED. Prostate-specific antigen density in patients with histologically proven prostate carcinoma. *Cancer* (1994) 74 (11):3002–9. doi: 10.1002/1097-0142(19941201)74:11<3002::AID-CNCR2820741118>3.0.CO;2-G

142. Chughtai B, Rojanasarot S, Neeser K, Gultyaev D, Fu S, Bhattacharyya SK, et al. A comprehensive analysis of clinical, quality of life, and cost-effectiveness outcomes of key treatment options for benign prostatic hyperplasia. *PloS One* (2022) 17(4): e0266824. doi: 10.1371/journal.pone.0266824

143. DeWitt-Foy ME, Gill BC, Ulchaker JC. Cost comparison of benign prostatic hyperplasia treatment options. *Curr Urol Rep* (2019) 20(8):45. doi: 10.1007/s11934-019-0907-3

144. Amenta M, Oliva F, Barone B, Corsaro A, Arcaniolo D, Scarpato A, et al. Minimally invasive simple prostatectomy: Robotic-assisted versus laparoscopy. A comparative study. *Arch Ital Urol Androl* (2022) 94(1):37–40. doi: 10.4081/aiua.2022.1.37

frontiers | Frontiers in Endocrinology

TYPE Original Research
PUBLISHED 24 November 2023
DOI 10.3389/fendo.2023.1257902

OPEN ACCESS

EDITED BY
Heidi de Wet,
University of Oxford, United Kingdom

REVIEWED BY
Corinna Geisler,
University Medical Center Schleswig-Holstein, Germany
Mengmeng Song,
University of California, San Francisco, United States

*CORRESPONDENCE
Joon Kim
joon08167@gm.gist.ac.kr
Shinje Moon
sinjei82@gmail.com

RECEIVED 13 July 2023
ACCEPTED 31 October 2023
PUBLISHED 24 November 2023

CITATION
Lee H, Chung HS, Kim YJ, Choi MK, Roh YK, Yu JM, Oh C-M, Kim J and Moon S (2023) Association between body composition and the risk of mortality in the obese population in the United States. *Front. Endocrinol.* 14:1257902. doi: 10.3389/fendo.2023.1257902

Association between body composition and the risk of mortality in the obese population in the United States

Heeso Lee[1], Hye Soo Chung[2], Yoon Jung Kim[2], Min Kyu Choi[1], Yong Kyun Roh[1], Jae Myung Yu[2], Chang-Myung Oh[3], Joon Kim[3]* and Shinje Moon[2]*

[1]Department of Family Medicine, Hallym University College of Medicine, Chuncheon, Republic of Korea, [2]Division of Endocrinology and Metabolism, Department of Internal Medicine, Hallym University College of Medicine, Chuncheon, Republic of Korea, [3]Department of Biomedical Science and Engineering, Gwangju Institute of Science and Technology, Gwangju, Republic of Korea

Background: Recent studies have presented the concept of the obesity paradox, suggesting that individuals with obesity have a lower risk of death than those without obesity. This paradox may arise because body mass index (BMI) alone is insufficient to understand body composition accurately. This study investigated the relationship between fat and muscle mass and the risk of mortality in individuals with overweight/obesity.

Methods: We used data from the National Health and Nutrition Examination Survey (NHANES) from 1999 to 2006 and 2011 to 2018, which were linked to mortality information obtained from the National Death Index. Multiple Cox regression analyses were performed to estimate mortality risk. Subgroup analysis was conducted using propensity score-matched (PSM) data for age, sex, and race/ethnicity.

Results: This study included 16,555 participants who were overweight/obese (BMI≥25 kg/m^2). An increase in appendicular skeletal muscle mass index was associated with a lower mortality risk (hazard ratio [HR]: 0.856; 95% confidence interval [CI]: 0.802–0.915). This finding was consistent with the subgroup analysis of the PSM data. Contrastingly, a high fat mass index was associated with an increased risk of mortality. Sarcopenic overweight/obesity was significantly associated with high mortality compared to obesity without sarcopenia (HR: 1.612, 95%CI: 1.328–1.957). This elevated risk was significant in both age- and sex-based subgroups. This finding was consistent with the subgroup analysis using PSM data.

Conclusion: In contrast to the obesity paradox, a simple increase in BMI does not protect against mortality. Instead, low body fat and high muscle mass reduce mortality risk.

KEYWORDS

sarcopenia, obesity, muscle, obesity paradox, mortality

Introduction

In 2016, the World Health Organization reported that 13% of the global population was obese and that the obesity rate has increased threefold over the past 30 years (1). Obesity is associated with various diseases, including cardiovascular disease (CVD), diabetes, cerebral infarction, and cancer, and is responsible for approximately 4.8% of deaths worldwide (2–6). Although it is important to diagnose obesity accurately, recent studies have indicated an obesity paradox, which states that obese individuals may have a lower mortality risk than those with normal weight (a finding in two representative studies). A review of 40 cohort studies found that individuals with body mass indices (BMIs) <20 kg/m^2 had a higher risk of total and cardiovascular mortality, whereas individuals who were overweight (BMI: 25–29.9 kg/m^2) had a lower risk of mortality than those with a normal BMI (7). Furthermore, individuals who were overweight (BMI: 25–30 kg/m^2) or obese (BMI: 30–35 kg/m^2) and had hypertension and coronary artery disease had a lower risk of all-cause mortality than those with a normal weight (BMI: 20–25 kg/m^2) (8). This paradox may be attributed to the use of BMI, which does not accurately measure body composition, to define obesity. To obtain precise measurements of body composition, including body fat and muscle mass, imaging tests such as computed tomography (CT), magnetic resonance imaging, dual-energy X-ray absorptiometry, and positron emission tomography/CT are required. However, these tests are expensive and not readily accessible. Therefore, BMI is commonly used to assess the severity of obesity. Nevertheless, BMI has limitations as it cannot accurately differentiate between fat, mineral, and muscle masses and has restrictions in measuring body fat (9–16). Consequently, BMI alone may not be sufficient for predicting the risk of CVD, diabetes, cerebral infarction, cancer, and mortality (17–19).

Although obesity is commonly believed to protect against sarcopenia by preserving muscle mass, it can impair muscle function and lead to functional limitations (20, 21). Moreover, sarcopenia can occur in individuals with obesity, resulting in sarcopenic obesity, in which individuals may have a high BMI but poor lean body mass, leading to increased disability, immobility, and metabolic dysfunction (22, 23). Due to its negative impact on quality of life, physical function, and mortality, the prevalence of sarcopenic obesity is concerning (24, 25). Therefore, clinicians and researchers need to recognize and address sarcopenic obesity as a distinct clinical entity to improve health outcomes and enhance the quality of life.

This study aimed to use data from the National Health and Nutrition Examination Survey (NHANES) to determine the prevalence of sarcopenic obesity and investigate the relationship between fat and muscle mass, particularly in relation to sarcopenic obesity and the risk of mortality.

Method and materials

Study population

The NHANES is a research program designed to assess the health and nutritional status of adults and children in the United States (26). This longitudinal study used baseline data from four NHANES cycles from 1999 to 2006 and 2011 to 2018, linked to mortality data from the National Death Index (27).

Measurements

The average of three blood pressure (BP) measurements, taken after at least 5 minutes in a seated position, was used as data. Fasting blood glucose and cholesterol levels were measured by enzymatic methods. The NHANES Laboratory Procedure Manual provides additional information on sample collection and testing methods (28). Whole-body DEXA was performed using a Hologic QDR 4500 A fan-beam X-ray bone densitometer (Hologic Inc., Marlborough, MA, USA). DEXA was also used to assess total and regional body composition.

Definition of obesity/overweight, underlying diseases, and sarcopenia

Obesity/overweight was defined as a BMI ≥25 kg/m^2. Participants were considered to have hypertension if they had systolic BP >140 mmHg, mean diastolic BP >90 mmHg, or were receiving treatment for hypertension. Diabetes mellitus was defined as a fasting blood glucose level >126 mg/dL, random blood glucose level >200 mg/dL, HbA1c level >6.5%, or treatment for diabetes. Patients with a fasting total cholesterol level of 240 mg/dL or receiving treatment for dyslipidemia were considered to have dyslipidemia. Cancer history was assessed using structured questionnaires as follows: "*Have you ever been told by a doctor or other health professional that you have cancer or a malignancy?*" Patients with one or more of the following conditions were considered to have a history of CVD: angina pectoris, myocardial infarction, coronary heart disease, congestive heart failure, and cerebrovascular disease. Appendicular skeletal mass was defined as the sum of the total lean mass, excluding the bone mineral content of all extremities. The appendicular skeletal mass index (ASMI) was defined as the value obtained by dividing the appendicular skeletal mass by the square of the height (m) (29). We defined low muscle mass as ASMI <7 kg/m^2 in men and <5.5 kg/m^2 in women, according to the European Working Group on Sarcopenia in Older People 2 (EWGSOP2) (30). Sarcopenic obesity/overweight was defined as a BMI ≥25 kg/m^2 with a low muscle mass. We also defined high fat mass as a fat mass index (FMI) ≥ 8.3 kg/m^2 in men and ≥ 11.8 kg/m^2 in women based on the study of Gonzalez et al. (31).

Study outcomes

We collected publicly available mortality data from the National Center for Health Statistics based on probabilistic matching of the NHANES and National Death Index death certificate records through December 31, 2019. The data included all-cause mortality and follow-up duration through the month (27).

Ethics statement

All the NHANES protocols conducted in the United States were authorized by the Research Ethics Review Board of the National Center for Health Statistics, U.S. Centers for Disease Control and Prevention (Protocol Number: 1999–2004, Protocol #98–12; 2005–2010, Protocol #2005–06; 2011–2016, Protocol #2011–17) and conducted in accordance with the principles of the Declaration of Helsinki. All participants provided informed consent prior to the study.

Statistical analysis

Continuous and categorical variables of demographic characteristics, underlying diseases, anthropometric indices, and blood test results are presented as means, standard deviations, and frequencies (%), respectively. Independent t-tests and Pearson's chi-square tests were used to compare results. Correlations between BMI, ASMI, and FMI were examined using Pearson's correlation coefficient. Multiple Cox regression analyses were performed to assess the hazard ratios (HR) of all-cause mortality after adjusting for age, sex, race, smoking status, alcohol consumption, hypertension, diabetes, hyperlipidemia, and previous CVD events. The time from the first anthropometric and clinical measurements to death or the last follow-up (December 31, 2019) was included in the calculation. In addition, we performed a subgroup analysis of the propensity score matching (PSM) data (1:4 matching), considering the heterogeneity of the demographic characteristics and underlying diseases of sarcopenia. The graphical association between HR for each obesity parameter and mortality was assessed using four-knot-restricted cubic spline plots. Statistical analyses were performed using the IBM Statistical Package for the Social Sciences Statistics version 24.0 (IBM Corporation, Armonk, NY, USA) and R version 4.2.2 (R Foundation for Statistical Computing, Vienna, Austria; www.r-project.org). Statistical significance was set at $p < 0.05$.

Results

Baseline characteristics

In this study, 80,630 participants were initially identified from the 1999–2006 and 2011–2018 NHANES datasets (Figure 1). After excluding 34,295 participants with missing mortality data, 23,693 with insufficient data, and 6,107 with BMIs <25 kg/m^2, the final analysis included 16,555 participants. Table 1 shows the baseline characteristics of the participants with obesity or overweight according to their sarcopenia status. The sarcopenia group (n=291) was older (61.7 ± 16.51 years), had a lower proportion of men (43.0%), and exhibited significant differences in race/ethnicity distribution compared to the group without sarcopenia (n=16,264). There were no significant differences in the triglyceride levels between the groups. The prevalence of smoking, cancer history, and systolic BP was higher, whereas the proportion of drinkers, BMI, and diastolic BP was lower in the sarcopenia group. Patients in the sarcopenia group had higher fasting glucose, HbA1c, total cholesterol, and high-density lipoprotein (HDL) cholesterol levels. In addition, the sarcopenia group had a higher prevalence of previous CVD, diabetes mellitus, hypertension, and dyslipidemia. The proportion of all-cause deaths was higher in the sarcopenia group. Finally, ASMI was lower in the sarcopenia group, whereas FMI was not significantly different between the two groups. BMI was positively correlated with ASMI (*Pearson correlation coefficient*: 0.524, $p<0.001$) and FMI (*Pearson correlation coefficient*: 0.831, $p<0.001$).

We also performed 1:4 PSM to minimize the impact of confounding variables in the data analysis. The factors accounted for in the PSM included diabetes mellitus, hypertension, dyslipidemia, previous CVD events, and ASMI or FMI, and they were matched for age, sex, ethnicity/race, smoking status, and alcohol consumption. Table 1 shows the baseline characteristics of propensity score-matched (PSM) participants with obesity or overweight status according to their sarcopenia status. There were no differences between the groups in age, sex, race, or medical

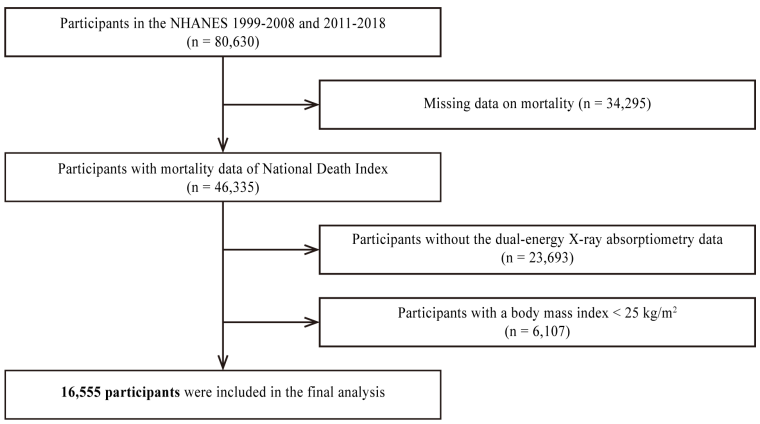

FIGURE 1
Flowchart for final selection. NHANES, National Health and Nutrition Examination Survey.

TABLE 1 Characteristics of whole and propensity score-matched participants with obesity/overweight according to sarcopenia.

	Whole dataset (N=16555)			PSM dataset (N=1385)		
	Without sarcopenia (N=16264)	Sarcopenia (N=291)	p	Without sarcopenia (N=1108)	Sarcopenia (N=277)	p
Age, years	42.97 ± 15.86	61.7 ± 16.51	< 0.001	62.2 ± 15.62	62.35 ± 15.70	0.883
Male sex, n (%)	8440 (51.9%)	125 (43.0%)	0.003	434 (39.2%)	121 (43.7%)	0.193
Race/Ethnicity, n (%)			< 0.001			< 0.778
Hispanic	5008 (30.8%)	111 (38.1%)		426 (38.4%)	106 (38.3%)	
Non-Hispanic White	6378 (39.2%)	155 (53.3%)		591 (53.3%)	151 (54.5%)	
Non-Hispanic Black	3565 (21.9%)	9 (3.1%)		42 (3.8%)	7 (2.5%)	
Other Race	1313 (8.1%)	16 (5.5%)		49 (4.4%)	13 (4.7%)	
Smokers, n (%)	6739 (43.5%)	160 (55.9%)	0.001	594 (53.6%)	154 (55.6%)	0.599
Drinkers, n (%)	10101 (68.0%)	166 (59.7%)	0.013	659 (59.5%)	166 (59.9%)	0.945
History of cancer, n (%)	839 (5.5%)	43 (15.0%)	< 0.001	150 (13.5%)	43 (15.6%)	0.436
BMI, kg/m^2	31.03 ± 5.08	26.5 ± 1.2	< 0.001	30.23 ± 4.30	26.46 ± 1.11	< 0.001
Systolic BP, mmHg	123.27 ± 17.72	133.17 ± 23.60	< 0.001	132.95 ± 21.26	133.70 ± 23.54	0.626
Diastolic BP, mmHg	72.17 ± 12.56	70.01 ± 12.18	0.006	70.79 ± 13.47	70.13 ± 12.26	0.487
Fasting glucose, mg/dL	107.91 ± 37.09	117.71 ± 50.37	0.001	114.87 ± 41.84	118.26 ± 51.25	0.410
HBA1c, %	5.66 ± 1.07	5.89 ± 1.21	< 0.001	5.86 ± 1.13	5.91 ± 1.22	0.595
Total cholesterol, mg/dL	198.29 ± 42.62	209.5 ± 43.88	< 0.001	205.98 ± 40.59	209.86 ± 43.91	0.173
Triglycerides, mg/dL	161.56 ± 159.77	153.35 ± 88.04	0.512	167.03 ± 123.17	154.85 ± 89.44	0.249
HDL-C, mg/dL	48.93 ± 13.67	55.26 ± 18.36	< 0.001	50.61 ± 14.19	54.79 ± 16.95	< 0.001
Previous CVD, n (%)	1076 (7.1%)	61 (21.6%)	< 0.001	176 (16.0%)	59 (21.7%)	< 0.032
Diabetes Mellitus, n (%)	2172 (13.7%)	65 (22.9%)	< 0.001	236 (21.6%)	63 (23.2%)	0.622
Hypertension, n (%)	6222 (40.1%)	184 (65.7%)	< 0.001	664 (63.8%)	177 (66.5%)	0.444
Dyslipidemia, n (%)	5993 (45.9%)	162 (63.3%)	< 0.001	563 (59.0%)	157 (63.3%)	0.241
All-cause death, n (%)	1794 (11.0%)	141 (48.5%)	< 0.001	461 (41.6%)	136 (49.1%)	0.029
ASMI, kg/m^2	8.38 ± 1.47	5.88 ± 0.75	< 0.001	7.50 ± 1.15	5.89 ± 0.75	< 0.001
FMI, kg/m^2	11.27 ± 3.86	10.90 ± 1.80	0.103	11.76 ± 3.42	10.85 ± 1.72	< 0.001

BMI, body mass index; HBA1c, hemoglobin A1c; HDL-C, high-density lipoprotein cholesterol; CVD, cardiovascular disease; ASMI, appendicular skeletal mass index; FMI, fat mass index.

history, except for CVD. The prevalence of CVD and HDL cholesterol was higher in the sarcopenia group, whereas BMI, ASMI, and FMI were lower in the sarcopenia group.

Association between body composition indices and mortality in participants with obesity/overweight

According to the results of the multiple Cox regression analyses, an increase in ASMI was significantly associated with a reduced risk of mortality (HR: 0.856, 95% confidence interval [CI]: 0.802–0.915, p=0.001; Table 2). This negative association was observed in both age subgroups, i.e., those aged ≤ 65 years (HR: 0.836, 95% CI: 0.760–0.919, p<0.001) and > 65 years (HR: 0.875, 95% CI: 0.798–0.960, p=0.005; Table 2). When stratified by sex, the negative association remained significant in both men (HR: 0.826; 95% CI: 0.758–0.900; p<0.001) and women (HR: 0.897; 95% CI: 0.806–0.998; p=0.046; Table 2). When stratified by cause of death, ASMI was negatively associated with death from cancer (HR: 0.829; 95% CI: 0.726–0.947; p=0.006) and non-cancer causes (HR: 0.867; 95% CI: 0.803–0.935; p<0.001), but not with death from CVD/cerebrovascular accident (HR: 0.974; 95% CI: 0.867–0.973; p=0.659). We further analyzed the PSM dataset. This subgroup analysis confirmed a negative association between ASMI and all-cause mortality (HR: 0.899; 95% CI: 0.830–0.973; p=0.008; Table 2). In contrast, a higher FMI

TABLE 2 The risk of mortality according to the body composition indices in participants with obesity/overweight.

	ASMI		FMI	
	HR (95% CI)	P-value	HR (95% CI)	P-value
Total	0.856 (0.802–0.915)	<0.001	1.045 (1.021–1.069)	<0.001
Subgroup by age				
Aged ≤ 65 years	0.836 (0.760–0.919)	<0.001	1.064 (1.029–1.099)	<0.001
Aged > 65 years	0.875 (0.798–0.960)	0.005	1.033 (1.001–1.066)	0.046
Subgroup by sex				
Men	0.826 (0.758–0.900)	<0.001	1.079 (1.043–1.116)	<0.001
Women	0.897 (0.806–0.998)	0.046	1.017 (0.984–1.051)	0.325
Subgroup by cause of death				
Cancer	0.829 (0.726–0.947)	0.006	1.057 (1.009–1.107)	0.019
Non-cancer	0.867 (0.803–0.935)	<0.001	1.041 (1.014–1.069)	0.003
CVD/CVA	0.974 (0.867–1.094)	0.659	1.027 (0.986–1.069)	0.204
PSM data*	0.899 (0.830–0.973)	0.008	0.955 (0.925–0.985)	0.004

ASMI, appendicular skeletal mass index; FMI, fat mass index; CVD, cardiovascular disease; CVA, cerebrovascular accident.
Adjusted for age, sex, ethnicity/race, smoking status, alcohol consumption, history of cancer at baseline, diabetes mellitus, hypertension, dyslipidemia, previous CVD events, and ASMI or FMI.
*Adjusted for diabetes mellitus, hypertension, dyslipidemia, previous CVD events, and ASMI or FMI in propensity score-matched data for age, sex, ethnicity/race, smoking status, and alcohol consumption.

was significantly correlated with an increased risk of mortality. (HR: 1.045, 95% CI: 1.021–1.069, p<0.001; Table 2). This association was consistent in participants aged ≤ 65 years (HR: 1.064; 95% CI: 1.029–1.099; p<0.001) and > 65 years (HR: 1.033; 95% CI: 1.001–1.066; p=0.046; Table 2). Among men, a higher FMI significantly increased the risk of mortality (HR: 1.079; 95% CI: 1.043–1.116; p<0.001). However, this association was not significant in women (HR: 1.017, 95% CI: 0.984–1.051, p=0.325; Table 2). In contrast to ASMI, when stratified by cause of death, FMI was positively associated with cancer (HR: 1.057; 95% CI: 1.009–1.107; p=0.019) and non-cancer mortality (HR: 1.041; 95% CI: 1.014–1.069; p=0.003), but not CVD/cerebrovascular accident (HR: 1.027; 95% CI: 0.986–1.069; p=0.204). In the PSM dataset, contrary to the total dataset, FMI and mortality were negatively correlated (HR: 0.955; 95% CI: 0.925–0.985; p=0.004). In the restricted cubic spline regression plot, the ASMI showed a negative association with the HR for mortality. Conversely, the HR for mortality continuously increased with FMI (Figure 2).

The risk of mortality in sarcopenic obesity/overweight

Kaplan–Meier survival curves showed a relationship between ASMI, FMI, and mortality, with the highest mortality rates in the low ASMI and high FMI groups (log-rank test, p<0.001) (Figure 3).

Table 3 presents the HR for mortality among individuals with sarcopenic obesity/overweight compared with those with obesity/overweight but sufficient ASMI, as determined by multiple Cox regression analyses. Sarcopenic obesity/overweight status was significantly associated with a higher risk of death. When analyzed by age subgroups, it was significantly associated with a higher risk of death in those ≤ 65 years of age (HR: 2.707; 95% CI: 1.813–4.043; p<0.001), but no significant association was found in those > 65 years of age (HR: 1.174; 95% CI: 0.982–1.404; p=0.079; Table 3). In the sex subgroups, the elevated risk was significant for both men and women (Table 3). In the subgroup analyses by cause of death, sarcopenic obesity/overweight was associated with an increased risk of cancer (HR: 1.541; 95% CI: 1.028–2.309; p=0.036) and non-cancer mortality (HR: 1.629; 95% CI: 1.306–2.031; p<0.001) but not CVD/cerebrovascular accident (HR: 1.367; 95% CI: 0.955–1.956; p=0.088; Table 3). In the analysis of PSM data, the risk of death in those with sarcopenic obesity/overweight was also significantly higher (HR: 1.481; 95% CI: 1.203–1.823; p<0.001; Table 3).

The sensitivity analysis of the Cox proportional hazards model by time of death

Tables 4 and 5 show the risk of all-cause mortality according to body composition indices and sarcopenic obesity/overweight status, respectively, considering the time of death. As shown in Table 4, ASMI and FMI were positively and negatively associated with the risk of all-cause mortality, respectively, independent of the time of death. However, when participants who died within the first 1, 2, and 3 years were excluded, the risk of all-cause mortality for sarcopenic obesity/overweight did not show a significant increase (Table 5).

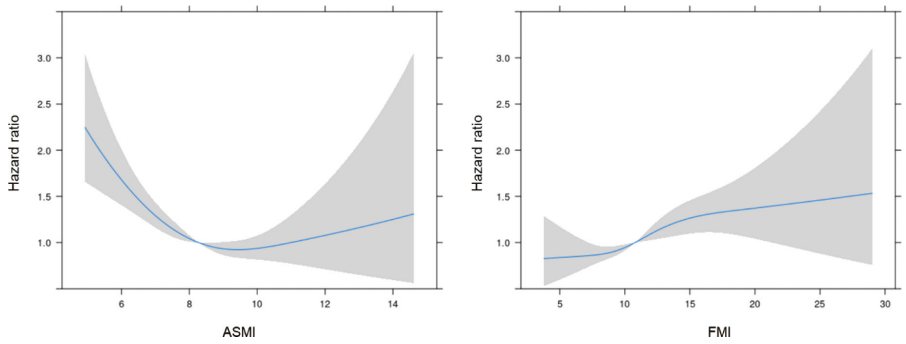

FIGURE 2
The hazard ratio for mortality according to ASMI and FMI. ASMI, appendicular skeletal mass index; FMI, fat mass index. Adjusted for age, sex, ethnicity/race, smoking status, alcohol consumption, history of cancer at baseline, diabetes mellitus, hypertension, dyslipidemia, previous CVD events, and ASMI or FMI.

Discussion

When food is consumed, it is converted into energy and used by the body; excess energy is converted into glycogen and triglycerides, which are stored in the body. Obesity develops when there is an imbalance between energy intake and expenditure. The risk factors for overweight/obesity include insufficient exercise, unhealthy eating habits, a lack of sufficient high-quality sleep, stress, diseases, genetics, and medications. Obesity is associated with diseases such as diabetes mellitus, CVD, stroke, hypertension, pulmonary disease, cancer, and NAFLD (non-alcoholic fatty liver disease) (32). Obesity is also associated with increased mortality (33). However, CVD-associated mortality decreases in the presence of obesity, a phenomenon known as the obesity paradox (34).

Sarcopenia is characterized by decreased muscle function and muscle mass (35). Muscle mass decreases by 3–8% every ten years after the age of 30 years, and this rate increases after 60 years of age (36). Sarcopenia has a prevalence of 6–15% in people aged > 65 years (37). The main causes of sarcopenia include reduced nutritional intake and activity, comorbidities, and drug use. Sarcopenia must be distinguished from malnutrition, cachexia, and senility before treatment. It is diagnosed based on reduced muscle strength, quantity, quality, and physical performance (30). Sarcopenia is associated with increased hospitalization duration, number of hospitalizations, and mortality (38).

This large-scale study aimed to determine the association between ASMI and FMI on mortality in participants with obesity. The HR for mortality increased as ASMI increased, which is consistent with previous studies suggesting that sarcopenia is associated with increased mortality (39, 40). In addition, the mortality risk increased proportionally with FMI, contrary to previous studies that found that being overweight was associated with decreased mortality (33, 41). However, this result is consistent with those of previous studies investigating the association between FMI, but not BMI, and mortality (42, 43). Furthermore, sarcopenia increases mortality risk in participants with obesity, reaffirming the

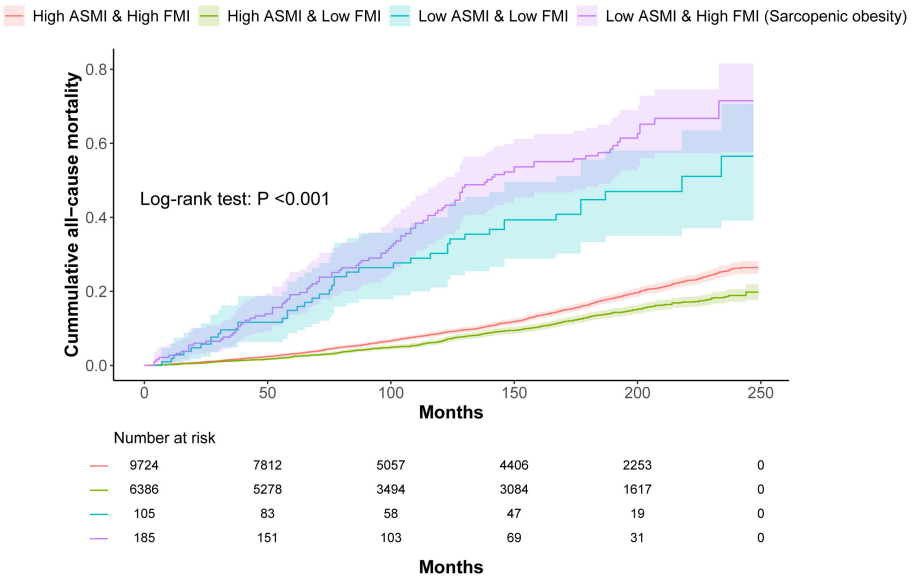

FIGURE 3
Kaplan–Meier plot of cumulative mortality by ASMI and FMI in participants with obesity.

TABLE 3 The hazard ratios for death in sarcopenic obesity/overweight compared to obesity/overweight with sufficient ASMI.

	Model 1		Model 2	
	HR (95% CI)	P-value	HR (95% CI)	P-value
Total	1.612 (1.328–1.957)	<0.001	1.481 (1.203–1.823)	<0.001
Subgroup by age				
Aged ≤ 65 years	2.707 (1.813–4.043)	<0.001		
Aged > 65 years	1.174 (0.982–1.404)	0.079		
Subgroup by sex				
Men	1.429 (1.101–1.854)	0.007		
Women	1.924 (1.435–2.581)	<0.001		
Subgroup by cause of death				
Cancer	1.541 (1.028–2.309)	0.036		
Non-cancer	1.629 (1.306–2.031)	<0.001		
CVD/CVA	1.367 (0.955–1.956)	0.088		

CVD, cardiovascular disease; CVA, cerebrovascular accident.
Model 1: Adjusted for age, sex, ethnicity/race, smoking status, alcohol consumption, history of cancer at baseline, diabetes mellitus, hypertension, dyslipidemia, and previous CVD events.
Model 2: Adjusted for diabetes mellitus, hypertension, dyslipidemia, and previous CVD events in propensity score-matched data for age, sex, ethnicity/race, smoking status, and alcohol consumption.

importance of sarcopenia in this population (44). Therefore, it is reasonable to assume that high muscle mass and low fat mass rather than high BMI are associated with reduced mortality.

Since the term "sarcopenic obesity" was first used by Heber et al. in 1996, it has become increasingly important. The incidence of sarcopenic obesity has increased owing to an increase in the older population and the presence of obesity, and sarcopenia exacerbates the adverse effects of obesity (45). Sarcopenic obesity has several causes. Aging causes changes in the body's composition. Fat mass increases with age, whereas muscle mass decreases after 40 years of age. The basal metabolic rate of older people is low because both the number and oxidative function of mitochondria in muscles are reduced. In addition, although the amount of thermogenic adipose tissue required for adaptive thermogenesis decreases (46), there is no significant change in the desire for food intake, which causes weight and fat gain. Hormones play a crucial role in muscle growth and strength. Testosterone, growth hormone, insulin, and thyroid hormones are associated with sarcopenia (47). Testosterone is a potent anabolic hormone that stimulates protein synthesis and inhibits protein degradation. Testosterone also increases the size of muscle fibers while inhibiting the differentiation of adipocyte progenitor cells. It also increases the levels of another anabolic hormone, insulin-like growth factor 1 (IGF-1), in the muscles. The growth hormone enhances protein turnover and muscle mass but does not increase muscle strength. Skeletal muscle is an important organ for insulin-induced glycemic control; thus, decreased muscle mass and quality lead to increased fat mass (48). Thyroid hormones are also involved in muscle growth and contraction (49). In older adults, the secretion of testosterone and growth hormones and the biological activity of thyroid hormones decrease, whereas insulin resistance increases, making them vulnerable to sarcopenic obesity (50). Adipose tissue inflammation is associated with sarcopenic obesity. Fat accumulation in the adipose tissue increases the release of free fatty acids and the production of leptin/monocyte

TABLE 4 Sensitivity analysis of the Cox proportional hazards model for all-cause mortality by time of death and body composition indices in participants with obesity/overweight.

	ASMI		FMI	
	HR (95% CI)	P-value	HR (95% CI)	P-value
Primary analysis	0.856 (0.802–0.915)	<0.001	1.045 (1.021–1.069)	<0.001
Excluding patients with event within the first year	0.857 (0.802–0.917)	<0.001	1.040 (1.016–1.065)	0.001
Excluding patients with event within 2 years	0.861 (0.803–0.922)	<0.001	1.040 (1.015–1.065)	0.001
Excluding patients with event within 3 years	0.864 (0.804–0.928)	<0.001	1.040 (1.015–1.066)	0.002

ASMI, appendicular skeletal mass index; FMI, fat mass index; CVD, cardiovascular disease; CVA, cerebrovascular accident.
Adjusted for age, sex, ethnicity/race, smoking status, alcohol consumption, history of cancer at baseline, diabetes mellitus, hypertension, dyslipidemia, previous CVD events, and ASMI or FMI.

TABLE 5 Sensitivity analysis of the Cox proportional hazards model for all-cause mortality by time to death and sarcopenia status in obese/overweight participants.

	Sarcopenia	
	HR (95% CI)	P-value
Primary analysis	1.612 (1.328–1.957)	<0.001
Excluding patients with events within the first year	1.348 (0.895–2.030)	0.152
Excluding patients with events within 2 years	1.321 (0.864–2.020)	0.199
Excluding patients with events within 3 years	1.243 (0.791–1.954)	0.345

Adjusted for age, sex, ethnicity/race, smoking status, alcohol consumption, history of cancer at baseline, diabetes mellitus, hypertension, dyslipidemia, previous CVD events, and ASMI or FMI.

chemoattractant protein 1 (MCP-1) and decreases adiponectin secretion. These adipokines recruit macrophages that undergo M1 polarization. Macrophages secrete tumor necrosis alpha (TNF-α), interleukin 6 (IL-6), and leptin, which are associated with the secretion of proinflammatory cytokines and decreased levels of IGF-1. Furthermore, TNF-α impedes mitochondrial biosynthesis and muscle development (51).

This study investigated the effect of obesity on mortality in a large sample and found that muscle and fat mass, but not BMI, were important for predicting mortality risk. ASMI was associated with a lower risk of mortality, independent of age and sex, while FMI was associated with a higher risk of mortality, independent of age, in men. Unexpectedly, in the PSM data, FMI was associated with a lower risk of mortality, which may reflect poor nutritional status in older patients with sarcopenia; however, further research is needed. In addition, when comparing participants with obesity and sarcopenia to participants with sarcopenia alone, the mortality rate was higher in the participants with obesity and sarcopenia. This effect was more significant in participants aged < 65 years. While other studies have investigated the effect of sarcopenia on mortality in older people (39, 40), this study revealed that sarcopenia was associated with increased mortality even in participants aged < 65 years. In the sensitivity analysis by time of death, when premature death was excluded, sarcopenic obesity/overweight was not associated with a significant increase in mortality, suggesting that sarcopenic obesity is associated with premature death. However, this study has several limitations. First, the effects of muscle strength or physical performance on mortality were not investigated. Secondly, the effects of sarcopenia management on mortality were not evaluated. Third, our study did not evaluate which type of fat (subcutaneous or visceral) influenced the mortality rate. Nevertheless, our study reaffirmed that sarcopenic obesity increases mortality rates.

Conclusions

These findings highlight the importance of maintaining muscle mass and managing fat mass to reduce mortality risk among people who are obese or overweight. In particular, this study provides evidence that the obesity paradox is incorrect by revealing that sarcopenia increases the mortality risk in individuals who are obese or overweight. Further investigations are warranted for the management of sarcopenic obesity/overweight.

Data availability statement

Publicly available datasets were analyzed in this study. This data can be found here: https://www.cdc.gov/nchs/nhanes/index.htm.

Ethics statement

All NHANES protocols conducted within the United States were authorized by the Research Ethics Review Board of the National Center for Health Statistics, U.S. Centers for Disease Control and Prevention (NCHS IRB/ERB Protocol Number: 1999–2004, Protocol #98–12; 2005–2010, Protocol #2005–06; 2011–2016, Protocol #2011–17) under the declaration of Helsinki. All participants provided informed consent prior to the study.

Author contributions

HL: Conceptualization, Formal analysis, Investigation, Methodology, Writing – original draft, Writing – review & editing. HC: Formal analysis, Investigation, Writing – review & editing. YK: Formal analysis, Investigation, Writing – review & editing. MC: Formal analysis, Investigation, Writing – review & editing. YR: Formal analysis, Investigation, Writing – review & editing. JY: Formal analysis, Investigation, Writing – review & editing. CO: Formal analysis, Investigation, Supervision, Writing – original draft, Writing – review & editing. JK: Formal analysis, Investigation, Supervision, Visualization, Writing – original draft, Writing – review & editing. SM: Conceptualization, Data curation, Formal analysis, Investigation, Methodology, Supervision, Visualization, Writing – original draft, Writing – review & editing.

Funding

The author(s) declare financial support was received for the research, authorship, and/or publication of this article. This research was supported by a "GIST Research Institute(GRI) IIBR" grant funded by the GIST in 2023 and by a grant from the MD-PhD/Medical Scientist Training Program through the Korea Health Industry Development Institute (KHIDI), funded by the Ministry of Health and Welfare, Republic of Korea.

Conflict of interest

The authors declare that the research was conducted in the absence of any commercial or financial relationships that could be construed as a potential conflict of interest.

Publisher's note

References

1. World Health Organization. *Fact sheet on obesity and overweight* (2021). Available at: https://www.who.int/en/news-room/fact-sheets/detail/obesity-and-overweight.

2. Solomon CG, Manson JE. Obesity and mortality: a review of the epidemiologic data. *Am J Clin Nutr* (1997) 66(4):1044S–50S. doi: 10.1093/ajcn/66.4.1044S

3. Krauss RM, Winston M, Fletcher BJ, Grundy SM. Obesity: impact on cardiovascular disease. *Circulation* (1998) 98(14):1472–6. doi: 10.1161/01.CIR.98.14.1472

4. Moon S, Oh C-M, Choi M-K, Park Y-K, Chun S, Choi M, et al. The influence of physical activity on risk of cardiovascular disease in people who are obese but metabolically healthy. *PLoS One* (2017) 12(9):e0185127. doi: 10.1371/journal.pone.0185127

5. Wallström P, Bjartell A, Gullberg B, Olsson H, Wirfält E. A prospective Swedish study on body size, body composition, diabetes, and prostate cancer risk. *Br J Cancer* (2009) 100(11):1799–805. doi: 10.1038/sj.bjc.6605077

6. World Health Organization. *Global health risks: mortality and burden of disease attributable to selected major risks*. Geneva, Switzerland: World Health Organization (2009). Available at: https://www.who.int/publications/i/item/9789241563871.

7. Romero-Corral A, Montori VM, Somers VK, Korinek J, Thomas RJ, Allison TG, et al. Association of bodyweight with total mortality and with cardiovascular events in coronary artery disease: a systematic review of cohort studies. *Lancet* (2006) 368 (9536):666–78. doi: 10.1016/S0140-6736(06)69251-9

8. Uretsky S, Messerli FH, Bangalore S, Champion A, Cooper-DeHoff RM, Zhou Q, et al. Obesity paradox in patients with hypertension and coronary artery disease. *Am J Med* (2007) 120(10):863–70. doi: 10.1016/j.amjmed.2007.05.011

9. Rahman M, Berenson AB. Accuracy of current body mass index obesity classification for white, black, and hispanic reproductive-age women. *Obstetrics Gynecology* (2010) 115(5):982–88. doi: 10.1097/AOG.0b013e3181da9423

10. Gurunathan U, Myles P. Limitations of body mass index as an obesity measure of perioperative risk. *Br J Anaesthesia* (2016) 116(3):319–21. doi: 10.1093/bja/aev541

11. Rothman KJ. BMI-related errors in the measurement of obesity. *Int J Obes* (2008) 32(3):S56–S9. doi: 10.1038/ijo.2008.87

12. Coutinho T, Goel K, Corrêa de Sá D, Carter RE, Hodge DO, Kragelund C, et al. Combining body mass index with measures of central obesity in the assessment of mortality in subjects with coronary disease: role of "normal weight central obesity". *J Am Coll Cardiol* (2013) 61(5):553–60. doi: 10.1016/j.jacc.2012.10.035

13. Gastaldelli A, Miyazaki Y, Pettiti M, Matsuda M, Mahankali S, Santini E, et al. Metabolic effects of visceral fat accumulation in type 2 diabetes. *J Clin Endocrinol Metab* (2002) 87(11):5098–103. doi: 10.1210/jc.2002-020696

14. Donohoe CL, Doyle SL, Reynolds JV. Visceral adiposity, insulin resistance and cancer risk. *Diabetol Metab Syndrome* (2011) 3:12. doi: 10.1186/1758-5996-3-12

15. Shimizu I, Yoshida Y, Minamino T. Maintenance of subcutaneous fat homeostasis improves systemic metabolic dysfunction in obesity. *Diabetes* (2015) 64 (12):3984–6. doi: 10.2337/dbi15-0013

16. Tran TT, Yamamoto Y, Gesta S, Kahn CR. Beneficial effects of subcutaneous fat transplantation on metabolism. *Cell Metab* (2008) 7(5):410–20. doi: 10.1016/j.cmet.2008.04.004

17. Romero-Corral A, Somers VK, Sierra-Johnson J, Thomas RJ, Collazo-Clavell M, Korinek J, et al. Accuracy of body mass index in diagnosing obesity in the adult general population. *Int J Obes* (2008) 32(6):959–66. doi: 10.1038/ijo.2008.11

18. Schneider HJ, Friedrich N, Klotsche J, Pieper L, Nauck M, John U, et al. The predictive value of different measures of obesity for incident cardiovascular events and mortality. *J Clin Endocrinol Metab* (2010) 95(4):1777–85. doi: 10.1210/jc.2009-1584

19. Flegal KM, Graubard BI, Williamson DF, Gail MH. Excess deaths associated with underweight, overweight, and obesity. *JAMA* (2005) 293(15):1861–7. doi: 10.1001/jama.293.15.1861

20. Cava E, Yeat NC, Mittendorfer B. Preserving healthy muscle during weight loss. *Adv Nutr* (2017) 8(3):511–9. doi: 10.3945/an.116.014506

21. Tallis J, James RS, Seebacher F. The effects of obesity on skeletal muscle contractile function. *J Exp Biol* (2018) 221(13):jeb163840. doi: 10.1242/jeb.163840

22. Barazzoni R, Bischoff S, Boirie Y, Busetto L, Cederholm T, Dicker D, et al. Sarcopenic obesity: time to meet the challenge. *Obes Facts* (2018) 11(4):294–305. doi: 10.1159/000490361

23. Park HM. Current Status of Sarcopenia in Korea: A focus on Korean geripausal women. *Ann Geriatric Med Res* (2018) 22(2):52–61. doi: 10.4235/agmr.2018.22.2.52

24. Bouchard DR, Dionne IJ, Brochu M. Sarcopenic/obesity and physical capacity in older men and women: data from the nutrition as a determinant of successful aging (NuAge)—the Quebec longitudinal study. *Obesity* (2009) 17(11):2082–8. doi: 10.1038/oby.2009.109

25. Rolland Y, Lauwers-Cances V, Cristini C, van Kan GA, Janssen I, Morley JE, et al. Difficulties with physical function associated with obesity, sarcopenia, and sarcopenic-obesity in community-dwelling elderly women: the EPIDOS (EPIDemiologie de l'OSteoporose) Study. *Am J Clin Nutr* (2009) 89(6):1895–900. doi: 10.3945/ajcn.2008.26950

26. CDC. *About the National Health and Nutrition Examination Survey* (2023). Available at: https://www.cdc.gov/nchs/nhanes/about_nhanes.htm.

27. National Center for Health Statistics. Office of analysis and epidemiology. In: *The Linkage of National Center for Health Statistics Survey Data to the National Death Index—2015 Linked Mortality File (LMF): Methodology Overview and Analytic Considerations*. Hyattsville, Maryland: National Center for Health Statistics (2019). Available at: https://www.cdc.gov/nchs/data-linkage/mortality-methods.htm.

28. CDC. *MEC Laboratory Procedures Manual* (2017). Available at: https://wwwn.cdc.gov/nchs/data/nhanes/2017-2018/manuals/2017_MEC_Laboratory_Procedures_Manual.

29. Van Ancum JM, Alcazar J, Meskers CG, Nielsen BR, Suetta C, Maier AB. Impact of using the updated EWGSOP2 definition in diagnosing sarcopenia: A clinical perspective. *Arch Gerontology Geriatrics* (2020) 90:104125. doi: 10.1016/j.archger.2020.104125

30. Cruz-Jentoft AJ, Bahat G, Bauer J, Boirie Y, Bruyère O, Cederholm T, et al. Sarcopenia: revised European consensus on definition and diagnosis. *Age Ageing* (2019) 48(4):16–31. doi: 10.1093/ageing/afy169

31. Gonzalez MC, Pastore CA, Orlandi SP, Heymsfield SB. Obesity paradox in cancer: new insights provided by body composition. *Am J Clin Nutr* (2014) 99(5):999–1005. doi: 10.3945/ajcn.113.071399

32. Haslam D, James W. Obesity. *Lancet* (2005) 366(9492):1197–209. doi: 10.1016/S0140-6736(05)67483-1

33. Flegal KM, Kit BK, Orpana H, Graubard BI. Association of all-cause mortality with overweight and obesity using standard body mass index categories. *JAMA* (2013) 309(1):71–82. doi: 10.1001/jama.2012.113905

34. Lavie CJ, Milani RV, Ventura HO. Obesity and cardiovascular disease: risk factor, paradox, and impact of weight loss. *J Am Coll Cardiol* (2009) 53(21):1925–32. doi: 10.1016/j.jacc.2008.12.068

35. Cruz-Jentoft AJ, Sayer AA. Sarcopenia. *Lancet* (2019) 393(10191):2636–46. doi: 10.1016/S0140-6736(19)31138-9

36. Volpi E, Nazemi R, Fujita S. Muscle tissue changes with aging. *Curr Opin Clin Nutr Metab Care* (2004) 7(4):405–10. doi: 10.1097/01.mco.0000134362.76653.b2

37. Iii LJM, Khosla S, Crowson CS, O'Connor MK, O'Fallon WM, Riggs BL. Epidemiology of sarcopenia. *J Am Geriatrics Society* (2000) 48(6):625–30. doi: 10.1111/j.1532-5415.2000.tb04719.x

38. Pacifico J, Reijnierse EM, Lim WK, Maier AB. The association between sarcopenia as a comorbid disease and incidence of institutionalisation and mortality in geriatric rehabilitation inpatients: REStORing health of acutely unwell adulTs (RESORT). *Gerontology* (2022) 68(5):498–508. doi: 10.1159/000517461

39. Xu J, Wan CS, Ktoris K, Reijnierse EM, Maier AB. Sarcopenia is associated with mortality in adults: a systematic review and meta-analysis. *Gerontology* (2022) 68 (4):361–76. doi: 10.1159/000517099

40. Zhang X, Wang C, Dou Q, Zhang W, Yang Y, Xie X. Sarcopenia as a predictor of all-cause mortality among older nursing home residents: a systematic review and meta-analysis. *BMJ Open* (2018) 8(11):e021252. doi: 10.1136/bmjopen-2017-021252

41. Bhaskaran K, Dos-Santos-Silva I, Leon DA, Douglas IJ, Smeeth L. Association of BMI with overall and cause-specific mortality: a population-based cohort study of 3·6 million adults in the UK. *Lancet Diabetes Endocrinol* (2018) 6(12):944–53. doi: 10.1016/s2213-8587(18)30288-2

42. Hu J, Chen X, Yang J, Giovannucci E, Lee DH, Luo W, et al. Association between fat mass and mortality: analysis of Mendelian randomization and lifestyle modification. *Metabolism* (2022) 136:155307. doi: 10.1016/j.metabol.2022.155307

43. Gnatiuc Friedrichs L, Wade R, Alegre-Díaz J, Ramirez-Reyes R, Garcilazo-Ávila A, Gonzáles-Carballo C, et al. Body composition and risk of vascular-metabolic

mortality risk in 113 000 mexican men and women without prior chronic disease. *J Am Heart Assoc* (2023) 12(3):e028263. doi: 10.1161/jaha.122.028263

44. Zhang X, Xie X, Dou Q, Liu C, Zhang W, Yang Y, et al. Association of sarcopenic obesity with the risk of all-cause mortality among adults over a broad range of different settings: a updated meta-analysis. *BMC Geriatrics* (2019) 19(1):183. doi: 10.1186/s12877-019-1195-y

45. Batsis JA, Villareal DT. Sarcopenic obesity in older adults: aetiology, epidemiology and treatment strategies. *Nat Rev Endocrinol* (2018) 14(9):513–37. doi: 10.1038/s41574-018-0062-9

46. da Nadyellem Silva G, Amato AA. Thermogenic adipose tissue aging: Mechanisms and implications. *Front Cell Dev Biol* (2022) 10:955612. doi: 10.3389/fcell.2022.955612

47. Gungor O, Ulu S, Hasbal NB, Anker SD, Kalantar-Zadeh K. Effects of hormonal changes on sarcopenia in chronic kidney disease: where are we now and what can we do? *J Cachexia Sarcopenia Muscle* (2021) 12(6):1380–92. doi: 10.1002/jcsm.12839

48. Cartee GD, Hepple RT, Bamman MM, Zierath JR. Exercise promotes healthy aging of skeletal muscle. *Cell Metab* (2016) 23(6):1034–47. doi: 10.1016/j.cmet.2016.05.007

49. Mullur R, Liu Y-Y, Brent GA. Thyroid hormone regulation of metabolism. *Physiol Rev* (2014) 94(2):355–82. doi: 10.1152/physrev.00030.2013

50. Michalakis K, Goulis D, Vazaiou A, Mintziori G, Polymeris A, Abrahamian-Michalakis A. Obesity in the ageing man. *Metabolism* (2013) 62(10):1341–9. doi: 10.1016/j.metabol.2013.05.019

51. Kalinkovich A, Livshits G. Sarcopenic obesity or obese sarcopenia: A cross talk between age-associated adipose tissue and skeletal muscle inflammation as a main mechanism of the pathogenesis. *Ageing Res Rev* (2017) 35:200–21. doi: 10.1016/j.arr.2016.09.008

frontiers | Frontiers in Endocrinology

TYPE Original Research
PUBLISHED 06 December 2023
DOI 10.3389/fendo.2023.1283795

OPEN ACCESS

EDITED BY
Kenju Shimomura,
Fukushima Medical University, Japan

REVIEWED BY
Nikolaos C. H. Syrmos,
Aristotle University of Thessaloniki, Greece
Maohua Lin,
Florida Atlantic University, United States

*CORRESPONDENCE
Sibo Wang
wangsbspine1@163.com

†These authors have contributed equally to this work and share first authorship

RECEIVED 27 August 2023
ACCEPTED 15 November 2023
PUBLISHED 06 December 2023

CITATION
Abudouaini H, Xu H, Yang J, Yi M, Lin K and Wang S (2023) Comparison of the effectiveness of zero-profile device and plate cage construct in the treatment of one-level cervical disc degenerative disease combined with moderate to severe paraspinal muscle degeneration. *Front. Endocrinol.* 14:1283795. doi: 10.3389/fendo.2023.1283795

Comparison of the effectiveness of zero-profile device and plate cage construct in the treatment of one-level cervical disc degenerative disease combined with moderate to severe paraspinal muscle degeneration

Haimiti Abudouaini†, Hui Xu†, Junsong Yang, Mengbing Yi, Kaiyuan Lin and Sibo Wang*

Department of Spine Surgery, Honghui Hospital, Xi'an Jiaotong University, Xi'an, Shanxi, China

Objective: Recent evidence indicates that cervical paraspinal muscle degeneration (PMD) is a prevalent and age-related condition in patients with cervical disc degenerative disease (CDDD). However, the relationship between surgery selection and post-operative outcomes in this population remains unclear. Consequently, this study aims to investigate the disparities in clinical outcomes, radiological findings, and complications between two frequently utilized anterior cervical surgical procedures. The objective is to offer guidance for the management of PMD in conjunction with CDDD.

Methods: A total of 140 patients who underwent single-level anterior cervical discectomy and fusion (ACDF) at our department were included in this study. The patients were divided into three groups based on the severity of PMD: mild (n=40), moderate (n=54), and severe (n=46), as determined by Goutalier fat infiltration grade. The subjects of interest were those with moderate-severe PMD, and their clinical outcomes, radiological parameters, and complications were compared between those who received a stand-alone zero-profile anchored cage (PREVAIL) and those who received a plate-cage construct (PCC).

Results: The JOA, NDI, and VAS scores exhibited significant improvement at all postoperative intervals when compared to baseline, and there were no discernible differences in clinical outcomes between the two groups. While the PCC group demonstrated more pronounced enhancements and maintenance of several sagittal alignment parameters, such as the C2-7 angle, FSU angle, C2-7 SVA, and T1 slope, there were no statistically significant differences between the two groups. The incidence of dysphagia in the zero-profile group was 22.41% at one week, which subsequently decreased to 13.79% at three months and 3.45% at the final follow-up. In contrast, the plate cage group exhibited a higher incidence of dysphagia, with rates of 47.62% at one week, 33.33% at three months, and 11.90% at the final follow-up. Notably, there were significant differences in the incidence of dysphagia between the two groups within the

10.3389/fendo.2023.1283795

first three months. However, the fusion rate, occurrence of implant subsidence, and adjacent segment degeneration (ASD) were comparable at the final follow-up.

Conclusion: For patients with one-level cervical disc degenerative disease combined with paraspinal muscle degeneration, both the zero-profile technique and PCC have demonstrated efficacy in ameliorating clinical symptoms and maintaining the postoperative sagittal balance. Although no significant disparities were observed between these two technologies in terms of complications such as adjacent segment degeneration and implant subsidence, the zero-profile technique exhibited superior performance over PCC in relation to dysphagia during the early stages of postoperative recovery. To validate these findings, studies with longer follow-up periods and evaluations of multilevel cervical muscles are warranted.

KEYWORDS

cervical paraspinal muscle, fatty infiltration, cross-sectional area, cervical disc degenerative disease, anterior cervical discectomy and fusion, stand-alone anchored cage

Introduction

Cervical degenerative disc disease (CDDD) is a pathological condition characterized by the degeneration of intervertebral discs and subsequent degeneration of the adjacent intervertebral joints, resulting in detrimental effects on the surrounding essential tissues, including the spinal cord, nerve roots, sympathetic nerves, and vertebral arteries (1, 2). It typically presents as discomfort in the neck and shoulders, accompanied by stiffness, radiating sensations towards the head, pillow, or upper limbs. In more severe instances, it may lead to spasms in both lower limbs, hindered mobility, quadriplegia, and other related symptoms (3–5). According to a cohort study involving 47,560 patients, the incidence of CDDD is 13.1% (6), with a peak incidence in the fourth and fifth decades of life (7). Reportedly, total annual treatment costs for neck pain were estimated at $686 million in Netherlands and $800 million in China (8, 9).

In cases where conservative treatments prove ineffective, surgical intervention is advised for patients with CDDD. Since anterior cervical discectomy and fusion (ACDF) was first reported by Smith and Cloward in 1958, the procedure has gradually become one of the dominant surgical strategies in the treatment of single and double level CDDD (10), and previous literature revealed that ACDF indeed could provide favorable clinical outcomes and maintain the reconstruction of the cervical spine (11–13). It was reported that more than 100 000 patients receive this treatment in the US annually (3) and is projected to increase by more than 10% in the next 20 years (14). The ACDF with traditional plate-cage construct (PCC) with screws was the primary spinal surgical approach for addressing symptomatic cervical disc disease. This method offers several benefits, including the preservation or enhancement of cervical sagittal alignment and stability, improved fusion rates, decreased likelihood of graft extrusion, as well as reduced micromotion and subsidence of implanted cages (15–18). The placement of an anterior cervical plate in close proximity to the esophagus may lead to mechanical irritation and subsequent soft tissue swelling, ultimately resulting in secondary dysphagia (19–21). Consequently, the utilization of a novel stand-alone device featuring a zero-profile device has become prevalent in ACDF procedures as a means of mitigating plate-related complications. The zero-profile devices represent a viable substitute for traditional ACDF implants, as they have demonstrated efficacy in diminishing the incidence of adjacent segment degeneration, circumventing contact with the cervical spine's anterior soft tissue, and potentially averting postoperative dysphagia (22). Nonetheless, scholars have discovered that patients who undergo ACDF with zero-profile device may encounter postoperative axial pain, loss of cervical curvature, and sagittal imbalance as a result of the absence of supplementary plate fixation (23).

The cervical paraspinal muscle (CPM) is a vital component of the dynamic spinal stabilization system, serving a critical function in preserving the stability and mobility of the neck (24). Through the recruitment of muscles and reflex responses of the nervous system, the neck muscles and tendons provide sufficient stability and regulate cervical motion. Recent research has revealed that degeneration of the CPM, in addition to bony structural alterations, is a significant contributor to persistent neck pain, sagittal imbalance, and the development of CDDD (25–27). Numerous patients with CDDD exhibit varying degrees of neck muscle degeneration, as evidenced by two abnormal indicators on MR images: a reduction in myofiber size (muscle atrophy) and an increase in fat deposition (fatty infiltration) (28). The co-occurrence of muscle atrophy and fatty infiltration is frequently

observed due to the inclination of myosatellite cells to differentiate into adipocytes under pathological conditions (29). However, there is a paucity of research investigating the correlation between surgical selection and postoperative outcomes among patients afflicted with concurrent CDDD and CPM degeneration.

Given the limited availability of clinical data in this domain, a retrospective analysis was conducted to determine the more advantageous surgical approach for these patients. Specifically, the clinical and radiological outcomes of ACDF with zero-profile device versus ACDF with PCC system were compared. The findings of this study are anticipated to furnish valuable insights and practical recommendations for the management of CDDD patients with CPM degeneration in the foreseeable future.

Materials and methods

Study design

In our department, a retrospective review was conducted on patients who underwent single-level ACDF from C3 to C7 between January 2016 and May 2020. The decision to proceed with surgery was determined by a clinical presentation that was consistent with recent magnetic resonance imaging (MRI) findings of root or spinal cord compression. This study received approval from the Medical Ethics Committee of our hospital and all patients provided informed consent for the analysis of their clinical data.

Inclusion and exclusion criteria for patients

The study's inclusion criteria encompassed patients who exhibited radiculopathy or myelopathy stemming from single-level cervical disc disease, with corresponding magnetic resonance imaging evidence and a lack of response to conservative treatment for a minimum of six weeks. Additionally, eligible patients were over 18 years of age and had undergone ACDF utilizing either the zero-profile device or PCC system from C3 to C7. Furthermore, patients were required to have comprehensive postoperative anteroposterior and lateral X-rays, as well as clinical data, and had agreed to participate in at least one year of follow-up. The present study employed specific exclusion criteria, which included the following: cervical disc replacement (CDR) or hybrid surgery (CDR with ACDF); ACDF utilizing alternative types of devices; multilevel surgery; local or systemic infection; severe osteoporosis (T score < -2.5); pathological vertebral fracture or spinal deformity; allergy to the device material; ankylosing spondylitis; rheumatoid arthritis; or prior cervical spine surgery.

All surgical procedures were performed by one senior spinal surgeon in our department using a standard, right Smith- Robinson approach after the induction of general anesthesia (30, 31). The selection of the zero-profile device or PCC device was based on the patient's condition and willingness. The zero-profile device group received a stand-alone cervical fusion implant (PREVAIL Medtronic Sofamor Danek, Memphis, TN) filled with a composite synthetic bone graft for ACDF, while the PCC group underwent ACDF using the VENTURE^{TM} anterior cervical plate system (Medtronic Sofamor Danek, Memphis, Tennessee, USA) with an allograft.

Clinical evaluation

The patients' arm and neck pain were evaluated using the visual analogue scale (VAS), which measures pain on a scale of 0 to 10 points, with 0 representing the absence of pain and 10 representing the highest level of pain. The neck disability index (NDI) scores were used to evaluate the function of the neck. The NDI is a validated 10-item questionnaire, with each item rated on a 6-point scale (32). This study used the Chinese version of the NDI proposed by Wu et al. (33), which is specifically targeted at Chinese-speaking individuals with neck pain. It also uses a 6-point Likert scale that ranges from 0 (no disability) to 5 (complete disability) for each item. Disability ratings are assigned as follows: 0 to 4, no disability; 5 to 14, mild disability; 15 to 24, moderate disability; 25 to 34, severe disability; and above 34, complete disability. The Japanese orthopedic association (JOA) scores were used to assess the neurological status of patients with myelopathy, the myelopathy severity is considered mild if the JOA score is higher than 13, moderate if the JOA score ranges from 9 to 13, and severe if the JOA score is lower than 9 (34).

Radiological evaluation

Evaluation of CPM degeneration

The study employed lateral X-ray images, computed tomography (CT) and MRI images to conduct radiological analysis. Prior to the operation, qualitative and quantitative evaluations of CPM were performed on an axial T2 weight section obtained from MRI. The degree of muscle fat infiltration at the C5/6 level was chosen as a representative measure of the cervical muscle, consistent with established practice in prior research (24, 35). The Goutallier classification was employed to assess the degree of fatty infiltration in the CPM prior to ACDF surgery, as documented in previous studies (24, 35). The Goutallier grading system utilizes scores ranging from 0 to 4, with 0 indicating the absence of visible fat streaks in the multifidus, 1 indicating minimal fatty streaks, 2 indicating a greater proportion of muscle than fat, 3 indicating equal amounts of fat and muscle, and 4 indicating a greater proportion of fat than muscle (Table 1, Figure 1). The multifidus muscles on both the right and left sides were evaluated separately, and the average of the scores was used for the final classification. Furthermore, the medial fascia boundaries of multifidus, semispinalis cervicis, semispinalis capitis, and splenius capitis at the C5-6 level on both sides were manually delineated using ImageJ software (v2.1.4.7; National Institutes of Health, USA) and quantified as the cross-sectional area (CSA) of each muscle Figure 2.

10.3389/fendo.2023.1283795

TABLE 1 The Goutallier fatty infiltration grade of paravertebral muscle degeneration.

Score	Severity	Fat infiltration
0	None	Absence of visible fat streaks
1	Mild	Minimal fatty streaks
2	Moderate	A greater proportion of muscle than fat
3	Moderate-Severe	Equal amounts of fat and muscle
4	Severe	A greater proportion of fat than muscle

Measurement of cervical sagittal alignment

The present study recorded various parameters related to cervical spine, including cervical lordosis (CL), range of motion (ROM) of C2-C7, functional spinal unit angle (FSUA), sagittal vertical axis (C2-7 SVA), center of the sella turcica–C7 sagittal vertical axis (St-SVA), and T1 slope. The measurement techniques employed in this study were consistent with those described in previous literature (36, 37). Specifically, CL was determined by measuring the angle between the inferior margin of the C2 vertebrae and the inferior margin of the C7 vertebrae. The calculation of the FSU angle involved the utilization of the Cobb angle of the vertebrae adjacent to the intervertebral disc in question. The determination of the C2-C7 SVA was based on the measurement of the distance between the posterosuperior corner of C7 and the vertical line originating from the center of the C2 body. The center of the St-SVA was established as the distance between a plumb line originating from the center of the sellar turcica and the center of the C7 body. The T1 slope was defined as the angle formed between the T1 superior endplate and a horizontal line (Figure 3).

Complications

The study documented postoperative complications, namely dysphagia, adjacent segment degeneration (ASD) and implant subsidence. Dysphagia was evaluated by using the Bazaz grading system and the scores of the Bazaz grading system were ranked as follows: 0-none, 1-mild, 2-moderate and 3-severe, representing no episodes of swallowing problems, rare episodes of dysphagia, occasional swallowing difficulties with specific foods and frequent swallowing difficulties with most foods, respectively. ASD was characterized by the emergence of new or enlarged ossification of the anterior longitudinal ligament, new or increased narrowing of the disc space by more than 30%, new or obvious enlarging osteophyte formation, and endplate sclerosis (38). Implant subsidence pertains to a reduction in the height of the functional spinal unit (FSU) by more than 2 mm (39).

Statistical analysis

The retrospective nature of the study predetermines the fixed sample size based on the available data. The statistical software SPSS

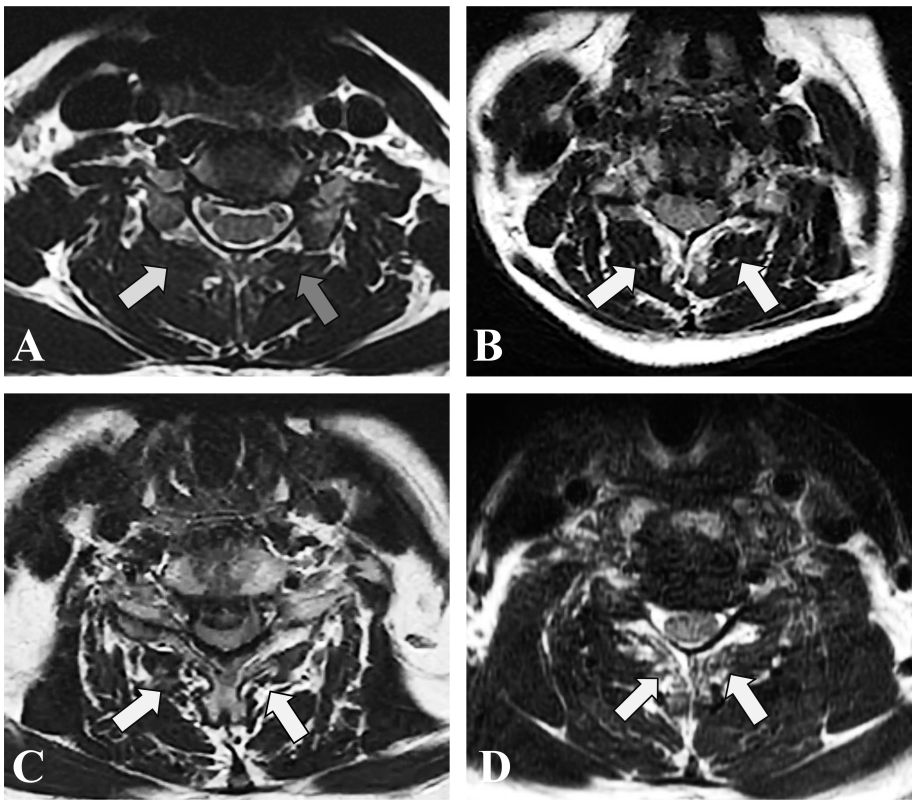

FIGURE 1
T2-weighted axial MRI section demonstrating fatty infiltration of muscle multifidus belly at C5/6. **(A)** Goutalier Grade 0 (white arrow), Goutalier Grade 1 (grey arrow); **(B)** Goutalier Grade 2. **(C)** Goutalier Grade 3. **(D)** Goutalier Grade 4.

10.3389/fendo.2023.1283795

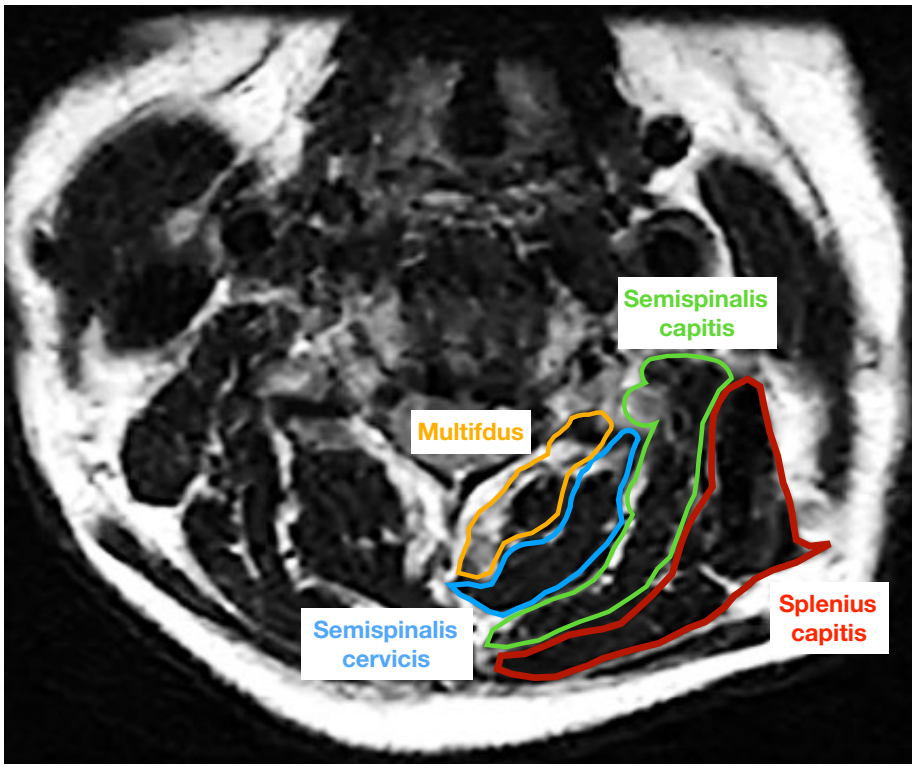

FIGURE 2
The cross-sectional area of multifdus (yellow), semispinalis cervicis (blue), semispinalis capitis (green), and splenius capitis (red) was measured on an axial T2 weighted image at the C5/6 level.

version 22.0 (IBM Corp., Armonk, NY) was utilized for all analyses. Continuous variables were presented as the mean ± standard deviation, while categorical variables were presented as the rate and ratio index. The normality of the parameters was assessed through a Shapiro-Wilk test. To examine significant differences among the groups, one-way analysis of variance (ANOVA) and Kruskal–Wallis tests were conducted based on the distribution of variables. The Chi-squared test was employed for categorical variables. The preoperative and post-operative parameters were compared using either the paired t-test or the Wilcoxon signed-rank test. Statistical significance was determined by a p-value of less than 0.05.

Results

Patient demographic data

The study consisted of a total of 140 patients, with 80 patients (43 men and 37 women) in the zero-profile group and 60 patients (38 men and 22 women) in the PCC group. The average age of the zero-profile group was 51.54 ± 9.19 years, while the average age of the PCC group was 52.30 ± 10.96 years. Statistical analysis revealed no significant differences between the two groups in terms of age, sex, body mass index (BMI), bone mineral density (BMD), operated level, intraoperative time, intraoperative blood loss, median time of hospital stay, or follow-up period (Table 2).

Degrees of fatty infiltration and grouping method

Table 3 displays the categorization of all patients based on the Goutallier classification, with three distinct groups established. The fatty infiltration of the multifidus was graded as 0-1 Goutallier grade for group A, 1.5-2 Goutalier grade for group B, and 2.5-4 Goutallier grade for group C. The patient population for group A consisted of 40 individuals (23 male and 17 females; average age=45.06 ± 6.31years), while group B comprised 54 patients (31 male and 23 female; average age = 43.21 ± 7.53 years), and group C included 46 patients (24 male and 22 female; average age = 46.51 ± 7.6 years). The study revealed that in Group A, 22 patients (55.0%) underwent ACDF with a zero-profile implant, while 18 patients (45.0%) received ACDF with a PCC fixation. Similarly, in Group B, 31 patients (57.41%) underwent ACDF with a zero-profile implant, and 23 patients (42.59%) received ACDF with a PCC fixation. In Group C, 27 patients (57.41%) underwent ACDF with a zero-profile implant, while 19 patients (42.59%) received ACDF with a PCC fixation.

Mean CSA of the paraspinal muscles

The mean CSA of the multifidus muscle was found to be 227.13 ± 75.88 mm^2 in group A, 222.69 ± 72.74 mm^2 in group B, and 219.54 ± 71.87 mm^2 in group C. Similarly, the CSA of the semispinalis cervicis muscle was 318.23 ± 93.51 mm^2 in group A,

10.3389/fendo.2023.1283795

TABLE 2 Comparison of general information between the zero-profile and the PCC group.

	zero-profile group (n=80)	PCC group (n=60)	p
Age (year)	51.59 ± 9.21	52.85 ± 11.206	0.164
Sex (male/female)	43/37	38/22	0.301
BMI (kg/m^2)	23.51 ± 2.84	23.18 ± 2.95	0.895
Preoperative symptom			0.749
Radiculopathy	33	27	
Myelopathy	37	24	
Radiculopathy and Myelopathy	10	9	
Operated segment			
C3-C4	7	8	
C4-C5	12	9	
C5-C6	52	36	
C6-C7	9	7	
Cage height	6.33 ± 0.73	6.28 ± 0.69	0.531
Intraoperative time (minute)	119.88 ± 18.33	121.83 ± 20.27	0.274
Estimated blood loss (milliliter)	72.13 ± 21.51	75.00 ± 27.02	0.468
T-score	0.22 ± 1.41	0.15 ± 1.31	0.111
Follow-up (month)	18.60 ± 7.37	17.90 ± 7.12	0.352

307.30 ± 97.27 mm^2 in group B, and 302.72 ± 103.53 mm^2 in group C. The CSA of the semispinalis capitis muscle was 361.15 ± 139.18 mm^2 in group A, 349.13 ± 148.31 mm^2 in group B, and 338.74 ± 111.55 mm^2 in group C. Lastly, the CSA of the splenius capitis muscle was 416.58 ± 150.20 mm^2 in group A, 402.41 ± 138.47 mm^2 in group B, and 395.26 ± 145.58 mm^2 in group C. No statistically significant differences were observed in the mean CSA of the paraspinal muscles across the three groups (Table 3).

Zero-profile versus PCC

To explore the most effective treatment strategy for patients with CDDD and severe CPM degeneration (Goutallier grade 1.5-2 and Goutallier grade 2.5-4), we conducted a comparative analysis of therapeutic efficacy, sagittal parameters, and complications between the zero-profile group and the PCC group.

Clinical outcomes

The preoperative clinical outcomes did not exhibit any significant differences between the two groups. However, all patients experienced a marked improvement in clinical symptoms following the operation. The mean JOA score increased in all groups, while the mean VAS score and NDI significantly decreased. Postoperative clinical outcomes did not demonstrate any significant differences between the zero-profile and PCC groups, as evidenced by Table 4.

Radiological findings

Table 5 presents the imaging results, indicating that, with the exception of St-SVA at the final follow-up, the other sagittal alignment parameters were comparable across various time points Figure 4. Specifically, the St-SVA in the zero-profile group remained stable from 28.11 ± 7.17 mm pre-surgery to 26.45 ± 9.42 mm at the last follow-up, with a mean change value of -0.28 ± 6.65 mm. In contrast, the PCC group experienced a decrease in St-SVA from 27.86 ± 7.55 mm pre-surgery to 21.91 ± 8.61 mm at the last follow-up, with a mean change value of 2.09 ± 13.31 mm. Notably, there were significant differences between the groups in the St-SVA at the last follow-up (p=0.023).

Complications

Over the course of several months following surgery, the overall occurrence of dysphagia exhibited a gradual decline in both groups. Specifically, the zero-profile group demonstrated a dysphagia incidence of 22.41% at one week, which decreased to 13.79% at three months and 3.45% at the final follow-up. In contrast, the plate cage group exhibited a dysphagia incidence of 47.62% at one week, which decreased to 33.33% at three months and 11.90% at the final follow-up. Notably, there were statistically significant differences between the groups in terms of dysphagia incidence within the initial three months (Table 6).

Discussion

Despite the widespread prevalence of cervical muscle degeneration, it has not garnered commensurate attention relative to the lumbar spine (40–44). He et al. observed a degeneration rate of 69.1% in the paraspinal muscles (Goutallier Grade ≥1.5) among patients with two-level cervical disc degenerative disease (24). They also identified a significant positive correlation between severe paraspinal muscle degeneration and postoperative sagittal balance disorder. Similarly, Wang et al. found that 67.33% (68/101) of patients with single-level cervical disc degenerative disease and severe fatty infiltration of paravertebral muscles experienced improved cervical sagittal alignment, which was comparable to those with strong cervical extensor muscles (39). The findings of our investigation align with prior research indicating that paraspinal muscle fatty degeneration can reach a prevalence of 71.43%. As a result, it is crucial to consider which ACDF procedure would be most advantageous for this demographic. Nevertheless, there is a dearth of literature on surgical decision-making for this cohort in previous studies.

The present study reports on the incidence of dysphagia in two groups, namely the zero-profile group and Plate group. The

10.3389/fendo.2023.1283795

TABLE 3 Comparison of baseline information between the three groups.

	Group A (n=40)	Group B (n=54)	Group C (n=46)	p
Goutalier grade	0-1	1.5-2	2.5-4	
Degree of fat infiltration	Normal-Mild	Moderate	Severe	
Age (year)	50.67 ± 10.01	53.23 ± 10.45	51.06 ± 8.30	0.879
Sex (male/female)	22/18	31/23	28/18	0.857
BMI (kg/m^2)	22.87 ± 2.71	23.50 ± 2.79	23.64 ± 3.11	0.420
Preoperative symptom				0.656
Radiculopathy	19	27	22	
Myelopathy	18	18	17	
Radiculopathy and Myelopathy	3	9	7	
Operated segment				0.102
C3-C4	9	2	3	
C4-C5	6	13	9	
C5-C6	20	33	28	
C6-C7	5	6	6	
Cage height	6.38 ± 0.74	6.26 ± 0.68	6.30 ± 0.73	0.738
Intraoperative time (minute)	128.50 ± 22.96	118.89 ± 19.80	126.20 ± 22.49	0.077
Estimated blood loss (milliliter)	71.75 ± 23.19	77.96 ± 26.66	76.30 ± 34.47	0.572
T-score	0.01 ± 1.43	0.29 ± 1.33	0.22 ± 1.36	0.602
Cross-sectional area (mm^2)				
Multifidus	227.13 ± 75.88	222.69 ± 72.74	219.54 ± 71.87	0.892
Semispinalis cervicis	318.23 ± 93.51	307.30 ± 97.27	302.72 ± 103.53	0.758
Semispinalis capitis	361.15 ± 139.18	349.13 ± 148.31	338.74 ± 111.55	0.744
Splenius capitis	416.58 ± 150.20	402.41 ± 138.47	395.26 ± 145.58	0.787
Follow-up (month)	18.45 ± 6.57	19.44 ± 8.87	16.83 ± 5.31	0.196
Implant type				0.941
zero-profile	22	31	27	
PCC	18	23	19	

incidence of dysphagia in the zero-profile group was found to be 22.41% and 47.62% at one week, 13.79% and 33.33% at three months, and 3.45% and 11.90% at the final follow-up, respectively. It is noteworthy that all cases of dysphagia were mild or moderate and showed a decreasing trend over time. However, the increasing use of zero-profile implant was found to be associated with a higher risk of kyphotic deformity and poor dynamic stability due to the lack of anterior support, as reported in previous studies (15, 45). Lee et al. conducted a comparative analysis of postoperative retention and motion stabilization following ACDF utilizing three distinct implants (46). Their findings suggested that patients requiring robust postoperative motion stabilization should receive a plate-cage construct rather than a Zero-profile implant. Our investigation found that a single-level ACDF procedure utilizing a zero-profile or plate cage construct, with varying degrees of multifidus fatty infiltration, did not impact sagittal balance. One possible explanation for why no differences were seen between groups is that anterior surgery results in less obstruction to the paraspinal muscle (47). ACDF has the advantage of preserving the posterior muscles and avoiding injuring the posterior structures, such as the posterior ligaments, compared with posterior surgery. In the previous literature, most of the results that paravertebral muscle fat infiltration has an effect on cervical curvature and sagittal position parameters mainly focus on posterior cervical surgery. Preserving of the posterior structures in turn has an enormous impact on the mechanical stability of the cervical spine (48, 49). Our other hypothesis is that although cross-sectional area and degree of fat infiltration are now commonly used to evaluate paravertebral muscle degeneration, whether these indicators fully reflect paravertebral muscle function remains to

10.3389/fendo.2023.1283795

TABLE 4 Comparison of clinical outcomes after ACDF with a zero-profile implant and PCC in patients with severe muscle degeneration.

	zero-profile group (n=58)	PCC group(n=42)	P
JOA scores			
preoperative	11.03 ± 1.34	10.88 ± 2.29	0.698
Last follow-up	15.62 ± 1.44	15.74 ± 1.40	0.684
VAS score			
preoperative	5.86 ± 1.12	6.10 ± 1.23	0.325
Last follow-up	1.72 ± 0.59	1.71 ± 0.60	0.271
NDI scores			
preoperative	28.14 ± 7.19	28.42 ± 7.01	0.843
Last follow-up	11.66 ± 5.27	12.44 ± 4.69	0.438

TABLE 5 Comparison of radiographic assessments after ACDF with a zero-profile implant and PCC in patients with severe muscle degeneration.

Group	zero-profile group (n=58)	PCC group (n=42)	p
$C_{2\text{-}7}$ angle (°)			
Preoperative	10.41 ± 7.92	9.39 ± 8.57	0.542
1 week	12.67 ± 7.63	14.67 ± 7.11	0.206
Last follow-upΔ	9.60 ± 7.25	12.00 ± 7.65	0.113
Δ $C_{2\text{-}7}$ angle	3.07 ± 5.84	2.56 ± 4.86	0.649
FSU angle (°)			
Preoperative	1.12 ± 1.99	1.44 ± 1.98	0.346
1 week	3.20 ± 1.86	3.67 ± 1.42	0.173
Last follow-up	2.90 ± 1.98	3.51 ± 1.61	0.088
Δ FSU angle	- 0.32 ± 2.83	- 0.15 ± 1.55	0.734
$C_{2\text{-}7}$ SVA (mm)			
Preoperative	19.83 ± 6.22	18.66 ± 6.04	0.351
1 week	22.41 ± 6.90	22.00 ± 5.02	0.748
Last follow-up	19.53 ± 6.56	20.33 ± 4.69	0.499
Δ $C_{2\text{-}7}$ SVA	2.88 ± 8.79	1.68 ± 0.94	0.378
St-SVA (mm)			
Preoperative	28.11 ± 7.17	27.86 ± 7.55	0.628
1 week	23.75 ± 7.67	24.65 ± 8.96	0.412
Last follow-up	26.45 ± 9.42	21.91 ± 8.61	0.023*
Δ St-SVA	-0.81 ± 11.00	2.09 ± 13.31	0.236
T_1 slope (°)			
preoperative	26.84 ± 6.88	27.31 ± 6.26	0.760
1 week	27.06 ± 5.64	26.72 ± 6.02	0.774
Last follow-up	26.54 ± 6.81	27.63 ± 6.46	0.421
Δ T_1 slope	0.51 ± 7.05	-0.92 ± 7.23	0.327

* Indicates statistically significant differences ($p<0.05$).

be verified. Therefore, the indicators that can reflect the paravertebral muscle function should be explored in the future studies. However, the parameters of the final follow-up indicated that the sagittal vertical axis (St-SVA) was worse. Our hypothesis posits that a novel sagittal balance is established following single-level anterior cervical discectomy and fusion, thereby preserving the optimal horizontal plane of the preoptic system and maintaining the head axis. The degeneration of a solitary muscle within a singular segment may not be adequate to disrupt and exacerbate the state of equilibrium. Therefore, a comprehensive and extensive study of multiple-level ACDF procedures involving multiple cervical muscles, with long-term follow-up, is imperative. Furthermore, notable advancements have been achieved in the advancement of finite element (FE) models pertaining to cervical spine in recent decades. Consequently, employing the FE model of ACDF surgery to investigate the impact of cervical paravertebral muscle degeneration on postoperative biomechanical characteristics and sagittal balance emerges as one of the crucial and efficacious avenues for future scholarly inquiry (50).

According to estimations, cervical paraspinal muscles maintain approximately 80% of the mechanical stability of the cervical spine (51), which is essential for holding posture and stabilizing the head. The cervical paraspinal muscle is categorized into superficial, intermediate, and deep layers, forming a crucial dynamic equilibrium system of the cervical spine (52). The superficial layer of cervical paraspinal muscles comprises the trapezius, rhomboid, and levator scapulae muscles, while the intermediate layer primarily consists of the head clamp muscle, neck clamp muscle, and longest neck muscle, the deep layer primarily comprises the semi-spinous muscle and neck multifidus muscle. The flexion of the neck is primarily regulated by muscles such as the scalene muscle, longissimus capitis, and longissimus cervicalis, while extension is mainly controlled by the multifidus muscle, longissimus capitis, and suboccipital muscle. Lateral flexion is primarily governed by the head clamp muscle, neck clamp muscle, sternocleidomastoid muscle, and scalene muscle. Additionally, the lateral rotation of the neck is predominantly controlled by the sternocleidomastoid muscle, multifidus muscle, erector spine muscle, and head and neck clamp muscle (53–56).

The comprehensive examination and investigation of the molecular mechanism governing adipogenesis in muscle cells will enhance our comprehension of the interconversion between muscle and adipose tissues, the metabolic roles of muscle tissues, and the etiology of muscular disorders. Despite an incomplete understanding of the molecular mechanism underlying the muscle-adipose conversion, recent advancements have provided us with fresh perspectives on adipogenesis in muscle cells. To the best of our understanding, the development of muscle, bone, and adipose tissues encompasses a complex series of steps, beginning with the

10.3389/fendo.2023.1283795

TABLE 6 Comparison of fusion rates and complications after ACDF with a zero-profile implant and PCC in patients with severe muscle degeneration.

	zero-profile group (n=58)	PCC group (n=42)	P
Fusion rate (%,n)	93.10% (54/58)	92.86% (39/42)	1.000
Subsidence (%,n)	12.07% (7/58)	9.52% (4/42)	0.757
Dysphagia(%,n)			
One week	22.41% (13/58)	47.62% (20/42)	0.010*
Three months	13.79% (8/58)	33.33% (14/42)	0.028*
Final follow-up	3.45% (2/58)	11.90% (5/42)	0.127
ASD (n,%)			
Superior	8.62% (5/58)	14.29% (6/42)	0.519
Inferior	15.52% (9/58)	19.05% (8/42)	0.788

*Indicates statistically significant differences ($p<0.05$).

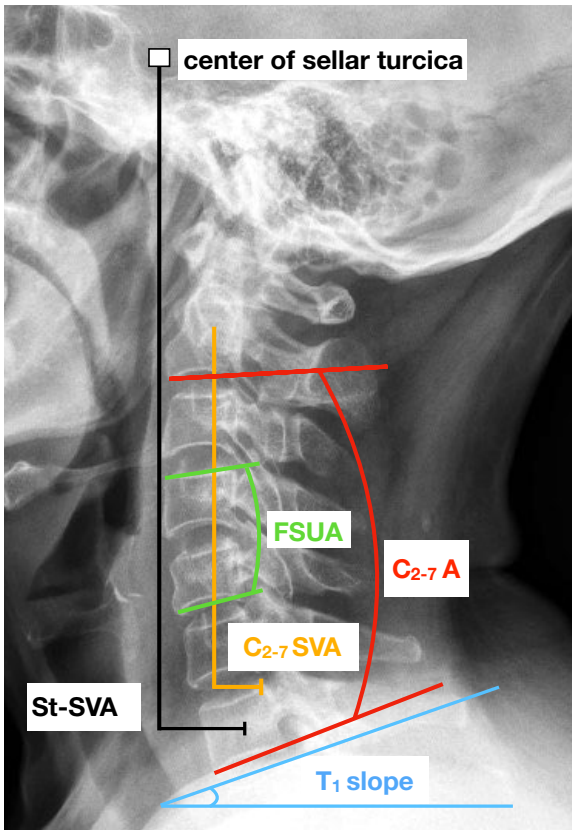

FIGURE 3
Lateral cervical spine radiograph with an illustration of key cervical sagittal alignment measurements. FSUA indicates the functional spinal unit angle. $C_{2\text{-}7}$ A represents the C2-C7 angle. $C_{2\text{-}7}$ SVA indicates the sagittal vertical axis and St-SVA indicates the center of the sella turcica – C7 sagittal vertical axis.

specification of a shared progenitor mesodermal cell towards a particular differentiation pathway, and subsequently leading to the manifestation of diverse terminal differentiation phenotypes (57). *In vitro* investigations have confirmed the pluripotent capacity of muscle-derived stem cells or precursor cells to differentiate in multiple directions (58, 59). To the best of our understanding, the development of muscle, bone, and adipose tissues encompasses a complex series of steps, beginning with the specification of a shared progenitor mesodermal cell towards a particular differentiation pathway, and subsequently leading to the manifestation of diverse terminal differentiation phenotypes (60). *In vitro* investigations have confirmed the pluripotent capacity of muscle-derived stem cells or precursor cells to differentiate in multiple directions. The multi-directional differentiation potential of muscle-derived stem cells or precursor cells has been demonstrated in *in vitro* studies (61). Additionally, lineage-tracing experiments have revealed that brown adipocytes, skeletal muscle cells, and dorsal dermal cells all originate from the same multi-potential progenitor cells derived from the central dermomyotome (62). Myoblasts have the potential to transdifferentiate into adipocytes or adipocyte-like cells under specific induction conditions (i.e., drug stimulation, cytokine treatment). Our findings also suggest that adipogenesis in muscle cells is prevalent among patients with cervical disc degenerative disease. Previous studies have reported the involvement of coding genes and non-coding genes, particularly miRNAs, in regulating the adipogenic transdifferentiation of myocytes (63). For example, miR-199a has been shown to regulate the transdifferentiation of C2C12 myoblasts by targeting the FATP1 gene (64). Moreover, the elimination of the interaction between slincRAD and the DNMT1 gene is anticipated to lead to impaired epigenetic regulation, thereby compromising the process of adipogenesis (65). Additionally, Qi et al. have documented that the lncRNA-GM43652 gene exhibits potential as a regulator of adipogenesis in muscle cells (66). However, this current level of understanding is insufficient to fully elucidate the regulatory functions of coding and non-coding genes in the process of transformation. Therefore, additional research is necessary to investigate the complex mechanisms involved in adipogenesis in muscle cells and to evaluate its association with prognostic outcomes in individuals suffering from cervical disc degenerative disease.

The current investigation is subject to certain limitations. Firstly, given that the study is retrospective, selection bias was unavoidable. Another limitation is the relatively small number of patients. Although we selected patients from January 2016 and May 2020, we limited the sample to only operations performed by the same doctor. Therefore, multicenter prospective design studies with a larger sample size are needed to verify our results. Secondly, the degree of muscle fat infiltration at the C5/6 level was exclusively chosen as a surrogate for the entirety of cervical muscle. While this approach has been employed in prior research (24, 35), it may not accurately reflect the actual mass of cervical muscles. Besides, although we measured muscle fat infiltration based on previously published reports, we acknowledge that potentially inherent radiographic imaging error might be a significant limitation. Another limitation of our study was the exact mechanism of the paraspinal muscle degeneration was did not explored. Additionally, the duration of the follow-up period was brief. Nonetheless, given

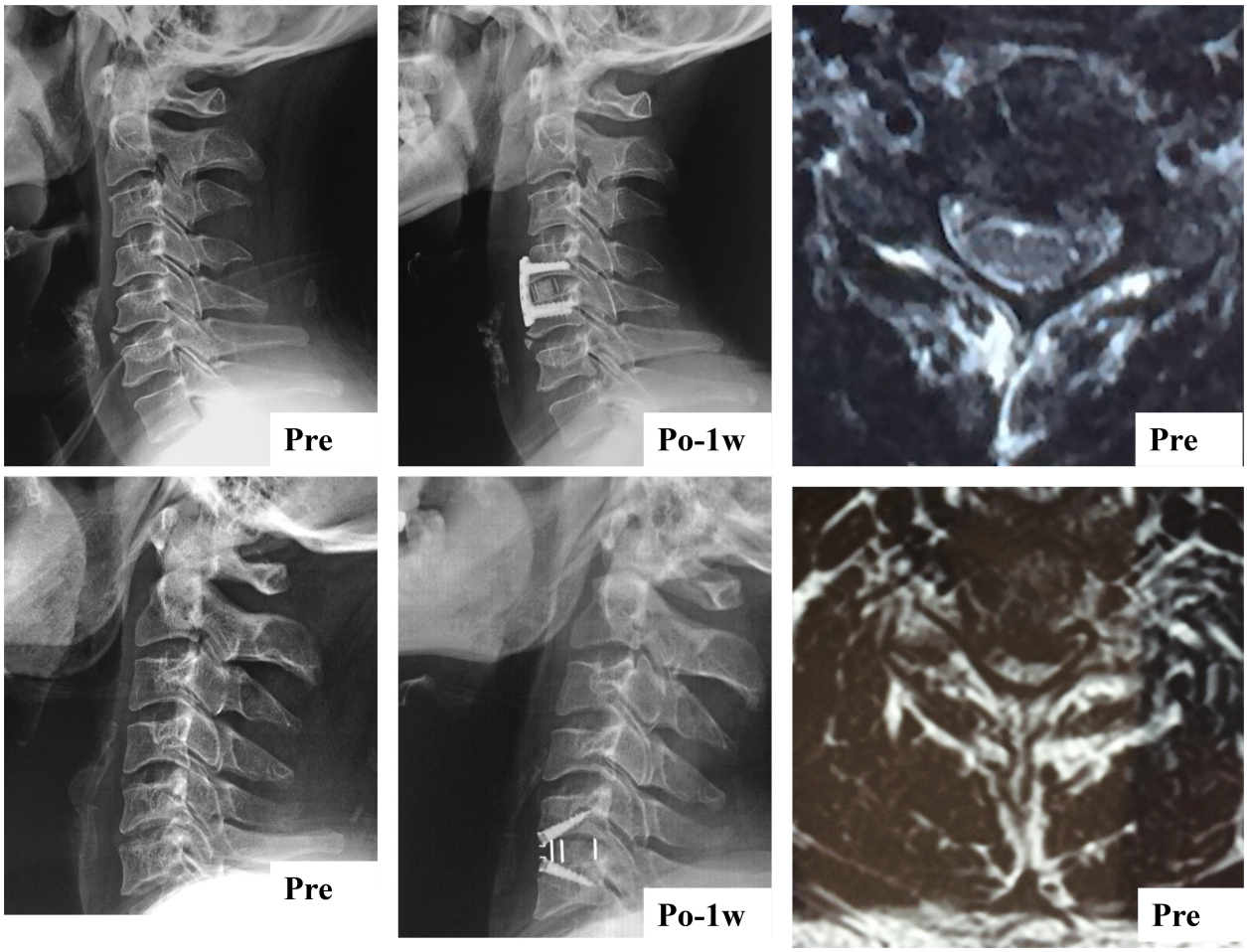

FIGURE 4
Sagittal parameters were improved whether cervical paraspinal muscle degeneration patients underwent ACDF using a Zero-profile device or conventional plate cage construct.

that clinical outcomes, radiological parameters, and fusion rates stabilized and complications such as dysphagia and subsidence manifested within 12 months, the timeframe was deemed adequate for assessing short-term outcomes. However, a more extensive duration of follow-up would be required to examine the degeneration of adjacent segments and assess the long-term results.

Conclusion

For patients with one-level cervical disc degenerative disease combined with paraspinal muscle degeneration, both the zero-profile technique and PCC have demonstrated efficacy in ameliorating clinical symptoms and maintaining the postoperative sagittal balance. Although no significant disparities were observed between these two technologies in terms of complications such as adjacent segment degeneration and implant subsidence, the zero-profile technique exhibited superior performance over PCC in relation to dysphagia during the early stages of postoperative recovery. To validate these findings, studies with longer follow-up periods and evaluations of multilevel cervical muscles are warranted.

Data availability statement

The raw data supporting the conclusions of this article will be made available by the authors, without undue reservation.

Ethics statement

The studies involving humans were approved by Medical Ethics Committee of Xi'an Jiaotong University. The studies were conducted in accordance with the local legislation and institutional requirements. The participants provided their written informed consent to participate in this study.

Author contributions

HA: Writing – original draft. HX:. JY: Resources, Supervision, Writing – review & editing. MY: Methodology, Validation, Writing – review & editing. KL: Methodology, Software, Writing – original

draft. SW: Formal analysis, Project administration, Resources, Supervision, Writing – review & editing.

Funding

The author(s) declare that no financial support was received for the research, authorship, and/or publication of this article.

Acknowledgments

HA and HX contributed equally to this work and they are the co-first authors of this study.

Conflict of interest

The authors declare that the research was conducted in the absence of any commercial or financial relationships that could be construed as a potential conflict of interest.

Publisher's note

References

1. Friedmann A, Baertel A, Schmitt C, Ludtka C, Milosevic J, Meisel HJ, et al. Intervertebral disc regeneration injection of a cell-loaded collagen hydrogel in a sheep model. *Int J Mol Sci* (2021) 22(8):4248. doi: 10.3390/ijms22084248

2. Sang D, Xiao B, Rong T, Wu B, Cui W, Zhang J, et al. Depression and anxiety in cervical degenerative disc disease: Who are susceptible? *Front Public Health* (2023) 10:1002837. doi: 10.3389/fpubh.2022.1002837

3. Johansen TO, Sundseth J, Fredriksli OA, Andresen H, Zwart JA, Kolstad F, et al. Effect of arthroplasty vs fusion for patients with cervical radiculopathy: A randomized clinical trial. *JAMA Netw Open* (2021) 4(8):e2119606. doi: 10.1001/jamanetworkopen.2021.19606

4. Tian X, Zhang L, Zhang X, Meng L, Li X. Correlations between preoperative diffusion tensor imaging and surgical outcome in patients with cervical spondylotic myelopathy. *Am J Transl Res* (2021) 13(10):11461–71.

5. Badhiwala JH, Ahuja CS, Akbar MA, Witiw CD, Nassiri F, Furlan JC, et al. Degenerative cervical myelopathy-update and future directions. *Nat Rev Neurol* (2020) 16:108–24. doi: 10.1038/s41582-019-0303-0

6. Schairer WW, Carrer A, Lu M, Hu SS. The increased prevalence of cervical spondylosis in patients with adult thoracolumbar spinal deformity. *J Spinal Disord Tech* (2014) 27:E305–8. doi: 10.1097/BSD.0000000000000119

7. Safaee MM, Nichols NM, Yerneni K, Zhang Y, Riew KD, Tan LA. Safety and efficacy of direct nerve root decompression via anterior cervical discectomy and fusion with uncinectomy for cervical radiculopathy. *J Spine Surg* (2020) 6(1):205–9. doi: 10.21037/jss.2019.12.04

8. Liu F, Fang T, Zhou F, Zhao M, Chen M, You J, et al. Association of depression/anxiety symptoms with neck pain: A systematic review and meta-analysis of literature in China. *Pain Res Manage* (2018) 2018:3259431. doi: 10.1155/2018/3259431

9. Miyamoto GC, Lin CC, Cabral CMN, van Dongen JM, van Tulder MW. Cost-effectiveness of exercise therapy in the treatment of non-specific neck pain and low back pain: a systematic review with meta-analysis. *Br J Sports Med* (2019) 53(3):172–81. doi: 10.1136/bjsports-2017-098765

10. Gendreau JL, Kim LH, Prins PN, D'Souza M, Rezaii P, Pendharkar AV, et al. Outcomes after cervical disc arthroplasty versus stand-alone anterior cervical discectomy and fusion: A meta-analysis. *Global Spine J* (2020) 10(8):1046–56. doi: 10.1177/2192568219888448

11. Sasso WR, Ye J, Foley DP, Vinayek S, Sasso RC. 20-year clinical outcomes of cervical disc arthroplasty: A prospective, randomized, controlled trial. *Spine (Phila Pa 1976).* (2023). doi: 10.1097/BRS.0000000000004811

12. Sheng XQ, Yang Y, Ding C, Wang BY, Hong Y, Meng Y, et al. Uncovertebral joint fusion versus end plate space fusion in anterior cervical spine surgery: A prospective randomized controlled trial. *J Bone Joint Surg Am* (2023) 105(15):1168–74. doi: 10.2106/JBJS.22.01375

13. Wang Y, Liu Y, Zhang A, Han Q, Jiao J, Chen H, et al. Biomechanical evaluation of a novel individualized zero-profile cage for anterior cervical discectomy and fusion: a finite element analysis. *Front Bioeng Biotechnol* (2023) 11:1229210. doi: 10.3389/fbioe.2023.1229210

14. Xu S, Liang Y, Zhu Z, Qian Y, Liu H. Adjacent segment degeneration or disease after cervical total disc replacement: a meta-analysis of randomized controlled trials. *J Orthop Surg Res* (2018) 13(1):244. doi: 10.1186/s13018-018-0940-9

15. Huang CY, Meng Y, Wang BY, Yu J, Ding C, Yang Y, et al. The effect of the difference in C2-7 angle on the occurrence of dysphagia after anterior cervical discectomy and fusion with the zero-profile implant system. *BMC Musculoskelet Disord* (2020) 21(1):649. doi: 10.1186/s12891-020-03691-7

16. Song KJ, Taghavi CE, Lee KB, Song JH, Eun JP. The efficacy of plate construct augmentation versus cage alone in anterior cervical fusion. *Spine (Phila Pa 1976)* (2009) 34(26):2886–92. doi: 10.1097/BRS.0b013e3181b64f2c

17. Abudouaini H, Huang C, Liu H, Hong Y, Wang B, Ding C, et al. Change in the postoperative intervertebral space height and its impact on clinical and radiological outcomes after ACDF surgery using a zero-profilerofile device: a single-Centre retrospective study of 138 cases. *BMC Musculoskelet Disord* (2021) 22(1):543. doi: 10.1186/s12891-021-04432-0

18. Lin M, Shapiro SZ, Doulgeris J, Engeberg ED, Tsai CT, Vrionis FD. Cage-screw and anterior plating combination reduces the risk of micromotion and subsidence in multilevel anterior cervical discectomy and fusion-a finite element study. *Spine J* (2021) 21(5):874–82. doi: 10.1016/j.spinee.2021.01.015

19. Li ZH, Zhao YT, Tang JG, Ren D, Guo J, Wang H. A comparison of a new zero-profile, stand-alone Fidji cervical cage and anterior cervical plate for single and multilevel ACDF: a minimum 2-year follow- up study. *Eur Spine J* (2017) 26 (4):1129–39. doi: 10.1007/s00586-016-4739-2

20. Min Y, Kim WS, Kang SS, Choi JM, Yeom JS, Paik NJ. Incidence of dysphagia and serial videofluoroscopic swallow study findings after anterior cervical discectomy and fusion: a prospective study. *Clin Spine Surg* (2016) 29(4):E177. doi: 10.1097/BSD.0000000000000060

21. Riley LH, Skolasky RL, Albert TJ, Vaccaro AR, Heller JG. Dysphagia after anterior cervical decompression and fusion: prevalence and risk fac- tors from a longitudinal cohort study. *Spine (Phila Pa 1976).* (2005) 30:2564–9. doi: 10.1097/01.brs.0000186317.86379.02

22. Abudouaini H, Wu T, Liu H, Wang B, Chen H, Li L. Comparison of the postoperative motion stabilization between anterior cervical decompression and fusion with a zero-profile implant system and a plate-cage construct. *World Neurosurg* (2022) 166:e484–e494.172-181. doi: 10.1016/j.wneu.2022.07.033

23. Li T, Yang JS, Wang XF, Meng CY, Wei JM, Wang YX, et al. Can zero-profile cage maintain the cervical curvature similar to plate-cage construct for single-level anterior cervical diskectomy and fusion? *World Neurosurg* (2020) 135:e300–6. doi: 10.1016/j.wneu.2019.11.153

24. He J, Wu T, Ding C, Wang B, Hong Y, Liu H. The fatty infiltration into cervical paraspinal muscle as a predictor of postoperative outcomes: A controlled study based on hybrid surgery. *Front Endocrinol (Lausanne).* (2023) 14:1128810. doi: 10.3389/fendo.2023.1128810

25. Peterson G, Leary SO, Nilsson D, Moodie K, Tucker K, Trygg J, et al. Ultrasound imaging of dorsal neck muscles with speckle tracking analyses - the relationship between muscle deformation and force. *Sci Rep* (2019) 9(1):13688. doi: 10.1038/s41598-019-49916-1

26. Fortin M, Wilk N, Dobrescu O, Martel P, Santaguida C, Weber MH, et al. Relationship between cervical muscle morphology evaluated by MRI, cervical muscle strength and functional outcomes in patients with degenerative cervical myelopathy. *Musculoskelet Sci Pract* (2018) 38:1–7. doi: 10.1016/j.msksp.2018.07.003

27. Tamai K, Grisdela P Jr, Romanu J, Paholpak P, Nakamura H, Wang JC, et al. The impact of cervical spinal muscle degeneration on cervical sagittal balance and spinal degenerative disorders. *Clin Spine Surg* (2019) 32(4):E206–13. doi: 10.1097/BSD.0000000000000789

28. Dallaway A, Kite C, Griffen C, Duncan M, Tallis J, Renshaw D, et al. Age-related degeneration of the lumbar paravertebral muscles: Systematic review and three-level meta-regression. *Exp Gerontol* (2020) 133:110856. doi: 10.1016/j.exger.2020.110856

29. Reza M, Subramaniyam N, Sim C, Ge X, Sathiakumar D, McFarlane C, et al. Irisin is a pro-myogenic factor that induces skeletal muscle hypertrophy and rescues denervation-induced atrophy. *Nat Commun* (2017) 8(1):1104. doi: 10.1038/s41467-017-01131-0

30. Deng Y, Wang B, Hong Y, Yang Y, Xing R, Wang X, et al. Anterior bone loss: A common phenomenon which should be considered as bone remodeling process existed not only in patients underwent cervical disk replacement but also those with anterior cervical diskectomy and fusion. *Eur Spine J* (2023) 32(3):977–85. doi: 10.1007/s00586-022-07504-4

31. Peng Z, Liu L, Sheng X, Liu H, Ding C, Wang B, et al. Risk factors of nonfusion after anterior cervical decompression and fusion in the early postoperative period: A retrospective study. *Orthop Surg* (2023) 15(10):2574–81. doi: 10.1111/os.13835

32. Vernon H. The neck disability index: state-of-the-art, 1991–2008. *J Manipulative Physiol Ther* (2008) 31(7):491–502. doi: 10.1016/j.jmpt.2008.08.006

33. Wu S, Ma C, Mai M, Li G. Translation and validation study of Chinese versions of the neck disability index and the neck pain and disability scale. *Spine J* (2010) 35 (16):1575–9. doi: 10.1097/BRS.0b013e3181c6ea1b

34. Li C, Mei Y, Li L, Li Z, Huang S. Posterior decompression and fusion with vertical pressure procedure in the treatment of multilevel cervical OPLL with kyphotic deformity. *Orthop Surg* (2022) 14(9):2361–8. doi: 10.1111/os.13433

35. Pinter ZW, Wagner SC, Fredericks DR Jr, Xiong A, Freedman BA, Elder BD, et al. Higher paraspinal muscle density effect on outcomes after anterior cervical discectomy and fusion. *Global Spine J* (2021) 11(6):931–5. doi: 10.1177/2192568220935108

36. Noh SH, Park JY. Association of complete uncinate process removal on 2-year assessment of radiologic outcomes: subsidence and sagittal balance in patients receiving one-level anterior cervical discectomy and fusion. *BMC Musculoskelet Disord* (2020) 21 (1):439. doi: 10.1186/s12891-020-03443-7

37. Abudouaini H, Wu T, Liu H, Wang B, Chen H, Huang C, et al. Partial uncinatectomy combined with anterior cervical discectomy and fusion for the treatment of one-level cervical radiculopathy: analysis of clinical efficacy and sagittal alignment. *BMC Musculoskelet Disord* (2021) 22(1):777. doi: 10.1186/s12891-021-04680-0

38. Robertson JT, Papadopoulos SM, Traynelis VC. Assessment of adjacent-segment disease in patients treated with cervical fusion or arthroplasty: a prospective 2-year study. *J Neurosurg Spine.* (2005) 3(6):417–23. doi: 10.3171/spi.2005.3.6.0417

39. Wang XJ, Huang KK, He JB, Wu TK, Rong X, Liu H. Fatty infiltration in cervical extensor muscle: is there a relationship with cervical sagittal alignment after anterior cervical discectomy and fusion? *BMC Musculoskelet Disord* (2022) 23(1):641. doi: 10.1186/s12891-022-05606-0

40. Park MW, Park SJ, Chung SG. Relationships between skeletal muscle mass, lumbar lordosis, and chronic low back pain in the elderly. *Neurospine* (2023) 20 (3):959–68. doi: 10.14245/ns.2346494.247

41. Schönnagel L, Guven AE, Camino-Willhuber G, Caffard T, Tani S, Zhu J, et al. Examining the role of paraspinal musculature in post-operative disability after lumbar fusion surgery for degenerative spondylolisthesis. *Spine (Phila Pa 1976)* (2023). doi: 10.1097/BRS.0000000000004840

42. Shahidi B, Padwal JA, Su JJ, Regev G, Zlomislic V, Allen RT, et al. The effect of fatty infiltration, revision surgery, and sex on lumbar multifidus passive mechanical properties. *JOR Spine* (2023) 6(3):e1266. doi: 10.1002/jsp2.1266

43. Song J, Shahsavarani S, Vatsia S, Katz AD, Ngan A, Fallon J, et al. Association between history of lumbar spine surgery and paralumbar muscle health: a propensity score-matched analysis. *Spine J* (2023) 11:S1529–9430(23)03260-6. doi: 10.1016/j.spinee.2023.07.004

44. Singh S, Shahi P, Asada T, Kaidi A, Subramanian T, Zhao E, et al. Poor muscle health and low preoperative ODI are independent predictors for slower achievement of MCID after minimally invasive decompression. *Spine J* (2023) 23(8):1152–60. doi: 10.1016/j.spinee.2023.04.004

45. Kaiser MG, Haid RW Jr, Subach BR, Barnes B, Rodts GE Jr. Anterior cervical plating enhances arthrodesis after discectomy and fusion with cortical allograft. *Neurosurgery* (2002) 50(2):229–36. doi: 10.1097/00006123-200202000-00001

46. Lee YS, Kim YB, Park SW. Does a zero-profilerofile anchored cage offer additional stabilization as anterior cervical plate? *Spine (Phila Pa 1976)* (2015) 40 (10):E563–70. doi: 10.1097/BRS.0000000000000864

47. Siasios I, Samara E, Fotiadou A, Tsoleka K, Vadikolias K, Mantatzis M, et al. The role of cervical muscles morphology in the surgical treatment of degenerative disc disease: clinical correlations based on magnetic resonance imaging studies. *J Clin Med Res* (2021) 13(7):367–76. doi: 10.14740/jocmr4551

48. Matsumoto M, Okada E, Ichihara D, Watanabe K, Chiba K, Toyama Y, et al. Changes in the cross-sectional area of deep posterior extensor muscles of the cervical spine after anterior decompression and fusion: 10-year follow-up study using MRI. *Eur Spine J* (2012) 21(2):304–8. doi: 10.1007/s00586-011-1978-0

49. Anderson JS, Hsu AW, Vasavada AN. Morphology, architecture, and biomechanics of human cervical multifidus. *Spine (Phila Pa 1976).* (2005) 30(4):E86–91. doi: 10.1097/01.brs.0000153700.97830.02

50. Lin M, Paul R, Dhar UK, Doulgeris J, O'Connor TE, Tsai CT, et al. A review of finite element modeling for anterior cervical discectomy and fusion. *Asian Spine J* (2023) 17(5):949–63. doi: 10.31616/asj.2022.0295

51. Gorla C, Martins TS, Florencio LL, Pinheiro-Araújo CF, Fernández-de-Las-Peñas C, Martins J, et al. Reference values for cervical muscle strength in healthy women using a hand-held dynamometer and the association with age and anthropometric variables. *Healthcare (Basel)* (2023) 11(16):2278. doi: 10.3390/healthcare11162278

52. Panjabi MM, Lydon C, Vasavada A, Grob D, Crisco JJ 3rd, Dvorak J. On the understanding of clinical instability. *Spine (Phila Pa 1976).* (1994) 19(23):2642–50. doi: 10.1097/00007632-199412000-00008

53. Suvarnnato T, Puntumetakul R, Uthaikhup S, Boucaut R. Effect of specific deep cervical muscle exercises on functional disability, pain intensity, craniovertebral angle, and neck-muscle strength in chronic mechanical neck pain: a randomized controlled trial. *J Pain Res* (2019) 12:915–25. doi: 10.2147/JPR.S190125

54. Jull GA, Falla D, Vicenzino B, Hodges PW. The effect of therapeutic exercise on activation of the deep cervical flexor muscles in people with chronic neck pain. *Man Ther* (2009) 14(6):696–701. doi: 10.1016/j.math.2009.05.004

55. Moon H, Lee SK, Kim WM, Seo YG. Effects of exercise on cervical muscle strength and cross-sectional area in patients with thoracic hyperkyphosis and chronic cervical pain. *Sci Rep* (2021) 11(1):3827. doi: 10.1038/s41598-021-83344-4

56. Lin IH, Chang KH, Liou TH, Tsou CM, Huang YC. Progressive shoulder-neck exercise on cervical muscle functions in middle-aged and senior patients with chronic neck pain. *Eur J Phys Rehabil Med* (2018) 54(1):13–21. doi: 10.23736/S1973-9087.17.04658-5

57. Frasch M. Dedifferentiation, redifferentiation, and transdifferentiation of striated muscles during regeneration and development. *Curr Top Dev Biol* (2016) 106:331–55. doi: 10.1016/bs.ctdb.2015.12.005

58. Jiang J, Zhou P, Ling H, Xu Z, Yi B, Zhu S. MiR-499/PRDM16 axis modulates the adipogenic differentiation of mouse skeletal muscle satellite cells. *Hum Cell* (2018) 31:282–91. doi: 10.1007/s13577-018-0210-5

59. Buckingham M. Gene regulatory networks and cell lineages that underlie the formation of skeletal muscle. *Proc Natl Acad Sci USA* (2017) 114:5831–7. doi: 10.1073/pnas.1610605114

60. Aguiari P, Leo S, Zavan B, Vindigni V, Rimessi A, Bianchi K, et al. High glucose induces adipogenic differentiation of muscle-derived stem cells. *Proc Natl Acad Sci USA* (2008) 105:1226–31. doi: 10.1073/pnas.0711402105

61. Kook SH, Choi KC, Son YO, Lee KY, Hwang IH, Lee HJ, et al. Satellite cells isolated from adult hanwoo muscle can proliferate and differentiate into myoblasts and adipose-like cells. *Mol Cells* (2006) 22:239–45.

62. Atit R, Sgaier SK, Mohamed OA, Taketo MM, Dufort D, Joyner AL, et al. Beta-catenin activation is necessary and sufficient to specify the dorsal dermal fate in the mouse. *Dev Biol* (2006) 296:164–76. doi: 10.1016/j.ydbio.2006.04.449

63. Wang H, Li X, Gao S, Sun X, Fang H. Transdifferentiation via transcription factors or microRNAs: Current status and perspective. *Differentiation* (2015) 90:69–76. doi: 10.1016/j.diff.2015.10.002

64. Qi R, Long D, Wang J, Wang Q, Huang X, Cao C, et al. MicroRNA-199a targets the fatty acid transport protein 1 gene and inhibits the adipogenic trans-differentiation of C2C12 myoblasts. *Cell Physiol Biochem* (2016) 39:1087–97. doi: 10.1159/000447817

65. Yi F, Zhang P, Wang Y, Xu Y, Zhang Z, Ma W, et al. Long non-coding RNA slincRAD functions in methylation regulation during the early stage of mouse adipogenesis. *RNA Biol* (2019) 19:1–13. doi: 10.1080/15476286.2019.1631643

66. Qi R, Qiu X, Zhang Y, Wang J, Wang Q, Wu M, et al. Comparison of lncRNA expression profiles during myogenic differentiation and adipogenic transdifferentiation of myoblasts. *Int J Mol Sci* (2019) 20(15):3725. doi: 10.3390/ijms20153725

frontiers | Frontiers in Endocrinology

TYPE Original Research
PUBLISHED 04 January 2024
DOI 10.3389/fendo.2023.1279493

OPEN ACCESS

EDITED BY
Kenju Shimomura,
Fukushima Medical University, Japan

REVIEWED BY
Cipta Pramana,
K.R.M.T. Wongsonegoro Hospital, Indonesia
Alan Decherney,
Clinical Center (NIH), United States

*CORRESPONDENCE
Zhiyong Yang
109872931@qq.com

RECEIVED 18 August 2023
ACCEPTED 06 December 2023
PUBLISHED 04 January 2024

CITATION
Su Q and Yang Z (2024) Age at first birth, age at menopause, and risk of ovarian cyst: a two-sample Mendelian randomization study. *Front. Endocrinol.* 14:1279493. doi: 10.3389/fendo.2023.1279493

Age at first birth, age at menopause, and risk of ovarian cyst: a two-sample Mendelian randomization study

Qian Su and Zhiyong Yang*

Clinical Medical College and Affiliated Hospital of Chengdu University, Chengdu University, Chengdu, China

Background: Increasing observational studies have indicated that hormonal reproductive factors were associated with ovarian cyst, a common gynecological disease. A two-sample Mendelian randomization (MR) was carried out by investigating the causality of reproductive factors including age at first birth (AFB), age at natural menopause (ANM), and age at menarche (AAM), and the risk of ovarian cyst (OC).

Method: Summary statistics were collected from a large genome-wide association study (GWAS), and we used a two-sample MR study to clarify the causal association between the exposure of AFB (N = 542,901), ANM (N = 69,360), and AAM (N = 29,346) and the outcome of the OC (N_{case} = 20,750, $N_{control}$ = 107,564). We separately selected 51, 35, and 6 single-nucleotide polymorphisms (SNPs) as instrumental variables (IVs) for assaying the influence of AFB, ANM, and AAM on OC, respectively. Then, the causal relationship was tested through multiple approaches including an inverse-variance weighted method, an MR-Egger regression, and a weighted median method. In addition, the MR-PRESSO method was also used to verify the horizontal pleiotropy. Subsequently, we adjust the confounders for MR design.

Results: The MR analysis results showed that AFB was negatively associated with the OC (IVW Beta: −0.09, OR: 0.91, 95% CI: 0.86–0.96, p = 0.00185), and the greater AAM decreased the risk of OC (IVW Beta: −0.10, OR: 0.91, 95% CI: 0.82–0.99, p = 0.0376). However, ANM has a positive correlation with the OC (IVW Beta: 0.05, OR: 1.05, 95% CI: 1.03–1.08, $p = 8.38 \times 10^{-6}$). After adjusting BMI, alcohol intake frequency, and ever smoked, we also obtained a negative relationship between AFB and OC ($p < 0.005$). Meanwhile, we adjusted weight, alcohol intake frequency, and height, and then found a causal relationship between older AMN and an increased risk of OC ($p < 0.005$).

Conclusion: A causal effect of reproductive factors on the development of OC, affected by AFB, ANM, and AAM, was found convincingly. After adjusting the confounders, we also successfully found the substantial causal effect of younger AFB, younger AAM, and older ANM on an increased risk of OC.

KEYWORDS

Mendelian randomization, ovarian cyst, age at first birth, age at natural menopause, genetic epidemiology

1 Introduction

Ovarian cysts (OCs) showed a high incidence of 21.2% among healthy postmenopausal women in Europe, which affect approximately 7% of women at some point around the world (1). As a result of ovulation, a fluid-filled sac known as an OC can form on one or both ovaries. It is not common to find adnexal masses or OCs in women, and approximately 20% of women developed at least one pelvic mass in their lifetime (2). The sample OC could be found by ultrasound, and the sample OC was fairly common and appear stable in a majority of postmenopausal women with no intervention measure (1). Nevertheless, multiple complications such as blood loss, cyst rupture, and pelvic pain could occur during the development of OC (2). In early studies, researchers found that a greater age at first birth (AFB) was the main risk factor associated with serous or mucinous OCs (3). Observational research identified the association between hormonal reproductive factors (such as AFB) and OC (4). Therefore, it will be of great use to test the causal effect between hormonal reproductive factors and OC.

AFB poses a substantial impact on health and evolutionary fitness. Pregnancy is an important factor that affected the future health status of women. Significant alterations in endocrine hormone profiles, endocrine gland morphology on imaging, and serum and urine electrolytes may occur due to the physiological changes in pregnancy (5). During pregnancy, estradiol levels, levels of progesterone and 17-hydroxyprogesterone, and testosterone levels progressively rise, while follicle-stimulating hormone and luteinizing hormone (LH) levels are low (5). Therefore, the changes in hormone level may affect the formation of OC. In addition, several studies have investigated the reproductive factors of AFB and the risk of disease. For example, Luo's group found that older AFB is associated with an increased risk of pancreatic cancer in women through a meta-analysis (6). Yang's group analyzed NHANES data, providing evidence that women with younger AFB have higher odds of non-alcoholic fatty liver disease in later life (7). Li's group carried out a meta-analysis to evaluate the melanoma risk correlated with AFB (8). However, researchers hardly focused on the AFB and the risk of OC.

Age at natural menopause (ANM) has implications for women's quality of life and health. Menopause causes changes in hormone levels, leading to some impact on women's lives. Specifically, with the decreasing estrogen, women have a higher risk of suffering from some illness such as osteoporosis. On the basis of the related research, during menopause transition, some sex hormones showed large fluctuations, such as sex hormone-binding globulin (SHBG) and bio-available testosterone, which may also be involved in menopause-related diseases (9). Later ANM was associated with higher bone mineral density, a longer life expectancy and lower risk of fracture, cardiovascular disease (CVD), all-cause mortality, and cardiovascular death, yet with greater breast and ovarian cancer risk (10). The increasing evidence supporting age at menopause onset as a marker of overall health calls for worldwide attention. Michael's cohort study included 144,260 postmenopausal women and found that menopause (before age 40 years) increased the risk for cardiovascular diseases (11). A Mendelian randomization (MR) also found the causal effect relationship between ANM and the risk of breast cancer (12). However, the real relationship between ANM and OC remains unclear.

Here, we conducted an MR to provide a reliable estimation between the reproductive factors (AFB, ANM, and AAM) and an outcome of OC. An MR study applied single-nucleotide polymorphisms (SNPs) as instrumental variables (IVs), which were from the genome-wide association study (GWAS) (13, 14). IV–exposure associations were extracted from the largest GWAS(s) accomplished in AFB (N = 542,901), AMN (N = 69,360), and AAM (N = 29,346) (15, 16), and the data source is shown in Supplementary Table S1. IV–outcome associations were extracted from a large GWAS accomplished in OC (N_{OC} = 20,750, $N_{control}$ = 107,564).

2 Methods

2.1 Study design

We carried out the two-sample MR analysis with the flow-process diagrams shown in Figure 1. To clarify the MR analysis, we should follow three important assumptions (13). Assumption 1 states that the IVs of SNPs should be strongly related to exposure ($p < 5 \times 10^{-8}$). Assumption 2 required the IVs to be irrelevant to any confounders and we should remove the SNPs associated with the

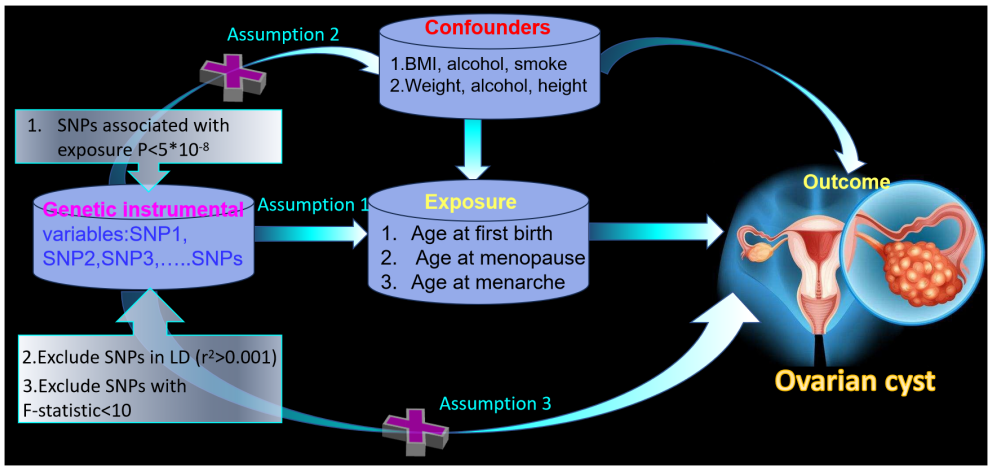

FIGURE 1
The framework of the two-sample Mendelian randomization study between age at first birth, age at menopause, age at menarche, and ovarian cyst.

outcome. Next, the IVs have an impact on the outcome only through the exposure in Assumption 3. Additionally, all SNPs possessed the *F*-statistic larger than 10 to confirm a robust IV. We decreased the population stratification by including only European ancestry.

2.2 Equation data sources

2.2.1 GWAS summary statistics of AFB and ANM

The genetic architecture of AFB has been collected by a GWAS of 542,901 individuals (n = 124,088 male individuals; n = 418,758 female individuals) from 36 studies; the age of AFB individuals ranged from those born before 1941 (0.60) to those born after 1960 (0.31). In addition, the GWAS was restricted to individuals of European ancestry who passed quality control, and the researcher found that polycystic ovarian syndrome may cause AFB later, which is associated with infertility (15). Individuals were eligible for inclusion in analyses if they met the following conditions: (a) have given birth to a child (parous), (b) all relevant covariates (year of birth) were available for the individual, (c) were successful genotypes genome-wide (recommended >95%), (d) passed the cohort-specific standard quality controls, and (e) were of European ancestry. The genetic architecture of ANM was obtained by a GWAS of up to 69,360 women of European ancestry, which identified the enrichment of signals in/near genes involved in delayed puberty and discovered the first molecular links between the onset and the end of reproductive lifespan (16). The research (16) included women with ANM who were 40–60 years of age, excluding those with menopause induced by hysterectomy, bilateral ovariectomy, radiation, or chemotherapy and those using hormone replacement therapy (HRT) before menopause. For AFB, ANM, AAM, BMI, alcohol intake frequency, ever smoked, and height, the GWAS data were from the publicly available IEU Open GWAS Project database (https://gwas.mrcieu.ac.uk/), and the detailed information is shown in Supplementary Table S1.

2.2.2 GWAS summary statistic of OC

GWAS summary statistics for OC were obtained from FinnGen consortium R9 release data (17). The GWAS included 128,314 Finnish adult female subjects and consisted of 20,750 cases and 107,564 controls.

2.3 Ethical approval

This MR study was conducted by virtue of publicly published studies or shared datasets, and the datasets had obtained ethical approval and informed consent. We did not have to make any additional ethics statement or consent.

2.4 Instrumental variable selection

Our independent IV was defined as follows: met the genome-wide significance threshold of $p < 5 \times 10^{-8}$, all of which was under the limited value ($r^2 < 0.001$ within a clumping window of 10,000 kb) in linkage disequilibrium (LD) analysis (18). Our analysis removed the palindromic SNPs, which was regardless of allele frequency (18). In addition, IVs were included only when they existed in the GWAS summary statistics of outcome, and our analysis did not include the proxy SNPs (19, 20). *F*-statistics ($F = \text{Beta}^2/\text{SE}^2$) were used to evaluate the power of each SNP (21). Eventually, all the SNPs were equipped with stronger statistical power (*F*-statistics > 10).

In this MR study, 51 SNPs for AFB and 35 SNPs for ANM were extracted from the GWAS summary statistics with the outcome of OC. The *F*-statistics of the above SNPs were in the range of 532.08–3,770.81, 349.41–8,923.43, and 30.25–119.80, respectively, for AFB, ANM, and AAM, showing the strong validity of the selected SNPs. Detailed information of all selected SNPs of AFB, ANM, and AAM can be found in Supplementary Tables S1-S5.

2.5 Mendelian randomization estimates

Several approaches were utilized to conduct the MR analysis, including an inverse-variance weighted approach (IVW), an MR-Egger regression, a weighted median approach, a weighted mode, and the MR-PRESSO method.

We applied the IVW method as the primary method for two-sample MR tests. The important condition for IVW estimates is that all instrumental variants are valid, while the weak IVs tend to underestimate the true variation (22). MR-Egger, MR-PRESSO, and the weight median were mutually complementary and estimated the horizontal pleiotropy (23). The MR-Egger approach provided a valid estimation of the null causal hypothesis and the causal effect fit well even with the invalid IVs. The weighted median method was identified as more robust to test the horizontal pleiotropy (24). When 50% of genetic variants were considered to be invalid, this method was robust to outliers and gave unanimous estimation (23). MR-PRESSO was used to evaluate the horizontal pleiotropy through three of its components: the global test, the outlier test, and the distortion test (25). Additionally, the weight mode method could test the causal effect of the subset with the largest number of SNPs by clustering the SNPs into subsets resting on the resemblance of causal effects (25).

Subsequently, for assaying the heterogeneity and pleiotropy, we applied leave-one-out sensitivity analysis, the MR-Egger intercept test, and Cochran's *Q* statistic (24). Then, we removed the confounders to analyze the direct effect of exposure on outcome. As for the causal effect of AFB and OC, we adjusted the BMI, alcohol intake frequency, and ever smoked. Investigating the causal effect of ANM and OC, we adjusted the weight, alcohol intake frequency, and height.

All analyses were performed using the TwoSampleMR (version 0.5.7), Mendelian Randomization (version 0.8.0), and MRPRESSO package (1.0) in R Software 4.3.1 (https://www.R-project.org). In addition, the *p*-value was less than 0.05 for statistical significance.

3 Results

3.1 Causal association of AFB on OC through two-sample MR

As shown in Table 1, there was convincing evidence to support a causal effect between the two hormone-related exposure and the risk of OC. In the main IVW analysis, per-year increase in AFB was associated with 0.09 standard deviation decrease in the risk of OC (OR = 0.91, 95% CI = 0.86–0.96, $p = 0.00185$). The test results kept significant by the other two methods ($OR_{\text{per-SD increment in AFB}}$ [95% CI] for weighted median 0.92 [0.85–0.99] and for MR-PRESSO 0.91 [0.86–0.97]). Meanwhile, the MR-Egger regression and weighted mode results were not significant. There seemed to be no apparent sign of pleiotropy (*p*-value of MR-Egger intercept = 0.362). In addition, MR-PRESSO estimation did not observe any outlier SNPs. Next, as depicted in Figure 2A, none of the SNPs crossed the zero line in the leave-one-out sensitivity analysis, which proved the non-heterogeneity of our study. Additionally, the MR-PRESSO global test has a *p*-value of 0.057, showing little pleiotropy.

As modifiable risk factors of OC, obesity (BMI), alcohol intake frequency, and ever smoked may play a significant role in the etiology of OC. Adjusting the effect of confounders including BMI, alcohol intake frequency, and ever smoked, we also found the causal effect between AFB and OC ($p < 0.005$) (Figure 3; Supplementary Table S4). Moreover, we found that alcohol intake frequency and ever smoked played an unimportant role in the etiology of OC through the two-sample MR analysis. Meanwhile, the obesity with higher BMI increased the risk of OC (Beta: 0.106, $p = 0.005$) by our MR test (Supplementary Table S4).

3.2 Causal association of ANM on OC through two-sample MR

Similarly, we have found convincing evidence to support the causal relationship of genetically instrumented ANM with OC. As shown in Table 1, per-year increase in ANM was related to a 0.05 standard deviation risk increase of OC (OR = 1.05, 95% CI = 1.03–1.08, $p = 8 \times 10^{-6}$). Meanwhile, the detection results remained consistent using different methods ($OR_{\text{per-SD increment in ANM}}$ [95% CI] was 1.08 [1.01–1.14] for MR-Egger regression, 1.06 [1.02–1.09] for weighted median, 1.06 [1.01–1.11] for weighted mode, and 1.05 [1.03–1.08] for MR-PRESSO). We did not identify any leverage points with a high influence in the leave-one-out sensitivity analysis (Figure 2B). Cochran's *Q* statistic illustrated no heterogeneity among SNPs of OC. As a supplement to the MR-Egger analysis, the MR-PRESSO global test with a *p* of 0.396 and no outlier SNPs demonstrated no directional pleiotropy.

Then, an IVW-based multivariable MR (mvMR) was conducted to test the direct effect of ANM on OC accounting for the confounding effect from weight, height, and ever smoked. The results of mvMR remained consistent with our primary findings ($p < 0.005$) (Figure 3; Supplementary Table S4). In addition, to estimate the weight and height using mvMR, we found that genetically predicted weight showed little influence on the risk of OC (OR = 1.00, 95% CI = 1.00–1.01, $p = 0.407$), so did weight (OR = 1.03, 95% CI = 0.95–1.11, $p = 0.495$).

3.3 Causal association of AAM on OC through two-sample MR

Meanwhile, for genetically predicted AAM, we only observed significant association with OC using IVW (OR = 0.91, 95% CI = 0.82–0.99, $p = 0.037648$) (Table 1), while MR-Egger regression ($OR_{\text{per-SD increment in AAM}}$ [95% CI], 0.96 [0.61–1.52]), weighted median approach ($OR_{\text{per-SD increment in AAM}}$ [95% CI], 0.93 [0.83–1.05]), and weighted mode ($OR_{\text{per-SD increment in AAM}}$ [95% CI], 0.95 [0.82–1.10]) remained non-significant. In addition, no heterogeneity and directional pleiotropy were found from the MR-Egger and MR-PRESSO test. Moreover, there are no confounding effect using the PhenoScanner method.

TABLE 1 Results of causal associations between age at first birth, age at menopause, age at menarche and ovarian cyst.

Exposure	Outcome	Method	No. of SNPs	Beta	SE	OR (95% CI)	*p*	Q stastistic	*p*-heterogeneity	*p*-intercept
Age at first birth	Ovarian cyst	Inverse variance weighted	51	-0.09	0.03	0.91 (0.86-0.96)	0.001854			
		MR Egger	51	-0.20	0.12	0.82 (0.64-1.04)	0.101932	65.64	0.056	0.362
		Weighted median	51	-0.09	0.04	0.92 (0.85-0.99)	0.032656			
		Weighted mode	51	-0.07	0.09	0.93 (0.77-1.12)	0.459661			
		MR Presso	51	-0.09	0.03	0.91 (0.86-0.97)	0.003064			0.057
Age at menopau se	Ovarian cyst	Inverse variance weighted	35	0.05	0.01	1.05 (1.03-1.08)	0.000008			
		MR Egger	35	0.07	0.03	1.08 (1.01-1.14)	0.021477	35.48	0.352	0.043
		Weighted median	35	0.06	0.02	1.06 (1.02-1.09)	0.000468			
		Weighted mode	35	0.06	0.02	1.06 (1.01-1.11)	0.022650			
		MR Presso	35	0.05	0.01	1.05 (1.03-1.08)	0.000086			0.396
Age at menarche	Ovarian cyst	Inverse variance weighted	6	-0.10	0.05	0.91 (0.82-0.99)	0.037648			
		MR Egger	6	-0.04	0.23	0.96 (0.61-1.52)	0.879696	4.19	0.381	0.798
		Weighted median	6	-0.07	0.06	0.93 (0.83-1.05)	0.252069			
		Weighted mode	6	-0.05	0.08	0.95 (0.82-1.10)	0.550588			
		MR Presso	6	-0.10	0.04	0.91 (0.83-0.99)	0.074255			0.578

4 Discussion

In this work, we tested a putative causal relationship between three hormonal reproductive traits (AFB, ANM, and AAM) and OC influencing many women for the first time, making use of SNPs of strong IVs related to exposure (*F*-statistics: 921.51 for AFB, 1,148.44 for ANM, and 56.32 for AAM). We have found reliable evidence to demonstrate the causal effects of AFB, ANM, and AAM on OC using the two-sample MR analysis. Specifically, we genetically predicted that delayed AFB and AAM were associated with a decreased risk of OC, and similarly, we genetically predicted that younger ANM was related to a lower risk of OC. Therefore, a shorter reproductive period is associated with a lower risk of OC. After adjusting the effect of confounders including obesity (BMI), alcohol intake frequency, and ever smoked for AFB and weight, height, and ever smoked for ANM, a consistent causal effect was identified through the mvMR, proving the robustness of our findings.

When considering clinical significance, it is important to assess the magnitude of the effect and its practical implications in a real-world setting. While confidence intervals of approximately 1 indicate uncertainty, it does not necessarily mean that the results are not clinically significant. To determine clinical significance, it would be helpful to have more information on the OC, the large number of population being studied, and the causal determination of risk factors at the genetic level. Additionally, the interpretation of clinical significance may change depending on the field of study and the specific outcome being assessed.

Previous studies have found that there may be a relationship between AFB and ovarian cancer, and late AFB was associated with increased risk (26). Conversely, researchers summarized the AFB with risk of cancer and found that younger age (typically defined as

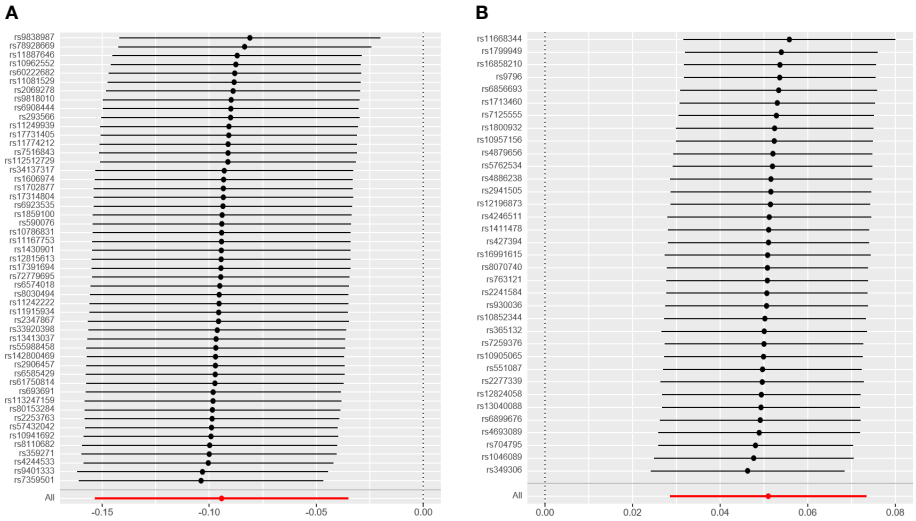

FIGURE 2
The leave-one-out analysis plot. **(A)** Leave-one-out plot for age at first birth and ovarian cyst. **(B)** Leave-one-out plot for age at menopause and ovarian cyst.

19 years or younger) at first birth is associated with an increased risk of cervical and endometrial cancers (27). Therefore, hormonal exposure of AFB has a strong correlation with ovarian disease due to certain reasons. First, reproductive factors such as AFB were very complicated and influenced more by environmental factors than by genetic factors. Second, estimates from previous epidemiologic studies are affected by confounders. For instance, smoking is one of the risk factors that have been considered for functional OCs, and a case–control study identified that the increase in BMI may reduce the adverse effect of smoking on the risk of functional OC (28). Thus, it is of vital importance to control the confounding factors in epidemiologic research. In our mvMR, we have controlled the effect of BMI, the alcohol intake frequency, and ever smoked, and we also obtained positive results after removing the confounders. Moreover, we tested the causal effect of confounders and outcome, showing a positive result for BMI with hundreds of IVs (Supplementary Table S4). Further investigations were needed to identify the causal relationship between BMI and OC.

As we all know, menopause was accompanied by the variation in hormone level, leading to many diseases in women. However, the biological mechanisms of hormonal factors on the influence of OC

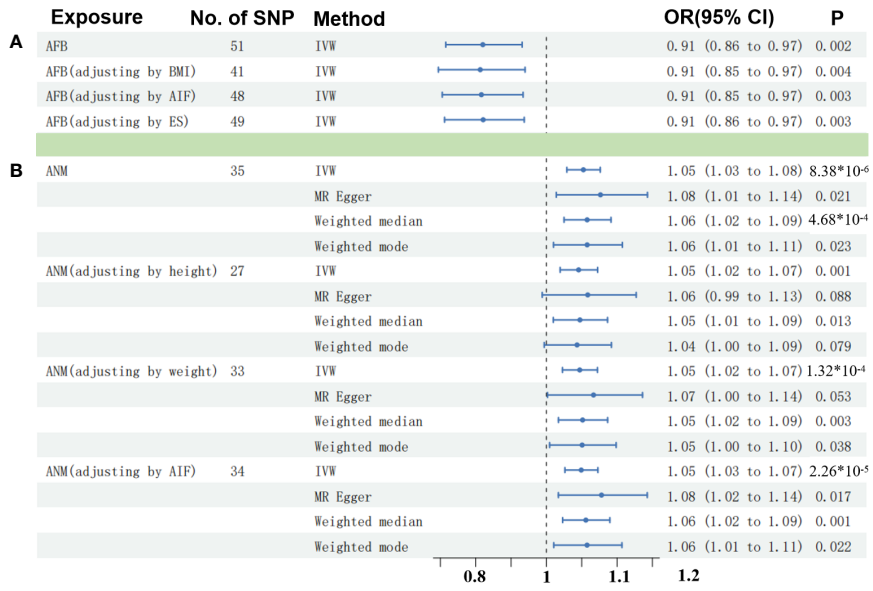

FIGURE 3
Comparisons of Mendelian randomization results. **(A)** Comparisons of Mendelian randomization results for AFB on OC. **(B)** Comparisons of Mendelian randomization results for ANM on OC. OC, ovarian cyst; AFB, age at first birth; ANM, age at natural menopause; BMI, body mass index; AIF, alcohol intake frequency; EK, ever smoked.

remain obscure. Recently, experimental research showed that the insufficient LH surge, intrafollicular changes in gonadotrophin receptors, and growth factors are the potential reasons leading to hormonally active OCs (4). During perimenopause, the hypothalamic arcuate nucleus and paraventricular nucleus are induced to pulse the secretion of gonadotropin-releasing hormone into the portal circulation due to the decrease in estrogen level, causing an increase in LH. Hence, older age of natural menopause may influence the LH level, thus leading to the elevated risk of OC.

As for the advantages of this study, an MR analysis was conducted to evaluate the causal effect between the reproductive factors and OC. Three distinct reproductive factors (AFB, ANM, and AAM) were incorporated to reflect the length of the reproductive period. The results clarified that prolonged exposure to estrogens as a consequence of a delayed menopause and early menarche increases the risk of the hormone-dependent disease of OC. Moreover, we performed a bidirectional two-sample MR analysis to avoid reverse causality, and the negative results were obtained as shown in Supplementary Table S4. Potential confounders such as BMI and ever smoked were also adjusted by mvMR, which makes the results more reliable and robust compared with observational studies.

As for the limitations of our study, at first, the number of our genetic instruments (SNPs) was less than 100, and further verification was needed to enhance the results. Second, participants of European ancestry were included in our MR analysis, which influenced our results' external validity to other ancestry groups. Third, our research was performed using the overall OC rather than distinguishing disease subtypes including functional cysts, endometriotic cysts/blood cysts, dermoid cysts, serous cysts, and mucinous cysts. AFB and ANM may have a different effect on the various subsets of OC. Fourth, the MR-PRESSO GLOBAL test results of AFB showed minimal pleiotropy, while another effective method, the MR-Egger test, served as a supplement to show no directional pleiotropy (29). Furthermore, other social factors such as education and financial state may also confound our results without consideration of our MR analysis. Therefore, further studies should investigate the variety of subsets and adjust the social factors.

5 Conclusion

In summary, our findings demonstrated that reproductive factors (AAM, AFB, and ANM) play an important role in the risk of OC. Further research such as clinical trials and observational studies is needed to learn more about the relevant mechanisms.

Data availability statement

The datasets presented in this study can be found in online repositories. The names of the repository/repositories and accession number(s) can be found in the article/Supplementary Material.

Ethics statement

Ethical approval was not required for the study involving humans in accordance with the local legislation and institutional requirements. Written informed consent to participate in this study was not required from the participants or the participants' legal guardians/next of kin in accordance with the national legislation and the institutional requirements.

Author contributions

QS: Conceptualization, Data curation, Investigation, Software, Writing – original draft, Writing – review & editing. ZY: Formal Analysis, Methodology, Supervision, Validation, Data curation, Writing – review & editing.

Funding

The author(s) declare financial support was received for the research, authorship, and/or publication of this article. This work was supported by scientific research projects of Clinical Medical College and Affiliated Hospital of Chengdu University (Y202229) and Medical Research Project of Chengdu (2021080).

Acknowledgments

We want to acknowledge the participants and investigators of the UK Biobank and FinnGen study.

Conflict of interest

The authors declare that the research was conducted in the absence of any commercial or financial relationships that could be construed as a potential conflict of interest.

Publisher's note

Supplementary material

The Supplementary Material for this article can be found online at: https://www.frontiersin.org/articles/10.3389/fendo.2023.1279493/full#supplementary-material

References

1. Farghaly SA. Current diagnosis and management of ovarian cysts. *Clin Exp Obstet Gynecol.* (2014) 41:609–12. doi: 10.12891/ceog20322014

2. Mobeen S, Apostol R. Ovarian cyst. *StatPearls* (2023). Treasure Island (FL): StatPearls Publishing.

3. Parazzini F, La Vecchia C, Franceschi S, Negri E, Cecchetti G. Risk factors for endometrioid, mucinous and serous benign ovarian cysts. *Int J Epidemiol.* (1989) 18:108–12. doi: 10.1093/ije/18.1.108

4. Sasidharan JK, Patra MK, Singh LK, Saxena AC, De UK, Singh V, et al. Ovarian cysts in the bitch: an update. *Top Companion Anim Med* (2021) 43:100511. doi: 10.1016/j.tcam.2021.100511

5. Morton A, Teasdale S. Physiological changes in pregnancy and their influence on the endocrine investigation. *Clin Endocrinol (Oxf).* (2022) 96:3–11. doi: 10.1111/cen.14624

6. Luo AJ, Feng RH, Wang XW, Wang FZ. Older age at first birth is a risk factor for pancreatic cancer: a meta-analysis. *Hepatobiliary Pancreat Dis Int* (2016) 15:125–30. doi: 10.1016/s1499-3872(16)60063-2

7. Yang HH, Chen GC, Zhou MG, Xie LF, Jin YY, Chen HT, et al. Association of age at first birth and risk of non-alcoholic fatty liver disease in women: evidence from the NHANES. *Hepatol Int* (2023) 17:303–12. doi: 10.1007/s12072-022-10429-1

8. Li Z, Gu M, Cen Y. Age at first birth and melanoma risk: a meta-analysis. *Int J Clin Exp Med* (2014) 7:5201–9.

9. Zhang X, Huangfu Z, Wang S. Review of mendelian randomization studies on age at natural menopause. *Front Endocrinol* (2023) 14:1234324. doi: 10.3389/fendo.2023.1234324

10. El Khoudary SR. Age at menopause onset and risk of cardiovascular disease around the world. *Maturitas* (2020) 141:33–8. doi: 10.1016/j.maturitas.2020.06.007

11. Honigberg MC, Zekavat SM, Aragam K, Finneran P, Klarin D, Bhatt DL, et al. Association of premature natural and surgical menopause with incident cardiovascular disease. *JAMA* (2019) 322:2411–21. doi: 10.1001/jama.2019.19191

12. Magnus MC, Borges MC, Fraser A, Lawlor DA. Identifying potential causal effects of age at menopause: a Mendelian randomization phenome-wide association study. *Eur J Epidemiol.* (2022) 37:971–82. doi: 10.1007/s10654-022-00903-3

13. Zhang N, Liao Y, Zhao H, Chen T, Jia F, Yu Y, et al. Polycystic ovary syndrome and 25-hydroxyvitamin D: A bidirectional two-sample Mendelian randomization study. *Front Endocrinol (Lausanne).* (2023) 14:1110341. doi: 10.3389/fendo.2023.1110341

14. Zhu J, Niu Z, Alfredsson L, Klareskog L, Padyukov L, Jiang X. Age at menarche, age at natural menopause, and risk of rheumatoid arthritis - a Mendelian randomization study. *Arthritis Res Ther* (2021) 23:108. doi: 10.1186/s13075-021-02495-x

15. Mills MC, Tropf FC, Brazel DM, van Zuydam N, Vaez AeQTLGen Consortium, et al. Identification of 371 genetic variants for age at first sex and birth linked to externalising behaviour. *Nat Hum Behav* (2021) 5:1717–30. doi: 10.1038/s41562-021-01135-3

16. Day FR, Ruth KS, Thompson DJ, Lunetta KL, Pervjakova N, Chasman DI, et al. Large-scale genomic analyses link reproductive aging to hypothalamic signaling, breast cancer susceptibility and BRCA1-mediated DNA repair. *Nat Genet* (2015) 47:1294–303. doi: 10.1038/ng.3412

17. Kurki MI, Karjalainen J, Palta P, Sipilä TP, Kristiansson K, Donner KM, et al. FinnGen provides genetic insights from a well-phenotyped isolated population. *Nature* (2023) 613:508–18. doi: 10.1038/s41586-022-05473-8

18. Hemani G, Zheng J, Elsworth B, Wade KH, Haberland V, Baird D, et al. The MR-Base platform supports systematic causal inference across the human phenome. *Elife* (2018) 7:e34408. doi: 10.7554/eLife.34408

19. Gill D, Karhunen V, Malik R, Dichgans M, Sofat N. Cardiometabolic traits mediating the effect of education on osteoarthritis risk: A mendelian randomization study. *Osteoarthritis Cartilage.* (2021) 29:365–71. doi: 10.1016/j.joca.2020.12.015

20. Yoshikawa M, Asaba K. Educational attainment decreases the risk of COVID-19 severity in the European population: A two-sample mendelian randomization study. *Front Public Health* (2021) 9:673451. doi: 10.3389/fpubh.2021.673451

21. Huang W, Xiao J, Ji J, Chen L. Association of lipid-lowering drugs with COVID-19 outcomes from a Mendelian randomization study. *Elife* (2021) 10:e73873. doi: 10.7554/eLife.73873

22. Burgess S, Davey Smith G, Davies NM, Dudbridge F, Gill D, Glymour MM, et al. Guidelines for performing Mendelian randomization investigations: update for summer 2023. *Wellcome Open Res* (2023) 4:186. doi: 10.12688/wellcomeopenres.15555.3

23. Verbanck M, Chen CY, Neale B, Do R. Detection of widespread horizontal pleiotropy in causal relationships inferred from mendelian randomization between complex traits and diseases. *Nat Genet* (2018) 50:693–8. doi: 10.1038/s41588-018-0099-7

24. Bowden J, Davey Smith G, Burgess S. Mendelian randomization with invalid instruments: effect estimation and bias detection through egger regression. *Int J Epidemiol.* (2015) 44:512–25. doi: 10.1093/ije/dyv080

25. Yin KJ, Huang JX, Wang P, Yang XK, Tao SS, Li HM, et al. No genetic causal association between periodontitis and arthritis: A bidirectional two-sample mendelian randomization analysis. *Front Immunol* (2022) 13:808832. doi: 10.3389/fimmu.2022.808832

26. La Vecchia C, Decarli A, Franceschi S, Regallo M, Tognoni G. Age at first birth and the risk of epithelial ovarian cancer. *J Natl Cancer Inst* (1984) 73:663–6.

27. Merrill RM, Fugal S, Novilla LB, Raphael MC. Cancer risk associated with early and late maternal age at first birth. *Gynecol Oncol* (2005) 96:583–93. doi: 10.1016/j.ygyno.2004.11.038

28. Holt VL, Cushing-Haugen KL, Daling JR. Risk of functional ovarian cyst: effects of smoking and marijuana use according to body mass index. *Am J Epidemiol.* (2005) 161:520–5. doi: 10.1093/aje/kwi080

29. Burgess S, Thompson SG. Interpreting findings from Mendelian randomization using the MR-Egger method. *Eur J Epidemiol.* (2017) 32:377–89. doi: 10.1007/s10654-017-0255-x

frontiers | Frontiers in Endocrinology

TYPE Original Research
PUBLISHED 31 January 2024
DOI 10.3389/fendo.2023.1331739

OPEN ACCESS

EDITED BY
Kenju Shimomura,
Fukushima Medical University, Japan

REVIEWED BY
Lubia Velázquez López,
Instituto Mexicano del Seguro Social, Mexico
Shun Matsuura,
Fujieda Municipal General Hospital, Japan

*CORRESPONDENCE
Lin Zhang
yaoran2008@163.com

RECEIVED 01 November 2023
ACCEPTED 26 December 2023
PUBLISHED 31 January 2024

CITATION
Wang Y, Zhang X, Li Y, Gui J, Mei Y, Yang X, Liu H, Guo L-l, Li J, Lei Y, Li X, Sun L, Yang L, Yuan T, Wang C, Zhang D, Li J, Liu M, Hua Y and Zhang L (2024) Obesity- and lipid-related indices as a predictor of type 2 diabetes in a national cohort study.
Front. Endocrinol. 14:1331739.
doi: 10.3389/fendo.2023.1331739

Obesity- and lipid-related indices as a predictor of type 2 diabetes in a national cohort study

Ying Wang[1], Xiaoyun Zhang[1], Yuqing Li[1], Jiaofeng Gui[1], Yujin Mei[1], Xue Yang[1], Haiyang Liu[2], Lei-lei Guo[3], Jinlong Li[4], Yunxiao Lei[5], Xiaoping Li[6], Lu Sun[6], Liu Yang[7], Ting Yuan[5], Congzhi Wang[7], Dongmei Zhang[8], Jing Li[9], Mingming Liu[9], Ying Hua[10] and Lin Zhang[7]*

[1]Department of Graduate School, Wannan Medical College, Wuhu, An Hui, China, [2]Student Health Center, Wannan Medical College, Wuhu, An Hui, China, [3]Department of Surgical Nursing, School of Nursing, Jinzhou Medical University, Linghe District, Jinzhou, Liaoning, China, [4]Department of Occupational and Environmental Health, Key Laboratory of Occupational Health and Safety for Coal Industry in Hebei Province, School of Public Health, North China University of Science and Technology, Tangshan, Hebei, China, [5]Obstetrics and Gynecology Nursing, School of Nursing, Wannan Medical College, Wuhu, An Hui, China, [6]Department of Emergency and Critical Care Nursing, School of Nursing, Wannan Medical College, Wuhu, An Hui, China, [7]Department of Internal Medicine Nursing, School of Nursing, Wannan Medical College, Wuhu, An Hui, China, [8]Department of Pediatric Nursing, School of Nursing, Wannan Medical College, Wuhu, An Hui, China, [9]Department of Surgical Nursing, School of Nursing, Wannan Medical College, 22 Wenchang West Road, Higher Education Park, Wuhu, An Hui, China, [10]Rehabilitation Nursing, School of Nursing, Wanna Medical College, 22 Wenchang West Road, Higher Education Park, Wuhu, An Hui, China

Objective: Type 2 diabetes mellitus (T2DM) remains a major and widespread public health concern throughout the world. The prevalence of T2DM in the elderly has risen to the top of the list of public health concerns. In this study, obesity- and lipid-related indices were used to predict T2DM in middle-aged and elderly Chinese adults.

Methods: The data came from the China Health and Retirement Longitudinal Study (CHARLS), including 7902 middle-aged and elderly participants aged 45 years or above. The study assessed the association of obesity- and lipid-related indices and T2DM by measuring 13 indicators, including body mass index (BMI), waist circumference(WC), waist-height ratio (WHtR), conicity index(CI), visceral adiposity index (VAI), Chinese visceral adiposity index (CVAI), lipid accumulation product (LAP), a body shape index (ABSI), body roundness index (BRI), triglyceride glucose index (TyG-index) and its correlation index (TyG-BMI, TyG-WC, TyG-WHtR). The association of 13 obesity- and lipid-related indices with T2DM was investigated by binary logistic regression. Additionally, the predictive anthropometric index was evaluated, and the ideal cut-off value was established using the receiver operating characteristic (ROC) curve analysis and area under the curve (AUC).

Results: The study included 7902 participants, of whom 3638(46.04) and 4264 (53.96) were male and female. The prevalence of T2DM in mid-aged and old adults in China was 9.02% in males and 9.15% in females. All the above 13 indicators show a modest predictive power (AUC>0.5), which was significant for predicting T2DM in adults (middle-aged and elderly people) in China (P<0.05).

The results revealed that TyG-WHtR [AUC =0.600, 95%CI: 0.566–0.634] in males and in females [AUC =0.664, 95%CI: 0.636–0.691] was the best predictor of T2DM (P<0.05).

Conclusion: Most obesity- and lipid-related indices have important value in predicting T2DM. Our results can provide measures for the early identification of T2DM in mid-aged and elderly Chinese to reduce the prevalence of T2DM and improve health.

KEYWORDS

type 2 diabetes, National cohort study, obesity, middle-aged and elderly, receiver operating characteristic curve

Introduction

The percentage of older adults (defined as those 60 years of age or older) is expected to increase and reach >20% by the year 2050. China has the world's largest elderly population, 201 million in 2015, which is expected to rise to 479 million by 2050 (1). Type 2 diabetes mellitus(T2DM) is a worldwide problem and the most prevalent metabolic disease affecting about 1 in 10 adults (10.5% of adults worldwide) (2). Over the last two years, the prevalence of T2DM has increased by 16%, which is an alarming increase (2). Without taking into account the risk of death associated with COVID-19, in 2021, approximately 12.2% of adult all-cause deaths worldwide will be due to diabetes and its complications (3). In addition, 10.6% of adults in the world have poor glucose tolerance, which puts them at high risk of developing T2DM (3). In parallel with the rise in prevalence, the economic costs of T2DM have also increased dramatically. Controlling the incidence of T2DM is the key to reducing the cost of global economic development and improving the health of individuals and communities.

T2DM is associated with a variety of factors. The increase in the incidence of T2DM is mainly due to changes in living conditions and habits, such as a sedentary lifestyle (4), physical inactivity (5), smoking (6), and alcohol consumption (7). Several epidemiological investigations have shown that obesity is the most important risk factor for T2DM, and it has a certain impact on the production of insulin resistance and disease progression (8). The epidemic of obesity contributes to the burden of T2DM in worldwide. In a meta-analysis of Mendelian randomization studies, the easiest and most generally used indicator of obesity, body mass index (BMI), was linked to a higher risk of T2DM (9). However, BMI is not entirely inclusive. Such as WC (waist circumference), waist-height ratio (WHtR), and lipid accumulation index (LAP) have been widely used in epidemiology to measure obesity or central obesity (10–13). We can use these indicators to explore the risk of developing T2DM.

It should be noted that no agreement has been reached on the association of obesity and lipid-associated indices with T2DM. For instance, the BMI is frequently used to estimate the likelihood of contracting chronic diseases including diabetes, hypertension, depression, and cancer (14–17). However, compared to other measurements like WC, WHR, and WHtR, BMI was the least accurate predictor for cardiovascular risk factors such as diabetes, hypertension, and dyslipidemia in the study conducted by Lee et al. (18). Some studies have suggested that WC appears to be a stronger predictor of diabetes than BMI in Western populations (19, 20), while the evidence on this remains contradictory in Asian populations (21, 22). Previous studies reported that the Chinese visceral adiposity index (CVAI) was superior to BMI, WC, or visceral adiposity index (VAI) for the diagnosis of diabetes and prediabetes (23, 24). Another study in Japan found that triglyceride glucose index (TyG-index) was linearly associated with the risk of T2DM in the population (25). From these studies, it can be concluded that obesity and lipid-related indices are closely related to T2DM. However, it is not clear which index performs better in predicting diabetes risk. Moreover, most of the research is carried out based on the West, and the results are different because of the differences in nationality and culture. Therefore, it is of great significance to further determine the correlation and predictive value between obesity and lipid-related indicators and T2DM in middle-aged and elderly people for guiding the prevention and treatment of T2DM in elderly people.

Abbreviations: T2DM, type 2 diabetes mellitus; BMI, body mass index; WC, waist circumference; WHtR, waist-height ratio; VAI, visceral adiposity index; CVAI, cardio-ankle vascular index; LAP, lipid accumulation product; ABSI, a body shape index; BRI, body roundness index; TyG, triglyceride glucose; TyG-WHtR, triglyceride glucose-waist-height ratio; TyG-BMI, triglyceride glucose-body mass index; TyG-WC, triglyceride glucose-waist circumference; CHARLS, China Health and Retirement Longitudinal Study; FPG, fasting plasma glucose; TG, triglyceride; HDL-c, high-density lipoprotein-cholesterol; LDL-c, low-density lipoprotein-cholesterol; SD, standard deviation; OR, odds ratio; 95% CI, 95% confidence intervals; ROC, receiver operator curve; AUC, area under curve; IR, insulin resistance.

Currently, only a small number of cross-sectional studies have investigated the relationship between obesity and T2DM in elderly Chinese adults, but few studies have explored multiple indicators to predict T2DM risk, so to fill these gaps, we conducted a national retrospective cohort study in older Chinese adults. The longitudinal effects of 13 indicators on the incidence of T2DM were examined to predict the incidence of T2DM. This study provides a theoretical basis for early detection of T2DM, advanced and scientific medical prevention, and avoiding the occurrence of complications of T2DM, significantly improving the living standards of the elderly and prolonging life.

Method

Study design and setting

For this national cohort study, we used data from the China Wave2011 Longitudinal Study of Health and Retirement, a national longitudinal study of middle-aged and older Chinese people and their spouses, who were evaluated at baseline and followed up for two years (26). Individuals without T2DM in baseline from the China Health and Retirement Longitudinal Study (CHARLS) Wave 2011 study were included in our analysis after excluding subjects with missing data. Data gathering was then carried out in 2015. We enrolled 7902 individuals over 45 years of age in our nationwide cohort. The CHARLS project received approval from Peking University's Biomedical Ethics Review Board, and each participant signed an informed consent form. The data and relevant data for this study are available at the CHARLS project website (http://charls.pku.edu.cn/).

Individuals

The subjects of this survey were selected from the CHARLS, Wave 1 (2011). The CHARLS Wave 2011 was used to select participants. Cohort studies are used in this investigation. In 2011, patients with undiagnosed T2DM were included in our follow-up cohort. Four years later, in 2015, the incident rate of those affected by 13 indicators was assessed.

Baseline characteristics

At baseline, trained researchers used a structured questionnaire to acquire sociodemographic status information and health-related indicators, including age, education, marriage, residence, drinking, smoking, activities, exercise, and chronic diseases. The majority of factors were based on our earlier research investigations (27–32).

Data collection and definitions

Fasting plasma glucose (FPG), HbA1c, TC, triglycerides (TG), high-density lipoprotein-cholesterol (HDL-c), and low-density lipoprotein-cholesterol (LDL-c) were measured by fasting blood samples. FPG, TG, TC, HDL-c, and LDL-c were determined by enzyme colorimetric assay, while the HbA1c test was carried out by high-performance liquid chromatography (HPLC) (33). T2DM was defined as *1*) self-reported doctor-diagnosed diabetes, *2*) fasting plasma glucose ≥7.0mmol/L, *3*) 2-h plasma glucose ≥11.1mmol/L, or *4*) HbA1c ≥6.5% (34). Participants with a diagnosis of T2DM at baseline were excluded from this analysis.

Measurements

The BMI was calculated based on the weight and height of the participants. According to the Chinese standard, BMI was classified into three categories: obesity (BMI ≥ 28 kg/m2), overweight (24 ≤ BMI< 28 kg/m2), and underweight and normal (BMI< 24 kg/m2) (35). The lower rib margin and the middle of the flexible measuring tape were used to determine the WC (32). Conicity Index (CI) was measured by WC, weight, and height (36). When calculating the Body shape Index (BSI), body roundness index (BRI), and VAI, it should be noted that VAI is not gender-specific like other measurements (37–39). WHtR is defined as the WC (m) divided by the height (m) (40). The LAP is calculated somewhat differently by subtracting from the WC (men: 65 cm, women: 58 cm) and multiplying it with TG (41). In order to create a more suitable metric for Chinese people, CVAI is built on VAI (42). The following formulas were used to measure the other anthropometric indexes (Equations 1-12).

$$BMI = \frac{Weight}{Height^2} \tag{1}$$

$$WHtR = \frac{WC}{Height} \tag{2}$$

$$\text{Males}: VAI = \frac{WC}{39.68 + (1.88 \times BMI)} \times \frac{TG}{0.81} \times \frac{1.52}{HDL} \tag{3}$$

$$\text{Females}: VAI = \frac{WC}{36.58 + (1.89 \times BMI)} \times \frac{TG}{0.81} \times \frac{1.52}{HDL}$$

$$ABSI = \frac{WC}{Height^{\frac{1}{2}} \times BMI^{\frac{2}{3}}} \tag{4}$$

$$\text{BRI} = 364.2 - 365.5\sqrt{1 - \left(\frac{WC \div (2\pi)^2}{(0.5 \times Height)^2}\right)} \tag{5}$$

$$\text{Males}: LAP = [WC\,(cm) - 65] \times TG\,(mmol/l) \tag{6}$$

$$\text{Females}: LAP = [WC\,(cm) - 58] \times TG\,(mmol/l)$$

$$CI = \frac{WC(m)}{0.019\sqrt{\frac{weight(kg)}{height(m)}}} \tag{7}$$

$$\text{Males}: CVAI = -267.93 + 0.68 \times age + 0.03 \times BMI\ (kg/m2) + 4.00 \times WC\ (cm) + 22.00 \times Log_{10}TG\ (mmol/l) - 16.32 \times HDL - C(mmol/l) \quad (8)$$

$$\text{Females}: CVAI = -187.32 + 1.71 \times age + 4.32 \times BMI\ (kg/m2) + 1.12 \times WC\ (cm) + 39.76 \times Log_{10}TG\ (mmol/l) - 11.66 \times HDL - C(mmol/l)$$

$$TyG\ index = Ln[(TG(mg/dl) \times glucose(mg/dl)/2)] \quad (9)$$

$$TyG - BMI = TyG \times BMI \quad (10)$$

$$TyG - WC = TyG \times WC \quad (11)$$

$$TyG - WHtR = TyG \times WHtR \quad (12)$$

Statistical analysis

All the statistical analyses were analyzed using STATA software version 25.0. Continuous variables were applied by mean (standard deviation, SD) depending on normal distribution or not, while the frequency with percentage was presented for categorical variables. A chi-squared test was run to compare dichotomous or categorical variables. Results from studies that were gender-specific are also included because the relationship between T2DM and obesity status varies between the sexes. The odds ratios (OR) and 95% confidence intervals (CI) for each of the 13 obesity- and lipid-related indices were calculated by binary logistic regression after adjusting for age, education, marital status, current residence, current smoking, alcohol consumption, activity participation, regular exercise, and chronic disease. The 13 indices were divided into two categories based on their optimal cutoff values. The P-value obtained by the statistical significance test is usually regarded as the statistical significance when $P< 0.05$, and the $P< 0.001$ is very significant. The ability of these indices to distinguish T2DM was tested by drawing the receiver operating curve (ROC curve) and AUC calculation. The ROC curve can be used to calculate the sensitivity, specificity, positive, negative, positive, positive, and negative. A Youden index (sensitivity + specificity 1) was used to select the cut-off points to evaluate classification accuracy.

Results

Table 1 shows the characteristics of the participants with complete samples. This study included 7902 patients, of which 3638 (46. 04%) were male, and 4 264 (53.96%) were female. Most of them were 45-64 years old, there were significant differences between men and women in age, education, marital status, current smoking, alcohol drinking, number of chronic diseases, WC, BMI, WHtR, VAI, ABSI, BRI, LAP, CI, CVAI, TyG index, TyG-BMI, TyG-WC and TyG-WHtR ($P< 0.05$). However, there was no statistical significance in the distribution of current residence, taking activities, and having regular exercises between the two groups ($P > 0.05$). Due to these marked gender differences ($P< 0.05$), the main analysis was conducted separately by gender.

Table 2 presents the baseline characteristics of T2DM and non-diabetic subjects by gender. Based on the findings, the percentage of women with T2DM was significantly higher (9.15% versus 9.02% for males). There were significant differences in WC, BMI, WHtR, VAI, ABSI, BRI, LAP, CI, CVAI, TyG, TyG-BMI, TyG-WC, and TyG-WHtR in men with T2DM ($P< 0.05$); There were significant differences in age, current residence, chronic illness, WC, BMI, WHtR, VAI, ABSI, BRI, LAP, CI, CVAI, CVAI, TyG-BMI, TyG-WC, and TyG-WHtR in women with T2DM ($P< 0.05$). There were no significant differences among T2DM subgroups, male or female, in terms of educational background, marital status, current smoking, alcohol drinking, taking activities, and having regular exercises ($P > 0.05$).

Table 3 illustrates the evaluation of the prediction using ROC curves and AUC. The ROC curves of each parameter for predicting the risk of T2DM are presented in Figures 1, 2. In men, the TyG -WHtR was the best predictor of T2DM in the middle-aged and elderly male population (AUC=0.600, SE=0.017, 95% CI=0.566-0.634, and optimal cut-off=4.769). Meanwhile, it can be observed from the table that WC (AUC = 0.583, S E = 0.018, 95% CI = 0.549-0.618, and optimal cut-off =88.850) and LAP (AUC = 0.583, S E = 0.017, 95% CI = 0.549-0.617, and optimal cut-off =28.333) had similar predictive values. Similarly, the predictive values were similar for the WHtR (AUC = 0.592, SE = 0.017, 95% CI =0.558-0.627, and optimal cut-off = 0.520), BRI (AUC = 0.592, SE = 0.017, 95% CI =0.558-0.627, and optimal cut-off =3.739) and TyG-WC (AUC = 0.592, SE = 0.017, 95% CI =0.558-0.626, and optimal cut-off = 765.677). In addition, in female patients, TyG -WHtR was also the best predictor of T2DM (AUC=0.664, SE=0.015, 95%CI 0.636-0.691, and optimal cut-off=5.031). Similarly, the predictive values were similar for the WHtR (AUC = 0.641, SE = 0.014, 95% CI =0.613-0.670, and optimal cut-off = 0.553), BRI (AUC = 0.641, SE = 0.014, 95% CI =0.613-0.670, and optimal cut-off =4.416). There was a statistical difference in all the indexes ($P< 0.05$). The results showed that the AUC of these 13 indexes was above 0.5, suggesting that they could predict the development of T2DM.

Table 4 shows the associations of obesity- and lipid-related indices with T2DM. In this survey, 13 obesity and lipid indices were converted into two categories according to the figures in Table 3. Table 4 is based on the transformed variables. In general, the greater the OR, the higher the risk. After adjusting for factors such as age, education, marital status, current residence, current smoking, alcohol drinking, taking activities, having regular exercises, and chronic diseases, both men's and women's odds of developing T2DM gradually increased with increasing obesity and lipid measurement units. After adjusting for all covariates, each unit rise in TyG -WHtR, for example, was related to a 2.249-fold (95%

TABLE 1 Characteristics of participants with full samples(N=7902).

Variables	Male	Female	Total	t/χ^2	P
	N (%)	N (%)	N (%)		
N	3638 (46.04)	4264 (53.96)	7902 (100)		
Age(years)					
45-54	1107 (30.43)	167 3(39.24)	2780 (35.18)	79.602	< 0.001
55-64	1420 (39.03)	1562 (36.63)	2982 (37.74)		
65-74	814 (22.37)	716 (16.79)	1530 (19.36)		
≥75	297 (8.16)	313 (7.34)	610 (7.72)		
Education					
Illiterate	501 (13.77)	1807 (42.38)	2308 (29.21)	796.902	< 0.001
Less than elementary school	2669 (73.36)	2173 (50.96)	4842 (61.28)		
High school	306 (8.41)	212 (4.97)	518 (6.56)		
Above vocational school	162 (4.45)	72 (1.69)	234(2.96)		
Marital status					
Single	337(9.26)	645 (15.13)	982 (12.43)	62.013	< 0.001
Married	3301(90.74)	3619 (84.87)	6920 (87.57)		
Current residence					
Rural	3363(92.44)	3968 (93.06)	7331 (92.77)	1.116	0.291
Urban	275(7.56)	296 (6.94)	571 (7.23)		
Current smoking					
No	893(24.55)	3937 (92.33)	4830 (61.12)	3796.205	< 0.001
Former smoke	585(16.08)	77 (1.81)	662(8.38)		
Current smoke	2160(59.37)	250 (5.86)	2410 (30.50)		
Alcohol drinking					
No	1592(43.76)	3730 (87.48)	5322 (67.35)	1771.074	< 0.001
Less than once a month	403(11.08)	215 (5.04)	618 (7.82)		
More than once a month	1643(45.16)	319 (7.48)	1962 (24.83)		
Taking activities					
No	1801(49.51)	2161 (50.68)	3962 (50.14)	1.084	0.298
Yes	1837(50.49)	2103 (49.32)	3940 (49.86)		
Having regular exercises					
No exercise	2245(61.71)	2596 (60.88)	4841 (61.26)	1.028	0.598
Less than exercises	686(18.86)	842 (19.75)	1528 (19.34)		
egular exercises	707(19.43)	826 (19.37)	1533 (19.40)		
Chronic diseases(counts)					
0	1267(34.83)	1322 (31.00)	2589 (32.76)	13.892	0.001
01-Feb	1820(50.03)	2226 (52.20)	4046 (51.20)		
Mar-14	551(15.15)	716 (16.79)	1267 (16.03)		
WC	84.22 ± 9.49	84.99 ± 10.05	84.63 ± 9.80	-3.487	< 0.001

(Continued)

TABLE 1 Continued

Variables	Male	Female	Total	t/χ^2	*P*
	N (%)	N (%)	N (%)		
BMI	22.72 ± 3.48	23.78 ± 3.92	23.29 ± 3.76	-12.738	< 0.001
WHtR	0.51 ± 0.06	0.56 ± 0.07	0.54 ± 0.06	-31.109	< 0.001
VAI	3.49 ± 3.35	5.47 ± 4.77	4.56 ± 4.29	-21.566	< 0.001
ABSI	0.08 ± 0.01	0.08 ± 0.01	0.08 ± 0.01	-9.591	< 0.001
BRI	3.69 ± 1.10	4.57 ± 1.41	4.16 ± 1.35	-31.091	< 0.001
LAP	27.05 ± 26.61	39.83 ± 30.87	33.95 ± 29.67	-19.758	< 0.001
CI	1.27 ± 0.08	1.30 ± 0.10	1.28 ± 0.09	-14.182	< 0.001
CVAI	91.47 ± 45.25	102.64 ± 42.06	97.49 ± 43.91	-11.295	< 0.001
TyG index	8.50 ± 0.56	8.60 ± 0.54	8.56 ± 0.55	-8.467	< 0.001
TyG-BMI	193.63 ± 35.46	205.10 ± 39.08	199.82 ± 37.89	-13.677	< 0.001
TyG-WC	717.41 ± 106.25	732.57 ± 108.26	725.59 ± 107.60	-6.26	< 0.001
TyG -WHtR	4.38 ± 0.62	4.80 ± 0.71	4.61 ± 0.70	-27.746	< 0.001

WC, waist circumference; BMI, body mass index; WHtR, waist to height ratio;VAI, visceral adiposity index; ABSI, A body shape index; BRI, body roundness index; LAP, lipid accumulation product; CVAI, cardio-ankle vascular index; CI, conicity index; TyG, triglyceride and glucose index; TyG-BMI, TyG related to BMI; TyG-WC, TyG related to WC; TyG-WHtR, TyG related to WHtR.

TABLE 2 Baseline characteristics of the study participants with and without T2DM by sex.

Variables	Male (N=3638)		$\chi2$	*P*	Female (N=4264)		$\chi2$	*P*
N (%)	With T2DM N (%)	Without T2DM N (%)			With T2DM N (%)	Without T2DM N (%)		
N	328 (9.02)	3310 (90.98)			390 (9.15)	3874 (90.85)		
Age(years)								
45-54	85 (25.91)	1022 (30.88)	3.745	0.290	126(32.31)	1547 (39.93)	15.792	0.001
55-64	140 (42.68)	1280 (38.67)			142 (36.41)	1420 (36.65)		
65-74	75 (22.87)	739 (22.33)			90 (23.08)	626 (16.16)		
≥75	28 (8.54)	269(8.13)			32 (8.21)	281 (7.25)		
Education								
Illiterate	38 (11.59)	463 (13.99)	3.632	0.304	177 (45.38)	1630 (42.08)	6.344	0.096
Less than elementary school	255 (77.74)	2414 (72.93)			198 (50.77)	1975 (50.98)		
High school	22 (6.71)	284 (8.58)			10 (2.56)	202 (5.21)		
Above vocational school	13 (3.96)	149 (4.50)			5 (1.28)	67 (1.73)		
Marital status								
Single	32 (9.76)	305 (9.21)	0.104	0.747	68(17.44)	577 (14.89)	1.783	0.182
Married	296 (90.24)	3005 (90.79)			322 (82.56)	3297 (85.11)		
Current residence								
Rural	300 (91.46)	3063 (92.54)	0.493	0.483	373 (95.64)	3595 (92.80)	4.433	0.035
Urban	28 (8.54)	247 (7.46)			17 (4.36)	279 (7.20)		

(Continued)

TABLE 2 Continued

Variables	Male (N=3638)		χ^2	P	Female (N=4264)		χ^2	P
N (%)	With T2DM N (%)	Without T2DM N (%)			With T2DM N (%)	Without T2DM N (%)		
Current smoking								
No	75 (22.87)	818 (24.71)	0.647	0.724	359 (92.05)	3578 (92.36)	0.638	0.727
Former smoke	52 (15.85)	533 (16.10)			9 (2.31)	68 (1.76)		
Current smoke	201 (61.28)	1959 (59.18)			22 (5.64)	228 (5.89)		
Alcohol drinking								
No	156 (47.56)	1436 (43.38)	2.117	0.347	352 (90.26)	3378 (87.20)	3.036	0.219
Less than once a month	34 (10.37)	369 (11.15)			15 (3.85)	200 (5.16)		
More than once a month	138 (42.07)	1505 (45.47)			23 (5.90)	296 (7.64)		
Taking activities								
No	158 (48.17)	1643 (49.64)	0.257	0.612	205 (52.56)	1956 (50.49)	0.610	0.435
Yes	170 (51.83)	1667 (50.36)			185 (47.44)	1918 (49.51)		
Having regular exercises								
No exercise	199 (60.67)	2046 (61.81)	0.173	0.917	231 (59.23)	2365 (61.05)	1.801	0.406
Less than exercises	64 (19.51)	622 (18.79)			87 (22.31)	755 (19.49)		
Regular exercises	65 (19.82)	642 (19.40)			72 (18.46)	754 (19.46)		
Chronic diseases(counts)								
0	106 (32.32)	1161 (35.08)	4.123	0.127	91 (23.33)	1231 (31.78)	13.312	0.001
1-2	160 (48.78)	1660 (50.15)			218 (55.90)	2008 (51.83)		
3-14	62 (18.90)	489 (14.77)			81 (20.77)	635 (16.39)		
WC	87.06 ± 10.68	83.94 ± 9.32	-5.113	< 0.001	89.61 ± 10.43	84.52 ± 9.89	-9.631	< 0.001
BMI	23.70 ± 4.28	22.62 ± 3.38	-4.417	< 0.001	25.31 ± 3.96	23.63 ± 3.89	-8.107	< 0.001
WHtR	0.53 ± 0.06	0.51 ± 0.05	-5.489	< 0.001	0.59 ± 0.07	0.55 ± 0.06	-9.528	< 0.001
VAI	4.39 ± 4.34	3.41 ± 3.22	-4.010	< 0.001	6.79 ± 5.28	5.34 ± 4.70	-5.201	< 0.001
ABSI	0.08 ± 0.01	0.08 ± 0.01	-2.120	0.034	0.08 ± 0.01	0.08 ± 0.01	-2.868	0.004
BRI	4.06 ± 1.28	3.65 ± 1.07	-5.559	< 0.001	5.22 ± 1.51	4.50 ± 1.39	-9.613	< 0.001
LAP	36.06 ± 37.00	26.16 ± 25.18	-4.738	< 0.001	52.43 ± 35.78	38.56 ± 30.05	-7.395	< 0.001
CI	1.29 ± 0.09	1.27 ± 0.08	-4.016	< 0.001	1.32 ± 0.09	1.29 ± 0.10	-5.943	< 0.001
CVAI	106.66 ± 51.51	89.96 ± 44.31	-5.669	< 0.001	124.29 ± 40.84	100.45 ± 41.56	-10.813	< 0.001
TyG index	8.64 ± 0.60	8.49 ± 0.55	-4.380	< 0.001	8.79 ± 0.52	8.58 ± 0.54	-7.249	< 0.001
TyG-BMI	205.33 ± 42.58	192.47 ± 34.47	-5.299	< 0.001	222.74 ± 38.60	203.33 ± 38.69	-9.447	< 0.001
TyG-WC	754.21 ± 122.30	713.76 ± 103.83	-5.787	< 0.001	788.49 ± 107.94	726.94 ± 106.70	-10.847	< 0.001
TyG -WHtR	4.61 ± 0.72	4.36 ± 0.61	-6.127	< 0.001	5.16 ± 0.69	4.76 ± 0.70	-10.813	< 0.001

WC, waist circumference; BMI, body mass index; WHtR, waist to height ratio; VAI, visceral adiposity index; ABSI, A body shape index; BRI, body roundness index; LAP, lipid accumulation product; CVAI, cardio-ankle vascular index; CI, conicity index; TyG, triglyceride and glucose index; TyG-BMI, TyG related to BMI; TyG-WC, TyG related to WC; TyG-WHtR, TyG related to WHtR.

CI=1.771-2.857) increase in the likelihood of developing T2DM in males. Each unit increase in TyG-WC was linked to a 2.761-fold (95% CI=2.223-3.430) increase in the likelihood of developing T2DM in females. Among the 13 indicators, the correlation between ABSI and T2DM was weakest in males (OR=1.637, 95% CI: 1.277-2.099) and females (OR=1.415, 95% CI: 1.117-1.791). After adjusting for confounding factors, all indicators were statistically significant ($P< 0.05$). Figure 3 illustrates the forest plot or values before and after adjustment for the confounding factors for men and women.

TABLE 3 Cut-off between area under curve, sensitivity, and specificity for obesity- and lipid-related indices to detect T2DM by sex.

N=7902	WC	BMI	WHtR	VAI	ABSI	BRI	LAP	CI	CVAI	TyG index	TyG-BMI	TyG-WC	TyG -WHtR
Male													
Area under curve	0.583	0.572	0.592	0.565	0.554	0.592	0.583	0.578	0.593	0.576	0.586	0.592	0.600
Std. Error	0.018	0.017	0.017	0.017	0.017	0.017	0.017	0.017	0.018	0.017	0.017	0.017	0.017
95%CI	0.549,0.618	0.538,0.606	0.558,0.627	0.531,0.599	0.521,0.587	0.558,0.627	0.549,0.617	0.544,0.612	0.559,0.628	0.543,0.609	0.552,0.620	0.558,0.626	0.566,0.634
P-value	< 0.001	< 0.001	< 0.001	< 0.001	0.001	< 0.001	< 0.001	< 0.001	< 0.001	< 0.001	< 0.001	< 0.001	< 0.001
Optimal cutoffs	88.850	23.082	0.520	4.573	0.085	3.739	28.333	1.307	99.429	8.762	207.797	765.677	4.769
J-Youden	0.151	0.135	0.160	0.113	0.114	0.160	0.151	0.145	0.166	0.126	0.154	0.171	0.173
Sensitivity (%)	44.21%	53.70%	57.01%	31.70%	38.41%	57.01%	46.34%	42.99%	55.18%	39.94%	44.51%	46.04%	41.46%
Specificity (%)	70.85%	59.80%	59.03%	79.60%	72.99%	59.03%	68.79%	71.45%	61.39%	72.66%	70.91%	71.06%	75.80%
(+) Likelihood ratio	1.516	1.336	1.392	1.554	1.422	1.392	1.485	1.506	1.429	1.461	1.530	1.591	1.713
(-) Likelihood ratio	0.788	0.774	0.728	0.858	0.844	0.728	0.780	0.798	0.730	0.827	0.783	0.759	0.772
Female													
Area under curve	0.640	0.625	0.641	0.608	0.559	0.641	0.643	0.601	0.663	0.610	0.647	0.662	0.664
Std. Error	0.015	0.015	0.014	0.015	0.015	0.014	0.014	0.015	0.014	0.014	0.015	0.014	0.014
95%CI	0.612,0.669	0.596,0.655	0.613,0.670	0.580,0.637	0.529,0.588	0.613,0.670	0.616,0.670	0.572,0.630	0.636,0.691	0.582,0.639	0.619,0.675	0.634,0.689	0.636,0.691
P-value	< 0.001	< 0.001	< 0.001	< 0.001	< 0.001	< 0.001	< 0.001	< 0.001	< 0.001	< 0.001	< 0.001	< 0.001	< 0.001
Optimal cutoffs	84.950	25.422	0.553	4.277	0.086	4.416	30.835	1.341	114.005	8.516	212.290	759.606	5.031
J-Youden	0.224	0.198	0.223	0.183	0.123	0.223	0.234	0.163	0.253	0.191	0.228	0.256	0.248
Sensitivity (%)	70.30%	48.72%	70.51%	63.33%	44.40%	70.51%	72.05%	44.90%	60.51%	72.10%	59.70%	61.28%	58.72%
Specificity (%)	52.10%	71.09%	51.83%	55.01%	67.90%	51.83%	51.34%	71.40%	64.79%	47.00%	63.10%	64.27%	66.06%
(+) Likelihood ratio	1.468	1.685	1.464	1.408	1.383	1.464	1.481	1.570	1.719	1.360	1.618	1.715	1.730
(-) Likelihood ratio	0.570	0.721	0.569	0.667	0.819	0.569	0.544	0.772	0.609	0.594	0.639	0.602	0.625

WC, waist circumference; BMI, body mass index; WHtR, waist to height ratio; VAI, visceral adiposity index; ABSI, A body shape index; BRI, body roundness index; LAP, lipid accumulation product; CVAI, cardio-ankle vascular index; CI, conicity index; TyG, triglyceride and glucose index; TyG-BMI, TyG related to BMI; TyG-WC, TyG related to WC; TyG-WHtR, TyG related to WHtR.

10.3389/fendo.2023.1331739

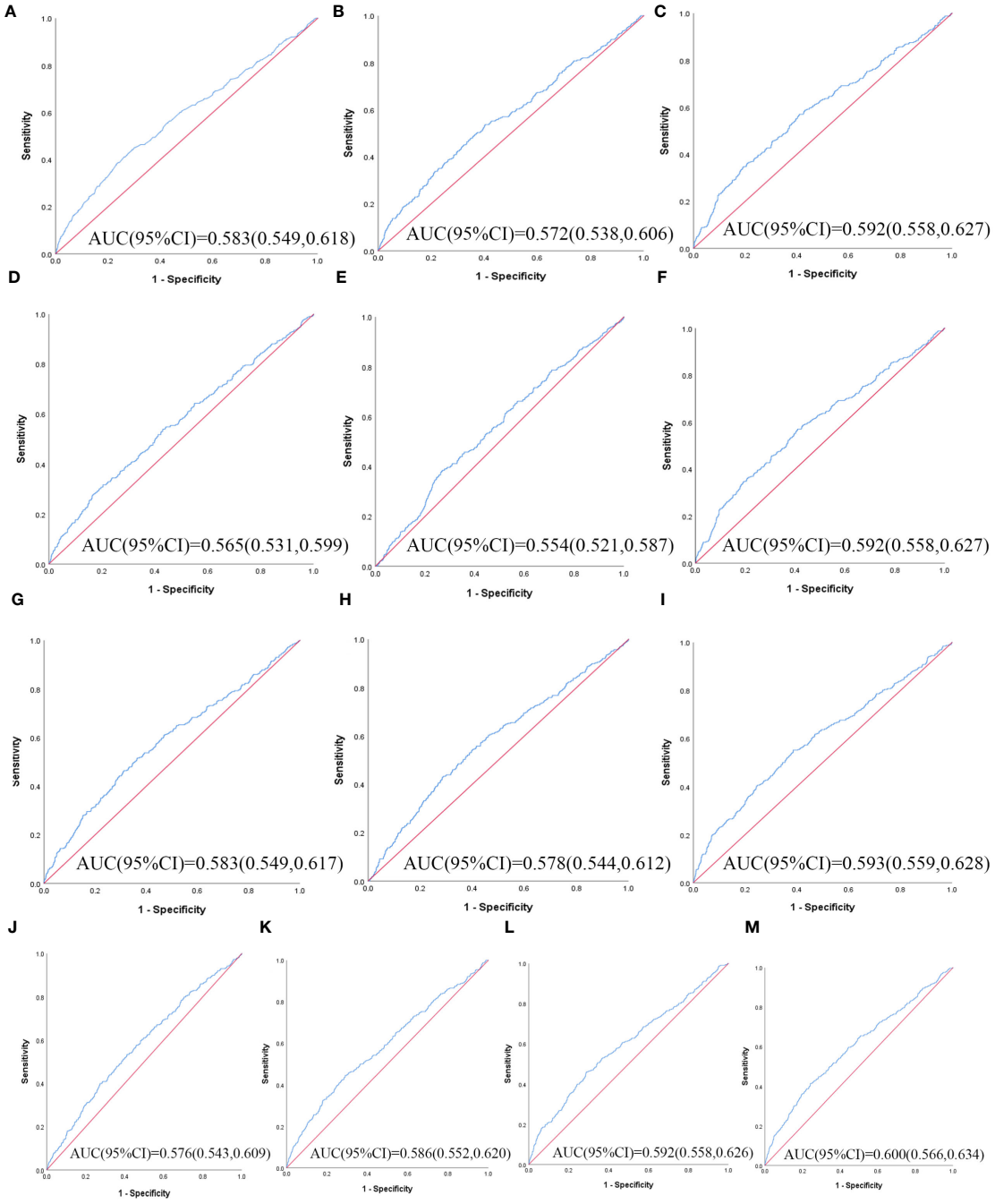

FIGURE 1
The ROC curves of each indicator in the prediction of T2DM risk in males. **(A)** WC, **(B)** BMI, **(C)** WHtR, **(D)** VAI, **(E)** ABSI, **(F)** BRI, **(G)** LAP, **(H)** CI, **(I)** CVAI, **(J)** TyG-index, **(K)** TyG-BMI, **(L)** TyG-WC, **(M)** TyG-WHtR.

Discussion

T2DM has been identified as a major public health problem with significant implications for people's lives and health spending. A significant risk factor for T2DM is obesity. Finding a quick and easy way to test for diabetes can therefore serve as a foundation for an early diagnosis of T2DM. This study evaluated the predictive power of 13 obesity- and lipid-related indices in identifying the risk of T2DM in middle-aged and old adults in China. In our study, a total of 7902 people participated in the study. After adjusting for population factors in our population-based cohort analysis, we found a statistically significant relationship between obesity and lipid-related indices and T2DM.

This study revealed that 13 obesity and lipid-related indicators are all related to the risk of T2DM. Similar to other studies, all 13 indicators play an important role in different populations (43–45). After adjusting for multiple covariates, as the 13 indicators increase, the prevalence of T2DM increases. Among them, TyG-WHtR and CVAI have a stronger correlation with the prevalence of T2DM.

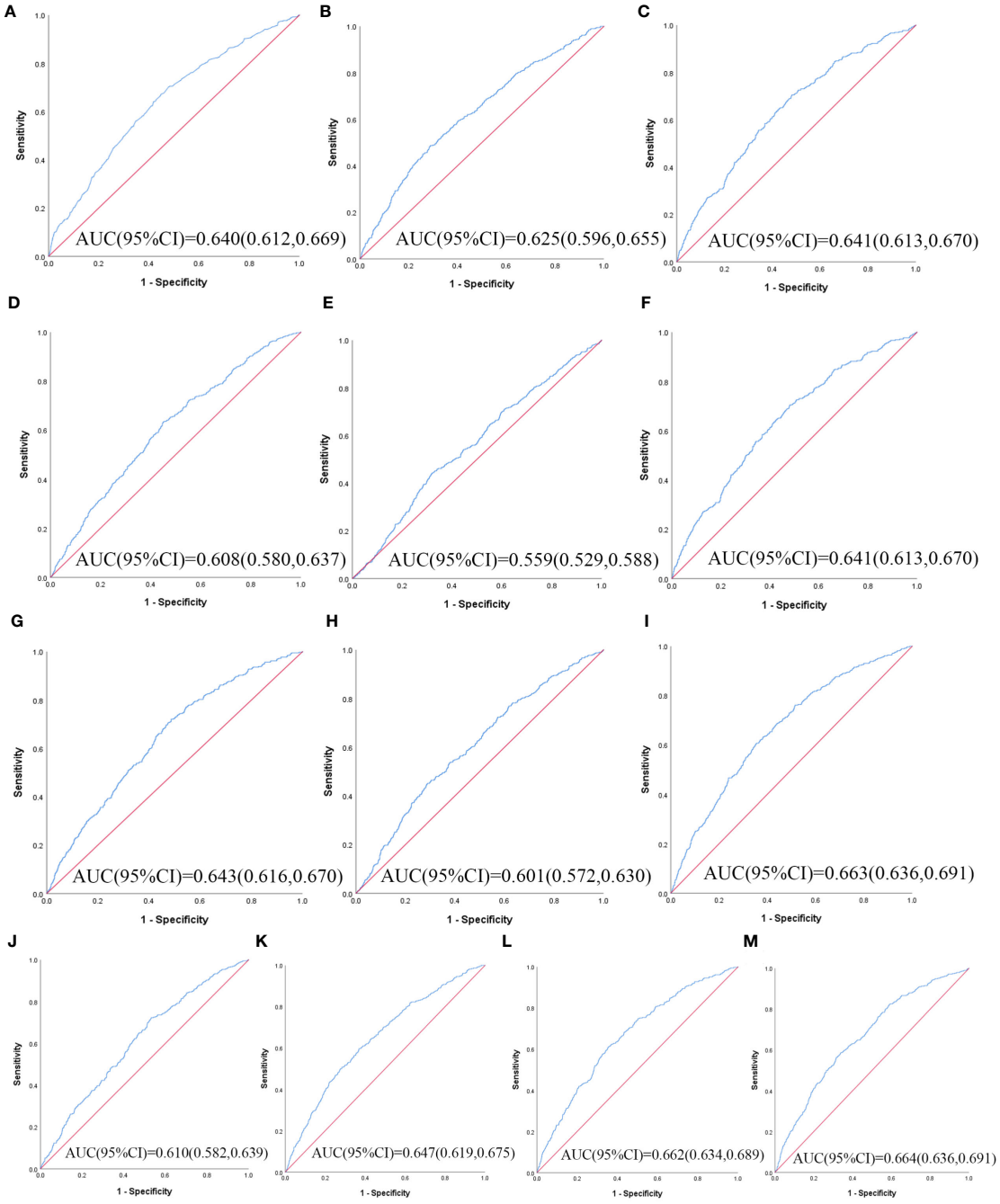

FIGURE 2
The ROC curves of each indicator in the prediction of T2DM risk in females. **(A)** WC, **(B)** BMI, **(C)** WHtR, **(D)** VAI, **(E)** ABSI, **(F)** BRI, **(G)** LAP, **(H)** CI, **(I)** CVAI, **(J)** TyG-index, **(K)** TyG-BMI, **(L)** TyG-WC, **(M)** TyG-WHtR.

As far as we know, insulin resistance (IR) and islet β-cell dysfunction are the main pathophysiology of T2DM (46–48). A great deal of hormones and cytokines are produced in adipose and adipose tissue, which are important in glucose metabolism and lipid metabolism (49). A characteristic of several metabolic diseases, including hyperglycemia and hypertriglyceridemia, is IR (50). Ahn et al. have shown that the TyG index is composed of factors related to fat and blood sugar, and it is a reliable indicator that has a good reflection of human IR (10). Studies have shown that the TyG index can be a cheap and reliable indicator for the diagnosis of IR, which is important for the early diagnosis of T2DM high-risk people (51). The TyG index, a new measure based on TG and FBG, has been shown to be a useful predictor of metabolic disorders and T2DM (52–54). Several studies have suggested that TyG index is significantly linked to the chance of acquiring T2DM in Singapore (55), Japan (56), Korea (57), and Thailand (58). Ferreira, J.R.S (59). has shown that the TyG-related factors are a useful tool to predict metabolic syndrome. So far, the majority of studies (60–62) have also demonstrated a strong relationship between the TyG-related factors and pre-diabetes/diabetes.

10.3389/fendo.2023.1331739

TABLE 4 Associations of obesity- and lipid-related indices with T2DM and its components.

T2DM	WC	BMI	WHtR	VAI	ABSI	BRI	LAP	CI	CVAI	TyG index	TyG-BMI	TyG-WC	TyG -WHtR
Male													
Unadjusted OR (95% CI)	1.925 (1.529,2.424) **	1.699 (1.353,2.133) **	1.888 (1.501,2.374) **	1.809 (1.413,2.317) **	1.662 (1.307,2.115) **	1.909 (1.518,2.401) **	1.904 (1.514,2.394)**	1.868 (1.482,2.353) **	1.958 (1.558,2.461)**	1.764 (1.397,2.229) **	1.955 (1.553,2.461)**	2.094 (1.665,2.635) **	2.191 (1.734,2.768) **
P value	<0.001	<0.001	<0.001	<0.001	<0.001	<0.001	<0.001	<0.001	<0.001	<0.001	<0.001	<0.001	<0.001
Adjusted OR (95% CI)	1.995 (1.573,2.530) **	1.803 (1.422,2.286) **	1.921 (1.521,2.426) **	1.838 (1.429,2.363) **	1.637 (1.277,2.099) **	1.943 (1.539,2.455) **	1.972 (1.557,2.497) **	1.840 (1.455,2.327) **	1.991 (1.575,2.517) **	1.804 (1.423,2.287) **	2.071 (1.629,2.633) **	2.188 (1.726,2.774) **	2.249 (1.771,2.857)**
P value	<0.001	<0.001	<0.001	<0.001	<0.001	<0.001	<0.001	<0.001	<0.001	<0.001	<0.001	<0.001	<0.001
Female													
Unadjusted OR (95% CI)	2.574 (2.053,3.226) **	2.333 (1.890,2.879) **	2.552 (2.035,3.201) **	2.110 (1.701,2.617) **	1.572 (1.269,1.948) **	2.571 (2.049,3.224) **	2.717 (2.159,3.420) **	2.019 (1.635,2.494) **	2.820 (2.278,3.491) **	2.255 (1.793,2.837) **	2.512 (2.031,3.107) **	2.848 (2.299,3.527) **	2.768 (2.239,3.422) **
P value	<0.001	<0.001	<0.001	<0.001	<0.001	<0.001	<0.001	<0.001	<0.001	<0.001	<0.001	<0.001	<0.001
Adjusted OR (95% CI)	2.505 (1.993,3.148) **	2.450 (1.972,3.043)**	2.409 (1.914,3.032) **	2.059 (1.656,2.560) **	1.415 (1.117,1.791) *	2.428 (1.929,3.056) **	2.662 (2.110,3.358) **	1.881 (1.500,2.360) **	2.717 (2.172,3.399)**	2.187 (1.735,2.757) **	2.607 (2.096,3.242) **	2.761 (2.223,3.430) **	2.613 (2.104,3.244) **
P value	<0.001	<0.001	<0.001	<0.001	0.004	<0.001	<0.001	<0.001	<0.001	<0.001	<0.001	<0.001	<0.001

WC, waist circumference; BMI, body mass index; WHtR, waist to height ratio; VAI, visceral adiposity index; ABSI, A body shape index; BRI, body roundness index; LAP, lipid accumulation product; CVAI, cardio-ankle vascular index; CI, conicity index; TyG, triglyceride and glucose index; TyG-BMI, TyG related to BMI; TyG-WC, TyG related to WC; TyG-WHtR, TyG related to WHtR.
Odds ratios were adjusted for age, educational levels, marital status, live place, current smoking, alcohol drinking, activities, exercises, chronic diseases.
*P<0.05, **P<0.001.

In fact, factors related to TyG played a far greater role in this study than other factors. In our study, TyG-related factors such as TyG-WHtR, TyG-BMI, and TyG-WC can provide a broader basis for obesity- and lipid-related indices to estimate T2DM. TyG-WHtR (AUC=0.600 in males and 0.664 in females) had greater efficacy in predicting T2DM symptoms than the TyG index alone. Many earlier several studies share similar views to our findings (63, 64). As the TyG index is a reliable and alternate indicator of IR, it may be used to assess the risk of T2DM. It is easy to get and calculate it in the clinic or large-scale epidemiological survey.

In addition, our study showed that women have a higher risk of developing T2DM than men. This may be because women lose more height than men and have more subcutaneous fat storage. One study showed that increased visceral fat levels were associated with about a threefold increased risk of T2DM in women, and a modest 20% increased risk in men (65). The central distribution of adipose tissue has a greater impact on the incidence of non-insulin-dependent T2DM in women than in men and may lead to an increased risk of T2DM (65, 66). Together, consistent with our study, older women have a higher risk of new-onset T2DM than men and are more sensitive to predicting the prevalence of T2DM in women with a higher area under the curve for most indicators.

Interestingly, in our study, women were 2.761 times more likely to develop T2DM for each unit increase in TyG-WC (95% CI=2.223-3.430), and a similar study reported a stronger correlation between visceral adiposity and serum TG in women than in men (67). This may be because women generally show higher hepatocyte lipids on an empty stomach and after a glucose and lipid load (68). Several studies (64, 69) have jointly shown that TyG-WC can be used as the main monitoring parameter for diabetes screening and clinical assessment/prediction of diabetes risk in the population, which also has certain reference value for our research.

BMI and WC are safe, easy, and cheap tools to evaluate a person's health status and make a rough estimate of the risk of obesity, including T2DM. In a retrospective study of 41, 242 people aged 45 or older, the relationship between BMI and WC and T2DM was higher than that of WHtR or TyG index (70). Qiwei Ge et al. (71) also found that WC was the best predictor of T2DM in elderly men. However, these studies' indicators differed from those in our analysis. In our research, BMI and WC were relatively weak in predicting T2DM. A Japanese cohort study (72) showed that BRI was superior to BMI and WC in predicting T2DM. Moreover, it is noteworthy that Jayedi et al.'s recent meta-analysis of 216 cohort studies, which was published in the BMJ, demonstrated that WHtR was more closely linked to T2DM in routine assessments than WC, waist-to-hip ratio, and BMI (73). With some reports demonstrate that WHtR had higher predictive power than WC and BMI (74, 75). The cut-off values for BMI and WC are greatly impacted by gender differences, and both BMI and WC have various limits (76). Perhaps in the future, BMI can be combined with WHtR and WC, which can improve the risk phenotype of T2DM and screen diabetic patients.

VAI is the visceral obesity index (77), which was often used in the past in Caucasians, and the correlation with the area of adipose tissue in the Chinese body is low, and the difference may be related to the different distribution of adipose tissue in the body of Caucasians and Asians, and Asians may be more prone to have visceral fat

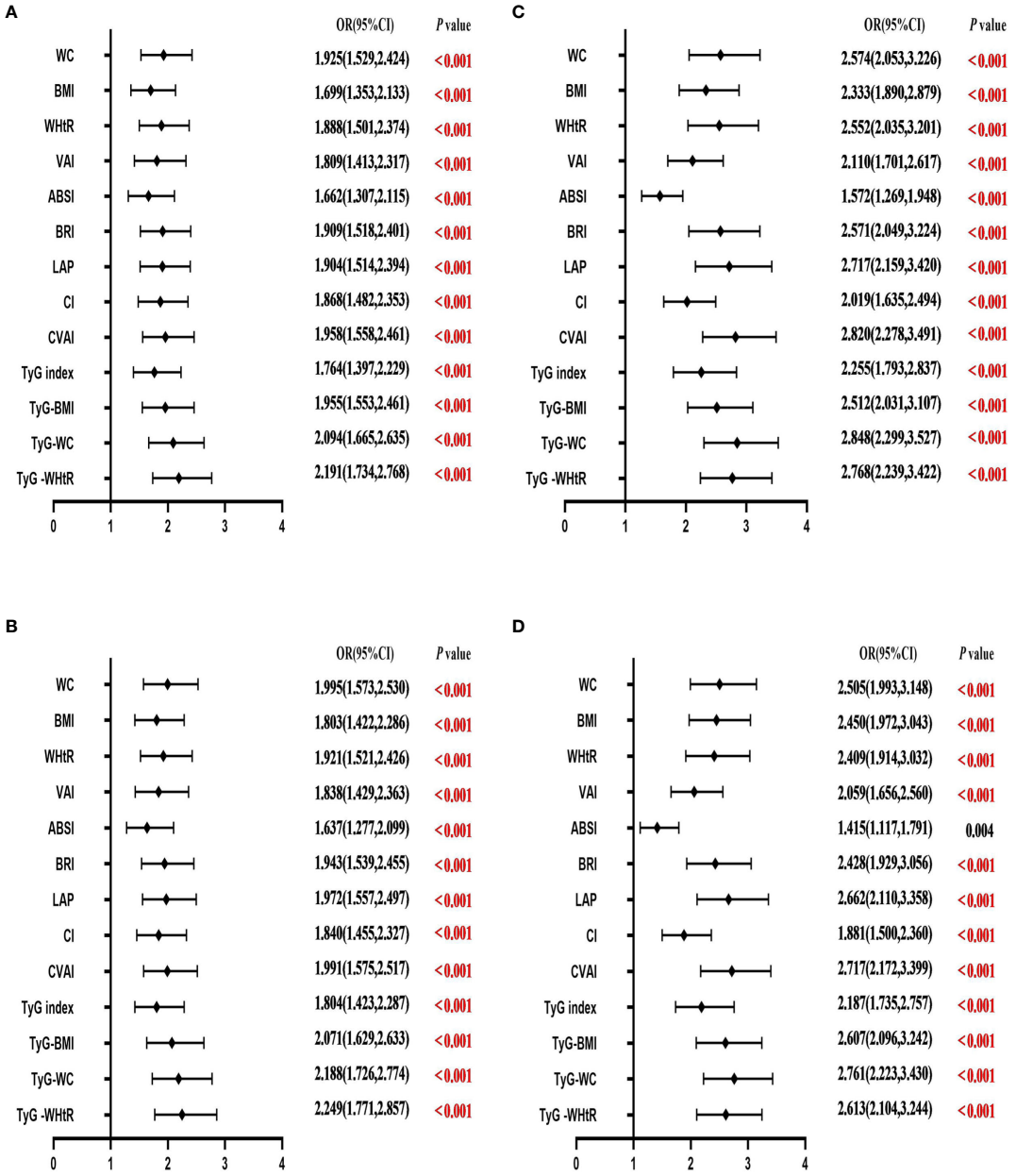

FIGURE 3
Forest diagram of OR before and after adjustment of confounding factors for males and females. **(A)** Male unadjusted; **(B)** male adjusted; **(C)** female unadjusted; **(D)** female adjusted. Adjusted OR: Adjusted for age, educational levels, marital status, live place, current smoking, alcohol drinking, activities, exercises, and chronic diseases.

accumulation, which may be related to different lifestyles. Therefore, in order to find an index that better represents the characteristics of body fat distribution and has a higher predictive value, CVAI is a new index for the evaluation of visceral adipose. Research indicates that among Chinese individuals, CVAI positively correlates with the risk of T2DM (23, 24, 78). The Japanese study indicated a significant association between CVAI and T2DM risk, which further confirmed the efficacy of CVAI in Asia, and was superior to BMI and WC in predicting T2DM. This could be due to the fact that CVAI is a composite of age, BMI, WC, and blood lipids. Therefore, it is superior to a single index. In our study, the AUC of CVAI was smaller than that of TyG-WHtR in middle-aged and older adults in both males (AUC = 0.593, Std. Error = 0.018, 95% CI = 0.559–0.628, and optimal cutoff value = 99.429) and female (AUC = 0.663, Std. Error = 0.014, 95% CI = 0.636–0.691, and optimal cutoff value = 114.005), making CVAI the second-best indicator after TyG-WHtR in this group. A 5-year prospective study in China showed that it was superior to VAI and anthropometric indicators in assessing metabolic risk (79). Similarly, Wei In reviewer *et al.* also found that CVAI outperformed WC, BMI, and ABSI in T2DM screening among Chinese adults (22).

Similarly, LAP is a good predictor of metabolic synthesis. LAP was found to be a strong predictor of insulin resistance (80, 81), indicating a significant relationship between LAP and T2DM. The greatest component in this study's ROC analysis of obesity- and lipid-

associated measurements for females was the AUC of LAP (AUC = 0.643, Std. Error = 0.014, 95% CI = 0.616-0.670, and optimal cut-off = 30.835), which was excepted for the TyG related factors and CVAI.

In this study, 13 obesity- and lipid-related indices were transformed into two categories based on the optimum cut-off point in Table 3. Table 4 is based on the transformed variables. In general, a higher OR indicates a greater risk factor. In Table 4, the ABSI OR was significantly lower than the other 12 indices (OR=1.637 in males and 1.415 in females), after adjustment for all confounding factors. According to ROC analysis, the AUC value of ABSI is lower than the other 12 indices (AUC=0.554 in males and 0.559 in females). Consistent with our research results, Chang et al. also found that in terms of predicting the existence of T2DM among the rural population in Northeast China, compared with BRI, ABSI has the weakest predictive ability (82).

In this study, the relationship between obesity and lipid-associated index and T2DM was discussed. These straightforward and easily measured indicators can assist middle-aged and elderly individuals in implementing early intervention measures, such as lifestyle modifications (balanced diet and appropriate physical activity), to prevent the occurrence of T2DM. Because T2DM is a chronic disease, early detection of potential risk factors and maintaining a healthy lifestyle are key to preventing it. In the field of public health, the results can be used as a reference for clinical practice, public health consultation, and for identifying high-risk groups for prevention.

Strengths and limitations of the study

Our research is based on a nationally representative longitudinal dataset. As far as we know, aging-related diseases are rapidly expanding among the elderly in China, and this is the first cohort study to evaluate the association between 13 obesity and lipid-related indicators and the prevalence of T2DM among the elderly in China. Secondly, the measurement methods of most indicators are simple to operate and can be popularized in clinical practice. In addition, this study included 7902 people aged 45 years and older, a large sample size, which provides a scientific basis and theoretical basis for the prevention and treatment of T2DM. The study does have some limitations. First of all, this study focuses on middle-aged and elderly people in China, and it is difficult to apply the conclusions of this study to elderly people in other countries when there are differences between the East and the West. Second, although we adjusted for multiple influencing factors such as education level, smoking status, drinking status, and chronic diseases, undetected residual factors may alter the relationship between obesity and T2DM or hinder its development.

Conclusions

In conclusion, our findings revealed that T2DM was connected to overall obesity- and lipid-related indicators. Additionally, the TyG-WHtR is the most accurate marker for detecting T2DM in both males and females. CVAI was a good predictor of T2DM in males and females. Our findings highlight the importance of increasing knowledge about T2DM and improving health care.

Data availability statement

The datasets presented in this study can be found in online repositories. The names of the repository/repositories and accession number(s) can be found in the article/supplementary material.

Ethics Statement

All data are openly published as microdata at http://opendata.pku.edu.cn/dataverse/CHARLS with no direct contact with all participants. Approval for this study was given by the medical ethics committee of Wannan medical college (approval number 2021–3).

Author contributions

YW: Writing – original draft, Writing – review & editing. XZ: Writing – review & editing. YQL: Writing – review & editing. JG: Writing – review & editing. YM: Writing – review & editing. XY: Writing – review & editing. HL: Writing – review & editing. L-LG: Writing – review & editing. JLL: Writing – review & editing. YXL: Writing – review & editing. XL: Writing – review & editing. LS: Writing – review & editing. LY: Writing – review & editing. TY: Writing – review & editing. CW: Writing – review & editing. DZ: Writing – review & editing. JL: Writing – review & editing. ML: Writing – review & editing. YH: Writing – review & editing. LZ: Methodology, Writing – review & editing.

Funding

The author(s) declare financial support was received for the research, authorship, and/or publication of this article. CHARLS was supported by the NSFC (70910107022, 71130002) and National Institute on Aging (R03-TW008358-01; R01-AG037031-03S1), and World Bank (7159234) and the Support Program for Outstanding Young Talents from the Universities and Colleges of Anhui Province for Lin Zhang (gxyqZD2021118).

Acknowledgments

We thank the members of the research as well as all participants for their contribution.

Conflict of interest

The authors declare that the research was conducted in the absence of any commercial or financial relationships that could be construed as a potential conflict of interest.

Publisher's note

References

1. Aiken-Morgan AT, Capuano AW, Arvanitakis Z, Barnes LL. Changes in body mass index are related to faster cognitive decline among african american older adults. *J Am Geriatrics Society* (2020) 68(11):2662–7. doi: 10.1111/jgs.16814

2. Diabetes is "a pandemic of unprecedented magnitude" now affecting one in 10 adults worldwide. *Diabetes Res Clin practice* (2021) 181:109133. doi: 10.1016/j.diabres.2021.109133

3. Nishi SK, Viguiliouk E, Kendall CWC, Jenkins DJA, Hu FB, Sievenpiper JL, et al. Nuts in the prevention and management of type 2 diabetes. *Nutrients* (2023) 15(4):878. doi: 10.3390/nu15040878

4. Li M, Jeeyavudeen MS, Arunagirinathan G, Pappachan J. Is type 2 diabetes mellitus a behavioural disorder? An evidence review for type 2 diabetes mellitus prevention and remission through lifestyle modification. *TouchREVIEWS endocrinology* (2023) 19(1):7–15. doi: 10.17925/EE.2023.19.1.7

5. Wu J, Wang Y, Xiao X, Shang X, He M, Zhang L. Spatial analysis of incidence of diagnosed type 2 diabetes mellitus and its association with obesity and physical inactivity. *Front endocrinology* (2021) 12:755575. doi: 10.3389/fendo.2021.755575

6. Jeong SM, Yoo JE, Park J, Jung W, Lee KN, Han K, et al. Smoking behavior change and risk of cardiovascular disease incidence and mortality in patients with type 2 diabetes mellitus. *Cardiovasc diabetology* (2023) 22(1):193. doi: 10.1186/s12933-023-01930-4

7. Cullmann M, Hilding A, Östenson CG. Alcohol consumption and risk of pre-diabetes and type 2 diabetes development in a Swedish population. *Diabetic Med J Br Diabetic Assoc* (2012) 29(4):441–52. doi: 10.1111/j.1464-5491.2011.03450.x

8. Tong Y, Xu S, Huang L, Chen C. Obesity and insulin resistance: Pathophysiology and treatment. *Drug Discovery Today* (2022) 27(3):822–30. doi: 10.1016/j.drudis.2021.11.001

9. Riaz H, Khan MS, Siddiqi TJ, Usman MS, Shah N, Goyal A, et al. Association between obesity and cardiovascular outcomes: A systematic review and meta-analysis of mendelian randomization studies. *JAMA network Open* (2018) 1(7):e183788. doi: 10.1001/jamanetworkopen.2018.3788

10. Ahn N, Baumeister SE, Amann U, Rathmann W, Peters A, Huth C, et al. Visceral adiposity index (VAI), lipid accumulation product (LAP), and product of triglycerides and glucose (TyG) to discriminate prediabetes and diabetes. *Sci Rep* (2019) 9(1):9693. doi: 10.1038/s41598-019-46187-8

11. Calderón-García JF, Roncero-Martín R, Rico-Martín S, De Nicolás-Jiménez JM, López-Espuela F, Santano-Mogena E, et al. Effectiveness of body roundness index (BRI) and a body shape index (ABSI) in predicting hypertension: A systematic review and meta-analysis of observational studies. *Int J Environ Res Public Health* (2021) 18 (21):11607. doi: 10.3390/ijerph182111607

12. Ho RC, Niti M, Kua EH, Ng TP. Body mass index, waist circumference, waist-hip ratio and depressive symptoms in Chinese elderly: a population-based study. *Int J geriatric Psychiatry* (2008) 23(4):401–8. doi: 10.1002/gps.1893

13. Jagadamba. SU. Influence of central obesity assessed by conicity index on lung age in young adults. *J Clin Diagn Res JCDR* (2017) 11(4):Cc09–cc12. doi: 10.7860/JCDR/2017/23428.9718

14. Khatib M, Badillo N, Kahar P, Khanna D. The risk of chronic diseases in individuals responding to a measure for the initial screening of depression and reported feelings of being down, depressed, or hopeless. *Cureus.* (2021) 13(9):e17634. doi: 10.7759/cureus.17634

15. Lu P, Zhang Y, Liu Q, Ding X, Kong W, Zhu L, et al. Association of BMI, diabetes, and risk of tuberculosis: a population-based prospective cohort. *Int J Infect Dis IJID Off Publ Int Soc Infect Diseases* (2021) 109:168–73. doi: 10.1016/j.ijid.2021.06.053

16. Oniszczenko W, Stanisławiak E. Association between sex and body mass index as mediated by temperament in a nonclinical adult sample. *Eating weight Disord EWD* (2019) 24(2):291–8. doi: 10.1007/s40519-018-0617-8

17. Sohn W, Lee HW, Lee S, Lim JH, Lee MW, Park CH, et al. Obesity and the risk of primary liver cancer: A systematic review and meta-analysis. *Clin Mol hepatology* (2021) 27(1):157–74. doi: 10.3350/cmh.2020.0176

18. Lee CM, Huxley RR, Wildman RP, Woodward M. Indices of abdominal obesity are better discriminators of cardiovascular risk factors than BMI: a meta-analysis. *J Clin Epidemiol* (2008) 61(7):646–53. doi: 10.1016/j.jclinepi.2007.08.012

19. Langenberg C, Sharp SJ, Schulze MB, Rolandsson O, Overvad K, Forouhi NG, et al. Long-term risk of incident type 2 diabetes and measures of overall and regional obesity: the EPIC-InterAct case-cohort study. *PloS Med* (2012) 9(6):e1001230. doi: 10.1371/journal.pmed.1001230

20. Nordström A, Hadrévi J, Olsson T, Franks PW, Nordström P. Higher prevalence of type 2 diabetes in men than in women is associated with differences in visceral fat mass. *J Clin Endocrinol Metab* (2016) 101(10):3740–6. doi: 10.1210/jc.2016-1915

21. Cheng YH, Tsao YC, Tzeng IS, Chuang HH, Li WC, Tung TH, et al. Body mass index and waist circumference are better predictors of insulin resistance than total body fat percentage in middle-aged and elderly Taiwanese. *Medicine.* (2017) 96(39):e8126. doi: 10.1097/MD.0000000000008126

22. Wei J, Liu X, Xue H, Wang Y, Shi Z. Comparisons of visceral adiposity index, body shape index, body mass index and waist circumference and their associations with diabetes mellitus in adults. *Nutrients.* (2019) 11(7):1580. doi: 10.3390/nu11071580

23. Wu J, Gong L, Li Q, Hu J, Zhang S, Wang Y, et al. A Novel Visceral Adiposity Index for Prediction of Type 2 Diabetes and Pre-diabetes in Chinese adults: A 5-year prospective study. *Sci Rep* (2017) 7(1):13784. doi: 10.1038/s41598-017-14251-w

24. Xia MF, Lin HD, Chen LY, Wu L, Ma H, Li Q, et al. Association of visceral adiposity and its longitudinal increase with the risk of diabetes in Chinese adults: A prospective cohort study. *Diabetes/metabolism Res Rev* (2018) 34(7):e3048. doi: 10.1002/dmrr.3048

25. Liu EQ, Weng YP, Zhou AM, Zeng CL. Association between triglyceride-glucose index and type 2 diabetes mellitus in the Japanese population: A secondary analysis of a retrospective cohort study. *BioMed Res Int* (2020) 2020:2947067. doi: 10.1155/2020/2947067

26. Zhao Y, Hu Y, Smith JP, Strauss J, Yang G. Cohort profile: the China health and retirement longitudinal study (CHARLS). *Int J Epidemiol* (2014) 43(1):61–8. doi: 10.1093/ije/dys203

27. Zhang L, Li JL, Guo LL, Li H, Li D, Xu G. The interaction between serum uric acid and triglycerides level on blood pressure in middle-aged and elderly individuals in China: result from a large national cohort study. *BMC Cardiovasc Disord* (2020) 20 (1):174. doi: 10.1186/s12872-020-01468-3

28. Zhang L, Li JL, Zhang LL, Guo LL, Li H, Li D. No association between C-reactive protein and depressive symptoms among the middle-aged and elderly in China: Evidence from the China Health and Retirement Longitudinal Study. *Medicine.* (2018) 97(38):e12352. doi: 10.1097/MD.0000000000012352

29. Zhang L, Li JL, Zhang LL, Guo LL, Li H, Li D. Body mass index and serum uric acid level: Individual and combined effects on blood pressure in middle-aged and older individuals in China. *Medicine.* (2020) 99(9):e19418. doi: 10.1097/MD.0000000000019418

30. Zhang L, Li JL, Zhang LL, Guo LL, Li H, Yan W, et al. Relationship between adiposity parameters and cognition: the "fat and jolly" hypothesis in middle-aged and elderly people in China. *Medicine.* (2019) 98(10):e14747. doi: 10.1097/MD.0000000000014747

31. Zhang L, Liu K, Li H, Li D, Chen Z, Zhang LL, et al. Relationship between body mass index and depressive symptoms: the "fat and jolly" hypothesis for the middle-aged and elderly in China. *BMC Public Health* (2016) 16(1):1201. doi: 10.1186/s12889-016-3864-5

32. Zhang L, Yang L, Wang C, Yuan T, Zhang D, Wei H, et al. Individual and combined association analysis of famine exposure and serum uric acid with hypertension in the mid-aged and older adult: a population-based cross-sectional study. *BMC Cardiovasc Disord* (2021) 21(1):420. doi: 10.1186/s12872-021-02230-z

33. Wu X, Gao Y, Wang M, Peng H, Zhang D, Qin B, et al. Atherosclerosis indexes and incident T2DM in middle-aged and older adults: evidence from a cohort study. *Diabetol Metab syndrome* (2023) 15(1):23. doi: 10.1186/s13098-023-00992-4

34. Yang H, Zhang M, Nie J, Zhang M, Lu G, Chen R, et al. Associations of obesity-related indices with prediabetes regression to normoglycemia among Chinese middle-aged and older adults: a prospective study. *Front Nutr* (2023) 10:1075225. doi: 10.3389/fnut.2023.1075225

35. Zhou BF. Effect of body mass index on all-cause mortality and incidence of cardiovascular diseases–report for meta-analysis of prospective studies open optimal cut-off points of body mass index in Chinese adults. *Biomed Environ Sci BES* (2002) 15 (3):245–52.

36. Rato Q. Conicity index: An anthropometric measure to be evaluated. *Rev portuguesa cardiologia orgao oficial da Sociedade Portuguesa Cardiologia = Portuguese J Cardiol an Off J Portuguese Soc Cardiol* (2017) 36(5):365–6. doi: 10.1016/j.repce.2017.04.006

37. Amato MC, Giordano C, Galia M, Criscimanna A, Vitabile S, Midiri M, et al. Visceral Adiposity Index: a reliable indicator of visceral fat function associated with cardiometabolic risk. *Diabetes Care* (2010) 33(4):920–2. doi: 10.2337/dc09-1825

38. Krakauer NY, Krakauer JC. A new body shape index predicts mortality hazard independently of body mass index. *PloS One* (2012) 7(7):e39504. doi: 10.1371/journal.pone.0039504

39. Thomas DM, Bredlau C, Bosy-Westphal A, Mueller M, Shen W, Gallagher D, et al. Relationships between body roundness with body fat and visceral adipose tissue emerging from a new geometrical model. *Obes (Silver Spring Md)* (2013) 21(11):2264–71. doi: 10.1002/oby.20408

40. Zhang FL, Ren JX, Zhang P, Jin H, Qu Y, Yu Y, et al. Strong association of waist circumference (WC), body mass index (BMI), waist-to-height ratio (WHtR), and waist-to-hip ratio (WHR) with diabetes: A population-based cross-sectional study in Jilin Province, China. *J Diabetes Res* (2021) 2021:8812431. doi: 10.1155/2021/8812431

41. Kahn HS. The "lipid accumulation product" performs better than the body mass index for recognizing cardiovascular risk: a population-based comparison. *BMC Cardiovasc Disord* (2005) 5:26. doi: 10.1186/1471-2261-5-26

42. Xia MF, Chen Y, Lin HD, Ma H, Li XM, Aleteng Q, et al. A indicator of visceral adipose dysfunction to evaluate metabolic health in adult Chinese. *Sci Rep* (2016) 6:38214. doi: 10.1038/srep38214

43. Feng X, Wang J, Wang S, Wu S, Wang Z, Wei Y, et al. Correlation analysis of anthropometric indices and type 2 diabetes mellitus in residents aged 60 years and older. *Front Public Health* (2023) 11:1122509. doi: 10.3389/fpubh.2023.1122509

44. Feng Y, Yang X, Li Y, Wu Y, Han M, Qie R, et al. Metabolic Score for Visceral Fat: a novel predictor for the risk of type 2 diabetes mellitus. *Br J Nutr* (2022) 128 (6):1029–36. doi: 10.1017/S0007114521004116

45. Wang L, Cong HL, Zhang JX, Hu YC, Wei A, Zhang YY, et al. Triglyceride-glucose index predicts adverse cardiovascular events in patients with diabetes and acute coronary syndrome. *Cardiovasc diabetology* (2020) 19(1):80. doi: 10.1186/s12933-020-01054-z

46. Galicia-Garcia U, Benito-Vicente A, Jebari S, Larrea-Sebal A, Siddiqi H, Uribe KB, et al. Pathophysiology of type 2 diabetes mellitus. *Int J Mol Sci* (2020) 21(17):6275. doi: 10.3390/ijms21176275

47. Gao R, Meng X, Xue Y, Mao M, Liu Y, Tian X, et al. Bile acids-gut microbiota crosstalk contributes to the improvement of type 2 diabetes mellitus. *Front Pharmacol* (2022) 13:1027212. doi: 10.3389/fphar.2022.1027212

48. Lee YS, Olefsky J. Chronic tissue inflammation and metabolic disease. *Genes Dev* (2021) 35(5-6):307–28. doi: 10.1101/gad.346312.120

49. Hajer GR, van Haeften TW, Visseren FL. Adipose tissue dysfunction in obesity, diabetes, and vascular diseases. *Eur Heart J* (2008) 29(24):2959–71. doi: 10.1093/eurheartj/ehn387

50. Samuel VT, Shulman GI. The pathogenesis of insulin resistance: integrating signaling pathways and substrate flux. *J Clin Invest* (2016) 126(1):12–22. doi: 10.1172/JCI77812

51. Jia W, Weng J, Zhu D, Ji L, Lu J, Zhou Z, et al. Standards of medical care for type 2 diabetes in China 2019. *Diabetes/metabolism Res Rev* (2019) 35(6):e3158. doi: 10.1002/dmrr.3158

52. Guo Y, Zhao J, Zhang Y, Wu L, Yu Z, He D, et al. Triglyceride glucose index influences platelet reactivity in acute ischemic stroke patients. *BMC neurology* (2021) 21(1):409. doi: 10.1186/s12883-021-02443-x

53. Zhao Y, Sun H, Zhang W, Xi Y, Shi X, Yang Y, et al. Elevated triglyceride-glucose index predicts risk of incident ischaemic stroke: The Rural Chinese cohort study. *Diabetes Metab* (2021) 47(4):101246. doi: 10.1016/j.diabet.2021.101246

54. Zhou Y, Pan Y, Yan H, Wang Y, Li Z, Zhao X, et al. Triglyceride glucose index and prognosis of patients with ischemic stroke. *Front neurology* (2020) 11:456. doi: 10.3389/fneur.2020.00456

55. Low S, Pek S, Moh A, Ang K, Khoo J, Shao YM, et al. Triglyceride-glucose index is prospectively associated with chronic kidney disease progression in Type 2 diabetes - mediation by pigment epithelium-derived factor. *Diabetes Vasc Dis Res* (2022) 19 (4):14791641221113784. doi: 10.1177/14791641221113784

56. Xuan X, Hamaguchi M, Cao Q, Okamura T, Hashimoto Y, Obora A, et al. U-shaped association between the triglyceride-glucose index and the risk of incident diabetes in people with normal glycemic level: A population-base longitudinal cohort study. *Clin Nutr (Edinburgh Scotland)* (2021) 40(4):1555–61. doi: 10.1016/j.clnu.2021.02.037

57. Yoon JS, Lee HJ, Jeong HR, Shim YS, Kang MJ, Hwang IT. Triglyceride glucose index is superior biomarker for predicting type 2 diabetes mellitus in children and adolescents. *Endocrine J* (2022) 69(5):559–65. doi: 10.1507/endocrj.EJ21-0560

58. Chamroonkiadtikun P, Ananchaisarp T, Wanichanon W. The triglyceride-glucose index, a predictor of type 2 diabetes development: A retrospective cohort study. *Primary Care diabetes* (2020) 14(2):161–7. doi: 10.1016/j.pcd.2019.08.004

59. Ferreira JRS, Zandonade E, de Paula Alves Bezerra OM, Salaroli LB. Cutoff point of TyG index for metabolic syndrome in Brazilian farmers. *Arch Endocrinol Metab* (2021) 65(6):704–12. doi: 10.20945/2359-3997000000401

60. Sánchez-García A, Rodríguez-Gutiérrez R, Mancillas-Adame L, González-Nava V, Díaz González-Colmenero A, Solis RC, et al. Diagnostic accuracy of the triglyceride and glucose index for insulin resistance: A systematic review. *Int J endocrinology* (2020) 2020:4678526. doi: 10.1155/2020/4678526

61. Ramdas Nayak VK, Satheesh P, Shenoy MT, Kalra S. Triglyceride Glucose (TyG) Index: A surrogate biomarker of insulin resistance. *JPMA J Pakistan Med Assoc* (2022) 72(5):986–8. doi: 10.47391/JPMA.22-63

62. Dikaiakou E, Vlachopapadopoulou EA, Paschou SA, Athanasouli F, Panagiotopoulos I, Kafetzi M, et al. Triglycerides-glucose (TyG) index is a sensitive marker of insulin resistance in Greek children and adolescents. *Endocrine.* (2020) 70 (1):58–64. doi: 10.1007/s12020-020-02374-6

63. Zeng ZY, Liu SX, Xu H, Xu X, Liu XZ, Zhao XX. Association of triglyceride glucose index and its combination of obesity indices with prehypertension in lean individuals: A cross-sectional study of Chinese adults. *J Clin hypertension (Greenwich Conn)* (2020) 22(6):1025–32. doi: 10.1111/jch.13878

64. Zheng S, Shi S, Ren X, Han T, Li Y, Chen Y, et al. Triglyceride glucose-waist circumference, a novel and effective predictor of diabetes in first-degree relatives of type 2 diabetes patients: cross-sectional and prospective cohort study. *J Trans Med* (2016) 14 (1):260. doi: 10.1186/s12967-016-1020-8

65. Kanaya AM, Harris T, Goodpaster BH, Tylavsky F, Cummings SR. Adipocytokines attenuate the association between visceral adiposity and diabetes in older adults. *Diabetes Care* (2004) 27(6):1375–80. doi: 10.2337/diacare.27.6.1375

66. Wu L, Liu H, Cui Z, Hou F, Gong X, Zhang Y, et al. Fluctuations in waist circumference increase diabetes risk: a 4-year cohort study in 61,587 older adults. *Nutr Metab* (2021) 18(1):99. doi: 10.1186/s12986-021-00627-3

67. Smith SR, Lovejoy JC, Greenway F, Ryan D, deJonge L, de la Bretonne J, et al. Contributions of total body fat, abdominal subcutaneous adipose tissue compartments, and visceral adipose tissue to the metabolic complications of obesity. *Metabolism: Clin experimental* (2001) 50(4):425–35. doi: 10.1053/meta.2001.21693

68. Machann J, Thamer C, Schnoedt B, Stefan N, Stumvoll M, Haring HU, et al. Age and gender related effects on adipose tissue compartments of subjects with increased risk for type 2 diabetes: a whole body MRI/MRS study. *Magma (New York NY)* (2005) 18(3):128–37. doi: 10.1007/s10334-005-0104-x

69. Kuang M, Yang R, Huang X, Wang C, Sheng G, Xie G, et al. Assessing temporal differences in the predictive power of baseline TyG-related parameters for future diabetes: an analysis using time-dependent receiver operating characteristics. *J Trans Med* (2023) 21(1):299. doi: 10.1186/s12967-023-04159-7

70. He K, Zhang W, Hu X, Zhao H, Song R, Bai K, et al. Stronger associations of body mass index and waist circumference with diabetes than waist-height ratio and triglyceride glucose index in the middle-aged and elderly population: A retrospective cohort study. *J Diabetes Res* (2022) 2022:9982390. doi: 10.1155/2022/9982390

71. Ge Q, Li M, Xu Z, Qi Z, Zheng H, Cao Y, et al. Comparison of different obesity indices associated with type 2 diabetes mellitus among different sex and age groups in Nantong, China: a cross-section study. *BMC geriatrics* (2022) 22(1):20. doi: 10.1186/s12877-021-02713-w

72. Zhao W, Tong J, Li J, Cao Y. Relationship between body roundness index and risk of type 2 diabetes in Japanese men and women: A reanalysis of a cohort study. *Int J endocrinology* (2021) 2021:4535983. doi: 10.1155/2021/4535983

73. Jayedi A, Soltani S, Motlagh SZ, Emadi A, Shahinfar H, Moosavi H, et al. Anthropometric and adiposity indicators and risk of type 2 diabetes: systematic review and dose-response meta-analysis of cohort studies. *BMJ (Clinical Res ed)* (2022) 376: e067516. doi: 10.1136/bmj-2021-067516

74. Lawal Y, Bello F, Anumah FE, Bakari AG. Waist-height ratio: How well does it predict glucose intolerance and systemic hypertension? *Diabetes Res Clin Pract* (2019) 158:107925. doi: 10.1016/j.diabres.2019.107925

75. Moosaie F, Fatemi Abhari SM, Deravi N, Karimi Behnagh A, Esteghamati S, Dehghani Firouzabadi F, et al. Waist-to-height ratio is a more accurate tool for predicting hypertension than waist-to-hip circumference and BMI in patients with type 2 diabetes: A prospective study. *Front Public Health* (2021) 9:726288. doi: 10.3389/fpubh.2021.726288

76. Tramunt B, Smati S, Grandgeorge N, Lenfant F, Arnal JF, Montagner A, et al. Sex differences in metabolic regulation and diabetes susceptibility. *Diabetologia.* (2020) 63 (3):453–61. doi: 10.1007/s00125-019-05040-3

77. Amato MC, Giordano C, Pitrone M, Galluzzo A. Cut-off points of the visceral adiposity index (VAI) identifying a visceral adipose dysfunction associated with cardiometabolic risk in a Caucasian Sicilian population. *Lipids Health Dis* (2011) 10:183. doi: 10.1186/1476-511X-10-183

78. Han M, Qin P, Li Q, Qie R, Liu L, Zhao Y, et al. Chinese visceral adiposity index: A reliable indicator of visceral fat function associated with risk of type 2 diabetes. *Diabetes/metabolism Res Rev* (2021) 37(2):e3370. doi: 10.1002/dmrr.3370

79. Qiao T, Luo T, Pei H, Yimingniyazi B, Aili D, Aimudula A, et al. Association between abdominal obesity indices and risk of cardiovascular events in Chinese populations with type 2 diabetes: a prospective cohort study. *Cardiovasc diabetology* (2022) 21(1):225. doi: 10.1186/s12933-022-01670-x

80. Anoop SS, Dasgupta R, Rebekah G, Jose A, Inbakumari MP, Finney G, et al. Lipid accumulation product (LAP) as a potential index to predict risk of insulin resistance in young, non-obese Asian Indian males from Southern India: observations from hyperinsulinemic-euglycemic clamp studies. *BMJ Open Diabetes Res Care* (2021) 9(1):e002414. doi: 10.1136/bmjdrc-2021-002414

81. Chen J, Sun H, Qiu S, Tao H, Yu J, Sun Z. Lipid accumulation product combined with urine glucose excretion improves the efficiency of diabetes screening in chinese adults. *Front endocrinology* (2021) 12:691849. doi: 10.3389/fendo.2021.691849

82. Chang Y, Guo X, Chen Y, Guo L, Li Z, Yu S, et al. A body shape index and body roundness index: two new body indices to identify diabetes mellitus among rural populations in northeast China. *BMC Public Health* (2015) 15:794. doi: 10.1186/s12889-015-2150-2

frontiers | Frontiers in Endocrinology

TYPE Original Research
PUBLISHED 10 May 2024
DOI 10.3389/fendo.2024.1374027

OPEN ACCESS

EDITED BY
Kenju Shimomura,
Fukushima Medical University, Japan

REVIEWED BY
Stefano Pagano,
University of Perugia, Italy
Takashi Taguchi,
Western University of Health Sciences, United States

*CORRESPONDENCE
Hongjiao Li
smmulhj@163.com

RECEIVED 21 January 2024
ACCEPTED 02 April 2024
PUBLISHED 10 May 2024

CITATION
Liu X and Li H (2024) Global trends in research on aging associated with periodontitis from 2002 to 2023: a bibliometric analysis.
Front. Endocrinol. 15:1374027.
doi: 10.3389/fendo.2024.1374027

Global trends in research on aging associated with periodontitis from 2002 to 2023: a bibliometric analysis

Xiaomeng Liu and Hongjiao Li*

Department of Stomatology, Xinhua Hospital, Shanghai Jiaotong University School of Medicine, Shanghai, China

Background: Aging has been implicated in many chronic inflammatory diseases, including periodontitis. Periodontitis is an inflammatory disease caused by long-term irritation of the periodontal tissues by the plaque biofilm on the surface of the teeth. However, only a few bibliometric analyses have systematically studied this field to date. This work sought to visualize research hot spots and trends in aging associated with periodontitis from 2002 to 2023 through bibliometric approaches.

Methods: Graphpad prism v8.0.2 was used to analyse and plot annual papers, national publication trends and national publication heat maps. In addition, CtieSpace (6.1.6R (64-bit) Advanced Edition) and VOSviewer (version 1.6.18) were used to analyse these data and visualize the scientific knowledge graph.

Results: The number of documents related to aging associated with periodontitis has steadily increased over 21 years. With six of the top ten institutions in terms of publications coming from the US, the US is a major driver of research in this area. journal of periodontology is the most published journal in the field. Tonetti MS is the most prolific authors and co-cited authors in the field. Journal of Periodontology and Journal of Clinical Periodontology are the most popular journals in the field with the largest literature. Periodontitis, Alzheimer's disease, and peri-implantitis are current hot topics and trends in the field. Inflammation, biomarkers, oxidative stress cytokines are current research hotspots in this field.

Conclusion: Our research found that global publications regarding research on aging associated with periodontitis increased dramatically and were expected to continue increasing. Inflammation and aging, and the relationship between periodontitis and systemic diseases, are topics worthy of attention.

KEYWORDS

periodontitis, bibliometric analysis, data visualization, inflammation, aging

1 Introduction

Periodontitis is an inflammatory disease resulting from infection with periodontal pathogenic microorganisms and dysregulation of the host immune system (1). More than 50% of adults worldwide are affected by different degrees of periodontitis (2, 3). Periodontitis is classified as mild, moderate or severe depending on the degree of inflammation of the disease (4). Severe periodontal tissue damage can lead to aesthetic complications that can be very disturbing to the patient, and new treatment techniques such as laser therapy and digital technology can improve patients' quality of life (5, 6). Aging underlies the pathogenesis of a range of systemic diseases and has a critical effect on the development of chronic inflammatory diseases (7), such as atherosclerosis and autoimmune (8, 9). Numerous studies have shown a close connection between periodontitis and aging (10–12). During the development of periodontitis, the periodontal tissues are attacked by a large number of free radicals, which intensifies oxidative stress and causes oxidative damage to DNA, consequently accelerating telomere shortening. Shortened telomere length can exert cytotoxic effects, leading not only to disruption of epithelial connective tissue continuity, but also to interference with cell growth and differentiation processes. At the same time, persistent stimulation of bacterial-derived lipopolysaccharide affects cellular senescence of osteoblasts, driving alveolar bone resorption (13, 14). In conclusion, Aging may be one of the key risk factors that promote periodontitis progression.

With time changes as well as functional deterioration, the organism develops a number of chronic and age-related conditions. This process is defined as aging (15). Aging affects normal metabolism as well as promotes the progression of inflammatory responses, disrupting bone remodeling and leading to increased levels of bone resorption (16). In addition, aging impairs the organism's immune system, mainly through damaging the physiological function of immune cells and weakening the immune effects of biomolecules. This causes a series of processes of immune senescence, immune activation, and inflammatory responses that ultimately result in older adults being more susceptible to autoimmune, and inflammatory diseases. Decreased immune responsiveness with chronic inflammation, which may accelerate the disease process (17–19). Periodontitis is a chronic inflammatory condition related to alterations in the oral microbiota (20). Notably, localized microecological dysregulation in the oral cavity is often caused by a high-inflammatory state in the host (21). Given that aging is related to a low-level "sterile" inflammatory state with no apparent infection, it is suggested that aging may influence the underlying process of periodontitis (22).

Bibliometrics allows for retrospective reviews to discover the relevance of data and make predictions for the future (23). Bibliometrics is a common method of measuring the academic impact of scientific and technical papers, and a means of demonstrating and encouraging emerging scholarship (24). Bibliometrics and visualization analysis can not only effectively integrate information and enhance understanding of research activities, but also analyze research hotspots and future trends in a certain field (25). In recent decades, Bibliometrics has been broadly used in the field of medicine, including obstetrics and gynecology, orthopedics, complementary medicine, and alternative medicine. It has promoted the development of medical research and clinical practice (26). However, the application of bibliometrics in dentistry is still limited at present, and there is a gap in the study of periodontitis related to aging. For this reason, this work intends to systematically sort out the aging research related to periodontitis, summarize the existing research results at home and abroad, assess their academic impact and characteristics, and provide new design ideas for further research.

2 Methods and materials

Web of Science Core Collection(WoSCC)has better accuracy in labeling literature types than any other database and is considered the best choice for literature analysis, therefore we chose to search in this database. We searched WOS for all articles related to periodontitis and aging from January 1, 2002 to October 25, 2023 with the following search formula (Figure 1): (((TS=(aging)) OR TS=(Senescence)) OR TS=(Biological Aging)) OR TS=(Aging, Biological) AND (((TS=(periodontitis)) OR TS=(Periodontitides)) OR TS=(Pericementitis)) OR TS=(Pericementitides) (Supplementary Table S1). Literature selection inclusion criteria for this study were as follows: (1) the full text of publications related to periodontitis and aging; (2) the articles and reviews manuscript category were in English; and (3) the article was published between January 1, 2002, and October 25, 2023. The criteria for exclusion were as follows (1) the topic was not related to periodontitis and aging, and (2) the article was a conference abstract, news, or briefing

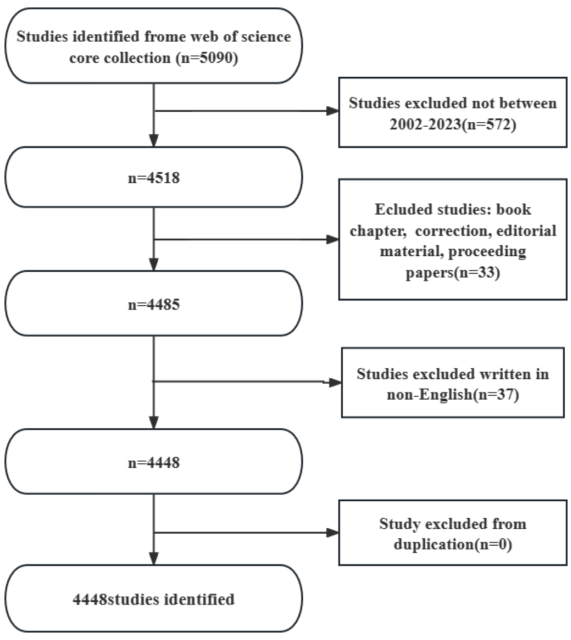

FIGURE 1
Literature screening flowchart.

paper. We exported the plain text version of the paper. Graphpad prism v8.0.2 was used to analyze and plot annual papers, national publication trends, and national publication heat maps. In addition, CtieSpace (6.1.6R (64-bit) Advanced Edition) and VOSviewer (version 1.6.18) were used to analyze these data and visualize the scientific knowledge graph. VOSviewer v.1.6.17, created by Waltman et al. in 2009, is a free JAVA-based software for analyzing large amounts of literature data and displaying it in a map format. In order to visualize the results of research in a particular field by mapping the literature co-citation network, Professor Chaomei Chen created the CiteSpace (6.1.6R) software, which envisions the use of an experimental framework for studying new concepts and evaluating existing technologies. This enables users to better understand areas of knowledge, research frontiers and trends, and to anticipate their future research progress.

3 Result

The results showed that from January 1, 2002 to October 25, 2023, the WoSCC database contained a total of 3,240 publications on periodontitis and aging-related literature, including 2,339 (%) articles and 901 reviews (%). The literature covers 120 countries and regions, 3807 institutions and 19263 authors. From 2002 to 2004, the number of articles per year was less than 100, suggesting that the field was not noticed, and after 2005 the number of articles had a yearly increase, which increased rapidly after 2017 and reached the highest value in 2022. It indicates that the correlation between aging and the progression of periodontitis is receiving widespread attention after 2017 (Figure 2A).

Research related to periodontitis and aging has been conducted in 120 countries and regions. Figures 2B, C show the heat map and line graph of the annual publication volume of the top 10 countries during the past 20 years, and the top 5 countries with the highest publication volume in this field are the United States, Brazil, China, Japan, and Germany. The U.S. accounts for 23.02% of the total number of papers published, which is far more than other countries.

Research related to periodontitis and aging has been conducted in 120 countries and regions. Figures 2B, C show the heat map and line graph of the annual publication volume of the top ten countries during the past 20 years. The top five countries with the highest publication volumes are the United States, Brazil, China, Japan and Germany. The percentage of papers published in the United States is 23.02%, far exceeding that of other countries.

The number of citations for papers published in the United States is 41,954 (Supplementary Table S2), significantly surpassing all other countries/regions. Additionally, the citation/publication ratio (40.97%) places the United States as the second highest globally. Although China has the third highest number of publications, its citation/publication ratio is only 17.26%, the lowest among the ten countries, which suggests that the quality of China's publications is not high. Despite a significant difference in the number of publications compared to the United States, the citation/publication ratio for the United Kingdom (56.03%) ranks first globally. This indicates the superior quality of materials published from the UK. The network of cooperation is shown in Figure 2D, with close cooperation between the US, the largest producer, and Korea and Japan. The US also has cooperative relationships with countries such as China, Germany and the UK. From the heat map of paper publications, it can be observed that since 2002, the United States has published a greater number of articles. However, the number of articles published by China has surged in recent years and caught up with the United States by 2021. The United States not only has a significantly larger number of publications compared to other countries, but its centrality value also reached 0.46, indicating a leadership role in the development of

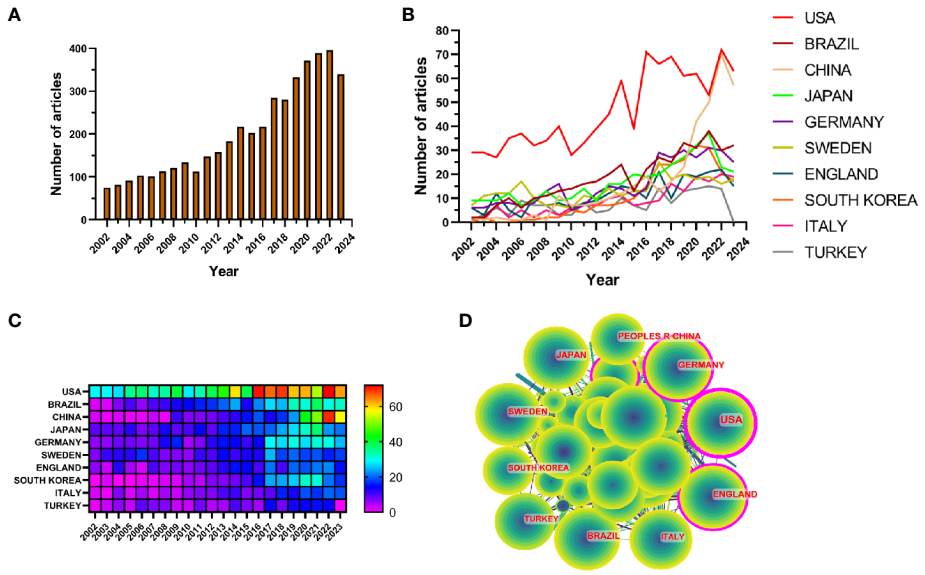

FIGURE 2
(A) Line graph of the volume of communications **(B)** Heat map of national issuances **(C)** Line graph of national issuances **(D)** Map of country cooperation network.

the field. The remaining countries are still in the process of development in this field.

3.1 Institutions

3807 organizations systematically published articles related to periodontitis and aging. Among the top 10 institutions with the highest number of publications, six are from the United States, two from Switzerland, one from Finland and one from South Korea. Karolinska Instiv has published the most literature in this field (116 papers, 3,351 citations, 21.86 citations per paper). Univ Helsinki (105 papers, 3,315 citations, 57.56/paper) ranked second and Univ Washington (86 papers, 8,051 citations, 16.37/paper) ranked third (Figure 4A). It can be seen that institutions between countries prefer to cooperate with their own domestic institutions and there is a lack of international cooperation, so we call for the strengthening of cooperation between domestic and foreign institutions to break down academic barriers.

3.2 Journal

The top 10 journals with the highest number of publications are presented in Supplementary Table S3 and Figure 3A. The *Journal of Periodontology* (522 articles, 11.74%) is the most published journal in this field. It was followed by *journal of clinical periodontology* (461 articles, 10.36%),*journal of periodontal research* (166 articles, 3.73%)和clinical oral investigations (138 articles, 3.10%). Among the 10 most prolific journals, journal of dental research had the highest IF of 7.6. 50% of the journals are categorized as Q1 and the remaining 50% are categorized as Q2.

The impact factor of a journal is determined by the frequency with which it is cited and reflects the significant impact the journal has had on the scientific community. The most cited journal was J PERIODONTOL (3601), followed by J CLIN PERIODONTOL (3466)and J DENT RES (2711) (Supplementary Table S5 and Figure 4B). Among the top 10 most co-cited journals, LANCET was cited 1062 times and had the highest impact factor (168.9). And 60% of the co-cited journals were first quarter journals.

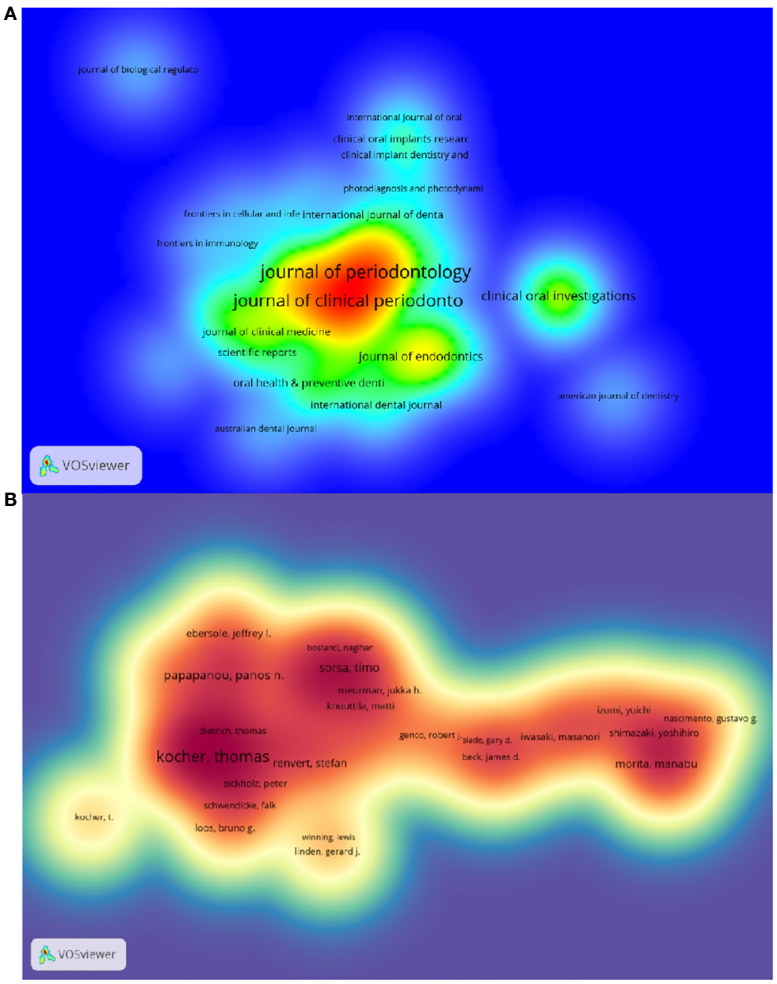

FIGURE 3
(A) Density map of journal postings. **(B)** Density map of author postings.

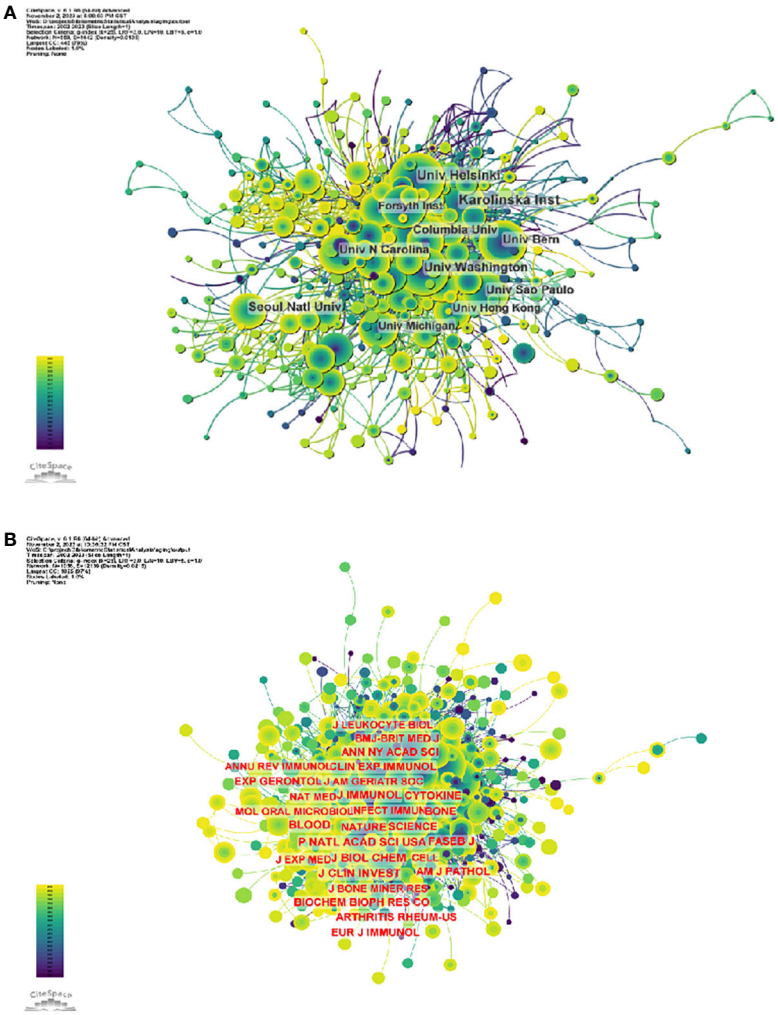

FIGURE 4
(A) Institutional Collaboration Network Diagram **(B)** Journal co-citation network diagram.

The thematic distribution of scholarly publications is shown by a double map overlay (Supplementary Figure S1). The colored tracks indicate citation links, with the citing journal on the left and the cited journal on the right. After analyzing the data, we have identified three primary citation paths, each color-coded for clarity. (1) Research published in molecular/biology/immunology journals is predominantly cited by studies in molecular/biology/genetics and health/nursing/medicine journals. (2) Research reports in medicine/health/clinical research receive the most citations from journals in molecular/biological/genetics, health/nursing/medicine, and dermatology/dentistry/surgery fields. (3) Research reports in the dentistry/dental/surgery field are cited by journals primarily in the medical/immunology field.

The top 10 authors with the highest number of publications related to periodontitis and aging are shown in Table S6 and Figure 3B. These authors have published a total of 276 papers, accounting for 6.21% of the total in the field. Kocher, Thomas (50 papers) published the most research papers, following papapanou, panos n. (31 papers) and holtfreter, birte (28 papers).

Figure 5A and Supplementary Table S1 respectively show the top 10 authors with the highest number of total citations and the highest number of total citations. 78 authors have a total of more than 100 citations, demonstrating the high reputation and impact of their research. The largest nodes are associated with the most co-cited authors, including TONETTI MS (698 citations), EKE PI (672 citations), and PAGE RC (534 citations).

3.3 Commonly cited references

Using a ten-year time slice with a time frame of 2013 to 2023, the co-cited reference network had 1453 nodes and 6745 links (Figure 5B). According to the top 10 most co-cited articles, the JOURNAL OF PERIODONTOLOGY (IF=6.7) entitled “Staging and grading of periodontitis: framework and proposal of a new classification and case definition” (12) was the most co-cited reference with Tonetti MS as the first author. We found that most of the 10 most co-cited articles were foundational literature related to periodontitis and aging.

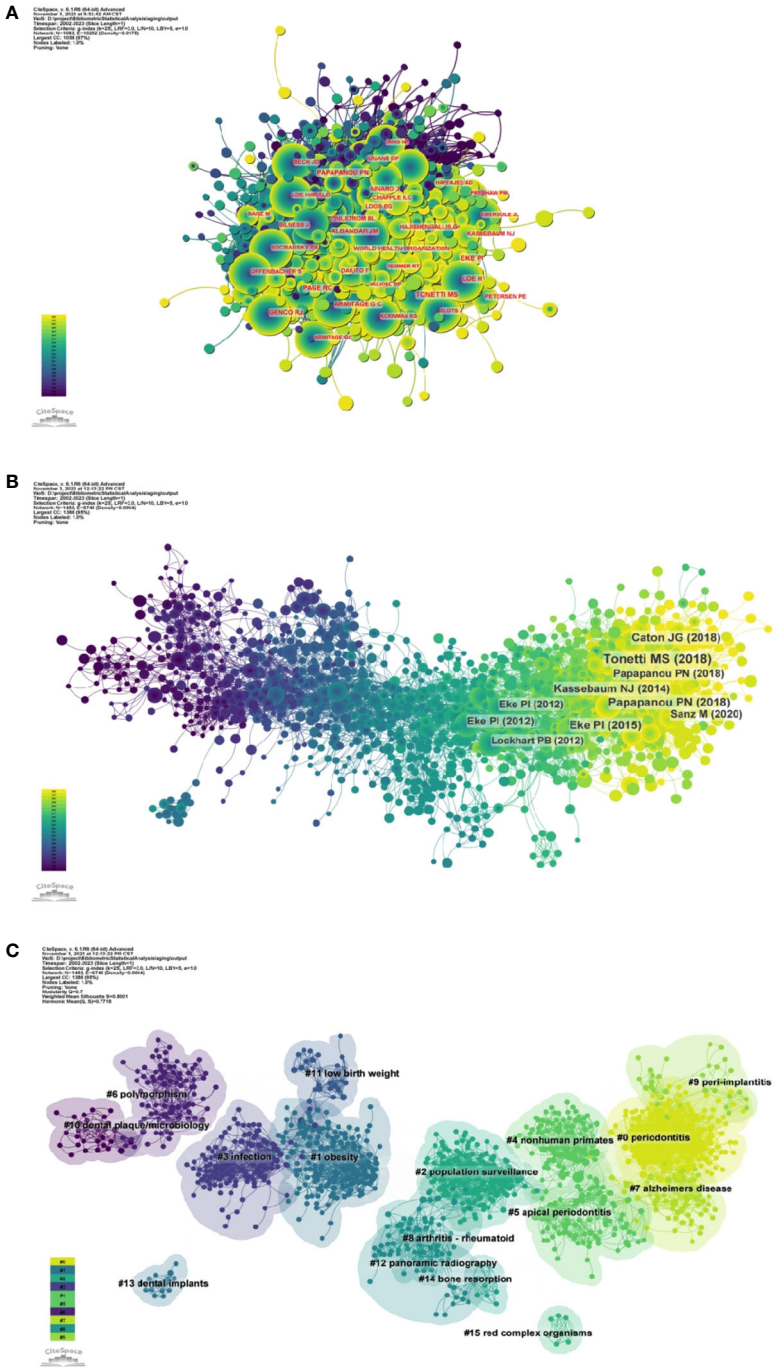

FIGURE 5
(A) Author co-citation network map. **(B)** Network diagram of co-cited literature. **(C)** Clustering map of co-cited literature.

We performed co-citation reference clustering and timeline analysis (Figures 5C, 6). We found that obesity (cluster1), infection (cluster3), polymorphism (cluster6), dental plaque/microbiology (cluster10), and low birth weight (cluster 11) were the population surveillance (cluster2), nonhuman primates (cluster4), apical periodontitis (cluster5), and arthritis-rheumatoid (cluster8), panoramic radiography (cluster12), dental implants (cluster13), and bone resorption (cluster14) are the hotspots of research in the mid-term, while periodontitis (cluster0), alzheimers Periodontitis (cluster0), alzheimers disease (cluster7), and peri-implantitis (cluster9) are the current hot topics and trends in this field.

3.4 Keyword analysis

By analyzing keywords, we can get a quick overview of a field and its direction. According to the co-occurrence of keywords in

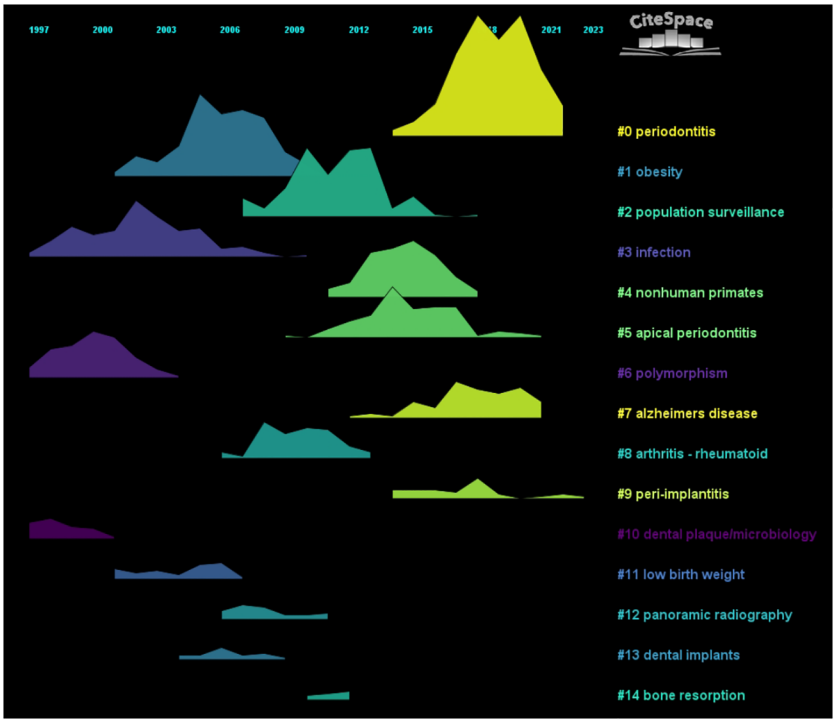

FIGURE 6
Volcano map of co-cited literature.

VOSwiever, the most popular keyword was PREVALENCE (747), followed by RISK (640), INFLAMMATION (600), and HEALTH (489) (Table 1 and Figures 7A, B). We constructed a network containing 217 keywords with at least 30 occurrences (Figure 8), yielding a total of 6 different clusters. Cluster 1 (red) had 76 keywords including inflammation, biomarkers, chronic periodontitis, oxidative stress, peophyromonas-gingivalis, subgingival microbiota, bone loss, cytokines. group 2 (green) has 67 keywords, including prevalence, epidemiology, tooth loss, oral health, global burden, risk-factors, nutrition. group 3 contains 32 keywords (blue), including therapy, dental implants. Includes therapy, dental implants, alveolar bone loss, diagnosis, radiography, apical periodontitis, surgery, management Group 4 contains 26 keywords (in yellow) and includes risk, diabetes, metabolic syndrome, blood pressure, insulin-resistance, c-reactive protein, markers, glycemic control. group 5 contains 11 keywords (purple), including obesity, risk factors, weight, overweight, body-mass-index. group 6 contains 5 keywords (sky blue), including cigarette-smoking, smokers, tobacco smoking, and young-adults. a volcano map to visualize the research hotspots over time (Figure 7C).

3.5 Co-cited references and keyword highlighting

Through CiteSpace, we derived the 50 most reliable citation bursts related to the field of periodontitis and aging (Figure 8). One of them, "Staging and grading of periodontitis: framework and proposal of a new classification and case definition" by Maurizio S. Tonetti (13), the reference with the highest burst intensity (61.64). Forty-eight of the 50 references were published between 2002 and 2023, indicating that these papers have been cited frequently over the past 20 years and that research on periodontitis and aging will remain of interest in the future.

Among the 50 strongest burst keywords in the field, we focused on those that will still be mutating in 2023 (Figure 9), including "cohort study" (7.38 burst intensity), "global burden" (16.64 burst intensity), peri implant disease (24.76 burst intensity), oral microbiome (7.8 bursts), prevention (6.89 bursts), public health (6.82 bursts), classification (55.8 bursts), consensus report (26.23 bursts), 2017 world workshop (14.47 burst intensity), workshop (9.3 burst intensity), cellular senescence (6.95 burst intensity), cary (6.66 burst intensity), oral microbiota (6.55 burst intensity), and periapical lesion (6.33 burst intensity). (6.33 burst intensity).

4 Discussion

In this work, we assessed research trends and hot topics in the field of aging and periodontitis over the last 20 years through bibliometric analysis. We searched 2,339 articles and 901 reviews published from January 1, 2002, to October 25, 2023, respectively. During that research phase, only a few papers were published in the field prior to 2004. The number of papers has increased every year since 2005, rapidly increasing after 2017 and peaking in 2022,

TABLE 1 Table of high-frequency keywords.

Rank	Keyword	Counts	Rank	Keyword	Counts
1	prevalence	747	11	therapy	269
2	risk	640	12	porphyromonas-gingivalis	266
3	inflammation	600	13	chronic periodontitis	265
4	health	489	14	risk-factors	265
5	epidemiology	485	15	gingival crevicular fluid	234
6	tooth loss	435	16	apical periodontitis	228
7	population	376	17	c-reactive protein	226
8	oral-health	323	18	classification	224
9	smoking	319	19	infection	221
10	adults	294	20	obesity	220

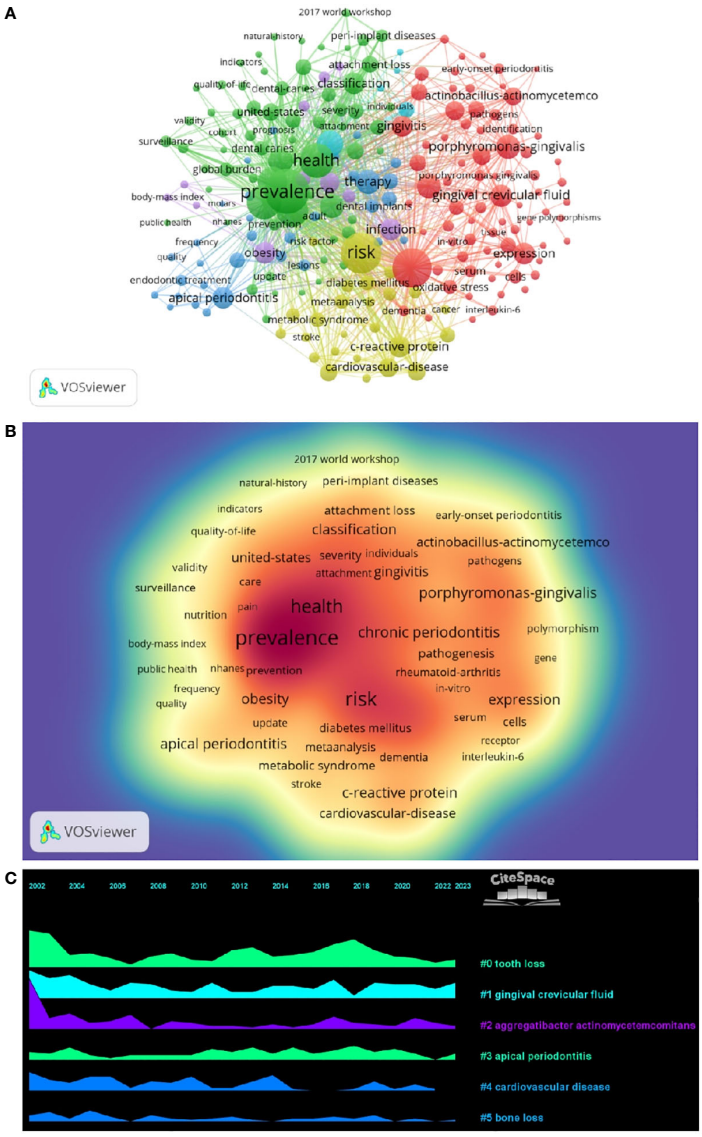

FIGURE 7
(A) Keyword clustering network diagram. **(B)** Keyword Density Map. **(C)** Keyword volcano map.

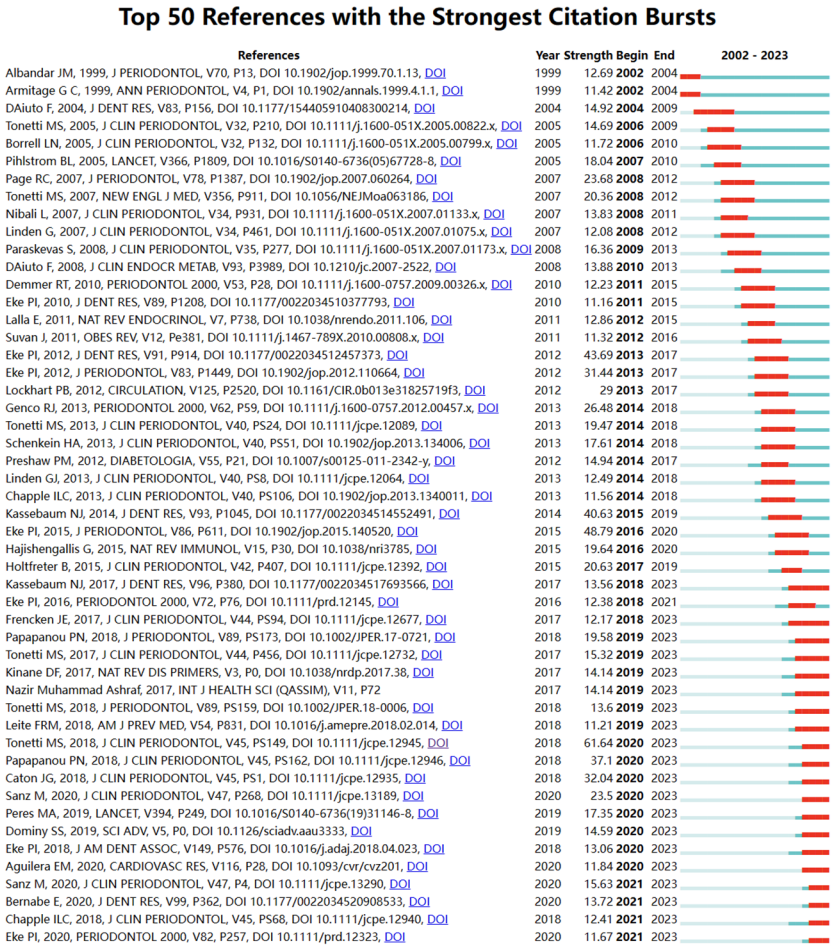

FIGURE 8
Co-cited literature emergence map.

indicating that the field is growing rapidly and maintaining strong research interest. Therefore, we may speculate that research related to aging and periodontitis remains a hot topic for the future.

In the field of periodontitis and aging research, papers published in the United States were cited 41,954 times, far exceeding all other countries/regions, and it also had the second highest citation/number of papers ratio (40.97%). A Although China has the third largest number of papers in this field in the world, its citation/publication ratio is only 17.26%, indicating that the quality of Chinese publications still needs improvement. It is worth noting that although the UK has a low number of publications, its citation/publication ratio (56.03%) is among the highest in the world, indicating the high quality of the material it publishes. The collaboration network indicates close cooperation between the United States, South Korea, and Japan, with the highest number of published papers. According to the heat map, it can be seen that in recent years, the U.S. has had a higher volume of publications since 2002, while China has seen a surge in publications in recent years and is gradually catching up with the U.S. by 2021. The United States not only has a much higher number of publications than other countries but also has a centrality score of 0.46, indicating its leading position in this field. The rest of the countries are far less than the United States, indicating that these countries are still in the process of development in this field.

In terms of institutions, 3807 institutions systematically published articles related to periodontitis and aging. Among the 10 institutions with the highest number of publications, six are from the United States, two from Switzerland, one from Finland, and the other from South Korea. Karolinska Instiv had the most publications in this area (116 papers, 3351 citations, 21.86 citations per paper). Univ Helsinki (105 papers, 3315 citations 57.56 citations/paper) ranked second and Univ Washington (86 papers, 8051 citations, 16.37 citations/paper) ranked third. It can be seen that institutions between countries prefer to cooperate with their own domestic institutions, and there is a lack of international cooperation, so we call for the strengthening of cooperation between domestic and foreign institutions to break down academic barriers. Among all the authors who have published literature related to periodontitis and aging, Table 2 and Figure 5B list the 10 authors who have published the most papers. The top 10 authors have collectively published 276 papers, accounting for 6.21% of all papers in this field. kocher, thomas (50 papers) published the most research papers, following by papapanou, panos n. (31 papers) and holtfreter, birte (28

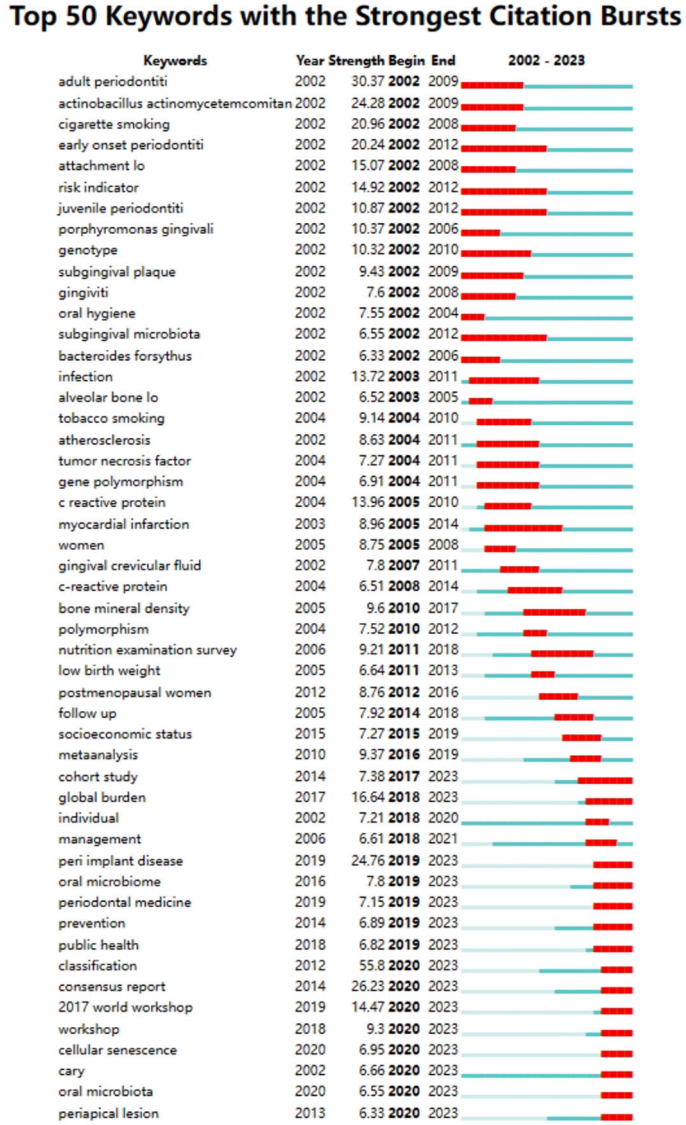

FIGURE 9
Keyword emergence map.

papers). According to the top 10 most co-cited articles (Table 3), the JOURNAL OF PERIODONTOLOGY (IF=6.7) entitled "Staging and grading of periodontitis: framework and proposal of a new classification and case definition" (18) was the most co-cited reference, demonstrating the importance of this journal among periodontal journals, with Tonetti MS as the first author, demonstrating his centrality to the field. We found that most of the 10 most co-cited articles were foundational literature related to periodontitis and aging.

In bibliometric analyses, keyword bursts usually reflect hot topics in the research field (83), and keyword volcano maps can show the evolution of new research hotspots (84, 85). We found that obesity, infection, polymorphism, dental plaque/microbiology, and low birth weight were early research hotspots, population surveillance, nonhuman primates, apical periodontitis, arthritis-rheumatoid, panoramic radiography, dental implants and bone resorption are mid-term hotspots. While periodontitis, alzheimers disease and peri-implantitis are current hot topics and trends in the field. In periodontitis, a large accumulation of microorganisms leads to the recruitment of polymorphonuclear neutrophils to the lesion site within the periodontal pocket. As the first line of defense against pathogens, the recruitment of neutrophils is influenced by various factors, including immune cell cytokines and chemotactic factors (86, 87). Early keyword hotspots reflect the exploration of periodontitis and the mechanisms of aging, and current keywords in the field reflect the aging phenomenon in which the possible link between disease and illness in the aging process and how to prevent and treat it will become a hotspot.

The analysis of co-occurring keywords indicates a close relationship between periodontitis and aging, consistent with previous research findings in recent years (88–90). Aging may trigger a decline in both innate and adaptive immune functions in

TABLE 2 Top 10 literature co-citation table.

Rank	Title	Journal IF(2021)	Author(s)	Total citations
1	Staging and grading of periodontitis: Framework and proposal of a new classification and case definition	JOURNAL OF CLINICAL PERIODONTOLOGY (IF=6.7)	Tonetti, Maurizio S.	239
2	Periodontitis: Consensus report of workgroup 2 of the 2017 World Workshop on the Classification of Periodontal and Peri-Implant Diseases and Conditions	JOURNAL OF CLINICAL PERIODONTOLOGY (IF=6.7)	Tonetti, Maurizio S.	148
3	A new classification scheme for periodontal and peri-implant diseases and conditions - Introduction and key changes from the 1999 classification	JOURNAL OF CLINICAL PERIODONTOLOGY (IF=6.7)	Tonetti, Maurizio S.	125
4	Update on Prevalence of Periodontitis in Adults in the United States: NHANES 2009 to 2012	JOURNAL OF PERIODONTOLOGY (IF=4.3)	Eke, Paul I.	123
5	Global Burden of Severe Periodontitis in 1990-2010: A Systematic Review and Metaregression	JOURNAL OF DENTAL RESEARCH(IF=7.6)	Kassebaum, N. J.	91
6	Prevalence of Periodontitis in Adults in the United States: 2009 and 2010	JOURNAL OF DENTAL RESEARCH(IF=7.6)	Forbes, Josephine M	90
7	Periodontitis: Consensus report of workgroup 2 of the 2017 World Workshop on the Classification of Periodontal and Peri-Implant Diseases and Conditions	JOURNAL OF PERIODONTOLOGY (IF=4.3)	Tonetti, Maurizio S.	80
8	Periodontitis and cardiovascular diseases: Consensus report	JOURNAL OF CLINICAL PERIODONTOLOGY (IF=6.7)	Sanz, Mariano	77
9	Update of the Case Definitions for Population-Based Surveillance of Periodontitis	JOURNAL OF PERIODONTOLOGY (IF=4.3)	Eke, Paul I.	65
10	Periodontal Disease and Atherosclerotic Vascular Disease: Does the Evidence Support an Independent Association? A Scientific Statement From the American Heart Association	CIRCULATION (IF=37.8)	Lockhart, Peter B	60

the body, as well as alterations in the functional efficacy of effector biomolecules, leading to immune aging, immune activation, and inflammatory processes. This may be one of the plausible mechanisms by which aging may lead to increased susceptibility to periodontitis (91). Notably, the *in vivo* microenvironment associated with aging may additionally increase the complexity of defects in innate immunity and adaptive function (92–94). In addition, the close relationship between aging and bone metabolism was analyzed by keywords. Many immune and non-immune cells in periodontal tissue interact with osteoblasts and osteoclasts, which can regulate the balance of physiological bone formation and bone resorption (95, 96). Therefore, bone metabolism is regulated by various factors, including aging. In particular, aging disrupts the balance between bone remodeling and metabolism, leading to increased bone resorption, changes in bone structure, and decreased fracture resistance (16).

Based on results from keyword co-occurrence analysis, we also identified several terms related to systemic diseases, such as Alzheimer's disease, atherosclerosis, and rheumatoid arthritis. These findings are consistent with recent research trends regarding the association between periodontitis and systemic diseases. These complex, multi-factorial diseases share common characteristics with periodontitis, including accelerated aging (97–99).

In recent years, Hajishengallis found that periodontitis can lead to dysbiosis, which is a serious risk to human health. In addition,

TABLE 3 Reported TLR9 -related content.

Drug (optimal dose)	Target	conclusion	References
Erythromycin (DPG3:10μg/ml) Tetracycline (MF1:1 μg/ml)	TLR2, -3, -4, -6, and -9	1.Sensitization of Human Aortic Endothelial Cells to Lipopolysaccharide via Regulation of Toll-Like Receptor 4 by Bacterial Fimbria-Dependent Invasion 2.invasive P. gingivalis infection of primary aortic endothelial cells results in increased TLR expression on the cell surface. 3.priming of endothelial cells by invasive P. gingivalis infection leads to increased binding of PAMPs and the induction of TLR-dependent inflammatory responses	Yumto H, et al, 2005 (69)
P. gingivalis LPS (HPLCs:10 mg/ml)	TLR2 and -4	Gram-negative periodontal bacteria or their LPS might play a role in triggering TLR2 and/or TLR4, and be of importance for the	Sun Y, et al, 2010 (70)

(Continued)

TABLE 3 Continued

Drug (optimal dose)	Target	conclusion	References
		immune responses in periodontitis	
Gingivalis (HGFs)	TLR2,-4 and -9	P. gingivalis infection induces TLR2 and TLR9 upregulation in patients with CP. P. gingivalis–induced TLR2 expression in HGFs is partially dependent on TNF-a and may lead to sensitization of HGFs to bacterial components encountered in the periodontal microenvironment	Wara-aswapati N, et al, 2013 (71)
P. gingivalis LPS (HPDLFs:10mg/L)	TLR2,-4 and MAPK	In hPDLFs, P. gingivalis LPS suppresses bone sialoprotein and enhances IL-8 gene and protein expression via TLR2 and ERK1/2 or the p38 MAPK signaling pathway, respectively.	Zhang Y, et al, 2015 (72)
	TLR2,-4,-5,-7,-9 and IFN-α1	The expression levels of TLR2, -4, -7, and -9 were significantly higher in periodontitis lesions than gingivitis lesions. The expression level of TLR5 was comparable to levels of TLR2 and -4; however, no significant difference was found between gingivitis and periodontitis. Although the expression of IFN-a1 mRNA was higher in periodontitis lesions compared with gingivitis lesions, the level was quite low. Only a few pDCs were found in some periodontitis specimens. No difference was found for antibody-positivity between gingivitis and periodontitis.	Kajita K, et al, 2007 (73)
live P. gingivalis (2x109 CFU)	TLR9	1.TLR9-mediated inflammation promotes P. gingivalis-induced periodontal bone loss. 2.Lack of TLR9 signaling suppresses inflammation in gingival tissues of P. gingivalis-infected mice. 3.Lack of TLR9 signaling leads to decreased cytokine production in splenocytes and macrophages challenged with P. gingivalis.	Kim PD, et al, 2015 (74)

(Continued)

TABLE 3 Continued

Drug (optimal dose)	Target	conclusion	References
		4.Lack of TLR9 signaling affects cytokine production in splenocytes and macrophages challenged with TLR2 and TLR4 agonists.	
	TLR9	The TLR9 haplotype has a protective effect against the development of CP and, in contrast, haplotype can increase the susceptibility of this disease in the Czech population.	Holla LI, et al, 2010 (75)
	TLR-9, AIM2 and DAI	This study is the first report of AIM2 and DAI receptor expression in periodontal tissues and further confirms increased TLR-9 expression, as well as reporting enhanced TLR-8 expression at CP sites.	Sahingur SE, et al. 2013 (76)
	TLR9	Expression of cytokeratin 19 (CK19) was markedly increased in the basement membranes of the oral epithelium and in all layers of the pocket epithelium where it caused evident cell proliferation and migration of sulcular epithelial cells into the lamina propria of periodontitis tissue. TLR4 and the cytoplasmic NLRP3 were expressed in all sections examined regardless of disease state. However, expression of TLR9-,CK19-and collagenolytic matrix metalloproteinase-13 and activated NF-kB subunit p65 was more commonly found in periodontitis tissues than in gingivitis tissues.	Chen YC, et al,2012 (77)
	TLR4, NOD1 and NOD2	Using human peripheral blood monocytes (HPBM) And murine bone-marrow-derived macrophages (BMDM) from wild-type (WT) and Toll-like receptor (TLR)-specific and MyD88 knockouts (KOs), we demonstrated that heat-killed Campylobacter concisus, Campylobacter rectus, Selenomonas infelix, Porphyromonas endodontalis, Porphyromonas	Marchesan J, et al, 2016 (78)

(Continued)

TABLE 3 Continued

Drug (optimal dose)	Target	conclusion	References
		gingivalis, and Tannerella forsythia mediate high immunostimulatory activity. Campylobacter concisus, C. rectus, and S. infelix exhibited robust TLR4 stimulatory activity. Studies using mesothelial cells from WT and NOD1-specific KOs and NOD2-expressing human embryonic kidney cells demonstrated that Eubacterium saphenum, Eubacterium nodatum and Filifactor alocis exhibit robust NOD1 stimulatory activity, and that Porphyromonas endodontalis and Parvimonas micra have the highest NOD2 stimulatory activity. T	
OMVs (HEK-Blue cells)	TLR2,-4,-7,-8,-9,NOD1 and NOD2	P. gingivalis OMVs induced strong TLR2 and TLR4-specific responses and moderate responses in TLR7, TLR8, TLR9, NOD1 and NOD2 expressing-HEK-Blue cells. Responses to T. forsythia OMVs were less than those of P. gingivalis and T. denticola OMVs induced only weak responses.	Cecil JD, et al, 2016 (79)
	TLR1,-2 and -4	Semiquantitative polymerase chain reaction and immunohistochemical analysis demonstrated that of 9 TLRs, the expression of TLR1, TLR2, and TLR4 was markedly enhanced in human atherosclerotic plaques. A considerable proportion of TLR-expressing cells were also activated, as shown by the nuclear translocation of nuclear factor-kB	Edfeldt K, et al, 2002 (80)
	TLR9	CpG DNA binds directly to TLR9 in ligand-binding studies. CpG DNA moves into early endosomes and is subsequently transported to a tubular lysosomal compartment. Concurrent with the movement of CpG DNA in cells, TLR9 redistributes from the ER to CpG DNA–containing structures, which also	Latz E, et al, 2004 (81)

(Continued)

TABLE 3 Continued

Drug (optimal dose)	Target	conclusion	References
		accumulate MyD88. Our data indicate a previously unknown mechanism of cellular activation involving the recruitment of TLR9 from the ER to sites of CpG DNA uptake, where signal transduction is initiated.	
	TLR2,-4 and-9	TLR9 activation by F. nucleatum and TLR2 activation by both bacteria appear to be involved in HIV-1 reactivation; however, TLR4 activation had no effect.	González OA, et al, 2010 (82)

localized treatment of periodontitis may serve as an additional indicator for the reduction of systemic inflammation and concomitant diseases (100, 101). There is substantial evidence suggesting that periodontitis may be influenced by systemic low-grade inflammation (102). Generally, periodontitis shows a bidirectional relationship with systemic inflammatory diseases. Aging is considered as a common factor that may explain the pathophysiological mechanisms underlying various inflammatory diseases (103–105). Therefore, aging may be a critical therapeutic target for inflammatory diseases.

Furthermore, citespace's keyword exploration also helps to reveal future trends. We conclude that macrophage imbalance, oxidative stress may be current research hotspots. Meanwhile, pyroptosis and TLR9 may be potential research directions and targets.

4.1 Macrophage imbalance

Macrophages, as part of the innate immune system, possess high plasticity. When exposed to local stimuli, macrophages can exhibit various active states, which are classified into 2 major subsets, depending on the stimuli: classically activated (M1) and alternatively activated (M2) (106–108). Dysfunction of macrophages has been recognized as a key factor in periodontitis. Understanding the roles of different macrophage phenotypes contributes to the comprehension of potential mechanisms underlying periodontitis and aids in the development of new therapeutic strategies. Pro-inflammatory M1-like macrophages and reparative M2-like macrophages play an important role in inflammation and tissue homeostasis in periodontitis. Periodontal pathogens can induce the differentiation of macrophages into M1 type by stimulating CD14, Toll-like receptors (TLRs), and NOD-like receptors (NLRs) on the surface of macrophages with LPS. M2 macrophages, on the other hand, exert anti-inflammatory effects and play a role in wound healing and tissue repair. In the early

stages of periodontitis, M1 macrophages dominate the infiltration of periodontal tissues, and the proportion of M1 is positively correlated with the progression of periodontal inflammation. There is evidence suggesting an increase in the abundance of M1 macrophages and a decrease in M2 counts in periodontal tissues from patients with periodontitis compared to healthy controls (109–112). During the progression of periodontitis, on one hand, periodontal pathogens may induce an excessive inflammatory response by modulating metabolic pathways to skew macrophage polarization towards M1, while on the other hand, sites of alveolar bone destruction accumulate large numbers of M1 macrophages, leading to the production of IL-1β and TNF-α, upregulation of RANKL expression, and increased bone resorption (113, 114). However, different studies have shown that no alterations in the M1/M2 ratio in periodontal tissues from patients with periodontitis (115, 116). Furthermore, the quantity of M1 macrophages notably decreases during the periodontitis stage. Therefore, in the pathogenesis of periodontitis, it is likely that the roles of M1 pro-inflammatory macrophages and M2 anti-inflammatory macrophages are not as straightforward as previously thought. They exist in a dynamic equilibrium, and disruption of this balance can lead to persistent inflammation (117, 118). During the natural healing process of periodontitis, M1 macrophages are capable of phagocytosing microorganisms and matrix debris. They exhibit a high antigen-presenting capacity during the early stages of healing. Consequently, the number of M1 macrophages increases in the early healing stages and then rapidly declines thereafter. M2 macrophages, on the other hand, peak in numbers during the later stages of healing (118–120). By producing IL-10 and reducing the expression of IL-6, M2 macrophages regulate the functions of Th17 and Treg cells, thereby influencing their anti-inflammatory and reparative properties (121, 122). In addition, the polarization of macrophages also undergoes changes with age. Research indicates that while there is no significant difference in the quantity of macrophages between young and old mice, the expression of M1-related markers, pro-inflammatory cytokines, and chemokines significantly increases in aged mice.[(112, 123) Therefore, the aging immune system may play a crucial role in alveolar bone loss (124). Interventions targeting the aging immune system could emerge as a novel approach to managing periodontitis in elderly patients. Currently, the standard treatment for periodontitis typically involves mechanical removal of disrupted biofilms to control inflammation (125). However, this approach doesn't always successfully halt the progression of the disease. Hence, exploring additional therapeutic targets contributes to the advancement of periodontal treatment. While therapeutic modulation of macrophage phenotypes has not yet been utilized in the treatment of periodontitis patients, inhibiting macrophage polarization to the M1 type or increasing the numbers and ratio of M2 macrophages may alleviate the progression of periodontitis. Therefore, the transition of macrophage phenotypes could potentially serve as a promising therapeutic target for periodontitis treatment, holding significant promise (Table 4).

4.2 Oxidative stress

Oxidative stress is an integral part of the pathogenesis of periodontitis and is the result of an imbalance between the oxidative and antioxidant systems in the body, an over-oxidized state caused by an overproduction of ROS and/or a lack of antioxidant defenses (126). A causal relationship between ROS-mediated oxidative stress and periodontal disease has been demonstrated (127, 128). Studies have shown that the serum levels of superoxide are significantly higher in periodontitis patients, especially in chronic periodontitis, than in healthy individuals. In addition, the levels of malondialdehyde (MDA), a biomarker of lipid peroxidation, and 8-hydroxydeoxyguanosine (8-OHdG), a marker of oxidative DNA damage, were significantly elevated in saliva and gingival sulcus of patients with chronic periodontitis compared with healthy periodontal tissues (3, 129). Oxidative stress induced by the antimicrobial response during periodontitis may be an important cause of tissue damage. ROS play an important role in the pathomechanism of periodontitis.Gram-negative anaerobes colonizing dental plaque trigger the recruitment and activation of neutrophils, which subsequently produce a range of antimicrobial factors during phagocytosis of periodontal pathogens and release an excess of ROS through the NADPH oxidase pathway (130, 131). During phagocytosis, free radicals are the end-products of functional roles played by the mitochondria of polymorphonuclear neutrophils, mainly through lipid peroxidation (132–134). This leads to an oxidative imbalance that triggers a pro-inflammatory mechanism, which in turn promotes osteoclastogenesis, thus leading to alveolar bone resorption in patients with periodontitis (127, 135–139). In addition, reactive oxygen species affect Nuclear factor-erythroid 2-related factor 2 (Nrf2),Nrf2 down-regulation is associated with the progression of periodontitis, and finally, through direct damage to extracellular connective tissues (in addition to the bone itself), the production of reactive oxygen species is responsible for the loss of attachment that leads to periodontal destruction (140, 141).At the same time, reactive oxygen species production activates the NF-κB signaling pathway, which mediates the phosphorylation and degradation of NF-κB inhibitor a of NF-κB (IκBα) and the nuclear translocation of P65, a subunit of NF-κB, which promotes proinflammatory cytokines (such as interleukin-1, interleu-kin-6, and tumor necrosis factor-alpha), which can act directly or indirectly on periodontal tissues to cause bone resorption (142–144).In addition, increased reactive oxygen species disrupt the homeostatic relationship between bone formation and resorption via the RANKL/osteopro-tegerin axis, and thus oxidative stress-mediated inflammation may be one of the pathways leading to the development of periodontal disease. This means that conventional prophylaxis and treatment focusing on bacterial infection-mediated periodontal disease seems to be insufficient, especially when initial periodontal treatment fails to alleviate inflammation, and antioxidant scavenging of ROS to reduce overburdened inflammation is considered to be an effective way to stop the progression of periodontitis (Table 5).

TABLE 4 Reported macrophage polarization-related content.

Drug (optimal dose)	Target	Conclusion	References
	P53	The activation of p53 gene could alleviate periodontitis by reducing M1-type macrophage polarization	Liu, T et al.2024 (27)
Dimethyloxalylglycine (C57BL/6 male mice:1.25 mg/kg)	HIF-1α	Dimethyloxalylglycine Inhibits M1-like Polarization of RAW264.7 Macrophages and Mouse Bone Marrow Macrophages (BMM) for the Treatment of Periodontitis	Chen, Mei-Hua et al.2021 (28)
Leptin (C57BL/6 male mice:40 ug/mouse, Qd, ip)	NLRP3	Leptin aggravates the periodontal response to the ligature by promoting M1 macrophage polarization via the NLRP3 inflammasome	Han, Y et al.2022 (29)
	UCP2	UCP2 controls M1 macrophage activation by modulating reactive oxygen species (ROS) production	Yan, X et al.2020 (30)
	A20	A20 inhibits periodontal bone resorption and NLRP3-mediated M1 macrophage polarization	Hou, Liguang et al.2020 (31)
	miR-143-3p	Inflammatory PDLSCs facilitate M1 macrophage polarization through the exosomal miR-143-3p-mediated regulation of PI3K/AKT/NF-κB signaling, providing a potential new target for periodontitis treatment.	Wang, Yazheng et al.2023 (32)
M2-exos male SD rats		M2-exos drive an appropriate and timely macrophage reprogramming from M1 to M2 type, which resolves chronic inflammation and accelerated periodontal healing.	Cui, Y et al.2023 (33)
Exo-TNF-α (C57BL/6NCrSlc female:20 μ g/ mouse,Qd)		TNF-α stimulation not only increased the amount of exosome secreted from GMSCs, but also enhanced the exosomal expression of CD73, thereby inducing anti-inflammatory M2	Nakao, Y et al.2020 (34)

(Continued)

TABLE 4 Continued

Drug (optimal dose)	Target	Conclusion	References
		macrophage polarization	
Mo-BGC (C57BL/6 mice:0.1μmol/mL)		Induced M2 polarization by enhancing the mitochondrial function of macrophages and promoted a cell metabolic shift from glycolysis toward mitochondrial oxidative phosphorylation.	He, X.T et al.2022 (35)
PDLSCs		PDLSCs were able to induce M2 macrophage polarization instead of M1 polarization, and capable of enhancing M2 macrophage polarization induced by IL-4 and IL-13.	Liu, J et al.2022 (36)
M2-Exo (C57BL/ 6mice:30ul,100 μg/ml)	IL-10/ IL-10R	The reparative M2-like macrophages could promote osteogenesis while inhibiting osteoclastogenesis *in vitro* as well as protect alveolar bone against resorption *in vivo* significantly.	Chen, Xutao et al.2022 (37)
Sulforaphene (SFE) (male C57BL/6 mice:20mg/kg, Qd, ip)	DCIR	SFE effectively inhibits M1 polarization while promoting M2 polarization, ultimately suppressing periodontitis.	Liao, Y et al.2023 (38)
G3@SeHANs (C57BL/6 male mice:30ul, 1 mg/mL)		G3@SeHANs regulates the mononuclear phagocyte system in the periodontitis environment and promotes M2 macrophage phenotype over M1 macrophage phenotype	Huang, H et al.2024 (39)
Interleukin-37 (RAW264.7 cells:50μL,20μg/mL)	NLRP3	IL-37 prevents the progression of periodontitis by suppressing NLRP3 inflammasome activation and mediating M1/M2 macrophage polarization.	Yang, L et al.2024 (40)
Glipizide (C57BL/6 male mice:10 mg/kg, Qd, ig)	.	Glipizide inhibited the LPS-induced migration of BMMs but promoted M2/M1 macrophage ratio in LPS-induced	Guo, Xet al.2023 (41)

(Continued)

TABLE 4 Continued

Drug (optimal dose)	Target	Conclusion	Referen-ces
		BMMs via activation of PI3K/AKT signaling	
Quercetin-Loaded Ceria Nanocomposite Potentiate Dual-Directional Immunoregulation (Rat:50 μg mL -1)		Such nanocomposite can control the phenotypic switch of macrophages by not only inhibition of M1 polarization for suppressing the damage in the destructive phase but also promotion of M2 polarization for regenerating the surrounding tissues in reparative phase of periodontal disease.	Wang, Y et al.2021 (42)
CMC2.24 (Rat Mφ:5 μM)		CMC2.24 appears to be a potent inhibitor of the pro-inflammatory M1 phenotype; and a promotor of the pro-resolving M2 phenotype, thus acting like a crucial "switch" to reduce inflammation.	Deng, J et al.2023 (43)
	RGS12	Knockdown of RGS12 in macrophages promotes macrophage reprogramming to M2 type, and macrophage migration in response to lipopolysaccharide stimulation	Yuan, G et al.2022 (44)
BMSC-sEVs (male SD rats:500 μg/mL)		Promoting periodontal regeneration by modulating transforming growth factor-β1 (TGF-β1) expression and the ratio of type 2 macrophages to type 1 macrophages (M2/M1)	Liu, L et al.2021 (45)

TABLE 5 Reported oxidative stress-related content.

Drug (optimal dose)	Target	conclusion	References
Silibinin (Rat:150 mg/kg)	NrF2	Silibinin exhibits anti-inflammatory and antioxidant properties against periodontitis by upregulating Nrf2 expression	Li, X et al., 2023 (46)
Curcumin (hPDLSCs:0.1 μM)	NrF2	Curcumin could promote the osteogenesis of hPDLSCs, and the	Xiong, Y.et al.2020 (47)

(Continued)

TABLE 5 Continued

Drug (optimal dose)	Target	conclusion	References
		effect is related to the PI3K/AKT/Nrf2 signaling pathway.	
Resveratrol (Rat:5mg/kg Hgfs:50μM)	NrF2	Resveratrol alone augmented HO-1 induction via Nrf2-mediated signaling.	Bhattarai, G.et al.2016 (48)
Metformin (hPDLSCs:100μM)	NrF2	Metformin activates the Nrf2 signaling pathway in PDLSCs, which not only promotes osteogenic differentiation of PDLSCs, but also protects PDLSCs from oxidative stress-induced injury	Jia, L.et al.2020 (49)
Quercetin (hPDLSCs:5 μM)	NrF2	quercetin activated NRF2 signaling in the periodontal ligaments, reduced the OS level of mice with periodontitis, and slowed the absorption of alveolar bone *in vivo*.	Wei, Y. et al.2021 (50)
Four-Octyl itaconate (C57BL/6 male mice:50 mg/kg)	NrF2	Four-Octyl itaconate attenuates inflammation and oxidative stress via disassociation of KEAP1-Nrf2 and activation of Nrf2 signaling cascade.	Xin, L et al.2022 (51)
N-Acetyl-l-cysteine-Derived Carbonized Polymer Dots (C57BL/6 male mice:100mg/kg)	NrF2	N-Acetyl-l-cysteine-Derived Carbonized Polymer Dots may regulate redox homeostasis and promote bone formation in the periodontitis microenvironment by modulating the kelch-like ECH-associated protein l (Keap1)/ nuclear factor erythroid 2-related factor 2 (Nrf2) pathway.	Liu, X et al.2023 (52)
Paeonol (Rat:80 mg/kg)	NrF2	paeonol protected against periodontitis-aggravated osteoclastogenesis and alveolar bone lesion via regulating Nrf2/NF-κB/ NFATc1 signaling pathway.	Li, Y et al.2019 (53)
Baicalein (Rat:200mg/kg)	NrF2	Baicalein attenuates alveolar bone loss by upregulating NRF2	Zhu, C et al.2020 (54)
Chlorogenic acid (Hgfs:40μM)	NrF2	Chlorogenic acid attenuates inflammation in human gingival	Huang, X et al.2022 (55)

(Continued)

TABLE 5 Continued

Drug (optimal dose)	Target	conclusion	References
		fibroblasts, possibly through CysLT1R/Nrf2/NLRP3 signaling.	
Notopterol (C57BL/6 male mice:20 mg/kg)	NrF2	Notopterol alleviates periodontal inflammation by activating the NRF2 signaling pathway	Zhou, J et al.2023 (56)
Epigallocatechin-3-gallate (Rat:200mg/kg)	NrF2	Epigallocatechin-3-gallate inhibits oxidative stress and inflammatory responses in the periodontitis model by modulating the Nrf2/HO-1/NLRP3/NF-κB p65 signaling pathway	Fan, Q et al.2023 (57)

4.3 Pyroptosis

Pyroptosis, a pro-inflammatory programmed cell death dependent on the Gasdermin family of proteins, plays an important role in the regulation of peridontal environmental homeostasis (145). Compared to apoptosis, pyroptosis occurs more rapidly as the cell swells until the membrane ruptures, releasing cellular contents and activating a strong inflammatory response (146, 147). Inflammatory mediators can cause collagen degradation and bone matrix resorption (148), causing destruction of periodontal hard and soft tissues. The initiation of cellular pyroptosis is dependent on the activation of intracellular inflammatory vesicles and their downstream cysteinyl aspartate-specific proteases1 (caspase-1), as well as the production of active fragments of the key pyroptosis protein Gasdermin. The invasion of periodontal pathogens induces an inflammatory response in the host, the molecular mechanism of which involves the activation of multiple inflammatory vesicles and triggers cellular pyroptosis, as well as the release of a large number of inflammatory factors, such as interleukin (IL)-1β, IL-18, and others, which mediate the destruction of periodontal tissues (149). The inflammatory response of periodontopathogenic bacteria in the periodontium is characterized by the release of a wide range of inflammatory factors. There is growing evidence that focal death plays a role in periodontitis pathology, such as Porphyromonas gingivalis, which can induce an inflammatory response through focal death. CASP4/GSDMD triggered by bacterial LPS leads to focal death of periodontal ligament stem cells in periodontitis patients (150). In the early stages of inflammation, gingival epithelial cell pyroptosis disrupts the epithelial barrier by interfering with intercellular junctions. When inflammation progresses, cell pyroptosis can further cause gingival fibroblast death, impaired migration of periodontal fibroblasts, impaired migration of osteoblasts, and active osteoclasts, which will be macroscopically manifested as loss of attachment and alveolar bone resorption. At the same time, the cellular contents released by pyroptosis, such as inflammatory factors and mtROS, can stimulate the production of MMP, causing collagen degradation in gingival and periodontal tissues. In summary elevated levels of focal death in periodontitis promote the secretion of active inflammatory factors (IL-1β, IL-18), which amplifies the inflammatory response and leads to an overactive immune response; this ultimately reduces bone formation, enhances bone resorption by up-regulating RANKL, exacerbates the destruction of periodontal tissues, and inhibits their regeneration. However, the regulation of cellular pyroptosis related to the osteoclastic mechanism needs to be further explored (Table 6).

4.4 TLR9

Periodontitis is a common chronic disease, and its progression may be regulated by interactions between host immunity and periodontal pathogens (151, 152). TLRs are type I transmembrane glycoproteins that belong to the pattern recognition receptor (PRR) class, which recognizes highly conserved structures on the surface of a large number of microorganisms and activates intrinsic immune cells through intercellular signaling pathways, thereby triggering an acquired immune response (153, 154).In recent years, many studies have revealed the ability of TLRs to recognize periodontal pathogens and modulate host innate immune responses to periodontal bacteria, including plasma membrane-associated TLR2, TLR4, and more recently the intrinsic intracellular sensor TLR9 (74, 76, 78, 155). *In vivo* evidence shows that TLR9-deficient (TLR9/) mice are resistant to periodontitis. This provides the first conceptual evidence for the involvement of nucleic acid sensors in periodontitis (101). In addition, TLR9 has been shown to modulate inflammation triggered by TLR2 and TLR4, suggesting possible crosstalk between these sensors during periodontal inflammation via downstream signaling pathways. Recent data suggest that TLR9 is one of the most up-regulated PRRs expressed in chronic periodontitis (156). DNA of the periodontal pathogen Porphyromonas gingivalis promotes its virulence in periodontitis by expressing inflammatory cytokines via the TLR9 signaling pathway (80, 156). TLR9 is present in gingival tissues, and nucleic acids significantly upregulate TLR9 gene expression in patients with periodontitis (76). TLRs signal through two pathways: a MyD88-dependent pathway and a MyD88-independent pathway.TLR9 recognizes viral nucleic acids through a MyD88-dependent pathway. The TLR9 signaling pathway activates the transcription factor NF-κB through inhibition of the nuclear factor-κB (i -κB) kinase (IKK) complex, leading to enhanced NF-κB signaling (157, 158). TLR9 is also present in macrophages and can sense bacterial DNA. in addition the distribution of TLR9 haplotypes and TLR9 (T1486C) genotypes may be associated with chronic periodontitis (75, 159). To model chronic periodontitis, TLR9 knockout mice or wild-type mice were exposed to Porphyromonas gingivalis. The data showed that bone loss was increased in wild-type mice compared with controls (not infected with Porphyromonas gingivalis), and no bone loss was detected in TLR9 knockout mice compared with controls, suggesting that alveolar bone loss in patients with periodontitis may be regulated by TLR9 (74). TLR9

TABLE 6 Reported pyroptosis -related content.

Drug (optimal dose)	Target	conclusion	References
MARK4 inhibitors (OTSSP167 and Compound 50) and small interference RNA)	MARK4	Inhibition of MARK4 decreased LDH release, IL-1β and IL-18 production, ASC speck formation, and the pyroptosis-related genes transcription.	Wang, L et al. (58)
Azgp1 knockout mice	NLRP3/ caspase-1	AZGP1 participates in the pathogenesis of periodontitis by aggravating macrophage M1 polarization and pyroptosis through the NLRP3/caspase-1 pathway.signaling pathway.	Yang, S et al. (59)
Eldecalcitol (Rat:5mg/kg Hgfs:5nM)	NLRP3	ED-71 inhibits cellular pyroptosis by decreasing the activation of NLRP3 inflammatory vesicles.	Huang, C et al. (60)
z-YVAD-FMK (hPDLSCs:2 mM)	caspase-1	The NLRP1 inflammasome led to the activation of caspase-1 and the subsequent activation and releasing of IL-1β, and initiated pyroptosis.	Zhao, D et al. (61)
Construction of DEC2 overexpression vector (RAW 264.7)	caspase-11	Dec2 overexpression reduces levels of IL-1β and sequentially regulates caspase-11, thereby inhibiting pyroptosis.	He, D et al. (62)
Kynurenic (RAW 264.7:100uM)	Caspase1/ NLRP3	Kynurenic significantly suppressed macrophage pyroptosis induced by LPS.	Gao, Y et al. (63)
Construction of TET1 overexpression vector (OCCM-30)	caspase-1	TET1 prevents the onset of cellular pyroptosis by inhibiting caspase-1 activation.	Peng, Y et al. (64)
Isoliquiritigenin (Hgfs:5μM)	NLRP3	Isoliquiritigenin attenuates Porphyromonas gingivalis-induced pyroptosis by inhibiting NLRP3 activation.	Lv, X et al. (65)
N-acetylcysteine (hPDLSCs:10mM)	NF-κB/ Caspase-1	N-acetylcysteine reduces cellular pyroptosis by inhibiting the NF-κB/ Caspase-1 signaling pathway.	Chu, Y et al. (66)
Metformin (mice:200mg/kg)	NEK7/ NLRP3	Metformin reduces cellular pyroptosis by inhibiting theNEK7/ NLRP3 signaling pathway.	Zhou, X et al. (67)
Synoviolin knockout mice	GSDMD	Synoviolin protected against periodontitis by regulating GSDMD	Pang, Y et al. (68)

(Continued)

TABLE 6 Continued

plays a key role in periodontitis, and aberrant expression of TLR9 can be observed in patients with periodontitis, thus TLR9 has the potential to serve as a diagnostic or prognostic biomarker for periodontitis. Understanding the mechanisms by which TLR9 promotes periodontal inflammation could provide important insights into how to control aberrant periodontal inflammation as well as identify therapeutic targets and disease biomarkers that are critical for local and systemic outcomes (Table 3).

This work demonstrates the dynamic evolutionary process and structural relationship between the fields related to periodontitis and aging by knowledge mapping and data visualization, and preliminarily analyzes the research frontiers in this field. This study will provide more theoretical basis for researchers in this field. In conclusion, we should place greater emphasis on research regarding the association between periodontal disease and aging. Additionally, it is important to strengthen communication and collaboration among research institutions to facilitate the development of this field.

Data availability statement

The raw data supporting the conclusions of this article will be made available by the authors, without undue reservation.

Author contributions

XL: Conceptualization, Data curation, Formal analysis, Investigation, Methodology, Software, Visualization, Writing – original draft, Writing – review & editing. HL: Funding acquisition, Supervision, Writing – review & editing.

Funding

The author(s) declare financial support was received for the research, authorship, and/or publication of this article. This study was supported by the National Natural Science Foundation of China (No. 81970938).

Conflict of interest

The authors declare that the research was conducted in the absence of any commercial or financial relationships that could be construed as a potential conflict of interest.

Publisher's note

Supplementary material

The Supplementary Material for this article can be found online at: https://www.frontiersin.org/articles/10.3389/fendo.2024.1374027/full#supplementary-material

SUPPLEMENTARY TABLE 1
Search strategy.

SUPPLEMENTARY TABLE 2
National communications scale.

SUPPLEMENTARY TABLE 3
Institutional issuance scale.

SUPPLEMENTARY TABLE 4
Scale of Journal Publications.

SUPPLEMENTARY FIGURE 1
Double stacked diagram of journals.

SUPPLEMENTARY TABLE 5
Table of Journal Commonly Cited.

SUPPLEMENTARY TABLE 6
Table of authors' publications and top 10 co-cited authors.

References

1. Ebersole JL, Kirakodu SS, Neumann E, Orraca L, Gonzalez Martinez J, Gonzalez OA. Oral microbiome and gingival tissue apoptosis and autophagy transcriptomics. *Front Immunol.* (2020) 11:585414. doi: 10.3389/fimmu.2020.585414

2. Eke PI, Borgnakke WS, Genco RJ. Recent epidemiologic trends in periodontitis in the USA. *Periodontol 2000.* (2020) 82:257–67. doi: 10.1111/prd.12323

3. Chen M, Cai W, Zhao S, Shi L, Chen Y, Li X, et al. Oxidative stress-related biomarkers in saliva and gingival crevicular fluid associated with chronic periodontitis: A systematic review and meta-analysis. *J Clin Periodontol.* (2019) 46:608–22. doi: 10.1111/jcpe.13112

4. Parameter on chronic periodontitis with advanced loss of periodontal support. *J Periodontol.* (2000) 71 Suppl 5S:856–8. doi: 10.1902/jop.2000.71.5-S.856

5. Valenti C, Pagano S, Bozza S, Ciurnella E, Lomurno G, Capobianco B, et al. Use of the er : YAG laser in conservative dentistry: evaluation of the microbial population in carious lesions. *Materials (Basel).* (2021) 14. doi: 10.3390/ma14092387

6. Ortensi L, Sigari G, La Rosa GRM, Ferri A, Grande F, Pedull E. Digital planning of composite customized veneers using Digital Smile Design: Evaluation of its accuracy and manufacturing. *Clin Exp Dent Res.* (2022) 8:537–43. doi: 10.1002/cre2.570

7. Fulop T, Larbi A, Pawelec G, Khalil A, Cohen AA, Hirokawa K, et al. Immunology of aging: the birth of inflammaging. *Clin Rev Allergy Immunol.* (2023) 64:109–22. doi: 10.1007/s12016-021-08899-6

8. Di Micco R, Krizhanovsky V, Baker D, d'Adda di Fagagna F. Cellular senescence in ageing: from mechanisms to therapeutic opportunities. *Nat Rev Mol Cell Biol.* (2021) 22:75–95. doi: 10.1038/s41580-020-00314-w

9. Ebersole JL, Graves CL, Gonzalez OA, Dawson D3rd, Morford LA, Huja PE, et al. Aging, inflammation, immunity and periodontal disease. *Periodontol 2000.* (2016) 72:54–75. doi: 10.1111/prd.12135

10. Eke PI, Dye BA, Wei L, Thornton-Evans GO, Genco RJ. Prevalence of periodontitis in adults in the United States: 2009 and 2010. *J Dent Res.* (2012) 91:914–20. doi: 10.1177/0022034512457373

11. Bertl K, Tangl S, Rybaczek T, Berger B, Traindl-Prohazka M, Schuller-Götzburg P, et al. Prevalence and severity of periodontal disease in a historical Austrian population. *J Periodontal Res.* (2020) 55:931–45. doi: 10.1111/jre.12785

12. Mack F, Mojon P, Budtz-Jørgensen E, Kocher T, Splieth C, Schwahn C, et al. Caries and periodontal disease of the elderly in Pomerania, Germany: results of the Study of Health in Pomerania. *Gerodontology.* (2004) 21:27–36. doi: 10.1046/j.1741-2358.2003.00001.x

13. Baima G, Romandini M, Citterio F, Romano F, Aimetti M. Periodontitis and accelerated biological aging: A geroscience approach. *J Dent Res.* (2022) 101:125–32. doi: 10.1177/00220345211037977

14. Albuquerque-Souza E, Crump KE, Rattanaprukskul K, Li Y, Shelling B, Xia-Juan X, et al. TLR9 mediates periodontal aging by fostering senescence and inflammaging. *J Dent Res.* (2022) 101:1628–36. doi: 10.1177/00220345221110108

15. LL.ez-Ot0. C, Blasco MA, Partridge L, Serrano M, Kroemer G. Hallmarks of aging: An expanding universe. *Cell.* (2023) 186:243–78. doi: 10.1016/j.cell.2022.11.001

16. Demontiero O, Vidal C, Duque G. Aging and bone loss: new insights for the clinician. *Ther Adv Musculoskelet Dis.* (2012) 4:61–76. doi: 10.1177/1759720x11430858

17. Franceschi C, Campisi J. Chronic inflammation (inflammaging) and its potential contribution to age-associated diseases. *J Gerontol A Biol Sci Med Sci.* (2014) 69 Suppl 1: S4–9. doi: 10.1093/gerona/glu057

18. Huttner EA, MaChado DC, de Oliveira RB, Antunes AG, Hebling E. Effects of human aging on periodontal tissues. *Spec Care Dentist.* (2009) 29:149–55. doi: 10.1111/j.1754-4505.2009.00082.x

19. Hajishengallis G. Too old to fight? Aging and its toll on innate immunity. *Mol Oral Microbiol.* (2010) 25:25–37. doi: 10.1111/j.2041-1014.2009.00562.x

20. Boutin S, Hagenfeld D, Zimmermann H, El Sayed N, Höpker T, Greiser HK, et al. Clustering of subgingival microbiota reveals microbial disease ecotypes associated with clinical stages of periodontitis in a cross-sectional study. *Front Microbiol.* (2017) 8:340. doi: 10.3389/fmicb.2017.00340

21. Van Dyke TE. Shifting the paradigm from inhibitors of inflammation to resolvers of inflammation in periodontitis. *J Periodontol.* (2020) 91 Suppl 1:S19–s25. doi: 10.1002/jper.20-0088

22. Franceschi C, Bonafe M, Valensin S, Olivieri F, De Luca M, Ottaviani E, et al. Inflamm-aging. An evolutionary perspective on immunosenescence. *Ann N Y Acad Sci.* (2000) 908:244–54. doi: 10.1111/j.1749-6632.2000.tb06651.x

23. Thompson DF, Walker CK. A descriptive and historical review of bibliometrics with applications to medical sciences. *Pharmacotherapy.* (2015) 35:551–9. doi: 10.1002/phar.1586

24. Akmal M, Hasnain N, Rehan A, Iqbal U, Hashmi S, Fatima K, et al. Glioblastome multiforme: A bibliometric analysis. *World Neurosurg.* (2020) 136:270–82. doi: 10.1016/j.wneu.2020.01.027

25. Ma C, Su H, Li H. Global research trends on prostate diseases and erectile dysfunction: A bibliometric and visualized study. *Front Oncol.* (2020) 10:627891. doi: 10.3389/fonc.2020.627891

26. Wang S, Zhou H, Zheng L, Zhu W, Zhu L, Feng D, et al. Global trends in research of macrophages associated with acute lung injury over past 10 years: A bibliometric analysis. *Front Immunol.* (2021) 12:669539. doi: 10.3389/fimmu.2021.669539

27. Liu T, Chen D, Tang S, Zou Z, Yang F, Zhang Y, et al. P53 alleviates the progression of periodontitis by reducing M1-type macrophage differentiation. *Inflammation.* (2024). doi: 10.1007/s10753-024-01968-w

28. Chen MH, Wang YH, Sun BJ, Yu LM, Chen QQ, Han XX, et al. HIF-1, activator DMOG inhibits alveolar bone resorption in murine periodontitis by regulating macrophage polarization. *Int Immunopharmacol.* (2021) 99:107901. doi: 10.1016/j.intimp.2021.107901

29. Han Y, Huang Y, Gao P, Yang Q, Jia L, Zheng Y, et al. Leptin aggravates periodontitis by promoting M1 polarization via NLRP3. *J Dent Res.* (2022) 101:675–85. doi: 10.1177/00220345211059418

30. Yan X, Yuan Z, Bian Y, Jin L, Mao Z, Lei J, et al. Uncoupling protein-2 regulates M1 macrophage infiltration of gingiva with periodontitis. *Cent Eur J Immunol.* (2020) 45:9–21. doi: 10.5114/ceji.2020.94664

31. Hou L, Ye Y, Gou H, Tang H, Zhou Y, Xu X, et al. A20 inhibits periodontal bone resorption and NLRP3-mediated M1 macrophage polarization. *Exp Cell Res.* (2022) 418:113264. doi: 10.1016/j.yexcr.2022.113264

32. Wang Y, Zhang X, Wang J, Zhang Y, Ye Q, Wang Y, et al. Inflammatory Periodontal Ligament Stem Cells Drive M1 Macrophage Polarization via Exosomal miR-143-3p-Mediated Regulation of PI3K/AKT/NF-ed Signaling. *Stem Cells.* (2023) 41:184–99. doi: 10.1093/stmcls/sxac087

33. Cui Y, Hong S, Xia Y, Li X, He X, Hu X, et al. Melatonin engineering M2 macrophage-derived exosomes mediate endoplasmic reticulum stress and immune

reprogramming for periodontitis therapy. *Adv Sci (Weinh)*. (2023) 10:e2302029. doi: 10.1002/advs.202302029

34. Nakao Y, Fukuda T, Zhang Q, Sanui T, Shinjo T, Kou X, et al. Exosomes from TNF-omes,2/a human gingiva-derived MSCs enhance M2 macrophage polarization and inhibit periodontal bone loss. *Acta Biomater*. (2021) 122:306–24. doi: 10.1016/j.actbio.2020.12.046

35. He XT, Li X, Zhang M, Tian BM, Sun LJ, Bi CS, et al. Role of molybdenum in material immunomodulation and periodontal wound healing: Targeting immunometabolism and mitochondrial function for macrophage modulation. *Biomaterials*. (2022) 283:121439. doi: 10.1016/j.biomaterials.2022.121439

36. Liu J, Wang H, Zhang L, Li X, Ding X, Ding G, et al. Periodontal ligament stem cells promote polarization of M2 macrophages. *J Leukoc Biol*. (2022) 111:1185–97. doi: 10.1002/jlb.1ma1220-853rr

37. Chen X, Wan Z, Yang L, Song S, Fu Z, Tang K, et al. Exosomes derived from reparative M2-like macrophages prevent bone loss in murine periodontitis models via IL-10 mRNA. *J Nanobiotechnol*. (2022) 20:110. doi: 10.1186/s12951-022-01314-y

38. Liao Y, Yan Q, Cheng T, Yao H, Zhao Y, Fu D, et al. Sulforaphene Inhibits Periodontitis through Regulating Macrophage Polarization via Upregulating Dendritic Cell Immunoreceptor. *J Agric Food Chem*. (2023) 71:15538–52. doi: 10.1021/acs.jafc.3c02619

39. Huang H, Pan W, Wang Y, Kim HS, Shao D, Huang B, et al. Nanoparticulate cell-free DNA scavenger for treating inflammatory bone loss in periodontitis. *Nat Commun*. (2022) 13:5925. doi: 10.1038/s41467-022-33492-6

40. Yang L, Tao W, Xie C, Chen Q, Zhao Y, Zhang L, et al. Interleukin-37 ameliorates periodontitis development by inhibiting NLRP3 inflammasome activation and modulating M1/M2 macrophage polarization. *J Periodontal Res*. (2024) 59:128–39. doi: 10.1111/jre.13196

41. Guo X, Huang Z, Ge Q, Yang L, Liang D, Huang Y, et al. Glipizide alleviates periodontitis pathogenicity via inhibition of angiogenesis, osteoclastogenesis and M1/M2 macrophage ratio in periodontal tissue. *Inflammation*. (2023) 46:1917–31. doi: 10.1007/s10753-023-01850-1

42. Wang Y, Li C, Wan Y, Qi M, Chen Q, Sun Y, et al. Quercetin-Loaded Ceria Nanocomposite Potentiate Dual-Directional Immunoregulation via Macrophage Polarization against Periodontal Inflammation. *Small*. (2021) 17:e2101505. doi: 10.1002/smll.202101505

43. Deng J, Golub LM, Lee HM, Bhatt HD, Johnson F, Xu TM, et al. A novel modified-curcumin 2.24 resolves inflammation by promoting M2 macrophage polarization. *Sci Rep*. (2023) 13:15513. doi: 10.1038/s41598-023-42848-x

44. Yuan G, Fu C, Yang ST, Yuh DY, Hajishengallis G, Yang S. RGS12 drives macrophage activation and osteoclastogenesis in periodontitis. *J Dent Res*. (2022) 101:448–57. doi: 10.1177/00220345211045303

45. Liu L, Guo S, Shi W, Liu Q, Huo F, Wu Y, et al. Bone marrow mesenchymal stem cell-derived small extracellular vesicles promote periodontal regeneration. *Tissue Eng Part A*. (2021) 27:962–76. doi: 10.1089/ten.TEA.2020.0141

46. Li X, Zhou R, Han Y, Zeng J, Shi L, Mao Y, et al. Silibinin attenuates experimental periodontitis by downregulation of inflammation and oxidative stress. *Oxid Med Cell Longev*. (2023) 2023:5617800. doi: 10.1155/2023/5617800

47. Xiong Y, Zhao B, Zhang W, Jia L, Zhang Y, Xu X. Curcumin promotes osteogenic differentiation of periodontal ligament stem cells through the PI3K/AKT/Nrf2 signaling pathway. *Iran J Basic Med Sci*. (2020) 23:954–60. doi: 10.22038/ijbms.2020.44070.10351

48. Bhattarai G, Poudel SB, Kook SH, Lee JC. Resveratrol prevents alveolar bone loss in an experimental rat model of periodontitis. *Acta Biomater*. (2016) 29:398–408. doi: 10.1016/j.actbio.2015.10.031

49. Jia L, Xiong Y, Zhang W, Ma X, Xu X. Metformin promotes osteogenic differentiation and protects against oxidative stress-induced damage in periodontal ligament stem cells via activation of the Akt/Nrf2 signaling pathway. *Exp Cell Res*. (2020) 386:111717. doi: 10.1016/j.yexcr.2019.111717

50. Wei Y, Fu J, Wu W, Ma P, Ren L, Yi Z, et al. Quercetin prevents oxidative stress-induced injury of periodontal ligament cells and alveolar bone loss in periodontitis. *Drug Des Devel Ther*. (2021) 15:3509–22. doi: 10.2147/dddt.S315249

51. Xin L, Zhou F, Zhang C, Zhong W, Xu S, Jing X, et al. Four-Octyl itaconate ameliorates periodontal destruction via Nrf2-dependent antioxidant system. *Int J Oral Sci*. (2022) 14:27. doi: 10.1038/s41368-022-00177-1

52. Liu X, Hou Y, Yang M, Xin X, Deng Y, Fu R, et al. N-acetyl-l-cysteine-derived carbonized polymer dots with ROS scavenging via keap1-nrf2 pathway regulate alveolar bone homeostasis in periodontitis. *Adv Healthc Mater*. (2023) 12:e2300890. doi: 10.1002/adhm.202300890

53. Li J, Li Y, Pan S, Zhang L, He L, Niu Y. Paeonol attenuates ligation-induced periodontitis in rats by inhibiting osteoclastogenesis via regulating Nrf2/NF-ngogenesi signaling pathway. *Biochimie*. (2019) 156:129–37. doi: 10.1016/j.biochi.2018.09.004

54. Zhu C, Zhao Y, Wu X, Qiang C, Liu J, Shi J, et al. The therapeutic role of baicalein in combating experimental periodontitis with diabetes via Nrf2 antioxidant signaling pathway. *J Periodontal Res*. (2020) 55:381–91. doi: 10.1111/jre.12722

55. Huang X, Liu Y, Shen H, Fu T, Guo Y, Qiu S. Chlorogenic acid attenuates inflammation in LPS-induced Human gingival fibroblasts via CysLT1R/Nrf2/NLRP3 signaling. *Int Immunopharmacol*. (2022) 107:108706. doi: 10.1016/j.intimp.2022.108706

56. Zhou J, Shi P, Ma R, Xie X, Zhao L, Wang J. Notopterol inhibits the NF-ib pathway and activates the PI3K/akt/nrf2 pathway in periodontal tissue. *J Immunol*. (2023) 211:1516–25. doi: 10.4049/jimmunol.2200727

57. Fan Q, Zhou XH, Wang TF, Zeng FJ, Liu X, Gu Y, et al. Effects of epigallocatechin-3-gallate on oxidative stress, inflammation, and bone loss in a rat periodontitis model. *J Dent Sci*. (2023) 18:1567–75. doi: 10.1016/j.jds.2023.02.019

58. Wang L, Pu W, Wang C, Lei L, Li H. Microtubule affinity regulating kinase 4 promoted activation of the NLRP3 inflammasome-mediated pyroptosis in periodontitis. *J Oral Microbiol*. (2022) 14:2015130. doi: 10.1080/20002297.2021.2015130

59. Yang S, Yin Y, Sun Y, Ai D, Xia X, Xu X, et al. AZGP1 aggravates macrophage M1 polarization and pyroptosis in periodontitis. *J Dent Res*. (2024), 220345241235616. doi: 10.1177/00220345241235616

60. Huang C, Zhang C, Yang P, Chao R, Yue Z, Li C, et al. Eldecalcitol inhibits LPS-induced NLRP3 inflammasome-dependent pyroptosis in human gingival fibroblasts by activating the nrf2/HO-1 signaling pathway. *Drug Des Devel Ther*. (2020) 14:4901–13. doi: 10.2147/dddt.S269223

61. Zhao D, Wu Y, Zhuang J, Xu C, Zhang F. Activation of NLRP1 and NLRP3 inflammasomes contributed to cyclic stretch-induced pyroptosis and release of IL-1a in human periodontal ligament cells. *Oncotarget*. (2016) 7:68292–302. doi: 10.18632/oncotarget.11944

62. He D, Li X, Zhang F, Wang C, Liu Y, Bhawal UK, et al. Dec2 inhibits macrophage pyroptosis to promote periodontal homeostasis. *J Periodontal Implant Sci*. (2022) 52:28–38. doi: 10.5051/jpis.2101380069

63. Gao Y, Guo X, Zhou Y, Du J, Lu C, Zhang L, et al. Kynurenic acid inhibits macrophage pyroptosis by suppressing ROS production via activation of the NRF2 pathway. *Mol Med Rep*. (2023) 28. doi: 10.3892/mmr.2023.13098

64. Peng Y, Wang H, Huang X, Liu H, Xiao J, Wang C, et al. Tet methylcytosine dioxygenase 1 modulates Porphyromonas gingivalis-triggered pyroptosis by regulating glycolysis in cementoblasts. *Ann N Y Acad Sci*. (2023) 1523:119–34. doi: 10.1111/nyas.14979

65. Lv X, Fan C, Jiang Z, Wang W, Qiu X, Ji Q. Isoliquiritigenin alleviates P. gingivalis-LPS/ATP-induced pyroptosis by inhibiting NF-ibi NLRP3/GSDMD signals in human gingival fibroblasts. *Int Immunopharmacol*. (2021) 101:108338. doi: 10.1016/j.intimp.2021.108338

66. Chu Y, Xu Y, Yang W, Chu K, Li S, Guo L. N-acetylcysteine protects human periodontal ligament fibroblasts from pyroptosis and osteogenic differentiation dysfunction through the SIRT1/NF-ontionetimp. signaling pathway. *Arch Oral Biol*. (2023) 148:105642. doi: 10.1016/j.archoralbio.2023.105642

67. Zhou X, Wang Q, Nie L, Zhang P, Zhao P, Yuan Q, et al. Metformin ameliorates the NLPP3 inflammasome mediated pyroptosis by inhibiting the expression of NEK7 in diabetic periodontitis. *Arch Oral Biol*. (2020) 116:104763. doi: 10.1016/j.archoralbio.2020.104763

68. Pang Y, Liu L, Wu S, Wang J, Liu L. Synoviolin alleviates GSDMD-mediated periodontitis by suppressing its stability. *Immun Inflammation Dis*. (2023) 11:e880. doi: 10.1002/iid3.880

69. Yumoto H, Chou HH, Takahashi Y, Davey M, Gibson FC 3rd, Genco CA. Sensitization of human aortic endothelial cells to lipopolysaccharide via regulation of Toll-like receptor 4 by bacterial fimbria-dependent invasion. *Infect Immun*. (2005) 73:8050–9. doi: 10.1128/iai.73.12.8050-8059.2005

70. Sun Y, Shu R, Li CL, Zhang MZ. Gram-negative periodontal bacteria induce the activation of Toll-like receptors 2 and 4, and cytokine production in human periodontal ligament cells. *J Periodontol*. (2010) 81:1488–96. doi: 10.1902/jop.2010.100004

71. Wara-aswapati N, Chayasadom A, Surarit R, Pitiphat W, Boch JA, Nagasawa T, et al. Induction of toll-like receptor expression by Porphyromonas gingivalis. *J Periodontol*. (2013) 84:1010–8. doi: 10.1902/jop.2012.120362

72. Zhang Y, Li X. Lipopolysaccharide-regulated production of bone sialoprotein and interleukin-8 in human periodontal ligament fibroblasts: the role of toll-like receptors 2 and 4 and the MAPK pathway. *J Periodontal Res*. (2015) 50:141–51. doi: 10.1111/jre.12193

73. Kajita K, Honda T, Amanuma R, Domon H, Okui T, Ito H, et al. Quantitative messenger RNA expression of Toll-like receptors and interferon-alpha1 in gingivitis and periodontitis. *Oral Microbiol Immunol*. (2007) 22:398–402. doi: 10.1111/j.1399-302X.2007.00377.x

74. Kim PD, Xia-Juan X, Crump KE, Abe T, Hajishengallis G, Sahingur SE. Toll-like receptor 9-mediated inflammation triggers alveolar bone loss in experimental murine periodontitis. *Infect Immun*. (2015) 83:2992–3002. doi: 10.1128/iai.00424-15

75. Holla LI, Vokurka J, Hrdlickova B, Augustin P, Fassmann A. Association of Toll-like receptor 9 haplotypes with chronic periodontitis in Czech population. *J Clin Periodontol*. (2010) 37:152–9. doi: 10.1111/j.1600-051X.2009.01523.x

76. Sahingur SE, Xia XJ, Voth SC, Yeudall WA, Gunsolley JC. Increased nucleic Acid receptor expression in chronic periodontitis. *J Periodontol*. (2013) 84:e48–57. doi: 10.1902/jop.2013.120739

77. Chen YC, Liu CM, Jeng JH, Ku CC. Association of pocket epithelial cell proliferation in periodontitis with TLR9 expression and inflammatory response. *J Formos Med Assoc*. (2014) 113:549–56. doi: 10.1016/j.jfma.2012.07.043

78. Marchesan J, Jiao Y, Schaff RA, Hao J, Morelli T, Kinney JS, et al. TLR4, NOD1 and NOD2 mediate immune recognition of putative newly identified periodontal pathogens. *Mol Oral Microbiol*. (2016) 31:243–58. doi: 10.1111/omi.12116

79. Cecil JD, O'Brien-Simpson NM, Lenzo JC, Holden JA, Chen YY, Singleton W, et al. Differential responses of pattern recognition receptors to outer membrane vesicles of three periodontal pathogens. *PloS One*. (2016) 11:e0151967. doi: 10.1371/journal.pone.0151967

80. Edfeldt K, Swedenborg J, Hansson GK, Yan ZQ. Expression of toll-like receptors in human atherosclerotic lesions: a possible pathway for plaque activation. *Circulation*. (2002) 105:1158–61.

81. Latz E, Schoenemeyer A, Visintin A, Fitzgerald KA, Monks BG, Knetter CF, et al. TLR9 signals after translocating from the ER to CpG DNA in the lysosome. *Nat Immunol*. (2004) 5:190–8. doi: 10.1038/ni1028

82. González OA, Li M, Ebersole JL, Huang CB. HIV-1 reactivation induced by the periodontal pathogens Fusobacterium nucleatum and Porphyromonas gingivalis involves Toll-like receptor 2 [corrected] and 9 activation in monocytes/macrophages. *Clin Vaccine Immunol*. (2010) 17:1417–27. doi: 10.1128/cvi.00009-10

83. Liu G, Jiang R, Jin Y. Sciatic nerve injury repair: a visualized analysis of research fronts and development trends. *Neural Regener Res*. (2014) 9:1716–22. doi: 10.4103/1673-5374.141810

84. Xiao F, Li C, Sun J, Zhang L. Knowledge domain and emerging trends in organic photovoltaic technology: A scientometric review based on citeSpace analysis. *Front Chem*. (2017) 5:67. doi: 10.3389/fchem.2017.00067

85. Ma L, Ma J, Teng M, Li Y. Visual analysis of colorectal cancer immunotherapy: A bibliometric analysis from 2012 to 2021. *Front Immunol*. (2022) 13:843106. doi: 10.3389/fimmu.2022.843106

86. Graves D. Cytokines that promote periodontal tissue destruction. *J Periodontol*. (2008) 79:1585–91. doi: 10.1902/jop.2008.080183

87. Sczepanik FSC, Grossi ML, Casati M, Goldberg M, Glogauer M, Fine N, et al. Periodontitis is an inflammatory disease of oxidative stress: We should treat it that way. *Periodontol 2000*. (2020) 84:45–68. doi: 10.1111/prd.12342

88. Clark D, Kotronia E, Ramsay SE. Frailty, aging, and periodontal disease: Basic biologic considerations. *Periodontol 2000*. (2021) 87:143–56. doi: 10.1111/prd.12380

89. Tan J, Dai A, Pan L, Zhang L, Wang Z, Ke T, et al. Inflamm-aging-related cytokines of IL-17 and IFN-7 accelerate osteoclastogenesis and periodontal destruction. *J Immunol Res*. (2021) 2021:9919024. doi: 10.1155/2021/9919024

90. Scannapieco FA, Cantos A. Oral inflammation and infection, and chronic medical diseases: implications for the elderly. *Periodontol 2000*. (2016) 72:153–75. doi: 10.1111/prd.12129

91. Hajishengallis G. Aging and its impact on innate immunity and inflammation: implications for periodontitis. *J Oral Biosci*. (2014) 56:30–7. doi: 10.1016/j.job.2013.09.001

92. Krabbe KS, Pedersen M, Bruunsgaard H. Inflammatory mediators in the elderly. *Exp Gerontol*. (2004) 39:687–99. doi: 10.1016/j.exger.2004.01.009

93. LeMaoult J, Szabo P, Weksler ME. Effect of age on humoral immunity, selection of the B-cell repertoire and B-cell development. *Immunol Rev*. (1997) 160:115–26. doi: 10.1111/j.1600-065x.1997.tb01032.x

94. Schou S, Holmstrup P, Kornman KS. Non-human primates used in studies of periodontal disease pathogenesis: a review of the literature. *J Periodontol*. (1993) 64:497–508. doi: 10.1902/jop.1993.64.6.497

95. Feng X, McDonald JM. Disorders of bone remodeling. *Annu Rev Pathol*. (2011) 6:121–45. doi: 10.1146/annurev-pathol-011110-130203

96. Ogura N, Matsuda U, Tanaka F, Shibata Y, Takiguchi H, Abiko Y. *In vitro* senescence enhances IL-6 production in human gingival fibroblasts induced by lipopolysaccharide from Campylobacter rectus. *Mech Ageing Dev*. (1996) 87:47–59. doi: 10.1016/0047-6374(96)01701-0

97. Chen LP, Chiang CK, Chan CP, Hung KY, Huang CS. Does periodontitis reflect inflammation and malnutrition status in hemodialysis patients? *Am J Kidney Dis*. (2006) 47:815–22. doi: 10.1053/j.ajkd.2006.01.018

98. Sanz M, Del Castillo AM, Jepsen S, Gonzalez-Juanatey JR, D'Aiuto F, Bouchard P, et al. Periodontitis and cardiovascular diseases. Consensus report. *Glob Heart*. (2020) 15:1. doi: 10.5334/gh.400

99. Kinane DF, Stathopoulou PG, Papapanou PN. Periodontal diseases. *Nat Rev Dis Primers*. (2017) 3:17038. doi: 10.1038/nrdp.2017.38

100. D'Aiuto F, Parkar M, Andreou G, Suvan J, Brett PM, Ready D, et al. Periodontitis and systemic inflammation: control of the local infection is associated with a reduction in serum inflammatory markers. *J Dent Res*. (2004) 83:156–60. doi: 10.1177/154405910408300214

101. Hajishengallis G. Interconnection of periodontal disease and comorbidities: Evidence, mechanisms, and implications. *Periodontol 2000*. (2022) 89:9–18. doi: 10.1111/prd.12430

102. Pink C, Kocher T, Meisel P, Dörr M, Markus MR, Jablonowski L, et al. Longitudinal effects of systemic inflammation markers on periodontitis. *J Clin Periodontol*. (2015) 42:988–97. doi: 10.1111/jcpe.12473

103. Sharma P, Fenton A, Dias IHK, Heaton B, Brown CLR, Sidhu A, et al. Oxidative stress links periodontal inflammation and renal function. *J Clin Periodontol*. (2021) 48:357–67. doi: 10.1111/jcpe.13414

104. Sari A, Davutoglu V, Bozkurt E, Taner IL, Erciyas K. Effect of periodontal disease on oxidative stress markers in patients with atherosclerosis. *Clin Oral Investig*. (2022) 26:1713–24. doi: 10.1007/s00784-021-04144-8

105. Rodrigues LP, Teixeira VR, Alencar-Silva T, Simonassi-Paiva B, Pereira RW, Pogue R, et al. Hallmarks of aging and immunosenescence: Connecting the dots. *Cytokine Growth Factor Rev*. (2021) 59:9–21. doi: 10.1016/j.cytogfr.2021.01.006

106. Martinez FO, Gordon S. The M1 and M2 paradigm of macrophage activation: time for reassessment. *F1000Prime Rep*. (2014) 6:13. doi: 10.12703/p6-13

107. Gordon S. Alternative activation of macrophages. *Nat Rev Immunol*. (2003) 3:23–35. doi: 10.1038/nri978

108. Zhuang Z, Yoshizawa-Smith S, Glowacki A, Maltos K, Pacheco C, Shehabeldin M, et al. Induction of M2 macrophages prevents bone loss in murine periodontitis models. *J Dent Res*. (2019) 98:200–8. doi: 10.1177/0022034518805984

109. Almubarak A, Tanagala KKK, Papapanou PN, Lalla E, Momen-Heravi F. Disruption of monocyte and macrophage homeostasis in periodontitis. *Front Immunol*. (2020) 11:330. doi: 10.3389/fimmu.2020.00330

110. Sloniak MC, Lepique AP, Nakao LYS, Villar CC. Alterations in macrophage polarization play a key role in control and development of periodontal diseases. *J Indian Soc Periodontol*. (2023) 27:578–82. doi: 10.4103/jisp.jisp_75_23

111. Yamamoto M, Fujihashi K, Hiroi T, McGhee JR, Van Dyke TE, Kiyono H. Molecular and cellular mechanisms for periodontal diseases: role of Th1 and Th2 type cytokines in induction of mucosal inflammation. *J Periodontal Res*. (1997) 32:115–9. doi: 10.1111/j.1600-0765.1997.tb01391.x

112. Yang J, Zhu Y, Duan D, Wang P, Xin Y, Bai L, et al. Enhanced activity of macrophage M1/M2 phenotypes in periodontitis. *Arch Oral Biol*. (2018) 96:234–42. doi: 10.1016/j.archoralbio.2017.03.006

113. Wang W, Zheng C, Yang J, Li B. Intersection between macrophages and periodontal pathogens in periodontitis. *J Leukoc Biol*. (2021) 110:577–83. doi: 10.1002/jlb.4mr0421-756r

114. Mosser DM, Edwards JP. Exploring the full spectrum of macrophage activation. *Nat Rev Immunol*. (2008) 8:958–69. doi: 10.1038/nri2448

115. Li W, Zhang Z, Wang ZM. Differential immune cell infiltrations between healthy periodontal and chronic periodontitis tissues. *BMC Oral Health*. (2020) 20:293. doi: 10.1186/s12903-020-01287-0

116. Zhou LN, Bi CS, Gao LN, An Y, Chen F, Chen FM. Macrophage polarization in human gingival tissue in response to periodontal disease. *Oral Dis*. (2019) 25:265–73. doi: 10.1111/odi.12983

117. Shapouri-Moghaddam A, Mohammadian S, Vazini H, Taghadosi M, Esmaeili SA, Mardani F, et al. Macrophage plasticity, polarization, and function in health and disease. *J Cell Physiol*. (2018) 233:6425–40. doi: 10.1002/jcp.26429

118. Atri C, Guerfali FZ, Laouini D. Role of human macrophage polarization in inflammation during infectious diseases. *Int J Mol Sci*. (2018) 19. doi: 10.3390/ijms19061801

119. Locati M, Curtale G, Mantovani A. Diversity, mechanisms, and significance of macrophage plasticity. *Annu Rev Pathol*. (2020) 15:123–47. doi: 10.1146/annurev-pathmechdis-012418-012718

120. Chen B, Li S, Chang Y, Zhang J, Liu J, Dong Y, et al. Macrophages contribute to periodontal wound healing mainly in the tissue proliferation stage. *J Periodontal Res*. (2023) 58:122–30. doi: 10.1111/jre.13074

121. Ortega-Gga-Gr A, Perretti M, Soehnlein O. Resolution of inflammation: an integrated view. *EMBO Mol Med*. (2013) 5:661–74. doi: 10.1002/emmm.201202382

122. Sun X, Gao J, Meng X, Lu X, Zhang L, Chen R. Polarized macrophages in periodontitis: characteristics, function, and molecular signaling. *Front Immunol*. (2021) 12:763334. doi: 10.3389/fimmu.2021.763334

123. Gibon E, Loi F, Córdova LA, Pajarinen J, Lin T, Lu L, et al. Aging affects bone marrow macrophage polarization: relevance to bone healing. *Regener Eng Transl Med*. (2016) 2:98–104. doi: 10.1007/s40883-016-0016-5

124. Zhou F, Wang Z, Zhang G, Wu Y, Xiong Y. Immunosenescence and inflammaging: Conspiracies against alveolar bone turnover. *Oral Dis*. (2023). doi: 10.1111/odi.14642

125. Pihlstrom BL, Michalowicz BS, Johnson NW. Periodontal diseases. *Lancet*. (2005) 366:1809–20. doi: 10.1016/s0140-6736(05)67728-8

126. Novakovii N, Cakik S, Todorovii T, Raicevii BA, Dozi; I, Petrovii V, et al. Antioxidative status of saliva before and after non-surgical periodontal treatment. *Srp Arh Celok Lek*. (2013) 141:163–8. doi: 10.2298/sarh1304163n

127. Ling MR, Chapple IL, Matthews JB. Neutrophil superoxide release and plasma C-reactive protein levels pre- and post-periodontal therapy. *J Clin Periodontol*. (2016) 43:652–8. doi: 10.1111/jcpe.12575

128. Shin MS, Shin HS, Ahn YB, Kim HD. Association between periodontitis and salivary 8-hydroxydeoxyguanosine among Korean rural adults. *Community Dent Oral Epidemiol*. (2016) 44:381–9. doi: 10.1111/cdoe.12225

129. Ohnishi T, Bandow K, Kakimoto K, Machigashira M, Matsuyama T, Matsuguchi T. Oxidative stress causes alveolar bone loss in metabolic syndrome model mice with type 2 diabetes. *J Periodontal Res*. (2009) 44:43–51. doi: 10.1111/j.1600-0765.2007.01060.x

130. Chapple IL, Matthews JB. The role of reactive oxygen and antioxidant species in periodontal tissue destruction. *Periodontol 2000*. (2007) 43:160–232. doi: 10.1111/j.1600-0757.2006.00178.x

131. Ramesh A, Varghese SS, Doraiswamy JN, Malaiappan S. Herbs as an antioxidant arsenal for periodontal diseases. *J Intercult Ethnopharmacol*. (2016) 5:92–6. doi: 10.5455/jice.20160122065556

132. Baňasová L, Kamodyov4 N, Janodyov4 K, T.;odyo Ľ, Stanko P, Turnk J, et al. Salivary DNA and markers of oxidative stress in patients with chronic periodontitis. *Clin Oral Investig*. (2015) 19:201–7. doi: 10.1007/s00784-014-1236-z

133. Su H, Gornitsky M, Velly AM, Yu H, Benarroch M, Schipper HM. Salivary DNA, lipid, and protein oxidation in nonsmokers with periodontal disease. *Free Radic Biol Med*. (2009) 46:914–21. doi: 10.1016/j.freeradbiomed.2009.01.008

134. Konopka T, Kr;o K, Kopep W, Gerber H. Total antioxidant status and 8-hydroxy-2'-deoxyguanosine levels in gingival and peripheral blood of periodontitis patients. *Arch Immunol Ther Exp (Warsz)*. (2007) 55:417–22. doi: 10.1007/s00005-007-0047-1

135. Yin KJ, Huang JX, Wang P, Yang XK, Tao SS, Li HM, et al. No genetic causal association between periodontitis and arthritis: A bidirectional two-sample mendelian randomization analysis. *Front Immunol*. (2022) 13:808832. doi: 10.3389/fimmu.2022.808832

136. Bartold PM, Marshall RI, Haynes DR. Periodontitis and rheumatoid arthritis: a review. *J Periodontol*. (2005) 76:2066–74. doi: 10.1902/jop.2005.76.11-S.2066

137. Boyce BF, Xing L. Biology of RANK, RANKL, and osteoprotegerin. *Arthritis Res Ther*. (2007) 9 Suppl 1:S1. doi: 10.1186/ar2165

138. Belibasakis GN, Bostanci N. The RANKL-OPG system in clinical periodontology. *J Clin Periodontol*. (2012) 39:239–48. doi: 10.1111/j.1600-051X.2011.01810.x

139. Baltaccltac E, Yuva P, Ayda,c G, Alver A, Kahraman C, Karabulut E, et al. Lipid peroxidation levels and total oxidant/antioxidant status in serum and saliva from patients with chronic and aggressive periodontitis. Oxidative stress index: a new biomarker for periodontal disease? *J Periodontol*. (2014) 85:1432–41. doi: 10.1902/jop.2014.130654

140. Ikeda E, Ikeda Y, Wang Y, Fine N, Sheikh Z, Viniegra A, et al. Resveratrol derivative-rich melinjo seed extract induces healing in a murine model of established periodontitis. *J Periodontol*. (2018) 89:586–95. doi: 10.1002/jper.17-0352

141. Chiu AV, Saigh MA, McCulloch CA, Glogauer M. The role of nrF2 in the regulation of periodontal health and disease. *J Dent Res*. (2017) 96:975–83. doi: 10.1177/0022034517715007

142. Vo TTT, Chu PM, Tuan VP, Te JS, Lee IT. The promising role of antioxidant phytochemicals in the prevention and treatment of periodontal disease via the inhibition of oxidative stress pathways: updated insights. *Antioxid (Basel)*. (2020) 9. doi: 10.3390/antiox9121211

143. Kanzaki H, Wada S, Narimiya T, Yamaguchi Y, Katsumata Y, Itohiya K, et al. Pathways that regulate ROS scavenging enzymes, and their role in defense against tissue destruction in periodontitis. *Front Physiol*. (2017) 8:351. doi: 10.3389/fphys.2017.00351

144. Wei SJ, Zhang Q, Xiang YJ, Peng LY, Peng W, Ren Q, et al. Guizhi-Shaoyao-Zhimu decoction attenuates bone erosion in rats that have collagen-induced arthritis via modulating NF-ul signalling to suppress osteoclastogenesis. *Pharm Biol*. (2021) 59:262–74. doi: 10.1080/13880209.2021.1876100

145. Quirke AM, Lugli EB, Wegner N, Hamilton BC, Charles P, Chowdhury M, et al. Heightened immune response to autocitrullinated Porphyromonas gingivalis peptidylarginine deiminase: a potential mechanism for breaching immunologic tolerance in rheumatoid arthritis. *Ann Rheum Dis*. (2014) 73:263–9. doi: 10.1136/annrheumdis-2012-202726

146. Mei YM, Li L, Wang XQ, Zhang M, Zhu LF, Fu YW, et al. AGEs induces apoptosis and autophagy via reactive oxygen species in human periodontal ligament cells. *J Cell Biochem*. (2020) 121:3764–79. doi: 10.1002/jcb.29499

147. Shi J, Gao W, Shao F. Pyroptosis: gasdermin-mediated programmed necrotic cell death. *Trends Biochem Sci*. (2017) 42:245–54. doi: 10.1016/j.tibs.2016.10.004

148. Franco C, Patricia HR, Timo S, Claudia B, Marcela H. Matrix metalloproteinases as regulators of periodontal inflammation. *Int J Mol Sci*. (2017) 18. doi: 10.3390/ijms18020440

149. Bostanci N, Emingil G, Saygan B, Turkoglu O, Atilla G, Curtis MA, et al. Expression and regulation of the NALP3 inflammasome complex in periodontal diseases. *Clin Exp Immunol*. (2009) 157:415–22. doi: 10.1111/j.1365-2249.2009.03972.x

150. Chen Q, Liu X, Wang D, Zheng J, Chen L, Xie Q, et al. Periodontal inflammation-triggered by periodontal ligament stem cell pyroptosis exacerbates periodontitis. *Front Cell Dev Biol*. (2021) 9:663037. doi: 10.3389/fcell.2021.663037

151. O'Brien-Simpson NM, Pathirana RD, Paolini RA, Chen YY, Veith PD, Tam V, et al. An immune response directed to proteinase and adhesin functional epitopes protects against Porphyromonas gingivalis-induced periodontal bone loss. *J Immunol*. (2005) 175:3980–9. doi: 10.4049/jimmunol.175.6.3980

152. Sorsa T, Tervahartiala T, Leppilahti J, Hernandez M, Gamonal J, Tuomainen AM, et al. Collagenase-2 (MMP-8) as a point-of-care biomarker in periodontitis and cardiovascular diseases. Therapeutic response to non-antimicrobial properties of tetracyclines. *Pharmacol Res*. (2011) 63:108–13. doi: 10.1016/j.phrs.2010.10.005

153. Flórez-Álvarez L, Ruiz-Perez L, Taborda N, Hernandez JC. Toll-like receptors as a therapeutic target in cancer, infections and inflammatory diseases. *Immunotherapy*. (2020) 12:311–22. doi: 10.2217/imt-2019-0096

154. Kumar V. Toll-like receptors in adaptive immunity. *Handb Exp Pharmacol*. (2022) 276:95–131. doi: 10.1007/164_2021_543

155. Crump KE, Sahingur SE. Microbial nucleic acid sensing in oral and systemic diseases. *J Dent Res*. (2016) 95:17–25. doi: 10.1177/0022034515609062

156. Crump KE, Oakley JC, Xia-Juan X, Madu TC, Devaki S, Mooney EC, et al. Interplay of toll-like receptor 9, myeloid cells, and deubiquitinase A20 in periodontal inflammation. *Infect Immun*. (2017) 85. doi: 10.1128/iai.00814-16

157. O'Neill LA. When signaling pathways collide: positive and negative regulation of toll-like receptor signal transduction. *Immunity*. (2008) 29:12–20. doi: 10.1016/j.immuni.2008.06.004

158. Karapetyan L, Luke JJ, Davar D. Toll-like receptor 9 agonists in cancer. *Onco Targets Ther*. (2020) 13:10039–60. doi: 10.2147/ott.S247050

159. Sahingur SE, Xia XJ, Gunsolley J, Schenkein HA, Genco RJ, De Nardin E. Single nucleotide polymorphisms of pattern recognition receptors and chronic periodontitis. *J Periodontal Res*. (2011) 46:184–92. doi: 10.1111/j.1600-0765.2010.01327.x

frontiers | Frontiers in Endocrinology

TYPE Original Research
PUBLISHED 11 June 2024
DOI 10.3389/fendo.2024.1380779

OPEN ACCESS

EDITED BY
Fumihiko Maekawa,
National Institute for Environmental Studies (NIES), Japan

REVIEWED BY
Toyoshi Umezu,
National Institute for Environmental Studies (NIES), Japan
Nang Thinn Thinn Htike,
Saitama University, Japan

*CORRESPONDENCE
Yuko Maejima
maejimay@fmu.ac.jp
Kenju Shimomura
shimomur@fmu.ac.jp

RECEIVED 05 February 2024
ACCEPTED 27 May 2024
PUBLISHED 11 June 2024

CITATION
Nakajima D, Yamachi M, Misaka S, Shimomura K and Maejima Y (2024) Sex differences in the effects of aromatherapy on anxiety and salivary oxytocin levels. *Front. Endocrinol.* 15:1380779. doi: 10.3389/fendo.2024.1380779

Sex differences in the effects of aromatherapy on anxiety and salivary oxytocin levels

Daisuke Nakajima[1,2], Megumi Yamachi[1], Shingen Misaka[1], Kenju Shimomura[1,3]* and Yuko Maejima[1,3]*

[1]Department of Bioregulation and Pharmacological Medicine, Fukushima Medical University School of Medicine, Fukushima City, Fukushima, Japan, [2]Medical Division, Nitto Boseki Co., Ltd., Koriyama Fukushima, Japan, [3]Departments of Obesity and Inflammation Research, Fukushima Medical University School of Medicine, Fukushima City, Fukushima, Japan

Objective: Aromatherapy is a holistic healing method to promote health and well-being by using natural plant extracts. However, its precise mechanism of action and influence on the endocrine system remains unclear. Since recent studies reported that a neuropeptide, oxytocin, can attenuate anxiety, we hypothesized that if oxytocin secretion is promoted through aromatherapy, it may improve mood and anxiety. The present study is aimed to investigate the relationship between oxytocin and the effects of aromatherapy with lavender oil on anxiety level, by measuring salivary oxytocin levels in healthy men and women.

Methods: We conducted a randomized open crossover trial in 15 men and 10 women. Each participant received a placebo intervention (control group) and aromatherapy with lavender oil (aromatherapy group). For the aromatherapy group, each participant spent a 30-min session in a room with diffused lavender essential oil, followed by a 10-min hand massage using a carrier oil containing lavender oil. Anxiety was assessed using the State-Trait Anxiety Inventory (STAI) before the intervention, 30-min after the start of intervention, and after hand massage, in both groups. Saliva samples were collected at the same time points of the STAI.

Results: In women, either aromatherapy or hand massage was associated with a reduction in anxiety levels, independently. Moreover, salivary oxytocin levels were increased after aromatherapy. On the other hand, in men, anxiety levels were decreased after aromatherapy, as well as after hand massage, regardless of the use of lavender oil. However, there were no significant differences in changes of salivary oxytocin levels between the control and aromatherapy groups during the intervention period. Interestingly, there was a positive correlation between anxiety levels and salivary oxytocin levels before the intervention, but a negative correlation was observed after hand massage with lavender oil.

Conclusion: The results of the present study indicate that in women, aromatherapy with lavender oil attenuated anxiety with increase in oxytocin

level in women, whereas in men, there was no clear relationship of aromatherapy with anxiety or oxytocin levels but, there was a change in correlation between anxiety and oxytocin. The results of the present study suggest that the effect of aromatherapy can vary depending on sex.

KEYWORDS

aromatherapy, hand massage, oxytocin, anxiety, stress, sex differences

1 Introduction

Aromatherapy is the use of essential oils extracted from plants for the treatment of physical and psychological health. It has been reported to have positive psychological therapeutic effects through inhaling aromatic plant-based compounds (aroma) (1). There are many kinds of aroma oils, and they are used selectively based on the purpose. For example, sweet marjoram aroma has been reported to have calming and sedative effects, and thus contributes to the relief of negative emotional states. On the other hand, lavender aroma has been reported to have positive effects on mood, stress, anxiety, depression and insomnia (1).

Aromatherapy has recently become popular, and is used by a wide range of generations, regardless of gender. The main reason for this popularity is the positive effect that aromatherapy has on mental stress. Stress is considered to play a bigger role in modern society than it ever has before. In particular, stress-related disorders became a global issue as a result of restrictions caused by the COVID-19 pandemic. The global population experiencing mood disorders and depression triggered by stress is increasing, and the incidence of depression is estimated to be 5% in adults, with a higher prevalence in women than in men (2). Therefore, aromatherapy is expected as a simple and effective method to improve mental illness and promote wellness. In addition, massage has been reported to contribute to reduce anxiety, heart rate and stress hormones levels (3). However, in order to apply aromatherapy and massage as possible mental therapies, proper academic evaluation and clarification of their mechanisms of action are necessary.

Oxytocin has been attracting attention as a hormone that attenuates anxiety and stress response (4). It is a peptide hormone consisting of nine amino acids that is secreted from the hypothalamus and acts in both the brain and the body. It was originally discovered as a hormone that promotes delivery and milk ejection in 1906 (5), and has long been regarded as important hormone only during the perinatal period in women. However, it has recently been reported that oxytocin also has functions on behaviors, such as maternal behavior (6), social behavior (7), and social communication regardless of sex (8). Our previous studies found the anti-obesity and anti-metabolic syndrome effects of oxytocin (9, 10). In addition, oxytocin has been reported to be associated with anxiety and stress in animals and humans. Oxytocin exerts a central anxiolytic-like effect on the endocrine system and on behavior (11). Compared to wild-type mice, oxytocin-deficient mice displayed more anxiety-related behaviors and released more corticosterone after experiencing a psychogenic stressor (12). There is a negative correlation between plasma oxytocin level and severity of anxiety in patients with major depression (13). Oxytocin is considered a suitable treatment option for human anxiety disorders, especially for those associated with socio-emotional dysfunctions (14).

Oxytocin is present in breast milk, cerebrospinal fluid, blood, and saliva (15, 16), and it has been reported that salivary and blood oxytocin concentrations increase with massage and/or aromatherapy (17–19). Given these findings, it is speculated that the stress-buffering effects of aromatherapy and/or massage are mediated by oxytocin secretion. Therefore, the present study is aimed to investigate changes in anxiety after aromatherapy and hand massage with aroma oil in men and women, and to elucidate the association with the changes in anxiety and salivary oxytocin levels. To the best of our knowledge, this is the first study to investigate the effects and underlying mechanistic factors of aromatherapy and hand massage by measuring changes in salivary oxytocin levels after these treatments in human men and women.

2 Materials and methods

2.1 Participants and experimental design

We conducted a 2 × 2 crossover trial in 15 men and 11 women in their 20s–40s. They received prior explanation about the interventions used in this study, and provided their written informed consent to participate in this study. Each participant underwent both interventions in two different days, and to avoid the influence of physiological diurnal variation in oxytocin levels, the interventions were conducted at the same time of day in each intervention. Only one female participant (one out of 25 participants: 4%) had experience of aromatherapy in the past. Thus, almost all participants (96%) have never experienced aromatherapy before and the present study was the first experience. There were no participants who experienced hand massage in the past. The interval between the two experimental days was set to be at least one week. The participants did not include

smokers, individuals with chronic illnesses, those taking medication (including traditional Chinese medicine), or those who were pregnant or lactating.

2.2 Intervention protocol

Anxiety was assessed using the State-Trait Anxiety Inventory (STAI) composed of State Anxiety Inventory (SAI) and Trait Anxiety Inventory (TAI) questionnaires freely available for academic use (20, 21) and the reference reported by Shimizu and Imae (22). SAI was evaluated for each intervention since it reflects current emotional state and ideal to evaluate time dependent change of emotion, while TAI was measured to evaluate general mood. Saliva samples were collected prior to intervention, and the participants were asked to complete the SAI and TAI questionnaires (1st assessment). Each participant subsequently received a placebo intervention (control group) or aromatherapy intervention (aromatherapy group). The participants in the aromatherapy group received a 30-min aromatherapy session in a private room with diffused aroma oil, as described in 2.3. During the session, they were prohibited from doing anything that could affect their anxiety state, such as using a smartphone, reading, or sleeping. After the session, saliva samples were collected, and the participants were asked to complete the SAI questionnaire again, and measure the heart rate (2nd assessment). This saliva sampling, completing SAI score questionnaire and pulse measurement were performed within 10 min (35-45 min in Figure 1). They then received a 10-min hand massage with aroma oil in the same room, followed by sample collection and the SAI questionnaire (3rd assessment). The participants in the control group stayed in a private room without diffused aroma oil for 30-min after the 1st assessment. Following the 2nd assessment, they received a 10-min hand massage using carrier oil without containing aroma oil, followed by the 3rd assessment. As described above, SAI evaluates current emotional state and TAI measures trait emotional mood. Thus, TAI test was performed only at the 1st assessment. The detailed protocol is illustrated in Figure 1.

2.3 Aromatherapy and hand massage

Aromatherapy was administered using authentic lavender essential oil (*Lavandula angustifolia*: from France, TREE OF LIFE Co., Ltd.), which was introduced into the room using a diffuser (Brezza Corporation Flavor Life, Tokyo, Japan). For hand massage, sweet almond oil (TREE OF LIFE Co., Ltd.) was used as the carrier oil. In the aromatherapy group, lavender oil concentration of 1% (v/v) was added to the carrier oil. All hand massages were administered for 10-min (5-min on each hand) by a nurse trained in lymphatic massage. In control intervention, the participants were not given both moisture diffuser and aroma oil and were asked to take rest in intervention room for 30 min. The participants received hand massage with almond oil without lavender essential oil in control intervention.

To ensure consistency in the interventional conditions, all hand massages were performed by the same nurse.

2.4 Measurement of heart rate

Heart rate was measured for 30-sec with the participant in a sitting position, using a pulse wave analyzer with a fingertip sensor (Act Medical Service Co., Fukushima, Japan). This measurement was performed 5-min after each of the 1st, 2nd, and 3rd saliva samplings (Figure 1).

2.5 Saliva collection and storage

Saliva was collected using a Salivette® tube (Sarstedt AG, Nümbrecht, Germany). In order to prevent degradation of oxytocin, aprotinin (600 KIU; 014-18113, FUJIFILM Tokyo, Japan) was added to the tube. The participants were not allowed to eat or drink anything except water from 2-h prior to the intervention. They rinsed their mouths thoroughly with water 10-min prior to the first saliva collection. Although drinking water was allowed during the intervention, it was prohibited for 10-min prior to each saliva collection. Samples were centrifuged (1000 × *g* for 5-

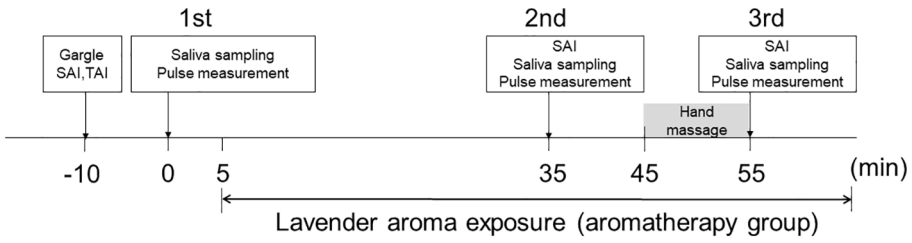

FIGURE 1
Protocol for interventions. The participants received two interventions (aromatherapy and control). Sample collection, SAI and TAI questionnaires, and pulse measurement were performed three times during each intervention (1st assessment, 2nd assessment, 3rd assessment). Prior to each intervention, the participants underwent the 1st assessment. They then spent 30-min in a room with diffused aroma (aromatherapy group) or without (control group), followed by the 2nd assessment. Saliva sampling, completing SAI score and pulse measurement were performed within 10 min (35-45 min). They subsequently received a 10-min hand massage with aroma oil (aromatherapy group) or without (control group), followed by the 3rd assessment.

min) after collection, and the supernatant was collected and stored at -80°C until the day of measurement.

2.6 Measurement of salivary oxytocin

At the measurements, 0.1 M HCl was added to the supernatant, and oxytocin was recovered by a C18 Sep-Pak column (Waters Co., Massachusetts, U.S.A.) and was extracted with methanol. Salivary oxytocin was measured using an ELISA kit (K048-H, ARBOR Assays Inc., Michigan, U.S.A). In order to minimize inter-measurement variation, samples from each participant were measured using the same assay plate. GraphPad Prism 7.0 (Dotmatics Co., Massachusetts, U.S.A.) was used for statistical analysis.

2.7 Statistical analysis

All data are presented as mean ± standard error. Comparison of the TAI and SAI scores between the control and aromatherapy groups was conducted using a paired *t*-test. Pearson's correlation coefficient was used to determine the correlation between SAI and TAI scores, and Spearman's rank correlation coefficient was used to analyze the correlation between SAI score and oxytocin concentration. Heart rate, SAI score, and oxytocin concentration at the 1st, 2nd, and 3rd assessments in the control and aromatherapy groups were analyzed by one-way ANOVA. Two-way ANOVA was used to compare the percentage of oxytocin concentrations, which were set as 100% at the 1st sampling, between the control and aromatherapy groups. All statistical tests were two-tailed, with p values of < 0.05 considered statistically significant.

3 Results

3.1 Participants

Fifteen men and 11 women participated in this study. One of the female participants was excluded from the analysis because the amount of saliva collected was not enough for assay. The mean age of the participants included in the analysis was 24.9 ± 0.8 years (21–32 years) and 26.5 ± 2.7 years (20–42 years) in the men and women, respectively. The mean BMI was 21.5 ± 0.7 (17.3–26.5) in the men, and that in the women was 22.3 ± 0.7 (20.0–27.4). The mean TAI scores in the control and aromatherapy groups were 40.9 ± 1.9 (31–55) and 44.0 ± 3.1 (32–66) in the men and women, respectively. The mean SAI score at before the intervention in control and aromatherapy groups were 32.7 ± 1.2 (23–41) and 36.8 ± 2.6 (25–55) in men and women, respectively. The mean salivary oxytocin levels before the intervention in the control and aromatherapy groups were 68.3 ± 19 (17.3-294) and 66.5 ± 8.3 (25-98.5) in men and women, respectively. There were no significant differences in SAI score and oxytocin levels before the intervention between men and women (Table 1). There were no significant differences in TAI or SAI scores between the control and aromatherapy groups (Figures 2A–D). Additionally, there was a significant positive correlation between the TAI and SAI scores at the 1st assessment in both men and women (r = 0.65, $p < 0.001$; $r = 0.74$, $p < 0.001$; respectively Figures 2E, F).

3.2 Relationships among aromatherapy, hand massage and SAI score

3.2.1 Aromatherapy with lavender oil had no effect on SAI scores in men

A significant decrease was observed in SAI scores at the 2nd and 3rd assessments in the men of both the control and aromatherapy groups. (Figures 3A, C). To evaluate the effect of each intervention on SAI scores, changes in the SAI scores from the 1st assessment [ΔSAI scores: 2nd score – 1st score (2nd point), 3rd score-1st score (3rd point)] were compared between the control and aromatherapy groups. There was no significant difference in ΔSAI score between the control (-3.1 ± 0.86) and aromatherapy (-4.1 ± 1.2) groups at the 2nd assessment. Similarly, there was also no significant difference in ΔSAI score between the control (-4.8 ± 1.0) and aromatherapy (-5.9 ± 1.3) groups at the 3rd assessment ($F_{1,28} = 0.5057$, $p = 0.48$, Figure 3E).

3.2.2 Aromatherapy with lavender oil and hand massage decreased SAI score in women

The SAI scores at the 2nd assessment were significantly decreased in women in the aromatherapy group (Figure 3D), whereas no significant changes were observed in the control group (Figure 3B). On the other hand, the SAI scores at the 3rd assessment were

TABLE 1 Participant characteristics.

	Men (n = 15)			Women (n = 10)			
	Mean	SE	Range	Mean	SE	Range	p-value
Age (years)	24.9	0.8	21-32	26.5	2.7	20-42	0.5246
Height (cm)	173.1	1.7	163-184	160.0	1.9	154-168	< 0.0001
Weight (kg)	64.5	2.4	50-84	57.1	2.0	51-71	< 0.05
BMI (kg/m²)	21.5	0.7	17.3-26.5	22.3	0.7	20.0-27.4	0.4221
TAI	40.5	1.7	31-55	43.6	2.8	32-66	0.3226
SAI 1st	32.7	1.2	23-41	36.8	2.6	25-55	0.1221
Oxytocin 1st (pg/ml)	68.3	19	17.3-294	66.5	8.3	25-98.5	0.9431

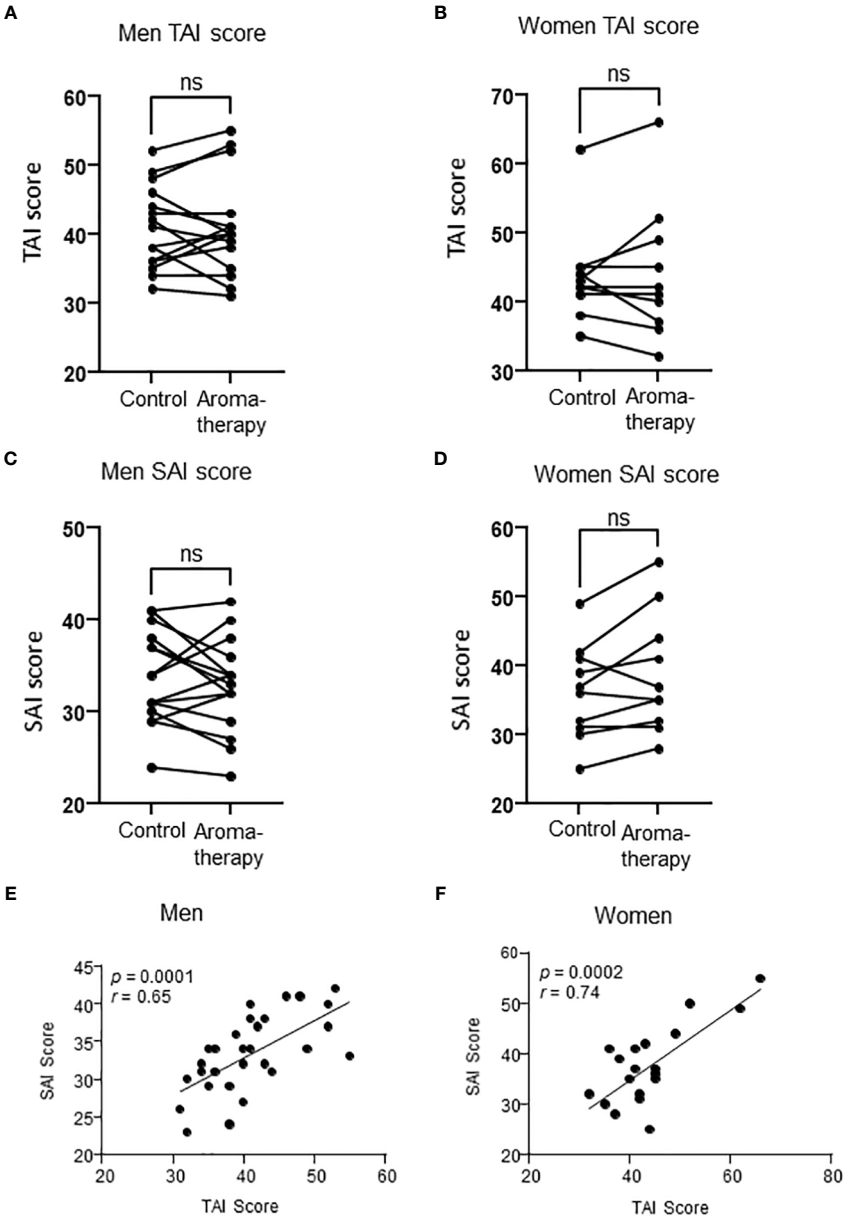

FIGURE 2
Relationship between TAI score and SAI score in men and women. **(A, B)** TAI scores in the control and aromatherapy groups in men (**A**, n = 15) and women (**B**, n = 10). ns: $p > 0.05$, paired t-test. **(C, D)** SAI score at the 1st assessment in the control and aromatherapy groups in men (**C**, n = 15) and women **(D)**, n = 10). ns: $p > 0.05$, paired t-test. **(E, F)** The correlation of SAI score and TAI score at the 1st assessment in the control and aromatherapy groups in men (**E**, n = 30) and women (**F**, n = 20). **(E, F)** analyzed by Pearson's correlation coefficient. ns, not significant.

significantly decreased in both groups (Figures 3B, D). There was a significant difference in the ΔSAI score: score at the 2nd assessment between the control (-0.3 ± 1.0) and aromatherapy (-6.5 ± 1.3) groups (Figure 3F). The ΔSAI score at the 3rd assessment was significantly lower in the aromatherapy group (-11.2 ± 1.5) compared with the control group (-5.8 ± 1.3) ($F_{1,18}$ = 12.87, p = 0.0021, Figure 3F).

3.3 Heart rate

There were no significant changes in heart rate in both men and women in the control and aromatherapy groups (Figure 4).

3.4 Relationships among aromatherapy, hand massage and salivary oxytocin

3.4.1 Salivary oxytocin levels were not changed by aromatherapy and hand massage in men

There were no significant changes in salivary oxytocin levels from the 1st to the 3rd assessment in men of either the control or aromatherapy group (Figures 5A, C). As shown in Figures 5A, C, the salivary oxytocin levels largely varied among individuals. Thus, we analyzed the individual changes by setting the salivary oxytocin levels at the 1st assessment as 100%. As shown in Figure 5E, no significant differences were found at any points between the

10.3389/fendo.2024.1380779

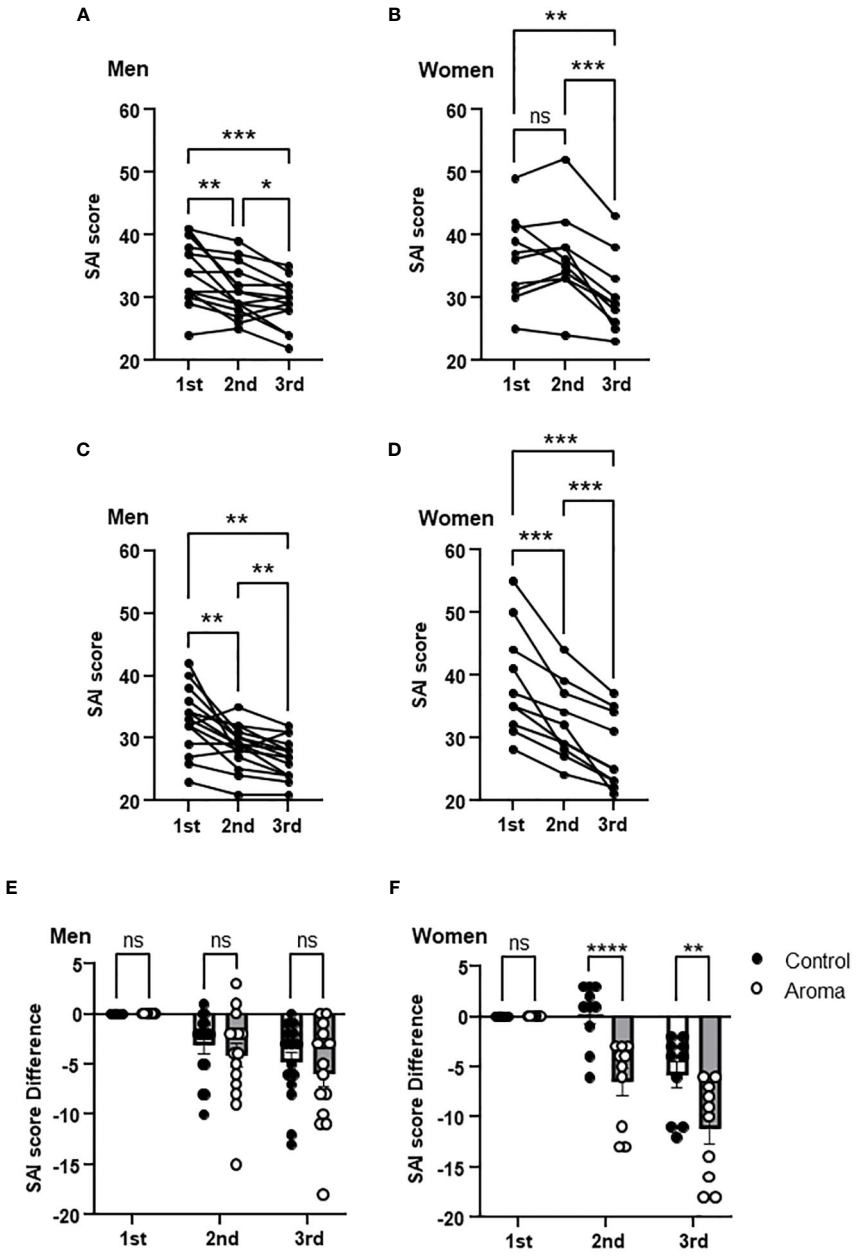

FIGURE 3
Change of SAI scores in the control and aromatherapy groups. **(A, B)** Change of SAI scores in the control group in men (**A**, n = 15) and women (**B**, n = 10). One-way ANOVA Holm-Sidak's multiple comparisons test. **(C, D)** Change of SAI scores in the aromatherapy group in men (**C**, n = 15) and women (**D**, n = 10). One-way ANOVA Holm-Sidak's multiple comparisons test. **(E, F)** Comparison of SAI score difference from 1st assessment at each assessment between the control and aromatherapy groups in men (**E**, n = 15) and women (**F**, n = 10). Two-way ANOVA followed by Sidak's multiple comparisons test. ns, $p > 0.05$; *$p < 0.05$; **$p < 0.005$; ***$p < 0.0005$; ****$p < 0.0001$. ns, not significant.

aromatherapy group (2nd, 145 ± 36%; 3rd, 70 ± 11%) and the control group (2nd, 121 ± 17%; 3rd, 91 ± 18%) ($F_{1,\ 28}$ = 0.0058, p = 0.71).

3.4.2 Salivary oxytocin levels were increased by aromatherapy in women

Although an increasing trend was observed in salivary oxytocin levels at the 2nd assessment in women of the aromatherapy group, there were no significant differences between the control and aromatherapy groups at any assessment point (Figures 5B, D). As in the case with men, we analyzed the individual changes by setting the salivary oxytocin levels at the 1st assessment as 100%, which showed a significantly higher percent increase at the 2nd assessment in the aromatherapy group (160 ± 42%) than the control group (75 ± 11%) ($F_{1,\ 18}$ = 7.8, p = 0.017, Figure 5F). Although there was no statistically significant difference in percent change of oxytocin levels between the control and aroma groups, the tendency of increased salivary oxytocin percentage was maintained after the hand massage (3rd point; 73 ± 15% in the control group; 137 ± 23% in the aromatherapy group, p = 0.0997).

10.3389/fendo.2024.1380779

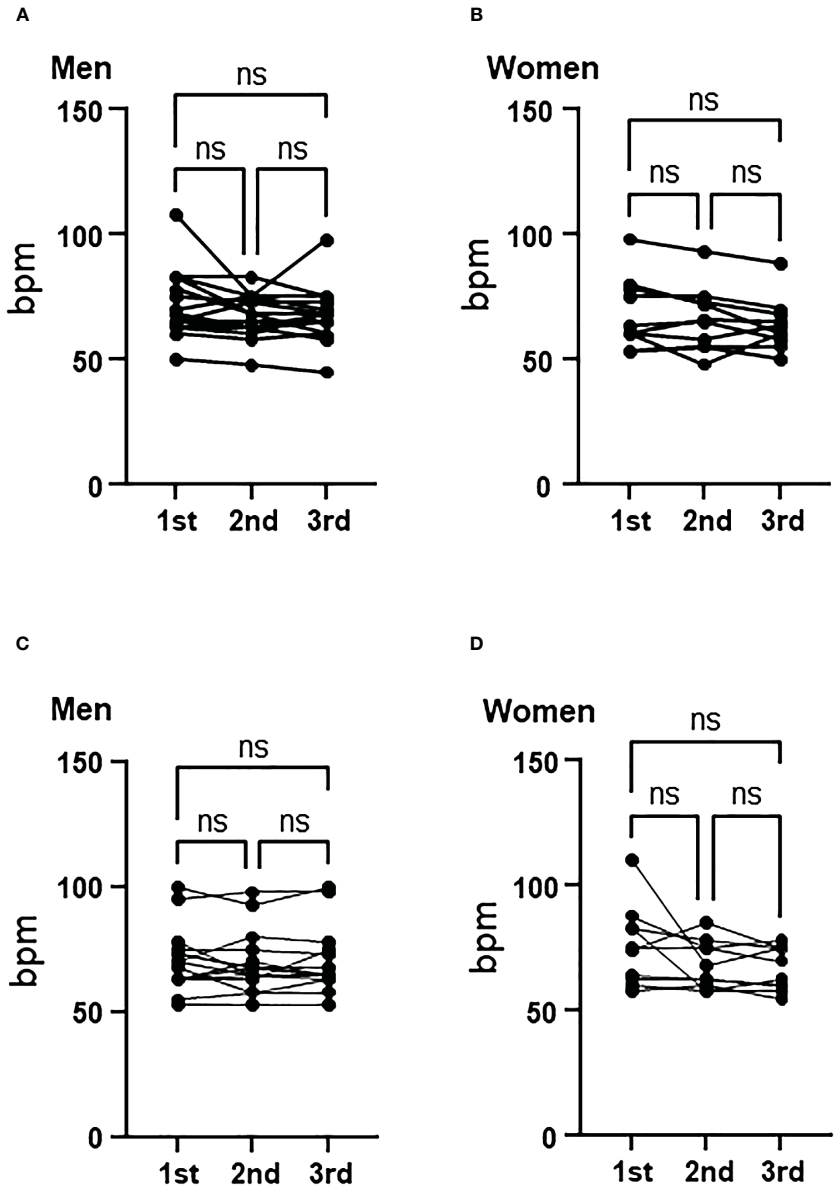

FIGURE 4
Change of heart rate in the control and aromatherapy groups. **(A, B)** Change of heart rate in the control group in men (**A**, *n* = 15) and women (**B**, *n* = 10). Related-samples Friedman's ANOVA test. **(C, D)** Change of heart rate in the aroma group in men (**C**, *n* = 15) and women (**D**, *n* = 10). Related-samples Friedman's ANOVA test. ns, not significant.

3.5 Relationships among anxiety and salivary oxytocin levels

3.5.1 Effect of hand massage with aroma oil on correlation between anxiety and oxytocin levels in men

The correlations between salivary oxytocin levels and SAI scores at each assessment were analyzed in the control (Figures 6A, C, G) and aromatherapy groups (Figures 6A, E, I). In men, a significant positive correlation was found at the 1st and 3rd assessments in the control group (Figures 6A, G) However, a tendency of negative correlation was observed at the 3rd assessment in the aromatherapy group (Figure 6I).

3.5.2 The relationship between SAI score and salivary oxytocin levels in women

In women, there was no significant correlation between the SAI scores and salivary oxytocin level at the 1st assessment (Figure 6B). Although a correlation was detected at the 2nd assessment in the control group (Figure 6D), there were no significant correlations between SAI score and oxytocin level at the 3rd assessment point in both the control and aromatherapy groups (Figures 6H, J, respectively).

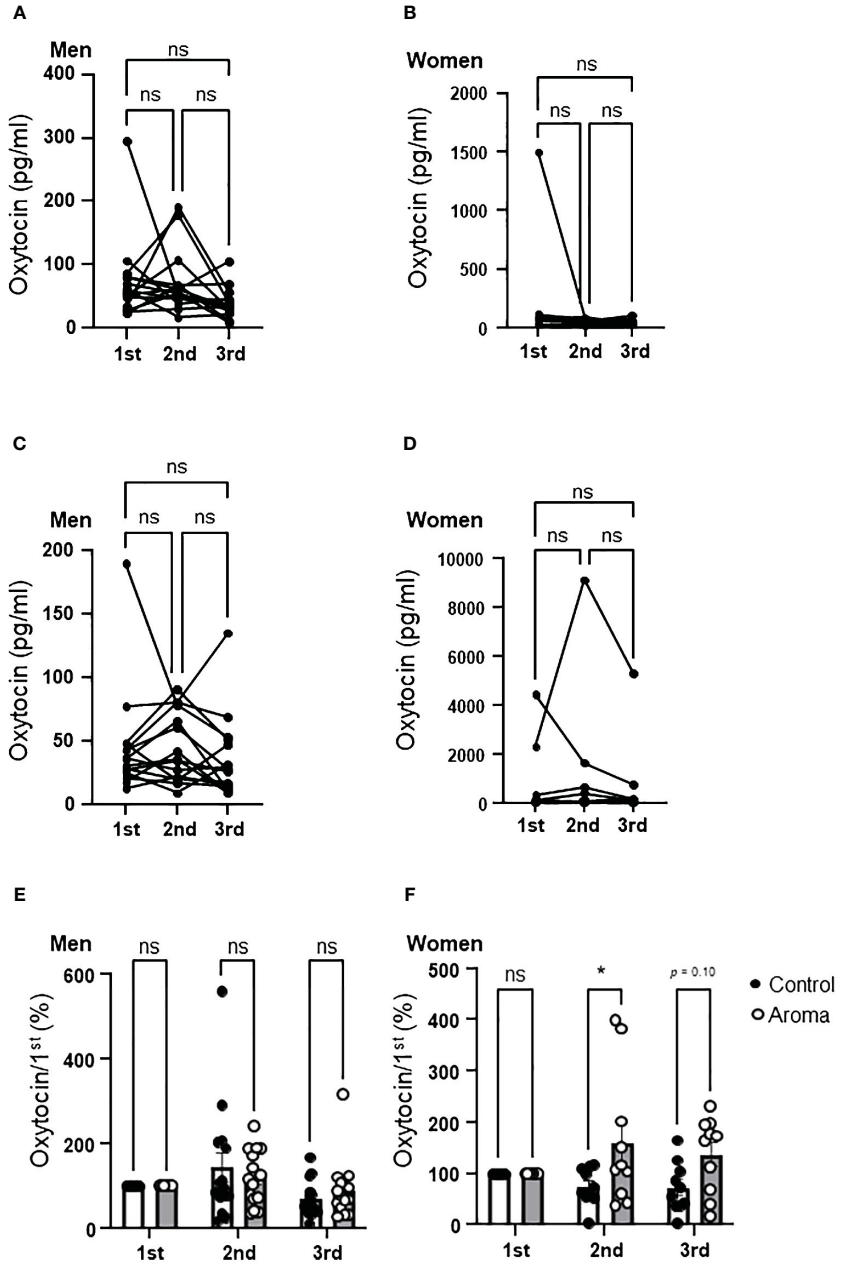

FIGURE 5
Change of salivary oxytocin levels in the control and aromatherapy groups. **(A, B)** Change of salivary oxytocin concentration (pg/ml) in the control group in men (**A**, *n* = 15) and women (**B**, *n* = 10). Related-samples Friedman's ANOVA test. **(C, D)** Change of salivary oxytocin concentration (pg/ml) in the aroma group in men (**C**, *n* = 15) and women (**D**, *n* = 10). Related-samples Friedman's ANOVA test. **(E, F)** Comparison of change of salivary oxytocin levels at each assessment between the control and aromatherapy groups in men (**E**, *n* = 15) and women (**F**, *n* = 10). The oxytocin levels at the 1st assessment is normalized as 100%. Two-way ANOVA followed by Sidak's multiple comparisons test. ns, $p > 0.05$; * $p < 0.05$. ns, not significant.

4 Discussion

Many studies have reported the positive effect of aromatherapy on anxiety reduction (23–31). Animal studies in the past have indicated that aromatherapy can provide psychological effects by acting on the central nervous system (32, 33).

In the present study, we examined the changes in anxiety and salivary oxytocin levels induced by aromatherapy and hand massage with aroma oil in individuals aged 20s–40s, including both men and women.

We used the STAI to evaluate the effect of aromatherapy and hand massage on anxiety levels. Previous studies have reported that aromatherapy with lavender oil significantly reduced anxiety in male as well as in female (23–29, 34). In the present study, the SAI scores decreased in both the control and the aromatherapy groups in men, and when considering only men with high initial anxiety

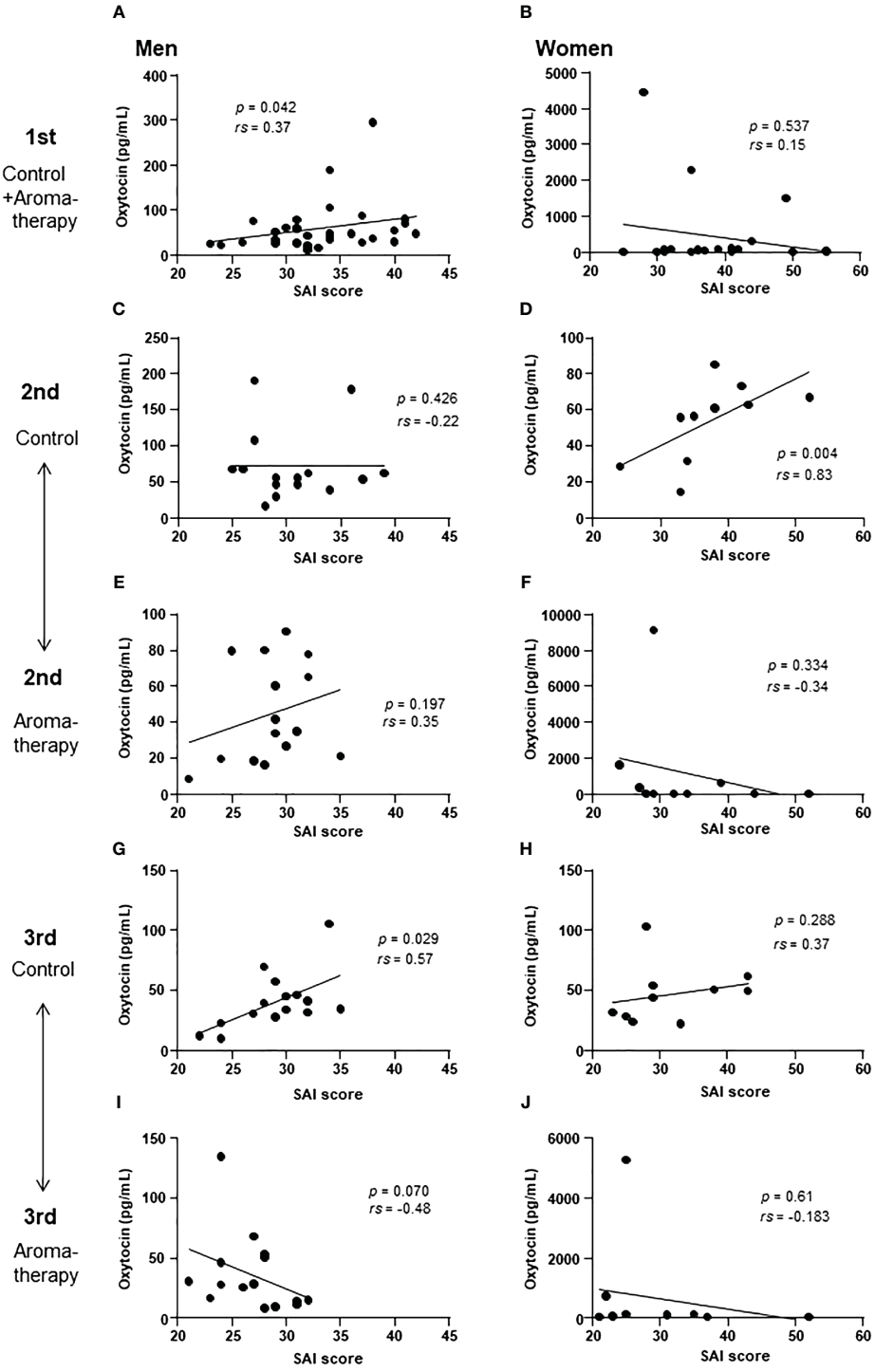

FIGURE 6
Correlation of salivary oxytocin level and SAI score at each assessment. **(A, B)** Correlation of salivary oxytocin levels and SAI scores at the 1st assessment in the control and aromatherapy groups in men (**A**, *n* = 30) and women (**B**, *n* = 20). **(C, D)** Correlation of salivary oxytocin levels and SAI scores at the 2nd assessment in the control group in men (**C**, *n* = 15) and women (**D**, *n* = 10). **(E, F)** Correlation of salivary oxytocin levels and SAI scores at the 2nd assessment in the aromatherapy group in men (**E**, *n* = 15) and women (**F**, *n* = 10). **(G, H)** Correlation of salivary oxytocin levels and SAI scores at the 3rd assessment in the control group in men (**G**, *n* = 15) and women (**H**, *n* = 10). **(I, J)** Correlation of salivary oxytocin levels and SAI scores at the 3rd assessment in the aromatherapy group in men (**I**, *n* = 15) and women (**J**, *n* = 10). **(A–J)** were analyzed using Spearman's rank correlation coefficient.

(SAI score > 36), a decrease in scores by ≥ 5 points was observed in 50% (3 out of 6) in the control group and 100% (4 out of 4) in the aromatherapy group. These results suggest that although there is no effect in salivary oxytocin levels, aromatherapy on its own may be useful in reducing anxiety in men with high anxiety levels. Further study is required to clarify this effect and its mechanisms.

The present study showed significant differences between the aromatherapy and control groups in SAI score changes from the 1st

to 2nd assessment among women. Although there were no significant changes in the SAI scores from the 1st and 2nd assessment in the control group (Figure 3B), a significant decrease was observed in the aromatherapy group (Figure 3D, 3F). These data suggest that, in contrast to men, simply resting in a quiet room alone does not significantly alter anxiety levels in women. However, exposure to lavender oil appears to have a pronounced anxiety-reducing effect in women. In addition, our results suggest that this reduction in anxiety may be further enhanced by the addition of hand massage.

We measured salivary oxytocin levels based on the hypothesis that the anxiety-reducing effects of aromatherapy and/or massages are mediated by oxytocin secretion. Oxytocin is mainly synthesized in the paraventricular and supraoptic nuclei in the hypothalamus. Oxytocin in the peripheral circulations is derived from oxytocin neurons in magnocellular subdivisions in the paraventricular nucleus and supraoptic nuclei that project to the posterior pituitary. On the other hand, oxytocin neurons in the parvocellular subdivision of paraventricular nucleus secrete oxytocin into the brain or cerebrospinal fluid (CSF) via their projection or dendritic release (35). The level of oxytocin in saliva is considered to reflect that in the CSF (36). Thus, the change of salivary oxytocin levels shown in the present study may reflect the change of oxytocin levels in the CSF. The secretion of oxytocin in the brain plays an important role in reducing stress responses (37). Upon stress, corticotropin-releasing hormone from the paraventricular nucleus of the hypothalamus stimulates the secretion of adrenocorticotropic hormone from the pituitary gland, and adrenocorticotropic hormone stimulates cortisol secretion from the adrenal gland. This axis, known as the hypothalamic-pituitary adrenal (HPA) axis, plays an important role in protecting animals, including humans, from stress. In response to activation of the HPA axis, oxytocin inhibits the expression and secretion of corticotropin-releasing hormone from the hypothalamic paraventricular nucleus, and prevents overactivation of the HPA axis, resulting in attenuation of stress response (37). Therefore, increase in salivary oxytocin level can be considered as an indicator for stress response attenuation.

A significant positive correlation was detected between the SAI scores and salivary oxytocin levels at the 1st assessment in men (Figure 6A). This result indicates that the participants with higher anxiety scores showed higher salivary oxytocin levels. Considering the role of oxytocin in stress response, its secretion could be increased to attenuate anxiety. In humans, oxytocin levels in saliva and peripheral blood increase due to factors such psychological stress, exercise, and noise stress (38–41). These findings are consistent with our results found in men, which showed a positive correlation between the SAI scores and salivary oxytocin levels. However, the positive correlation between the SAI scores and salivary oxytocin levels was maintained to some extent at the 3rd assessment in men of the control group (Figure 6G). In contrast, there was a tendency of negative correlation at the 3rd assessment in the aromatherapy group (Figure 6I). The physiological role of this invert from positive correlation to negative correlation remains unknown. Further study is required to clarify the link between anxiety attenuation and its involvement of oxytocin.

One possible mechanism of oxytocin to attenuate stress is its effect on the amygdala (42, 43). The amygdala is a region of the cerebral limbic system that governs emotions, especially anxiety. Oxytocin receptors are abundantly expressed in this region (44). It has been reported that there is a positive correlation between salivary oxytocin levels and the size of the amygdala in men (45). Furthermore, nasal oxytocin administration attenuates the activation of the amygdala's response to fearful facial expressions in men (46). In addition, oxytocin can modulate amygdala reactivity in response to social threat and attenuate anxiety (42). Thus, it is possible that higher oxytocin levels contributed to attenuation of anxiety in men with higher anxiety scores in the present study.

Interestingly, contrary to men, there is a negative correlation between salivary oxytocin levels and amygdala volume in women (45). Shou et al. speculated that high oxytocin levels increase amygdala volume by activating this brain region with a high frequency in men, while in women it reduces amygdala volume by suppressing its activation (45). Taking into account this report and our results, it is possible that there is a sex difference in the mechanism of action of oxytocin on anxiety reduction in humans.

Although present study is based on small number of participants, it demonstrated a possible sex difference in the effect of aromatherapy on salivary oxytocin levels. There were no significant differences in the changes of salivary oxytocin levels between the control and aromatherapy groups in the men (Figure 5E), while the change of salivary oxytocin levels of the aromatherapy group was significantly larger than that of the control group in the women (Figure 5F). In the present study, salivary oxytocin levels at the 2nd assessment in female aromatherapy group increased by approximately 1.5 times differ from to those of the control group, which is a similar level of increase in salivary oxytocin reported in a previous study which postmenopausal women were exposed to lavender essential oil for 20-min (19). The female participant of present study is all premenopausal women and our results suggest that the effectiveness of aromatherapy for anxiety reduction with possible interaction with oxytocin secretion is limited to women.

Although many mechanisms can be speculated for its effectiveness on women, one possible mechanism can be the differences in the olfactory system. The sense of smell in women has been reported to be more sensitive than in men (47). The olfactory bulb is an initial brain region that receives olfactory stimuli from olfactory receptors. A previous postmortem brain study reported that the number of neurons and glial cells in the olfactory bulb of women were 40%–50% higher than those in men (48). Given these findings, the sex difference in the response to aromatherapy may be linked to the sex differences in the olfactory system.

Regarding the levels of oxytocin with the sex difference in the response to aromatherapy, the neurons in olfactory bulb which project to various brain regions related to the stress responses, including hypothalamus, bed nucleus of the stria terminalis and medial amygdala (49–51), may contribute to the results shown in this study. Since, the number of neurons and glial cells in the olfactory bulb of women are higher than those of men (48), the input from olfactory neurons in women may have stronger effects of aromatic effects on enhancing oxytocin response. On the other hand, it has been reported that lavender essential oil inhalation to mice decreased

an anxiolytic-like behavior via serotonergic neuronal system (52). Oxytocin increases the release of serotonin and availability of 5-HT1A receptors (53). In addition to these reports, estrogen increases oxytocin receptors expressions in neurons (54).

Considering from these reports, olfactory systems in female can enhance aromatherapy effects via neuronal projection from olfactory neurons than male. In addition, serotonin and estrogen, which have important role in regulating physiology of women, are also known to enhance the oxytocin effect. It is possible to consider that in addition to enhanced olfactory systems, serotonin and estrogen systems further enhanced the role of oxytocin in response to aromatherapy in decreasing anxiety.

Interestingly, in the present study, an additive effect on the increase in salivary oxytocin levels by hand massage was not observed in either sex. According to previous studies, salivary oxytocin levels increase with stroking head (55). On the other hand, oxytocin levels in the blood increase with massage on the back and feet (18, 56). The secretion of oxytocin into saliva and blood depends on the type of stimulus and does not always occur in parallel (57); therefore, it is plausible that the hand massage in the present study did not contribute to an increase in salivary oxytocin levels. Further investigation into this is required.

4.1 Limitations

Oxytocin has been reported to be secreted in response to stress, and its secretion in the central and peripheral regions is not necessarily consistent and depends largely on the type of stress (57). Therefore, in the present study, we measured oxytocin level in saliva but not in blood. In addition, given that the oxytocin levels in premenopausal women fluctuate according to the estrous cycle, the correlation between the SAI scores and oxytocin levels in women of the present study may have been interfered by factors other than anxiety. Also, present study is based on relatively small number of participants and further study with larger scale is required.

4.2 Conclusion

The results of the present study suggest that aromatherapy with lavender oil attenuated anxiety with increase in oxytocin secretion in women but not in men. This indicates the possibility that attenuation of anxiety by aromatherapy with lavender oil in women may partially depend on oxytocin secretion. However, further research is needed to determine the significant roles of oxytocin in change of anxiety score by aromatherapy and hand massage in men with high anxiety score.

Data availability statement

The raw data supporting the conclusions of this article will be made available by the authors, without undue reservation.

Ethics statement

The studies involving humans were approved by General Ethics Committee of Fukushima Medical University. The studies were conducted in accordance with the local legislation and institutional requirements. The participants provided their written informed consent to participate in this study.

Author contributions

DN: Formal analysis, Writing – original draft, Writing – review & editing. MY: Investigation, Writing – review & editing. SM: Methodology, Supervision, Writing – review & editing. KS: Investigation, Methodology, Supervision, Writing – original draft, Writing – review & editing. YM: Funding acquisition, Investigation, Methodology, Project administration, Supervision, Writing – original draft, Writing – review & editing.

Funding

The author(s) declare financial support was received for the research, authorship, and/or publication of this article. This work was supported by a grant from Aroma Environment Association of Japan and Grant-Aid for Scientific Research (C) (18K08483, 22K11755 to YM, 26461366 to KS).

Acknowledgments

The authors thank Shoko Yokota, Fumi Saitoh and Rie Ohashi for their technical support.

Conflict of interest

Author DN was employed by Nitto Boseki Co., Ltd.

The remaining authors declare that the research was conducted in the absence of any commercial or financial relationships that could be construed as a potential conflict of interest.

Publisher's note

References

1. Herz RS. Aromatherapy facts and fictions: A scientific analysis of olfactory effects on mood, physiology and behavior. *Int J Neurosci*. (2009) 119:263–90. doi: 10.1080/00207450802333953

2. World Health Organization. *Depressive disorder (depression)* (2024). Available online at: https://www.who.int/news-room/fact-sheets/detail/depression (Accessed Feb 2, 2024)

3. Field T. Massage therapy research review. *Complement. Ther Clin Pract*. (2016) 24:19–31. doi: 10.1016/j.ctcp.2016.04.005

4. McCall C, Singer T. The animal and human neuroendocrinology of social cognition, motivation and behavior. *Nat Neurosci*. (2012) 15:681–8. doi: 10.1038/nn.3084

5. Dale HH. On some physiological actions of ergot. *J Physiol (Lond.)*. (1906) 34:163–206. doi: 10.1113/jphysiol.1906.sp001148

6. Jin D, Liu HX, Hirai H, Torashima T, Nagai T, Lopatina O, et al. CD38 is critical for social behaviour by regulating oxytocin secretion. *Nature*. (2007) 446:41–5. doi: 10.1038/nature05526

7. Bartz JA, Zaki J, Bolger N, Ochsner KN. Social effects of oxytocin in humans: context and person matter. *Trends. Cogn. Sci*. (2011) 15:301–9. doi: 10.1016/j.tics.2011.05.002

8. Domes G, Heinrichs M, Michel A, Berger C, Herpertz SC. Oxytocin improves "mind-reading" in humans. *Biol Psychiatry*. (2007) 61:731–3. doi: 10.1016/j.biopsych.2006.07.015

9. Maejima Y, Iwasaki Y, Yamahara Y, Kodaira M, Sedbazar U, Yada T. Peripheral oxytocin treatment ameliorates obesity by reducing food intake and visceral fat mass. *Aging*. (2011) 3:1169–77. doi: 10.18632/aging.100408

10. Maejima Y, Aoyama M, Sakamoto K, Jojima T, Aso Y, Takasu K, et al. Impact of sex, fat distribution and initial body weight on oxytocin's body weight regulation. *Sci Rep*. (2017) 7:8599. doi: 10.1038/s41598-017-09318-7

11. Windle RJ, Shanks N, Lightman SL, Ingram CD. Central oxytocin administration reduces stress-induced corticosterone release and anxiety behavior in rats. *Endocrinology*. (1997) 138:2829–34. doi: 10.1210/endo.138.7.5255

12. Amico JA, Mantella RC, Vollmer RR, Li X. Anxiety and stress responses in female oxytocin deficient mice. *J Neuroendocrinol*. (2004) 16:319–24. doi: 10.1111/j.0953-8194.2004.01161.x

13. Scantamburlo G, Hansenne M, Fuchs S, Pitchot W, Maréchal P, Pequeux C, et al. Plasma oxytocin levels and anxiety in patients with major depression. *Psychoneuroendocrinology*. (2007) 32:407–10. doi: 10.1016/j.psyneuen.2007.01.009

14. Naja WJ, Aoun MP. Oxytocin and anxiety disorders: translational and therapeutic aspects. *Curr Psychiatry Rep*. (2017) 19:67. doi: 10.1007/s11920-017-0819-1

15. Kuwabara Y, Takeda S, Mizuno M, Sakamoto S. Oxytocin levels in maternal and fetal plasma, amniotic fluid, and neonatal plasma and urine. *Arch Gynecol. Obstet*. (1987) 241:13–23. doi: 10.1007/BF00931436

16. White-Traut R, Watanabe K, Pournajafi-Nazarloo H, Schwertz D, Bell A, Carter CS. Detection of salivary oxytocin levels in lactating women. *Dev Psychobiol*. (2009) 51:367–73. doi: 10.1002/dev.20376

17. Tsuji S, Yuhi T, Furuhara K, Ohta S, Shimizu Y, Higashida H. Salivary oxytocin concentrations in seven boys with autism spectrum disorder received massage from their mothers: a pilot study. *Front Psychiatry*. (2015) 6:58. doi: 10.3389/fpsyt.2015.00058

18. Li Q, Becker B, Wernicke J, Chen Y, Zhang Y, Li R, et al. Foot massage evokes oxytocin release and activation of orbitofrontal cortex and superior temporal sulcus. *Psychoneuroendocrinology*. (2019) 99:193–203. doi: 10.1016/j.psyneuen.2018.11.016

19. Tarumi W, Shinohara K. The effects of essential oil on salivary oxytocin concentration in postmenopausal women. *J Altern. Complement. Med*. (2020) 26:226–30. doi: 10.1089/acm.2019.0361

20. Spielberger CD. *State-trait anxiety inventory: bibliography (2nd ed.)*. Palo Alto, CA: Consulting Psychologists Press (1989).

21. Spielberger CD, Gorsuch RL, Lushene R, Vagg PR, Jacobs GA. *Manual for the state-trait anxiety inventory*. Palo Alto, CA: Consulting Psychologists Press (1983).

22. Shimizu H, Imae K. Creation of STATE-TRAIT ANXIETY INVENTORY in Japanese for university students (STATE-TRAIT ANXIETY INVENTORY no nihongoban (daigakuseiyou) no sakusei) (in Japanese). *Japanese Jounal Educate Psycholosy*. (1981) 29-4:348–53. doi: 10.5926/jjep1953.29.4_348

23. Yoo O, Park SA. Anxiety-reducing effects of lavender essential oil inhalation: A systematic review. *Healthcare (Basel Switzerland)*. (2023) 11:2978. doi: 10.3390/healthcare11222978

24. Perry R, Terry R, Watson LK, Ernst E. Is lavender an anxiolytic drug? A systematic review of randomised clinical trials. *Phytomedicine Int J phytotherapy phytopharmacology*. (2012) 19:825–35. doi: 10.1016/j.phymed.2012.02.013

25. Kang HJ, Nam ES, Lee Y, Kim M. How strong is the evidence for the anxiolytic efficacy of lavender?: systematic review and meta-analysis of randomized controlled trials. *Asian Nurs Res*. (2019) 13:295–305. doi: 10.1016/j.anr.2019.11.003

26. Donelli D, Antonelli M, Bellinazzi C, Gensini GF, Firenzuoli F. Effects of lavender on anxiety: A systematic review and meta-analysis. *Phytomedicine Int J phytotherapy phytopharmacology*. (2019) 65:153099. doi: 10.1016/j.phymed.2019.153099

27. Shamabadi A, Hasanzadeh A, Ahmadzade A, Ghadimi H, Gholami M, Akhondzadeh S. The anxiolytic effects of Lavandula angustifolia (lavender): An overview of systematic reviews. *J Herbal Med*. (2023) 40:100672. doi: 10.1016/j.hermed.2023.100672

28. Kim M, Nam ES, Lee Y, Kang HJ. Effects of lavender on anxiety, depression, and physiological parameters: systematic review and meta-analysis. *Asian Nurs Res*. (2021) 15:279–90. doi: 10.1016/j.anr.2021.11.001

29. Koulivand PH, Khaleghi Ghadiri M, Gorji A. Lavender and the nervous system. *Evidence-Based complementary Altern Med eCAM*. (2013) 2013:681304. doi: 10.1155/2013/681304

30. Gong M, Dong H, Tang Y, Huang W, Lu F. Effects of aromatherapy on anxiety: A meta-analysis of randomized controlled trials. *J Affect. Disord*. (2020) 274:1028–40. doi: 10.1016/j.jad.2020.05.118

31. Li D, Li Y, Bai X, Wang M, Yan J, Cao Y. The effects of aromatherapy on anxiety and depression in people with cancer: A systematic review and meta-analysis. *Front Public. Health*. (2022) 10:853056. doi: 10.3389/fpubh.2022.853056

32. Re L, Barocci S, Sonnino S, Mencarelli A, Vivani C, Paolucci G, et al. Linalool modifies the nicotinic receptor-ion channel kinetics at the mouse neuromuscular junction. *Pharmacol Res*. (2000) 42:177–81. doi: 10.1006/phrs.2000.0671

33. Kim Y, Kim M, Kim H, Kim K. Effect of lavender oil on motor function and dopamine receptor expression in the olfactory bulb of mice. *J Ethnopharmacol*. (2009) 125:31–5. doi: 10.1016/j.jep.2009.06.017

34. Ebrahimi A, Eslami J, Darvishi I, Momeni K, Akbarzadeh M. An overview of the comparison of inhalation aromatherapy on emotional distress of female and male patients in preoperative period. *J Complement. Integr Med*. (2022) 19:111–9. doi: 10.1515/jcim-2020-0464

35. Dölen G. Oxytocin: parallel processing in the social brain? *J Neuroendocrinol*. (2015) 27:516–35. doi: 10.1111/jne.12284

36. Martin J, Kagerbauer SM, Gempt J, Podtschaske A, Hapfelmeier A, Schneider G. Oxytocin levels in saliva correlate better than plasma levels with concentrations in the cerebrospinal fluid of patients in neurocritical care. *J Neuroendocrinol*. (2018) 30:e12596. doi: 10.1111/jne.12596

37. Winter J, Jurek B. The interplay between oxytocin and the CRF system: regulation of the stress response. *Cell Tissue. Res*. (2019) 375:85–91. doi: 10.1007/s00441-018-2866-2

38. Jong TR, Menon R, Bludau A, Grund T, Biermeier V, Klampfl SM, et al. Salivary oxytocin concentrations in response to running, sexual self-stimulation, breastfeeding and the TSST: The Regensburg Oxytocin Challenge (ROC) study. *Psychoneuroendocrinology*. (2015) 62:381–8. doi: 10.1016/j.psyneuen.2015.08.027

39. Landgraf R, Häcker R, Buhl H. Plasma vasopressin and oxytocin in response to exercise and during a day-night cycle in man. *Endokrinologie*. (1982) 79:281–91. doi: 10.1007/BF02337184

40. Pierrehumbert B, Torrisi R, Laufer D, Halfon O, Ansermet F, Beck Popovic M. Oxytocin response to an experimental psychosocial challenge in adults exposed to traumatic experiences during childhood or adolescence. *Neuroscience*. (2010) 166:168–77. doi: 10.1016/j.neuroscience.2009.12.016

41. Sanders G, Freilicher J, Lightman SL. Psychological stress of exposure to uncontrollable noise increases plasma oxytocin in high emotionality women. *Psychoneuroendocrinology*. (1990) 15:47–58. doi: 10.1016/0306-4530(90)90046-C

42. Gorka SM, Fitzgerald DA, Labuschagne I, Hosanagar A, Wood AG, Nathan PJ, et al. Oxytocin modulation of amygdala functional connectivity to fearful faces in generalized social anxiety disorder. *Neuropsychopharmacology*. (2015) 40:278–86. doi: 10.1038/npp.2014.168

43. Labuschagne I, Phan KL, Wood A, Angstadt M, Chua P, Heinrichs M, et al. Oxytocin attenuates amygdala reactivity to fear in generalized social anxiety disorder. *Neuropsychopharmacology*. (2010) 35:2403–13. doi: 10.1038/npp.2010.123

44. Rokicki J, Kaufmann T, de Lange AG, van der Meer D, Bahrami S, Sartorius AM, et al. Oxytocin receptor expression patterns in the human brain across development. *Neuropsychopharmacology*. (2022) 47:1550–60. doi: 10.1038/s41386-022-01305-5

45. Shou Q, Yamada J, Nishina K, Matsunaga M, Matsuda T, Takagishi H. Association between salivary oxytocin levels and the amygdala and hippocampal volumes. *Brain. Struct Funct*. (2022) 227:2503–11. doi: 10.1007/s00429-022-02543-5

46. Domes G, Heinrichs M, Gläscher J, Büchel C, Braus DF, Herpertz SC. Oxytocin attenuates amygdala responses to emotional faces regardless of valence. *Biol Psychiatry*. (2007) 62:1187–90. doi: 10.1016/j.biopsych.2007.03.025

47. Seo HS, Guarneros M, Hudson R, Distel H, Min BC, Kang JK, et al. Attitudes toward olfaction: A cross-regional study. *Chem Senses*. (2011) 36:177–87. doi: 10.1093/chemse/bjq112

48. Oliveira-Pinto AV, Santos RM, Coutinho RA, Oliveira LM, Santos GB, Alho AT, et al. Sexual dimorphism in the human olfactory bulb: females have more neurons and glial cells than males. *PLoS. One*. (2014) 9:e111733. doi: 10.1371/journal.pone.0111733

49. Lebow MA, Chen A. Overshadowed by the amygdala: the bed nucleus of the stria terminalis emerges as key to psychiatric disorders. *Mol Psychiatry*. (2016) 21:450–63. doi: 10.1038/mp.2016.1

50. Imamura F, Ito A, LaFever BJ. Subpopulations of projection neurons in the olfactory bulb. *Front Neural circuits*. (2020) 14:561822. doi: 10.3389/fncir.2020.561822

51. Murata K, Kinoshita T, Fukazawa Y, Kobayashi K, Kobayashi K, Miyamichi K, et al. GABAergic neurons in the olfactory cortex projecting to the lateral hypothalamus in mice. *Sci Rep*. (2019) 9:7132. doi: 10.1038/s41598-019-43580-1

52. Chioca LR, Ferro MM, Baretta IP, Oliveira SM, Silva CR, Ferreira J, et al. Anxiolytic-like effect of lavender essential oil inhalation in mice: participation of serotonergic but not GABAA/benzodiazepine neurotransmission. *J ethnopharmacology*. (2013) 147:412–8. doi: 10.1016/j.jep.2013.03.028

53. Lefevre A, Richard N, Jazayeri M, Beuriat PA, Fieux S, Zimmer L, et al. Oxytocin and serotonin brain mechanisms in the nonhuman primate. *J Neurosci Off J Soc Neurosci*. (2017) 37:6741–50. doi: 10.1523/JNEUROSCI.0659-17.2017

54. Sharma K, LeBlanc R, Haque M, Nishimori K, Reid MM, Teruyama R. Sexually dimorphic oxytocin receptor-expressing neurons in the preoptic area of the mouse brain. *PloS One*. (2019) 14:e0219784. doi: 10.1371/journal.pone.0219784

55. Tomosugi N, Koshino Y. Gentle, massage-like, head stroking provokes salivary oxytocin release. *Altern. Ther Health Med*. (2023) 29:188–91.

56. Morhenn V, Beavin LE, Zak PJ. Massage increases oxytocin and reduces adrenocorticotropin hormone in humans. *Altern. Ther Health Med*. (2012) 18:11–8.

57. Engelmann M, Landgraf R, Wotjak CT. The hypothalamic-neurohypophysial system regulates the hypothalamic-pituitary-adrenal axis under stress: an old concept revisited. *Front Neuroendocrinol*. (2004) 25:132–49. doi: 10.1016/j.yfrne.2004.09.001/j.yfrne.2004.09.001

frontiers | Frontiers in Endocrinology

TYPE Original Research
PUBLISHED 19 June 2024
DOI 10.3389/fendo.2024.1308841

OPEN ACCESS

EDITED BY
Kenju Shimomura,
Fukushima Medical University, Japan

REVIEWED BY
Pengpeng Ye,
Chinese Center For Disease Control and Prevention, China
Hongmei Wu,
Tianjin Medical University, China
Yang Xia,
ShengJing Hospital of China Medical University, China
Lixing Zhou,
Sichuan University, China

*CORRESPONDENCE
Qi Guo
guoqijp@gmail.com

†These authors have contributed equally to this work and share first authorship

RECEIVED 07 October 2023
ACCEPTED 04 June 2024
PUBLISHED 19 June 2024

CITATION
Han P, Chen X, Liang Z, Liu Y, Yu X, Song P, Zhao Y, Zhang H, Zhu S, Shi X and Guo Q (2024) Metabolic signatures and risk of sarcopenia in suburb-dwelling older individuals by LC-MS–based untargeted metabonomics. *Front. Endocrinol.* 15:1308841. doi: 10.3389/fendo.2024.1308841

Metabolic signatures and risk of sarcopenia in suburb-dwelling older individuals by LC-MS–based untargeted metabonomics

Peipei Han[1,2,3†], Xiaoyu Chen[2†], Zhenwen Liang[2†], Yuewen Liu[2], Xing Yu[2], Peiyu Song[3], Yinjiao Zhao[3], Hui Zhang[3], Shuyan Zhu[2], Xinyi Shi[2] and Qi Guo[1,2,3*]

[1]Department of Rehabilitation Medicine, Shanghai University of Medicine and Health Sciences Affiliated Zhoupu Hospital, Shanghai, China, [2]College of Rehabilitation Sciences, Shanghai University of Medicine and Health Sciences, Shanghai, China, [3]Jiangwan Hospital of Shanghai Hongkou District, Shanghai University of Medicine and Health Science Affiliated First Rehabilitation Hospital, Shanghai, China

Background: Untargeted metabonomics has provided new insight into the pathogenesis of sarcopenia. In this study, we explored plasma metabolic signatures linked to a heightened risk of sarcopenia in a cohort study by LC-MS-based untargeted metabonomics.

Methods: In this nested case–control study from the Adult Physical Fitness and Health Cohort Study (APFHCS), we collected blood plasma samples from 30 new-onset sarcopenia subjects (mean age 73.2 ± 5.6 years) and 30 healthy controls (mean age 74.2 ± 4.6 years) matched by age, sex, BMI, lifestyle, and comorbidities. An untargeted metabolomics methodology was employed to discern the metabolomic profile alterations present in individuals exhibiting newly diagnosed sarcopenia.

Results: In comparing individuals with new-onset sarcopenia to normal controls, a comprehensive analysis using liquid chromatography-mass spectrometry (LC-MS) identified a total of 62 metabolites, predominantly comprising lipids, lipid-like molecules, organic acids, and derivatives. Receiver operating characteristic (ROC) curve analysis indicated that the three metabolites hypoxanthine (AUC=0.819, 95% CI=0.711–0.927), L-2-amino-3-oxobutanoic acid (AUC=0.733, 95% CI=0.598–0.868) and PC(14:0/20:2(11Z,14Z)) (AUC= 0.717, 95% CI=0.587–0.846) had the highest areas under the curve. Then, these significant metabolites were observed to be notably enriched in four distinct metabolic pathways, namely, "purine metabolism"; "parathyroid hormone synthesis, secretion and action"; "choline metabolism in cancer"; and "tuberculosis".

Conclusion: The current investigation elucidates the metabolic perturbations observed in individuals diagnosed with sarcopenia. The identified metabolites hold promise as potential biomarkers, offering avenues for exploring the underlying pathological mechanisms associated with sarcopenia.

KEYWORDS

LC-MS, risk, sarcopenia, untargeted metabonomics, Chinese

Introduction

Sarcopenia, defined by the gradual decline in skeletal muscle mass, muscle strength, and physical performance (1), is closely linked to the aging process and adverse health outcomes, including disability, diabetes, metabolic syndrome, poor quality of life, and increased mortality (2). Despite the severity of its symptoms and associated side effects, the pathophysiological mechanisms driving sarcopenia remain inadequately elucidated, and current pharmacotherapies demonstrate limited efficacy (3). Therefore, there exists a pressing imperative to uncover novel, clinically significant biomarkers, delineate high-risk populations, and attain a more profound understanding of the underlying pathological mechanisms to mitigate the onset and progression of sarcopenia.

Metabonomics emerges as a potent methodology capable of furnishing intricate insights into biological pathways, pivotal genes, and mutations, thus elucidating the mechanisms underlying disease progression and revealing diagnostic biomarkers Metabonomics analysis can be performed using untargeted or targeted approaches. Most of the current metabonomics studies were targeted metabonomics analyses (4–6).

Nevertheless, while targeted metabonomics offers precision, it inherently limits the potential for discovering novel biomarkers and unveiling previously unrecognized pathways in sarcopenia development. Untargeted metabolomic analysis emerges as essential for functional research, facilitating the integration of comprehensive metabolic profiles with biological insights (7).

Several integrated studies investigating the relationship between blood and fecal untargeted metabolomics and sarcopenia have been published. These studies involve untargeted profiling to discern trait-specific or shared metabolites linked with muscle mass and strength (8), comparing the plasma metabolome (9, 10), as well as analyzing the differences in fecal metabolites (11–13). Blood metabolomics primarily reflects systemic metabolic changes and can capture metabolites related to muscle metabolism, hormonal regulation, and systemic inflammation, which are directly relevant to the pathophysiology of sarcopenia. In contrast, fecal metabolomics offers insights into gut microbiota composition and activity, which, while important for overall health, may be less directly connected to muscle metabolism. The systemic nature of blood metabolomics makes it particularly valuable for identifying biomarkers that are directly associated with muscle mass and strength, and for understanding the systemic metabolic disturbances underlying sarcopenia.

Multiple studies have proposed that the characterization of metabolic signatures holds promise as a biomarker for investigating the physical debilitation associated with sarcopenia (14). However, research on metabolomic analysis in sarcopenia remains in its incipient stages. More research is needed to identify more valuable potential markers, especially by untargeted metabonomics. Furthermore, studies using untargeted metabonomics approaches have predominantly been conducted in Western populations (8, 9, 15, 16). Asians and Westerners differ in lifestyle factors such as exercise habits, sleep quality, stress levels, etc. These lifestyle factors potentially influence metabolic processes, thereby contributing to differences in metabolomic profiles.

Data from Asian populations are scarce and predominantly derived from cross-sectional studies, which are vulnerable to reverse causation and hinder the establishment of temporal and causal relationships. To our knowledge, only two studies have been conducted on Asian populations (17, 18).

Here, the objective of this study was to pinpoint potential plasma metabolite biomarkers linked with sarcopenia. These findings will enrich our understanding of sarcopenia's progression and may aid in identifying new molecular targets for the treatment of this condition.

Materials and methods

Study, setting, and design

The study design entailed a nested case-control approach derived from the Adult Physical Fitness and Health Cohort Study (APFHCS) [ChiCTR1900024880]. The APFHCS is a substantial prospective, open, and dynamic cohort study primarily examining the correlation between physical fitness and health status within a broad adult population residing in Tianjin and Shanghai, China. All participants enrolled in the National Free Physical Examination Program were recruited for comprehensive annual health assessments. Subsequently, they were instructed to fill out detailed questionnaires regarding their lifestyle and medical history. Subsequently, they were subjected to lifelong follow-up through periodic visits. The characteristics of the study participants have been delineated in our prior investigation (19).

Subjects in this study participated in September 2019 (baseline) and September 2020 (follow-up) in Shanghai. A total of 380 subjects had a plasma sample available at baseline. Participants who met any of the following conditions were excluded from the study: (1) inability to provide informed consent; (2) inability to undergo anthropometric measurements; and (3) diagnosis of sarcopenia using the AWGS criteria. Among the 380 subjects, 48 individuals diagnosed with sarcopenia in 2019 were excluded from the analysis. Subsequently, 30 subjects who developed new-onset sarcopenia in 2020 were matched with non-sarcopenic individuals based on age, sex, BMI, lifestyle, and comorbidities using propensity score matching. Nearest neighbor matching without replacement was employed in a 1:1 manner, with a caliper set at 0.02 standard deviations of the logit of the propensity score. This study was approved by the Ethics Committee of Shanghai University of Medicine and Health Sciences. All study participants voluntarily participated by providing written informed consent and completing comprehensive questionnaires encompassing demographic variables, including age, sex, lifestyle behaviors, and medical history. The measurement methods were detailed in our previous cross-sectional study (19).

Assessment of sarcopenia

Sarcopenia was defined according to the Asian Working Group for Sarcopenia (AWGS) criteria (20), in which a person who has low

muscle mass, low muscle strength and/or low physical performance was identified as having sarcopenia. Low muscle mass was classified as a relative skeletal muscle mass index (ASM/ht^2) less than 7.0 kg/m2 and 5.7 kg/m2 in men and women, respectively; low muscle strength was defined as grip strength <28 kg or <18 kg for males and females, respectively; and low physical performance was defined as walking speed <1.0 m/s for both males and females.

Muscle mass was quantified employing direct segmental multi-frequency bioelectrical impedance analysis (BIA) (In-Body720; Biospace Co., Ltd,Seoul, Korea). Assessment of muscle strength involved measuring grip strength using a dynamometer (GRIP-D; Takei Ltd, Niigata, Japan) while standing, with the arm fully extended straight down by the side. The participant received instructions to exert maximal effort by squeezing the handle of the dynamometer for a duration of 3–5 seconds, accompanied by standard encouragement to ensure maximal performance. Following this, the measurement was repeated after a 30-second interval to allow for recovery. The usual walking speed, measured in meters per second (m/s), was utilized as an objective indicator of physical performance, conducted along a 4-meter course. The methodology for this measurement has been previously elucidated in our prior study (21).

Sample collection and processing

Each plasma sample was procured from the study participants under fasting conditions in the morning. Subsequently, the samples were separated and preserved in freezers at a temperature of -80°C until the commencement of the metabonomics assay. Thawing of the samples was conducted at room temperature prior to analysis. Initially, 150 µl of plasma was aliquoted into a new Eppendorf tube, followed by the addition of 10 µl of L-2-chlorophenylalanine (0.3 mg/ml) dissolved in methanol as the internal standard. Subsequently, a 450-µl mixture of methanol/acetonitrile (2/1) was added and vortexed for 1 minute. The entire samples underwent extraction by ultrasonication for 10 minutes and were then stored at -20°C for 30 minutes. The resulting extract was centrifuged for 10 minutes at 4°C (13,000 rpm). A volume of 200 µl of supernatant was then subjected to drying in a freeze concentration centrifugal dryer, followed by resolubilization with 300 µl of methanol/water (1/4) and vortexing for 30 seconds. Subsequent extraction by ultrasonication for 3 minutes was performed. After thorough mixing, the samples were centrifuged at 4°C (13,000 rpm) for 10 minutes, and 150 µl of supernatant was filtered through 0.22-µm microfilters before being transferred to LC vials. The vials were stored at -80°C prior to analysis by LC-MS.

Metabolic profiling

Plasma metabolomic profiling analysis was conducted in accordance with previously established methodologies (22). In brief, LC-MS analysis was executed utilizing an ACQUITY ultra-performance liquid chromatography (UPLC) I-Class coupled with a VION IMS QT high-resolution mass spectrometer (Waters Corporation, Milford, USA). Metabolic profiles were obtained through electrospray ionization (ESI) in both positive and negative ion modes. Sample separation was conducted using an ACQUITY UPLC BEH C18 column (Waters Corporation; particle size: 1.7 µm, dimensions: 100 × 2.1 mm) at a flow rate of 0.4 ml/min. The column temperature was held constant at 45°C, while the sample chamber temperature was maintained at 4°C, and a 1 µl injection volume was employed. The mobile phases consisted of two solutions: solution A comprised water with 0.1% formic acid, while solution B consisted of a mixture of acetonitrile and methanol in a ratio of 2:3 (vol/vol) with 0.1% formic acid. The gradient elution program was as follows: from 0 to 1 minute, the composition was 30% solution B; from 1 to 2.5 minutes, the composition increased from 30% to 60% solution B; from 2.5 to 6.5 minutes, it increased from 60% to 90% solution B; from 6.5 to 8.5 minutes, it increased from 90% to 100% solution B; at 8.5 to 10.7 minutes, the composition remained at 100% solution B; from 10.7 to 10.8 minutes, it decreased from 100% to 1% solution B; and finally, from 10.8 to 13 minutes, the composition was maintained at 1% solution B. The LC-MS system was operated under optimized conditions, including an ion source temperature of 150°C, capillary voltage set to 2.5 kV, desolvation gas flow maintained at 900 L/h, declustering potential set at 40V, collision energy at 4 eV, a mass scan range from m/z 50 to 1,000, and a scan time of 0.2 s (22).

Data processing and analysis

The LC-MS data underwent processing using Progenesis QI version 2.3 software (Nonlinear Dynamics, Newcastle, UK) to facilitate meaningful data analysis, encompassing peak alignment, selection, normalization, and retention time (RT) correction. The resultant feature matrix comprised information on mass-to-charge ratio (m/z), RT, and peak intensities. Compound identification relied on precise m/z values, secondary fragments, and isotopic distribution, with reference to databases such as the Human Metabolome Database (HMDB) (http://www.hmdb.ca/), LIPID MAPS (version 2.3) (http://www.lipidmaps.org/), Metabolite Mass Spectral Database (METLIN) (http://metlin.scripps.edu/), and internally curated databases (EMDB) for qualitative analysis.

In order to delineate differences in metabolic profiles between the control group and individuals with newly diagnosed sarcopenia, orthogonal projection to latent structure with discriminant analysis (OPLS-DA) was utilized as a statistical approach. Simultaneously, the OPLS-DA model underwent validation using a 200-fold permutation test. This permutation test was evaluated through cross-validation, during which the correlation coefficients R2 and Q2 derived from the cross-validation procedure were examined to determine the likelihood of overfitting (23).

Variations in expression between groups were evaluated employing both multidimensional and single-dimensional analyses. The variable importance in projection (VIP) scores derived from OPLS-DA were employed to identify metabolites demonstrating significant biological disparities. Additionally, the statistical significance of these differentially expressed metabolites was confirmed through Student's t-test. Metabolites with VIP scores

10.3389/fendo.2024.1308841

exceeding 1.0 and P-values below 0.05 were considered potential biomarkers indicative of sarcopenia. The predictive accuracy of the model was assessed via the computation of the area under the receiver operating characteristic (ROC) curve (AUC). Furthermore, to elucidate the underlying mechanisms driving metabolic pathway alterations across distinct sample groups, the differentially expressed metabolites underwent metabolic pathway enrichment analysis utilizing the Kyoto Encyclopedia of Genes and Genomes (KEGG) database (http://www.kegg.jp/kegg/pathway.html).

The baseline sociodemographic characteristics of both the control and newly diagnosed sarcopenia cohorts were juxtaposed employing an independent t-test for numerical variables and the chi-squared test for categorical variables. Data exhibiting a normal distribution were depicted as the mean along with the standard deviation (SD), whereas categorical variables were delineated as proportions. Statistical assessments were conducted using SPSS version 26.0 (SPSS Incorporation, Chicago, IL, USA), with significance threshold established at $p < 0.05$.

Results

Participants

During this study, 30 new-onset sarcopenia subjects and 30 non-sarcopenia subjects (control group) were eventually incorporated into our study. The primary characteristics of the population are delineated based on the cases and controls in Table 1. There were no statistically significant discrepancies noted in age, gender distribution, BMI, or other pertinent indicators across the groups, implying that individuals within each group were similar in baseline characteristics.

Multivariate statistical analysis

To analyze the metabolic changes between the new-onset sarcopenia and matched control groups, nontargeted metabonomics analysis was performed using LC–MS. OPLS-DA serves as a suitable model for discerning distinct origins in scenarios where multiple factors may influence metabolite profiles. Consequently, we established an OPLS-DA model utilizing the metabolic spectrum, revealing an evident tendency for segregation, as illustrated in Figure 1. Furthermore, additional permutation tests illustrated that the model was not overfitted, with R2= (0.0, 0.51) and Q2= (0.0, -0.42) (Figure 2). Taken together, these findings suggest a significant metabolic alteration between the new-onset sarcopenia group and the matched control group.

Metabolomic differences between the studied groups

As shown in Table 2, a total of 62 differentially expressed metabolites, including 34 downregulated and 28 upregulated differentially expressed metabolites, contributed significantly to the

TABLE 1 Baseline characteristics of the matched groups.

Characteristic	New-onset Sarcopenia Group (n=30)	Control Group (n=30)	*P* value
Age (years)	73.2 ± 5.6	74.2 ± 4.6	0.483
Sex			1.000
Male (%)	40.0	40.0	
Female (%)	60.0	60.0	
BMI (kg/m2)	22.7 ± 2.7	22.9 ± 2.6	0.778
MNA (score)	12.4 ± 1.6	12.9 ± 1.1	0.122
IPAQ (Met-min/wk)	5313(643–9571)	6294 (1195–13440)	0.438
GDS (score)	5.6 ± 3.7	5.4 ± 3.7	0.848
Sleep quality (score)	0.37 ± 0.68	0.42 ± 0.74	0.764
Illiteracy (%)			0.299
No	76.7	90.0	
Yes	23.3	10.0	
Widowed (%)			0.209
No	70.0	86.7	
Yes	30.0	13.3	
Farming (%)			0.781
No	30.0	33.3	
Yes	70.0	66.7	
Smoking (%)			0.688
No	90.0	86.7	
Yes	10.0	13.3	
Drinking (%)			0.417
No	70.0	60.0	
Yes	30.0	40.0	
Diabetes (%)			0.145
No	79.3	93.3	
Yes	20.7	6.7	
Hypertension (%)			1.000
No	23.3	23.3	
Yes	76.7	76.7	
Hyperlipidemia (%)			0.422
No	56.7	70.0	
Yes	43.3	30.0	
Heart disease (%)			0.795
No	58.6	53.3	
Yes	41.4	46.7	

BMI, Body mass index; MNA, Mini nutritional assessment; IPAQ, International physical activity questionnaires; GDS, Geriatric depression scale.

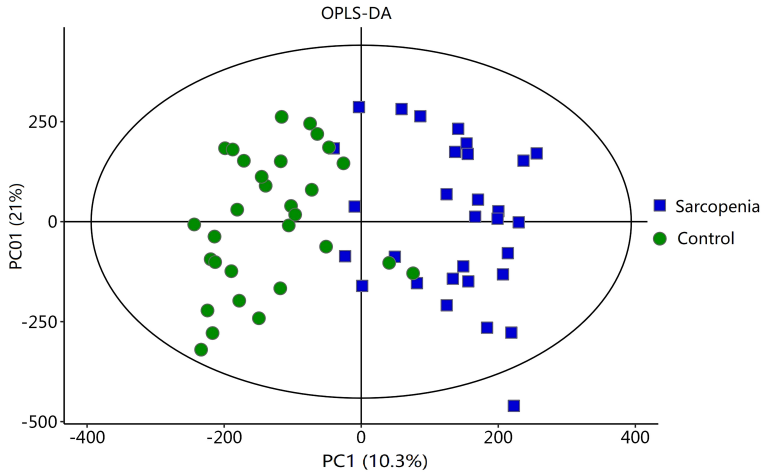

FIGURE 1
OPLS-DA score plot comparing the new-onset sarcopenia group with the matched control group.

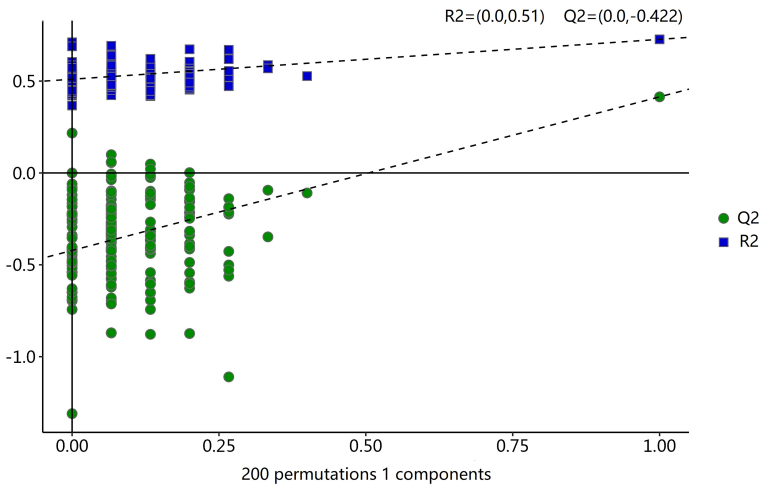

FIGURE 2
Statistical validation of the OPLS-DA model by permutation testing with 200 iterations.

distinction between the control group and the new-onset sarcopenia group. The volcano plot displays both the p-value and fold change value (Figure 3), thereby substantiating the efficacy of differential metabolites. The majority of these distinct metabolites were identified as lipids and lipid-like molecules, along with organic acids and derivatives, which accounted for 45.2% and 24.2%, respectively (Figure 4). Hierarchical clustering was performed using the expression profiles of all metabolites demonstrating significant disparities (Figure 5). In this visualization, colors indicate elevated (red) or diminished (blue) levels of abundance, with intensity correlating to the respective concentration. These findings provide a more direct depiction of the associations among samples and the variations in metabolite expression across different samples.

Evaluation of the metabolite panel for the diagnosis of sarcopenia

Univariate ROC curve analysis was conducted for the top 10 potential biomarkers. Among these, five metabolites exhibited areas under the ROC curve (AUCs) of at least 0.7 (Table 3). Notably, the three most discriminative metabolites with the highest accuracy were identified as hypoxanthine (AUC=0.819, 95% CI=0.711–0.927), L-2-amino-3-oxobutanoic acid (AUC=0.733, 95% CI=0.598–0.868), and PC(14:0/20:2(11Z,14Z)) (AUC= 0.717, 95% CI=0.587–0.846). We conducted a further analysis of the correlation between these three metabolites and the components of sarcopenia (muscle mass, grip strength, and walking speed). The

10.3389/fendo.2024.1308841

TABLE 2 The 62 differential metabolites associated with risk of sarcopenia.

m/z	Ion mode	Metabolite	kegg	Status	VIP	p value	log2(FC)
758.569	pos	PC(14:0/20:2(11Z,14Z))	C00157	↓	44.90	0.002	-0.35
784.583	pos	PC(16:0/20:3(8Z,11Z,14Z))	C00157	↓	21.12	0.011	-0.23
802.560	neg	PC(18:1(11Z)/16:1(9Z))	C00157	↓	18.26	0.001	-0.28
137.046	pos	Hypoxanthine	C00262	↑	9.00	<0.001	1.95
235.092	pos	L-2-Amino-3-oxobutanoic acid	C03508	↓	6.45	0.004	-0.27
273.072	neg	Deoxyuridine	C00526	↓	6.01	0.003	-0.13
742.540	neg	PC(15:0/18:2(9Z,12Z))	C00157	↓	5.12	0.001	-0.32
850.560	neg	PC(22:5(4Z,7Z,10Z,13Z,16Z)/16:1(9Z))	C00157	↓	4.81	0.048	-0.14
792.586	pos	PC(18:1(9Z)/P-18:1(9Z))	C00157	↓	4.31	0.036	-0.22
160.060	pos	Sumiki's acid	C20448	↓	3.98	0.042	-0.12
885.551	neg	PI(20:4(8Z,11Z,14Z,17Z)/18:0)	C00626	↓	3.94	0.018	-0.29
348.070	pos	2'-Deoxyguanosine 5'-monophosphate	C00362	↑	3.54	<0.001	1.51
538.315	neg	LysoPC(16:1(9Z)/0:0)	C04230	↓	3.26	0.004	-0.50
247.093	neg	Serylproline		↓	3.25	0.005	-0.12
766.541	neg	PC(20:4(5Z,8Z,11Z,14Z)/15:0)	C00157	↓	3.11	0.030	-0.16
194.082	neg	2-Phenyl-1,3-propanediol monocarbamate	C16586	↓	2.41	<0.001	-0.09
478.294	neg	PC(15:1(9Z)/0:0)		↓	2.37	0.005	-0.45
128.035	neg	(3R,5S)-1-pyrroline-3-hydroxy-5-carboxylic Acid	C04281	↑	2.35	<0.001	1.14
346.056	neg	3'-AMP	C01367	↑	2.34	<0.001	1.48
159.114	neg	N(6)-Methyllysine	C02728	↓	2.33	0.005	-0.13
378.242	neg	Sphingosine 1-phosphate	C06124	↓	2.29	0.001	-0.43
348.070	pos	Adenosine monophosphate	C00020	↑	2.24	<0.001	1.56
542.324	pos	LysoPC(20:5(5Z,8Z,11Z,14Z,17Z))	C04230	↓	2.23	0.014	-0.77
217.082	pos	Clavulanate	C06662	↓	2.19	0.004	-0.27
885.550	neg	PI(18:1(9Z)/20:3(8Z,11Z,14Z))	C00626	↓	2.10	0.019	-0.24
318.300	pos	Phytosphingosine	C12144	↓	2.09	<0.001	-0.74
812.581	neg	PC(P-16:0/20:3(8Z,11Z,14Z))		↓	2.05	0.012	-0.28
347.042	neg	Quercetin	C00389	↑	2.04	<0.001	1.99
249.054	pos	Paracetamol sulfate		↑	1.92	0.015	1.21
204.123	pos	L-Acetylcarnitine	C02571	↑	1.92	0.006	0.41
288.203	pos	Arginyl-Leucine		↑	1.89	<0.001	2.72
130.050	pos	Pyroglutamic acid	C01879	↑	1.89	<0.001	1.23
175.025	neg	Malonic semialdehyde	C00222	↑	1.86	0.003	0.94
124.007	neg	Taurine	C00245	↑	1.81	<0.001	0.78
347.040	neg	Inosinic acid	C00130	↑	1.81	<0.001	2.37
203.052	pos	D-Glucose	C00221	↓	1.79	<0.001	-0.99
162.112	pos	L-Carnitine	C00318	↓	1.76	0.036	-0.22
132.077	pos	L-3-Cyanoalanine	C02512	↑	1.62	0.010	0.44

(Continued)

TABLE 2 Continued

m/z	Ion mode	Metabolite	kegg	Status	VIP	p value	log2(FC)
184.073	pos	Tryptophanol	C00955	↓	1.50	0.025	-0.33
249.054	pos	Benzeneacetamide-4-O-sulphate		↑	1.48	0.023	1.12
567.318	neg	Deoxycholic acid 3-glucuronide	C03033	↑	1.45	0.012	0.83
189.087	pos	Tetrahydrodipicolinate	C03972	↓	1.42	0.002	-0.20
247.092	pos	5,6-Dihydrouridine		↓	1.41	0.043	-0.11
425.215	pos	5S-HETE di-endoperoxide		↑	1.37	0.001	0.48
130.050	pos	1-Pyrroline-4-hydroxy-2-carboxylate	C04282	↑	1.34	<0.001	1.09
295.228	neg	12,13-EpOME	C14826	↑	1.34	0.017	0.24
145.062	neg	L-Glutamine	C00064	↓	1.30	<0.001	-0.35
489.359	neg	Conicasterol D		↑	1.29	0.002	0.45
104.107	pos	Pentanal		↑	1.26	<0.001	0.37
910.722	pos	PC(25:0/18:0)		↑	1.25	<0.001	1.13
528.310	neg	PE(22:4(7Z,10Z,13Z,16Z)/0:0)		↓	1.23	0.005	-0.25
362.326	pos	Phytophthora mating hormone alpha1		↓	1.18	<0.001	-0.98
923.803	pos	TG(17:0/18:2(9Z,12Z)/20:0)[iso6]		↓	1.17	0.002	-0.53
453.334	pos	24-methylene-cholest-5-en-3beta,7beta,19-triol		↓	1.15	<0.001	-0.48
445.332	neg	25(OH)D3	C01561	↑	1.14	0.048	0.30
282.279	pos	Oleamide	C19670	↑	1.13	0.008	0.88
264.269	pos	5-propylideneisolongifolane		↓	1.10	0.001	-0.47
466.330	pos	PE(P-18:0/0:0)		↑	1.09	0.023	0.41
187.072	neg	N-Acetylglutamine		↓	1.08	0.008	-0.11
123.055	pos	Niacinamide	C00153	↑	1.06	<0.001	1.64
517.390	neg	Theonellasterol D		↑	1.03	0.006	0.47
146.046	neg	L-Glutamic acid	C00302	↑	1.01	<0.001	0.77

Relative concentrations compared to control group: ↑, upregulated; ↓, downregulated.

results indicated that hypoxanthine is negatively correlated with walking speed, whereas L-2-amino-3-oxobutanoic acid and PC (14:0/20:2(11Z,14Z)) are positively correlated with both grip strength and walking speed.

Metabolic enrichment analysis and pathway analysis

We examined the metabolic pathways potentially implicated in the observed changes in metabolic profiles associated with new-onset sarcopenia. Through pathway enrichment analysis, we demonstrated that “purine metabolism”, “parathyroid hormone synthesis, secretion and action”, “choline metabolism in cancer”, and “tuberculosis” emerged as the most significantly perturbed pathways in new-onset sarcopenia (Figure 6).

Discussion

In this prospective study, we systematically present the results of our longitudinal investigation into the associations between plasma metabolites and the onset of sarcopenia utilizing LC-MS-based untargeted metabonomics. This investigation includes a nested case–control study that specifically targets new-onset sarcopenia within a cohort study. We identified 62 metabolites that were correlated with an increased risk of developing new-onset sarcopenia. Among these, lipids and lipid-like molecules, as well as organic acids and derivatives, emerged as the predominant altered metabolites in individuals with new-onset sarcopenia compared to the control group. Currently, the few existing studies on non-targeted metabolomics of sarcopenia have yielded inconsistent results (8, 9, 15–18). The reason for the discrepancy is likely due to differences in lifestyle, such as exercise, sleep, diet, and

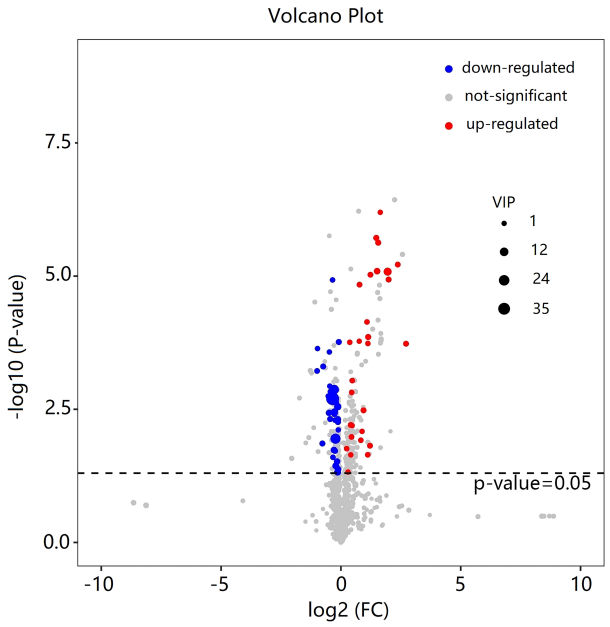

FIGURE 3
Volcano plot of the differential metabolites filtered by the univariate analysis between the new-onset sarcopenia and matched control groups.

psychological factors, as well as variations in populations and ethnicity. The top three metabolites demonstrating the highest discriminatory power between the groups were hypoxanthine, L-2-amino-3-oxobutanoic acid, and PC(14:0/20:2(11Z,14Z)). In summary, our study delineates a panel of 62 metabolic signatures,

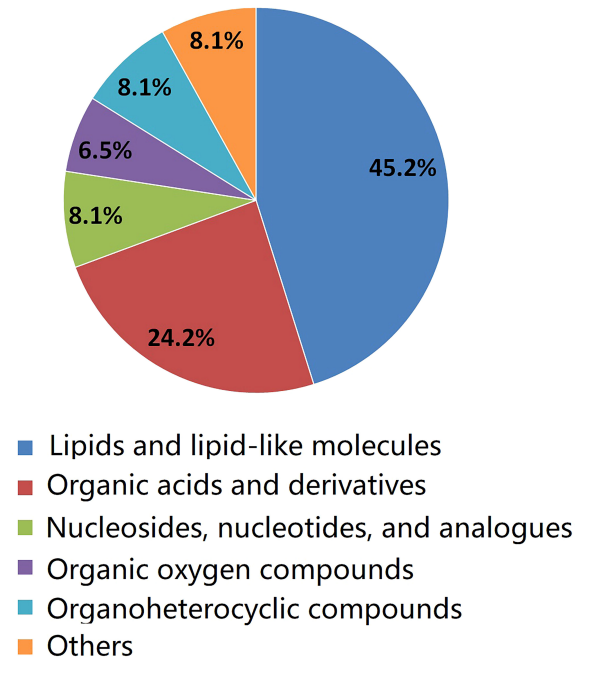

FIGURE 4
The pie chart illustrates the classification and quantity of significantly disturbed metabolites.

which can be broadly classified into four pathways: (1) purine metabolism; (2) parathyroid hormone synthesis, secretion and action; (3) choline metabolism in cancer; and (4) tuberculosis.

Relationship between the top three metabolites and sarcopenia

In this study, it was discovered that hypoxanthine levels were significantly elevated in the new-onset sarcopenia group compared to the control group, rendering it the most discriminative metabolite. Similarly, the studies by Shida T et al. (24) and Zhou J et al. (12) also observed higher hypoxanthine levels in the sarcopenia group compared to the non-sarcopenia group. Animal models of diabetes corroborate this hypothesis, as metabonomics analysis of atrophied quadriceps femoris muscles demonstrated significantly higher levels of hypoxanthine (25). In addition, previous investigations have reported that increases in circulating AdN degradation products are distinctive features of human sarcopenia (26–28), and hypoxanthine was one of the important AdN degradation products. Given that hypoxanthine originates from inosine metabolized by purine nucleoside phosphorylase activity (29), the observed elevations in the levels of inosine, xanthine, and hypoxanthine collectively indicate signs of oxidative stress within the muscle tissues of mice. Oxidative stress is recognized to play a pivotal role in the pathogenesis of sarcopenia (30).

L-2-amino-3-oxobutanoic acid emerged as the second metabolite with the highest discriminatory power between the groups. To our knowledge, there have been no previous reports of direct observations of L-2-amino-3-oxobutanoic acid in the context of sarcopenia. Previous research has indicated that L-2-amino-3-oxobutanoic acid is a downstream metabolite of glycine metabolism (31), and glycine has been shown in rodent models to reduce plasma insulin levels and decrease fat mass (32). Thus, we hypothesize that L-2-amino-3-oxobutanoic acid may be involved in the pathogenesis of sarcopenia through the modulation of glycine metabolism, potentially affecting insulin sensitivity, antioxidative, and anti-inflammatory capacities. However, we also note that only a few studies have linked L-2-amino-3-oxobutanoic acid to other metabolic diseases such as diabetes (33) and liver injury (31). Therefore, further research is warranted to elucidate the exact role and mechanisms of L-2-amino-3-oxobutanoic acid in the pathogenesis of sarcopenia.

In addition to hypoxanthine and L-2-amino-3-oxobutanoic acid, PC(14:0/20:2(11Z,14Z)) was also among the top three metabolites capable of discriminating between groups with the highest accuracy. It was found that lipids and lipid-like molecules emerged as the predominant altered metabolites in individuals with new-onset sarcopenia compared to the control group. These findings are consistent with the study by Chi JL et al. (3) and Zhou J et al. (12). In our cohort study, we observed that the abundances of nine PC species [for example, PC(14:0/20:2 (11Z,14Z)), PC (16:0/20:3(8Z,11Z,14Z)), and PC (18:1(11Z)/16:1 (9Z))] were markedly reduced in subjects with sarcopenia compared to those in the control group. Nonetheless, a prior

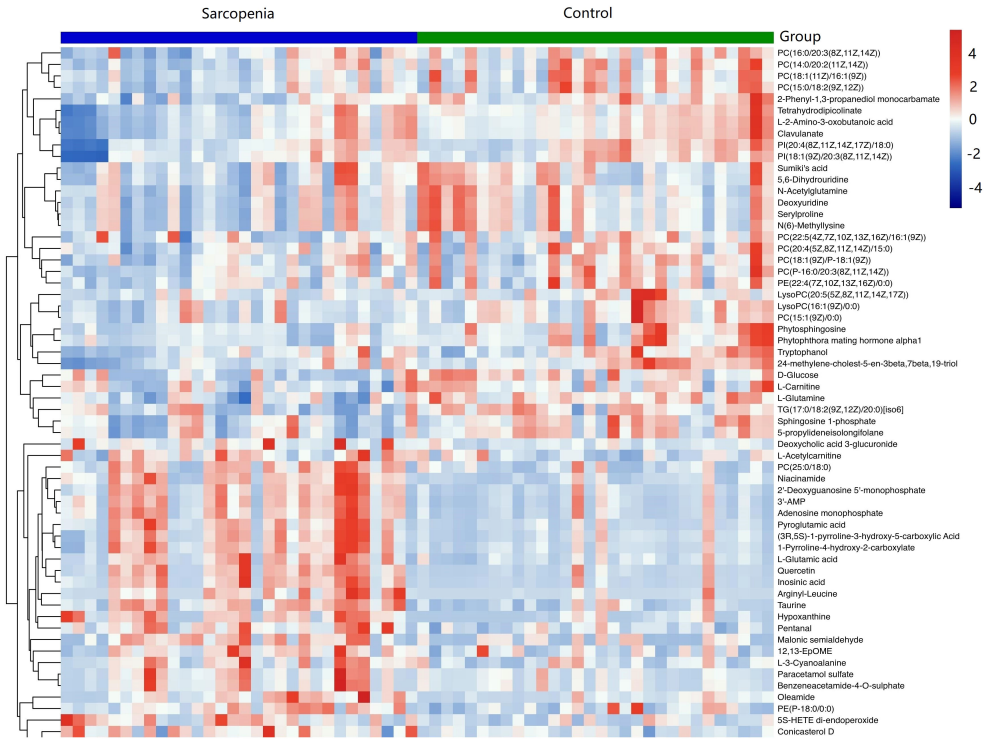

FIGURE 5
Hierarchical clustering revealed the profiles of important differential metabolites in samples from the new-onset sarcopenia and matched control groups. Blue indicates decreased levels, while red indicates increased levels.

investigation exploring the association between resting phosphorus metabolites and skeletal muscle mass noted that older adults with sarcopenia exhibited heightened levels of PCs (34). The variability in PCs levels may be attributed to the presence of unsaturated double bonds. Wang et al. suggested that a decline in the levels of PCs with greater unsaturated double bonds could be closely associated with an elevated risk of sarcopenia in elderly populations (35). Diminished levels of PCs may potentially contribute to the buildup of enlarged mitochondria, which could become impaired and resistant to standard degradation processes via the autophagosomal/lysosomal pathway. This could result in heightened production of reactive oxygen species, thereby potentially exacerbating the aging process. However, additional evidence is necessary to substantiate this novel speculation.

TABLE 3 The AUC values for metabolites.

Metabolite	AUC	95%CI	P
Hypoxanthine	0.819	0.711–0.927	<0.001
L-2-Amino-3-oxobutanoic acid	0.733	0.598–0.868	0.002
PC(14:0/20:2(11Z,14Z))	0.717	0.587–0.846	0.004
Deoxyuridine	0.713	0.581–0.846	0.005
PC(15:0/18:2(9Z,12Z))	0.710	0.578–0.842	0.005
PC(18:1(11Z)/16:1(9Z))	0.693	0.559–0.828	0.010
PC(16:0/20:3(8Z,11Z,14Z))	0.687	0.550–0.823	0.013
PC(22:5(4Z,7Z,10Z,13Z,16Z)/16:1(9Z))	0.667	0.526–0.807	0.071
Sumiki's acid	0.666	0.527–0.804	0.070
PC(18:1(9Z)/P-18:1(9Z))	0.643	0.502–0.784	0.071

Relationship between the four enriched pathways and sarcopenia

In a previous study, it was suggested that metabolites showed remarkable enrichment of purine metabolism for KEGG pathway analysis (12), which supports our findings. Purine metabolism is integral to numerous physiological and pathological processes in mammals, encompassing the inflammatory response, oxidative stress reactions, and cancer (36, 37). The significance of inflammation and oxidative stress as pivotal factors in the pathogenesis of sarcopenia is widely acknowledged (38). KEGG pathway enrichment analysis indicated that hypoxanthine participated in this metabolic pathway. No study has investigated the role of parathyroid hormone synthesis in sarcopenia until now. Parathyroid hormone is a key regulator of calcium and phosphorus homeostasis. KEGG pathway enrichment indicated that 25(OH)D3 participates in this metabolic pathway. In our study, we observed higher plasma 25(OH)D3 levels in subjects with sarcopenia compared to healthy controls. This finding contradicts the findings of most studies, which have reported low 25(OH)D3 levels attributed to chronic inflammation or bacterial

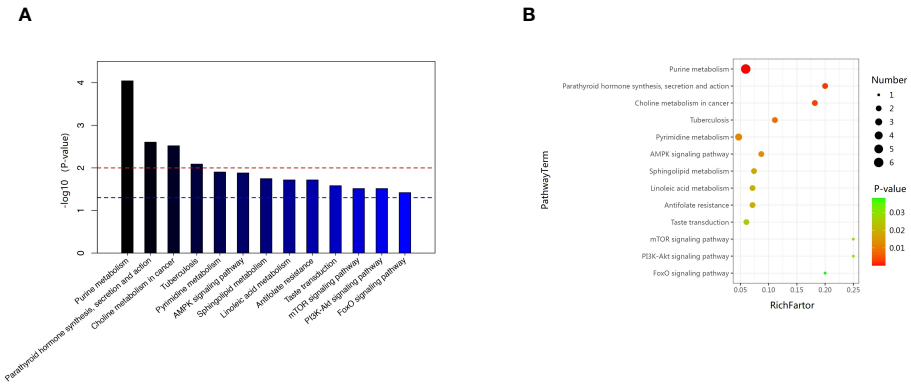

FIGURE 6
(A) Pathway analysis indicates that sphingolipid metabolism is the most statistically enriched pathway. **(B)** Metabolic pathway analysis based on plasma metabolites.

etiology (39). However, Zielińska et al. also found that 25(OH)D3 levels are elevated in inflammatory bowel diseases (40). Moreover, in an experimental model using C57BL/6 mice with induced muscle injury, the administration of excessive doses of 1α,25(OH)D3 or its intramuscular delivery did not show beneficial effects on muscle regeneration.it was observed to potentially have detrimental effects on satellite cell activity, ultimately compromising muscle fiber formation (41). In addition, the differentially expressed metabolite 25(OH)D3 also participates in the pathway of tuberculosis. The pathogenesis of sarcopenia in tuberculosis remains unknown. A thorough comprehension of the parathyroid hormone pathway's involvement in tuberculosis can enhance our understanding of sarcopenia's pathogenesis. In cancer, elevated levels of phosphocholine and total choline-containing compounds characterize the choline metabolite profile. Additionally, several studies have identified connections between choline metabolism in muscle tissue and both muscle protein synthesis and degradation. Therefore, further investigation into these metabolic pathways can advance our understanding of the pathological mechanisms underlying sarcopenia, thereby facilitating the development of more effective treatments.

Strengths and limitations

This study represents one of the initial attempts to explore the connections between plasma metabolic signatures and the susceptibility to sarcopenia in Asian populations using an untargeted metabonomics platform. The untargeted metabonomics approach facilitates the identification of a wide array of metabolites, which will enhance our comprehension of the comprehensive landscape of crucial metabolic pathway alterations in sarcopenia. However, it is important to acknowledge several limitations of our study. Firstly, our findings were derived from a single cohort with a restricted number of cases and controls. Due to the small sample size, the analysis was not adjusted for multiple comparisons. Future research endeavors should incorporate more targeted omics analyses in other thoroughly characterized cohorts or larger validation cohorts to corroborate these findings, while implementing multiple comparison correction techniques. Second, further investigations are warranted to elucidate the precise molecular mechanisms underlying the observed results. Specifically, the role of metabolites such as PCs in sarcopenia remains to be evaluated, and mechanistic studies are imperative to delineate the exact contribution of these metabolites to the pathogenesis of sarcopenia. Additionally, we did not observe significant associations between amino acid metabolism pathways and sarcopenia, possibly due to the relatively small sample size. Sarcopenia is a complex condition influenced by various genetic, lifestyle, and environmental factors. A relatively small sample size may limit the ability to capture the full spectrum of metabolic changes associated with sarcopenia. Finally, the short follow-up time was also a major limitation of this study. Consequently, we plan to extend the follow-up duration in future research to enhance the power to evaluate the risk factors.

Conclusion

In conclusion, we examined the connections between metabolic profiles and the susceptibility to sarcopenia utilizing LC-MS-based untargeted metabolomics methodologies. This investigation unveiled 62 early metabolic signatures and identified four metabolic pathways associated with sarcopenia, potentially enhancing the prognostication and prevention of sarcopenia in Chinese suburb-dwelling older adults. Notably, the top three metabolites, hypoxanthine, L-2-amino-3-oxobutanoic acid, and PC(14:0/20:2(11Z,14Z)), exhibit promise as novel plasma biomarkers for diagnosing sarcopenia. Nonetheless, these findings stem from a single, limited cohort, underscoring the necessity for future validation through robust, large-scale studies.

Data availability statement

The original contributions presented in the study are included in the article/supplementary material. Further inquiries can be directed to the corresponding author.

Ethics statement

The studies involving humans were approved by Ethics Committee of Shanghai University of Medicine and Health Sciences. The studies were conducted in accordance with the local legislation and institutional requirements. The participants provided their written informed consent to participate in this study.

Author contributions

PH: Funding acquisition, Methodology, Formal Analysis, Writing – original draft. XC: Writing – original draft, Investigation, Validation. ZL: Validation, Writing – original draft, Methodology. YL: Data curation, Resources, Writing – review & editing. XY: Data curation, Writing – review & editing, Methodology, Software. PS: Data curation, Writing – review & editing, Formal Analysis. YZ: Data curation, Writing – review & editing, Methodology. HZ: Data curation, Methodology, Writing – review & editing, Investigation. SZ: Investigation, Writing – review & editing. XS: Writing – review & editing. QG: Writing – review & editing, Funding acquisition, Methodology, Supervision, Validation.

Funding

The author(s) declare financial support was received for the research, authorship, and/or publication of this article. This work was supported by the National Natural Science Foundation of China (82202814; 82172552); Shanghai Municipal Health Commission (GWVI-11.2-YQ08; 20214Y0329; 202240367); and Academic Mentorship for Scientific Research Cadre Project (AMSCP-23-03-01).

Acknowledgments

We thank all patients and families for their study participation, and Xiaoyue Gu from the Chongming public health center for providing place and organization.

Conflict of interest

The authors declare that the research was conducted in the absence of any commercial or financial relationships that could be construed as a potential conflict of interest.

Publisher's note

All claims expressed in this article are solely those of the authors and do not necessarily represent those of their affiliated organizations, or those of the publisher, the editors and the reviewers. Any product that may be evaluated in this article, or claim that may be made by its manufacturer, is not guaranteed or endorsed by the publisher.

References

1. Delmonico MJ, Harris TB, Visser M, Park SW, Conroy MB, Velasquez-Mieyer P, et al. Longitudinal study of muscle strength, quality, and adipose tissue infiltration. *Am J Clin Nutr*. (2009) 90:1579–85. doi: 10.3945/ajcn.2009.28047

2. Fielding RA, Vellas B, Evans WJ, Bhasin S, Morley JE, Newman AB, et al. Sarcopenia: an undiagnosed condition in older adults. Current consensus definition: prevalence, etiology, and consequences. International working group on sarcopenia. *J Am Med Directors Assoc*. (2011) 12:249–56. doi: 10.1016/j.jamda.2011.01.003

3. Morley JE. Pharmacologic options for the treatment of sarcopenia. *Calcif Tissue Int*. (2016) 98:319–33. doi: 10.1007/s00223-015-0022-5

4. Zhao Q, Shen H, Liu J, Chiu CY, Su KJ, Tian Q, et al. Pathway-based metabolomics study of sarcopenia-related traits in two US cohorts. *Aging (Albany NY)*. (2022) 14:2101–12. doi: 10.18632/aging.v14i5

5. Meng L, Yang R, Wang D, Wu W, Shi J, Shen J, et al. Specific lysophosphatidylcholine and acylcarnitine related to sarcopenia and its components in older men. *BMC Geriatr*. (2022) 22:249. doi: 10.1186/s12877-022-02953-4

6. Gonzalez-Freire M, Moaddel R, Sun K, Fabbri E, Zhang P, Khadeer M, et al. Targeted metabolomics shows low plasma lysophosphatidylcholine 18:2 predicts greater decline of gait speed in older adults: the baltimore longitudinal study of aging. *J Gerontol A Biol Sci Med Sci*. (2019) 74:62–7. doi: 10.1093/gerona/gly100

7. Liu JC, Dong SS, Shen H, Yang DY, Chen BB, Ma XY, et al. Multi-omics research in sarcopenia: Current progress and future prospects. *Ageing Res Rev*. (2022) 76:101576. doi: 10.1016/j.arr.2022.101576

8. Zhao Q, Shen H, Su KJ, Tian Q, Zhao LJ, Qiu C, et al. A joint analysis of metabolomic profiles associated with muscle mass and strength in Caucasian women. *Aging (Albany NY)*. (2018) 10:2624–35. doi: 10.18632/aging.v10i10

9. Opazo R, Angel B, Marquez C, Lera L, Cardoso Dos Santos GR, Monnerat G, et al. Sarcopenic metabolomic profile reflected a sarcopenic phenotype associated with amino acid and essential fatty acid changes. *Metabolomics*. (2021) 17:83. doi: 10.1007/s11306-021-01832-0

10. Shin HE, Won CW, Kim M. Metabolomic profiles to explore biomarkers of severe sarcopenia in older men: A pilot study. *Exp Gerontol*. (2022) 167:111924. doi: 10.1016/j.exger.2022.111924

11. Lu Y, Karagounis LG, Ng TP, Carre C, Narang V, Wong G, et al. Systemic and metabolic signature of sarcopenia in community-dwelling older adults. *J Gerontol A Biol Sci Med Sci*. (2020) 75:309–17. doi: 10.1093/gerona/glz001

12. Zhou J, Liu J, Lin Q, Shi L, Zeng Z, Guan L, et al. Characteristics of the gut microbiome and metabolic profile in elderly patients with sarcopenia. *Front Pharmacol*. (2023) 14:1279448. doi: 10.3389/fphar.2023.1279448

13. He Y, Cui W, Fang T, Zhang Z, Zeng M. Metabolites of the gut microbiota may serve as precise diagnostic markers for sarcopenia in the elderly. *Front Microbiol*. (2023) 14:1301805. doi: 10.3389/fmicb.2023.1301805

14. Lu Y, Karagounis LG, Ng TP, Carre C, Narang V, Wong G, et al. Systemic and metabolic signature of sarcopenia in community-dwelling older adults. *J Gerontol A Biol Sci Med Sci*. (2020) 75:309–17. doi: 10.1093/gerona/glz001

15. Korostishevsky M, Steves CJ, Malkin I, Spector T, Williams FM, Livshits G. Genomics and metabolomics of muscular mass in a community-based sample of UK females. *Eur J Hum Genet*. (2016) 24:277–83. doi: 10.1038/ejhg.2015.85

16. Murphy RA, Moore SC, Playdon M, Meirelles O, Newman AB, Milijkovic I, et al. Metabolites associated with lean mass and adiposity in older black men. *J Gerontol A Biol Sci Med Sci*. (2017) 72:1352–9. doi: 10.1093/gerona/glw245

17. Lo CJ, Ko YS, Chang SW, Tang HY, Huang CY, Huang YC, et al. Metabolic signatures of muscle mass loss in an elderly Taiwanese population. *Aging (Albany NY)*. (2020) 13:944–56. doi: 10.18632/aging.v13i1

18. Liu H, Lin X, Gong R, Shen H, Qu Z, Zhao Q, et al. Identification and functional characterization of metabolites for skeletal muscle mass in early postmenopausal chinese women. *J Gerontol A Biol Sci Med Sci*. (2022) 77:2346–55. doi: 10.1093/gerona/glac075

19. Ma W, Zhang H, Wu N, Liu Y, Han P, Wang F, et al. Relationship between obesity-related anthropometric indicators and cognitive function in Chinese suburb-dwelling older adults. *PloS One*. (2021) 16:e0258922. doi: 10.1371/journal.pone.0258922

20. Chen LK, Woo J, Assantachai P, Auyeung TW, Chou MY, Iijima K, et al. Asian working group for sarcopenia: 2019 consensus update on sarcopenia diagnosis and treatment. *J Am Med Directors Assoc*. (2020) 21:300–307 e302. doi: 10.1016/j.jamda.2019.12.012

21. Han P, Kang L, Guo Q, Wang J, Zhang W, Shen S, et al. Prevalence and factors associated with sarcopenia in suburb-dwelling older chinese using the asian working group for sarcopenia definition. *J Gerontol A Biol Sci Med Sci*. (2016) 71:529–35. doi: 10.1093/gerona/glv108

22. Zhao Y, Song P, Zhang H, Chen X, Han P, Yu X, et al. Alteration of plasma metabolic profile and physical performance combined with metabolites is more sensitive to early screening for mild cognitive impairment. *Front Aging Neurosci*. (2022) 14:951146. doi: 10.3389/fnagi.2022.951146

23. Wang W, Yang GJ, Zhang J, Chen C, Jia ZY, Li J, et al. Plasma, urine and ligament tissue metabolite profiling reveals potential biomarkers of ankylosing spondylitis using NMR-based metabolic profiles. *Arthritis Res Ther*. (2016) 18:244. doi: 10.1186/s13075-016-1139-2

24. Shida T, Yoshida Y, Ohta T, Kojima N, Osuka Y, Takekoshi K, et al. Identification of a novel biomarker for sarcopenia diagnosis using serum metabolomic analysis: a pilot study. *Eur Geriatr Med*. (2024) 15:571–7. doi: 10.1007/s41999-023-00914-7

25. Xiang L, Zhang H, Wei J, Tian XY, Luan H, Li S, et al. Metabolomics studies on db/db diabetic mice in skeletal muscle reveal effective clearance of overloaded intermediates by exercise. *Anal Chim Acta*. (2018) 1037:130–9. doi: 10.1016/j.aca.2017.11.082

26. Durham WJ, Casperson SL, Dillon EL, Keske MA, Paddon-Jones D, Sanford AP, et al. Age-related anabolic resistance after endurance-type exercise in healthy humans. *FASEB J*. (2010) 24:4117–27. doi: 10.1096/fj.09-150177

27. Beavers KM, Beavers DP, Serra MC, Bowden RG, Wilson RL. Low relative skeletal muscle mass indicative of sarcopenia is associated with elevations in serum uric acid levels: findings from NHANES III. *J nutrition Health Aging*. (2009) 13:177–82. doi: 10.1007/s12603-009-0054-5

28. Lawton KA, Berger A, Mitchell M, Milgram KE, Evans AM, Guo L, et al. Analysis of the adult human plasma metabolome. *Pharmacogenomics*. (2008) 9:383–97. doi: 10.2217/14622416.9.4.383

29. Yegutkin GG. Enzymes involved in metabolism of extracellular nucleotides and nucleosides: functional implications and measurement of activities. *Crit Rev Biochem Mol Biol*. (2014) 49:473–97. doi: 10.3109/10409238.2014.953627

30. Derbre F, Gratas-Delamarche A, Gomez-Cabrera MC, Vina J. Inactivity-induced oxidative stress: a central role in age-related sarcopenia? *Eur J Sport Sci*. (2014) 14 Suppl 1:S98–108. doi: 10.1080/17461391.2011.654268

31. Yao W, Gu H, Zhu J, Barding G, Cheng H, Bao B, et al. Integrated plasma and urine metabolomics coupled with HPLC/QTOF-MS and chemometric analysis on potential biomarkers in liver injury and hepatoprotective effects of Er-Zhi-Wan. *Anal Bioanal Chem*. (2014) 406:7367–78. doi: 10.1007/s00216-014-8169-x

32. El Hafidi M, Perez I, Zamora J, Soto V, Carvajal-Sandoval G, Banos G. Glycine intake decreases plasma free fatty acids, adipose cell size, and blood pressure in sucrose-fed rats. *Am J Physiol Regul Integr Comp Physiol*. (2004) 287:R1387–1393. doi: 10.1152/ajpregu.00159.2004

33. Gu X, Al Dubayee M, Alshahrani A, Masood A, Benabdelkamel H, Zahra M, et al. Distinctive metabolomics patterns associated with insulin resistance and type 2 diabetes mellitus. *Front Mol Biosci*. (2020) 7:609806. doi: 10.3389/fmolb.2020.609806

34. Hinkley JM, Cornnell HH, Standley RA, Chen EY, Narain NR, Greenwood BP, et al. Older adults with sarcopenia have distinct skeletal muscle phosphodiester, phosphocreatine, and phospholipid profiles. *Aging Cell*. (2020) 19:e13135. doi: 10.1111/acel.13135

35. Wang X, Xiao R, Li H, Li T, Guan L, Ding H, et al. Correlation between mild cognitive impairment and sarcopenia: the prospective role of lipids and basal metabolic rate in the link. *Nutrients*. (2022) 14:1–19. doi: 10.2139/ssrn.4099408

36. Antonioli L, Blandizzi C, Pacher P, Hasko G. Immunity, inflammation and cancer: a leading role for adenosine. *Nat Rev Cancer*. (2013) 13:842–57. doi: 10.1038/nrc3613

37. Antonioli L, Colucci R, Pellegrini C, Giustarini G, Tuccori M, Blandizzi C, et al. The role of purinergic pathways in the pathophysiology of gut diseases: pharmacological modulation and potential therapeutic applications. *Pharmacol Ther*. (2013) 139:157–88. doi: 10.1016/j.pharmthera.2013.04.002

38. Nishikawa H, Fukunishi S, Asai A, Yokohama K, Nishiguchi S, Higuchi K. Pathophysiology and mechanisms of primary sarcopenia (Review). *Int J Mol Med*. (2021) 48. doi: 10.3892/ijmm

39. Mangin M, Sinha R, Fincher K. Inflammation and vitamin D: the infection connection. *Inflammation Res*. (2014) 63:803–19. doi: 10.1007/s00011-014-0755-z

40. Zielinska A, Sobolewska-Wlodarczyk A, Wisniewska-Jarosinska M, Gasiorowska A, Fichna J, Salaga M. The 25(OH)D3, but not 1,25(OH)2D3 levels are elevated in IBD patients regardless of vitamin D supplementation and do not associate with pain severity or frequency. *Pharm (Basel)*. (2021) 14:1–14. doi: 10.3390/ph14030284

41. Srikuea R, Hirunsai M. Effects of intramuscular administration of 1alpha,25 (OH)2D3 during skeletal muscle regeneration on regenerative capacity, muscular fibrosis, and angiogenesis. *J Appl Physiol (1985)*. (2016) 120:1381–93. doi: 10.1152/japplphysiol.01018.2015

frontiers | Frontiers in Endocrinology

TYPE Original Research
PUBLISHED 22 July 2024
DOI 10.3389/fendo.2024.1398235

OPEN ACCESS

EDITED BY
Kenju Shimomura,
Fukushima Medical University, Japan

REVIEWED BY
Jinhui Zhou,
Chinese Center for Disease Control and Prevention, China
Guoxin Ni,
First Affiliated Hospital of Xiamen University, China
Giuseppe Battaglia,
University of Palermo, Italy

*CORRESPONDENCE
Lijie Qin
qinlijie1819@163.com
Juan Xu
sophia2932@163.com

†These authors have contributed equally to this work and share first authorship

RECEIVED 09 March 2024
ACCEPTED 08 July 2024
PUBLISHED 22 July 2024

CITATION
Bai W, An S, Jia H, Xu J and Qin L (2024) Relationship between triglyceride-glucose index and cognitive function among community-dwelling older adults: a population-based cohort study. *Front. Endocrinol.* 15:1398235. doi: 10.3389/fendo.2024.1398235

Relationship between triglyceride-glucose index and cognitive function among community-dwelling older adults: a population-based cohort study

Weimin Bai[1†], Shuang An[2†], Hui Jia[3†], Juan Xu[4*] and Lijie Qin[1*]

[1]Department of Emergency, Henan Provincial People's Hospital, People's Hospital of Zhengzhou University, People's Hospital of Henan University, Zhengzhou, China, [2]Department of Pediatric Rehabilitation, Henan Children's Hospital Zhengzhou Children's Hospital, Children's Hospital Affiliated to Zhengzhou University, Zhengzhou, China, [3]Department of Convalescent Four Areas Nine Departments, Navy Qingdao Special Service Recuperation Center, Qingdao, China, [4]Department of General Surgery, Affiliated Xiaoshan Hospital, Hangzhou Normal University, Hangzhou, China

Background: The global increase in the aging population presents considerable challenges, particularly regarding cognitive impairment, a major concern for public health. This study investigates the association between the triglyceride-glucose (TyG) index, a measure of insulin resistance, and the risk of cognitive impairment in the elderly.

Methods: This prospective cohort study enrolled 2,959 participants aged 65 and above from the 2015 and 2020 waves of the China Health and Retirement Longitudinal Study (CHARLS). The analysis employed a logistic regression model to assess the correlation between the TyG index and cognitive impairment.

Results: The study included 2,959 participants, with a mean age of 71.2 ± 5.4 years, 49.8% of whom were female. The follow-up in 2020 showed a decrease in average cognitive function scores from 8.63 ± 4.61 in 2015 to 6.86 ± 5.45. After adjusting for confounding factors, a significant association was observed between TyG index quartiles and cognitive impairment. Participants in the highest quartile (Q4) of baseline TyG had a higher risk of cognitive impairment compared to those in the lowest quartile (Q1) (odds ratio [OR]: 1.97, 95% confidence intervals [CI]: 1.28–2.62, P<0.001).

Conclusion: The study highlights a significant connection between elevated TyG index levels and cognitive impairment among older adults in China. These findings suggest that targeted interventions to reduce the TyG index could mitigate cognitive impairment and potentially lower the incidence of dementia.

KEYWORDS

triglyceride glucose, cognitive impairment, elderly, insulin resistance, CHARLS

1 Introduction

The global aging phenomenon poses unprecedented challenges, notably in aggravating concerns associated with cognitive impairment (1–5). Cognitive impairment encompasses the reception and processing of information, characterized by memory loss, diminished understanding, impaired focus, and difficulties in calculation (6, 7). These cognitive alterations are regarded as the preclinical phase of dementia, possibly affected by factors like fasting glucose levels, physical performance, and other variables, highlighting its significance as a major public health concern (3, 8–10). Therefore, identifying risk factors to prevent cognitive impairment at early stages is essential (3, 6, 11–13).

There is growing evidence supporting the association between insulin resistance (IR) and the risk of cognitive decline (14–17). However, previous studies have primarily relied on the gold standard methods of insulin clamp and intravenous glucose tolerance test for diagnosing IR, which are not commonly performed in clinical settings (18–20).

The triglyceride-glucose (TyG) index, a readily available and cost-effective metric derived from triglyceride (TG) and fasting blood glucose (FBG) levels, has been recognized as a promising surrogate marker for IR (14, 18, 19, 21). Extensive epidemiological research has indicated significant links between the TyG index and various diseases, including cardiovascular diseases, cancers, and diabetes (22, 23). Nonetheless, the validity of the TyG index as an alternative indicator of IR in assessing its relationship with cognitive impairment is still in question. Prior investigations have largely concentrated on the TyG and cognitive function relationship within specific demographics, such as non-diabetic, gender-specific cohorts, or individuals living in rural areas, often focusing on specific cognitive domains (24–27).

This study, grounded in population-based research, seeks to explore the relationship between the TyG index and the occurrence of cognitive impairment in a wider elderly population. Utilizing the most recent cognitive function follow-up data from the 2020 China Health and Retirement Longitudinal Study (CHARLS) database, our work aims to offer an exhaustive and prolonged examination of this association across the entire elderly cohort. The study hypothesis is that elevated TyG index may be associated with cognitive impairment among older adults in China.

2 Materials and methods

2.1 Study population

The CHARLS is a comprehensive national study comprising five waves aimed at collecting health and social data from Chinese citizens aged 45 years and older (28). The CHARLS project aims to analyze the issue of population aging in China and promote interdisciplinary research on aging. CHARLS is a recurring survey conducted every 2 to 3 years. CHARLS employs a multi-stage probability proportional to size sampling approach, encompassing a sample frame of 450 villages, 150 counties, and 28 provinces. The study involves participation from over 20,000 individuals residing in approximately 10,000 households. Participants undergo face-to-face interviews at home using computer-assisted personal interviewing technology. Survey topics include basic demographic information of respondents and their families, intergenerational transfers within households, health status, medical insurance coverage, employment, income, expenditures, and assets. Additionally, CHARLS includes physical measurements and blood sample collection. Detailed information about CHARLS has been published in previous literature, and the CHARLS dataset is available for download on the CHARLS homepage at http://charls.pku.edu.cn/en. For our study, we used data from the 2015 and 2020 CHARLS surveys, with the former serving as the baseline. Initially, 5,511 participants aged 65 and older were selected from the database (25). To ensure the integrity of the data, we applied specific exclusion criteria: (1) participants with missing data on TG and FBG in 2015 (n = 1,844); (2) participants with missing data on cognitive function in 2015 and 2020 (n = 99); (3) participants with cognitive impairment in 2015 (n = 400); (4) ever having memory disorders or mental health conditions (n = 209). As a result, 2,959 participants satisfied all inclusion criteria and were incorporated into the study (Figure 1).

CHARLS received ethical approval from the Ethical Review Committee of Peking University (IRB00001052-11015). All participants provided informed consent by signing consent forms before taking part in the study.

2.2 Measurement of cognitive function and TyG index

Assessments of cognitive function were conducted during the follow-up surveys in 2015 and 2020, incorporating tests for episodic memory and mental acuity using a method akin to that employed in the American Health and Retirement Study (28). Participants were first asked to remember a list of ten words immediately after an interviewer read them aloud. Approximately 4 minutes later, they were asked to recall these words once more (delayed recall). The evaluation of episodic memory was based on the average scores from both the immediate and delayed recall tasks, with possible scores ranging from 0 to 10. For assessing mental acuity, participants completed a series of tasks including drawing a specific figure accurately, answering questions regarding the current date, season, and day of the week, and performing a serial subtraction task (subtracting 7 from 100 in five consecutive attempts). Each correct answer earned one point, culminating in a maximum possible score of 11 points (29, 30). The aggregate of these scores represented the participant's overall cognitive status, with total scores varying between 0 and 21, where higher scores signified superior cognitive function. According to previous research, cognitive impairment was determined as a score 1.0 standard deviation or more below the mean value of cognitive function (31–33).

TG and FBG levels were measured using a standard enzymatic colorimetric method. The TyG index was computed as ln (fasting TG [mg/dL] × FBG [mg/dL]/2) (14, 34). Participants were categorized into four groups (Q1, Q2, Q3, and Q4) based on quartiles of their TyG index.

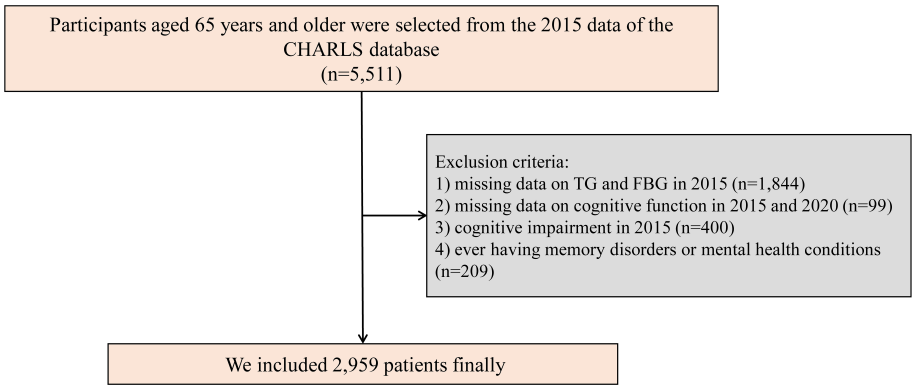

FIGURE 1
Study flowchart. CHARLS, China Health and Retirement Longitudinal Study; TG, triglyceride; FBG, fasting blood glucose.

2.3 Covariates

Covariates were selected based on previous research, baseline differences, and clinical significance (26, 33, 35). The potential confounders considered included age, gender, body mass index (BMI), educational level (illiterate, elementary school, middle school, and higher), place of residence (urban and rural), alcohol consumption (more than once a month, less than once a month, never), smoking status (current, former, never), hypertension (yes/no), diabetes (yes/no), overall health status (poor, fair, good, very good, and higher), and cognitive function in 2015.

2.4 Statistical analysis

Descriptive statistics were employed to summarize the data, presented as the mean (standard deviation [SD]), median (interquartile range [IQR]), or count and percentage, as appropriate. The chi-square test was used to examine differences among categorical variables. For continuous variables adhering to a normal distribution, one-way analysis of variance (ANOVA) was utilized. When continuous variables did not follow a normal distribution, the Kruskal–Wallis test was applied. These statistical methods aimed to evaluate the disparities and relationships between variables in the study.

Participants were categorized into four groups based on quartiles of the TyG index: Q1 (<8.21), Q2 (≥8.21–8.55), Q3 (≥8.55–8.97), and Q4 (≥8.97). A logistic regression model was used to investigate the independent associations between the TyG index and cognitive impairment, with results presented as adjusted odds ratios (OR) with 95% confidence intervals (CI). Covariates were selected based on previous literature and clinical insight (26, 33, 35). Model 1 was unadjusted; Model 2 adjusted for age and gender; and Model 3 further adjusted for age, gender, BMI, educational level, residence, drinking and smoking status, hypertension, diabetes, overall health, and cognitive function in 2015. We have also utilized Cox regression as a sensitivity analysis to further bolster our research findings. A subgroup analysis also explored the relationship between the TyG index and cognitive impairment across specific subgroups, including gender (male and female), age (65–75 years and ≥75 years), BMI (<24 kg/m^2 and ≥24 kg/m^2) (25), presence of chronic diseases (0 and ≥1), and diabetes (yes and no).

The statistical significance was determined using two-tailed tests, with a significance threshold of < 0.05 for the p values. All statistical analyses were performed using R software, version 4.2.2, developed by the R Foundation for Statistical Computing, based in Vienna, Austria.

3 Results

3.1 Baseline characteristics

The current study comprised a cohort of 2,959 participants. The participants' mean age was 71.2 ± 5.4 years, with 49.8% being female (n = 1,475). They were categorized into four groups according to the quartiles of the TyG index: Q1 (739), Q2 (740), Q3 (740), and Q4 (740). A majority of the participants lived in rural areas (59.5%) and had attained an elementary school level of education (47.8%). The average BMI was recorded at 23.85 ± 7.68 kg/m^2, and the mean score for depressive symptoms was 8.05 ± 6.50. Furthermore, 32.8% of the participants reported a history of chronic diseases, whereas 56.1% identified as current smokers. Participants in the highest TyG index group displayed a higher BMI, a greater proportion of females, and a more prevalent history of ≥2 chronic diseases, notably diabetes and hypertension. Table 1 details the baseline characteristics more comprehensively.

3.2 Association between TyG index and cognition function

In the cognitive function assessments conducted in 2015, the average score was 8.63 ± 4.61. A follow-up visit in 2020 indicated a progressive decline in cognitive function scores to 6.86 ± 5.45

10.3389/fendo.2024.1398235

TABLE 1 Baseline characteristics according to TyG index level at 2015 wave.

Characteristic	TyG index level					P-value
	Overall	Q1 (<8.21)	Q2 (≥8.21, <8.55)	Q3 (≥8.55, <8.97)	Q4 (≥8.97)	
	N= 2959	N = 739	N = 740	N = 740	N = 740	
Female, n (%)	1475 (49.8)	246 (33.3)	335 (45.3)	419 (56.6)	475 (64.2)	<0.001
Age, years	71.2 (5.4)	71.3 (5.4)	71.4 (5.3)	71.2 (5.4)	70.9 (5.4)	0.327
BMI, kg/m^2	23.85 (7.68)	22.58 (8.63)	22.52 (3.54)	24.09 (7.54)	26.22 (8.75)	<0.001
Residence, n (%)						0.344
Rural	1441 (59.5)	360 (61.5)	374 (61.1)	352 (58.0)	355 (57.4)	
Urban	981 (40.5)	225 (38.5)	238 (38.9)	255 (42.0)	263 (42.6)	
Educational, n (%)						0.632
Illiterate	1038 (35.1)	251 (34.0)	266 (35.9)	264 (35.7)	257 (34.7)	
Elementary school	1414 (47.8)	367 (49.7)	354 (47.8)	335 (45.3)	358 (48.4)	
Middle school and above	507 (17.1)	121 (16.4)	120 (16.2)	141 (19.1)	125 (16.9)	
Health, n (%)						0.069
Poor	140 (4.8)	29 (4.0)	31 (4.3)	33 (4.5)	47 (6.5)	
Fair	575 (19.9)	133 (18.5)	148 (20.4)	139 (19.1)	155 (21.5)	
Good	1552 (53.6)	384 (53.5)	381 (52.4)	395 (54.3)	392 (54.4)	
Very good and above	627 (21.7)	172 (24.0)	167 (23.0)	161 (22.1)	127 (17.6)	
Marital status, n (%)						0.223
Single	780 (26.4)	189 (25.6)	213 (28.8)	179 (24.2)	199 (26.9)	
Married	2179 (73.6)	550 (74.4)	527 (71.2)	561 (75.8)	541 (73.1)	
History of smoke, n (%)						<0.001
Current	782 (56.1)	248 (57.7)	242 (64.0)	154 (51.5)	138 (48.1)	
Cessation	513 (36.8)	145 (33.7)	125 (33.1)	123 (41.1)	120 (41.8)	
Never	99 (7.1)	37 (8.6)	11 (2.9)	22 (7.4)	29 (10.1)	
History of drink, n (%)						<0.001
More than once a month	742 (25.1)	254 (34.4)	198 (26.8)	164 (22.2)	126 (17.0)	
Less than once a month	214 (7.2)	56 (7.6)	56 (7.6)	45 (6.1)	57 (7.7)	
Never	2002 (67.7)	429 (58.1)	486 (65.7)	530 (71.7)	557 (75.3)	
Depressive score	8.05 (6.50)	7.99 (6.54)	7.98 (6.50)	8.13 (6.60)	8.11 (6.38)	0.960
Chronic diseases, n (%)						0.040
0	1988 (67.2)	523 (70.8)	508 (68.6)	482 (65.1)	475 (64.2)	
1	523 (17.7)	113 (15.3)	125 (16.9)	144 (19.5)	141 (19.1)	
≥2	448 (15.1)	103 (13.9)	107 (14.5)	114 (15.4)	124 (16.7)	
Diabetes, n (%)	318 (10.7)	67 (9.1)	76 (10.3)	76 (10.3)	99 (13.4)	<0.001
Hypertension, n (%)	1223 (41.3)	291 (39.4)	301 (40.7)	307 (41.5)	324 (43.8)	<0.001
Cognitive function in 2015	8.63 (4.61)	8.92 (4.64)	8.67 (4.58)	8.60 (4.59)	8.32 (4.58)	0.031
Cognitive function in 2020	6.86 (5.45)	7.12 (5.47)	7.04 (5.45)	6.87 (5.42)	6.38 (5.32)	0.007

Continuous variables were shown in mean (SD) and categorical variables were shown in percentages.
TyG index, Triglyceride glucose index; BMI, body mass index.

(Table 1). After adjusting for confounding variables, a significant relationship emerged between the TyG index quartiles and cognitive impairment. Participants in Q4 were found to have a higher risk of cognitive impairment compared to those in Q1 (OR: 1.97, 95% CI: 1.28–2.62, $P < 0.001$). Nevertheless, the associations between the TyG index in Q2 and Q3 quartiles and cognitive impairment did not reach statistical significance in the 2020 follow-up ($P > 0.05$) (Table 2).

3.3 Subgroup and sensitivity analyses

The subgroup analysis demonstrated consistent outcomes across various stratified subgroups, such as gender, age, BMI, chronic diseases, and diabetes, with no significant interaction effects observed (P-interaction > 0.05). Participants in the highest quartile of the TyG index (Q4) exhibited an increased risk of cognitive impairment, with the exception of individuals characterized by a lower BMI, absence of chronic diseases, and male gender (Table 3). The sensitivity analysis yielded results consistent with the main findings, indicating a significant correlation between TyG index and cognitive impairment (Additional Table 1).

4 Discussion

In this study, we observed a significant association between a higher TyG index and cognitive impairment in older adults (aged 65 years and above). A follow-up visit in 2020 revealed a gradual decline in cognitive function scores compared to the baseline in 2015. Stratified analysis by age, gender, BMI, chronic diseases, and diabetes showed that individuals with a higher TyG index faced a greater risk of cognitive impairment, with the exception of those with lower BMI, those without chronic diseases, and males. These findings suggest that a higher TyG index could be a potential risk factor for cognitive impairment in older adults, particularly in females and in those with higher BMI and chronic diseases.

The aging global population presents an unprecedented challenge, raising significant concerns (1–3). The rapid pace of aging intensifies the challenges associated with cognitive impairment (4, 5). The age-related decline in cognitive function has become a significant public health issue, leading to adverse health outcomes (11, 13). Cognitive impairment often manifests years before the onset of dementia, underscoring the need to explore its mechanisms and to implement preventive measures aimed at risk factors. Previous research has identified several key factors contributing to cognitive decline, including genetic predisposition, cardiovascular disease, and exposure to air pollution (36–40).

IR is characterized by reduced sensitivity and responsiveness to the effects of insulin, acting as a central factor in the emergence of various health issues, such as diabetes, cardiovascular diseases, and cognitive decline (3, 14). Moreover, some evidence suggests that IR is linked to an increased risk of cognitive decline (14–16). The hyperinsulinemic euglycemic clamp, despite its exceptional sensitivity in assessing the body's response to insulin, is costly and complex, limiting its use in clinical environments. The homeostasis model assessment of insulin resistance (HOMA-IR), based on FPG and insulin measurements, is considered the gold standard for evaluating insulin sensitivity. However, the measurement of insulin levels is not commonly included in routine clinical practice, thereby restricting the use of HOMA-IR in such contexts. The TyG index, a practical measure of IR derived from TG and FBG levels, offers a cost-effective and accessible alternative for IR assessment, gaining widespread adoption in research (14, 18, 19). Epidemiological studies have linked the TyG index to various conditions, including cardiovascular diseases, cancers, and diabetes. Yet, the effectiveness of the TyG index as an indirect marker for IR in exploring its association with cognitive impairment remains to be fully ascertained.

Previous research on the TyG index and cognitive function has predominantly focused on specific demographic groups, such as non-diabetic individuals, gender-specific populations, and rural dwellers, often categorizing cognitive function into distinct domains (24–27). Utilizing data from the National Health and Nutrition Examination Survey (NHANES), Wei et al. found a

TABLE 2 The association between TyG index (quartiles) and the risk of cognitive impairment in 2020.

	Event (%)	Model 1 [a]		Model 2 [b]		Model 3 [c]	
		OR (95% CI)	P Value	OR (95% CI)	P Value	OR (95% CI)	P Value
2020 cognitive impairment							
Q1	160 (21.7)	Ref.		Ref.		Ref.	
Q2	168 (22.7)	0.91 (0.72-1.15)	0.436	0.86 (0.69-1.13)	0.330	0.75 (0.47-1.20)	0.231
Q3	176 (23.8)	1.01 (0.72-1.41)	0.671	1.03 (0.73-1.57)	0.609	1.11 (0.70-1.69)	0.634
Q4	188 (25.4)	1.14 (1.02-2.03)	0.014	1.52 (1.19-2.20)	<0.001	1.97 (1.28-2.62)	<0.001
P value for trend			0.007		<0.001		<0.001

TyG index, triglyceride glucose index; OR, odds ratios; CI, confidence intervals.
[a]unadjusted.
[b]adjusted for age, gender.
[c]adjusted for age, gender, body mass index, educational level, residence, drinking status, smoking status, hypertension, diabetes, health status, cognitive function in 2015.

10.3389/fendo.2024.1398235

TABLE 3 Subgroup and interaction analysis between the TyG index and cognitive impairment in 2020 across various subgroups.

Subgroups	TyG	Event (%)	OR (95% CI)	P Value		TyG	Event (%)	OR (95% CI)	P Value	P-interaction
Gender										0.531
Male	Q1	104 (21.1)	Ref.		Female	Q1	56 (22.8)	Ref.		
	Q2	88 (21.7)	0.73 (0.39-1.28)	0.261		Q2	80 (23.9)	1.34 (0.29-2.95)	0.731	
	Q3	85 (26.5)	0.86 (0.52-1.69)	0.653		Q3	91 (21.7)	1.45 (0.32-3.17)	0.639	
	Q4	70 (26.4)	1.05 (0.59-2.07)	0.118		Q4	118 (25.9)	1.15 (1.05-1.27)	0.003	
Age										0.443
65-75 years	Q1	101 (18.2)	Ref.		≥75 years	Q1	59 (32.0)	Ref.		
	Q2	102 (18.3)	0.81 (0.43-1.49)	0.486		Q2	66 (36.3)	0.62 (0.30-1.24)	0.179	
	Q3	106 (18.9)	1.18 (0.58-2.41)	0.637		Q3	70 (39.1)	1.34 (0.69-2.19)	0.193	
	Q4	116 (20.2)	1.25 (1.01-2.59)	<0.001		Q4	72 (43.6)	1.76 (1.09-3.12)	<0.001	
BMI										0.544
<24 kg/m^2	Q1	130 (21.4)	Ref.		≥24 kg/m^2	Q1	30 (24.0)	Ref.		
	Q2	109 (21.5)	0.97 (0.59-1.68)	0.803		Q2	59 (26.5)	1.09 (0.85-1.62)	0.721	
	Q3	93 (24.3)	1.13 (0.90-2.59)	0.523		Q3	83 (23.9)	1.15 (0.78-2.13)	0.565	
	Q4	69 (25.5)	1.46 (0.67-3.51)	0.901		Q4	119 (26.0)	1.51 (1.11-3.52)	<0.001	
Chronic diseases										0.902
0	Q1	130 (21.8)	Ref.		>=1	Q1	30 (20.8)	Ref.		
	Q2	126 (21.7)	0.87 (0.48-1.58)	0.656		Q2	42 (26.3)	0.80 (0.27-2.32)	0.692	
	Q3	122 (22.0)	1.03 (0.66-1.92)	0.271		Q3	54 (29.0)	1.01 (0.32-3.29)	0.753	
	Q4	128 (23.4)	1.20 (0.97-2.05)	0.924		Q4	60 (31.0)	1.23 (1.13-2.78)	<0.001	
Diabetes										0.815
No	Q1	145 (20.5)	Ref.		Yes	Q1	15 (22.4)	Ref.		
	Q2	156 (22.5)	0.93 (0.49-1.78)	0.851		Q2	12 (15.8)	1.02 (0.32-2.01)	0.383	
	Q3	159 (23.7)	1.25 (0.74-2.10)	0.165		Q3	17 (22.4)	1.19 (0.82-2.89)	0.820	
	Q4	156 (27.4)	1.53 (1.17-2.35)	<0.001		Q4	32 (32.3)	1.69 (1.05-3.07)	<0.001	

Adjusted OR in cognitive impairment across quantiles of TyG index by gender, age, BMI, chronic diseases, and diabetes groups. TyG, triglyceride-glucose; BMI, body mass index; OR, odds ratios; CI, confidence intervals.

notable correlation between a high TyG index and reduced cognitive function, as determined by the CERAD test, in non-diabetic elderly individuals in the United States (24). Similarly, a study among elderly residents in rural China linked elevated TyG index values with diminished cognitive performance and brain atrophy (25).

Our population-based study aimed to explore the relationship between the TyG index and cognitive impairment among the elderly population in China. Utilizing data from a continuous cohort, we collected information from consecutive cognitive assessments conducted in 2020. We found a significant association between a higher TyG index and cognitive impairment in older adults during the follow-up visits in 2020, especially pronounced in females, individuals with a higher BMI, and those suffering from chronic conditions. Additionally, our findings showed that cognitive function scores were lower in females than in males. These results align with previous research. Earlier investigations have consistently indicated that females are at a greater risk of cognitive impairments compared to males (3, 41, 42). A study examining a 5-year change in the TyG index and its impact on cognitive function found that females in the second quartile of longitudinal TyG index change exhibited a significant association with reduced cognitive performance as measured by the CERAD test (26). Moreover, it was noted that females have a higher vulnerability to cognitive impairment compared to males (3).

Several factors might elucidate the observed results, necessitating consideration of the underlying mechanisms. Insulin possesses the ability to traverse the blood-brain barrier through specific receptors, affecting both behavioral and metabolic functions (17, 43). IR represents a unique metabolic disorder often

characterized by increased insulin levels, which can lead to neurodegeneration and persistent memory impairments due to prolonged exposure of brain neurons to elevated insulin levels (44). Furthermore, IR could diminish cerebral glucose metabolism in particular brain regions, possibly adversely affecting memory function in individuals (45). Some clinical studies have indicated that TG can cross the blood-brain barrier, potentially impairing cognitive function by inducing insulin receptor resistance (46). In our study, most female participants were postmenopausal, a phase associated with reduced estrogen levels. Previous research has identified estrogen as vital for learning and memory, providing neuroprotection and potentially enhancing cognitive function through estrogen therapy (47, 48). This could explain the more pronounced cognitive decline observed in females compared to males in our study. In the BMI-stratified analysis, the link between an elevated TyG index and cognitive impairment was observed solely in overweight and obese individuals, highlighting IR's traditional association with obesity, which is closely related to brain atrophy (25). Additionally, a study examining the relationship between the TyG index and lower brain volume found this association exclusively in individuals with a BMI ≥24 kg/m^2 (25).

The issue of cognitive impairment is becoming increasingly evident as the population ages. Serving as an early indicator of dementia, cognitive impairment is associated with a notably adverse prognosis, affecting individual quality of life and placing burdens on families and society. The early prevention of cognitive impairment is thus critical and urgent. Our research suggests that the TyG index could serve as an alternative marker of IR for predicting cognitive impairment in individuals over 65 years old in China, with a significant relationship observed between high TyG index and cognitive impairment. Targeted interventions could help in mitigating cognitive impairment, potentially decreasing the incidence of dementia. Additionally, further exploration into identifying more predictive risk factors for cognitive impairment is necessary to achieve the objective of early prevention.

This study has several limitations. First, it is important to recognize that the study was observational. Despite efforts to adjust for known confounders, the potential impact of unmeasured confounders on the outcomes cannot be disregarded. Therefore, the applicability of our findings may be somewhat restricted. Moreover, we evaluate cognitive function using episodic memory and mental acuity rather than clinical diagnosis. Comprehensive assessment across multiple dimensions is crucial for understanding overall cognitive function, highlighting limitations when evaluating solely based on episodic memory and mental acuity. However, these neuropsychological tests are widely regarded as reliable screening tools for measuring cognitive function and are extensively used in clinical practice (49). Finally, due to data availability limitations, our analysis was confined to a 5-year follow-up period from 2015 to 2020. Future studies should consider employing repeated-measures designs over longer durations and examining more potential pathways. Subsequent research is warranted to refine these findings further.

5 Conclusion

The results of this study reveal a notable association between elevated TyG index levels and the occurrence of cognitive impairment among the elderly Chinese demographic. The initiation of targeted intervention strategies may effectively mitigate cognitive impairment, potentially decreasing the prevalence of dementia.

Data availability statement

The datasets presented in this study can be found in online repositories. The names of the repository/repositories and accession number(s) can be found below: http://charls.pku.edu.cn/pages/data/111/zhcn.html.

Ethics statement

The studies involving humans were approved by the Ethical Review Committee of Peking University (IRB00001052-11015). The studies were conducted in accordance with the local legislation and institutional requirements. Written informed consent for participation was not required from the participants or the participants' legal guardians/next of kin in accordance with the national legislation and institutional requirements.

Author contributions

WMB: Data curation, Formal analysis, Investigation, Methodology, Validation, Writing – original draft. SA: Data curation, Investigation, Project administration, Validation, Writing – original draft. HJ: Data curation, Formal analysis, Investigation, Project administration, Software, Writing – original draft. JX: Conceptualization, Formal analysis, Methodology, Resources, Supervision, Writing – review & editing. LJQ: Data curation, Formal analysis, Investigation, Methodology, Resources, Supervision, Writing – review & editing.

Funding

The author(s) declare that no financial support was received for the research, authorship, and/or publication of this article.

Acknowledgments

We extend our sincere gratitude to Peking University for granting access to the CHARLS database, and we appreciate the participation of all individuals included in the database.

Conflict of interest

The authors declare that the research was conducted in the absence of any commercial or financial relationships that could be construed as a potential conflict of interest.

Publisher's note

All claims expressed in this article are solely those of the authors and do not necessarily represent those of their affiliated organizations, or those of the publisher, the editors and the reviewers. Any product that may be evaluated in this article, or claim that may be made by its manufacturer, is not guaranteed or endorsed by the publisher.

Supplementary material

The Supplementary Material for this article can be found online at: https://www.frontiersin.org/articles/10.3389/fendo.2024.1398235/full#supplementary-material

References

1. Beard JR, Officer A, de Carvalho IA, Sadana R, Pot AM, Michel JP, et al. The World report on ageing and health: a policy framework for healthy ageing. *Lancet*. (2016) 387:2145–54. doi: 10.1016/S0140-6736(15)00516-4

2. Gerland P, Raftery AE, Sevčíková H, Li N, Gu D, Spoorenberg T, et al. World population stabilization unlikely this century. *Science*. (2014) 346:234–7. doi: 10.1126/science.1257469

3. Jia L, Du Y, Chu L, Zhang Z, Li F, Lyu D, et al. Prevalence, risk factors, and management of dementia and mild cognitive impairment in adults aged 60 years or older in China: a cross-sectional study. *Lancet Public Health*. (2020) 5:e661–71. doi: 10.1016/S2468-2667(20)30185-7

4. Hebert LE, Weuve J, Scherr PA, Evans DA. Alzheimer disease in the United States (2010-2050) estimated using the 2010 census. *Neurology*. (2013) 80:1778–83. doi: 10.1212/WNL.0b013e31828726f5

5. Weuve J, Hebert LE, Scherr PA, Evans DA. Deaths in the United States among persons with Alzheimer's disease (2010-2050). *Alzheimer's Dementia J Alzheimer's Assoc*. (2014) 10:e40–46. doi: 10.1016/j.jalz.2014.01.004

6. Global, regional, and national burden of Alzheimer's disease and other dementias, 1990-2016: a systematic analysis for the Global Burden of Disease Study 2016. *Lancet Neurol*. (2019) 18:88–106. doi: 10.1016/S1474-4422(18)30403-4

7. McArdle JJ, Ferrer-Caja E, Hamagami F, Woodcock RW. Comparative longitudinal structural analyses of the growth and decline of multiple intellectual abilities over the life span. *Dev Psychol*. (2002) 38:115–42. doi: 10.1037/0012-1649.38.1.115

8. Aarsland D, Creese B, Politis M, Chaudhuri KR, Ffytche DH, Weintraub D, et al. Cognitive decline in Parkinson disease. *Nat Rev Neurol*. (2017) 13:217–31. doi: 10.1038/nrneurol.2017.27

9. Bianco A, Pomara F, Thomas E, Paoli A, Battaglia G, Petrucci M, et al. Type 2 diabetes family histories, body composition and fasting glucose levels: a cross-section analysis in healthy sedentary male and female. *Iranian J Public Health*. (2013) 42:681–90.

10. Patti A, Bianco A, Karsten B, Montalto MA, Battaglia G, Bellafiore M, et al. The effects of physical training without equipment on pain perception and balance in the elderly: A randomized controlled trial. *Work*. (2017) 57:23–30. doi: 10.3233/WOR-172539

11. Yuan L, Zhang X, Guo N, Li Z, Lv D, Wang H, et al. Prevalence of cognitive impairment in Chinese older inpatients and its relationship with 1-year adverse health outcomes: a multi-center cohort study. *BMC Geriatrics*. (2021) 21:595. doi: 10.1186/s12877-021-02556-5

12. Seshadri S, Wolf PA. Lifetime risk of stroke and dementia: current concepts, and estimates from the Framingham Study. *Lancet Neurol*. (2007) 6:1106–14. doi: 10.1016/S1474-4422(07)70291-0

13. 2021 Alzheimer's disease facts and figures. *Alzheimer's Dementia J Alzheimer's Assoc*. (2021) 17:327–406. doi: 10.1002/alz.12328

14. Hong S, Han K, Park CY. The insulin resistance by triglyceride glucose index and risk for dementia: population-based study. *Alzheimer's Res Ther*. (2021) 13:9. doi: 10.1186/s13195-020-00758-4

15. Hooshmand B, Rusanen M, Ngandu T, Leiviskä J, Sindi S, von Arnim CAF, et al. Serum insulin and cognitive performance in older adults: A longitudinal study. *Am J Med*. (2019) 132:367–73. doi: 10.1016/j.amjmed.2018.11.013

16. Neergaard JS, Dragsbæk K, Christiansen C, Nielsen HB, Brix S, Karsdal MA, et al. Metabolic syndrome, insulin resistance, and cognitive dysfunction: does your metabolic profile affect your brain? *Diabetes*. (2017) 66:1957–63. doi: 10.2337/db16-1444

17. Kullmann S, Heni M, Hallschmid M, Fritsche A, Preissl H, Häring HU. Brain insulin resistance at the crossroads of metabolic and cognitive disorders in humans. *Physiol Rev*. (2016) 96:1169–209. doi: 10.1152/physrev.00032.2015

18. Brito ADM, Hermsdorff HHM, Filgueiras MS, Suhett LG, Vieira-Ribeiro SA, Franceschini S, et al. Predictive capacity of triglyceride-glucose (TyG) index for insulin resistance and cardiometabolic risk in children and adolescents: a systematic review. *Crit Rev Food Sci Nutr*. (2021) 61:2783–92. doi: 10.1080/10408398.2020.1788501

19. Minh HV, Tien HA, Sinh CT, Thang DC, Chen CH, Tay JC, et al. Assessment of preferred methods to measure insulin resistance in Asian patients with hypertension. *J Clin Hypertension (Greenwich Conn)*. (2021) 23:529–37. doi: 10.1111/jch.14155

20. Wallace TM, Levy JC, Matthews DR. Use and abuse of HOMA modeling. *Diabetes Care*. (2004) 27:1487–95. doi: 10.2337/diacare.27.6.1487

21. García AG, Urbina Treviño MV, Villalpando Sánchez DC, Aguilar CA. Diagnostic accuracy of triglyceride/glucose and triglyceride/HDL index as predictors for insulin resistance in children with and without obesity. *Diabetes Metab Syndrome*. (2019) 13:2329–34. doi: 10.1016/j.dsx.2019.05.020

22. Won KB, Lee BK, Park HB, Heo R, Lee SE, Rizvi A, et al. Quantitative assessment of coronary plaque volume change related to triglyceride glucose index: The Progression of AtheRosclerotic PlAque DetermIned by Computed TomoGraphic Angiography IMaging (PARADIGM) registry. *Cardiovasc Diabetol*. (2020) 19:113. doi: 10.1186/s12933-020-01081-w

23. Fritz J, Bjørge T, Nagel G, Manjer J, Engeland A, Häggström C, et al. The triglyceride-glucose index as a measure of insulin resistance and risk of obesity-related cancers. *Int J Epidemiol*. (2020) 49:193–204. doi: 10.1093/ije/dyz053

24. Wei B, Dong Q, Ma J, Zhang A. The association between triglyceride-glucose index and cognitive function in nondiabetic elderly: NHANES 2011-2014. *Lipids Health Dis*. (2023) 22:188. doi: 10.1186/s12944-023-01959-0

25. Tian N, Song L, Hou T, Fa W, Dong Y, Liu R, et al. Association of triglyceride-glucose index with cognitive function and brain atrophy: A population-based study. *Am J Geriatric Psychiatry Off J Am Assoc Geriatric Psychiatry*. (2024) 32:151–62. doi: 10.1016/j.jagp.2023.09.007

26. Wang K, Xu L, Liu L, Zhan S, Wang S, Song Y. Sex differences in the association between the change in triglyceride–glucose index and cognitive decline: A population-based cohort study. *J Affect Disord*. (2022) 316:42–9. doi: 10.1016/j.jad.2022.08.014

27. Li S, Deng X, Zhang Y. The triglyceride-glucose index is associated with longitudinal cognitive decline in a middle-aged to elderly population: A cohort study. *J Clin Med*. (2022) 11(23):7153. doi: 10.3390/jcm11237153

28. Zhao Y, Hu Y, Smith JP, Strauss J, Yang G. Cohort profile: the China health and retirement longitudinal study (CHARLS). *Int J Epidemiol*. (2014) 43:61–8. doi: 10.1093/ije/dys203

29. Ding R, He P. Associations between childhood adversities and late-life cognitive function: Potential mechanisms. *Soc Sci Med*. (2021) 291:114478. doi: 10.1016/j.socscimed.2021.114478

30. Lu N, Wu B, Pei Y. Exploring the reciprocal relationship between cognitive function and edentulism among middle-aged and older adults in China. *Age Ageing*. (2021) 50:809–14. doi: 10.1093/ageing/afaa173

31. Bai A, Shi H, Huang X, Xu W, Deng Y. Association of C-reactive protein and motoric cognitive risk syndrome in community-dwelling older adults: the China health and retirement longitudinal study. *J Nutrition Health Aging*. (2021) 25:1090–5. doi: 10.1007/s12603-021-1678-3

32. Jak AJ, Bondi MW, Delano-Wood L, Wierenga C, Corey-Bloom J, Salmon DP, et al. Quantification of five neuropsychological approaches to defining mild cognitive impairment. *Am J Geriatric Psychiatry Off J Am Assoc Geriatric Psychiatry*. (2009) 17:368–75. doi: 10.1097/JGP.0b013e31819431d5

33. Chai S, Zhao D, Gao T, Wang X, Wang X, Luo J, et al. The relationship between handgrip strength and cognitive function among older adults in China: Functional

limitation plays a mediating role. *J Affect Disord*. (2024) 347:144–9. doi: 10.1016/j.jad.2023.11.056

34. Wang A, Tian X, Zuo Y, Chen S, Meng X, Wu S, et al. Change in triglyceride-glucose index predicts the risk of cardiovascular disease in the general population: a prospective cohort study. *Cardiovasc Diabetol*. (2021) 20:113. doi: 10.1186/s12933-021-01305-7

35. Pan X, Luo Y, Zhao D, Zhang L. Associations among drinking water quality, dyslipidemia, and cognitive function for older adults in China: evidence from CHARLS. *BMC Geriatrics*. (2022) 22:683. doi: 10.1186/s12877-022-03375-y

36. Schram MT, Euser SM, de Craen AJ, Witteman JC, Frölich M, Hofman A, et al. Systemic markers of inflammation and cognitive decline in old age. *J Am Geriatrics Society*. (2007) 55:708–16. doi: 10.1111/j.1532-5415.2007.01159.x

37. Baumgart M, Snyder HM, Carrillo MC, Fazio S, Kim H, Johns H. Summary of the evidence on modifiable risk factors for cognitive decline and dementia: A population-based perspective. *Alzheimer's Dementia J Alzheimer's Assoc*. (2015) 11:718–26. doi: 10.1016/j.jalz.2015.05.016

38. Griffiths CJ, Mudway IS. Air pollution and cognition. *BMJ*. (2018) 363:k4904. doi: 10.1136/bmj.k4904

39. Paul KC, Haan M, Mayeda ER, Ritz BR. Ambient air pollution, noise, and late-life cognitive decline and dementia risk. *Annu Rev Public Health*. (2019) 40:203–20. doi: 10.1146/annurev-publhealth-040218-044058

40. Schikowski T, Altuğ H. The role of air pollution in cognitive impairment and decline. *Neurochem Int*. (2020) 136:104708. doi: 10.1016/j.neuint.2020.104708

41. Cnop M, Havel PJ, Utzschneider KM, Carr DB, Sinha MK, Boyko EJ, et al. Relationship of adiponectin to body fat distribution, insulin sensitivity and plasma lipoproteins: evidence for independent roles of age and sex. *Diabetologia*. (2003) 46:459–69. doi: 10.1007/s00125-003-1074-z

42. Meyer MR, Clegg DJ, Prossnitz ER, Barton M. Obesity, insulin resistance and diabetes: sex differences and role of oestrogen receptors. *Acta Physiol*. (2011) 203:259–69. doi: 10.1111/apha.2011.203.issue-1

43. Soto M, Cai W, Konishi M, Kahn CR. Insulin signaling in the hippocampus and amygdala regulates metabolism and neurobehavior. *Proc Natl Acad Sci United States America*. (2019) 116:6379–84. doi: 10.1073/pnas.1817391116

44. Blázquez E, Velázquez E, Hurtado-Carneiro V, Ruiz-Albusac JM. Insulin in the brain: its pathophysiological implications for States related with central insulin resistance, type 2 diabetes and Alzheimer's disease. *Front Endocrinol*. (2014) 5:161. doi: 10.3389/fendo.2014.00161

45. Willette AA, Bendlin BB, Starks EJ, Birdsill AC, Johnson SC, Christian BT, et al. Association of insulin resistance with cerebral glucose uptake in late middle-aged adults at risk for alzheimer disease. *JAMA Neurol*. (2015) 72:1013–20. doi: 10.1001/jamaneurol.2015.0613

46. Banks WA, Farr SA, Salameh TS, Niehoff ML, Rhea EM, Morley JE, et al. Triglycerides cross the blood-brain barrier and induce central leptin and insulin receptor resistance. *Int J Obes*. (2018) 42:391–7. doi: 10.1038/ijo.2017.231

47. Engler-Chiurazzi EB, Singh M, Simpkins JW. From the 90's to now: A brief historical perspective on more than two decades of estrogen neuroprotection. *Brain Res*. (2016) 1633:96–100. doi: 10.1016/j.brainres.2015.12.044

48. Hara Y, Waters EM, McEwen BS, Morrison JH. Estrogen effects on cognitive and synaptic health over the lifecourse. *Physiol Rev*. (2015) 95:785–807. doi: 10.1152/physrev.00036.2014

49. Patnode CD, Perdue LA, Rossom RC, Rushkin MC, Redmond N, Thomas RG, et al. Screening for cognitive impairment in older adults: updated evidence report and systematic review for the US preventive services task force. *Jama*. (2020) 323:764–85. doi: 10.1001/jama.2019.22258

frontiers | Frontiers in Endocrinology

TYPE Original Research
PUBLISHED 22 July 2024
DOI 10.3389/fendo.2024.1432928

OPEN ACCESS

EDITED BY
Heidi de Wet,
University of Oxford, United Kingdom

REVIEWED BY
Fanny V. Langlet,
Université de Lausanne, Switzerland
Nerys Astbury,
University of Oxford, United Kingdom

*CORRESPONDENCE
James E. Blevins
jeblevin@uw.edu

†These authors have contributed equally to this work and share last authorship

RECEIVED 15 May 2024
ACCEPTED 25 June 2024
PUBLISHED 22 July 2024

CITATION
Blevins JE, Honeycutt MK, Slattery JD, Goldberg M, Rambousek JR, Tsui E, Dodson AD, Shelton KA, Salemeh TS, Elfers CT, Chichura KS, Ashlaw EF, Zraika S, Doyle RP and Roth CL (2024) The novel chimeric multi-agonist peptide (GEP44) reduces energy intake and body weight in male and female diet-induced obese mice in a glucagon-like peptide-1 receptor-dependent manner.
Front. Endocrinol. 15:1432928.
doi: 10.3389/fendo.2024.1432928

The novel chimeric multi-agonist peptide (GEP44) reduces energy intake and body weight in male and female diet-induced obese mice in a glucagon-like peptide-1 receptor-dependent manner

James E. Blevins[1,2*], Mackenzie K. Honeycutt[1], Jared D. Slattery[1], Matvey Goldberg[1], June R. Rambousek[1], Edison Tsui[1], Andrew D. Dodson[1], Kyra A. Shelton[1], Therese S. Salemeh[3], Clinton T. Elfers[3], Kylie S. Chichura[4], Emily F. Ashlaw[4], Sakeneh Zraika[1,2], Robert P. Doyle[4,5†] and Christian L. Roth[3,6†]

[1]VA Puget Sound Health Care System, Office of Research and Development Medical Research Service, Department of Veterans Affairs Medical Center, Seattle, WA, United States, [2]Division of Metabolism, Endocrinology and Nutrition, Department of Medicine, University of Washington School of Medicine, Seattle, WA, United States, [3]Seattle Children's Research Institute, Seattle, WA, United States, [4]Department of Chemistry, Syracuse University, Syracuse, NY, United States, [5]Departments of Medicine and Pharmacology, State University of New York (SUNY) Upstate Medical University, Syracuse, NY, United States, [6]Department of Pediatrics, University of Washington School of Medicine, Seattle, WA, United States

We recently reported that a novel chimeric peptide (GEP44) targeting both the glucagon-like peptide-1 receptor (GLP-1R) and neuropeptide Y1- and Y2 receptor (Y1R and Y2R) reduced energy intake and body weight (BW) in diet-induced obese (DIO) rats. We hypothesized that GEP44 reduces energy intake and BW primarily through a GLP-1R dependent mechanism. To test this hypothesis, GLP-1R$^{+/+}$ mice and GLP-1R null (GLP-1R$^{-/-}$) mice were fed a high fat diet for 4 months to elicit diet-induced obesity prior to undergoing a sequential 3-day vehicle period, 3-day drug treatment (5, 10, 20 or 50 nmol/kg; GEP44 vs the selective GLP-1R agonist, exendin-4) and a 3-day washout. Energy intake, BW, core temperature and activity were measured daily. GEP44 (10, 20 and 50 nmol/kg) reduced BW after 3-day treatment in DIO male GLP-1R$^{+/+}$ mice by -1.5 ± 0.6, -1.3 ± 0.4 and -1.9 ± 0.4 grams, respectively (P<0.05), with similar effects being observed in female GLP-1R$^{+/+}$ mice. These effects were absent in male and female DIO GLP-1R$^{-/-}$ mice suggesting that GLP-1R signaling contributes to GEP44-elicited reduction of BW. Further, GEP44 decreased energy intake in both male and female DIO GLP-1R$^{+/+}$ mice, but GEP44 appeared to produce more consistent effects across multiple doses in males. In GLP-1R$^{-/-}$ mice, the effects of GEP44 on energy intake were only observed in males and not females, suggesting that GEP44 may reduce energy intake, in part, through a GLP-1R independent mechanism in males. In addition, GEP44 reduced core temperature and activity in both male and female GLP-1R$^{+/+}$ mice suggesting that it may also reduce energy expenditure. Lastly, we show that GEP44 reduced fasting blood glucose in DIO male and female mice through

GLP-1R. Together, these findings support the hypothesis that the chimeric peptide, GEP44, reduces energy intake, BW, core temperature, and glucose levels in male and female DIO mice primarily through a GLP-1R dependent mechanism.

KEYWORDS

obesity, multi-agonist, GLP-1, PYY, IWAT, IBAT

Introduction

Obesity is a major worldwide health concern as it increases the risk of cardiovascular disease, obstructive sleep apnea, cancer, osteoarthritis, depression, COVID-19 related hospitalizations and type 2 diabetes. According to the NCD Risk Factor Collaboration, more than one billion people are obese worldwide (1). Approximately 1 in 2 US adults are predicted to have obesity by 2030 (2) and the costs to treat obesity in the US are estimated to be approximately 3 trillion/year by 2030 (3). More recently developed monotherapies to treat obesity such as the long-acting glucagon-like peptide-1 receptor (GLP-1R) agonists, liraglutide and semaglutide (4), produce more pronounced effects on weight loss relative to previous analogues. Weight loss in response to once-weekly treatment with semaglutide has ranged from ≈6.7% over 40 weeks (5) to ≈14.9% weight loss over 68 weeks (4). However, improvements still need to be made in terms of improving overall weight loss effectiveness over more prolonged periods [≈10.2% weight loss over 208 weeks (6)]. Furthermore, there is rapid recovery of weight when discontinued (7). This is likely due to the activation of counter-regulatory orexigenic mechanisms that increase energy intake and/or reduce energy expenditure to promote weight regain (8).

Recent studies suggest that combination therapy aimed at suppressing energy intake and/or increasing energy expenditure at low-dose or subthreshold dose combinations may be more effective for producing sustained weight loss than monotherapy (9) and may minimize the potential for unwanted side effects. The overall ineffectiveness of monotherapies to evoke prolonged weight loss in humans with obesity is assumed to occur, in part, by recruitment of robust orexigenic mechanisms that drive energy intake and decrease energy expenditure, resulting in body weight (BW) gain and thus preventing further weight loss. In addition to combination therapy, a recent innovative approach involves the targeting of two or more signaling pathways using a single compound such as monomeric multi-agonists (dual- or triple-agonists) based on glucose-dependent insulinotropic polypeptide (GIP) and GLP-1R agonists, with and without glucagon receptor (GCGR) agonism. One such drug, tirzepatide (Zepbound™), which targets both GLP-1R and and the GIP receptor (GIPR), was found to elicit a robust 20.9% and 25.3% weight loss in humans with obesity over 72- (10) and 88-week periods (11), and was recently approved by the FDA for weight management. Recent data indicate that the triple-agonist, retatrutide, which targets GLP-1R, GIPR and GCGR, was able to elicit 24.2% weight loss over 48-week period (12) (2 to 12 mg). While such therapies show considerable promise for effective and sustained reduction of BW during drug treatment, there are still mild to moderate adverse gastrointestinal side effects including nausea, diarrhea, abdominal pain and vomiting (10). Given the rise of the obesity epidemic in the US and worldwide, there remains an urgent need to develop newer and more effective anti-obesity treatment strategies in order to reduce obesity rates across a broader spectrum of the population. We recently designed the novel chimeric peptide, GEP44, which binds to GLP-1R, Y1R and Y2R (13). We found that systemic administration of GEP44 reduced energy intake and BW in both lean (14) and diet-induced obese rats (13, 14). Importantly, GEP44 also reduced energy intake at doses that were not associated with significant pica behavior (kaolin intake) in rats (14) or emesis in musk shrews (14). A critical remaining question is whether GEP44 reduces energy intake, BW, impacts thermogenesis and improves glucose homeostasis in a GLP-1R dependent manner, either alone or in-part. Given the role of GLP-1R in the control of energy intake and BW, we hypothesized that chimeric peptide GEP44 reduces energy intake and BW through a GLP-1R dependent mechanism. To test this hypothesis, we determined the extent to which GEP44 reduces energy intake and BW, impacts core temperature (core temperature as surrogate marker of energy expenditure) and gross motor activity and improves fasting blood glucose in male and female DIO mice that lack GLP-1R (GLP-1R$^{-/-}$) relative to age-matched cohorts of male and female GLP-1R$^{+/+}$ mice. Male and female mice were also weight-matched within a given cohort of GLP-1R$^{-/-}$ and GLP-1R$^{+/+}$ mice prior to treatment. The selective GLP-1R agonist, exendin-4, was included as a control to assess GLP-1R mediated effects on energy intake (15).

Methods

Animals

GLP-1R$^{+/-}$ mice were initially obtained from Dr. Daniel Drucker (University of Toronto, Canada) and bred by Dr. Sakeneh Zraika at the Veterans Affairs Puget Sound Health Care System (VAPSHCS) to obtain GLP-1R$^{+/+}$ and GLP-1R$^{-/-}$ (GLP-1R null) mice. Adult male and female mice (age: ~5.5-10 weeks) weighed, on average, 18.04 ± 0.04

grams and were 10.9 ± 0.03% fat at the time of body composition measurements prior to diet intervention. Mice were initially maintained on a chow diet [PicoLab® Rodent Diet 20 (5053)] (LabDiet®, St. Louis, MO; 13% kcal from fat). Mice were subsequently placed on a high fat diet (HFD) [60% kcal from fat; Research Diets, Inc., D12492i, New Brunswick, NJ] for approximately 4 months at which time body composition measurements were completed. Mice weighed, on average, 39.3 ± 0.04 grams and were 39.8 ± 0.03% fat at the time of body composition measurements prior to drug intervention. All animals were housed individually in Plexiglas cages in a temperature-controlled room (22 ± 2°C) under a 12:12-h light-dark cycle. All mice were maintained on a 11 a.m./11 p.m. reverse light cycle (lights off at 11 a.m./lights on at 11 p.m.). Mice had *ad libitum* access to water and HFD. The research protocols were approved both by the Institutional Animal Care and Use Committee of the Veterans Affairs Puget Sound Health Care System (VAPSHCS) and the University of Washington in accordance with NIH Guidelines for the Care and Use of Animals.

Drug preparation

GEP44 was synthesized in the Doyle lab as previously described (13). Fresh solutions of GEP44 and exendin-4 (ENZO; Farmingdale, NY) were prepared, frozen and thawed prior to the onset of each experiment (Study 1).

Implantation of G2 E-Mitter telemetry devices into abdominal cavity

At the age of 27-31.5 weeks (average age 28.8 ± 0.01 weeks), animals were anesthetized with isoflurane and subsequently underwent a sham surgery (no implantation) or received implantations of a sterile G2 E-Mitter (15.5 mm long x 6.5 mm wide; Starr Life Sciences Company) into the intraperitoneal cavity. The abdominal opening was closed with 5-0 Vicryl® absorbable suture and the skin was closed with Nylon sutures (5-0). Vetbond glue was used to seal the wound and bind any tissue together between the sutures. Sutures were removed within two weeks after the G2 E-Mitter implantation. All G2 E-Mitters were confirmed to have remained within the abdominal cavity at the conclusion of the study. Animals were grouped by genotype and sex and matched for body weight (Table 1), adiposity and post-surgical weight change prior to drug intervention.

Acute SC injections of GEP44 and Exendin-4

GEP44 (or saline vehicle; 3 mL/kg injection volume) or exendin-4 were administered immediately prior to the start of the dark cycle following 2 h of food deprivation. Mice underwent all treatments (unless otherwise noted). The study design consisted of sequential rounds of a 3-day baseline phase (vehicle treated), a 3-day treatment phase (single dose repeated over 3 days), and a washout phase (3 days). The 3-day treatment phase consisted of a dose escalation design beginning with the low dose (5 nmol/kg) over week 1 and ending with the high dose (50 nmol/kg) over the final week of the study (5, 10, 20 and 50 nmol/kg; GEP44 vs the selective GLP-1R agonist, exendin-4). A separate set of age- and weight-matched mice were treated with vehicle in place of drug in order to determine the impact of drug treatment on tail vein glucose, plasma hormones and thermogenic gene expression. BW was assessed daily approximately 3-h prior to the start of the dark cycle.

Body composition

Determinations of lean body mass and fat mass were made on conscious mice by quantitative magnetic resonance using an EchoMRI 4-in-1-700™ instrument (Echo Medical Systems, Houston, TX) at the VAPSHCS Rodent Metabolic Phenotyping Core.

Study protocols

Changes of BW and energy intake

DIO GLP-1R$^{+/+}$ and GLP-1R$^{-/-}$ mice underwent a 3-day vehicle period, 3-day dose escalation drug treatment (5, 10, 20 and 50 nmol/kg; GEP44 vs the selective GLP-1R agonist, exendin-4) and a 3-day washout in sequential order with the same mice receiving the escalating dose. The selective GLP-1R agonist, exendin-4, was included as a control to assess GLP-1R mediated effects on energy intake (15). BW and energy intake were measured daily. BW change reflects the total change over each sequential 3-day vehicle and 3-day drug treatment period. Energy intake data was averaged throughout each sequential 3-day vehicle and 3-day drug treatment period. Note that energy intake was averaged across two-day vehicle treatments (prior to 20 and 50 nmol/kg) for one of the four cohorts used in the dose escalation studies.

TABLE 1 Body weight (grams) in adult Male and Female GLP-1R$^{+/+}$ and GLP-1R$^{-/-}$ mice post-dietary intervention at study onset.

	GEP44	Exendin-4		GEP44	Exendin-4
Male WT	44.1 ± 2.6	43.8 ± 1.9	**Female WT**	32.7 ± 2.8	31.8 ± 1.8
Male GLP-1R$^{-/-}$	40.0 ± 1.6	38.0 ± 1.7	**Female GLP1R$^{-/-}$**	28.1 ± 1.2	27.6 ± 1.9

Male GLP-1R$^{+/+}$ GEP44 vs exendin-4 (P=NS); Male GLP-1R$^{-/-}$ GEP44 vs exendin-4 (P=NS).
Female GLP-1R$^{+/+}$ GEP44 vs exendin-4 (P=NS); Female GLP-1R$^{-/-}$ GEP44 vs exendin-4 (P=NS).
N=9-11/group.

Changes of core temperature and gross motor activity

Telemetry recordings of core temperature (surrogate marker of energy expenditure) and gross motor activity were measured from each mouse in the home cage immediately prior to injections and for a 6-, 12-, and 24-h period after injections. Core temperature and gross motor activity were recorded every 15 sec. The last hour of the light cycle (during which time energy intake, BW and drug administration occurred) was excluded from the telemetry analysis.

Core temperature and activity were averaged throughout each sequential 3-day vehicle and 3-day drug treatment period. Note that core temperature and activity energy intake were averaged across two-day vehicle treatments (prior to 20 and 50 nmol/kg) for one of the four cohorts used in the dose escalation studies.

Tissue collection for quantitative real-time PCR

Tissue [interscapular brown adipose tissue (IBAT) was collected from 3-h fasted mice at 2-h post-injection. Mice were euthanized with an overdose of ketamine cocktail at 2-h post-injection. Tissue was rapidly removed, wrapped in foil and frozen in liquid N2. Samples were stored frozen at -80°C until analysis. IBAT was collected within a 5-h window towards the end of the light cycle (9:00 a.m.-2:00 p.m.) as previously described in DIO CD® IGS/Long-Evans rats and C57BL/6J mice (16–18).

Blood collection

Blood samples [up to 1 mL] were collected by cardiac stick in chilled K2 EDTA Microtainer Tubes (Becton-Dickinson, Franklin Lakes, NJ) at 2-h post-injection. Whole blood was centrifuged at 6,000 rpm for 1.5-min at 4°C; plasma was removed, aliquoted and stored at −80°C for subsequent analysis.

Blood glucose measurements

Blood was collected at 2-h post-injection in a subset of mice for glucose measurements by tail vein nick and measured using a glucometer (AlphaTRAK 2, Abbott Laboratories, Abbott Park, IL) (16, 17).

Plasma hormone measurements

Plasma leptin, insulin and glucagon were measured using electrochemiluminescence detection [leptin/insulin: Meso Scale Discovery (MSD®), Rockville, MD] or (glucagon: Mercodia, Uppsala, Sweden) using established procedures (17, 19). Intra-assay coefficient of variation (CV) were 5.9%, 1.6% and 5.7% for leptin, insulin and glucagon. The range of detectability for the assays are as follows: 0.137-100 ng/mL (leptin), 0.069-50 ng/mL (insulin) and 0.002-0.183 ng/mL (glucagon). The data were normalized to historical values using a pooled plasma quality control sample that was assayed in each plate.

qPCR

RNA extracted from samples of IBAT was analyzed using the RNeasy Lipid Mini Kit (Qiagen Sciences Inc, Germantown, MD) followed by reverse transcription into cDNA using a high-capacity cDNA archive kit (Applied Biosystems, Foster City, CA). Quantitative analysis for relative levels of mRNA in the RNA extracts was measured in duplicate by qPCR on an Applied Biosystems 7500 Real-Time PCR system (Thermo Fisher Scientific, Waltham, MA) using the following TaqMan® probes (Thermo Fisher Scientific Gene Expression Assay probes): mouse Nono (catalog no. Mm00834875_g1), mouse UCP-1 (catalog no. Mm01244861_m1), mouse type 2 deiodinase (D2) (Dio2; catalog no. Mm00515664_m1), mouse G-protein coupled receptor 120 (Gpr120; catalog no. Mm00725193_m1), mouse cell death-inducing DNA fragmentation factor alpha-like effector A (Cidea; catalog no. Mm00432554_m1) and mouse peroxisome proliferator-activated receptor gamma coactivator 1 alpha (Ppargc1a; catalog no. Mm01208835_m1). Relative amounts of target mRNA were determined using the Comparative C_T or $2^{-\Delta\Delta C}{}_T$ method (20) following adjustment for the housekeeping gene, Nono. Specific mRNA levels of all genes of interest were normalized to the cycle threshold value of Nono mRNA in each sample and expressed as changes normalized to controls (vehicle treatment).

Statistical analyses

All results are expressed as mean ± SE. Planned comparisons within respective genotypes and sex between vehicle and drug (plasma measures, tail vein glucose, and gene expression data) involving between subjects design were made using one-way ANOVA. Planned comparisons within respective genotypes and sex to examine treatment means of vehicle and drug (BW change, energy intake, core temperature, activity and T_{IBAT}) involving within-subjects designs were made using a one-way repeated-measures ANOVA. A two-way ANOVA was used to examine sex*drug interactive effects on BW change and energy intake. In addition, planned comparisons were used to examine sex differences on BW change and energy intake using a one-way ANOVA. Analyses were performed using the statistical program SYSTAT (Systat Software, Point Richmond, CA). Differences were considered significant at $P<0.05$, 2-tailed.

Results

The overall goal of these studies was to use the GLP-$1R^{-/-}$ mouse as a strategy to determine the extent to which chimeric peptide, GEP44, reduces BW and energy intake, impacts core temperature (as surrogate for energy expenditure) and activity, and improves

glucose homeostasis through the GLP-1R in both male and female DIO mice. In addition, we incorporated use of the selective GLP-1R agonist, exendin-4, to assess GLP-1R mediated effects on BW, energy intake, core temperature, activity, and glucose levels in male and female DIO mice. DIO GLP-1R$^{+/+}$ and GLP-1R$^{-/-}$ mice underwent a 3-day vehicle period, 3-day dose escalation drug treatment (5, 10, 20 and 50 nmol/kg; GEP44 vs the selective GLP-1R agonist, exendin-4) and a 3-day washout in sequential order with the same mice receiving the escalating dose. Energy intake, core temperature and activity were averaged throughout each sequential 3-day vehicle and 3-day drug treatment period. Note that energy intake, core temperature and activity were averaged across two-day vehicle treatments (prior to 20 and 50 nmol/kg) for one of the four cohorts used in the dose escalation studies.

Baseline BW-matching in Male and Female DIO GLP-1R$^{+/+}$ and GLP-1R$^{-/-}$ Mice at Study Onset (post-dietary intervention/pre-drug treatment). By design, there were no differences in baseline BW between designated drug treatment groups (GEP44 vs exendin-4) of male GLP-1R$^{+/+}$ mice [F(1,19) = 0.009, *P*=NS] or male GLP-1R$^{-/-}$ mice [F(1,18) = 0.682, *P*=NS] prior to drug treatment (Table 1). Similarly, there were also no differences in baseline BW between designated treatment groups (GEP44 vs exendin-4) of female GLP-1R$^{+/+}$ mice [F(1,18) = 0.071, *P*=NS] or GLP-1R$^{-/-}$ mice [F(1,16) = 0.037, P=NS] prior to drug treatment (Table 1).

Body weight

Both male and female GLP-1R$^{+/+}$ and GLP-1R$^{-/-}$ mice were weight-matched within respective groups prior to treatment onset (Table 1). GEP44 treatment reduced cumulative 3-day BW in both male (Figures 1A, B) and female DIO GLP-1R$^{+/+}$ mice (Figures 1C, D), but these effects were absent in male and female DIO GLP-1R$^{-/-}$ mice. Specifically, GEP44 (10, 20 and 50 nmol/kg), reduced 3-day BW in DIO male GLP-1R$^{+/+}$ mice by -1.5 ± 0.6, -1.3 ± 0.4 and -1.9 ± 0.4 grams, respectively (Figures 1A, B; *P*<0.05). GEP44 also reduced 3-day BW (10,

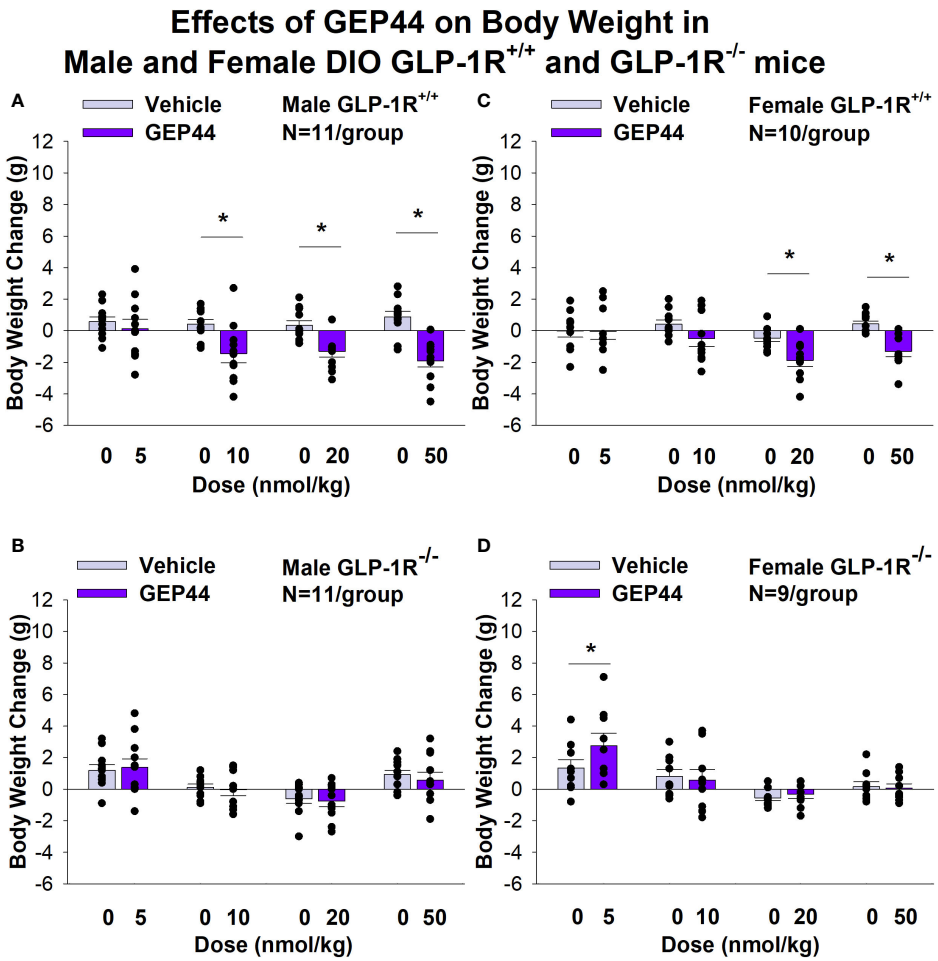

FIGURE 1
(A–D) Effects of the chimeric peptide, GEP44, on BW in male and female DIO GLP-1R$^{+/+}$ and GLP-1R$^{-/-}$ mice. Mice were maintained on HFD (60% kcal from fat; N=10-11/group) for approximately 4 months prior to receiving SC injections of vehicle (sterile saline/water) followed by escalating doses of GEP44 (5, 10, 20 and 50 nmol/kg; 3 mL/kg injection volume). **(A)** Effect of GEP44 on change in BW in male HFD-fed DIO GLP-1R$^{+/+}$ mice; **(B)** Effect of GEP44 on change in BW in male HFD-fed DIO GLP-1R $^{-/-}$ mice; **(C)** Effect of GEP44 on change in BW in female HFD-fed DIO GLP-1R$^{+/+}$ mice; **(D)** Effect of GEP44 on change in BW in female HFD-fed DIO GLP-1R$^{-/-}$ mice. BW change reflects the total change over each sequential 3-day vehicle and 3-day drug treatment period. Data are expressed as mean ± SEM. *P<0.05 GEP44 vs. vehicle.

20 and 50 nmol/kg) in female GLP-1R$^{+/+}$ mice by -0.5 ± 0.5 (P=0.053), -1.9 ± 0.4 and -1.3 ± 0.3 grams, respectively (Figures 1C, D; P<0.05).

Similarly, the selective GLP-1R agonist, exendin-4, reduced BW only in male (Figures 2A, B; P<0.05) and female DIO GLP-1R$^{+/+}$ mice (Figures 2C, D; P<.05) but not in male and female DIO GLP-1R $^{-/-}$ mice. Specifically, exendin-4 (5, 10, 20 and 50 nmol/kg) reduced BW in DIO male GLP-1R$^{+/+}$ mice by -0.7 ± 0.5, -1.0 ± 0.4, -1.4 ± 0.3, and -1.5 ± 0.2 grams, respectively (Figures 1A, B; P<0.05). Exendin-4 also reduced BW (10, 20 and 50 nmol/kg) in female GLP-1R$^{+/+}$ mice by -0.9 ± 0.6, -0.9 ± 0.3 and -1.5 ± 0.2 grams, respectively (Figures 1C, D; P<0.05).

Energy intake

GEP44 treatment significantly reduced energy intake only in male (Figures 3A, B) and female DIO GLP-1R$^{+/+}$ mice (Figures 3C, D) but not in male (with exception of the lowest and highest dose) and female DIO GLP-1R $^{-/-}$ mice. GEP44 treatment decreased energy intake (10, 20 and 50 nmol/kg); P<0.005) in both male and female mice. Similar results on FI were obtained when normalizing to BW (Supplementary Figures 1A–D).

Exendin-4 treatment also significantly reduced energy intake in male (Figures 4A, B) and female DIO GLP-1R$^{+/+}$ mice (Figures 4C, D) but not in male (with exception of the lowest dose) and female DIO GLP-1R $^{-/-}$ mice. Specifically, exendin-4 treatment decreased energy intake (10, 20 and 50 nmol/kg; P<0.05) in male GLP-1R$^{+/+}$ mice and also tended to decrease energy intake at the low dose (5 nmol/kg) in male GLP-1R $^{-/-}$ mice (P=0.055). However, exendin-4 reduced energy intake in female GLP-1R$^{+/+}$ mice across all doses (5, 10, 20 and 50 nmol/kg; P<0.05).

Similar results on energy intake were obtained when normalizing to BW (Supplementary Figures 2A–D).

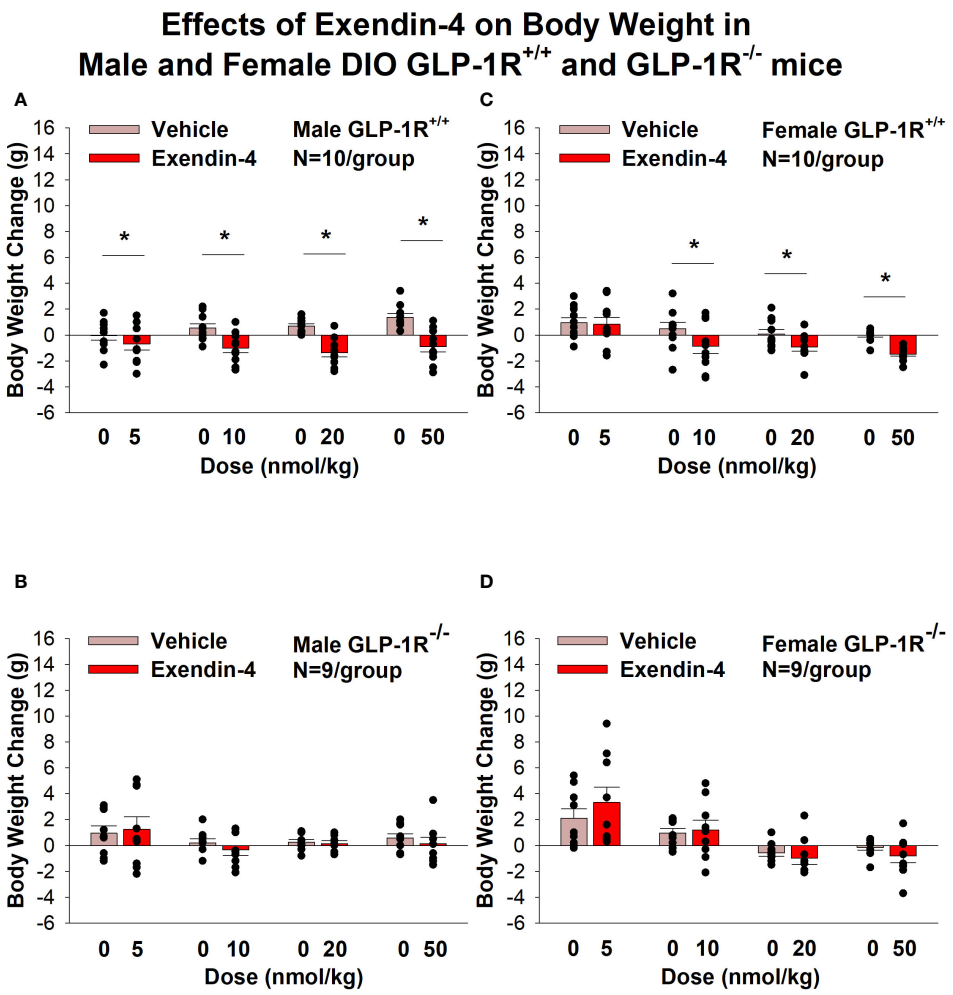

FIGURE 2
(A–D) Effects of the selective GLP-1R agonist, exendin-4, on BW in male and female DIO GLP-1R$^{+/+}$ and GLP-1R$^{-/-}$ mice. Mice were maintained on HFD (60% kcal from fat; N=9-11/group) for approximately 4 months prior to receiving SC injections of vehicle (sterile saline/water) followed by escalating doses of exendin-4 (5, 10, 20 and 50 nmol/kg; 3 mL/kg injection volume). **(A)** Effect of exendin-4 on change in BW in male HFD-fed DIO GLP-1R$^{+/+}$ mice; **(B)** Effect of exendin-4 on change in BW in male HFD-fed DIO GLP-1R$^{-/-}$ mice; **(C)** Effect of exendin-4 on change in BW in female HFD-fed DIO GLP-1R$^{+/+}$ mice; **(D)** Effect of exendin-4 on change in BW in female HFD-fed DIO GLP-1R$^{-/-}$ mice. BW change reflects the total change over each sequential 3-day vehicle and 3-day drug treatment period. Data are expressed as mean ± SEM. *P<0.05 exendin-4 vs. vehicle.

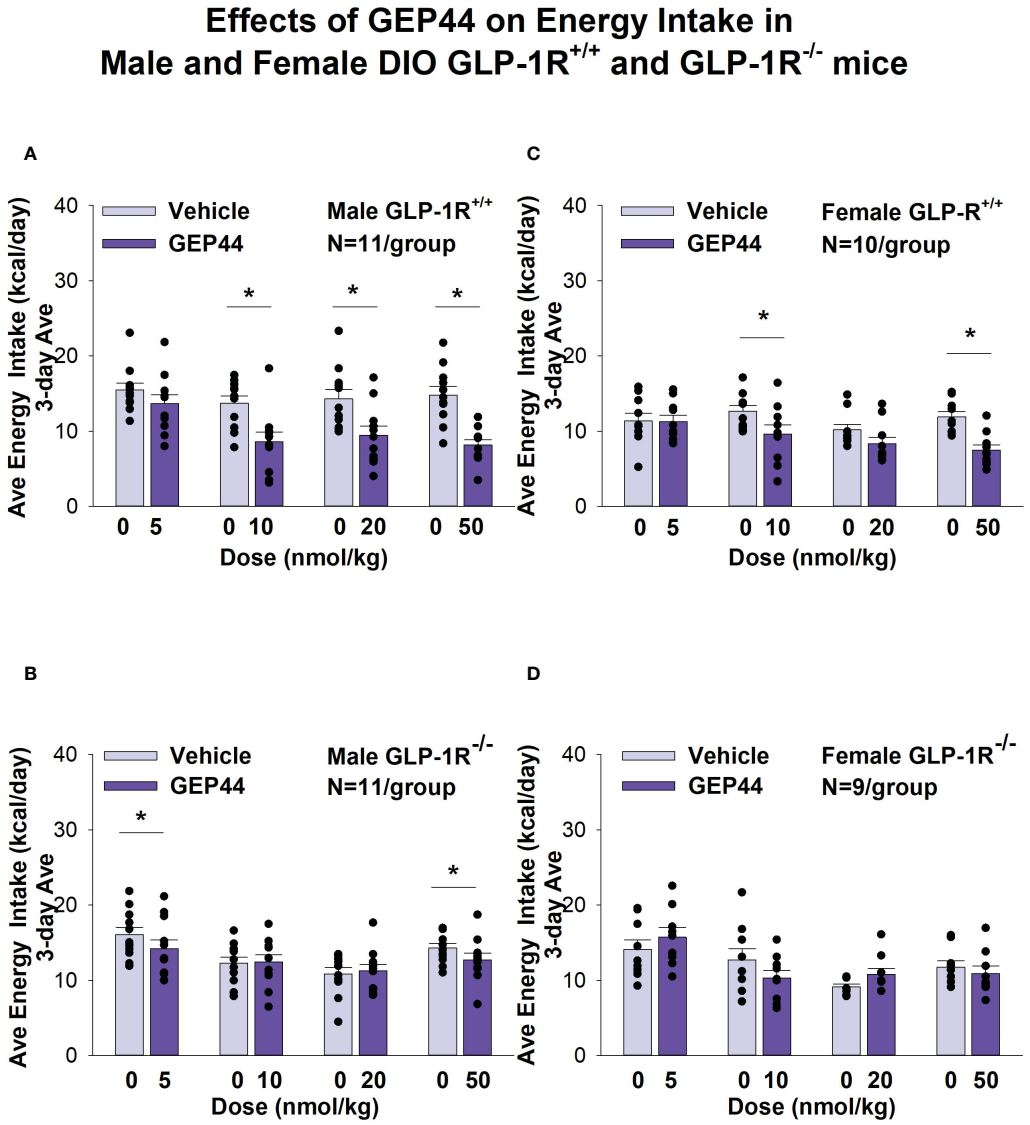

FIGURE 3
(A–D) Effects of the chimeric peptide, GEP44, on energy intake (kcal/day) in male and female DIO GLP-1R$^{+/+}$ and GLP-1R $^{-/-}$ mice. Mice were maintained on HFD (60% kcal from fat; N=10-11/group) for approximately 4 months prior to receiving SC injections of vehicle (sterile saline/water) followed by escalating doses of GEP44 (5, 10, 20 and 50 nmol/kg; 3 mL/kg injection volume). **(A)** Effect of GEP44 on energy intake in male HFD-fed DIO GLP-1R$^{+/+}$ mice; **(B)** Effect of GEP44 on change on energy intake in male HFD-fed DIO GLP-1R$^{-/-}$ mice; **(C)** Effect of GEP44 on energy intake in male HFD-fed DIO GLP-1R$^{+/+}$ mice; **(D)** Effect of GEP44 on energy intake in male HFD-fed DIO GLP-1R$^{-/-}$ mice. Energy intake was averaged throughout each sequential 3-day vehicle and 3-day drug treatment period. Data are expressed as mean ± SEM. *P<0.05 GEP44 vs. vehicle.

Sex differences linked to effects of GEP44 and Exendin-4 on body weight and energy intake

There was a significant difference in the effectiveness of GEP44 to suppress energy intake in male and female GLP-1R$^{+/+}$ mice with males showing the more pronounced effect of GEP44 to reduce energy intake at both 20 [F(1,19)= 6.524, P=0.019] and 50 nmol/kg [F(1,13)= 4.880, P=0.046]. Two-way repeated-measures ANOVA revealed a significant effect of sex [F(1,26) = 8.292, P=0.008] and treatment with GEP44 (20 nmol/kg) [F(1,26)= 32.110, P<0.01] on energy intake and a near significant interaction between sex and GEP44 on energy intake [F(1,26) = 3.112, P=0.089]. At the higher dose (50 nmol/kg) of GEP44, there was also a near significant effect of sex [F(1,26) = 3.902, P=0.059] and treatment with GEP44 [F(1,26) = 48.490, P<0.01] on energy intake but there was no significant interactive effect between sex and GEP44.

There was also a significant difference in the effectiveness of exendin-4 (5 nmol/kg) to reduce BW in male and female GLP-1R$^{+/+}$ mice with males showing the more heightened effect [F(1,18) = 4.698, P=0.044]. Two-way ANOVA revealed, however, that despite the overall effect of sex [(F1,26) = 6.954, P=0.014], there was no overall significant effect of exendin-4 treatment [(F1,26) = 1.052, P=0.314] and no interactive effect between sex and exendin-4 treatment [(F1,26) = 0.460, P=0.504].

10.3389/fendo.2024.1432928

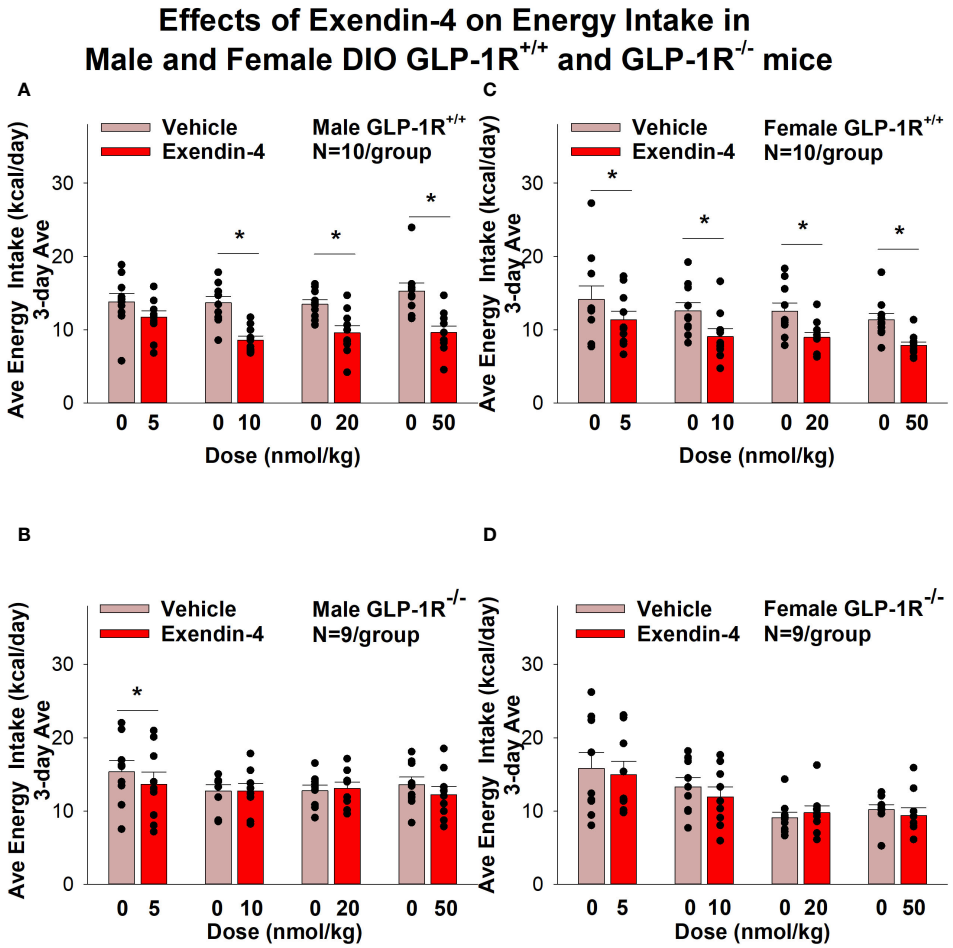

FIGURE 4
(A–D) Effects of the selective GLP-1R agonist, exendin-4, on energy intake (kcal/day) in male and female DIO GLP-1R$^{+/+}$ and GLP-1$^{-/-}$ mice. Mice were maintained on HFD (60% kcal from fat; N=9-11/group) for approximately 4 months prior to receiving SC injections of vehicle followed by escalating doses of GEP44 (5, 10, 20 and 50 nmol/kg; 3 mL/kg injection volume). **(A)** Effect of GEP44 on energy intake in male HFD-fed DIO GLP-1R$^{+/+}$ mice; **(B)** Effect of GEP44 on change on energy intake in male HFD-fed DIO GLP-1R$^{-/-}$ mice; **(C)** Effect of GEP44 on energy intake in male HFD-fed DIO GLP-1R$^{+/+}$ mice; **(D)** Effect of GEP44 on energy intake in male HFD-fed DIO GLP-1R$^{-/-}$ mice. Energy intake was averaged throughout each sequential 3-day vehicle and 3-day drug treatment period. Data are expressed as mean ± SEM. *P<0.05 exendin-4 vs. vehicle.

Changes of core temperature and gross motor activity

The analysis focused on the effects of GEP44 and exendin-4 on core temperature and activity at 6-h post-injection (dark cycle). We also discuss the extent to which these effects carried into the 12-h dark cycle, 11-h light cycle and 23-h post-injection period. Note that the last hour of the light cycle (hour 12) was excluded from the core temperature and activity analysis as this was during the time that the animals were being handled and injected.

Core temperature

GEP44 and exendin-4 both reduced core temperature over the 6-h post-injection period in male (Figure 5A; P<0.05) and female DIO GLP-1R$^{+/+}$ mice (Figure 5C; P<0.05). Notably, similar results were observed during the 12-h dark cycle in response to GEP44 (10 and 20 nmol/kg) in male DIO GLP-1R$^{+/+}$ mice (P<0.05; data not shown). GEP44 (10 nmol/kg) also reduced core temperature in male GLP-1R$^{+/+}$ mice during the 23-h post-injection period (P<0.05; data not shown). However, the effect of GEP44 to reduce core temperature was observed only at the high dose in male GLP-1R$^{-/-}$ mice (50 nmol/kg; Figure 5B; P<0.05). GEP44 was unable to reduce core temperature in female GLP-1R$^{-/-}$ mice (Figure 5D; P=NS). However, GEP44 produced an unexpected stimulation of core temperature at the low dose in female GLP-1R$^{-/-}$ mice (Figure 5D; P<0.05). There was an effect of exendin-4 to reduce core temperature in male (Figure 6A; P<0.05) or female GLP-1R$^{+/+}$ mice (Figure 6C; P<0.05) but not in GLP-1R$^{-/-}$ mice (Figures 6B, D; P=NS). Exendin-4 was largely without effect on core temperature during the 12-h dark, 11-h light and 23-h post-injection period in male DIO GLP-1R$^{+/+}$ mice. It did, however, produce a slight elevation of core temperature during the light cycle (20 nmol/kg; P<0.05). GEP44 produced opposing effects on core temperature during the dark (decrease) and light (increase) cycles (20 nmol/kg) but was otherwise ineffective at altering core temperature during the 12-h dark, 11-h light and 23-h post-injection period in female DIO GLP-1R$^{+/+}$ mice (P=NS).

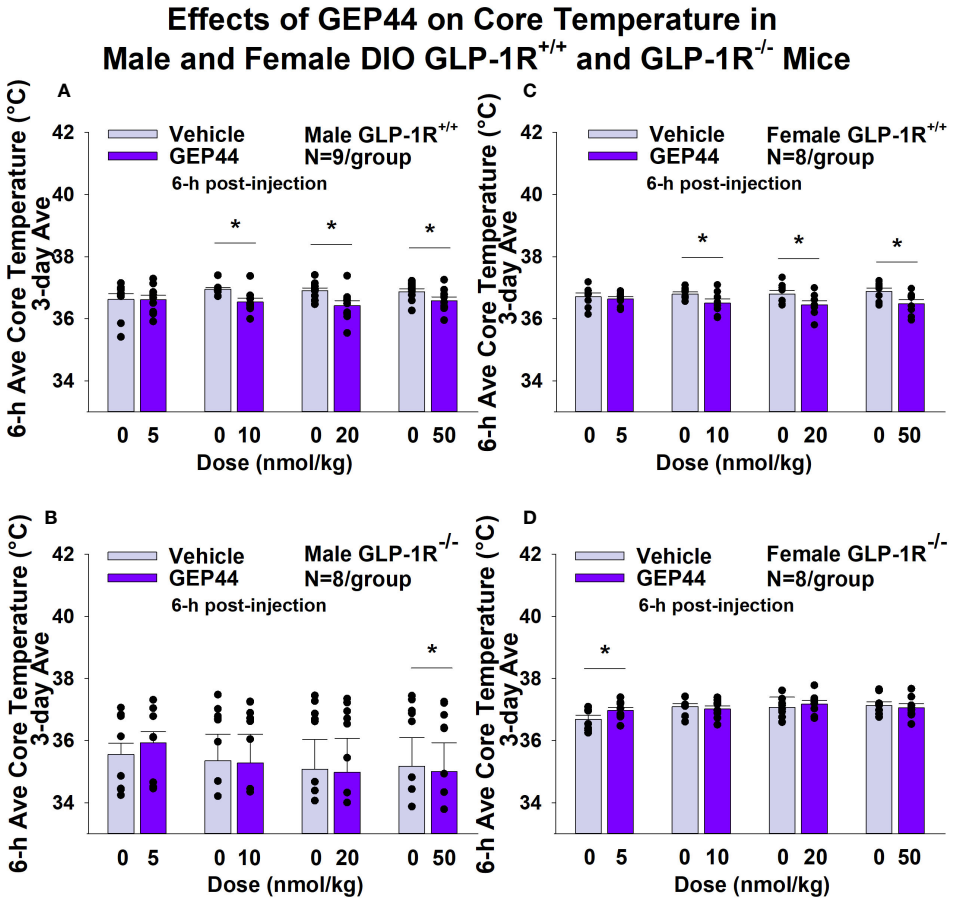

FIGURE 5
(A–D). Effects of the chimeric peptide, GEP44, on core temperature in male and female DIO GLP-1R$^{+/+}$ and GLP-1R$^{-/-}$ mice. Mice were maintained on HFD (60% kcal from fat; N=8-9/group) for approximately 4 months prior to receiving SC injections of vehicle (sterile saline/water) followed by escalating doses of GEP44 (5, 10, 20 and 50 nmol/kg; 3 mL/kg injection volume). **(A)** Effect of GEP44 on change in core temperature in male HFD-fed DIO GLP-1R$^{+/+}$ mice; **(B)** Effect of GEP44 on change in core temperature in male HFD-fed DIO GLP-1R $^{-/-}$ mice; **(C)** Effect of GEP44 on change in core temperature in female HFD-fed DIO GLP-1R$^{+/+}$ mice; **(D)** Effect of GEP44 on change in core temperature in female HFD-fed DIO GLP-1R$^{-/-}$ mice. Core temperature was averaged throughout each sequential 3-day vehicle and 3-day drug treatment period. Data are expressed as mean ± SEM. *P<0.05 GEP44 vs. vehicle.

Activity

GEP44 and exendin-4 both reduced activity over 6-h post-injection in male (Figure 7A; P<0.05) and female DIO GLP-1R$^{+/+}$ mice (Figure 7C; P<0.05). Similar results also observed over the 12-h dark cycle in response to GEP44 in male and female DIO GLP-1R$^{+/+}$ mice (P<0.05; data not shown). GEP44 (50 nmol/kg) also reduced activity during the 12-h dark and 23-h post-injection period in female DIO GLP-1R$^{+/+}$ mice (P<0.05) but had no effect during the 11-h light post-injection period. The lower dose of GEP44 (20 nmol/kg) reduced activity only during the 12-h dark period (P<0.05). In addition, GEP44 continued to reduce core temperature during the 12-h dark (10 nmol/kg, 20 and 50 nmol/kg), 11-h light (5 nmol/kg) and 23-h post-injection periods (5, 10, and 50 nmol/kg) in female DIO GLP-1R$^{+/+}$ mice (P<0.05). However, the effect of GEP44 to reduce activity was observed only at the low and high dose in male GLP-1R$^{-/-}$ mice (Figure 7B; P<0.05) and not in female GLP-1R$^{-/-}$ mice (Figure 7D; P=NS). There was an effect of exendin-4 to reduce activity in male (Figure 8A; P<0.05) and female GLP-1R$^{+/+}$ mice (Figure 8C; P=NS) but not in GLP-1R$^{-/-}$ mice (Figures 8B, D; P=NS). Exendin-4 had no effect on activity in male GLP-1R$^{+/+}$ during the 12-h dark, 11-h light or 23-h post-injection period. In contrast, exendin-4 reduced activity in female GLP-1R$^{+/+}$ during the 12-h dark (20 and 50 nmol/kg; P<0.05), 11-h light [5 nmol/kg (P><0.05) and 20 nmol/kg (P=0.050)], and 23-h post-injection period (20 and 50 nmol/kg; P<0.05).

Tissue collection for quantitative real-time PCR

As an additional readout of GEP44 and exendin-4-elicited thermogenic effects in IBAT, relative levels of mRNA for UCP-1, Gpr120, Ppargc1a, Cidea, and Dio2 were compared by PCR in response to GEP44 (50 nmol/kg) and exendin-4 (50 nmol/kg) or vehicle treatment at 2-h post-injection in male (Table 2A) and female GLP-1R$^{+/+}$ mice (Table 2C). We found that GEP44 increased Ppargc1a in male GLP-1R$^{+/+}$ mice [F(1,20) = 7.506, P=0.013]. Similarly, GEP44 increased Ppargc1a in female GLP-

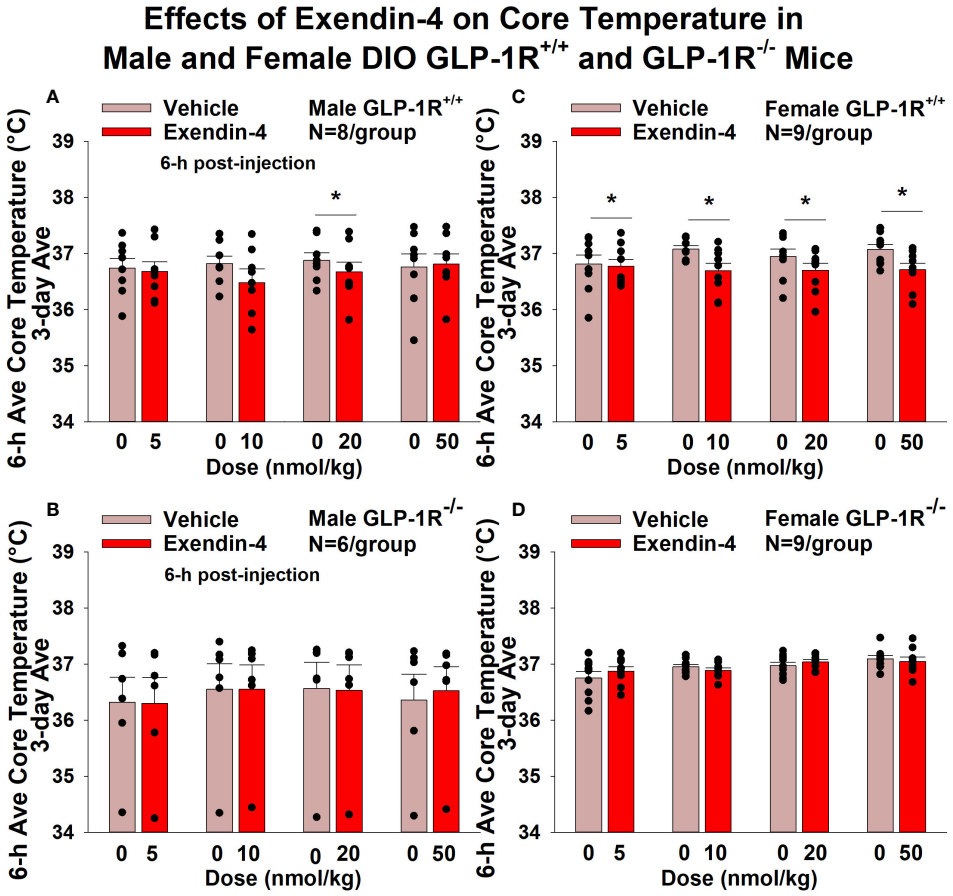

FIGURE 6
(A–D) Effects of the selective GLP-1R agonist, exendin-4, on core temperature in male and female DIO GLP-1R$^{+/+}$ and GLP-1R$^{-/-}$ mice. Mice were maintained on HFD (60% kcal from fat; N=6-9/group) for approximately 4 months prior to receiving SC injections of vehicle (sterile saline/water) followed by escalating doses of GEP44 (5, 10, 20 and 50 nmol/kg; 3 mL/kg injection volume). **(A)** Effect of exendin-4 on change in core temperature in male HFD-fed DIO GLP-1R$^{+/+}$ mice; **(B)** Effect of exendin-4 on change in core temperature in male HFD-fed DIO GLP-1R$^{-/-}$ mice; **(C)** Effect of exendin-4 on change in core temperature in female HFD-fed DIO GLP-1R$^{+/+}$ mice; **(D)** Effect of exendin-4 on change in core temperature in female HFD-fed DIO GLP-1R$^{-/-}$ mice. Core temperature was averaged throughout each sequential 3-day vehicle and 3-day drug treatment period. Data are expressed as mean ± SEM. *P<0.05 exendin-4 vs. vehicle.

1R$^{+/+}$ mice [F(1,18) = 36.773, P<0.001]. In contrast, the effects of GEP44 on thermogenic gene expression were largely absent in male GLP-1R$^{-/-}$ mice (Table 2B). In addition, GEP44 stimulated GPR120 in female GLP-1R$^{-/-}$ mice (Table 2D).

In female GLP-1R$^{+/+}$ mice, exendin-4 increased UCP-1 [F(1,18) = 5.967, P=0.025], Gpr120 [F(1,18) = 10.744, P=0.004], and Ppargc1a [F (1,18) = 19.767, P<0.001] while the effects of exendin-4 on thermogenic gene expression were absent in male and female GLP-1R$^{-/-}$ mice.

We also implanted a subset of mice with temperature transponders (HTEC IPTT-300; BIO MEDIC DATA SYSTEMS, INC, Seaford, DE) underneath both IBAT pads in order to obtain a more functional measure of IBAT thermogenesis [IBAT temperature (T_{IBAT})] as previously described (17, 18). T_{IBAT} was measured at 2, 3, 4, 5 and 6-h post-injection and averaged throughout each sequential 3-day vehicle and 3-day drug treatment period. Note that T_{IBAT} was averaged across two-day vehicle treatments (prior to 20 and 50 nmol/kg) for one of the four cohorts used in the dose escalation studies. Similar to what we found with GEP44-elicited increases in IBAT thermogenic gene expression, we found that GEP44 (50 nmol/kg) also increased T_{IBAT} at 240-min post-injection in male DIO GLP-1R$^{+/+}$ mice (N=3/group; P<0.05) (Figure 9A). Likewise, exendin-4 (50 nmol/kg) also increased T_{IBAT} at 180 and 360-min post-injection (N=4/group; P<0.05) (Figure 9B).

Lower doses of exendin-4 largely reproduced the effects found at the higher dose (50 nmol/kg). Namely, exendin-4 (10 nmol/kg) tended to increase T_{IBAT} at 300-min post-injection (P<0.05; data not shown) while the slightly higher dose (20 nmol/kg) increased T_{IBAT} at 240-min post-injection (P<0.05; data not shown). Exendin-4 (20 nmol/kg) appeared to produce a reduction of T_{IBAT} at 120-min post-injection (P<0.05; data not shown), but this was not observed at other doses. In contrast, GEP44 failed to produce significant effects on T_{IBAT} at lower doses (data not shown).

Together, our findings suggest that while both GEP44 and exendin-4 increase BAT thermogenesis, the effects of exendin-4 on BAT thermogenesis (T_{IBAT}) appeared to be longer lasting relative to GEP44.

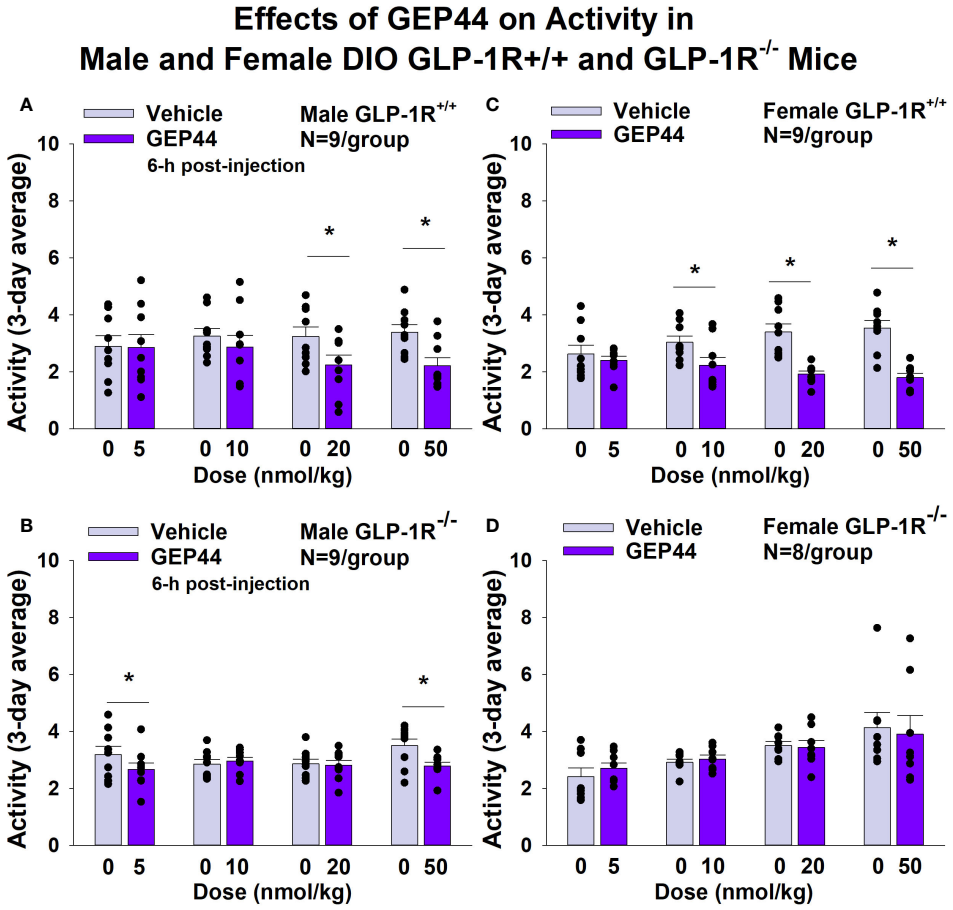

FIGURE 7
(A–D). Effects of the chimeric peptide, GEP44, on activity in male and female DIO GLP-1R$^{+/+}$ and GLP-1R$^{-/-}$ mice. Mice were maintained on HFD (60% kcal from fat; N=7-9/group) for approximately 4 months prior to receiving SC injections of vehicle (sterile saline/water) followed by escalating doses of GEP44 (5, 10, 20 and 50 nmol/kg; 3 mL/kg injection volume). **(A)** Effect of GEP44 on change in activity in male HFD-fed DIO GLP-1R$^{+/+}$ mice; **(B)** Effect of GEP44 on change in activity in male HFD-fed DIO GLP-1R$^{-/-}$ mice; **(C)** Effect of GEP44 on change in activity in female HFD-fed DIO GLP-1R$^{+/+}$ mice; **(D)** Effect of GEP44 on change in activity in female HFD-fed DIO GLP-1R$^{-/-}$ mice. Activity was averaged throughout each sequential 3-day vehicle and 3-day drug treatment period. Data are expressed as mean ± SEM. *P<0.05 GEP44 vs. vehicle.

Blood glucose and plasma hormones

Consistent with previous findings in rats, we found that that GEP44 also reduced tail vein glucose (collected at 2-h post-injection) in both male (Figure 10A) [F(1,14) = 39.938, P<0.05)] and female GLP-1R$^{+/+}$ DIO mice (Figure 10B) [F(1,10) = 6.954, P<0.05]. Moreover, the effects of GEP44 to reduce tail vein glucose were absent in both male [F(1,5) = 28.122, P<0.05] and female GLP-1R$^{-/-}$ mice [F(1,2) = 28.189, P<0.05]. In addition, exendin-4 reduced fasting tail vein glucose in both male (Figure 10B) [F(1,14) = 41.690, P<0.05] and female GLP-1R$^{+/+}$ DIO mice (Figure 10B) [F(1,9) = 7.241, P<0.05]. The reduction on blood glucose in response to GEP44 in both male and female GLP-1R$^{+/+}$ mice appear to be mediated, at least in part, by a reduction of glucagon (Tables 3A, B). As was the case with GEP44, the effects of exendin-4 to reduce tail vein blood glucose were also blocked in male GLP-1R$^{-/-}$ mice [F(1,4) = 54.475, P<0.05]. The effect of exendin-4 to reduce glucose also appeared to be impaired in female GLP-1R$^{-/-}$ mice [F(1,1) = 78.797, P=0.071]. In addition, exendin-4 reduced plasma leptin in male DIO mice [F(1,12) = 8.522, P<0.05] (Table 3A) and tended to reduce leptin in female DIO mice [F(1,15) = 4.157, P=0.059] (Table 3B). Furthermore, GEP44 tended to reduce plasma leptin in female DIO mice [F(1,14) = 3.325, P=0.09] (Table 3B). In contrast, both GEP44 and exendin-4 failed to reduce plasma leptin in both male and female GLP-1R$^{-/-}$ mice (P=NS). Both GEP44 [F(1,14) = 5.405, P<0.05] and exendin-4 [F(1,15) = 5.151, P<0.05] also reduced total cholesterol in female DIO mice (Table 3B). These effects on total cholesterol also tended to be observed in response to both exendin-4 [F(1,14) = 5.169, P<0.05] and GEP44 [F(1,13) = 3.805, P=0.073] in female GLP-1R$^{-/-}$ mice (Table 3B).

Discussion

Here we report effects of the novel chimeric peptide (GEP44), which targets GLP-1R, Y1R and Y2R, on energy intake, BW, thermoregulation (core temperature) and gross motor activity in DIO mice and characterize the extent to which these effects are mediated through GLP-1R. We tested the hypothesis that GEP44

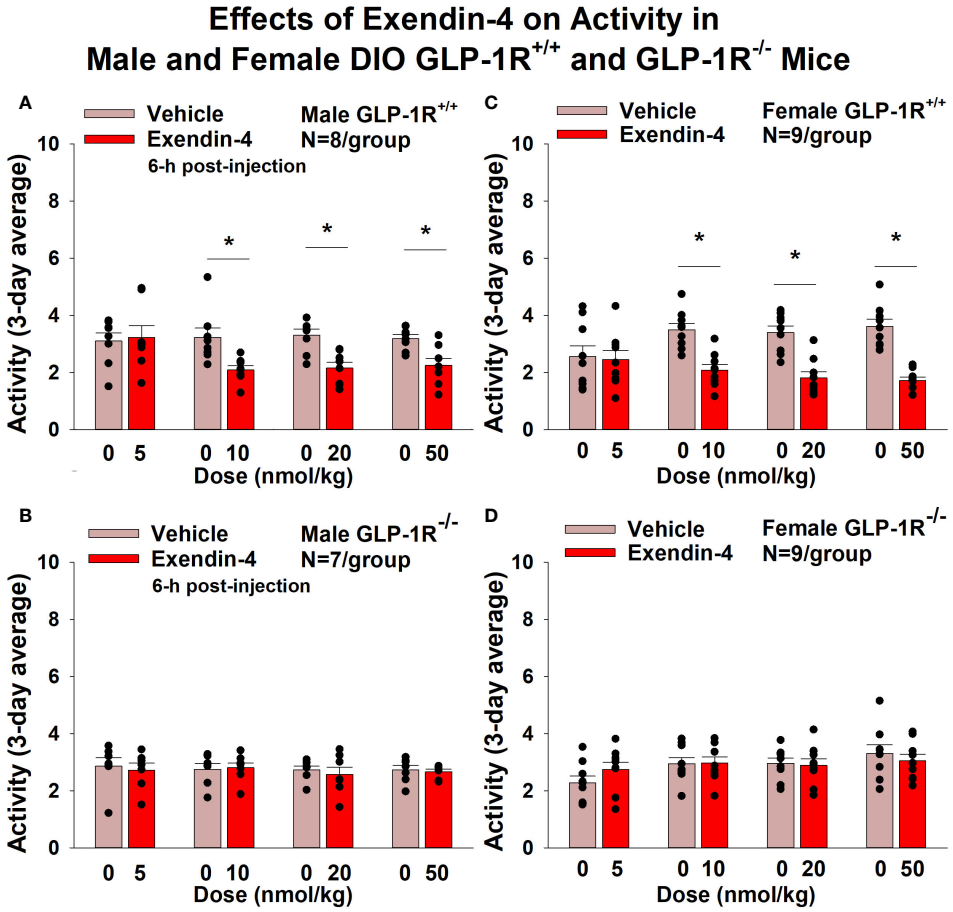

FIGURE 8
(A–D) Effects of the selective GLP-1R agonist, exendin-4, on activity in male and female DIO GLP-1R$^{+/+}$ and GLP-1R$^{-/-}$ mice. Mice were maintained on HFD (60% kcal from fat; N=8-9/group) for approximately 4 months prior to receiving SC injections of vehicle (sterile saline/water) followed by escalating doses of GEP44 (5, 10, 20 and 50 nmol/kg; 3 mL/kg injection volume). **(A)** Effect of exendin-4 on change in activity in male HFD-fed DIO GLP-1R$^{+/+}$ mice; **(B)** Effect of exendin-4 on change in activity in male HFD-fed DIO GLP-1R$^{-/-}$ mice; **(C)** Effect of exendin-4 on change in activity in female HFD-fed DIO GLP-1R$^{+/+}$ mice; **(D)** Effect of exendin-4 on change in activity in female HFD-fed DIO GLP-1R$^{-/-}$ mice. Activity was averaged throughout each sequential 3-day vehicle and 3-day drug treatment period. Data are expressed as mean ± SEM. *P<0.05 exendin-4 vs. vehicle.

reduces energy intake and BW through a GLP-1R dependent mechanism. We found that GEP44 reduced BW in both male and female DIO male GLP-1R$^{+/+}$ mice whereas these effects were absent in male and female DIO GLP-1R$^{-/-}$ mice. These findings suggest that GLP-1R signaling contributes to GEP44-elicited reduction of BW in both male and female mice. Additionally, GEP44 decreased energy intake in both male and female DIO GLP-1R$^{+/+}$ mice, but GEP44 produced more robust effects across multiple doses in males. These findings suggest that 1) GEP44 reduces BW, in part, through reductions in energy intake in DIO mice and 2) male mice might have enhanced sensitivity to the anorexigenic effects of GEP44. In GLP-1R$^{-/-}$ mice, the effects on energy intake were observed only at low and high doses in males suggesting that GEP44 may reduce energy intake in males, in part, through a GLP-1R independent mechanism. GEP44 reduced both core temperature and activity in both male and female GLP-1R$^{+/+}$ mice suggesting that reductions in energy expenditure and/or spontaneous activity-induced thermogenesis may also contribute to the weight lowering effects of GEP44 in mice. Lastly, we show that GEP44 reduced fasting blood glucose in DIO male and female mice through GLP-1R signaling. Together, these findings support the hypothesis that the chimeric peptide, GEP44, reduces energy intake, BW, core temperature, and glucose levels, in part, through a GLP-1R dependent mechanism.

We extend previous findings from our laboratory (13, 14) and demonstrate that the effects of GEP44 to elicit weight loss in both male and female mice are primarily driven by GLP-1R. These effects are mediated, at least in part, by reductions of energy intake. Similar to GLP-1R driven effects of GEP44 on BW, based on our findings in both male and female GLP-1R$^{-/-}$ mice, the ability of GEP44 to reduce energy intake also appears to be largely mediated by GLP-1R. However, the finding that the low and high dose of GEP44 also reduced energy intake in male GLP-1R$^{-/-}$ mice suggests other mechanisms are involved in contributing to these effects. Given the role of Y2R in the control of energy intake and BW (21), and results showing synergism/additive effects between co-administered GLP-1R and Y2-R agonists (22, 23), it is likely that the Y2R is also playing a role in the beneficial effects of GEP44 in terms of BW.

We incorporated the use of exendin-4 as a positive control for GLP-1R mediated effects on both food intake and BW. Similar to

10.3389/fendo.2024.1432928

what others have reported (15, 24), we also report that exendin-4 reduced BW and energy intake in both male and female DIO mice through GLP-1R signaling. Exendin-4 treatment appeared to be more effective at reducing BW in males at the lowest dose (5 nmol/kg). These findings are consistent with previous findings from Baggio and colleagues who reported that a single dose of exendin-4 (1.5 µg or 0.356 nmol/mouse) failed to reduce chow diet intake in male GLP-1R$^{-/-}$ mice (15). Another study also found that chronic subcutaneous administration of a single dose (0.126 mg/kg/day or 30 nmol/kg/day) also failed to reduce high fat diet intake and BW (vehicle corrected) in male GLP-1R$^{-/-}$ mice (24). In contrast to our studies, only a single dose of exendin-4 was examined in male mice in both studies (15, 24) and neither study examined the effects of exendin-4 in male and female DIO mice.

We also extend previous findings from our laboratory (13, 14) to demonstrate that GEP44 reduces core temperature (surrogate measure of energy expenditure) in both male and female mice, similar to what we described earlier herein following exendin-4 treatment. These data are also consistent with a previous report by Hayes and colleagues showing that the GLP-1R agonist, exendin-4, produced a long-lasting reduction of core temperature (hypothermia) that lasted for 4 hours following systemic [intraperitoneal (IP)] injections in rats (25). The hypothermic effects may be due, in part, to the reduced thermic effect of food (diet-induced thermogenesis) in exendin-4 and GEP44 treated mice. Furthermore, Baggio and colleagues (15) found that central

TABLE 2 (A–D) Changes in IBAT gene expression following GEP44 and Exendin-4 treatment in male and female DIO GLP-1R$^{+/+}$ and GLP-1R$^{-/-}$ mice.

TABLE 2A Changes in IBAT gene expression following GEP44 and Exendin-4 in male DIO GLP-1R$^{+/+}$ mice.

DIO GLP-1R$^{+/+}$ Mice				
Treatment	VEH	GEP44	VEH	Exendin-4
IBAT				
UCP1	1.0 ± 0.2^a	1.9 ± 0.5^a	1.0 ± 0.1^a	1.6 ± 0.4^a
Gpr120	1.0 ± 0.2^a	1.8 ± 0.4^a	1.0 ± 0.2^a	1.2 ± 0.3^a
Ppargc1a	1.0 ± 0.1^a	1.7 ± 0.2^b	1.0 ± 0.1^a	1.3 ± 0.2^a
Cidea	1.0 ± 0.2^a	1.2 ± 0.2^a	1.0 ± 0.2^a	1.6 ± 0.6^a
Dio2	1.0 ± 0.3^a	0.8 ± 0.3^a	1.0 ± 0.3^a	0.7 ± 0.2^a

Different letters denote significant differences between treatments (VEH vs GEP44/VEH vs Exendin-4; $P<0.05$).
Shared letters are not significantly different from one another (VEH vs GEP44/VEH vs Exendin-4).
IBAT was collected at 2-h post-injection of VEH, exendin-4 (50 nmol/kg) or GEP44 (50 nmol/kg).
Data are expressed as mean ± SEM.
N=5-12/group.

TABLE 2B Changes in IBAT gene expression following GEP44 and Exendin-4 in male DIO GLP-1R$^{-/-}$ mice.

DIO GLP-1R$^{-/-}$ Mice				
Treatment	VEH	GEP44	VEH	Exendin-4
IBAT				
UCP1	1.0 ± 0.2^a	1.7± 0.4^a	1.0 ± 0.2^a	1.7± 0.5^a
Gpr120	1.0 ± 0.3^a	1.0 ± 0.2^a	1.0 ± 0.3^a	1.2 ± 0.3^a
Ppargc1a	1.0 ± 0.2^a	1.2 ± 0.1^a	1.0 ± 0.2^a	1.6 ± 0.4^a
Cidea	1.0 ± 0.3^a	1.4 ± 0.3^a	1.0 ± 0.3^a	1.8 ± 0.4^a
Dio2	1.0 ± 0.4^a	0.9 ± 0.2^a	1.0 ± 0.4^a	1.2 ± 0.4^a

Different letters denote significant differences between treatments (VEH vs GEP44/VEH vs Exendin-4; $P<0.05$).
Shared letters are not significantly different from one another (VEH vs GEP44/VEH vs Exendin-4).
IBAT was collected at 2-h post-injection of VEH, exendin-4 (50 nmol/kg) or GEP44 (50 nmol/kg).
Data are expressed as mean ± SEM.
N=4-11/group.

TABLE 2C Changes in IBAT gene expression following GEP44 and Exendin-4 in female DIO GLP-1R$^{+/+}$ mice.

DIO GLP-1R$^{+/+}$ Mice				
Treatment	VEH	GEP44	VEH	Exendin-4
IBAT				
UCP1	1.0 ± 0.1^a	1.4 ± 0.2^a	1.0 ± 0.1^a	1.9 ± 0.4^b
Gpr120	1.0 ± 0.2^a	1.7 ± 0.4^a	1.0 ± 0.2^a	2.7 ± 0.5^b
Ppargc1a	1.0 ± 0.1^a	2.1 ± 0.2^b	1.0 ± 0.1^a	2.7 ± 0.4^b
Cidea	1.0 ± 0.2^a	0.8 ± 0.2^a	1.0 ± 0.2^a	1.6 ± 0.6^a
Dio2	1.0 ± 0.2^a	1.4 ± 0.4^a	1.0 ± 0.3^a	0.7 ± 0.2^a

Different letters denote significant differences between treatments (VEH vs GEP44 or Exendin-4; $P<0.05$).
Shared letters are not significantly different from one another (VEH vs GEP44 or Exendin-4).
IBAT was collected at 2-h post-injection of VEH, exendin-4 (50 nmol/kg) or GEP44 (50 nmol/kg).
Data are expressed as mean ± SEM. *P<0.05 GEP44 or exendin-4 vs. vehicle.
N=3-10/group.

TABLE 2D Changes in IBAT gene expression following GEP44 and Exendin-4 in female DIO GLP-1R$^{-/-}$ mice.

DIO GLP-1R$^{-/-}$ Mice				
Treatment	VEH	GEP44	VEH	Exendin-4
IBAT				
UCP1	1.0 ± 0.1^a	1.9 ± 0.5^a	1.0 ± 0.1^a	1.7 ± 0.3^a
Gpr120	1.0 ± 0.2^a	2.0 ± 0.4^b	1.0 ± 0.2^a	1.5 ± 0.3^a
Ppargc1a	1.0 ± 0.1^a	1.1 ± 0.1^a	1.0 ± 0.1^a	1.4 ± 0.1^a
Cidea	1.0 ± 0.2^a	1.3 ± 0.2^a	1.0 ± 0.2^a	2.0 ± 0.6^a
Dio2	1.0 ± 0.2^a	1.6 ± 0.7^a	1.0 ± 0.2^a	1.5 ± 0.3^a

Different letters denote significant differences between treatments (VEH vs GEP44/VEH vs Exendin-4; $P<0.05$).
Shared letters are not significantly different from one another (VEH vs GEP44/VEH vs Exendin-4).
IBAT was collected at 2-h post-injection of VEH, exendin-4 (50 nmol/kg) or GEP44 (50 nmol/kg).
Data are expressed as mean ± SEM.
N=3-9/group.

10.3389/fendo.2024.1432928

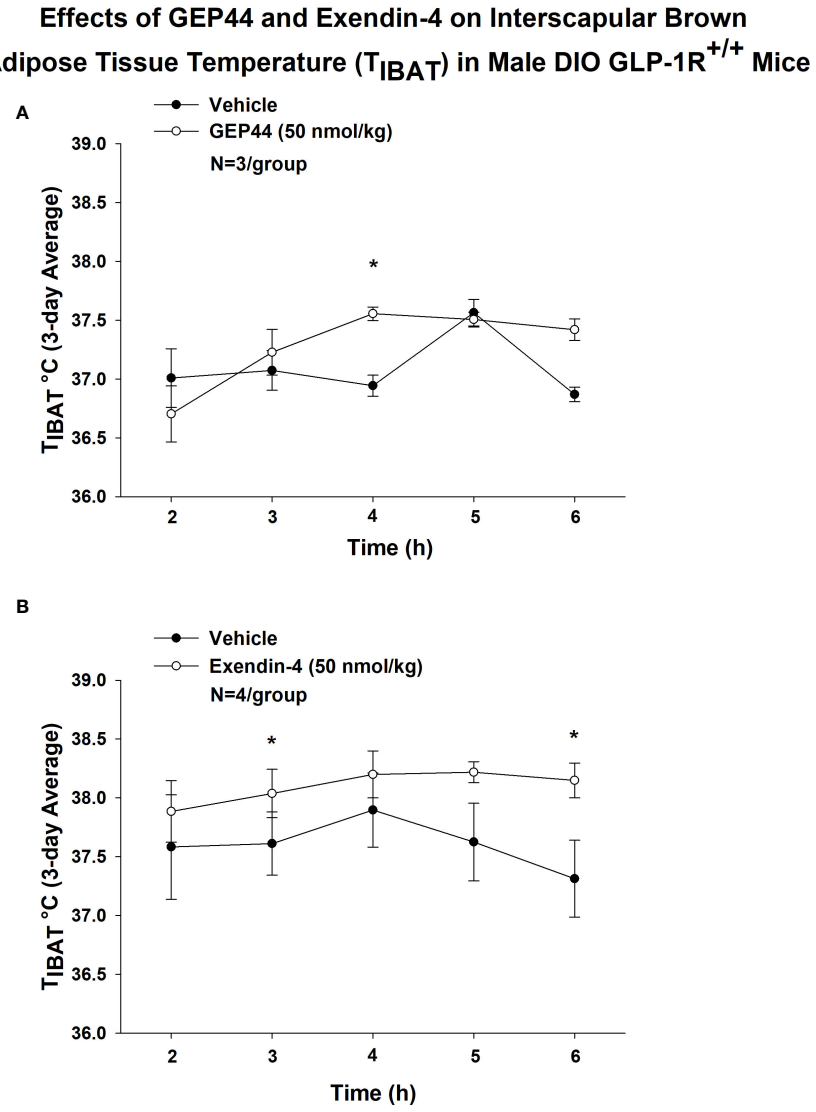

FIGURE 9
(A, B) Effects of GEP44 and exendin-4 on IBAT temperature (T_{IBAT}) in male DIO GLP-1R$^{+/+}$ mice. **(A)** Effect of GEP44 on T_{IBAT} in male DIO GLP-1R$^{+/+}$ mice; **(B)** Effect of exendin-4 on T_{IBAT} in male DIO GLP-1R$^{+/+}$ mice. T_{IBAT} data were collected at 2, 3, 4, 5 and 6-h post-injection and averaged throughout each sequential 3-day vehicle and 3-day drug treatment period. Data are expressed as mean ± SEM. *P<0.05 GEP44 or exendin-4 vs. vehicle.

and peripheral (IP; 1.5 µg or 0.356 nmol/mouse) administration of exendin-4 reduced VO2 and resting energy expenditure in adult male wild-type mice. These effects occurred over 2 and 21 hours following peripheral and central administration, respectively. Similarly, Krieger and colleagues found that peripheral exendin-4 reduced energy expenditure over 4-h post-injection in rats (26). In addition, van Eyk and colleagues found that liraglutide treatment reduced resting energy expenditure after 4 weeks of treatment in humans with type 2 diabetes (27). Gabery initially found that semaglutide reduced energy expenditure during the dark phase in DIO mice through treatment day 6 but these differences were no longer significant after adjusting for lean mass (28). Similarly, Blundell and colleagues initially found that semaglutide reduced resting energy expenditure after 12 weeks of treatment in humans but these effects were no longer significant after adjusting for lean mass (29). Despite previous reports indicating that acute central (ICV) administration of GLP-1 increases core temperature over 4-h post-injection (30), IBAT temperature over 6-h post-injection (31) and activates SNS fibers that innervate BAT (31), to our knowledge, the majority of studies that administered GLP-1R agonists peripherally have either found a reduction or no change in energy expenditure. Given the dearth of studies that have measured both core temperature and energy expenditure in the same group of animals, it will be important to measure both endpoints simultaneously in the same animal model. Ongoing studies are currently in the process of addressing the extent to which systemic administration of GEP44 and exendin-4 alters core temperature and more directly impacts energy expenditure (measured by indirect calorimetry) in male and female DIO rats.

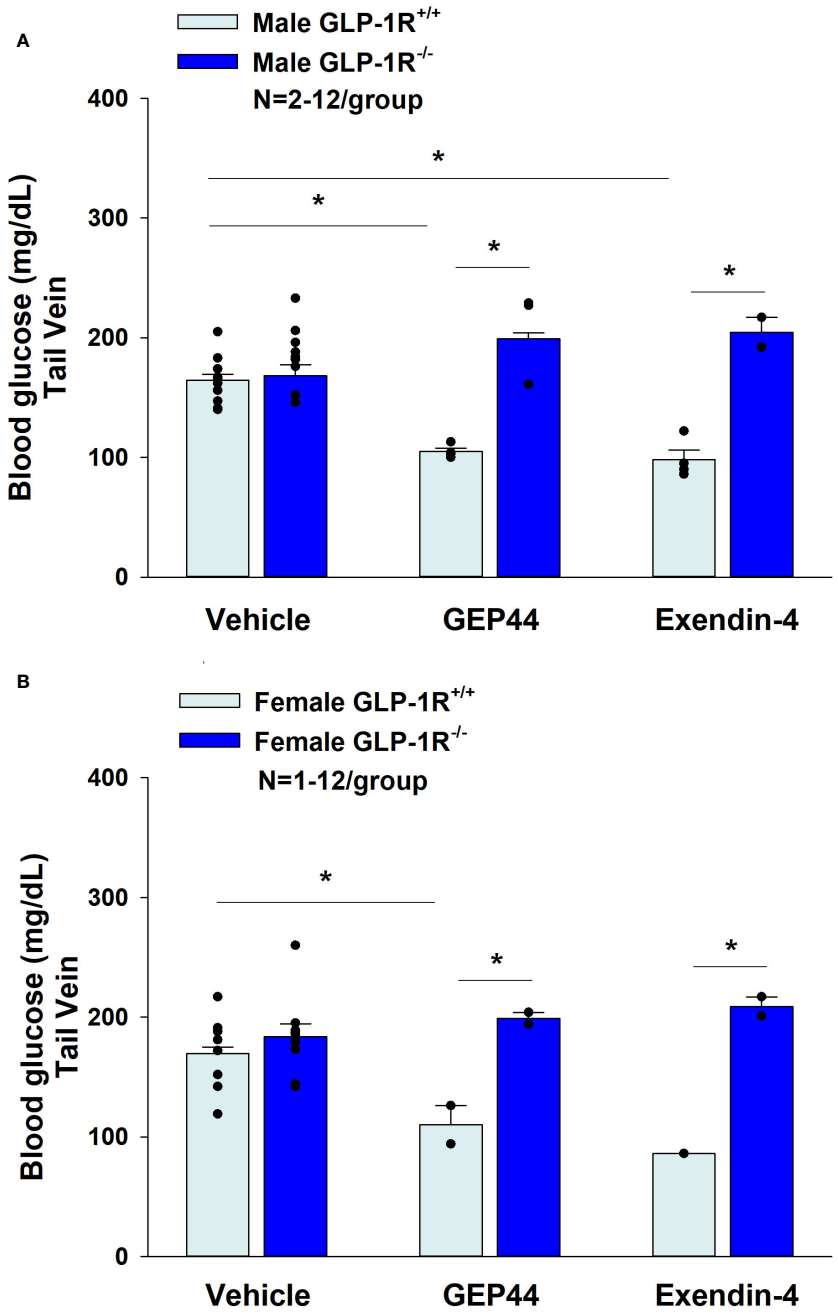

FIGURE 10
(A, B) Effects of GEP44 and exendin-4 on tail vein glucose in male and female DIO GLP-1R$^{+/+}$ and GLP-1R$^{-/-}$ mice. **(A)** Effect of GEP44 and exendin-4 on tail vein glucose in male DIO GLP-1R$^{+/+}$ and GLP-1R$^{-/-}$ mice; **(B)** Effect of GEP44 and exendin-4 on tail vein glucose in female DIO GLP-1R$^{+/+}$ and GLP-1R$^{-/-}$ mice. Blood was collected by tail vein nick (glucose) at 2-h post-injection of VEH, exendin-4 (50 nmol/kg) or GEP44 (50 nmol/kg). Tail vein glucose was measured at 2-h post-injection in conscious mice. Data are expressed as mean ± SEM. *P<0.05 GEP44 or exendin-4 vs. vehicle.

In contrast to the effects of GEP44 and exendin-4 to reduce core temperature, we found that both GEP44 and exendin-4 stimulated thermogenic markers (biochemical readout of BAT thermogenesis) within IBAT and T_{IBAT} (functional readout of BAT thermogenesis). It is not clear why GEP44 and exendin-4 elicited opposing effects on core temperature and T_{IBAT} given that BAT thermogenesis helps maintain core temperature in other contexts such as fever or stress (32, 33). Future studies that examine temporal profile will help identify if the elevated BAT thermogenesis may be in response to the reduction of core temperature. Our findings, however, that exendin-4 stimulated thermogenic markers within IBAT and IBAT temperature are consistent with what others have found following systemic (intraperitoneal) exendin-4 (34) or liraglutide (35) administration in mice. On the other hand, Krieger (26) found that systemic (IP) exendin-4 reduced BAT thermogenesis, skin temperature above the interscapular area over 2-h post-injection

TABLE 3 (A, B) Effects of the chimeric peptide, GEP44 (50 nmol/kg) and the selective GLP-1R agonist, exendin-4 (50 nmol/kg), on plasma leptin, insulin, and total cholesterol in (A) male and (B) female DIO GLP-1R$^{+/+}$ and GLP-1R$^{-/-}$ mice.

TABLE 3A Plasma Measurements Following SC Administration of GEP44 or Exendin-4 in Male DIO Mice.

	GLP-1R$^{+/+}$			GLP-1R$^{-/-}$		
SC Treatment	Vehicle	GEP44	Exendin-4	Vehicle	GEP44	Exendin-4
Leptin (ng/mL)	38.3 ± 3.7	29.8 ± 6.9	29.8 ± 6.0	36.1 ± 5.8	33.4 ± 4.8	34.5 ± 5.6
Insulin (ng/mL)	1.5 ± 0.5	4.4 ± 1.3*	1.5 ± 0.4	1.7 ± 0.5	1.5± 0.3	1.6 ± 0.5
Glucagon (pmol/L)	20.5 ± 5.9	6.1 ± 1.4*				
Total Cholesterol (mg/dL)	189.4 ± 23.2	159.1 ± 10.9	166.6 ± 11.4	186.0 ± 21.1	174.6 ± 6.7	184.7 ± 8.7

Blood was collected by tail vein nick (glucose) or cardiac stick (leptin, insulin, total cholesterol) at 2-h post-injection of VEH, exendin-4 (50 nmol/kg) or GEP44 (50 nmol/kg).
Data are expressed as mean ± SEM. *P <0.05 GEP44 or exendin-4 vs. vehicle.
N=6-10/group.

TABLE 3B Plasma Measurements Following SC Administration of GEP44 or Exendin-4 in Female DIO Mice.

	GLP-1R$^{+/+}$			GLP-1R$^{-/-}$		
SC Treatment	Vehicle	GEP44	Exendin-4	Vehicle	GEP44	Exendin-4
Leptin (ng/mL)	34.1 ± 4.3	18.5 ± 5.1*	17.7 ± 4.7*	19.8 ± 2.7	15.2 ± 3.2	14.0 ± 4.1
Insulin (ng/mL)	1.4 ± 0.4	1.1 ± 0.3	1.0 ± 0.3	0.5 ± 0.1	0.5 ± 0.1	0.5 ± 0.1
Glucagon (pmol/L)	14.7 ± 3.0	5.5 ± 1.8*				
Total Cholesterol (mg/dL)	170.9 ± 18.0	116.5 ± 6.5*	122.9 ± 7.0*	132.7 ± 11.3	105.0 ± 6.4*	102.7 ± 7.7*

Blood was collected by tail vein nick (glucose) or cardiac stick (leptin, insulin, total cholesterol) at 2-h post-injection of VEH, exendin-4 (50 nmol/kg) or GEP44 (50 nmol/kg).
Data are expressed as mean ± SEM. *P <0.05 GEP44 or exendin-4 vs. vehicle.
N=7-10/group.

and BAT Adrb3 in a rat model. Note that measurements of skin temperature above the interscapular area might not necessarily reflect T_{IBAT} as the interscapular subcutaneous area may also be influenced by heating and cooling of the skin temperature. We found that the majority of thermogenic genes in IBAT were elevated in response to both GEP44 and exendin-4. Furthermore, our findings suggest that GEP44 may also elicit BAT thermogenesis through similar mechanisms (PPargc1a) in both male and female GLP-1R$^{+/+}$ mice while exendin-4 may increase BAT thermogenesis via multiple thermogenic genes (UCP-1, Gpr120, and Ppargc1a) in female mice. In contrast to the effects of exendin-4 in GLP-1R$^{+/+}$ mice, the chimeric peptide, GEP44, appears to promote BAT thermogenesis in both male and female GLP-1R$^{+/+}$ mice through different genes. In contrast, GEP44 stimulated GPR120 only in female GLP-1R$^{-/-}$ mice raising the possibility that other receptor subtypes may contribute to these effects at the high dose in female mice. Overall, our findings suggest that systemic administration of both GEP44 and exendin-4 may promote BAT thermogenesis through different mechanisms in a mouse model. It will be important in future studies to examine if SNS outflow to BAT is a predominant mediator of GEP44 or exendin-4-elicited weight loss in male and female DIO mice.

Our findings also demonstrate that GEP44 reduced gross motor activity through what appears to be both GLP-1R and Y2R signaling in male mice; while this effect appears to be entirely mediated by GLP-1R in female mice. In contrast, we found that exendin-4 treatment reduces activity strictly through GLP-1R in both male and female mice, as anticipated. Similarly, others have also found that exendin-4 at lower [0.5-5 µg/kg (0.2-2 µg/rat, IP)] (36) or higher doses [30 µg/kg (9 µg/rat, IP)] (37) reduces locomotor activity in lean male Sprague Dawley rats (36, 37). While Hayes and colleagues (25) did not find any change in activity in response to exendin-4 at [3 µg/kg (0.9 µg/rat, IP)] in lean male Sprague-Dawley rats, it might be possible that differences in paradigm and/or timing of injections may account for discrepancies between studies. Given that we found reductions in both core temperature and gross motor activity, our data raise the possibility that reductions in spontaneous physical activity-induced thermogenesis (38) and/or shivering and non-shivering thermogenesis in skeletal muscle (39) may have contributed to the hypothermic effects of both GEP44 and exendin-4. Moreover, our findings indicate that GEP44 may produce GLP-1R independent effects on 1) activity in male mice and 2) core temperature in both male and female mice while exendin-4 appears to impact both activity and core temperature through GLP-1R dependent mechanism in both male and female mice.

We have now extended our previous findings on glucoregulation (14) by showing that the effects of GEP44 to reduce fasting blood glucose in DIO male and female mice were mediated, in part, by GLP-1R. In addition, the effects of peripheral GEP44 and exendin-4 to reduce cholesterol in female GLP-1R$^{+/+}$ and GLP-1R$^{-/-}$ mice are also consistent with the potential GLP-1R and/or Y2-receptor

mediated cholesterol lowering effects observed following the GLP-1R agonists, liraglutide (40) and exendin-4 (41, 42), Y2 receptor agonist, lipidated PYY_{3-36} analog, [Lys_7(C16- γGlu)PYY3–36] (similar potency on Y2R as PYY_{3-36}) (40), and dual GLP-1R/Y2 receptor agonists, 6q and peptide 19 (40), in DIO rodents.

One limitation to our studies is the lack of weight restricted or pair-fed controls for studies that assessed the effects of GEP44 and exendin-4 on gene expression as well as plasma measurements (total cholesterol, leptin, and glucose) in adult DIO male and female mice. As a result, it is possible that the effects of GEP44 and exendin-4 on thermogenic gene expression or glucose, total cholesterol or leptin lowering in DIO mice may also be due, in part, to the weight loss in response to GEP44 or exendin-4 treatment. In addition, we only collected T_{IBAT} between 120 and 360 min-post-injection. It is possible that, due to absence of being able to measure T_{IBAT} at earlier time points, we might have missed any potential hypothermic effects that might have preceded the elevations of T_{IBAT} that occurred at the later time points. In addition, we were unable to assess the roles of Y1R or Y2R signaling more fully in contributing to the effects of GEP44. Future studies incorporating the use of Y2R deficient mice will be helpful in more fully establishing the role of Y2R signaling in the anorectic response to GEP44.

In summary, the results presented in this manuscript highlight the beneficial effects of the dual-agonist, GEP44, on BW, energy intake, and glucoregulation in adult male and female DIO mice at doses that have not been found to elicit visceral illness in rats or emesis in shrews (13, 14). Our findings further demonstrate that effects on changes of BW, energy intake, activity, and glucose levels are largely mediated through GLP-1R signaling. However, given that GEP44 may also elicit GLP-1R independent effects on 1) activity in male mice and 2) core temperature in both male and female mice, it is possible that other receptor subtypes, including the Y1R (43) and Y2R, may contribute to these effects. The findings to date indicate that GEP44 is a promising drug targeting limitations associated with current GLP-1R agonist medications (5, 44) for the treatment of obesity and/or T2DM.

Data availability statement

All relevant data is contained within the article: The original contributions presented in the study are included in the article/Supplementary Material, further inquiries can be directed to the corresponding author/s.

Ethics statement

The animal study was approved by VA Puget Sound Health Care System IACUC and the US Army Medical Research and Development Command (USAMRDC) Animal Care and Use Review Office (ACURO). The study was conducted in accordance with the local legislation and institutional requirements.

Author contributions

JB: Writing – review & editing, Writing – original draft, Supervision, Resources, Project administration, Methodology, Investigation, Formal analysis, Data curation, Conceptualization. MH: Writing – review & editing, Writing – original draft, Resources, Project administration, Methodology, Investigation, Data curation. JS: Writing – review & editing, Writing – original draft, Resources, Project administration, Methodology, Investigation, Data curation. MG: Writing – review & editing, Writing – original draft, Resources, Project administration, Methodology, Investigation, Data curation. JR: Writing – review & editing, Writing – original draft, Resources, Project administration, Methodology, Investigation, Data curation. ET: Writing – review & editing, Writing – original draft, Resources, Project administration, Methodology, Investigation, Data curation. AD: Writing – review & editing, Writing – original draft, Resources, Project administration, Methodology, Investigation, Data curation. KS: Writing – review & editing, Writing – original draft, Project administration, Investigation. TS: Writing – review & editing, Writing – original draft, Methodology, Investigation, Conceptualization. CE: Writing – review & editing, Writing – original draft, Methodology, Investigation, Funding acquisition, Conceptualization. KC: Writing – review & editing, Writing – original draft, Resources, Methodology, Investigation. EA: Writing – review & editing, Writing – original draft, Resources, Methodology, Investigation. SZ: Writing – review & editing, Writing – original draft, Resources, Project administration, Methodology, Investigation. RD: Writing – review & editing, Writing – original draft, Supervision, Resources, Project administration, Methodology, Investigation, Funding acquisition, Conceptualization. CR: Writing – review & editing, Writing – original draft, Supervision, Resources, Project administration, Methodology, Investigation, Funding acquisition, Conceptualization.

Funding

The author(s) declare financial support was received for the research, authorship, and/or publication of this article. This material was based upon work supported by the Office of Research and Development, Medical Research Service, Department of Veterans Affairs (VA) and the VA Puget Sound Health Care System Rodent Metabolic Phenotyping Core and the Metabolic and Cellular Phenotyping Core of the Diabetes Research Center at the University of Washington and supported by National Institutes of Health (NIH) grant P30DK017047. This work was supported by Department of Defense Grant 6W81XWH201029901 to CR and RD (JB, subaward PI). This work was also supported by the VA Merit Review Award 5I01BX004102, from the United States (U.S.) Department of Veterans Affairs Biomedical Laboratory Research and Development Service. Research reported in this publication is a project of the Seattle Institute for Biomedical and Clinical Research, supported by the National Institute of Diabetes and Digestive and Kidney Diseases of the National Institutes of Health under Award Number R01DK115976 (JB) and R01DK135125 (CR, RD, SZ). The

content is solely the responsibility of the authors and does not necessarily represent the official views of the National Institutes of Health. The contents do not represent the views of the U.S. Department of Veterans Affairs or the United States Government.

Acknowledgments

Plasma sample analysis was performed by the UC Davis MMPC Live M&MH Core (NIH U2CDK135074). The authors thank the technical support of Dr. Tami Wolden-Hanson with body composition measurements and James Graham and Dr. Peter Havel for plasma analyses.

Conflict of interest

The authors declare that the research was conducted in the absence of any commercial or financial relationships that could be construed as a potential conflict of interest.

The author(s) declared that they were an editorial board member of Frontiers, at the time of submission. This had no impact on the peer review process and the final decision.

Publisher's note

All claims expressed in this article are solely those of the authors and do not necessarily represent those of their affiliated organizations, or those of the publisher, the editors and the reviewers. Any product that may be evaluated in this article, or claim that may be made by its manufacturer, is not guaranteed or endorsed by the publisher.

Supplementary material

The Supplementary Material for this article can be found online at: https://www.frontiersin.org/articles/10.3389/fendo.2024.1432928/full#supplementary-material

SUPPLEMENTARY FIGURE 1

(A–D) Effects of the chimeric peptide, GEP44, on energy intake (kcal/gram BW) in male and female DIO GLP-1R$^{+/+}$ and GLP-1R$^{-/-}$ mice. Mice were maintained on HFD (60% kcal from fat; N=10-11/group) for approximately 4 months prior to receiving SC injections of vehicle (sterile saline/water) followed by escalating doses of GEP44 (5, 10, 20 and 50 nmol/kg; 3 mL/kg injection volume). **(A)** Effect of GEP44 on energy intake in male HFD-fed DIO GLP-1R$^{+/+}$ mice; **(B)** Effect of GEP44 on change on energy intake in male HFD-fed DIO GLP-1R$^{-/-}$ mice; **(C)** Effect of GEP44 on energy intake in male HFD-fed DIO GLP-1R$^{+/+}$ mice; **(D)** Effect of GEP44 on energy intake in male HFD-fed DIO GLP-1R $^{-/-}$ mice. Energy intake (kcal/gram BW) was averaged throughout each sequential 3-day vehicle and 3-day drug treatment period. Data are expressed as mean ± SEM. *P<0.05 GEP44 vs. vehicle.

SUPPLEMENTARY FIGURE 2

(A–D) Effects of the selective GLP-1R agonist, exendin-4, on energy intake (kcal/gram BW) in male and female DIO GLP-1R$^{+/+}$ and GLP-1R$^{-/-}$ mice. Mice were maintained on HFD (60% kcal from fat; N=9-11/group) for approximately 4 months prior to receiving SC injections of vehicle followed by escalating doses of GEP44 (5, 10, 20 and 50 nmol/kg; 3 mL/kg injection volume). **(A)** Effect of GEP44 on energy intake in male HFD-fed DIO GLP-1R$^{+/+}$ mice; **(B)** Effect of GEP44 on change on energy intake in male HFD-fed DIO GLP-1R$^{-/-}$ mice; **(C)** Effect of GEP44 on energy intake in male HFD-fed DIO GLP-1R$^{+/+}$ mice; **(D)** Effect of GEP44 on energy intake in male HFD-fed DIO GLP-1R$^{-/-}$ mice. Energy intake (kcal/gram BW) was averaged throughout each sequential 3-day vehicle and 3-day drug treatment period. Data are expressed as mean ± SEM. *P<0.05 exendin-4 vs. vehicle.

References

1. N.C.D.R.F. Collaboration. Worldwide trends in underweight and obesity from 1990 to 2022: a pooled analysis of 3663 population-representative studies with 222 million children, adolescents, and adults. *Lancet*. (2024) 403:1027–50. doi: 10.1016/S0140-6736(23)02750-2

2. Ward ZJ, Bleich SN, Cradock AL, Barrett JL, Giles CM, Flax C, et al. State-level prevalence of adult obesity and severe obesity. *N Engl J Med*. (2019) 381:2440–50. doi: 10.1056/NEJMsa1909301

3. Okunogbe A, Nugent R, Spencer G, Powis J, Ralston J, Wilding J. Economic impacts of overweight and obesity: current and future estimates for 161 countries. *BMJ Glob Health*. (2022) 7:e009773. doi: 10.1136/bmjgh-2022-009773

4. Wilding JPH, Batterham RL, Calanna S, Davies M, Van Gaal LF, Lingvay I, et al. Once-weekly semaglutide in adults with overweight or obesity. *N Engl J Med*. (2021) 384:989. doi: 10.1056/NEJMoa2032183

5. Frias JP, Davies MJ, Rosenstock J, Perez Manghi FC, Fernandez Lando L, Bergman BK, et al. Tirzepatide versus semaglutide once weekly in patients with type 2 diabetes. *N Engl J Med*. (2021) 385:503–15. doi: 10.1056/NEJMoa2107519

6. Ryan DH, Lingvay I, Deanfield J, Kahn SE, Barros E, Burguera B, et al. Long-term weight loss effects of semaglutide in obesity without diabetes in the SELECT trial. *Nat Med*. (2024). doi: 10.1038/s41591-024-02996-7

7. Wilding JPH, Batterham RL, Davies M, Van Gaal LF, Kandler K, Konakli K, et al. Weight regain and cardiometabolic effects after withdrawal of semaglutide: The STEP 1 trial extension. *Diabetes Obes Metab*. (2022) 24:1553–64. doi: 10.1111/dom.14725

8. Myers MG Jr., Leibel RL, Seeley RJ, Schwartz MW. Obesity and leptin resistance: distinguishing cause from effect. *Trends Endocrinol Metab*. (2010) 21:643–51. doi: 10.1016/j.tem.2010.08.002

9. Rodgers RJ, Tschop MH, Wilding JP. Anti-obesity drugs: past, present and future. *Dis Model Mech*. (2012) 5:621–6. doi: 10.1242/dmm.009621

10. Jastreboff AM, Aronne LJ, Ahmad NN, Wharton S, Connery L, Alves B, et al. Tirzepatide once weekly for the treatment of obesity. *N Engl J Med*. (2022) 387:205–16. doi: 10.1056/NEJMoa2206038

11. Aronne LJ, Sattar N, Horn DB, Bays HE, Wharton S, Lin WY, et al. Continued treatment with tirzepatide for maintenance of weight reduction in adults with obesity: the SURMOUNT-4 randomized clinical trial. *Clinical Trial*. (2024) 331:38–48. doi: 10.1001/jama.2023.24945

12. Jastreboff AM, Kaplan LM, Hartman ML. Triple-hormone-receptor agonist retatrutide for obesity. *Reply N Engl J Med*. (2023) 389:1629–30. doi: 10.1056/NEJMc2310645

13. Chichura KS, Elfers CT, Salameh TS, Kamat V, Chepurny OG, McGivney A, et al. A peptide triple agonist of GLP-1, neuropeptide Y1, and neuropeptide Y2 receptors promotes glycemic control and weight loss. *Sci Rep*. (2023) 13:9554. doi: 10.1038/s41598-023-36178-1

14. Milliken BT, Elfers C, Chepurny OG, Chichura KS, Sweet IR, Borner T, et al. Design and evaluation of peptide dual-agonists of GLP-1 and NPY2 receptors for glucoregulation and weight loss with mitigated nausea and emesis. *J Med Chem*. (2021) 64:1127–38. doi: 10.1021/acs.jmedchem.0c01783

15. Baggio LL, Huang Q, Brown TJ, Drucker DJ. Oxyntomodulin and glucagon-like peptide-1 differentially regulate murine food intake and energy expenditure. *Gastroenterology*. (2004) 127:546–58. doi: 10.1053/j.gastro.2004.04.063

16. Blevins JE, Thompson BW, Anekonda VT, Ho JM, Graham JL, Roberts ZS, et al. Chronic CNS oxytocin signaling preferentially induces fat loss in high fat diet-fed rats by enhancing satiety responses and increasing lipid utilization. *Am J Physiol Regul Integr Comp Physiol*. (2016) 310:R640–58. doi: 10.1152/ajpregu.00220.2015

17. Roberts ZS, Wolden-Hanson TH, Matsen ME, Ryu V, Vaughan CH, Graham JL, et al. Chronic hindbrain administration of oxytocin is sufficient to elicit weight loss in

diet-induced obese rats. *Am J Physiol Regul Integr Comp Physiol*. (2017) 313:R357–71. doi: 10.1152/ajpregu.00169.2017

18. Edwards MM, Nguyen HK, Herbertson AJ, Dodson AD, Wietecha T, Wolden-Hanson T, et al. Chronic hindbrain administration of oxytocin elicits weight loss in male diet-induced obese mice. *Am J Physiol Regul Integr Comp Physiol*. (2021) 320: R471–87. doi: 10.1152/ajpregu.00294.2020

19. Bremer AA, Stanhope KL, Graham JL, Cummings BP, Wang W, Saville BR, et al. Fructose-fed rhesus monkeys: a nonhuman primate model of insulin resistance, metabolic syndrome, and type 2 diabetes. *Clin Transl Sci*. (2011) 4:243–52. doi: 10.1111/cts.2011.4.issue-4

20. Livak KJ, Schmittgen TD. Analysis of relative gene expression data using real-time quantitative PCR and the 2(-Delta Delta C(T)) Method. *Methods*. (2001) 25:402–8. doi: 10.1006/meth.2001.1262

21. Naveilhan P, Hassani H, Canals JM, Ekstrand AJ, Larefalk A, Chhajlani V, et al. Normal feeding behavior, body weight and leptin response require the neuropeptide Y Y2 receptor. *Nat Med*. (1999) 5:1188–93. doi: 10.1038/13514

22. Neary NM, Small CJ, Druce MR, Park AJ, Ellis SM, Semjonous NM, et al. Peptide YY3-36 and glucagon-like peptide-17-36 inhibit food intake additively. *Endocrinology*. (2005) 146:5120–7. doi: 10.1210/en.2005-0237

23. Boland BB, Laker RC, O'Brien S, Sitaula S, Sermadiras I, Nielsen JC, et al. Peptide-YY(3-36)/glucagon-like peptide-1 combination treatment of obese diabetic mice improves insulin sensitivity associated with recovered pancreatic beta-cell function and synergistic activation of discrete hypothalamic and brainstem neuronal circuitries. *Mol Metab*. (2022) 55:101392. doi: 10.1016/j.molmet.2021.101392

24. Tatarkiewicz K, Sablan EJ, Polizzi CJ, Villescaz C, Parkes DG. Long-term metabolic benefits of exenatide in mice are mediated solely *via* the known glucagon-like peptide 1 receptor. *Am J Physiol Regul Integr Comp Physiol*. (2014) 306:R490–8. doi: 10.1152/ajpregu.00495.2013

25. Hayes MR, Skibicka KP, Grill HJ. Caudal brainstem processing is sufficient for behavioral, sympathetic, and parasympathetic responses driven by peripheral and hindbrain glucagon-like-peptide-1 receptor stimulation. *Endocrinology*. (2008) 149:4059–68. doi: 10.1210/en.2007-1743

26. Krieger JP, Santos da Conceicao EP, Sanchez-Watts G, Arnold M, Pettersen KG, Mohammed M, et al. Glucagon-like peptide-1 regulates brown adipose tissue thermogenesis *via* the gut-brain axis in rats. *Am J Physiol Regul Integr Comp Physiol*. (2018) 315:R708–20. doi: 10.1152/ajpregu.00068.2018

27. van Eyk HJ, Paiman EHM, Bizino MB, I.J. SL, Kleiburg F, Boers TGW, et al. Liraglutide decreases energy expenditure and does not affect the fat fraction of supraclavicular brown adipose tissue in patients with type 2 diabetes. *Nutr Metab Cardiovasc Dis*. (2020) 30:616–24. doi: 10.1016/j.numecd.2019.12.005

28. Gabery S, Salinas CG, Paulsen SJ, Ahnfelt-Ronne J, Alanentalo T, Baquero AF, et al. Semaglutide lowers body weight in rodents *via* distributed neural pathways. *JCI Insight*. (2020) 5:e133429. doi: 10.1172/jci.insight.133429

29. Blundell J, Finlayson G, Axelsen M, Flint A, Gibbons C, Kvist T, et al. Effects of once-weekly semaglutide on appetite, energy intake, control of eating, food preference and body weight in subjects with obesity. *Diabetes Obes Metab*. (2017) 19:1242–51. doi: 10.1111/dom.12932

30. Lee SJ, Sanchez-Watts G, Krieger JP, Pignalosa A, Norell PN, Cortella A, et al. Loss of dorsomedial hypothalamic GLP-1 signaling reduces BAT thermogenesis and increases adiposity. *Mol Metab*. (2018) 11:33–46. doi: 10.1016/j.molmet.2018.03.008

31. Lockie SH, Heppner KM, Chaudhary N, Chabenne JR, Morgan DA, Veyrat-Durebex C, et al. Direct control of brown adipose tissue thermogenesis by central nervous system glucagon-like peptide-1 receptor signaling. *Diabetes*. (2012) 61:2753–62. doi: 10.2337/db11-1556

32. Morrison SF, Madden CJ, Tupone D. Central neural regulation of brown adipose tissue thermogenesis and energy expenditure. *Cell Metab*. (2014) 19:741–56. doi: 10.1016/j.cmet.2014.02.007

33. Kataoka N, Hioki H, Kaneko T, Nakamura K. Psychological stress activates a dorsomedial hypothalamus-medullary raphe circuit driving brown adipose tissue thermogenesis and hyperthermia. *Cell Metab*. (2014) 20:346–58. doi: 10.1016/j.cmet.2014.05.018

34. Wei Q, Li L, Chen JA, Wang SH, Sun ZL. Exendin-4 improves thermogenic capacity by regulating fat metabolism on brown adipose tissue in mice with diet-induced obesity. *Ann Clin Lab Sci*. (2015) 45:158–65.

35. Oliveira FCB, Bauer EJ, Ribeiro CM, Pereira SA, Beserra BTS, Wajner SM, et al. Liraglutide activates type 2 deiodinase and enhances beta3-adrenergic-induced thermogenesis in mouse adipose tissue. *Front Endocrinol (Lausanne)*. (2021) 12:803363. doi: 10.3389/fendo.2021.803363

36. Mack CM, Moore CX, Jodka CM, Bhavsar S, Wilson JK, Hoyt JA, et al. Antiobesity action of peripheral exenatide (exendin-4) in rodents: effects on food intake, body weight, metabolic status and side-effect measures. *Int J Obes (Lond)*. (2006) 30:1332–40. doi: 10.1038/sj.ijo.0803284

37. Erreger K, Davis AR, Poe AM, Greig NH, Stanwood GD, Galli A. Exendin-4 decreases amphetamine-induced locomotor activity. *Physiol Behav*. (2012) 106:574–8. doi: 10.1016/j.physbeh.2012.03.014

38. Kotz CM, Perez-Leighton CE, Teske JA, Billington CJ. Spontaneous physical activity defends against obesity. *Curr Obes Rep*. (2017) 6:362–70. doi: 10.1007/s13679-017-0288-1

39. Periasamy M, Herrera JL, Reis FCG. Skeletal muscle thermogenesis and its role in whole body energy metabolism. *Diabetes Metab J*. (2017) 41:327–36. doi: 10.4093/dmj.2017.41.5.327

40. Yang Q, Tang W, Sun L, Yan Z, Tang C, Yuan Y, et al. Design of xenopus GLP-1-based long-acting dual GLP-1/Y(2) receptor agonists. *J Med Chem*. (2022) 65:14201–20. doi: 10.1021/acs.jmedchem.2c01385

41. Parthsarathy V, Hogg C, Flatt PR, O'Harte PM. Beneficial long-term antidiabetic actions of N- and C-terminally modified analogues of apelin-13 in diet-induced obese diabetic mice. *Diabetes Obes Metab*. (2018) 20:319–27. doi: 10.1111/dom.13068

42. Alves PL, Abdalla FMF, Alponti RF, Silveira PF. Anti-obesogenic and hypolipidemic effects of a glucagon-like peptide-1 receptor agonist derived from the saliva of the Gila monster. *Toxicon*. (2017) 135:1–11. doi: 10.1016/j.toxicon.2017.06.001

43. Heath ME, Neuropeptide Y. and Y1-receptor agonists increase blood flow through arteriovenous anastomoses in rat tail. *J Appl Physiol (1985)*. (1998) 85:301–9. doi: 10.1152/jappl.1998.85.1.301

44. Muller TD, Bluher M, Tschop MH, DiMarchi RD. Anti-obesity drug discovery: advances and challenges. *Nat Rev Drug Discov*. (2022) 21:201–23. doi: 10.1038/s41573-021-00337-8

frontiers | Frontiers in Endocrinology

TYPE Original Research
PUBLISHED 31 July 2024
DOI 10.3389/fendo.2024.1440070

OPEN ACCESS

EDITED BY
Yuko Maejima,
Fukushima Medical University, Japan

REVIEWED BY
Yoichi Ueta,
University of Occupational and Environmental Health Japan, Japan
Taka-aki Koshimizu,
Jichi Medical University, Japan

*CORRESPONDENCE
James E. Blevins
jeblevin@uw.edu

RECEIVED 28 May 2024
ACCEPTED 28 June 2024
PUBLISHED 31 July 2024

CITATION
Edwards MM, Nguyen HK, Dodson AD, Herbertson AJ, Wolden-Hanson T, Wietecha TA, Honeycutt MK, Slattery JD, O'Brien KD, Graham JL, Havel PJ, Mundinger TO, Sikkema CL, Peskind ER, Ryu V, Taborsky GJ Jr. and Blevins JE (2024) Sympathetic innervation of interscapular brown adipose tissue is not a predominant mediator of oxytocin-elicited reductions of body weight and adiposity in male diet-induced obese mice.
Front. Endocrinol. 15:1440070.
doi: 10.3389/fendo.2024.1440070

Sympathetic innervation of interscapular brown adipose tissue is not a predominant mediator of oxytocin-elicited reductions of body weight and adiposity in male diet-induced obese mice

Melise M. Edwards[1], Ha K. Nguyen[1], Andrew D. Dodson[1], Adam J. Herbertson[1], Tami Wolden-Hanson[1], Tomasz A. Wietecha[2,3], Mackenzie K. Honeycutt[1], Jared D. Slattery[1], Kevin D. O'Brien[2,3], James L. Graham[4], Peter J. Havel[4,5], Thomas O. Mundinger[6], Carl L. Sikkema[1,7], Elaine R. Peskind[1,7], Vitaly Ryu[8], Gerald J. Taborsky Jr.[1,6] and James E. Blevins[1,6]*

[1]VA Puget Sound Health Care System, Office of Research and Development Medical Research Service, Department of Veterans Affairs Medical Center, Seattle, WA, United States, [2]Division of Cardiology, Department of Medicine, University of Washington School of Medicine, Seattle, WA, United States, [3]UW Medicine Diabetes Institute, University of Washington School of Medicine, Seattle, WA, United States, [4]Department of Nutrition, University of California, Davis, Davis, CA, United States, [5]Department of Molecular Biosciences, School of Veterinary Medicine, University of California, Davis, Davis, CA, United States, [6]Division of Metabolism, Endocrinology and Nutrition, Department of Medicine, University of Washington School of Medicine, Seattle, WA, United States, [7]Department of Psychiatry and Behavioral Sciences, University of Washington School of Medicine, Seattle, WA, United States, [8]Department of Medicine and Pharmacological Sciences, Icahn School of Medicine at Mount Sinai, New York, NY, United States

Previous studies indicate that CNS administration of oxytocin (OT) reduces body weight in high fat diet-induced obese (DIO) rodents by reducing food intake and increasing energy expenditure (EE). We recently demonstrated that hindbrain (fourth ventricular [4V]) administration of OT elicits weight loss and elevates interscapular brown adipose tissue temperature (T_{IBAT}, a surrogate measure of increased EE) in DIO mice. What remains unclear is whether OT-elicited weight loss requires increased sympathetic nervous system (SNS) outflow to IBAT. We hypothesized that OT-induced stimulation of SNS outflow to IBAT contributes to its ability to activate BAT and elicit weight loss in DIO mice. To test this hypothesis, we determined the effect of disrupting SNS activation of IBAT on the ability of 4V OT administration to increase T_{IBAT} and elicit weight loss in DIO mice. We first determined whether bilateral surgical SNS denervation to IBAT was successful as noted by ≥ 60% reduction in IBAT norepinephrine (NE) content in DIO mice. NE content was selectively reduced in IBAT at 1-, 6- and 7-weeks post-denervation by 95.9 ± 2.0, 77.4 ± 12.7 and 93.6 ± 4.6% ($P<0.05$), respectively and was unchanged in inguinal white adipose tissue, pancreas or liver. We subsequently measured the effects of acute 4V OT (1, 5 µg ≈ 0.99, 4.96 nmol)

10.3389/fendo.2024.1440070

on T_{IBAT} in DIO mice following sham or bilateral surgical SNS denervation to IBAT. We found that the high dose of 4V OT (5 μg ≈ 4.96 nmol) elevated T_{IBAT} similarly in sham mice as in denervated mice. We subsequently measured the effects of chronic 4V OT (16 nmol/day over 29 days) or vehicle infusions on body weight, adiposity and food intake in DIO mice following sham or bilateral surgical denervation of IBAT. Chronic 4V OT reduced body weight by 5.7 ± 2.23% and 6.6 ± 1.4% in sham and denervated mice ($P<0.05$), respectively, and this effect was similar between groups (P=NS). OT produced corresponding reductions in whole body fat mass ($P<0.05$). Together, these findings support the hypothesis that sympathetic innervation of IBAT is not necessary for OT-elicited increases in BAT thermogenesis and reductions of body weight and adiposity in male DIO mice.

KEYWORDS

obesity, brown adipose tissue (BAT), white adipose tissue (WAT), oxytocin, food intake

Introduction

While the hypothalamic neuropeptide, oxytocin (OT), has a more clearly established role in the control of reproductive behavior (1) and prosocial behavior (2, 3), it has also been recognized as having an important role in the control of food intake and body weight (4–7). Although OT reduces body weight in part by decreasing energy intake, pair-feeding studies indicate that OT-elicited reductions of weight gain or weight loss cannot be fully explained by its ability to decrease energy intake (8–10). In these studies, pair-feeding appears to account for approximately 50% of the reduction of weight gain and/or weight loss observed with OT treatment (8–10)

Indeed, recent studies have shown that OT increases energy expenditure (EE) (11–14). While brown adipose tissue thermogenesis (BAT) is important in the control of EE [for review see (15, 16)], it is unclear whether OT's effects on EE result primarily from 1) activation of non-shivering BAT thermogenesis, 2) spontaneous physical activity-induced thermogenesis (17), 3) shivering and non-shivering thermogenesis in skeletal muscle (18), or 4) endocrine factors [e.g. thyroid hormone, fibroblast growth factor-21, irisin (for review see (19, 20))]. We have found that acute third (3V) and fourth ventricular (4V) injections of OT increase interscapular BAT temperature (T_{IBAT}), a functional readout of BAT thermogenesis in mice and rats (21, 22). Furthermore, the effects of chronic CNS administration of OT on T_{IBAT} coincide with OT-elicited weight loss in diet-induced obese (DIO) rats (21). Sutton and colleagues demonstrated that use of designer drugs (DREADDs) technology to chemogenetically activate hypothalamic paraventricular nucleus (PVN) OT neurons increases both EE and tends to increase subcutaneous BAT temperature (P=0.13) in *Oxytocin-Ires-Cre* mice (23). Furthermore, Yuan et al. recently reported that peripheral administration of OT promotes BAT differentiation *in vitro* and the expression of genes involved in thermogenesis in IBAT in high fat diet-fed mice (24). On the other hand, reduced OT signaling is associated with obesity (14, 25–27), reductions of EE (13, 14, 27, 28) and deficits in BAT thermogenesis (28–31) in mice. Collectively, these findings support a role for increased BAT thermogenesis in OT-elicited weight loss in mice. What remains unclear is whether OT-elicited weight loss requires increased sympathetic nervous system (SNS) outflow to IBAT and whether this effect involves hindbrain OT receptors (OTRs). Here, we sought to clarify the role of SNS outflow to IBAT in mediating the effects of hindbrain OTR stimulation on both weight loss and BAT thermogenesis.

We hypothesized that OT-induced stimulation of SNS outflow to IBAT contributes to its ability to stimulate non-shivering BAT thermogenesis and elicit weight loss in DIO mice. We first confirmed the success of the IBAT denervation procedure by measuring IBAT norepinephrine (NE) content at 1-week post-denervation in lean mice. We subsequently determined if these effects can be translated to DIO mice at 1, 6 and 7-weeks post-sham/denervation. To assess the role of SNS innervation of BAT in contributing to OT-elicited increases in non-shivering thermogenesis in IBAT (as surrogate measure of energy expenditure), we examined the effects of acute 4V OT (1, 5 μg) on T_{IBAT} in DIO mice following bilateral surgical SNS denervation to IBAT. We next determined if SNS innervation to IBAT contributes to OT-induced weight loss by measuring the effect of bilateral surgical or sham denervation of IBAT on the ability of chronic 4V OT (16 nmol/day over 29 days) or vehicle administration to reduce body weight and adiposity. We subsequently determined if these effects were associated with a reduction of adipocyte size and energy intake.

Methods

Animals

Adult male C57BL/6J mice were initially obtained from Jackson Laboratory [strain # 000664 (lean) or 380050 (DIO); Bar Harbor, ME] after having been maintained on a chow diet (~16 weeks; 25-35 grams upon arrival) or the high fat diet (HFD) for 4 months starting at 6 weeks of age (~22 weeks; 40-50 grams upon arrival). The chow diet provided 16% kcal from fat (~0.62% sucrose) (5LG4; LabDiet®, St. Louis, MO). The HFD provided 60% kcal from fat (~ 6.8% kcal from sucrose and 8.9% of the diet from sucrose) (Research Diets, Inc., D12492i, New Brunswick, NJ). All animals were housed individually in Plexiglas cages in a temperature-controlled room (22 ± 2°C) under a 12:12-h light-dark cycle. All mice were maintained on a 6 a.m./6 p.m. light cycle. Mice had *ad libitum* access to water and HFD. The research protocols were approved both by the Institutional Animal Care and Use Committee of the Veterans Affairs Puget Sound Health Care System (VAPSHCS) and the University of Washington in accordance with NIH Guidelines for the Care and Use of Animals.

Drug preparation

Fresh solutions of OT acetate salt were prepared the day of each experiment (Study 5). Fresh solutions of OT acetate salt (Bachem Americas, Inc., Torrance, CA) were solubilized in sterile water, loaded into Alzet® minipumps (model 2004; DURECT Corporation, Cupertino, CA) and subsequently primed in sterile 0.9% saline at 37° C for approximately 40 hours prior to minipump implantation based on manufacturer's recommended instructions (Study 6-7). The beta 3 adrenergic receptor (β3-AR) agonist, CL 316243 (Tocris/Bio-Techne Corporation, Minneapolis, MN), was solubilized in sterile water each day of each experiment (Study 4).

SNS denervation procedure

A dissecting microscope (Leica M60/M80; Leica Microsystems, Buffalo Grove, IL) was used throughout the procedure. A 1" midline incision was made in the skin dorsally at the level of the thorax and continued rostrally to the base of the skull. Connective tissue was blunt dissected away from the adipose tissue with care to avoid cutting the large thoracodorsal artery that is located medially to both pads. Both left and right fat pads were separated from the mid line. Each fat pad was lifted up and the intercostal nerve bundles were located below. Once the nerves were located, a sharp point forceps was used to pull the nerve bundles straight up while using a 45 degree scissors to cut and remove 3-5 mm of nerves. The interscapular incision was closed with 4-0 non-absorbable monofilament Ethilon (nylon) sutures or with standard metal wound clips. Nerves were similarly identified but not cut for sham operated animals. Mice were treated pre-operatively with the analgesic ketoprofen (2 mg/kg; Fort Dodge Animal Health) prior to the completion of the denervation or sham procedure. This procedure was combined with transponder implantations for studies that involved IBAT temperature measurements in response to acute 4V injections (Study 5). Animals were allowed to recover for approximately 5-7 days prior to implantation of 4V cannulas. Note that surgical denervation was used in place of chemical denervation because chemical denervation can result in SNS terminal recovery within IBAT (32, 33) within only 10 days post-chemical denervation (32).

4V cannulations for acute injections

Animals were implanted with a cannula (P1 Technologies, Roanoke, VA) that was directed towards the 4V as previously described (22). Briefly, mice under isoflurane anesthesia were placed in a stereotaxic apparatus with the incisor bar positioned 4.5 mm below the interaural line. A 26-gauge cannula (P1 Technologies) was stereotaxically positioned into the 4V (5.9 mm caudal to bregma; 0.4 mm lateral to the midline, and 2.7 mm ventral to the skull surface) and secured to the surface of the skull with dental cement and stainless-steel screws.

4V cannulations for chronic infusions

Mice were implanted with a cannula within the 4V with a side port that was connected to an osmotic minipump (model 2004, DURECT Corporation) as previously described (22). Mice under isoflurane anesthesia were placed in a stereotaxic apparatus with the incisor bar positioned 4.5 mm below the interaural line. A 30-gauge cannula (P1 Technologies) was stereotaxically positioned into the 4V (5.9 mm caudal to bregma; 0.4 mm lateral to the midline, and 3.7 mm ventral to the skull surface) and secured to the surface of the skull with dental cement and stainless steel screws. A 1.2" piece of plastic Tygon™ Microbore Tubing (0.020" x 0.060"OD; Cole-Parmer) was tunneled subcutaneously along the midline of the back and connected to the 21-gauge sidearm osmotic minipump-cannula assembly. A stainless steel 22-gauge pin plug (Instech Laboratories, Inc.) was temporarily inserted at the end of the tubing during a two week postoperative recovery period, after which it was replaced by an osmotic minipump (DURECT Corporation) containing saline or OT. Mice were treated with the analgesic ketoprofen (5 mg/kg; Fort Dodge Animal Health) and the antibiotic enrofloxacin (5 mg/kg; Bayer Healthcare LLC., Animal Health Division Shawnee Mission, KS) at the completion of the 4V cannulations and were allowed to recover at least 10 days prior to implantation of osmotic minipumps.

Implantation of temperature transponders underneath IBAT

Animals were anesthetized with isoflurane and had the dorsal surface along the upper midline of the back shaved. The area was subsequently scrubbed with 70% ethanol followed by betadine swabs to sterilize/clean the area before a one-inch incision was

made at the midline of the interscapular area. The temperature transponder (14 mm long/2 mm wide) (HTEC IPTT-300; BIO MEDIC DATA SYSTEMS, INC, Seaford, DE) was implanted underneath both IBAT pads as previously described (22) and secured in place by suturing it to the brown fat pad with sterile silk suture. HTEC IPTT-300 transponders were used in place of IPTT-300 transponders to enhance accuracy in our measurements. The IPTT-300 transponders are specified to be accurate to ± 0.4°C between 35°C and 39°C (± 1.0°C between 32°C and 42°C) while the HTEC IPTT-300 transponders are accurate to ± 0.2°C between 32°C and 42°C (personal communication with Geoff Hunt from BIO MEDIC DATA SYSTEMS). The interscapular incision was closed with Nylon sutures (5-0), which were removed in awake animals 10-14 days after surgery.

Acute 4V injections and measurements of T_{IBAT}

OT (or saline vehicle; 1 µL injection volume) was administered into the 4V immediately prior to the start of the dark cycle following 4 hours of food deprivation. Animals remained without access to food for an additional 4 h during the T_{IBAT} measurements to prevent the confounding effects of diet-induced thermogenesis on T_{IBAT}. A handheld reader (DAS-8007-IUS Reader System; BIO MEDIC DATA SYSTEMS, INC) was used to collect measurements of T_{IBAT}. The 4V injections were administered at 1 µL/min using an injection pump (Harvard Apparatus Pump II Elite; Harvard Apparatus, Holliston, MA) via a 33-gauge injector (P1 Technologies) connected by polyethylene 20 tubing to a 10-µL Hamilton syringe. Mice underwent all treatments (unless otherwise noted) in a randomized order separated by at least 48 hours between treatments.

Body composition

Determinations of lean body mass and fat mass were made on un-anesthetized mice by quantitative magnetic resonance using an EchoMRI 4-in-1-700™ instrument (Echo Medical Systems, Houston, TX) at the VAPSHCS Rodent Metabolic Phenotyping Core. Measurements were taken prior to 4V cannulations and minipump implantations as well as at the end of the infusion period.

Tissue collection for NE content measurements

Mice were euthanized by rapid conscious decapitation at 1-week (Studies 1-3), 6-weeks (Study 2), 7-weeks (Study 2, Study 6), 9-weeks (Study 4) or 10-11 weeks (Study 5) post-sham or denervation procedure. Trunk blood and tissues (IBAT, EWAT, IWAT, liver or pancreas) were collected from 4-h fasted mice. Tissue was rapidly removed, wrapped in foil and frozen in liquid N2. Samples were stored frozen at -80°C until analysis. Note that anesthesia was not used when collecting tissue for NE content as it can cause the release of NE from SNS terminals within the tissue (33). Thus, animals were euthanized by rapid conscious decapitation.

Norepinephrine content measurements (biochemical confirmation of IBAT denervation procedure)

NE content was measured in IBAT, EWAT, IWAT, liver and/or pancreas using previously established techniques (34). Successful denervation was noted by ≥ 60% reduction in IBAT NE content as previously noted (35). Experimental animals that did not meet this criterion were excluded from the data analysis.

Study protocols

Study 1A: determine the success of the surgical denervation procedure at 1-week post-sham or denervation in lean mice by measuring NE content

Mice underwent sham or bilateral surgical SNS denervation procedures and, to prevent the confounder of anesthesia on NE content, animals were euthanized by rapid conscious decapitation at 1-week post-sham or denervation procedure.

Study 1B: determine the success of the surgical denervation procedure at 10-12 weeks post-sham or denervation in lean mice by measuring thermogenic gene expression

Mice underwent sham or bilateral surgical SNS denervation procedures and were euthanized by rapid conscious decapitation at 1-week post-sham or denervation procedure.

Study 2: determine the success of the surgical denervation procedure at 1-, 6- and 7-weeks post-sham or denervation in DIO mice by measuring NE content

Mice were fed *ad libitum* and maintained on HFD for approximately 4.25 months prior to underdoing sham or SNS denervation procedures. In addition to weekly body weight measurements, body composition measurements were obtained at baseline and at 6 and 7-weeks post-denervation/sham procedures. Mice were euthanized by rapid conscious decapitation 1-, 6- and 7-weeks post-sham or denervation procedure.

Study 3: determine if SNS innervation of IBAT is reduced in age-matched obese mice relative to lean mice by measuring NE content

Chow-fed and HFD-fed mice were age-matched (~22 weeks; 30-35 grams or 40-50 grams upon arrival). Age-matched chow-fed and DIO mice were fed *ad libitum* and maintained on chow or HFD for 4.5 months and matched for both body weight and adiposity prior to undergoing sham (N=5/diet) or SNS denervation (N=5/diet) procedures. Mice were euthanized by rapid conscious decapitation at 1-week post-sham or denervation procedure.

Study 4: determine if surgical denervation of IBAT compromises the ability of the β3-AR agonist, CL 316243, to increase T_{IBAT} in DIO mice

Mice were fed *ad libitum* and maintained on HFD for 4.5 months prior to underdoing sham or SNS denervation procedures and implantation of temperature transponders underneath the left IBAT depot. Mice were allowed to recover for at least 1 week during which time they were adapted to a daily 4-h fast, handling and mock injections. On an experimental day, 4-h fasted mice received CL 316243 (0.1 or 1 mg/kg; IP) or vehicle (sterile water; 1.5 mL/kg injection volume) during the early part of the light cycle in order to maximize the effects of CL 316243 during a time when circulating NE levels (36) and IBAT catecholamine levels are lower (37). Injections were completed in a crossover design at 7-day intervals such that each animal served as its own control (approximately 4-6 weeks post-sham or denervation procedures). T_{IBAT} was measured at baseline (-2 h; 8:00 a.m.), immediately prior to IP injections (0 h; 9:45-10:00 a.m.), and at 0.25, 0.5, 0.75, 1, 1.25, 1.5, 2, 3, 4, and 24-h post-injection (9:45-10:00 a.m.). Food intake and body weight were measured daily. This dose range was based on doses of CL 316243 found to be effective at reducing food intake and weight gain in rats (22, 38) (IP) and stimulating IBAT temperature in rats (22, 39) (IV, IP) and mice (IV) (40). Animals were euthanized by rapid conscious decapitation at 9-weeks post-sham or denervation procedure. Similar studies were also performed in lean mice (data not shown).

Likewise, we also examined the effects of systemic administration of the transient receptor potential channel melastatin family member 8 (TRPM8) agonist, icilin, which, may activate IBAT through a direct (41) or indirect mechanism (42) (data not shown). In addition, the effects of the sympathomimetic, tyramine, was also examined on T_{IBAT} in DIO mice with intact or impaired SNS innervation of IBAT (Supplementary Study 1).

Study 5: determine the extent to which 4V OT-induced activation of sympathetic outflow to IBAT contributes to its ability to increase T_{IBAT} in DIO mice

Mice were fed *ad libitum* and maintained on HFD for 4.25 months prior to undergoing sham or SNS denervation procedures and implantation of temperature transponders underneath the left IBAT depot. Mice were subsequently implanted 1 week later with 4V cannulas. Mice were allowed to recover for at least 2 weeks during which time they were adapted to a daily 4-h fast, handling and mock injections. On an experimental day, 4-h fasted mice received OT (1 or 5 μg/μl) or vehicle during the early part of the light cycle in order to maximize the effects of OT (14, 22) during a time when circulating NE levels (36) and IBAT catecholamine levels are lower (37). Injections were completed in a crossover design at approximately 48-h intervals such that each animal served as its own control (approximately 7-8 weeks post-sham or denervation procedures). T_{IBAT} was measured at baseline (-2 h; 9:00 a.m.), immediately prior to 4V injections (0 h; 9:45-10:00 a.m.), and at 0.25, 0.5, 0.75, 1, 1.25, 1.5, 2, 3, 4, and 24-h post-injection (10:00 a.m.). Food intake and body weight were measured daily. This dose range was based on doses of 4V OT found to be effective at stimulating T_{IBAT} in DIO mice in previous studies (22). Mice were euthanized by rapid conscious decapitation at 10-11 weeks post-sham or denervation procedure.

Similar studies were also performed in lean mice (Supplementary Study 2). In addition, we examined the effectiveness of a systemic dose to recapitulate the effects of a 4V dose to increase T_{IBAT} in lean mice (Supplementary Study 3). We next determined if the melanocortin 3/4 receptor (MC3/4R) agonist, melanotan II (MTII), which, along with the endogenous MC3/4R agonist, alpha-MSH, activate PVN OT neurons (43, 44) and act, in part, through OT signaling (43, 45), could recapitulate the effects of systemic OT on T_{IBAT} in lean mice with intact or impaired SNS innervation of IBAT (data not shown).

Study 6A: determine the extent to which OT-induced activation of sympathetic outflow to IBAT contributes to its ability to elicit weight loss in DIO mice

Mice were fed *ad libitum* and maintained on HFD for 4.25-4.5 months prior to prior to undergoing sham or SNS denervation procedures and implantation of temperature transponders underneath the left IBAT depot. Mice subsequently received 4V cannulas and minipumps to infuse vehicle or OT (16 nmol/day) over 28 days as previously described (22). This dose was selected based on a dose of 4V OT found to be effective at reducing body weight in DIO mice (22). Daily food intake and body weight were also tracked for 28 days. Animals were euthanized by rapid conscious decapitation at 7 weeks post-sham or denervation procedure.

Study 6B: determine the extent to which OT-induced activation of sympathetic outflow to IBAT impacts thermogenic gene expression in IBAT, IWAT, and EWAT in DIO mice

Mice from Study 6A were used for these studies. All mice were euthanized by rapid conscious decapitation following a 4-h fast at 2-h post-injection.

Study 7: determine the extent to which systemic (subcutaneous) infusion of a centrally effective dose of OT (16 nmol/day) elicits weight loss in DIO mice

Mice were fed *ad libitum* and maintained on HFD for 4-4.25 months prior to prior to being implanted with a temperature transponder underneath the left IBAT depot. Mice were subsequently maintained on a daily 4-h fast and received minipumps to infuse vehicle or OT (16 nmol/day) over 28 days (22). This dose was selected based on a dose of 4V OT found to be effective at reducing body weight in DIO mice (22). Daily food intake and body weight were also tracked for 28 days. Mice were euthanized with intraperitoneal injections of ketamine cocktail [ketamine hydrochloride (390 mg/kg), xylazine (26.4mg/kg) in an injection volume up to 1 mL/mouse] prior to collection of blood (cardiac stick) and tissues (IBAT, EWAT, IWAT, gastrocnemius and brain). Tissue was otherwise treated identically to Studies 1-4 or processed for subsequent measurements of adipocyte size and UCP-1 (see below).

Blood collection

Blood samples [trunk blood (Study 3-6) or cardiac stick (Study 7)] were collected from 4-h (Study 2-7) or 6-h (Study 1B) fasted mice within a 2-h window towards the beginning of the light cycle (10:00 a.m.-12:00 p.m.) as previously described in DIO CD ® IGS and Long-Evans rats and C57BL/6J mice (21, 22, 46). Treatment groups were counterbalanced at time of euthanasia to avoid time of day bias. Blood samples [up to 1 mL] were collected by trunk blood or cardiac stick in chilled K2 EDTA Microtainer Tubes (Becton-Dickinson, Franklin Lakes, NJ). Whole blood was centrifuged at 6,000 rpm for 1.5-min at 4°C; plasma was removed, aliquoted and stored at −80°C for subsequent analysis.

Plasma hormone measurements

Plasma leptin and insulin were measured using electrochemiluminescence detection [Meso Scale Discovery (MSD®), Rockville, MD] using established procedures (21, 47). Intra-assay coefficient of variation (CV) for leptin was 4.2% and 1.9% for insulin. The range of detectability for the leptin assay is 0.137-100 ng/mL and 0.069-50 ng/mL for insulin. Plasma fibroblast growth factor-21 (FGF-21) (R&D Systems, Minneapolis, MN) and irisin (AdipoGen, San Diego, CA) levels were determined by ELISA. The intra-assay CV for FGF-21 and irisin were 2.3% and 9.3%, respectively; the ranges of detectability were 31.3-2000 pg/mL (FGF-21) and 0.078-5 µg/mL (irisin). Plasma adiponectin was determined by ELISA [Millipore Sigma (Burlington, MA)]. Intra-assay CV for adiponectin was 4.2%. The range of detectability for the adiponectin assay is 2.8-178 ng/mL. The data were normalized to historical values using a pooled plasma quality control sample that was assayed in each plate.

Blood glucose and lipid measurements

Blood was collected for glucose measurements by tail vein nick in 4-h fasted mice and measured with a glucometer using the AlphaTRAK 2 blood glucose monitoring system (Abbott Laboratories, Abbott Park, IL) (21, 48). Total cholesterol (TC) [Fisher Diagnostics (Middletown, VA)], free fatty acids (FFAs) [Wako Chemicals USA, Inc., Richmond, VA)] and free glycerol (FG) (Millipore Sigma) were measured using an enzymatic-based kits. Intra-assay CVs for TC, FFAs and FG were 1.5, 2.9, and 2.2%, respectively. These assay procedures have been validated for rodents (49).

Adipose tissue processing for adipocyte size

Adipose tissue depots were collected at the end of the infusion period from a subset of DIO mice from Study 6 (IBAT, IWAT, EWAT) and Study 7 (EWAT and IWAT). IBAT, IWAT, and EWAT depots were dissected and placed in 4% paraformaldehyde-PBS for 24 h and then placed in 70% ethanol (EtOH) prior to paraffin embedding. Sections (5 µm) sampled were obtained using a rotary microtome, slide-mounted using a floatation water bath (37°C), and baked for 30 min at 60°C to give approximately 15-16 slides/fat depot with two sections/slide.

Adipocyte size analysis

Adipocyte size analysis was performed on deparaffinized and digitized IWAT and EWAT sections. The average cell area from two randomized photomicrographs was determined using the built-in particle counting method of ImageJ software (National Institutes of Health, Bethesda, MD). Fixed (4% PFA), paraffin-embedded adipose tissue was sectioned. Slides were visualized using bright field on an Olympus BX51 microscope (Olympus Corporation of the Americas; Center Valley, PA) and photographed using a Canon EOS 5D SR DSLR (Canon U.S.A., Inc., Melville, NY) camera at 100X magnification. Values for each tissue within a treatment were averaged to obtain the mean of the treatment group.

Tissue collection for NE content measurements

Mice were euthanized by rapid conscious decapitation at 1-week (Studies 1-3), 6-weeks (Study 2), 7-weeks (Study 2, Study 6), 9-weeks (Study 4) or 10-11 weeks (Study 5) post-sham or denervation procedure. Trunk blood and tissues (IBAT, EWAT, IWAT, liver or pancreas) were collected from 4-h (Study 2-7) or 6-h (Study 1B) fasted mice. Tissue was rapidly removed, wrapped in foil and frozen in liquid N2. Samples were stored frozen at -80°C until analysis. Note that anesthesia was not used when collecting tissue for NE content as it can cause the release of NE from SNS terminals within the tissue (33).

Tissue collection for quantitative real-time PCR

Tissue (IBAT, IWAT and EWAT) was collected from a subset of 4-h (Study 2-7) or 6-h (Study 1B) fasted mice in Study 4-7. In addition, mice from Study 7 were euthanized with an overdose of ketamine cocktail prior to tissue collection. IBAT, IWAT, EWAT, gastrocnemius and brains were collected within a 2-h window towards the start of the light cycle (10:00 a.m.-12:00 p.m.) as previously described in DIO CD ® IGS/Long-Evans rats and C57BL/6J mice (21, 22, 46). Tissue was rapidly removed, wrapped in foil and frozen in liquid N2. Samples were stored frozen at -80°C until analysis.

qPCR

RNA extracted from samples of IBAT and IWAT (Studies 4-7) were analyzed using the RNeasy Lipid Mini Kit (Qiagen Sciences Inc, Germantown, MD) followed by reverse transcription into

cDNA using a high-capacity cDNA archive kit (Applied Biosystems, Foster City, CA). Quantitative analysis for relative levels of mRNA in the RNA extracts was measured in duplicate by qPCR on an Applied Biosystems 7500 Real-Time PCR system (Thermo Fisher Scientific, Waltham, MA) and normalized to the cycle threshold value of Nono mRNA in each sample. The TaqMan® probes used in the study were Thermo Fisher Scientific Gene Expression Assay probes. The probe for mouse Nono (Mm00834875_g1), UCP-1 (catalog no. Mm01244861_m1), UCP-2 (catalog no. Mm00627599_m1), UCP-3 (catalog no. Mm01163394_m1), β1-AR (Adrb1; catalog no. Mm00431701_s1), β2-AR (Adrb2; catalog no. Mm02524224_s1), β3-AR (Adrb3; catalog no. Mm02601819_g1), alpha-2 adrenergic receptor (Adra2a; catalog no. Mm07295458_s1),type 2 deiodinase (D2) (Dio2; catalog no. Mm00515664_m1), cytochrome c oxidase subunit 8b (Cox8b; catalog no. Mm00432648_m1), G-protein coupled receptor 120 (Gpr120; catalog no. Mm00725193_m1), bone morphogenetic protein 8b (bmp8b; catalog no. Mm00432115_g1), cell death-inducing DNA fragmentation factor alpha-like effector A (Cidea; catalog no. Mm00432554_m1), peroxisome proliferator-activated receptor gamma coactivator 1 alpha (Ppargc1a; catalog no. Mm01208835_m1) were acquired from Thermo Fisher Scientific. Relative amounts of target mRNA were determined using the Comparative C_T or $2^{-\Delta\Delta CT}$ method (50) following adjustment for the housekeeping gene, Nono.

Transponder placement

All temperature transponders were confirmed to have remained underneath the IBAT depot at the conclusion of the study.

Statistical analyses

All results are expressed as means ± SE. Comparisons between multiple groups involving between subjects design were made using one-way ANOVA as appropriate, followed by a *post-hoc* Fisher's least significant difference test. Comparisons involving within-subjects designs were made using a one-way repeated-measures ANOVA followed by a *post-hoc* Fisher's least significant difference test. Analyses were performed using the statistical program SYSTAT (Systat Software, Point Richmond, CA). Differences were considered significant at $P<0.05$, 2-tailed.

Results

Study 1A: determine the success of the surgical denervation procedure at 1-week post-sham or denervation in lean mice

The goal of this study was to verify the success of the SNS denervation of IBAT procedure in lean mice by confirming a reduction of NE content that was specific to IBAT relative to other tissues (IWAT and liver). By design, mice were lean as determined by body weight (25.4 ± 0.3 g). There was no difference in body weight between sham and denervation groups prior to surgery (sham: 25.8 ± 0.3 g vs denervation: 25.1 ± 0.5 g) [($F(1,8) = 1.923$, $P=0.203$)] or at 1-week post-surgery (sham: 26.3 ± 0.4 g vs denervation: 26.1 ± 0.7 g) [($F(1,8) = 0.021$, $P=0.888$)].

IBAT NE content was reduced by 99.6 ± 0.2% at 1-week post-denervation [($F(1,8) = 12.358$, $P=0.008$)] (Figure 1) relative to IBAT from sham operated mice. In contrast, NE content was unchanged in IWAT or liver in denervated mice relative to sham mice (P=NS). We also repeated this study in a separate group of lean mice and found a similar reduction of IBAT NE content (99.2 ± 0.4%) at 1-week post-denervation relative to sham operated mice [($F(1,8) = 73.438$, $P=0.000$)].

Study 1B: verify the success of the surgical denervation procedure at 10-12 weeks after IBAT surgical denervation or sham denervation in lean mice by measuring thermogenic gene expression

The goal of this study was to determine the 1) verify the success of the SNS denervation of IBAT procedure in lean mice using a separate biochemical marker (IBAT thermogenic gene expression) and 2) confirm that these changes would persist for extended periods of time out to 10-12 weeks. There was no difference in body weight between sham and denervation groups prior to surgery (sham: 43.8 ± 1.3 g vs denervation: 43.0 ± 0.98 g) [($F(1,17) = 0.238$, $P=0.632$)] or at 10-12 weeks post-surgery (sham: 50.5 ± 2.0 g vs denervation: 49.3 ± 1.1 g) [($F(1,17) = 0.292$, $P=0.596$)].

IBAT NE content was reduced in denervated mice by 96.1 ± 3.3% at 10-12 weeks after IBAT surgical denervation relative to sham-operated control mice [($F(1,2) = 87.393$, $P=0.011$). Only a subset of samples (N=4 out of 20) were able to be screened for NE content but all tissue samples were included in the IBAT (N=20 out of 20), IWAT (N=9 out of 20) and EWAT (N=9 out of 20) gene expression analysis.

IBAT

There was a reduction of 9 out of the 13 measured mRNA levels of genes from IBAT of denervated mice relative to IBAT from sham operated mice ($P<0.05$; Table 1A).There were significant reductions of IBAT UCP-1 [($F(1,7) = 38.1$, $P<0.001$)], Dio2 [($F(1,7) = 12.669$, $P=0.009$)], Gpr120 [($F(1,7) = 65.965$, $P<0.001$)], Adrb3 [($F(1,7) = 65.916$, $P<0.001$)], Adrb1 [($F(1,7) = 8.015$, $P=0.025$)], Acox1 [($F(1,7) = 58.261$, $P<0.001$)], bmp8b [($F(1,7) = 19.636$, $P=0.003$)], cox8b [($F(1,6) = 16.403$, $P=0.007$)] and UCP-3 mRNA expression [($F(1,7) = 57.665$, $P<0.001$)]. There were no significant differences in IBAT CIDEA, PPARGC1, PPARA and PRDM16 mRNA expression between sham and denervation groups (P=NS).

The findings pertaining to IBAT UCP-1 gene expression in surgically denervated mice is consistent with what others have reported with IBAT UCP-1 protein expression from hamsters

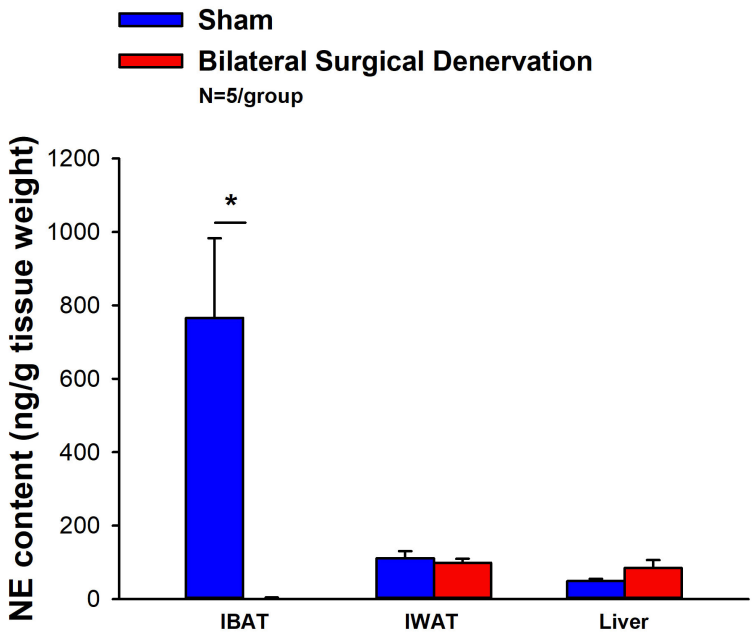

FIGURE 1
Effect of IBAT surgical denervation procedure on IBAT NE content at 1-week post-sham or IBAT denervation in lean mice. Mice were maintained on chow for approximately 2.5 months prior to undergoing a sham (N=5/group) or bilateral surgical IBAT denervation (N=5/group) procedures and were euthanized at 1-week post-sham or denervation procedure. NE content was measured from IBAT, IWAT and liver. Data are expressed as mean ± SEM. *P<0.05 denervation vs sham.

(51) and mice (52) following chemical (6-OHDA)-induced denervation of IBAT relative to control animals. Similarly, there was a reduction of IBAT UCP-1 mRNA following unilateral or bilateral surgical denervation in hamsters (53) and mice (54, 55), respectively. Similar to our findings, others also found a reduction of IBAT Dio2 and Adrb3 following bilateral surgical denervation in mice (54).

IWAT

IWAT UCP-1 [(F(1,2) = 11.131, P=0.079)] tended to be elevated in denervated mice relative to sham operated mice (Table 1B). There were no significant differences in the mRNAs of any of the other thermogenic markers (P=NS; Table 1B).

EWAT

There tended to be a reduction of UCP-1 in denervated mice compared to sham operated mice [(F(1,2) = 7.000, P=0.118)] (Table 1C). There were no significant differences in the mRNA levels of any of the other thermogenic genes (P=NS; Table 1C).

Study 2: determine the success of the surgical denervation procedure at 1, 6 and 7-weeks post-sham or denervation in DIO mice

The goal of this study was to 1) verify the success of the SNS denervation procedure in DIO mice by confirming a reduction of NE content that was specific to IBAT relative to other tissues (IWAT, liver and pancreas) and 2) confirm that these changes would persist for 7 weeks. By design, DIO mice were obese as determined by both body weight (45.1 ± 1.1 g) and adiposity (14.9 ± 0.8 g fat mass; 32.9 ± 1.3% adiposity) after maintenance on the HFD for approximately 4.5 months prior to sham/denervation procedures. Sham and denervation groups were matched for body weight, fat mass and lean mass such that there were no differences in baseline body weight, lean mass or fat mass between groups prior to surgery (data not shown; P=NS).

IBAT NE content was reduced by 95.9 ± 2.0, 77.4 ± 12.7 and 93.6 ± 4.6% at 1- [(F(1,8) = 19.636, P=0.002)], 6- [(F(1,8) = 20.532, P=0.002)] and 7-weeks [(F(1,8) = 34.586, P<0.0001)] post-denervation (Figure 2) relative to IBAT from sham operated mice. In contrast, NE content was unchanged in IWAT, liver or pancreas in denervated mice relative to sham mice (P=NS).

There were no significant differences in baseline body weights [(F(5,24) = 0.322, P=NS), fat mass [(F(5,24) = 0.106, P=NS), or lean mass [(F(5,24) = 0.304, P=NS) between sham and denervation groups. In addition, there were also no significant differences in body weights between sham and denervation groups at 1- [(F(1,8) = 0.353, P=NS), 6- [(F(1,8) = 1.230, P=NS) and 7-weeks [(F(1,8) = 0.109, P=NS) post-surgeries. In addition, there were also no significant differences in fat mass at 1- [(F(1,8) = 0.353, P=NS), 6- [(F(1,8) = 1.230, P=NS) and 7-weeks [(F(1,8) = 0.109, P=NS) post-denervation relative to sham operated mice. Similarly, no differences were found in lean mass at 1- [(F(1,8) = 0.141, P=NS)], 6- [(F(1,8) = 0.015, P=NS)] and 7-weeks [(F(1,8) = 0.009, P=NS)] post-

10.3389/fendo.2024.1440070

TABLE 1A Changes in IBAT mRNA expression following IBAT denervation.

Treatment	SHAM	DENERVATION
IBAT	4V VEH	4V VEH
Adrb1	1.0 ± 0.1[a]	0.6 ± 0.1[b]
Adrb3	1.0 ± 0.1[a]	0.3 ± 0.03[b]
Acox1	1.0 ± 0.1[a]	0.4 ± 0.03[b]
UCP1	1.0 ± 0.1[a]	0.3 ± 0.1[b]
UCP3	1.0 ± 0.04[a]	0.4 ± 0.1[b]
bmp8b	1.0 ± 0.2[a]	0.2 ± 0.1[b]
Cidea	1.0 ± 0.1[a]	0.9 ± 0.1[a]
Gpr120	1.0 ± 0.1[a]	0.1 ± 0.03[b]
Cox8b	1.0 ± 0.1[a]	0.7 ± 0.1[b]
DIO2	1.0 ± 0.2[a]	0.3± 0.1[b]
PRDM16	1.0 ± 0.2[a]	0.8 ± 0.1[a]
Ppargc1a	1.0 ± 0.1[a]	0.7 ± 0.1[a]
Ppara	1.0 ± 0.1[a]	0.8 ± 0.1[a]

IBAT was collected at 2-h post-injection of 4V Vehicle (VEH).
Different letters denote significant differences between treatments.
Shared letters are not significantly different from one another.
Data are expressed as mean ± SEM.
N=3-6/group.

TABLE 1B Changes in IWAT mRNA expression following IBAT denervation.

Treatment	SHAM	DENERVATION
IBAT	4V VEH	4V VEH
Adrb1	1.0 ± 0.1[a]	0.7 ± 0.1[a]
Adrb3	1.0 ± 0.5[a]	0.9 ± 0.2[a]
Acox1	1.0 ± 0.6[a]	1.0 ± 0.6[a]
UCP1	1.0 ± 0.2[a]	13.6 ± 3.8[a]
UCP3	1.0 ± 0.4[a]	1.1 ± 0.03[a]
bmp8b	1.0 ± 0.5[a]	1.3 ± 0.6[a]
Cidea	1.0 ± 0.4[a]	1.5 ± 0.3[a]
Gpr120	1.0 ± 0.2[a]	0.9 ± 0.1[a]
Cox8b	1.0 ± 0.1[a]	2.5 ± 1.6[a]
DIO2	1.0 ± 0.01[a]	4.0 ± 2.4[a]
Ppargc1a	1.0 ± 0.7[a]	0.9 ± 1.1[a]
Ppara	1.0 ± 0.7[a]	0.8 ± 0.8[a]

IWAT was collected at 2-h post-injection of 4V Vehicle (VEH).
Different letters denote significant differences between treatments.
Shared letters are not significantly different from one another.
Data are expressed as mean ± SEM.
N=2/group.

TABLE 1C Changes in EWAT mRNA expression following IBAT denervation.

Treatment	SHAM	DENERVATION
IBAT	4V VEH	4V VEH
Adrb1	1.0 ± 0.4[a]	1.0 ± 0.2[a]
Adrb3	1.0 ± 0.4[a]	1.1 ± 0.1[a]
Acox1	1.0 ± 0.2[a]	1.1 ± 0.01[a]
UCP1	1.0 ± 0.04[a]	0.7 ± 0.1[a]
UCP3	1.0 ± 0.4[a]	0.9 ± 0.01[a]
bmp8b	1.0 ± 0.2[a]	0.9 ± 0.1[a]
Cidea	1.0 ± 0.6[a]	1.5 ± 0.4[a]
Gpr120	1.0 ± 0.1[a]	1.0 ± 0.1[a]
Cox8b	1.0 ± 0.3[a]	1.9 ± 0.6[a]
DIO2	1.0 ± 0.2[a]	1.7 ± 0.4[a]
Ppargc1a	1.0 ± 0.4[a]	1.3 ± 0.03[a]

EWAT was collected at 2-h post-injection of 4V Vehicle (VEH).
Different letters denote significant differences between treatments.
Shared letters are not significantly different from one another.
Data are expressed as mean ± SEM.
N=2/group.

denervation relative to sham operated mice. These findings are in agreement with others who have reported no difference in body weight (51, 52, 54–56) or fat mass (52, 55) in hamsters or mice following bilateral surgical or chemical denervation of IBAT.

Study 3: determine if SNS innervation of IBAT is reduced in age-matched obese mice relative to lean mice

The goal of this study was to determine if SNS innervation to IBAT is reduced in the obese state relative to lean animals. Given that SNS activation of BAT and BAT activity decline with age [(57); for review see (58)], DIO mice were age-matched to lean chow-fed control mice. By design, DIO mice were obese as determined by both body weight (46.4 ± 1.2 g) and adiposity (17.8 ± 0.7 g fat mass; 38.3 ± 0.8% adiposity) relative to age-matched chow-fed control mice (33.1 ± 0.4 g) and adiposity (6.3 ± 0.4 g fat mass; 18.9 ± 1.1% adiposity) after maintenance on the HFD and chow, respectively, for approximately 4.5 months prior to sham procedures.

IBAT NE content was reduced by 38.9 ± 9.8% relative in lean mice relative to age-matched DIO mice [($F(1,8) = 10.757$, $P=0.011$)] (Figure 3). In addition, NE content in IWAT [($F(1,8) = 19.363$, $P=0.002$)] and liver [($F(1,8) = 14.516$, $P=0.005$)] was reduced in lean mice compared to age-matched DIO mice. NE content in pancreas also appeared to be reduced in lean mice relative to DIO mice [($F(1,8) = 4.233$, $P=0.074$)] while there was no significant difference in NE from EWAT (P=NS).

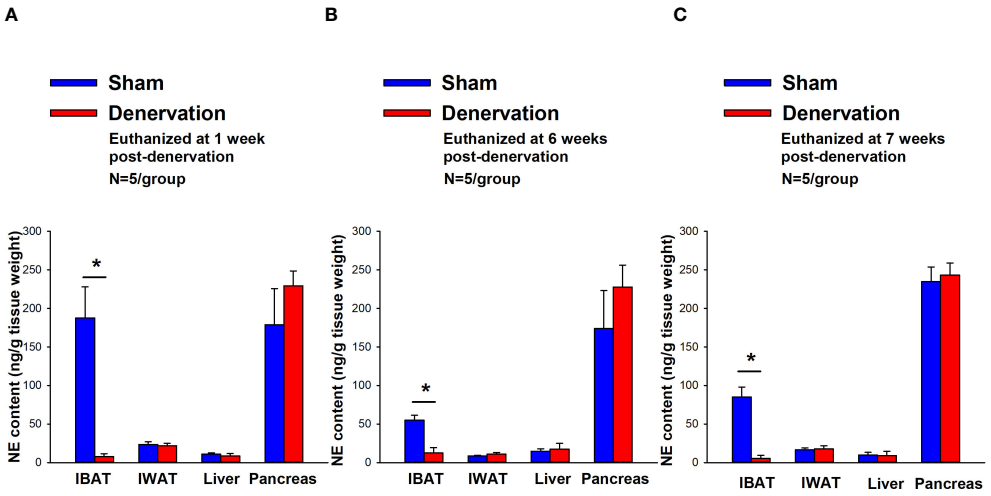

FIGURE 2
Effect of IBAT surgical denervation procedure on IBAT NE content at 1-, 6- and 7-weeks post-sham or IBAT denervation in DIO mice. Mice were maintained on a HFD (60% kcal from fat) for approximately 4.25 months prior to undergoing sham (N=5/group) or bilateral surgical IBAT denervation (N=5/group) procedures and were euthanized at **(A)** 1-, **(B)** 6- and **(C)** 7-weeks post-sham (N=15/group) or denervation procedures (N=15/group). NE content was measured from IBAT, IWAT, liver and pancreas. Data are expressed as mean ± SEM. *P<0.05, †0.05<P<0.1 denervation vs sham.

Study 4: determine if surgical denervation of IBAT changes the ability of the β3-AR agonist, CL 316243, to increase T_{IBAT} in DIO mice

The goal of this study was to verity that there was no change in the ability of IBAT to respond to direct β3-AR stimulation as a result of the denervation procedure relative to sham operated animals. By design, DIO mice were obese as determined by both body weight (44.2 ± 0.6 g) and adiposity (13.9 ± 0.8 g fat mass; 31.2 ± 1.4% adiposity) after maintenance on the HFD for approximately 4.5 months prior to sham/denervation procedures. The mice used in this study were identical to those used in Study 1B.

In sham mice, CL 316243 (1 mg/kg) increased T_{IBAT} at 0.25, 0.75, 1, 2, 3 and 4-h post-injection. The lowest dose (0.1 mg/kg) also stimulated T_{IBAT} at 0.25, 0.75, 1, 2, 3 and 4-h post-injection (P<0.05; Figure 4A). In addition, similar findings were apparent when measuring change in T_{IBAT} relative to baseline T_{IBAT} (Figure 4B). CL 316243 also stimulated T_{IBAT} and T_{IBAT} relative to baseline at 24-h post-injection at the high dose (P<0.05; data not shown).

IBAT NE content was reduced in denervated mice by 97.8 ± 0.5% in denervated mice relative to sham-operated control mice [(F(1,17) = 73.270, P<0.001). In contrast, there was no difference in NE content in IWAT, EWAT, liver or pancreas between sham or denervation groups (P=NS).

In denervated mice, CL 316243 (1 mg/kg) increased T_{IBAT} at 0.25, 0.5, 0.75, 1, 1.25, 1.5, 1.75, 2, 3 and 4-h post-injection. The lowest dose (0.1 mg/kg) also stimulated T_{IBAT} at 0.25, 0.5, 0.75, 1, 2, 3 and 4-h post-injection ((P<0.05; Figure 4C). CL 316243 also stimulated T_{IBAT} at 24-h post-injection at the high dose (P<0.05; data not shown). Similar findings were apparent when measuring change in T_{IBAT} relative to baseline T_{IBAT} through 240-min post-injection (Figure 4D). CL 316243 (1 mg/kg) also tended to stimulate the change in T_{IBAT} relative to baseline T_{IBAT} at 24-h post-injection (P=0.050).

Importantly, there was no difference in the T_{IBAT} response to CL 316243 (0.1 or 1 mg/kg) when the data were averaged over the 1-h or 4-h post-injection period between sham and denervated mice (P=NS).

Overall, these findings indicate that IBAT denervation did not change the ability of CL 316243 to increase BAT thermogenesis (surrogate measure of EE) in DIO mice relative to sham operated mice.

Energy intake

In sham mice, CL 316243 reduced daily energy intake at both 0.1 and 1 mg/kg by 25.3 and 51% (P<0.05). Similarly, in denervated mice, CL 316243 also reduced daily energy intake at both 0.1 and 1 mg/kg (P<0.05) by 34 and 57.1% relative to vehicle (Figure 4E).

Body weight

CL 316243 did not reduce overall body weight in either group. However, the high dose reduced body weight gain in both sham and denervated mice (P<0.05; Figure 4F) while the low dose also reduced body weight gain in the denervated mice (P<0.05; Figure 4F).

Importantly, there was no difference in the effectiveness of CL 316243 (0.1 or 1 mg/kg) to reduce energy intake or weight gain between sham and denervated mice (P=NS). However, there appeared to be a more enhanced effect of CL 316243 (0.1 mg/kg) to reduce weight gain (P=0.091) in the denervated group relative to the sham group.

Furthermore, there was no difference in energy intake [sham: 14.7 ± 0.98 kcal; denervation: 14.8 ± 0.8 kcal] or change in body weight [sham: -0.1± 0.2g; denervation: -0.1 ± 0.2 g] following acute IP vehicle injections in sham or denervated mice (P=NS).

Overall, these findings indicate that IBAT denervation did not change the ability of CL 316243 to reduce food intake or body weight gain in DIO mice relative to sham operated mice.

Similar results were also found in lean mice (data not shown). The sympathomimetic, icilin, which may act indirectly to stimulate BAT thermogenesis through SNS outflow to IBAT, increased T_{IBAT}

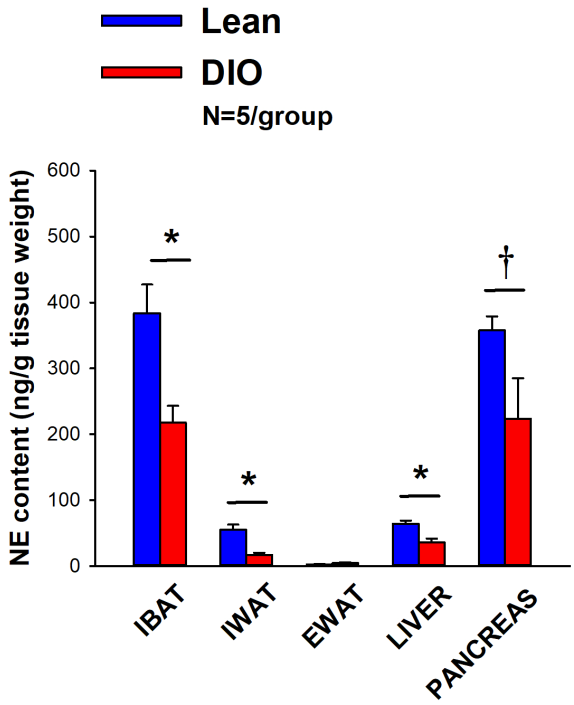

FIGURE 3
Effect of diet-induced obesity (DIO) on SNS Innervation (NE content) of IBAT, IWAT, EWAT, liver and pancreas at 1-week post-sham in age-matched lean and DIO mice. Age-matched mice were maintained on either chow (16% kcal from fat) or HFD (60% kcal from fat) for approximately 4.5 months prior to undergoing a sham denervation (N=5/group) procedure and were euthanized at 1-week post-sham (N=5/group). NE content was measured from IBAT, IWAT, EWAT, liver and pancreas. Data are expressed as mean ± SEM. *P<0.05, †0.05<P<0.1 lean vs DIO.

(P<0.05) throughout the measurement period in both sham and IBAT denervated mice (P<0.05; data not shown).

The effects of the sympathomimetic, tyramine (Supplementary Study 1), was also examined on T_{IBAT} in DIO mice with intact or impaired SNS innervation of IBAT. Tyramine (19.2 mg/kg) increased T_{IBAT} during the initial part of the measurement period in both sham and IBAT denervated mice (P<0.05; Supplementary Figures 1A–D).

There was no difference in the T_{IBAT} response to tyramine (19.2 mg/kg) when the data were averaged over the 0.25-h post-injection period between sham and denervated mice (P=NS). Similar findings were also observed when comparing T_{IBAT} or change from baseline T_{IBAT} at 0.25-h and 0.5-h post-injection between sham and denervated mice (P=NS).

Overall, these findings demonstrate there is not a functional change in the ability of IBAT to respond to direct β3-AR stimulation or other agents, including icilin, that may activate BAT through a direct non-β3-AR mechanism in denervated mice relative to sham animals.

Study 5: determine the extent to which OT-induced activation of sympathetic outflow to IBAT contributes to its ability to increase T_{IBAT} in DIO mice

After having confirmed there was no functional defect in the ability of IBAT to respond to direct β3-AR stimulation (Study 4), the goal of this study was to determine if OT-elicited elevation of T_{IBAT} requires intact SNS outflow to IBAT. By design, DIO mice were obese as determined by both body weight (43.6 ± 0.7 g) and adiposity (13.8 ± 0.6 g fat mass; 31.5 ± 1.1% adiposity) after maintenance on the HFD for approximately 4.25 months prior to sham/denervation procedures. There was no difference in body weight between sham and denervation groups prior to surgery (sham: 43.0 ± 1.1 g vs denervation: 42.9 ± 1.1 g) [($F(1,19)$ = 0.005, P=0.943] or at 10-11 weeks post-surgery (sham: 44.8 ± 1.8 g vs denervation: 43.9 ± 2.8 g) [($F(1,19)$ = 0.069, P=0.796]. Note that the T_{IBAT} data from sham-operated DIO mice has been previously published (22).

IBAT NE content was reduced by 94.9 ± 3.3% in denervated mice relative to sham-operated control mice [($F(1,19)$ = 33.427, P<0.001). In contrast, there was no difference in NE content in IWAT, EWAT, liver or pancreas between sham or denervation groups (P=NS).

In sham mice, 4V OT (5 µg) increased T_{IBAT} at 1 and 1.25-h post-injection (P<0.05) and tended to stimulate T_{IBAT} at 0.75, 1.5 and 1.75-h post-injection (0.05<P<0.1). The lowest dose (1 µg) also stimulated T_{IBAT} at 0.75 and 1-h post-injection and tended to stimulate T_{IBAT} at 1.25-h post-injection (0.05<P<0.1; Figure 5A). Similar findings were apparent when measuring change in T_{IBAT} relative to baseline T_{IBAT} (Figure 5B).

In denervated mice, OT (5 µg) increased T_{IBAT} at 0.75, 1, 1.25, 1.5, 2 and 3-h post-injection (P<0.05). The lowest dose (1 µg) tended to stimulate T_{IBAT} at 4-h and 24-h post-injection

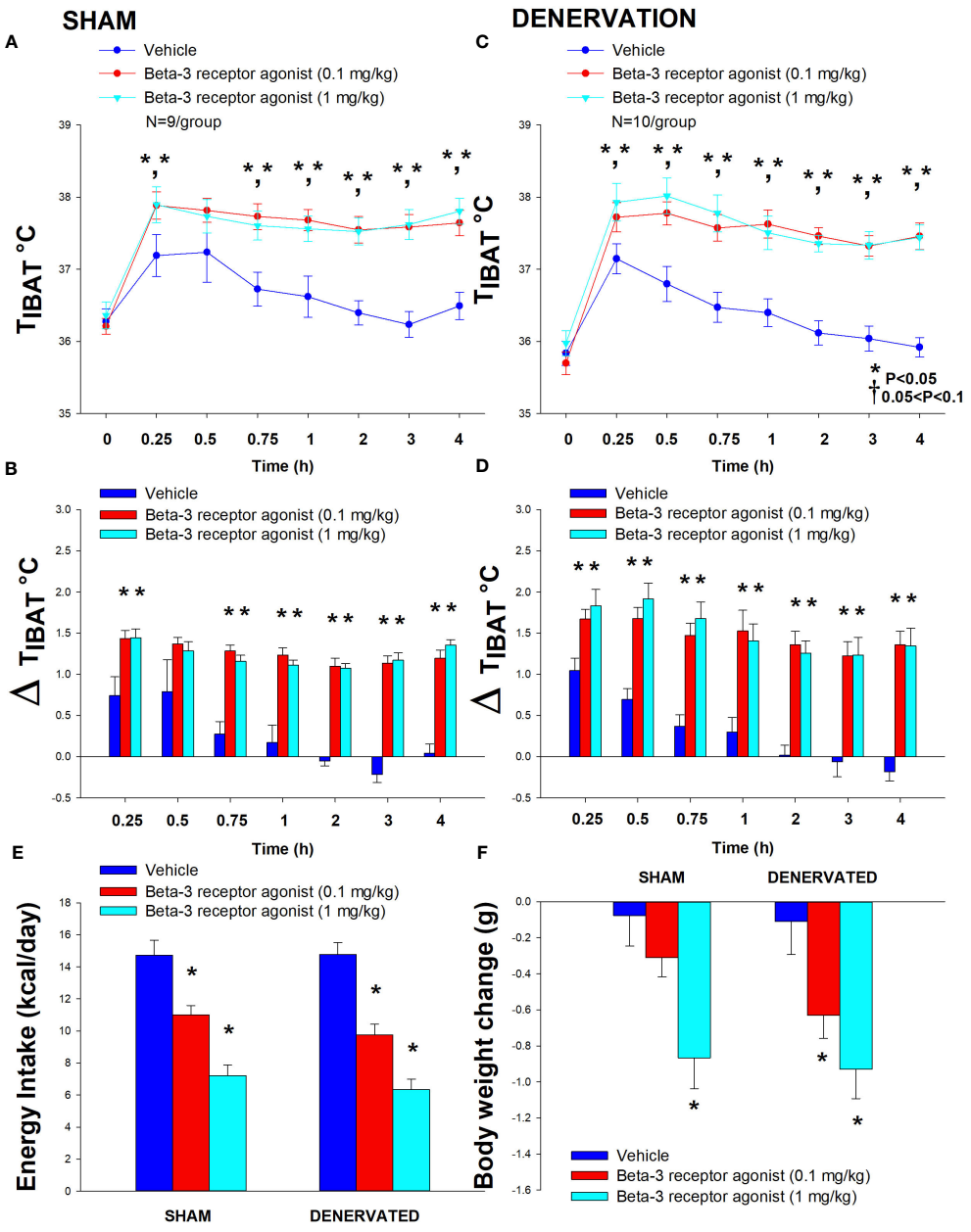

FIGURE 4
(A–F) Effect of systemic beta-3 receptor agonist (CL 316243) administration (0.1 and 1 mg/kg) on IBAT temperature (T_{IBAT}), energy intake and body weight post-sham or IBAT denervation in DIO mice. Mice were maintained on HFD (60% kcal from fat; N=9-10/group) for approximately 4.5 months prior to undergoing a sham or bilateral surgical IBAT denervation and implantation of temperature transponders underneath IBAT. Animals were subsequently adapted to a 4-h fast prior to receiving IP injections of (CL 316243) (0.1 or 1 mg/kg, IP) or vehicle (sterile water) where each animal received each treatment at approximately 7-day intervals. **(A, C)**, Effect of CL 316243 on T_{IBAT} in **(A)** sham operated or **(C)** IBAT denervated DIO mice; **(B, D)**, Effect of CL 316243 on change in T_{IBAT} relative to baseline T_{IBAT} (delta T_{IBAT}) in **(B)** sham operated or **(D)** IBAT denervated DIO mice; **(E)**, Effect of CL 316243 on change in energy intake in sham or IBAT denervated DIO mice; **(F)**, Effect of CL 316243 on change in body weight in sham or IBAT denervated DIO mice. Data are expressed as mean ± SEM. *P<0.05, †0.05<P<0.1 CL 316243 vs. vehicle.

(0.05<P<0.1; Figure 5C). Similar findings were apparent when measuring change in T_{IBAT} relative to baseline T_{IBAT} (Figure 5D). In addition, 4V OT elevated T_{IBAT} in lean denervated mice (data not shown).

There was no effect of acute 4V OT administration to reduce daily energy intake or body weight (P=NS) in either sham or denervated mice. Furthermore, there was no difference in energy intake [sham: 11.3 ± 1.2 kcal; denervation: 10.2 ± 1.9 kcal] or change in body weight [sham: 0.3± 0.1g; denervation: 0.4 ± 0.3 g] following acute 4V vehicle injections between sham or denervated mice (P=NS).

Overall, these findings demonstrate that SNS innervation of IBAT is not a predominant mediator of OT-elicited elevations of BAT thermogenesis.

In contrast to the pattern observed following 4V administration, systemic administration of OT produced an initial reduction of T_{IBAT} (P<0.05) followed by an increase in T_{IBAT} (P<0.05;

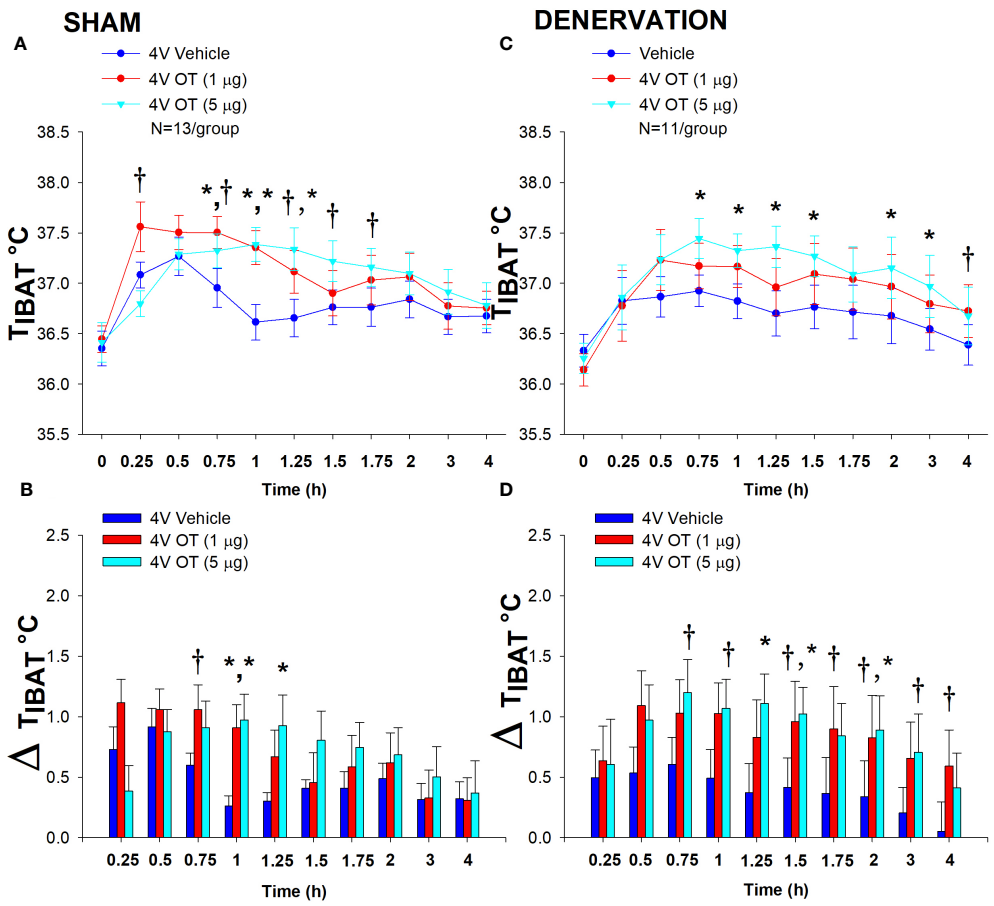

FIGURE 5
(A–D) Effect of acute 4V OT administration (1 and 5 µg) on T_{IBAT} post-sham or IBAT denervation in male DIO mice. Mice were maintained on HFD (60% kcal from fat; N=11-13/group) for approximately 4.25 months prior to undergoing a sham or bilateral surgical IBAT denervation and implantation of temperature transponders underneath IBAT. Mice were subsequently implanted with 4V cannulas and allowed to recover for 2 weeks prior to receiving acute 4V injections of OT or vehicle. Animals were subsequently adapted to a 4-h fast prior to receiving acute 4V injections of OT or vehicle **(A, C)**, Effect of acute 4V OT on T_{IBAT} in **(A)** sham operated or **(C)** IBAT denervated DIO mice; **(B, D)**, Effect of acute 4V OT on change in T_{IBAT} relative to baseline $T_{IBA}T$ (delta T_{IBAT}) in **(B)** sham operated or **(D)** IBAT denervated DIO mice; Data are expressed as mean ± SEM. *P<0.05, †0.05<P<0.1 OT vs. vehicle. The T_{IBAT} data from sham-operated DIO mice has been previously published (22).

Supplementary Figures 3A–D). Similar to OT, the melanocortin 3/4 receptor agonist, melanotan II (MTII), produced an initial reduction of T_{IBAT} (P<0.05; data not shown) followed by a subsequent increase in T_{IBAT} (data not shown; P<0.05).

Study 6A: determine the extent to which sympathetic outflow to IBAT contributes to the ability of OT to elicit weight loss in DIO mice

The goal of this study was to determine if OT-elicited weight loss requires intact SNS outflow to IBAT. By design, DIO mice were obese as determined by both body weight (47.9 ± 0.6 g) and adiposity (17.7 ± 0.5 g fat mass; 36.9 ± 0.7% adiposity) after maintenance on the HFD for approximately 4.25-4.5 months prior to sham/denervation procedures. There was no difference in body weight between sham and denervation groups prior to surgery (sham: 46.3 ± 1.0 g vs denervation: 47.9 ± 0.8 g) [(F(1,28) = 1.532, P=NS)].

IBAT NE content was reduced in denervated mice by 93.9 ± 2.3% in denervated mice relative to sham-operated control mice [(F(1,28) = 23.306, P=0.000). In contrast, there was no difference in NE content in IWAT, EWAT, liver or pancreas between sham or denervation groups (P=NS)

Chronic 4V OT reduced body weight by 5.7 ± 2.23% and 6.6 ± 1.4% in sham and denervated mice (P<0.05), respectively, and this effect was similar between groups (P=NS). OT produced corresponding reductions in fat mass (P<0.05) and this effect was also similar between groups (P=NS).

As expected, 4V vehicle resulted in 7.5 ± 3.0% weight gain relative to vehicle pre-treatment [(F(1,8) = 5.677, P=0.044)]. In contrast, 4V OT reduced body weight by 5.7 ± 2.23% relative to OT pre-treatment [(F(1,7) = 5.903, P=0.045)] (Figure 6A) and reduced weight gain (Figure 6B) between days 4-29 of the infusion period (P<0.05). 4V OT tended to reduce weight gain between days 2-3 (0.05<P<0.1). OT produced a corresponding reduction in fat mass [(F(1,13) = 5.190, P=0.040)] (Figure 6C) with no effect on lean body mass (P=NS). These effects were mediated, at least in part, by a modest reduction of

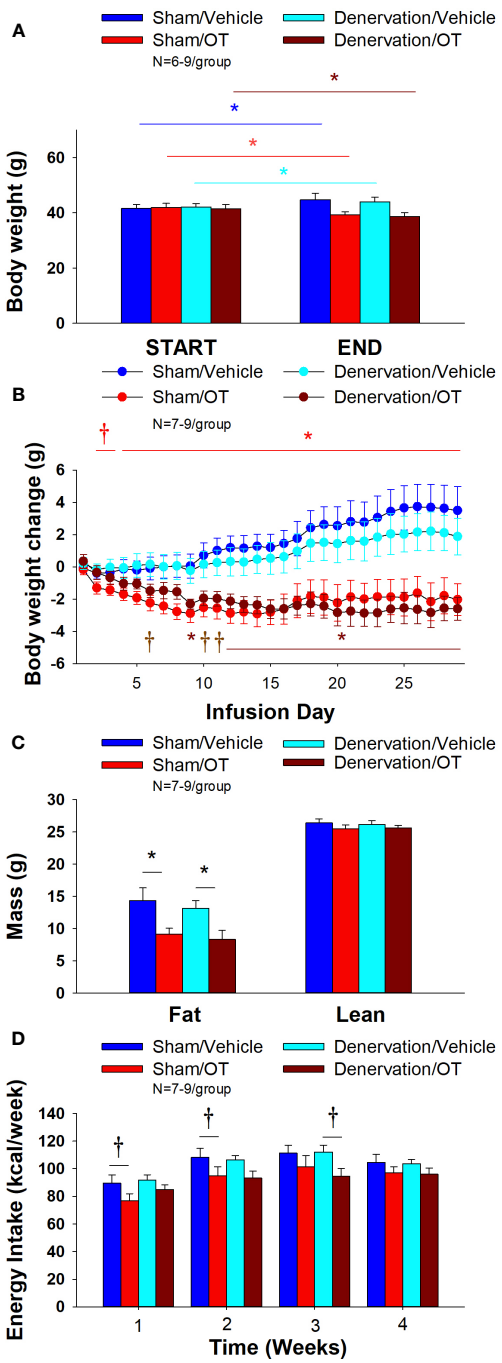

FIGURE 6
(A–D) Effect of chronic 4V OT infusions (16 nmol/day) on body weight, adiposity and energy intake post-sham or IBAT denervation in male DIO mice. **(A)**, Mice were maintained on HFD (60% kcal from fat; N=7-9/group) for approximately 4.25-4.5 months prior to undergoing a sham or bilateral surgical IBAT denervation. Mice were subsequently implanted with 4V cannulas and allowed to recover for 2 weeks prior to being implanted with subcutaneous minipumps that were subsequently attached to the 4V cannula. *A*, Effect of chronic 4V OT or vehicle on body weight in sham operated or IBAT denervated DIO mice; **(B)**, Effect of chronic 4V OT or vehicle on body weight change in sham operated or IBAT denervated DIO mice; **(C)**, Effect of chronic 4V OT or vehicle on adiposity in sham operated or IBAT denervated DIO mice; **(D)**, Effect of chronic 4V OT or vehicle on adiposity in sham operated or IBAT denervated DIO mice. Data are expressed as mean ± SEM. **P*<0.05, †0.05<*P*<0.1 OT vs. vehicle.

energy intake that tended to be present during weeks 1 (*P*=0.067; Figure 6D) and 2 (*P*=0.092).

In denervated mice, 4V vehicle treatment resulted in 4.3 ± 2.6% weight gain relative to vehicle pre-treatment [(F(1,5) = 17.371, *P*=0.009)]. In contrast, 4V OT reduced body weight by 6.6 ± 1.4% relative to OT pre-treatment [(F(1,5) = 15.883, *P*=0.010)] (Figure 6A) and it reduced weight gain (Figure 6B) throughout the 29-day infusion period. OT treatment reduced weight gain on days 9 and 12-29 (*P*<0.05) and it tended to reduce weight gain on days 6 (*P*=0.095), 10 (*P*=0.059) and 11 (*P*=0.055). OT produced a

corresponding reduction in fat mass [(F(1,11) = 7.101, P=0.022)] (Figure 6C) with no effect on lean body mass (P=NS). These effects were mediated, at least in part, by a modest reduction of energy intake that tended to be present during weeks 2 (P=0.147) and 3 (P=0.064; Figure 6D).

Furthermore, there was no difference in total 4-week energy intake [sham: 413.5 ± 21.9 kcal; denervation: 414.1 ± 10.6 kcal] or 4-week change in body weight [sham: 3.6± 1.4 g; denervation: 2.1 ± 1.1 g] following chronic 4V vehicle infusion between sham or denervated mice (P=NS).

Based on these collective findings, we conclude that SNS innervation of IBAT is not a predominant contributor of oxytocin-elicited increases in BAT thermogenesis (surrogate measure of EE), weight loss and reduction of fat mass.

Adipocyte size

Sham

There was a significant effect of 4V OT to reduce EWAT adipocyte size in sham operated mice [(F(1,13) = 5.729, P=0.032)] (Figure 7B) while it had no significant effect on IWAT adipocyte size (P=NS) (Figure 7A).

Denervation

In contrast to the effects observed in sham mice, 4V OT had no significant effect on EWAT adipocyte size in IBAT denervated mice (P=NS) (Figure 7B). However, there was a tendency of 4V OT to reduce IWAT adipocyte size in IBAT denervated mice [(F(1,11) = 4.233, P=0.064)] (Figure 7A).

Plasma hormone concentrations

To characterize the endocrine and metabolic effects between sham and denervated DIO mice, we measured blood glucose levels and plasma concentrations of leptin, insulin, FGF-21, irisin, adiponectin, FFA, free glycerol (FG) and total cholesterol (TC) post-sham and denervation procedure. We found an overall effect of 4V OT to reduce plasma leptin [(F(3,26) = 3.839, P=0.021)]. Specifically, 4V OT treatment was associated with a reduction of plasma leptin in the sham group (P<0.05; Table 2) which coincided with OT-elicited reductions in fat mass. We also found that 4V OT treatment tended to reduce plasma insulin in the denervation group relative to the 4V vehicle sham group (P=0.081; Table 2). In addition, there was an overall effect of OT to reduce plasma total cholesterol [(F(3,26) = 5.806, P=0.004)]. 4V OT treatment was associated with a significant reduction of total cholesterol in both groups (P<0.05; Table 2).

Study 6B: determine the extent to which sympathetic outflow to IBAT contributes to the ability of OT to impact thermogenic gene expression in IBAT, IWAT and EWAT in DIO mice

IBAT

There was a reduction of IBAT UCP-1 [(F(1,7) = 38.1, P<0.001)], DIO2 [(F(1,7) = 12.669, P=0.009)], Gpr120 [(F(1,7) = 65.965, P<0.001)], Adrb3 [(F(1,7) = 65.916, P=0.000)], Adrb1 [(F(1,7) = 8.015, P=0.025)], Acox1 [(F(1,7) = 58.261, P<0.001)], bmp8b [(F(1,7) = 19.636, P=0.003)], cox8b [(F(1,6) = 16.403, P=0.007)] and UCP-3 mRNA expression [(F(1,7) = 57.665, P<0.001)] in denervated mice relative to IBAT from sham operated mice (P<0.05; Table 3A). There were no significant differences in IBAT CIDEA, PPARGC1, PPARA and PRDM16 mRNA expression between sham and denervation groups (P=NS).

The findings pertaining to IBAT UCP-1 gene expression in surgically denervated mice are consistent with what others have reported with IBAT UCP-1 protein expression from hamsters (51) and mice (52) following chemical (6-OHDA)-induced denervation of IBAT relative to control animals. Similarly, there was a reduction of IBAT UCP-1 mRNA following unilateral or bilateral surgical denervation in hamsters (53) and mice (54, 55), respectively. Similar to our findings, others also found a reduction of IBAT Dio2 and Adrb3 following bilateral surgical denervation in mice (54). The findings pertaining to IBAT UCP-1 gene expression in denervated mice are consistent with what others have reported with IBAT UCP-1 protein expression from hamsters (51) and mice (52) with chemical (6-OHDA)-induced denervation of IBAT relative to control animals.

IWAT

IWAT UCP-1 [(F(1,2) = 11.131, P=0.079)] tended to be elevated in denervated mice relative to sham operated mice (Table 3B). There were no significant differences in any of the other thermogenic markers (P=NS; Table 3B).

EWAT

There tended to be a reduction of UCP-1 in denervated mice compared to sham operated mice [(F(1,2) = 7.000, P=0.118)] (Table 3C). There were no significant differences in any of the other thermogenic markers (P=NS; Table 3C).

Study 7: determine the extent to which systemic (subcutaneous) infusion of a centrally effective dose of OT (16 nmol/day) elicits weight loss in DIO mice

As expected, weight gain of DIO mice increased over the month of vehicle treatment relative to pre-treatment [(F(1,10) = 16.901, P=0.002)] (Figure 8A). In contrast to the weight lowering effects of 4V OT (16 nmol/day), systemic OT (16 nmol/day) resulted in a significant elevation of body weight relative to OT pre-treatment [(F(1,12) = 11.138, P=0.006)] (Figure 8A; P<0.05). Furthermore, SC OT, at a 3-fold higher dose (50 nmol/day), also resulted in a significant elevation of body weight relative to pre-treatment [(F(1,12) = 10.424, P=0.007)]. However, SC OT (16 and 50 nmol/day) was able to reduce weight gain (Figure 8B) relative to vehicle treatment throughout the 28-day infusion period. SC OT (50 nmol/day), at a dose that was at least 3-fold higher than the centrally effective dose (16 nmol/day), reduced weight gain throughout the entire 28-day infusion period. SC OT (16 nmol/day) treated mice had reduced weight gain between days 17-28 (P<0.05) but did not have the net weight loss seen when this dose

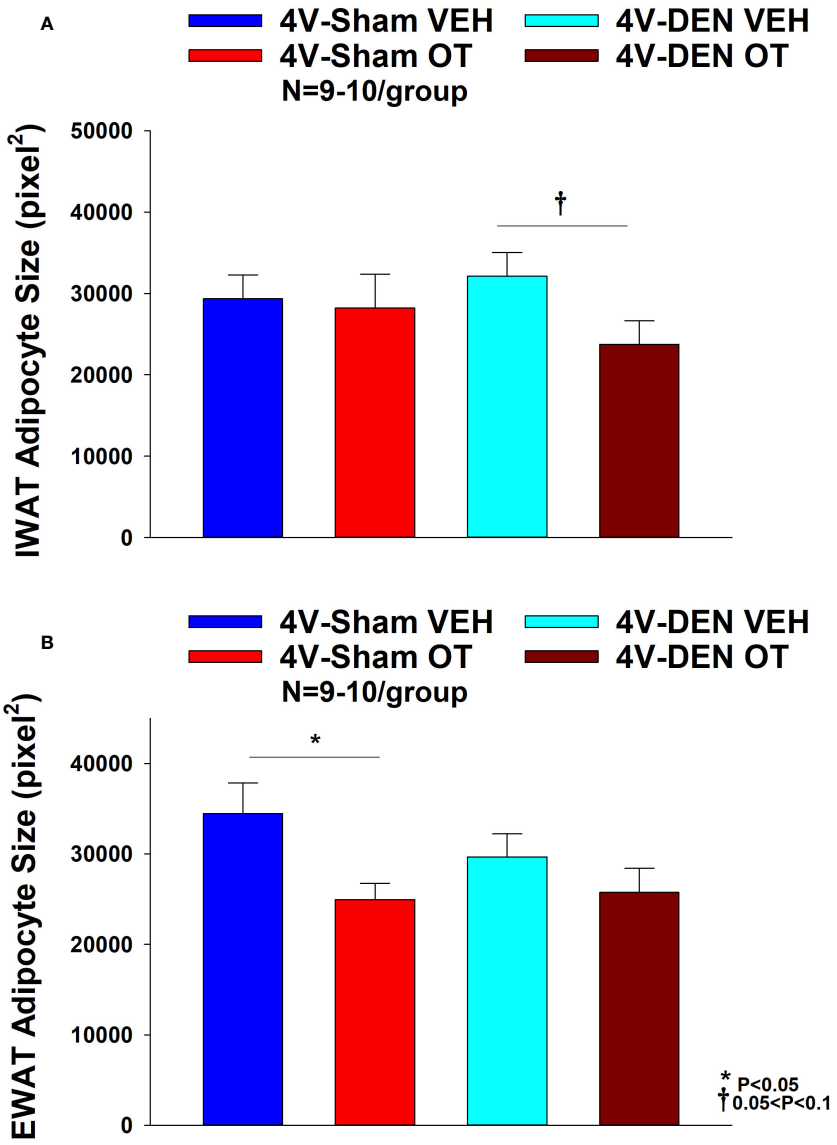

FIGURE 7
(A, B) Effect of chronic 4V OT infusions (16 nmol/day) on adipocyte size post-sham or IBAT denervation in male DIO mice. **(A)**, Adipocyte size (pixel^2) was measured in IWAT from mice that received chronic 4V infusion of OT (16 nmol/day) or vehicle (VEH) in sham or IBAT denervated DIO mice (N=9-10/group). **(B)**, Adipocyte size was measured in EWAT from mice that received chronic 4V infusion of OT (16 nmol/day) or vehicle in sham operated or IBAT denervated mice (N=9-10/group). Data are expressed as mean ± SEM. *P<0.05 OT vs. vehicle.

was given centrally. SC OT (16 and 50 nmol/day) reduced fat mass [(F(2,35) = 5.558, P=0.008)] (Figure 8C; P<0.05) and produced a corresponding reduction of plasma leptin [(F(2,35) = 3.890, P=0.03)], (Table 4) with no effect on lean body mass (P=NS). These effects that were mediated, at least in part, by a modest reduction of energy intake that was apparent during week 3 of SC OT (50 nmol/day) treatment (Figure 8D; P<0.05).

Discussion

The goal of the current studies was to determine if sympathetic innervation of IBAT is required for OT to increase non-shivering BAT thermogenesis and reduce body weight and adiposity in male DIO mice. To assess if OT-elicited changes in non-shivering BAT thermogenesis require intact SNS outflow to IBAT, we examined the effects of acute 4V OT (1, 5 µg) on T_{IBAT} in DIO mice following bilateral surgical SNS denervation to IBAT. We found that the high dose (5 µg) elevated T_{IBAT} similarly in sham mice as in denervated mice. We subsequently determined if OT-elicited reductions of body weight and adiposity require intact SNS outflow to IBAT. To accomplish this, we determined the effect of bilateral surgical denervation of IBAT on the ability of chronic 4V OT (16 nmol/day) administration to reduce body weight, adiposity and food intake in DIO mice. We found that chronic 4V OT produced comparable reductions of body weight and adiposity in denervated mice, as well as sham mice (P<0.05), supporting the hypothesis that sympathetic innervation of IBAT is not a predominant mediator of

TABLE 2 Plasma Measurements Following 4V Infusions of Oxytocin or Vehicle in Sham and Denervated DIO Mice.

4V Treatment	Vehicle	OT	Vehicle	OT
	Sham	Sham	Denervation	Denervation
Leptin (ng/mL)	36.5 ± 9.7[a]	13.4 ± 2.6[b]	23.1 ± 2.9[a]	9.7 ± 2.3[ab]
Insulin (ng/mL)	2.5 ± 0.5[a]	1.6 ± 0.2[ab]	1.8 ± 0.2[ab]	1.4 ± 0.3[bc]
FGF-21 (pg/mL)	856.4 ± 172[a]	679 ± 57.3[a]	698.4 ± 87.1[a]	505.5 ± 112.2[a]
Irisin (μg/mL)	3.3 ± 0.7[a]	2.6 ± 0.3[a]	3.1 ± 0.6[a]	2.0 ± 0.1[a]
Adiponectin (μg/mL)	11.3 ± 1.2[a]	10.0 ± 1.0[a]	14.0 ± 2.1[a]	12.1 ± 2.7[a]
Blood Glucose (mg/dL)	169.5 ± 5.5	156.6 ± 4.8	168.6 ± 5.6	158.3 ± 8.3
FFA (mEq/L)	0.5 ± 0.02[a]	0.5 ± 0.04[a]	0.5 ± 0.02[a]	0.6 ± 0.09[a]
Free Glycerol (mg/dL)	40.3 ± 1.7[a]	42.1 ± 1.9[a]	44.6 ± 2.3[a]	40.5 ± 3.9[a]
Total Cholesterol (mg/dL)	253.9 ± 7.4[a]	214.2 ± 12.6[b]	229.6 ± 7.8[a]	198.3 ± 10.9[b]

Blood was collected by tail vein nick (blood glucose) or from the trunk following a 4-h fast.
Different letters denote significant differences between treatments.
Shared letters are not significantly different from one another.
Data are expressed as mean ± SEM.
N=6-9/group.

OT-elicited increases of non-shivering BAT thermogenesis and reductions of body weight and adiposity in male DIO mice.

Our finding that OT produced these effects when given into the hindbrain (4V) suggest that hindbrain populations and/or spinal cord populations may contribute to the effects of OT-elicited thermogenesis and browning of WAT in mice. Recent findings highlight the presence of both overlapping and nonoverlapping CNS circuits that control SNS outflow to IWAT and IBAT (51). Namely, parvocellular PVN OT neurons have multi-synaptic projections to IBAT (59, 60), IWAT (59, 61) and EWAT (61, 62). A small subset of parvocellular PVN OT neurons overlap and project to both IBAT and IWAT (59). OT neurons are anatomically situated to control SNS outflow to IBAT and IWAT and increase BAT thermogenesis and browning of IWAT, respectively. It is not clear if these effects are mediated by the same OT neurons or through distinct OT neurons that project to the hindbrain nucleus of the solitary tract or nucleus tractus solitarius (NTS) (63, 64) and/or spinal cord (64), both of which are sites that can control SNS outflow to IBAT and BAT thermogenesis (65, 66). Ong and colleagues recently found that viral-elicited knockdown of OTR mRNA within the dorsal vagal complex was unable to block the effects of 4V OT to increase core temperature (67) suggesting that other OTRs within other areas of the hindbrain and/or spinal cord may contribute to these effects in a rat model. It will be important to determine whether 4V OT-elicited BAT thermogenesis is mediated by OTRs within regions of the NTS not targeted by Ong and colleagues (67), other hindbrain areas such as the raphe pallidus (29, 66, 68–70) or spinal cord (23).

One outstanding question is how 4V OT is activating IBAT if not through SNS outflow to IBAT. Our findings that 1) systemic administration of OT, at a dose that stimulated T_{IBAT} when given into the 4V, did not fully recapitulate the temporal profile we found following 4V administration and 2) 4V administration failed to reproduce the reduction of T_{IBAT} observed following systemic administration suggest that 4V OT is not likely leaking into the periphery to act at peripheral OTRs. One possibility might be that 4V OT activates OTRs within the hindbrain and/or spinal cord that results in the stimulation of epinephrine from the adrenal gland and subsequent activation of IBAT. Epinephrine has been previously found to stimulate both lipolysis and respiration from brown adipocytes derived from rat IBAT (71) and it has only a 2.5-fold lower affinity for recombinant β3-AR in CHO cells than NE (72). In addition, mice that lack epinephrine are able to maintain body temperature in response to cold stress but fail to show an increase in IBAT UCP-1 or PGC1-alpha (73) suggesting that non-UCP mechanisms may be involved to increase or retain heat. However, while it is clear that the hindbrain and spinal cord are part of a multi-synaptic projection to the adrenal gland (74, 75), only 1% of PVN OT neurons within either the parvocellular PVN or magnocellular PVN were found to have multi-synaptic projections to the adrenal gland (74). Whether 4V OT activates a hindbrain or spinal cord projection to the adrenal gland resulting in the release of epinephrine and subsequent activation of IBAT will need to be examined in future studies.

One other possibility is that acute 4V OT could be activating IBAT secondary to stimulating locomotor activity. We have found the high dose (5 μg) given acutely into the 4V stimulated IBAT temperature (21) at doses that increased gross motor activity in DIO rats during the first 2-h post-injection ($P<0.05$; unpublished findings). In addition, Sakamoto and colleagues found that intracerebroventricular (ICV) administration of OT (0.5 μg) stimulated activity levels in mice (76). Similarly, Noble and colleagues found that acute ventromedial hypothalamic injections of OT (1 nmol ≈ 1.0072 μg) also stimulated short-term physical activity at 1-h post-injection in rats (12). Sutton and colleagues also reported that acute DREADD-elicited stimulation of OT neurons within the PVN produced an increase in locomotor activity, energy expenditure and subcutaneous IBAT temperature (23) in Oxytocin IRES-Cre mice whose transponders were placed above the IBAT

10.3389/fendo.2024.1440070

TABLE 3A Changes in mRNA Expression Following 4V Infusions of OT or VEH in Male DIO Mice.

4V Treatment	VEH	OT	VEH	OT
	Sham	Sham	Denervation	Denervation
IBAT				
Adrb1	1.0 ± 0.1^{a}	0.7 ± 0.1^{ab}	0.5 ± 0.1^{b}	1.5 ± 0.5^{c}
Adrb3	1.0 ± 0.1^{a}	0.7 ± 0.2^{ab}	0.3 ± 0.1^{b}	0.9 ± 0.2^{a}
Acox1	1.0 ± 0.1^{a}	1.2 ± 0.3^{a}	0.4 ± 0.1^{b}	0.2 ± 0.1^{b}
UCP1	1.0 ± 0.3^{a}	0.8 ± 0.2^{ab}	0.1 ± 0.01^{b}	0.6 ± 0.5^{ab}
UCP3	1.0 ± 0.1^{ab}	1.4 ± 0.5^{a}	0.2 ± 0.1^{b}	0.3 ± 0.1^{b}
Cidea	1.0 ± 0.1^{a}	0.8 ± 0.2^{a}	0.3 ± 0.1^{b}	0.3 ± 0.1^{b}
Cox8b	1.0 ± 0.1^{a}	1.0 ± 0.1^{a}	0.2 ± 0.1^{b}	0.5 ± 0.1^{b}
DIO2	1.0 ± 0.2^{a}	0.6 ± 0.1^{b}	0.1 ± 0.1^{c}	1.2 ± 0.1^{a}
Ppara	1.0 ± 0.1^{a,b}	1.7 ± 0.6^{a}	0.5 ± 0.1^{b}	0.2 ± 0.1^{b}

IBAT was collected following a 4-h fast.
Different letters denote significant differences between treatments.
Shared letters are not significantly different from one another.
Data are expressed as mean ± SEM.
N=3-8/group.

TABLE 3B Changes in mRNA Expression Following Acute 4V OT or VEH Injections in Male DIO Mice.

4V Treatment	VEH	OT	VEH	OT
	Sham	Sham	Denervation	Denervation
IWAT				
Adra2a	1.0 ± 0.2^{a}	2.1 ± 1.0^{a}	0.8 ± 0.2^{a}	0.9 ± 0.3^{a}
Adrb3	1.0 ± 0.1^{a}	1.8 ± 0.5^{a}	1.7 ± 0.6^{a}	2.1 ± 0.7^{a}
Acox1	1.0 ± 0.3^{a}	0.7 ± 0.2^{a}	1.3 ± 0.2^{a}	1.3 ± 0.2^{a}
UCP1	1.0 ± 0.4^{ab}	1.4 ± 0.7^{a,b}	0.6 ± 0.1^{a}	2.9 ± 0.9^{bc}
DIO2	1.0 ± 0.3^{a}	0.2 ± 0.1^{a}	0.6 ± 0.1^{a}	1.3 ± 1.0^{a}
Ppara	1.0 ± 0.2^{a}	0.8 ± 0.3^{a}	1.5 ± 0.4^{a}	1.7 ± 0.2^{a}

IWAT was collected following a 4-h fast.
Different letters denote significant differences between treatments.
Shared letters are not significantly different from one another.
Data are expressed as mean ± SEM.
N=3-7/group.

TABLE 3C Changes in mRNA Expression Following Acute 4V OT or VEH Injections in Male DIO Mice.

4V Treatment	VEH	OT	VEH	OT
	Sham	Sham	Denervation	Denervation
EWAT				
Adra2a	1.0 ± 0.5^{a}	0.4 ± 0.1^{a}	1.1 ± 0.4^{a}	0.8 ± 0.2^{a}
Adrb3	1.0 ± 0.3^{a}	4.1 ± 1.2^{b}	0.4 ± 0.1^{a}	3.4 ± 1.3^{a,b}
Acox1	1.0 ± 0.1^{a,b}	1.1 ± 0.1^{a,b}	0.7 ± 0.2^{a}	1.4 ± 0.1^{b}
DIO2	1.0 ± 0.3^{a}	0.7 ± 0.1^{a}	0.6 ± 0.4^{a}	1.7 ± 0.8^{a}

EWAT was collected following a 4-h fast.
Different letters denote significant differences between treatments.
Shared letters are not significantly different from one another.
Data are expressed as mean ± SEM.
N=3-5/group.

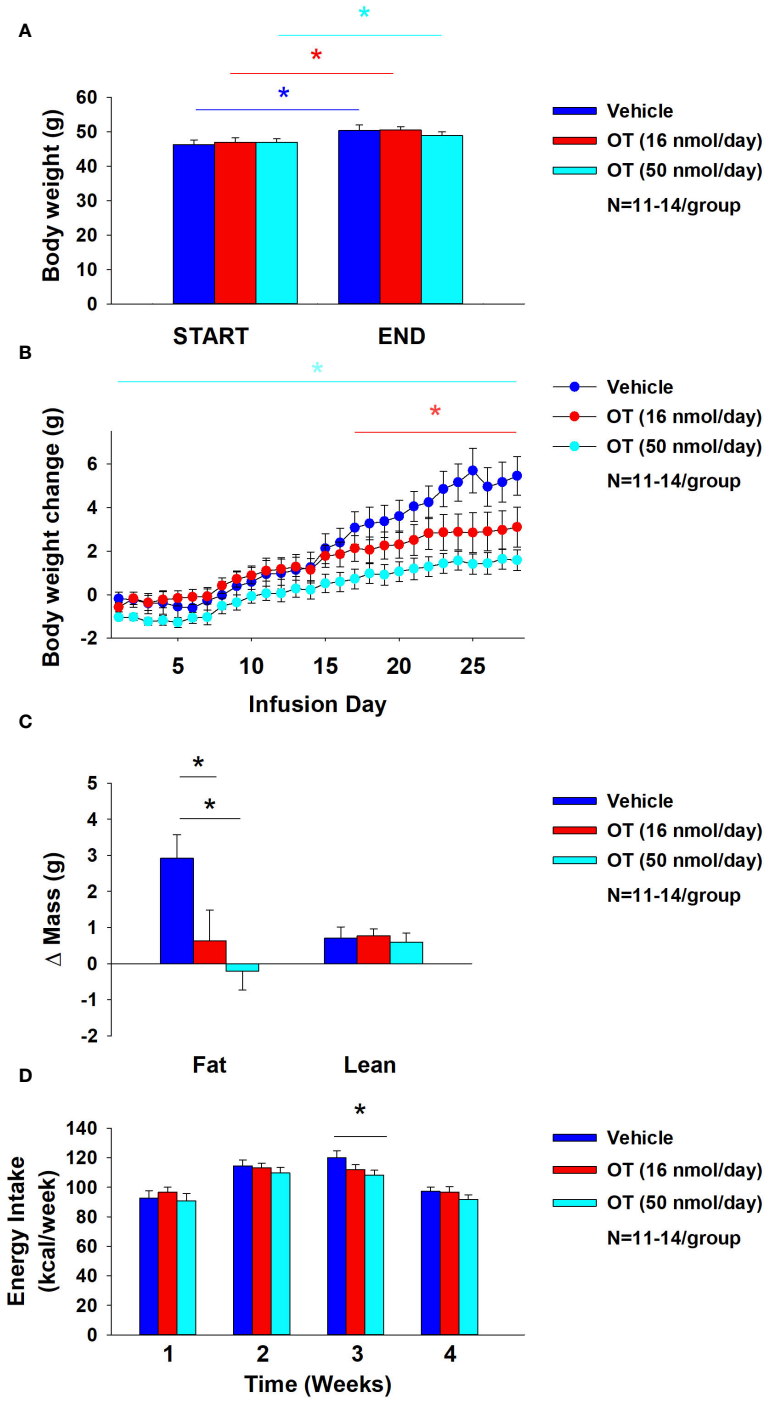

FIGURE 8
(A–D) Effect of chronic subcutaneous OT infusions (16 and 50 nmol/day) on body weight, adiposity and energy intake in male DIO mice. **(A)**, Mice were maintained on HFD (60% kcal from fat; N=11-14/group) for approximately 4-4.25 months prior to being implanted with temperature transponders and allowed to recover for 1-2 weeks prior to being implanted with subcutaneous minipumps. **(A)**, Effect of chronic subcutaneous OT or vehicle on body weight in DIO mice; **(B)**, Effect of chronic subcutaneous OT or vehicle on body weight change in DIO mice; **(C)**, Effect of chronic subcutaneous OT or vehicle on adiposity in DIO mice; **(D)**, Effect of chronic subcutaneous OT or vehicle on adiposity in DIO mice. Data are expressed as mean ± SEM. *P<0.05, †0.05<P<0.1 OT vs. vehicle.

pad. This finding raises that possibility that endogenous OT may also elicit increases in activity. Studies aimed at blocking endogenous OTR signaling prior to DREADD activation of PVN OT neurons will help determine the extent to which these effects are mediated by OT. Future studies will be required in order to examine the extent to which locomotor activity may contribute to the effects of acute 4V on T_{IBAT} in DIO mice

Recent findings also implicate a potentially important role of peripheral OT receptors in the control of body weight in rodents. Similar to our studies, Yuan and colleagues found systemic OT (100

10.3389/fendo.2024.1440070

TABLE 4 Plasma measurements following SC infusions of oxytocin or vehicle in DIO mice.

SC Treatment	Vehicle	OT (16 nmol/day)	OT (50 nmol/day)
Leptin (ng/mL)	90.4 ± 7.8[a]	68 ± 3.6[b]	69.9 ± 6.5[b]
FGF-21 (pg/mL)	2387.3 ± 250[a]	3087.4 ± 414.2[a]	3084.1 ± 520[a]
Irisin (μg/mL)	3.5 ± 0.3[a]	3.7 ± 0.3[a]	4.2 ± 0.4[a]
Adiponectin (μg/mL)	14.1 ± 0.7[a]	11.4 ± 1.0[b]	12.1 ± 0.9[ab]
Blood Glucose (mg/dL)	226.5 ± 12.2[a]	234.5 ± 12.7[a]	209.3 ± 11.0[a]
FFA (mEq/L)	0.1 ± 0.02[a]	0.1 ± 0.01[a]	0.1 ± 0.01[a]
Glycerol (mg/dL)	20.2 ± 0.7[a]	23.8 ± 1.5[a]	20.3 ± 1.8[a]
Total Cholesterol (mg/dL)	242.5 ± 7.2[a]	227.7 ± 9.4[a]	227.3 ± 9.2[a]

Blood was collected by tail vein nick (blood glucose) or from the trunk following a 4-h fast.
Different letters denote significant differences between treatments.
Shared letters are not significantly different from one another.
Data are expressed as mean ± SEM.
N=11-14/group.

nmol/day ≈ 100.72 μg/day) reduced weight gain in high fat diet-fed mice and these effects were associated with decreased adipocyte size (IWAT and EWAT). Asker and colleagues extended these findings and reported that a novel BBB-impermeable OT analog, OT-B12, reduced food intake in rats, thus providing additional evidence for the importance of peripheral OTRs in the control of food intake (77). These findings are in line with earlier studies by Iwasaki and colleagues who found that the effects of peripheral OT to reduce food intake were attenuated in vagotomized mice (78, 79). Similarly, previous findings from our lab also indicated that peripheral administration of a non-BBB penetrant OTR antagonist, L-371257, resulted in a modest stimulation of food intake and body weight gain in rats (80). These findings suggest that, in addition to a central mechanism mediated through hindbrain and/or spinal cord OTRs, OT may also act peripherally to reduce adipocyte size through a direct action on OTRs found on adipocytes (9, 81, 82).

The role of peripheral OTR in the control of BAT thermogenesis is not entirely clear but recent studies raise the possibility that systemic OT may impact BAT thermogenesis through a direct mechanism. Yuan and colleagues found that slow continuous systemic infusion of OT (100 nmol/day) elevated rectal temperature (single time point), UCP-1 protein and UCP-1 mRNA in IBAT and IWAT of high fat diet-fed mice (24) where OTR are expressed (24). In contrast, we found that a single acute bolus injection of lower doses of OT (5 and 10 μg/μL) elicited an initial reduction of T_{IBAT} prior to a subsequent elevation of T_{IBAT}. Similarly, others have found that peripheral administration of higher doses of OT (1 mg/kg) elicited a robust hypothermic response (83). Similar doses (1, 3 and 10 mg/kg, IP) were also found to block stress-induced stimulation of core temperature (84). Kohli reported that pretreatment with arginine vasopressin receptor 1A (AVPR1A) antagonist can reduce OT-mediated hypothermia, while pretreatment with OTR antagonist does not (85). Similar to systemic OT, we and others have demonstrated that systemic MTII produces an initial reduction of T_{IBAT} and/or core temperature (86, 87) followed by a subsequent elevation of T_{IBAT} or core temperature (87). Like OT, MTII-elicited reduction of body temperature was found to be blunted in response to the AVPR1A antagonist (86). In addition to a mechanism involving AVPV1A, MTII-elicited hypothermia is also due, in part, to mast cell activation (88). Together, these findings suggest that the hypothermia in response to high doses of systemic OT might be mediated, in part, by arginine vasopressin (AVP) receptor V1A rather than through OTR. It remains to be determined whether the hypothermic effects of systemic OT are also mediated, in part, by activation of mast cells.

To our knowledge, this is the first time that SNS innervation of IBAT (NE content) has been found to be reduced in DIO rodents relative to age-matched lean control mice. These findings are consistent with the reduction of IBAT NE content in obese *fa/fa* Zucker rats relative to lean homo- (*Fa/Fa*) or heterozygous (*Fa/fa*) rats (89). Similarly, tyrosine hydroxylase (TH; rate limiting enzyme to synthesis of catecholamines) was found to be reduced in obese relative to lean animals (90). The same group also found a reduction of IBAT NE content, NE turnover and activity of dopamine-β-hydroxylase (rate limiting enzyme to synthesis of NE) in young *fa/fa* Zucker rats prior to obesity onset (91). Previous studies have found that the IBAT from humans with obesity appears to be hypoactive (92, 93) although it isn't clear if this is due to reduced SNS innervation of IBAT or reduced sensitivity to endogenous catecholamines (94). Consistent with these findings, obese offspring also show reductions of IBAT temperature (95). Defects in BAT activity are associated with impairments of both the structure and function of BAT mitochondria (96). Furthermore, the IBAT of obese animals was associated with enlarged lipid droplets (97), indicative of hypoactivity of IBAT. Together, our data support the hypothesis that impaired activation of IBAT in the context of DIO may be due, in part, to reduced SNS innervation of IBAT.

Our findings showing a reduction of IBAT UCP-1, Dio2, and Adbr3 in denervated mice is consistent with what has been reported from IBAT of denervated mice or hamsters (51–55). In addition, we found a reduction of IBAT Adrb1, Acox1, UCP-3, bmp8b, Gpr120, and Cox8b in denervated mice. We also found that 4V OT blocked the reduction of Adrb1, Adrb3 and Dio2 in IBAT of denervated mice. Whether these genes contributed to the ability of OT to increase T_{IBAT} in denervated mice is unclear. What was also unexpected was that the β3-AR agonist, CL 316243, was able to produce comparable effects on T_{IBAT} in both groups of mice despite there being a reduction of IBAT Adrb3. However, we have found that chronic 1x daily administration of CL 316243 produced similar effects on stimulation of T_{IBAT} on treatment day 1 vs day 19 despite there being a reduction of IBAT Adrb3 mRNA at the end of the study (98). It is possible that the presence of even a reduced level of the β3-AR in IBAT is sufficient to contribute to the effects of CL 316243 on IBAT temperature at the pharmacological doses used in our studies. It is not as likely that the effects of CL 316243 on IBAT temperature in denervated mice was due to action at other adrenergic receptors in IBAT because CL 316243 is highly

selective to the β3-AR [128-fold higher selectivity to human β3-AR vs β1-AR (99)]. Furthermore, CL 316,243 appears to be more selective to the mouse β3-AR relative to the human β3-AR based on stimulation of cAMP formation in transfected CHO cells (pEC_{50} 8.7 vs. 4.3) (100). In addition, CL 316243 is ineffective at increasing free fatty acids, insulin secretion, energy expenditure, and reducing food intake in β3-AR deficient mice (101) indicating that these effects of CL 316243 are mediated by β3-AR. Furthermore, the effects of CL 316243 on oxygen consumption, insulin secretion and food intake were completely restored with re-expression of β3-AR in brown and white adipocytes (102) indicating that these CL 316243-elicited effects are mediated by β3-AR specifically in BAT and/or WAT.

One limitation of our study is that restraint stress may have limited our ability to observe larger effects on T_{IBAT} (103) during the time period when the effect of the drug is relatively short-lived or small. We aimed to minimize the impact of restraint stress by adapting the animals to handling and mock injections during the week prior to the experiment and by administering the drugs during the early part of the light cycle when catecholamine levels (36) and IBAT temperature are lower (22). Despite these adjustments to protocol, we failed to observe an obvious impairment in the ability of the sympathomimetic, tyramine, to stimulate T_{IBAT} in denervated mice even though there was clear evidence that IBAT NE content was lower in mice whose IBAT was denervated. While the effects of OT and CL 316243 continued well beyond the short-lived effects of restraint/vehicle stress on T_{IBAT} in our mouse studies (~30-45 minutes), the effects of tyramine were relatively short-lived and may have been masked by restraint stress. Thus, stress-induced epinephrine, from the adrenal medulla, or global release of NE from SNS nerve terminals (in response to tyramine) (104–106), may have activated β3-AR in IBAT to stimulate T_{IBAT}, even in denervated mice.

We also acknowledge that the focus of this study was on IBAT given that IBAT is most well characterized BAT depot "because of its size, accessibility and clear innervation IBAT" (107). However, IBAT is thought to contribute to approximately 45% of total thermogenic capacity of BAT (54) or ≥ 70% of total BAT mass (108). Thus, it is possible that the other BAT depots (axillary, cervical, mediastinal and perirenal depots), all of which show elevated UCP-1 in response to cold (109), might have contributed to the effects of OT to elicit weight loss in IBAT denervated mice. Moreover, we acknowledge the potential contribution of IWAT and EWAT given that chronic 4V OT was able to elevate IWAT UCP-1 and EWAT Acox1 in a limited number of IBAT denervated mice. As mentioned earlier, previous findings demonstrate crosstalk between SNS circuits that innervate IBAT and WAT (51). In addition, there is increased NE turnover and IWAT UCP-1 mRNA expression in IBAT denervated hamsters (51). It will be important to 1) confirm our IWAT and WAT gene expression findings in a larger group of animals and 2) develop a model to assess the effectiveness of denervation of all BAT and specific WAT depots in order to more fully understand the importance of BAT and WAT depots in contributing to the effects of OT to elicit weight loss in rodent models.

In summary, our findings demonstrate that acute 4V OT (5 μg) produced comparable increases in T_{IBAT} in both denervated and sham mice. We subsequently found that chronic 4V OT produced similar reductions of body weight and adiposity in both sham and denervated mice. Importantly, our findings suggest that there is no change or obvious functional impairment in the response of the β3-AR agonist, CL 316243, to activate IBAT in mice with impaired SNS innervation of IBAT in comparison to sham-operated mice. Together, these findings support the hypothesis that sympathetic innervation of IBAT is not a predominant mediator of OT-elicited increases in non-shivering BAT thermogenesis and reductions of body weight and adiposity in male DIO mice.

Data availability statement

All relevant data is contained within the article: The original contributions presented in the study are included in the article/Supplementary Material, further inquiries can be directed to the corresponding author/s.

Ethics statement

The animal study was approved by VA Puget Sound Health Care System IACUC. The study was conducted in accordance with the local legislation and institutional requirements.

Author contributions

ME: Conceptualization, Data curation, Investigation, Methodology, Project administration, Supervision, Writing – review & editing. HN: Conceptualization, Data curation, Formal analysis, Investigation, Methodology, Project administration, Validation, Writing – review & editing. AD: Conceptualization, Data curation, Formal analysis, Investigation, Methodology, Project administration, Validation, Writing – review & editing. AH: Data curation, Formal analysis, Investigation, Methodology, Project administration, Writing – review & editing. TW-H: Data curation, Formal analysis, Investigation, Methodology, Project administration, Validation, Writing – review & editing. TW: Data curation, Formal analysis, Investigation, Methodology, Writing – review & editing. MH: Data curation, Formal analysis, Investigation, Methodology, Project administration, Supervision, Validation, Writing – review & editing. JS: Data curation, Formal analysis, Investigation, Methodology, Project administration, Supervision, Validation, Writing – review & editing. KO'b: Data curation, Formal analysis, Methodology, Project administration, Supervision, Writing – review & editing. JG: Data curation, Formal analysis, Investigation, Methodology, Project administration, Validation, Writing – review & editing. PH: Conceptualization, Data curation, Formal analysis, Methodology, Project administration, Resources, Supervision, Validation, Writing – review & editing. TM: Methodology, Project administration, Supervision, Validation, Writing – original draft, Writing – review & editing. CS: Data curation, Formal

analysis, Investigation, Methodology, Validation, Writing – review & editing. EP: Project administration, Resources, Supervision, Validation, Writing – review & editing. VR: Methodology, Supervision, Validation, Writing – review & editing. GT: Conceptualization, Methodology, Supervision, Validation, Writing – original draft, Writing – review & editing. JB: Conceptualization, Data curation, Formal analysis, Funding acquisition, Investigation, Methodology, Project administration, Resources, Supervision, Validation, Writing – original draft, Writing – review & editing.

Funding

The author(s) declare financial support was received for the research, authorship, and/or publication of this article. This material was based upon work supported by the Office of Research and Development, Medical Research Service, Department of Veterans Affairs (VA) and the VA Puget Sound Health Care System Rodent Metabolic Phenotyping Core and the Cellular and Molecular Imaging Core of the Diabetes Research Center at the University of Washington and supported by National Institutes of Health (NIH) grant P30DK017047. This work was also supported by the VA Merit Review Award 5 I01BX004102 (JB), from the United States (U.S.) Department of Veterans Affairs Biomedical Laboratory Research and Development Service. Research reported in this publication is a project of the Seattle Institute for Biomedical and Clinical Research, supported by the National Institute of Diabetes and Digestive and Kidney Diseases of the National Institutes of Health under Award Number R01DK115976 (JB). PH's research program also received research support during the project period from NIH grants DK-095980, HL-091333, HL-107256 and a Multi-campus grant from the University of California Office of the President.

Acknowledgments

The authors thank the technical support of Nishi Ivanov. In addition, the authors are appreciative of the efforts by Dr. Michael Schwartz and Dr. Dianne Lattemann for providing feedback throughout the course of these studies.

Conflict of interest

JB had a financial interest in OXT Therapeutics, Inc., a company developing highly specific and stable analogs of oxytocin to treat obesity and metabolic disease. The authors' interests were reviewed and are managed by their local institutions in accordance with their conflict of interest policies.

The remaining authors declare that the research was conducted in the absence of any commercial or financial relationships that could be construed as a potential conflict of interest.

The author(s) declared that they were an editorial board member of Frontiers, at the time of submission. This had no impact on the peer review process and the final decision.

Publisher's note

Author disclaimer

The content is solely the responsibility of the authors and does not necessarily represent the official views of the National Institutes of Health. The contents do not represent the views of the U.S. Department of Veterans Affairs or the United States Government.

Supplementary material

The Supplementary Material for this article can be found online at: https://www.frontiersin.org/articles/10.3389/fendo.2024.1440070/full#supplementary-material

SUPPLEMENTAL STUDY 1

Determine if surgical denervation of IBAT changes the ability of IP tyramine to increase T_{IBAT} in DIO mice. The goal of this study was to determine if IP tyramine-elicited increase in T_{IBAT} requires intact SNS outflow to IBAT in DIO mice. We selected doses of tyramine based on previous studies (105). By design, mice were DIO as determined by both body weight (49.5 ± 1.1 g) and adiposity (13.9 ± 0.8 g fat mass; 31.2 ± 1.4% adiposity) after maintenance on the HFD (60% kcal from fat; N=9-10/group) for approximately 4.25 months prior to sham/denervation procedures and implantation of temperature transponders underneath IBAT. Mice from Study 4 were used in this study and were otherwise treated identically to those used in Study 4. Supplemental Study 1. In sham mice, tyramine (6.4 mg/kg) increased T_{IBAT} at 0.25-h post-injection while the higher dose (19.2 mg/kg) increased T_{IBAT} at 0.25 and 0.5-h post-injection ($P<0.05$; Supplementary Figure 1A). The lower dose also reduced T_{IBAT} at 0.75, 1, 1.25, 1.75, and 3-h post-injection and tended to reduce T_{IBAT} at 2-h post-injection. The higher dose reduced T_{IBAT} at 1, 1.25 and 1.75-h post-injection. Similar findings were apparent when measuring change in T_{IBAT} relative to baseline T_{IBAT} (Supplementary Figure 1B). In denervated mice, tyramine (6.4 mg/kg) was not effective at increasing T_{IBAT} but tended to reduce T_{IBAT} at 0.75-h post-injection ($P<0.05$; Supplementary Figure 1C). The higher dose (19.2 mg/kg) stimulated T_{IBAT} at 0.25 and 0.5-h post-injection and reduced T_{IBAT} at 1.25, 1.5, 1.75 and 2-h post-injection ($P<0.05$). Similar findings were also apparent when measuring change in T_{IBAT} relative to baseline T_{IBAT} (Supplementary Figure 1D).

SUPPLEMENTAL STUDY 2

Determine if surgical denervation of IBAT changes the ability of 4V OT to increase T_{IBAT} in lean mice. The goal of this study was to determine if OT- elicited increase in T_{IBAT} requires intact SNS outflow to IBAT in lean mice. By design, mice were lean as determined by both body weight (29.5 ± 0.7 g) and adiposity (3.3 ± 0.3 g fat mass; 10.4 ± 0.8% adiposity) after maintenance on the chow (16% kcal from fat; N=10/group) for approximately 4-4.25 months prior to sham/denervation procedures and implantation of temperature transponders underneath IBAT. Mice were otherwise treated identically to those used in Study 4. Supplemental Study 2. Only a subset of samples from Study 1B were able to be screened for NE content but all mice were otherwise included in the analysis. In sham mice, 4V OT (5 μg/μL) increased T_{IBAT} at 0.5, 0.75, 1 and 3-h post-injection ($P<0.05$; Suplemental Figure 2A) and tended to stimulate T_{IBAT} at 0.75 (1 μg/μL) and 1.25 (5 μg/μL) h-post-injection. In addition, we found similar findings were apparent when measuring change in T_{IBAT} relative to baseline T_{IBAT} (Supplementary Figure 2B). Similarly, in denervated mice, 4V OT (5 μg/μL) increased T_{IBAT} at 0.75, 1, 1.25 and 3-h post-injection ($P<0.05$; Supplementary Figure 2C) and tended

to stimulate T_{IBAT} at 1.25 (1 μg/μL) -h post-injection. In contrast, 4V OT was unable to stimulate a change in T_{IBAT} relative to baseline T_{IBAT} (Supplementary Figure 2D).

SUPPLEMENTAL STUDY 3

Determine if a centrally (4V) effective dose of OT can increase T_{IBAT} when given into the periphery of lean mice. The goal of this study was to determine if systemic administration of OT (IP) can increase T_{IBAT} at a dose that was effective when given into the 4V in lean mice. By design, mice were lean (31.2 ± 0.8 g) at study onset after maintenance on the chow (16% kcal from fat; N=10/group) for approximately 5 months. Mice did not undergo sham or SNS IBAT denervation procedures but were implanted with temperature transponders underneath IBAT and were otherwise treated similarly to those used in Study 4.Supplemental Study 3. In contrast to the more immediate elevation of T_{IBAT} in response to 4V OT (5 μg/μL), IP OT (5 μg/0.200 mL) resulted in a reduction of T_{IBAT} at 0.25-h post-injection followed by increases in T_{IBAT} at 1.25 and 3-h post-injection ($P<0.05$; Supplementary Figure 3A). IP OT (5 μg/0.200 mL) also tended to stimulate T_{IBAT} at 1.25, 2 and 4-h post-injection. In addition, we found similar findings were apparent when measuring change in T_{IBAT} relative to baseline T_{IBAT} (Supplementary Figure 3B). In addition, a higher dose of OT (10 μg/0.200 mL) produced a similar reduction of T_{IBAT} at 15-min post-injection followed by increases in T_{IBAT} at 1.25, 1.5, 2, and 3-h post-injection ($P<0.05$; Supplementary Figure 3A). IP OT (10 μg/0.200 mL) also tended to stimulate T_{IBAT} at 105 min-post-injection. In addition, we found similar findings were apparent when measuring change in T_{IBAT} relative to baseline T_{IBAT} (Supplementary Figure 3B).

SUPPLEMENTARY FIGURE 1

(A-D). Effect of IP Tyramine on IBAT temperature (T_{IBAT}) in DIO mice (0927.23F). Mice were fed *ad libitum* and maintained on HFD (N=9-10/group) for 4.25 months prior to underdoing sham or SNS denervation procedures and implantation of temperature transponders underneath the left IBAT depot. Mice were allowed to recover for at least 1 week during which time they were adapted to a daily 4-h fast, handling and mock injections. Following completion of Supplemental Study 5, mice subsequently received IP injections (1.5 mL/kg; ≈ 0.07-0.09 mL/mouse) of tyramine (6.4 and 19.4 mg/kg) or vehicle (DMSO) where each animal received each treatment at least 48-h intervals. **(A, C)**, Effect of tyramine on T_{IBAT} in **(A)** sham operated or **(C)** IBAT denervated lean mice; **(B, D)**, Effect of tyramine on change in T_{IBAT} relative to baseline $T_{IBA}T$ (delta T_{IBAT}) in **(B)** sham operated or **(D)** IBAT denervated DIO mice. Data are expressed as mean ± SEM. $^*P<0.05$, $^\dagger 0.05<P<0.1$ tyramine vs. vehicle.

SUPPLEMENTARY FIGURE 2

(A-D) Effect of 4V OT on IBAT temperature (T_{IBAT}) post-sham or IBAT denervation in lean mice. Mice were maintained on chow (16% kcal from fat; N=10/group) for approximately for approximately 4-4.25 months prior to undergoing a sham or bilateral surgical IBAT denervation and implantation of temperature transponders underneath IBAT. Mice were subsequently implanted with 4V cannulas and allowed to recover for 3-4 weeks prior to receiving 4V injections of OT (1 or 5 μg/μL) or vehicle (sterile water) where each animal received each treatment at approximately 48-h intervals. *A/C*, Effect of OT on T_{IBAT} in **(A)** sham operated or **(C)** IBAT denervated lean mice; **(B, D)**, Effect of OT on change in T_{IBAT} relative to baseline $T_{IBA}T$ (delta T_{IBAT}) in **(B)** sham operated or **(D)** IBAT denervated lean mice. Data are expressed as mean ± SEM. $^*P<0.05$, $^\dagger 0.05<P<0.1$ OT vs. vehicle.

SUPPLEMENTARY FIGURE 3

(A-D) Effect of IP OT on IBAT temperature (T_{IBAT}) in lean mice. Mice were maintained on chow (16% kcal from fat; N=9-10/group) for approximately for approximately 2.5 months prior to implantation of temperature transponders underneath IBAT. Mice were subsequently implanted with 4V cannulas and allowed to recover for approximately 2 weeks prior to receiving acute 4V injections of OT or vehicle [data previously published (22)]. Mice subsequently received IP injections of OT (5 μg/0.200 μL or 10 μg/0.200 μL) or vehicle (sterile water) where each animal received each treatment at approximately 48-h intervals. **(A, C)**, Effect of **(A)** lower and **(C)** higher dose of IP OT on T_{IBAT} in lean mice; **(B, D)**, Effect of **(B)** lower and **(D)** higher dose of IP OT on change in T_{IBAT} relative to baseline $T_{IBA}T$ (delta T_{IBAT}) in lean mice. Data are expressed as mean ± SEM. $^*P<0.05$, $^\dagger 0.05<P<0.1$ OT vs. vehicle.

References

1. Gimpl G, Fahrenholz F. The oxytocin receptor system: structure, function, and regulation. *Physiol Rev*. (2001) 81:629–83. doi: 10.1152/physrev.2001.81.2.629

2. Kosfeld M, Heinrichs M, Zak PJ, Fischbacher U, Fehr E. Oxytocin increases trust in humans. *Nature*. (2005) 435:673–6. doi: 10.1038/nature03701

3. Striepens N, Kendrick KM, Maier W, Hurlemann R. Prosocial effects of oxytocin and clinical evidence for its therapeutic potential. *Front Neuroendocrinol*. (2011) 32:426–50. doi: 10.1016/j.yfrne.2011.07.001

4. Blevins JE, Baskin DG. Translational and therapeutic potential of oxytocin as an anti-obesity strategy: Insights from rodents, nonhuman primates and humans. *Physiol Behav*. (2015) 152(Pt B):438–49. doi: 10.1016/j.physbeh.2015.05.023

5. Lawson EA. The effects of oxytocin on eating behaviour and metabolism in humans. *Nat Rev Endocrinol*. (2017) 13:700–9. doi: 10.1038/nrendo.2017.115

6. Lawson EA, Olszewski PK, Weller A, Blevins JE. The role of oxytocin in regulation of appetitive behaviour, body weight and glucose homeostasis. *J Neuroendocrinol*. (2020) 32:e12805. doi: 10.1111/jne.12805

7. McCormack SE, Blevins JE, Lawson EA. Metabolic effects of oxytocin. *Endocrine Rev*. (2020) 41:121–45. doi: 10.1210/endrev/bnz012

8. Altirriba J, Poher AL, Rohner-Jeanrenaud F. Chronic oxytocin administration as a treatment against impaired leptin signaling or leptin resistance in obesity. *Front Endocrinol*. (2015) 6:119. doi: 10.3389/fendo.2015.00119

9. Deblon N, Veyrat-Durebex C, Bourgoin L, Caillon A, Bussier AL, Petrosino S, et al. Mechanisms of the anti-obesity effects of oxytocin in diet-induced obese rats. *PloS One*. (2011) 6:e25565. doi: 10.1371/journal.pone.0025565

10. Morton GJ, Thatcher BS, Reidelberger RD, Ogimoto K, Wolden-Hanson T, Baskin DG, et al. Peripheral oxytocin suppresses food intake and causes weight loss in diet-induced obese rats. *Am J Physiol-Endoc M*. (2012) 302:E134–44. doi: 10.1152/ajpendo.00296.2011

11. Blevins JE, Graham JL, Morton GJ, Bales KL, Schwartz MW, Baskin DG, et al. Chronic oxytocin administration inhibits food intake, increases energy expenditure, and produces weight loss in fructose-fed obese rhesus monkeys. *Am J Physiol Regul Integr Comp Physiol*. (2015) 308:R431–8. doi: 10.1152/ajpregu.00441.2014

12. Noble EE, Billington CJ, Kotz CM, Wang C. Oxytocin in the ventromedial hypothalamic nucleus reduces feeding and acutely increases energy expenditure. *Am J Physiol Regul Integr Comp Physiol*. (2014) 307:R737–45. doi: 10.1152/ajpregu.00118.2014

13. Zhang G, Bai H, Zhang H, Dean C, Wu Q, Li J, et al. Neuropeptide exocytosis involving synaptotagmin-4 and oxytocin in hypothalamic programming of body weight and energy balance. *Neuron*. (2011) 69:523–35. doi: 10.1016/j.neuron.2010.12.036

14. Zhang G, Cai D. Circadian intervention of obesity development via resting-stage feeding manipulation or oxytocin treatment. *Am J Physiol Endocrinol Metab*. (2011) 301:E1004–12. doi: 10.1152/ajpendo.00196.2011

15. Cannon B, Nedergaard J. Brown adipose tissue: function and physiological significance. *Physiol Rev*. (2004) 84:277–359. doi: 10.1152/physrev.00015.2003

16. Morrison SF, Madden CJ, Tupone D. Central neural regulation of brown adipose tissue thermogenesis and energy expenditure. *Cell Metab*. (2014) 19:741–56. doi: 10.1016/j.cmet.2014.02.007

17. Kotz CM, Perez-Leighton CE, Teske JA, Billington CJ. Spontaneous physical activity defends against obesity. *Curr Obes Rep*. (2017) 6:362–70. doi: 10.1007/s13679-017-0288-1

18. Periasamy M, Herrera JL, Reis FCG. Skeletal muscle thermogenesis and its role in whole body energy metabolism. *Diabetes Metab J*. (2017) 41:327–36. doi: 10.4093/dmj.2017.41.5.327

19. Cereijo R, Villarroya J, Villarroya F. Non-sympathetic control of brown adipose tissue. *Int J Obes Supplments*. (2015) 5:S40–4. doi: 10.1038/ijosup.2015.10

20. Lopez M, Alvarez CV, Nogueiras R, Dieguez C. Energy balance regulation by thyroid hormones at central level. *Trends Mol Med*. (2013) 19:418–27. doi: 10.1016/j.molmed.2013.04.004

21. Roberts ZS, Wolden-Hanson TH, Matsen ME, Ryu V, Vaughan CH, Graham JL, et al. Chronic hindbrain administration of oxytocin is sufficient to elicit weight loss in diet-induced obese rats. *Am J Physiol Regul Integr Comp Physiol*. (2017) 313(4):R357–71. doi: 10.1152/ajpregu.00169.2017

22. Edwards MM, Nguyen HK, Herbertson AJ, Dodson AD, Wietecha T, Wolden-Hanson T, et al. Chronic hindbrain administration of oxytocin elicits weight loss in male diet-induced obese mice. *Am J Physiol Regul Integr Comp Physiol*. (2021) 320(4):R471–87. doi: 10.1152/ajpregu.00294.2020

23. Sutton AK, Pei H, Burnett KH, Myers MG Jr., Rhodes CJ, Olson DP. Control of food intake and energy expenditure by Nos1 neurons of the paraventricular hypothalamus. *J Neurosci*. (2014) 34:15306–18. doi: 10.1523/JNEUROSCI.0226-14.2014

24. Yuan J, Zhang R, Wu R, Gu Y, Lu Y. The effects of oxytocin to rectify metabolic dysfunction in obese mice are associated with increased thermogenesis. *Mol Cell Endocrinol*. (2020) 514:110903. doi: 10.1016/j.mce.2020.110903

25. Camerino C. Low sympathetic tone and obese phenotype in oxytocin-deficient mice. *Obesity*. (2009) 17:980–4. doi: 10.1038/oby.2009.12

26. Takayanagi Y, Kasahara Y, Onaka T, Takahashi N, Kawada T, Nishimori K. Oxytocin receptor-deficient mice developed late-onset obesity. *Neuroreport*. (2008) 19:951–5. doi: 10.1097/WNR.0b013e3283021ca9

27. Wu Z, Xu Y, Zhu Y, Sutton AK, Zhao R, Lowell BB, et al. An obligate role of oxytocin neurons in diet induced energy expenditure. *PloS One*. (2012) 7:e45167. doi: 10.1371/journal.pone.0045167

28. Kasahara Y, Sato K, Takayanagi Y, Mizukami H, Ozawa K, Hidema S, et al. Oxytocin receptor in the hypothalamus is sufficient to rescue normal thermoregulatory function in male oxytocin receptor knockout mice. *Endocrinology*. (2013) 154:4305–15. doi: 10.1210/en.2012-2206

29. Kasahara Y, Tateishi Y, Hiraoka Y, Otsuka A, Mizukami H, Ozawa K, et al. Role of the oxytocin receptor expressed in the rostral medullary raphe in thermoregulation during cold conditions. *Front Endocrinol*. (2015) 6:180. doi: 10.3389/fendo.2015.00180

30. Harshaw C, Leffel JK, Alberts JR. Oxytocin and the warm outer glow: Thermoregulatory deficits cause huddling abnormalities in oxytocin-deficient mouse pups. *Hormones Behav*. (2018) 98:145–58. doi: 10.1016/j.yhbeh.2017.12.007

31. Xi D, Long C, Lai M, Casella A, O'Lear L, Kublaoui B, et al. Ablation of oxytocin neurons causes a deficit in cold stress response. *J Endocrine Soc*. (2017) 1:1041–55. doi: 10.1210/js.2017-00136

32. Thureson-Klein A, Mill-Hyde B, Barnard T, Lagercrantz H. Ultrastructrual effects of chemical sympathectomy on brown adipose tissue. *J Neurocytol*. (1976) 5:677–90. doi: 10.1007/BF01181581

33. Depocas F, Foster DO, Zaror-Behrens G, Lacelle S, Nadeau B. Recovery of function in sympathetic nerves of interscapular brown adipose tissue of rats treated with 6-hydroxydopamine. *Can J Physiol Pharmacol*. (1984) 62:1327–32. doi: 10.1139/y84-222

34. Wang LY, Murphy RR, Hanscom B, Li G, Millard SP, Petrie EC, et al. Cerebrospinal fluid norepinephrine and cognition in subjects across the adult age span. *Neurobiol Aging*. (2013) 34:2287–92. doi: 10.1016/j.neurobiolaging.2013.04.007

35. Williams DL, Bowers RR, Bartness TJ, Kaplan JM, Grill HJ. Brainstem melanocortin 3/4 receptor stimulation increases uncoupling protein gene expression in brown fat. *Endocrinology*. (2003) 144:4692–7. doi: 10.1210/en.2003-0440

36. De Boer SF, van der Gugten J. Daily variations in plasma noradrenaline. *Adrenaline Corticosterone Concentrations Rats Physiol Behav*. (1987) 40:323–8. doi: 10.1016/0031-9384(87)90054-0

37. Davidovic V, Petrovic VM. Diurnal variations in the catecholamine content in rat tissues Effects of exogenous noradrenaline. *Arch Iniernationales Physiologie Biochimie*. (1981) 89:457–60. doi: 10.3109/13813458109082642

38. Suarez J, Rivera P, Arrabal S, Crespillo A, Serrano A, Baixeras E, et al. Oleoylethanolamide enhances beta-adrenergic-mediated thermogenesis and white-to-brown adipocyte phenotype in epididymal white adipose tissue in rat. *Dis Models Mech*. (2014) 7:129–41. doi: 10.1242/dmm.013110

39. Malinowska B, Schlicker E. Further evidence for differences between cardiac atypical beta-adrenoceptors and brown adipose tissue beta3-adrenoceptors in the pithed rat. *Br J Pharmacol*. (1997) 122:1307–14. doi: 10.1038/sj.bjp.0701516

40. Lateef DM, Abreu-Vieira G, Xiao C, Reitman ML. Regulation of body temperature and brown adipose tissue thermogenesis by bombesin receptor subtype-3. *Am J Physiol Endocrinol Metab*. (2014) 306:E681–7. doi: 10.1152/ajpendo.00615.2013

41. Ma S, Yu H, Zhao Z, Luo Z, Chen J, Ni Y, et al. Activation of the cold-sensing TRPM8 channel triggers UCP1-dependent thermogenesis and prevents obesity. *J Mol Cell Biol*. (2012) 4:88–96. doi: 10.1093/jmcb/mjs001

42. Liskiewicz D, Zhang Q, Barthem CS, Jastroch M, Liskiewicz A, Khajavi N, et al. Neuronal loss of TRPM8 leads to obesity and glucose intolerance in male mice. *Mol Metab*. (2023) 72:101714. doi: 10.1016/j.molmet.2023.101714

43. Modi ME, Inoue K, Barrett CE, Kittelberger KA, Smith DG, Landgraf R, et al. Melanocortin receptor agonists facilitate oxytocin-dependent partner preference formation in the prairie vole. *Neuropsychopharmacology: Off Publ Am Coll Neuropsychopharmacol*. (2015) 40:1856–65. doi: 10.1038/npp.2015.35

44. Olszewski PK, Wirth MM, Shaw TJ, Grace MK, Billington CJ, Giraudo SQ, et al. Role of alpha-MSH in the regulation of consummatory behavior: immunohistochemical evidence. *Am J Physiol Regul Integr Comp Physiol*. (2001) 281: R673–80. doi: 10.1152/ajpregu.2001.281.2.R673

45. Semple E, Shalabi F, Hill JW. Oxytocin neurons enable melanocortin regulation of male sexual function in mice. *Mol Neurobiol*. (2019) 56:6310–23. doi: 10.1007/s12035-019-1514-5

46. Blevins JE, Thompson BW, Anekonda VT, Ho JM, Graham JL, Roberts ZS, et al. Chronic CNS oxytocin signaling preferentially induces fat loss in high fat diet-fed rats by enhancing satiety responses and increasing lipid utilization. *Am J Physiol-Reg I*. (2016) 310(7):R640–58. doi: 10.1152/ajpregu.00220.2015

47. Bremer AA, Stanhope KL, Graham JL, Cummings BP, Wang W, Saville BR, et al. Fructose-fed rhesus monkeys: a nonhuman primate model of insulin resistance, metabolic syndrome, and type 2 diabetes. *Clin Trans Sci*. (2011) 4:243–52. doi: 10.1111/cts.2011.4.issue-4

48. Blevins JE, Moralejo DH, Wolden-Hanson TH, Thatcher BS, Ho JM, Kaiyala KJ, et al. Alterations in activity and energy expenditure contribute to lean phenotype in Fischer 344 rats lacking the cholecystokinin-1 receptor gene. *Am J Physiol Regul Integr Comp Physiol*. (2012) 303:R1231–40. doi: 10.1152/ajpregu.00393.2012

49. Cummings BP, Digitale EK, Stanhope KL, Graham JL, Baskin DG, Reed BJ, et al. Development and characterization of a novel rat model of type 2 diabetes mellitus: the UC Davis type 2 diabetes mellitus UCD-T2DM rat. *Am J Physiol Regul Integr Comp Physiol*. (2008) 295:R1782–93. doi: 10.1152/ajpregu.90635.2008

50. Livak KJ, Schmittgen TD. Analysis of relative gene expression data using real-time quantitative PCR and the 2(-Delta Delta C(T)) Method. *Methods*. (2001) 25:402–8. doi: 10.1006/meth.2001.1262

51. Nguyen NL, Barr CL, Ryu V, Cao Q, Xue B, Bartness TJ. Separate and shared sympathetic outflow to white and brown fat coordinately regulate thermoregulation and beige adipocyte recruitment. *Am J Physiol Regul Integr Comp Physiol*. (2016) 312 (1):R132–45. doi: 10.1152/ajpregu.00344.2016

52. Cao Q, Jing J, Cui X, Shi H, Xue B. Sympathetic nerve innervation is required for beigeing in white fat. *Physiol Rep*. (2019) 7:e14031. doi: 10.14814/phy2.14031

53. Klingenspor M, Meywirth A, Stohr S, Heldmaier G. Effect of unilateral surgical denervation of brown adipose tissue on uncoupling protein mRNA level and cytochrom-c-oxidase activity in the Djungarian hamster. *J Comp Physiol B*. (1994) 163:664–70. doi: 10.1007/BF00369517

54. Fischer AW, Schlein C, Cannon B, Heeren J, Nedergaard J. Intact innervation is essential for diet-induced recruitment of brown adipose tissue. *Am J Physiol Endocrinol Metab*. (2019) 316:E487–503. doi: 10.1152/ajpendo.00443.2018

55. Bajzer M, Olivieri M, Haas MK, Pfluger PT, Magrisso IJ, Foster MT, et al. Cannabinoid receptor 1 (CB1) antagonism enhances glucose utilisation and activates brown adipose tissue in diet-induced obese mice. *Diabetologia*. (2011) 54:3121–31. doi: 10.1007/s00125-011-2302-6

56. Labbe SM, Caron A, Festuccia WT, Lecomte R, Richard D. Interscapular brown adipose tissue denervation does not promote the oxidative activity of inguinal white adipose tissue in male mice. *Am J Physiol Endocrinol Metab*. (2018) 315:E815–24. doi: 10.1152/ajpendo.00210.2018

57. Bahler L, Verberne HJ, Admiraal WM, Stok WJ, Soeters MR, Hoekstra JB, et al. Differences in sympathetic nervous stimulation of brown adipose tissue between the young and old, and the lean and obese. *J Nucl medicine: Off publication Soc Nucl Med*. (2016) 57:372–7. doi: 10.2967/jnumed.115.165829

58. Zoico E, Rubele S, De Caro A, Nori N, Mazzali G, Fantin F, et al. Brown and beige adipose tissue and aging. *Front Endocrinol*. (2019) 10:368. doi: 10.3389/fendo.2019.00368

59. Doslikova B, Tchir D, McKinty A, Zhu X, Marks DL, Baracos VE, et al. Convergent neuronal projections from paraventricular nucleus, parabrachial nucleus, and brainstem onto gastrocnemius muscle, white and brown adipose tissue in male rats. *J Comp Neurol*. (2019) 527:2826–42. doi: 10.1002/cne.24710

60. Oldfield BJ, Giles ME, Watson A, Anderson C, Colvill LM, McKinley MJ. The neurochemical characterisation of hypothalamic pathways projecting polysynaptically to brown adipose tissue in the rat. *Neuroscience*. (2002) 110:515–26. doi: 10.1016/S0306-4522(01)00555-3

61. Shi H, Bartness TJ. Neurochemical phenotype of sympathetic nervous system outflow from brain to white fat. *Brain Res Bull*. (2001) 54:375–85. doi: 10.1016/S0361-9230(00)00455-X

62. Stanley S, Pinto S, Segal J, Perez CA, Viale A, DeFalco J, et al. Identification of neuronal subpopulations that project from hypothalamus to both liver and adipose tissue polysynaptically. *Proc Natl Acad Sci U.S.A*. (2010) 107:7024–9. doi: 10.1073/pnas.1002790107

63. Rinaman L. Oxytocinergic inputs to the nucleus of the solitary tract and dorsal motor nucleus of the vagus in neonatal rats. *J Comp Neurol*. (1998) 399:101–9. doi: 10.1002/(ISSN)1096-9861

64. Sawchenko PE, Swanson LW. Immunohistochemical identification of neurons in the paraventricular nucleus of the hypothalamus that project to the medulla or to the spinal cord in the rat. *J Comp Neurol*. (1982) 205:260–72. doi: 10.1002/cne.902050306

65. Bamshad M, Song CK, Bartness TJ. CNS origins of the sympathetic nervous system outflow to brown adipose tissue. *Am J Physiol*. (1999) 276:R1569–78. doi: 10.1152/ajpregu.1999.276.6.R1569

66. Cano G, Passerin AM, Schiltz JC, Card JP, Morrison SF, Sved AF. Anatomical substrates for the central control of sympathetic outflow to interscapular adipose tissue during cold exposure. *J Comp Neurol*. (2003) 460:303–26. doi: 10.1002/cne.10643

67. Ong ZY, Bongiorno DM, Hernando MA, Grill HJ. Effects of endogenous oxytocin receptor signaling in nucleus tractus solitarius on satiation-mediated feeding and thermogenic control in male rats. *Endocrinology*. (2017) 158:2826–36. doi: 10.1210/en.2017-00200

68. Kong D, Tong Q, Ye C, Koda S, Fuller PM, Krashes MJ, et al. GABAergic RIP-Cre neurons in the arcuate nucleus selectively regulate energy expenditure. *Cell*. (2012) 151:645–57. doi: 10.1016/j.cell.2012.09.020

69. Morrison SF, Nakamura K. Central neural pathways for thermoregulation. *Front bioscience*. (2011) 16:74–104. doi: 10.2741/3677

70. Morrison SF. Central control of body temperature. *F1000Research*. (2016) 5. doi: 10.12688/f1000research

71. Reed N, Fain JN. Stimulation of respiration in brown fat cells by epinephrine, dibutyryl-3',5'-adenosine monophosphate, and m-chloro(carbonyl cyanide) phenylhydrazone. *J Biol Chem*. (1968) 243:2843–8. doi: 10.1016/S0021-9258(18)93348-X

72. Strosberg AD. Structure and function of the beta 3-adrenergic receptor. *Annu Rev Pharmacol Toxicol*. (1997) 37:421–50. doi: 10.1146/annurev.pharmtox.37.1.421

73. Sharara-Chami RI, Joachim M, Mulcahey M, Ebert S, Majzoub JA. Effect of epinephrine deficiency on cold tolerance and on brown adipose tissue. *Mol Cell Endocrinol*. (2010) 328:34–9. doi: 10.1016/j.mce.2010.06.019

74. Strack AM, Sawyer WB, Platt KB, Loewy AD. CNS cell groups regulating the sympathetic outflow to adrenal gland as revealed by transneuronal cell body labeling with pseudorabies virus. *Brain Res*. (1989) 491:274–96. doi: 10.1016/0006-8993(89)90063-2

75. Dum RP, Levinthal DJ, Strick PL. The mind-body problem: Circuits that link the cerebral cortex to the adrenal medulla. *Proc Natl Acad Sci U.S.A*. (2019) 116:26321–8. doi: 10.1073/pnas.1902297116

76. Sakamoto T, Sugimoto S, Uekita T. Effects of intraperitoneal and intracerebroventricular injections of oxytocin on social and emotional behaviors in pubertal male mice. *Physiol Behav*. (2019) 212:112701. doi: 10.1016/j.physbeh.2019.112701

77. Asker M, Krieger JP, Liles A, Tinsley IC, Borner T, Maric I, et al. Peripherally restricted oxytocin is sufficient to reduce food intake and motivation, while CNS entry is required for locomotor and taste avoidance effects. *Diabetes Obes Metab*. (2023) 25:856–77. doi: 10.1111/dom.14937

78. Iwasaki Y, Kumari P, Wang L, Hidema S, Nishimori K, Yada T. Relay of peripheral oxytocin to central oxytocin neurons via vagal afferents for regulating feeding. *Biochem Biophys Res Commun*. (2019) 519:553–8. doi: 10.1016/j.bbrc.2019.09.039

79. Iwasaki Y, Maejima Y, Suyama S, Yoshida M, Arai T, Katsurada K, et al. Peripheral oxytocin activates vagal afferent neurons to suppress feeding in normal and leptin-resistant mice: a route for ameliorating hyperphagia and obesity. *Am J Physiol Regul Integr Comp Physiol*. (2015) 308:R360–9. doi: 10.1152/ajpregu.00344.2014

80. Ho JM, Anekonda VT, Thompson BW, Zhu M, Curry RW, Hwang BH, et al. Hindbrain oxytocin receptors contribute to the effects of circulating oxytocin on food intake in male rats. *Endocrinology*. (2014) 155:2845–57. doi: 10.1210/en.2014-1148

81. Schaffler A, Binart N, Scholmerich J, Buchler C. Hypothesis paper Brain talks with fat–evidence for a hypothalamic-pituitary-adipose axis? *Neuropeptides*. (2005) 39:363–7. doi: 10.1016/j.npep.2005.06.003

82. Yi KJ, So KH, Hata Y, Suzuki Y, Kato D, Watanabe K, et al. The regulation of oxytocin receptor gene expression during adipogenesis. *J Neuroendocrinol*. (2015) 27:335–42. doi: 10.1111/jne.12268

83. Hicks C, Ramos L, Reekie T, Misagh GH, Narlawar R, Kassiou M, et al. Body temperature and cardiac changes induced by peripherally administered oxytocin, vasopressin and the non-peptide oxytocin receptor agonist WAY 267,464: a biotelemetry study in rats. *Br J Pharmacol*. (2014) 171:2868–87. doi: 10.1111/bph.12613

84. Ring RH, Malberg JE, Potestio L, Ping J, Boikess S, Luo B, et al. Anxiolytic-like activity of oxytocin in male mice: behavioral and autonomic evidence, therapeutic implications. *Psychopharmacology*. (2006) 185:218–25. doi: 10.1007/s00213-005-0293-z

85. Kohli S, King MV, Williams S, Edwards A, Ballard TM, Steward LJ, et al. Oxytocin attenuates phencyclidine hyperactivity and increases social interaction and nucleus accumben dopamine release in rats. *Neuropsychopharmacology: Off Publ Am Coll Neuropsychopharmacol*. (2019) 44:295–305. doi: 10.1038/s41386-018-0171-0

86. Xu Y, Kim ER, Fan S, Xia Y, Xu Y, Huang C, et al. Profound and rapid reduction in body temperature induced by the melanocortin receptor agonists. *Biochem Biophys Res Commun*. (2014) 451:184–9. doi: 10.1016/j.bbrc.2014.07.079

87. Lute B, Jou W, Lateef DM, Goldgof M, Xiao C, Pinol RA, et al. Biphasic effect of melanocortin agonists on metabolic rate and body temperature. *Cell Metab*. (2014) 20:333–45. doi: 10.1016/j.cmet.2014.05.021

88. Jain S, Panyutin A, Liu N, Xiao C, Pinol RA, Pundir P, et al. Melanotan II causes hypothermia in mice by activation of mast cells and stimulation of histamine 1 receptors. *Am J Physiol Endocrinol Metab*. (2018) 315:E357–66. doi: 10.1152/ajpendo.00024.2018

89. Blouquit MF, Koubi H, Geloen A, Gripois D. Norepinephrine content in the brown adipose tissue of the developing obese Zucker rat. *Hormone Metab Res = Hormon- und Stoffwechselforschung = Hormones metabolisme*. (1991) 23:239. doi: 10.1055/s-2007-1003662

90. Blouquit MF, Gripois D. Tyrosine hydroxylase activity in the brown adipose tissue of the obese Zucker rat during development. *Hormone Metab Res = Hormon- und Stoffwechselforschung = Hormones metabolisme*. (1990) 22:123. doi: 10.1055/s-2007-1004865

91. Blouquit MF, Geloen A, Koubi H, Edwards D, Gripois D. Decreased norepinephrine turnover rate in the brown adipose tissue of pre-obese fa/fa Zucker rats. *J Dev Physiol*. (1993) 19:247–51.

92. Leitner BP, Huang S, Brychta RJ, Duckworth CJ, Baskin AS, McGehee S, et al. Mapping of human brown adipose tissue in lean and obese young men. *Proc Natl Acad Sci U.S.A*. (2017) 114:8649–54. doi: 10.1073/pnas.1705287114

93. Vijgen GH, Bouvy ND, Teule GJ, Brans B, Schrauwen P, van Marken Lichtenbelt WD. Brown adipose tissue in morbidly obese subjects. *PloS One*. (2011) 6:e17247. doi: 10.1371/journal.pone.0017247

94. Valentine JM, Ahmadian M, Keinan O, Abu-Odeh M, Zhao P, Zhou X, et al. beta3-Adrenergic receptor downregulation leads to adipocyte catecholamine resistance in obesity. *J Clin Invest*. (2022) 132. doi: 10.1172/JCI153357

95. de Almeida DL, Fabricio GS, Trombini AB, Pavanello A, Tofolo LP, da Silva Ribeiro TA, et al. Early overfeed-induced obesity leads to brown adipose tissue hypoactivity in rats. *Cell Physiol Biochemistry: Int J Exp Cell Physiology Biochemistry Pharmacol*. (2013) 32:1621–30. doi: 10.1159/000356598

96. Lerea JS, Ring LE, Hassouna R, Chong AC, Szigeti-Buck K, Horvath TL, et al. Reducing adiposity in a critical developmental window has lasting benefits in mice. *Endocrinology*. (2016) 157:666–78. doi: 10.1210/en.2015-1753

97. Rangel-Azevedo C, Santana-Oliveira DA, Miranda CS, Martins FF, Mandarim-de-Lacerda CA, Souza-Mello V. Progressive brown adipocyte dysfunction: Whitening and impaired nonshivering thermogenesis as long-term obesity complications. *J Nutr Biochem*. (2022) 105:109002. doi: 10.1016/j.jnutbio.2022.109002

98. Edwards MM, Nguyen HK, Dodson AD, Herbertson AJ, Wietecha TA, Wolden-Hanson T, et al. Effects of combined oxytocin and beta-3 receptor agonist (CL 316243) treatment on body weight and adiposity in male diet-induced obese rats. *Front Physiol*. (2021) 12. doi: 10.3389/fphys.2021.725912

99. Baker JG. The selectivity of beta-adrenoceptor antagonists at the human beta1, beta2 and beta3 adrenoceptors. *Br J Pharmacol*. (2005) 144:317–22. doi: 10.1038/sj.bjp.0706048

100. Hutchinson DS, Chernogubova E, Sato M, Summers RJ, Bengtsson T. Agonist effects of zinterol at the mouse and human beta(3)-adrenoceptor. *Naunyn Schmiedebergs Arch Pharmacol*. (2006) 373:158–68. doi: 10.1007/s00210-006-0056-3

101. Susulic VS, Frederich RC, Lawitts J, Tozzo E, Kahn BB, Harper ME, et al. Targeted disruption of the beta 3-adrenergic receptor gene. *J Biol Chem*. (1995) 270:29483–92. doi: 10.1074/jbc.270.49.29483

102. Grujic D, Susulic VS, Harper ME, HimmsHagen J, Cunningham BA, Corkey BE, et al. beta 3-adrenergic receptors on white and brown adipocytes mediate beta 3-selective agonist-induced effects on energy expenditure, insulin secretion, and food intake - A study using transgenic and gene knockout mice. *J Biol Chem*. (1997) 272:17686–93. doi: 10.1074/jbc.272.28.17686

103. Ootsuka Y, Blessing WW, Nalivaiko E. Selective blockade of 5-HT2A receptors attenuates the increased temperature response in brown adipose tissue to restraint stress in rats. *Stress*. (2008) 11:125–33. doi: 10.1080/10253890701638303

104. Harris WH, Foster DO, Ma SW, Yamashiro S, Langlais-Burgess LA. The noradrenaline content and innervation of brown adipose tissue in the young rabbit. *Can J Physiol Pharmacol*. (1986) 64:561–7. doi: 10.1139/y86-093

105. Taborsky GJ Jr., Mei Q, Hackney DJ, Figlewicz DP, LeBoeuf R, Mundinger TO. Loss of islet sympathetic nerves and impairment of glucagon secretion in the NOD mouse: relationship to invasive insulitis. *Diabetologia*. (2009) 52:2602–11. doi: 10.1007/s00125-009-1494-5

106. Gilliam LK, Palmer JP, Taborsky GJ Jr. Tyramine-mediated activation of sympathetic nerves inhibits insulin secretion in humans. *J Clin Endocrinol Metab*. (2007) 92:4035–8. doi: 10.1210/jc.2007-0536

107. Bartness TJ, Vaughan CH, Song CK. Sympathetic and sensory innervation of brown adipose tissue. *Int J Obes (Lond)*. (2010) 34 Suppl 1:S36–42. doi: 10.1038/ijo.2010.182

108. Bal NC, Maurya SK, Singh S, Wehrens XH, Periasamy M. Increased reliance on muscle-based thermogenesis upon acute minimization of brown adipose tissue function. *J Biol Chem*. (2016) 291:17247–57. doi: 10.1074/jbc.M116.728188

109. de Jong JM, Larsson O, Cannon B, Nedergaard J. A stringent validation of mouse adipose tissue identity markers. *Am J Physiol Endocrinol Metab*. (2015) 308:E1085–105. doi: 10.1152/ajpendo.00023.2015

frontiers | Frontiers in Endocrinology

TYPE Original Research
PUBLISHED 20 August 2024
DOI 10.3389/fendo.2024.1390564

OPEN ACCESS

EDITED BY
Heidi de Wet,
University of Oxford, United Kingdom

REVIEWED BY
Elif Bulbul,
University of Health Sciences, Türkiye
Carlos Manuel Zapata-Martín del Campo,
National Institute of Cardiology Ignacio Chavez, Mexico

*CORRESPONDENCE
Hong Qi
1529821185@qq.com

†These authors have contributed equally to this work and share first authorship

RECEIVED 28 March 2024
ACCEPTED 18 July 2024
PUBLISHED 20 August 2024

CITATION
Gan Y, Tian F, Fan X, Wang H, Zhou J, Yang N and Qi H (2024) A study of the relationship between social support, depression, alexithymia and glycemic control in patients with type 2 diabetes mellitus: a structural equation modeling approach.
Front. Endocrinol. 15:1390564.
doi: 10.3389/fendo.2024.1390564

A study of the relationship between social support, depression, alexithymia and glycemic control in patients with type 2 diabetes mellitus: a structural equation modeling approach

Yuqin Gan[1,2,3†], Fengxiang Tian[3†], Xinxin Fan[2,3], Hui Wang[4], Jian Zhou[5], Naihui Yang[3] and Hong Qi[1*]

[1]Clinical Medical College of Chengdu Medical College, First Affiliated Hospital, Chengdu, China, [2]The Fourth Hospital of West China, Sichuan University, Chengdu, China, [3]School of Nursing, Chengdu Medical College, Chengdu, China, [4]Nursing Department, First Affiliated Hospital of Chengdu Medical College, Chengdu, China, [5]Department of Rheumatology and Immunology, The First Affiliated Hospital of Chengdu Medical College, Chengdu, China

Aim: The aim of this research was to ascertain the correlations between alexithymia, social support, depression, and glycemic control in patients diagnosed with type 2 diabetes mellitus. Additionally, this study sought to delve into the potential mediating effects of social support and depression in the relationship between alexithymia and glycemic control.

Method: A purposive sampling methodology was employed to select a cohort of 318 patients afflicted with type 2 diabetes mellitus, hailing from a care establishment situated in Chengdu City. This investigation embraced a cross-sectional framework, wherein instruments such as the General Information Questionnaire, the Toronto Alexithymia Scale 20, the Social Support Rating Scale, and the Hamilton Depression Scale were judiciously administered. The primary objective of this endeavor was to unravel the interplay that exists amongst alexithymia, social support, depression, and glycemic control. The inquiry discerned these interrelationships through both univariate and correlational analyses, subsequently delving into a comprehensive exploration of the mediating ramifications engendered by social support and depression in the nexus between alexithymia and glycemic control.

Results: The HbA_{1c} level of patients diagnosed with type 2 diabetes mellitus was recorded as (8.85 ± 2.107), and their current status with regards to alexithymia, social support, and depression were measured as (58.05 ± 4.382), (34.29 ± 4.420), and (7.17 ± 3.367), respectively. Significant correlations were found between HbA_{1c} and alexithymia (R=0.392, P<0.01), social support (R=-0.338, P<0.01), and depression (R=0.509, P<0.01). Moreover, alexithymia correlation with social support (R=-0.357, P<0.01) and with depression (R=0.345, P<0.01). Regarding the mediation analysis, the direct effect of alexithymia on HbA_{1c} was calculated to be 0.158, while the indirect effect through social support and

depression were 0.086 and 0.149, respectively. The total effect value was determined to be 0.382, with the mediating effect accounting for 59.95%, and the direct effect accounting for 40.31%.

Conclusion: Alexithymia exerts both direct and indirect adverse effects on glycemic control, thereby exacerbating disease outcomes. Hence, it is imperative to prioritize the mental health status of individuals with type 2 diabetes to enhance overall well-being, ameliorate diabetes-related outcomes, elevate patients' quality of life, and alleviate the psychological distress and financial burden associated with the condition.

KEYWORDS

type 2 diabetes mellitus, glycemic control, alexithymia, social support, depression, structural equation modeling

1 Introduction

In accordance with a survey conducted by the International Diabetes Federation(IDF) (1), the global prevalence of diabetes mellitus is anticipated to reach approximately 10.5% (536.6 million) in 2021, projecting an escalation to 12.2% (783.2 million) by the year 2045. In tandem with the rapid advancement of China's economy and urbanization, coupled with elevated living standards and population aging, among other factors, the annual increment in the prevalence of diabetes mellitus has become discernible (2). The prevalence of diabetes mellitus among individuals aged 18 years and above is presently documented at 11.2%, representing the highest prevalence nationwide, with type 2 diabetes mellitus (T2DM) constituting over 90% of these cases (3). Enhancing the degree of glycemic control to impede the progression of complications stands as the principal therapeutic objective for individuals with diabetes (4). It serves as the quintessential standard for averting both microvascular and macrovascular complications in the context of diabetes mellitus (5). Clinically, glycated hemoglobin (HbA_{1c}) emerges as the prevailing benchmark for assessing glycemic control, with a diagnostic threshold set at 7.0% (6). Maintaining blood glucose concentrations within the normative range has the potential to diminish both the frequency and severity of diabetic complications. Conversely, an elevated HbA_{1c} level signifies suboptimal glycemic control over the preceding 2-3 months, thereby escalating the susceptibility to complications, encompassing both microvascular and macrovascular manifestations (7). Prolonged hyperglycemia not only heightens the risk of such complications but also amplifies the likelihood of mortality among affected individuals. Notably, the glycemic control rate among Chinese diabetic patients stands at a modest 50.1% (6), indicating a subpar level that warrants further enhancement. Henceforth, it becomes imperative to ameliorate the degree of glycemic control among individuals afflicted with T2DM with the dual objective of impeding the progression of diabetic complications and concurrently mitigating the psychological burden borne by the patients. Such interventions aim to actualize the enhancement of patients' quality of life and the alleviation of the associated economic burdens.

T2DM exerts a substantial financial encumbrance upon individuals and their families, owing to its irreversible nature, protracted duration, recurring nature, myriad complications, and the elevated costs associated with its treatment. Liu et al. (8) prognosticate that the aggregate expenditure for adult diabetes in China will surge from US$250.2 billion in 2020 to US$460.4 billion in 2030. This escalation, reflecting an annual growth rate of 6.32% over the period from 2020 to 2030 (5.99% - 6.65%), surpasses the rate of Gross Domestic Product (GDP) growth. This financial burden encompasses both direct costs linked to the prevention and treatment of diabetes and its associated complications, as well as indirect costs encompassing disability, loss of work productivity, and mortality (9). Moreover, the enduring nature of diabetes treatment elevates the susceptibility of patients to psychological disorders (10). These psychological disturbances, in turn, precipitate diminished adherence to treatment regimens and self-management protocols, thereby fostering suboptimal glycemic control. Consequently, the escalated risk of diabetes-related complications and mortality ensues, culminating in a deterioration of patients' quality of life and an augmentation of healthcare expenditures (11). The involvement of psychological factors in the etiopathogenesis of chronic diseases is awakening the interest of the scientific community (12). Empirical investigations (13) delineate that the incidence of psychological disorders among diabetic patients surpasses that of their non-diabetic counterparts by more than twofold. Consequently, there exists an exigency to enhance the mental well-being of diabetic patients with a view to ameliorating their quality of life and alleviating the associated economic burdens. The prevalence of alexithymia among diabetic patients exceeds that observed in the general population (14). Notably, its detection rate reaches as high as 75.8% in diabetic patients from foreign cohorts (15), and up to 45% among older people diabetic individuals in China, reflecting an

upward trajectory (16, 17). Alexithymia exerts adverse effects on clinical manifestations, disease perception, severity, progression, and treatment adherence. These repercussions, in turn, contribute to unfavorable disease outcomes, a diminished quality of life for patients (18, 19), and an augmented risk of mortality (20). Fares et al. (21) discerned a positive correlation between alexithymia and glycemic control in patients diagnosed with T2DM. Notably, the incidence of severe hyperglycemic episodes was threefold higher among individuals with alexithymia compared to those devoid of this psychological disposition. Furthermore, hospitalizations due to hyperglycemia were five times more frequent in patients exhibiting alexithymia compared to their counterparts lacking this psychological trait.

Social support assumes a buffering role in mental health, serving as a protective mechanism against the onset of physical and psychological disorders induced by heightened stress (22). It constitutes a pivotal element in fostering the treatment efficacy and recuperative processes in individuals diagnosed with diabetes (23). Furthermore, social support facilitates enhanced self-management strategies, thereby ameliorating patients' lifestyles and fortifying disease management, ultimately contributing to an augmentation in glycemic control (24). Its affirmative impact is conspicuous in the context of disease treatment and recuperation (23). Diminished levels of social support can amplify the incidence of alexithymia by constricting the patient's social milieu, inducing feelings of isolation, and curtailing the capacity to engage in dialogue or express emotions during periods of heightened psychological stress (25).

Concurrently, the progression of diabetes mellitus, coupled with the protracted course of treatment, precipitates the development of complications and an escalation in treatment expenses. Consequently, there is a commensurate augmentation in the psychological burden borne by the patient, with depression emerging as one of the most prevalent negative emotional outcomes (26). The prevalence of depression in individuals with diabetes ranges from 22% to 62% and, in some instances, may ascend to 73% (27), reflecting a prevalence approximately fivefold higher than that observed in the general population (28). Depression is associated with an elevated incidence of complications in diabetic patients, contributing to an increased disability rate and a curtailed life expectancy (29, 30). Moreover, it amplifies mortality rates by approximately 110% (31). Depression further engenders the manifestation of severe psychological symptoms in individuals with T2DM, fostering diminished treatment adherence, exerting a discernible impact on glycemic control, and augmenting the prevalence of alexithymia (32, 33).

In conclusion, a correlation exists among social support, depression, alexithymia, and glycemic control in patients diagnosed with T2DM; however, no study has systematically investigated the precise mechanistic pathways interconnecting these four variables. The current study delved into elucidating the roles of social support, depression, and alexithymia in influencing glycemic control, thereby establishing a foundational framework for clinical practitioners to enhance glycemic control strategies for individuals with T2DM.

2 Materials and methods

2.1 Study design and participants

This study is of a cross-sectional nature, and it recruited individuals diagnosed with T2DM who sought medical care within the endocrine inpatient department and outpatient clinic of a tertiary healthcare facility situated in Chengdu during the period spanning from October 2022 to June 2023.Inclusion criteria: ① Patients who conformed to the diagnostic standards set forth by the World Health Organization in 1999 for T2DM (34). ② Patients with a confirmed T2DM diagnosis for a duration of no less than 6 months. ③Age range: 18 years to 80 years. ④Cognitively sound, capable of regular communication, and possessing a comprehensive understanding of the questionnaire's content. ⑤Individuals who have provided informed consent and willingly enrolled in this investigation. Exclusion criteria: ① Patients presenting severe chronic ailments, such as those affecting the cardiovascular, cerebral, hepatic, renal, or pulmonary systems; ② Patients afflicted with psychiatric disorders or cognitive impairments (excluding depressed patients); ③ Patients in critical medical states, precluding their ability to collaborate with the investigative procedures.

Sample size calculation:In accordance with the Kendall sample size estimation method, the sample size was determined to be a minimum of ten times the number of variables (35). This study incorporated four research instruments, which included a 12-item General Information Questionnaire, a 3-item Social Support Rating Scale, and a 5-item Hamilton Depression Scale, a 3-item Toronto Narrative Alexithymia Scale, totaling 23 items. Hence, the total sample size comprised 230 cases. To safeguard against potential sample attrition influencing the study outcomes, a 20% sample loss margin was incorporated, resulting in a final sample size of 276 cases, as dictated by the requirements of structural equation modeling. The final sample size of 318 cases was included in conjunction with the actual clinical survey

2.2 Data collection

Prior to commencing the survey, the researcher (XF) engaged in a comprehensive review of the questionnaire's content. Additionally, any queries or uncertainties were addressed through consultation with pertinent experts or professionals. Throughout the survey process, the researcher elucidated the study's protocol to the participating patients. Those who consented to participate formally by signing the written informed consent document were subsequently entrusted to independently complete the questionnaires following standardized instructions provided by the researcher. In instances where participants encountered difficulties during the questionnaire completion, the researcher offered appropriate assistance. Upon the conclusion of the questionnaire administration, the researcher collected the completed forms on-site to ensure their comprehensive fulfillment and promptly addressed any vacancies requiring supplementation.

2.3 Ethics approval

The study was approved by the Ethics Committee of the First Affiliated Hospital of Chengdu Medical College (2022CYFYIRB-BA-Oct19), and the subjects signed an informed consent form before the investigation.

2.4 Research instruments

2.4.1 General information questionnaire

12 entries, including gender, age, education, marital status, occupation, per capita monthly household income, presence of health insurance, duration of illness, treatment modalities, presence of complications, co-morbidities, HAb_{1c}.

2.4.2 The social support rating scale

Devised by Chinese psychologist Xiao Shuiyuan (36) in 1986 for the assessment of individual social support, exhibits commendable psychometric properties. The scale contains three dimensions of objective support (3 entries), subjective support (4 entries), and utilization of social support (3 entries), for a total of 10 entries, demonstrates a high level of internal consistency with Cronbach's alpha coefficients ranging from 0.89 to 0.94 for both the overall scale and its constituent dimensions, alongside an impressive retest reliability of 0.92. Huang Zizin et al. (25) applied this scale to patients with T2DM, revealing a slightly reduced but still acceptable Cronbach's alpha coefficient of 0.72 for the overall scale. In the present study, the Cronbach's alpha coefficients for both the total scale and its dimensions ranged from 0.828 to 0.952, reaffirming its reliability. Interpretation of the questionnaire scores is as follows: Scores between 12 and 22 are indicative of a low level of social support, scores ranging from 23 to 43 denote a moderate level of social support, and scores falling within the range of 44 to 66 signify a high level of social support.

2.4.3 The Hamilton depression scale

Employed to assess the degree of patients' depressive condition, comprises 17 items distributed with 17 entries and 5 factors, i.e., somatization of anxiety, weight, cognitive impairment, silted up, and sleep disturbance. As originally reported by Hamilton himself, the scale exhibits a Cronbach's alpha coefficients of 0.90, while foreign studies attest to a validity exceeding 0.84. The reliability of the 1988 Chinese version of this scale demonstrates excellence, with empirical veracity coefficients within domestic literature reflecting a substantial clinical symptom severity coefficient of 0.92. Interpretation of the questionnaire's total score is as follows: Scores falling within the range of ≤ 7 points are indicative of a normal state, while scores ranging from 8 to 17 points denote mild depression, scores of 18 to 24 points represent moderate depression, and scores equal to or exceeding 25 points signify severe depression.

2.4.4 Toronto alexithymia scale 20

The TAS-20, developed by Taylor et al. (37) in 1984 and subsequently adapted by Bagby et al. (38) to create the Toronto Alexithymia Scale TAS-26, underwent translation and revision to yield the Chinese version by Yao Shuqiao et al. (39). The scale exhibits commendable psychometric properties, boasting a Cronbach's alpha coefficient of 0.83 and retest reliability of 0.87. The scale consists of 20 entries with 3 factors: identifying affective disorders (7 entries), describing affective disorders (5 entries) and extraverted thinking (8 entries). The TAS-20 serves as a universally applicable and widely employed tool for assessing alexithymia, characterized by robust reliability and validity. A questionnaire score equal to or below 60 signifies the absence of alexithymia, whereas a score equal to or exceeding 61 indicates the presence of alexithymia.

2.5 Statistical analysis

The data were exported from the EpiData management software (Chinese version) and subjected to analysis using IBM SPSS 26.0 software. Quantitative data were presented as mean ± standard deviation (`x ± s), while qualitative data were expressed in terms of case count and percentage (%). Linear regression was employed to scrutinize the impact of social support, depression, and alexithymia on glycemic control, and Pearson's correlation was utilized to investigate the interrelations among these variables. The construction of a structural equation model for factors impacting glycemic control in patients with type 2 diabetes mellitus was executed using AMOS 26.0 software. This encompassed an evaluation based on several goodness-of-fit indices, namely Goodness of Fit Index (GFI), Incremental Fit Index (IFI), Comparative Fit Index (CFI), Standardized Fit Index (NFl), Relative Fit Index (RFI), Non-normalized Fit Index (TLI), Normed Fit Index (NFl), and Root Mean Square Error of Approximation. The indices IFI, CFI, NFI, RFI, and TLI all exceeded 0.9, with RMSEA below 0.08, and 2/DF below 3, adhering to accepted standards (40). A statistically significant difference was ascribed to instances with a P-value less than 0.05.

3 Results

3.1 Participant characteristics

A total of 318 study participants were enrolled in this investigation, comprising 152 males (47.8%) and 166 females (52.2%). Their age distribution was as follows: 22 individuals (6.9%) aged 18-44, 174 individuals (54.7%) aged 45-64, and 122 individuals (38.4%) aged 65 and above. In terms of marital status, 267 participants (84.0%) were married, while 51 participants (16.0%) were not. Employment status revealed 98 participants (30.8%) were employed, and 220 participants (69.2%) were not actively working. Health insurance coverage was prevalent, with 295 participants (92.8%) having it, while 23 participants (7.2%) did not possess health insurance. Additional demographic details of the study cohort are delineated in Table 1.

3.2 Current status of glycemic control, alexithymia, social support and depression in T2DM patients

The glycemic control level among T2DM patients was determined to be (8.85 ± 2.107), while the indices for alexithymia, social support, and depression were measured at (58.05 ± 4.382), (34.29 ± 4.420), and (7.17 ± 3.367), respectively. Notably, suboptimal glycemic control was evident in 75.47% of cases, with 31.13% of participants exhibiting alexithymia, and a significant 94.97% experiencing an intermediate level of social support. Furthermore, depressive symptoms were reported by 45.6% of the participants. Detailed findings are presented in Table 2.

3.3 Univariate analysis of factors influencing glycemic control in T2DM patients

A linear regression analysis concerning alterations in HbA_{1c} was performed, with HbA_{1c} serving as the dependent variable and alexithymia, social support, and depression acting as independent variables. The findings underscored that alexithymia, social support, and depression emerged as significant determinants influencing HbA_{1c} levels in patients diagnosed with T2DM (P<0.05). Elaborative outcomes are delineated in Table 3.

3.4 Analysis of the correlation between glycemic control, alexithymia, social support and depression in T2DM patients

Pearson correlation analysis was employed to scrutinize the associations among social support, depression, alexithymia, and blood glucose control in individuals diagnosed with T2DM. The outcomes revealed that HbA_{1c} exhibited a positive correlation with both alexithymia (r=0.392, P<0.01) and depression (r=0.509, P<0.01), while demonstrating a negative correlation with social support (r=-0.338, P<0.01). Furthermore, alexithymia displayed a negative correlation with social support (r=-0.357, P<0.01) and a positive correlation with depression (r=0.345, P<0.01). Notably, social support exhibited no significant association with depression (r=-0.095, P>0.05). Comprehensive details are available in Table 4.

3.5 Structural equation modeling between for the study of glycemic control in T2DM patients

Derived from the initial model outcomes, inoperative paths were excised, and the initial model underwent refinement through amalgamation with correction indices. This culminated in the formulation of the definitive structural equation model delineating glycemic control in individuals diagnosed with T2DM, as elucidated in Figure 1. The model, presented in a standardized format, encompasses standardized path coefficients. Subsequently, the revised model was re-fitted to the dataset employing the maximum likelihood method. The ensuing results indicated commendable fit indices, including RMSEA=0.043 (<0.08), $\chi 2/df$=2.577 (<3), GFI=0.973 (>0.9), AGFI=0.948 (>0.9),

TABLE 1 Sociodemographic characteristics.

Characteristics	Category	n(%)
Gender	Man	152(47.8)
	Woman	166(52.2)
Age (years)	18-44	22(6.9)
	45-64	174(54.7)
	≥65	122(38.4)
Education level	Primary and below	132(41.5)
	middle school	114(35.8)
	high school or junior college	48(15.1)
	college and above	24(7.5)
Marital status	marriage	267(84.0)
	non-marital	51(16.0)
Career	incumbency	98(30.8)
	non-working	220(69.2)
Monthly per capita family income	<3000	139(43.7)
	3000-5000	103(32.4)
	>5000	76(23.9)
Medical insurance	Yes	295(92.8)
	No	23(7.2)
Course of disease(year)	1-10	203(63.8)
	11-20	88(27.7)
	≥21	27(8.5)
Treatment	dietary control only	24(7.5)
	antihyperglycemic drug	165(51.9)
	insulin	43(13.5)
	glucose-lowering drugs and insulin	86(27.0)
Complications	Yes	113(35.5)
	No	205(64.5)
Co-morbidity	Yes	166(52.2)
	No	152(47.8)
HbA_{1c}	≤7.0	78(24.5)
	>7.0	240(75.5)

TABLE 2 Glycemic control, alexithymia, social support and depression scores in T2DM patients (M ± SD).

	Current situation	M ± SD	Entry M ± SD
HAb_{1c}	<7.0% (78,24.53%) ≥7.0% (240,75.47%)	8.85 ± 2.107	—
Alexithymia	No(219,68.87%) Yes(99,31.13%)	58.05 ± 4.382	—
DIF		18.31 ± 3.153	2.62 ± 0.450
DDF		14.39 ± 1.718	2.88 ± 0.344
EOT		25.35 ± 1.897	3.17 ± 0.237
Social support	Low level (1,0.31%) Medium level (302,94.97%) High level(15,4.72%)	34.29 ± 4.420	—
OS		10.02 ± 2.264	3.34 ± 0.755
SS		19.36 ± 2.684	4.84 ± 0.671
USS		4.92 ± 1.658	1.64 ± 0.553
Depression	No(173,54.40%) Mildly (140,44.03%) Moderately (5,1.57%)	7.17 ± 3.367	—
SA		2.02 ± 1.475	0.40 ± 0.295
W		1.22 ± 1.533	1.22 ± 1.533
CI		0.64 ± 0.788	0.21 ± 0.263
SU		0.82 ± 1.145	0.21 ± 0.286
SD		2.37 ± 1.493	0.79 ± 0.498

DIF, Difficulty Identifying Feelings; DDF, Difficulty Describing Feelings; EOT, Externally-Oriented Thinking; OS, objective support; SS, subjective support; USS, utilization of social support; SA, Somatization of anxiety; W, weight; CI, cognitive impairment; SU, silted up; SD, sleep disorder.

IFI=0.952 (>0.9), TLI=0.918 (>0.9), and CFI=0.949 (>0.9), all well within the normative range of values. Additionally, NFI=0.878 (<0.9) and RFI=0.804 (<0.9), though marginally below 0.9, still fall within the acceptable threshold, affirming the enhanced fit of the refined model. For comprehensive specifics, refer to Table 5.

3.6 Effect analysis of structural equation modeling variables

The refined model exhibited fitting indices within acceptable parameters. The model outcomes indicated that social support manifested a negative association with depression (β=-0.336, t=-2.398, P=0.016), and likewise, social support displayed a negative correlation with alexithymia (β=-0.405, t=-3.566, P<0.001). Moreover, social support revealed an inverse relationship with glycemic control (β=-0.346, t=-3.437, P<0.001). Conversely, depression exhibited a positive connection with alexithymia (β=0.318, t=3.233, P=0.001) and also demonstrated a positive correlation with glycemic control (β=0.434, t=4.168, P<0.001). Notably, alexithymia exhibited no statistically significant relationship with glycemic control (P>0.05), as elucidated in Table 6.

4 Discussion

The study findings indicated that social support exerts a direct and indirect impact on glycemic control through depression. Social support was observed to have a direct effect on alexithymia. Depression exhibited direct influences on both alexithymia and glycemic control. Furthermore, a correlation was established between alexithymia and glycemic control; however, the specific pathways connecting these two variables remain unconfirmed within the scope of this investigation. This study establishes a theoretical foundation for elucidating the impact of social support, depression, and alexithymia on glycemic control through an examination of the intricate pathways interconnecting social support, depression, and alexithymia with glycemic control. Furthermore, it furnishes theoretical substantiation for enhancing glycemic control in individuals with T2DM with the ultimate goal of ameliorating the overall glycemic control in T2DM patients. The overarching objective is to impede the progression of complications, thereby enhancing the quality of life for patients, while concurrently mitigating the perceptual and economic burdens associated with the disease.

4.1 Current status of social support in T2DM patients

The study results revealed that the comprehensive social support score for patients diagnosed with T2DM was (34.29 ±

TABLE 3 Linear regression analysis of factors affecting HbA_{1c} in patients with type 2 diabetes mellitus.

Dependent variable	Independent variable	β	standardized coefficient β	t	P-Value	β95%CI	
						Lower	Upper
HbA_{1c}	alexithymia	0.189	0.392	7.578	<0.001	0.140	0.237
	social support	-0.161	-0.338	-6.375	<0.001	-0.211	-0.111
	depression	0.318	0.509	10.510	<0.001	0.259	0.378

TABLE 4 Correlations between social support, depression, alexithymia, and glycemic control in patients with type 2 diabetes mellitus.

	HbA_{1c}	alexithymia	social support	depression
HbA_{1c}	1			
alexithymia	0.392**	1		
social support	-0.338**	-0.357**	1	
depression	0.509**	0.345**	-0.095	1

**P<0.01.

4.42), indicating a moderate level. This finding aligns with the research conducted by Al-Dwaikat et al. (41) and contrasts with the outcomes reported by Qin Wen et al. (42) (39.27 ± 8.82), where social support levels were higher. Specifically, the subjective support score ranked highest, followed by the objective support score, while the social support utilization score was the lowest. This pattern resonates with the outcomes of a social support survey for diabetic patients conducted by Liu Qing et al. (43). Notably, patients exhibited a relatively high subjective perception of acquiring social support; however, the practical benefits derived from this assistance were diminished, impeding their ability to fully harness external aid. This suboptimal utilization of support resulted in consequences such as social isolation and delayed medical intervention (44), thereby influencing the efficacy of disease treatment. Social support not only exerts a direct positive influence on well-being but also functions as a buffer, shielding individuals from health issues induced by excessive stress (22). Adequate social support not only serves as a protective factor for individuals navigating health crises across diverse medical conditions but also correlates with a reduction in medication dependency, expedited recuperation, and enhanced adherence to therapeutic regimens (45). It is imperative to enhance objective support mechanisms and optimize the utilization of social support by patients, thereby maximizing the efficacy of such support systems and mitigating the burden of disease.

4.2 Current status of glycemic control in T2DM patients

The investigation revealed that the glycemic control level among patients with T2DM was (8.85 ± 2.107), surpassing that observed in Polish diabetic cohorts as reported by Cyranka et al. (46) (7.11 ± 1.0) and falling below the corresponding level found in Turkish diabetic subjects in the investigation by Celik et al. (23) (9.98 ± 1.80). This discrepancy underscores the discernible variability in the prevailing state of glycemic control among patients across diverse geographic regions. Notwithstanding the intermediary status of glycemic control observed in the subjects of this investigation, it demonstrated a noteworthy elevation compared to the established normative threshold (7.0%) (6). Nonetheless, the incidence of suboptimal glycemic control persisted at a considerable level. Prolonged exposure to elevated blood glucose levels in patients is known to instigate the onset of macrovascular complications, such as cardiovascular diseases (47), microvascular complications, including retinopathy and nephropathy (48), thereby amplifying the overall risk of mortality (49). Hence, it is recommended that clinical practitioners fortify the regimen of glycemic control in diabetic cohorts to ameliorate adverse pathological outcomes, augment the quality of life for patients, and mitigate the economic burdens associated with the condition.

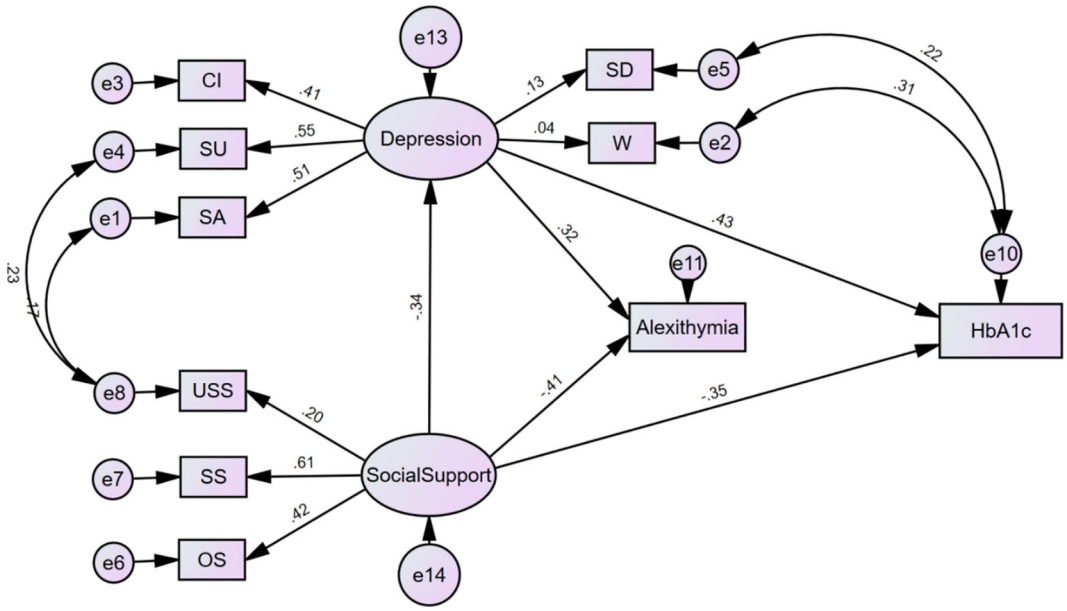

FIGURE 1
Modified model of glycemic control in patients with types 2 diabetes mellitus. USS, utilization of social support; SS, subjective support; OS, objective support; Cl, cognitive impairment; SU, silted up; SA, somatization of anxiety; SD, sleep disorder; W, weight.

TABLE 5 Evaluation results of the optimal model fit goodness-of-fit.

Adaptation index	χ^2/df	GFI	NFI	RFI	IFI	TLI	CFI	RMSEA
Reference value	<3.00	>0.9	>0.9	>0.9	>0.9	>0.9	>0.9	<0.08
Model test value	1.577	0.973	0.878	0.804	0.952	0.918	0.949	0.043

4.3 Impact of alexithymia on glycemic control in patients with T2DM

The current investigation elucidated a positive correlation between alexithymia and glycemic control among patients diagnosed with T2DM, aligning with the findings reported by Celik et al. (23). This concordance implies that individuals exhibiting alexithymic traits tend to manifest inferior glycemic control in comparison to their non-alexithymic counterparts. The failure to recognize body symptoms and emotion perceptions could lead to a further incomprehensible psychological and physical suffering, due to poorly regulated diabetes, which may limit the ability to manage their metabolic disease (50). Within the diabetic population, heightened psychological stress may recurrently or persistently activate glucose metabolic pathways, culminating in aberrant glucose concentrations beyond the normative spectrum. Such perturbations in metabolic homeostasis contribute to an inability to sustain glucose levels within physiological bounds, thereby fostering suboptimal glycemic control. Furthermore, psychological stress exerts a deleterious influence on patient self-management, diminishing adherence to therapeutic regimens and consequently engendering compromised glycemic control (51). Alexithymia emerges as a significant psychological determinant contributing to compromised glycemic control (52). Individuals characterized by alexithymic features tend to defer their pursuit of assistance, owing to challenges in articulating and discerning their personal emotional states. This delay, coupled with a reduction in others' capacity to perceive the patient's needs accurately, results in a lapse in the timely fulfillment of the patient's requisites. This circumstance amplifies the psychological burden borne by the patient and diminishes adherence to the prescribed therapeutic interventions, ultimately culminating in suboptimal glycemic control (23). Nevertheless, in the investigations conducted by Mnif and Hintistan et al (15, 53) concerning alexithymia and glycemic control in T2DM patients, the establishment of a conclusive correlation between glycemic control and alexithymia has not been discerned. This absence of a clear association may be attributed to idiosyncrasies within the sampled populations and variances in the methodologies employed for measurement. Consequently, the inquiry into the interrelation between alexithymia and glycemic control necessitates augmentation through additional related studies to enhance the overall persuasiveness of the research.

TABLE 6 Parameter estimation of a modified model of social support, depression, alexithymia and glycemic control in patients with type 2 diabetes mellitus.

	Standardized coefficient	S.E.	C.R.	*P*
depression<—social support	-0.336	0.112	-2.398	0.016
alexithymia<—social support	-0.405	0.530	-3.566	***
HAb_{1c}<—social support	-0.346	0.225	-3.437	***
alexithymia<—depression	0.318	0.570	3.233	0.001
HAb_{1c}<—depression	0.434	0.290	4.168	***

SE denotes standard error, C.R. denotes critical ratio, i.e., t-value, and *** is P < 0.001.

4.4 Impact of social support on glycemic control in patients with T2DM

The study findings indicate an inverse relationship between glycemic control and social support; specifically, a diminished level of social support correlates with a deterioration in glycemic control among diabetic patients. This concurrence aligns with the outcomes reported by Castillo-Hernandez et al. (54). Psychosocial stressors may also lead to decreased immune surveillance as well as abnormal activation of the autonomic nervous system (ANS) and the hypothalamic-pituitary-adrenal axis (HPA), which may affect the patient's control of the disease (12). In the context of T2DM, social support encompasses emotional, material, and informational facets, serving as a facilitator for enhancing patient adherence to medication protocols, blood glucose monitoring, and lifestyle modifications (e.g., dietary control, physical exercise) (55). This multifaceted support structure aims to ameliorate patients' self-management proficiency and, consequently, elevate glycemic control, thereby augmenting the overall efficacy of disease management. Conversely, a paucity of social support may engender a deficiency in requisite medical information and assistance for patients, diminishing their cognizance of the ailment. This may result in a procrastination of disease intervention, thereby impinging upon patients' self-management capabilities and exerting a deleterious impact on glycemic control.

Furthermore, social support may exert a detrimental impact on glycemic control through its association with depression, a phenomenon akin to the observations made by Burns et al. (56) in diabetic patient cohorts. Beyond the direct provision of tangible and spiritual support, the influence of social support on patients' psychological state emerges as an additional mechanism by which it can affect glycemic control. Social support serves to mitigate

psychological stress, assuage adverse emotional states, empower individuals to confront challenges, and enhance self-efficacy in surmounting obstacles (57). Conversely, inadequate social support may precipitate feelings of isolation, helplessness, and anxiety in recipients, potentially culminating in depressive states. Patients enduring chronic depression may experience a decline in confidence regarding their therapeutic regimen, fostering a lack of motivation for self-management and control. This, in turn, can contribute to suboptimal glycemic control.

4.5 Effect of depression on glycemic control in T2DM patients

The findings further revealed a positive association between depression and blood glucose control, indicating that elevated depression scores correlate with a deterioration in blood glucose regulation, consistent with the observations of Gonzalez et al. (58). Depression may precipitate physiological alterations in patients, contributing to suboptimal glycemic control in diabetic individuals. Mechanistically, this influence is manifested through the activation of the hypothalamo-pituitary-adrenal axis, stimulation of the sympathetic nervous system, and an escalation in inflammatory responses and platelet aggregation (59). Furthermore, depression may exacerbate the clinical condition and heighten the susceptibility to complications. Secondly, depression can instigate alterations in patients' attitudes and behaviors towards the ailment, diminishing their inclination to actively engage in treatment and detrimentally impacting self-management facets such as dietary practices, exercise, glucose monitoring, and medication adherence (60, 61). This, in turn, exerts an adverse influence on glycemic control, potentially escalating the severity of the disease, amplifying medical expenditures, and heightening the likelihood of diabetic complications and mortality (62). Moreover, depression may disrupt patients' social functioning, with chronically depressed individuals experiencing a reduction in social engagement and a decline in overall quality of life. These factors may further compromise the proficiency of glycemic control.

4.6 Limitations

This study constitutes a single-center cross-sectional investigation, potentially compromising the representativeness of the encompassed population. Furthermore, the limited sample size may pose a constraint on the generalizability of the findings. To enhance the robustness of future inquiries, multicenter studies incorporating a more diverse diabetic population could be considered, thereby bolstering the external validity of the results. Additionally, intervention studies investigating the impact of alexithymia on glycemic control could be undertaken to augment the persuasiveness of the outcomes.

4.7 Conclusions

In this investigation, we formulated a structural equation model encompassing social support, depression, alexithymia, and glycemic control. We scrutinized the intricate pathways through which these factors exert influence on glycemic regulation in diabetic patients. Our findings suggest that enhancing the level of social support and conducting timely assessments of mental health are imperative measures. These interventions aim to ameliorate the physical and psychological stress experienced by patients, subsequently elevating patients' adherence to treatment and self-management practices. This, in turn, contributes to an enhancement in glycemic control among individuals afflicted with T2DM and those at risk. The optimization of glucose control not only serves to retard the progression of complications and mitigate the risk of mortality but also endeavors to enhance the overall quality of life for patients. Simultaneously, such interventions aspire to alleviate both social and economic burdens associated with T2DM.

Data availability statement

The original contributions presented in the study are included in the article/Supplementary Material. Further inquiries can be directed to the corresponding author.

Ethics statement

The studies involving human participants were reviewed and approved by the Ethics Committee of the First Affiliated Hospital of Chengdu Medical College (2022CYFYIRB-BA-Oct19). The patients/participants provided their written informed consent to participate in this study.

Author contributions

YG: Conceptualization, Writing – original draft. FT: Data curation, Writing – original draft, Writing – review & editing. XF: Data curation, Methodology, Writing – original draft. HW: Conceptualization, Investigation, Writing – original draft. JZ: Investigation, Methodology, Writing – original draft. NY: Conceptualization. HQ: Writing – review & editing.

Funding

The author(s) declare financial support was received for the research, authorship, and/or publication of this article. This research was funded by Chengdu Medical College (Project No. YCX2023-01-57).

Acknowledgments

The authors would like to thank all study participants as well as all participants participating in the study's development, revision, and coaching. The final manuscript was read and approved by all writers.

Conflict of interest

The authors declare that the research was conducted in the absence of any commercial or financial relationships that could be construed as a potential conflict of interest.

Publisher's note

Supplementary material

The Supplementary Material for this article can be found online at: https://www.frontiersin.org/articles/10.3389/fendo.2024.1390564/full#supplementary-material

References

1. Sun H, Saeedi P, Karuranga S, Pinkepank M, Ogurtsova K, Duncan BB, et al. IDF Diabetes Atlas: Global, regional and country-level diabetes prevalence estimates for 2021 and projections for 2045. *Diabetes Res Clin Pract*. (2022) 183:109119. doi: 10.1016/j.diabres.2021.109119

2. Zhang X, Xu X, Dong T, Deng Y, Zeng J, Yi G, et al. Prevalence and influencing factors of adult diabetes mellitus in Sichuan Province in 2018. *Modern Prev Med*. (2022) 49(11):1931–6.

3. Zhong H. Guideline for the prevention and treatment of type 2 diabetes mellitus in China edition) (Part 1). *Chin J Pract Internal Med*. (2021) 41:668–95.

4. Cardoso C, Leite NC, Moram C, Salles GF. Long-term visit-to-visit glycemic variability as predictor of micro- and macrovascular complications in patients with type 2 diabetes: The Rio de Janeiro Type 2 Diabetes Cohort Study. *Cardiovasc Diabetol*. (2018) 17:33. doi: 10.1186/s12933-018-0677-0

5. Klein KR, Buse JB. The trials and tribulations of determining HbA(1c) targets for diabetes mellitus. *Nat Rev Endocrinol*. (2020) 16:717–30. doi: 10.1038/s41574-020-00425-6

6. Wang L, Peng W, Zhao Z, Zhang M, Shi Z, Song Z, et al. Prevalence and treatment of diabetes in China 2013-2018. *JAMA*. (2021) 326(24):2498–506. doi: 10.1001/jama.2021.22208

7. Kim KJ, Choi J, Bae JH, Kim KJ, Yoo HJ, Seo JA, et al. Time to reach target glycosylated hemoglobin is associated with long-term durable glycemic control and risk of diabetic complications in patients with newly diagnosed type 2 diabetes mellitus: A 6-year observational study. *Diabetes Metab J*. (2021) 45:368–78. doi: 10.4093/dmj.2020.0046

8. Liu J, Liu M, Chai Z, Li C, Wang Y, Shen M, et al. Projected rapid growth in diabetes disease burden and economic burden in China: a spatio-temporal study from 2020 to 2030. *Lancet Reg Health West Pac*. (2023) 33:100700. doi: 10.1016/j.lanwpc.2023.100700

9. Ettaro L, Songer TJ, Zhang P, Engelgau MM. Cost-of-illness studies in diabetes mellitus. *Pharmacoeconomics*. (2004) 22:149–64. doi: 10.2165/00019053-200422030-00002

10. Zhong H. Guideline for the prevention and treatment of type 2 diabetes mellitus in China, (2020 edition). *Chin J Diabetes*. (2021) 13:12–50.

11. Ali S, Stone M, Skinner TC, Robertson N, Davies M, Khunti K. The association between depression and health-related quality of life in people with type 2 diabetes: a systematic literature review. *Diabetes Metab Res Rev*. (2010) 26:75–89. doi: 10.1002/dmrr.1065

12. Conversano C, Di Giuseppe M. Psychological factors as determinants of chronic conditions: clinical and psychodynamic advances. *Front Psychol*. (2021) 12635708. doi: 10.3389/fpsyg.2021.635708

13. Naicker K, Johnson JA, Skogen JC, Manuel D, Øverland S, Sivertsen B, et al. Type 2 diabetes and comorbid symptoms of depression and anxiety: longitudinal associations with mortality risk. *Diabetes Care*. (2017) 40:352–8. doi: 10.2337/dc16-2018

14. Stingl M. Alexithymia in type I and type II diabetes. *Interventions Obes Diabetes*. (2018) 1:1–4. doi: 10.31031/IOD

15. Hintistan S, Cilingir D, Birinci N. Alexithymia among older people patients with diabetes. *Pakistan J Med Sci*. (2013) 29:1344. doi: 10.12669/pjms.296.2159

16. Housiaux M, Luminet O, Van Broeck N, DORCHY H. Alexithymia is associated with glycaemic control of children with type 1 diabetes. *Diabetes Metab*. (2010) 36:455–62. doi: 10.1016/j.diabet.2010.06.004

17. Xue J, Sun J, Tian C. Analysis of alexithymia status and influencing factors in older people patients with diabetes mellitus. *Modern Prev Med*. (2020) 47:305–9.

18. Avci D, Kelleci M. Alexithymia in patients with type 2 diabetes mellitus: the role of anxiety, depression, and glycemic control. *Patient Prefer Adherence*. (2016) 10:1271–7. doi: 10.2147/PPA

19. Martino G, Catalano A, Bellone F, Russo GT, Vicario CM, Lasco A, et al. As time goes by: anxiety negatively affects the perceived quality of life in patients with type 2 diabetes of long duration. *Front Psychol*. (2019) 10. doi: 10.3389/fpsyg.2019.01779

20. Terock J, Klinger-König J, Janowitz D, Nauck M, Völzke H, Grabe HJ. Alexithymia is associated with increased all-cause mortality risk in men, but not in women: A 10-year follow-up study. *J Psychosomatic Res*. (2021) 143:110372. doi: 10.1016/j.jpsychores.2021.110372

21. Fares C, Bader R, Ibrahim JN. Impact of alexithymia on glycemic control among Lebanese adults with type 2 diabetes. *J Diabetes Metab Disord*. (2019) 18:191–8. doi: 10.1007/s40200-019-00412-3

22. Kojima M, Senda Y, Nagaya T, Tokudome S, Furukawa TA. Alexithymia, depression and social support among Japanese workers. *Psychother Psychosom*. (2003) 72:307–14. doi: 10.1159/000073027

23. Celik S, Taskin YF, Yurtsever CS, Anataca G, Bulbul E. Alexithymia in diabetes patients: its relationship with perceived social support and glycaemic control. *J Clin Nurs*. (2022) 31(17-18):2612–20. doi: 10.1111/jocn.16088

24. Williams JS, Walker RJ, Egede LE. Gender invariance in the relationship between social support and glycemic control. *PloS One*. (2023) 18:e0285373. doi: 10.1371/journal.pone.0285373

25. Huang Z, Wang X, Han Q, Li Y. The mediating effect of psychological resilience between social support and narrative impairment in middle-aged and older people patients with type 2 diabetes mellitus. *Chin J Prev Control Chronic Dis*. (2020) 28:774–7. doi: 10.16386/j.cjpccd.issn.1004-6194.2020.10.013

26. Jinhua J, Jianjun X, Dan L, Lina J, Hailin Z. Depression status and its influencing factors among the older people with type 2 diabetes mellitus in urban communities of Fuzhou City. *Modern Prev Med*. (2022) 49:2381–7.

27. Zhang T, Xiang Y, Song X, Yang Y, Qiu X, Li P. The mediating role of illness perception and illness distress on glycemic control and depression among people with type 2 diabetes. *Chin J Behav Med Brain Sci*. (2020) 29:620–3.

28. Pan J, Xue X, Ma T, Lu Y. Treatment of diabetic depression with traditional chinese medicine: a review. *Chin J Exp Traditional Med Formulae*. (2022) 28:266–72.

29. Ismail K, Winkley K, Stahl D, Chalder T, Edmonds M. A cohort study of people with diabetes and their first foot ulcer: the role of depression on mortality. *Diabetes Care*. (2007) 30:1473–9. doi: 10.2337/dc06-2313

30. Sartorius N. Depression and diabetes. *Dialogues Clin Neurosci*. (2022) 20:47–52. doi: 10.31887/DCNS.2018.20.1/nsartorius

31. Naicker K, Øverland S, Johnson JA, Manuel D, Skogen JC, Sivertsen B, et al. Symptoms of anxiety and depression in type 2 diabetes: Associations with clinical diabetes measures and self-management outcomes in the Norwegian HUNT study. *Psychoneuroendocrinology*. (2017) 84:116–23. doi: 10.1016/j.psyneuen.2017.07.002

32. Melin EO, Thunander M, Svensson R, Landin-Olsson M, Thulesius HO. Depression, obesity, and smoking were independently associated with inadequate glycemic control in patients with type 1 diabetes. *Eur J Endocrinol*. (2013) 168:861–9. doi: 10.1530/EJE-13-0137

33. Whitworth SR, Bruce DG, Starkstein SE, Davis WA, Davis T, Bucks RS. Lifetime depression and anxiety increase prevalent psychological symptoms and worsen glycemic control in type 2 diabetes: the Fremantle Diabetes Study Phase II. *Diabetes Res Clin Pract*. (2016) 122:190–7. doi: 10.1016/j.diabres.2016.10.023

34. Drouin P, Blicklé JF, Charbonnel B, Eschwege E, Guillausseau P, Plouin P, et al. Diagnostic et classification du diabète sucré: les nouveaux critères [Diagnosis and classification of diabetes mellitus: the new criteria]. *Diabetes Metab*. (1999) 25:72–83.

35. Ni P, Chen J, Liu N. The sample size estimation hi quantitative nursing research. *Chin J Nurs*. (2010) 45:378–80.

36. Xiao S. Theoretical basis and research applications of the Social Support Rating Scale. *J Clin Psychiatry*. (1994) 02:98–100.

37. Taylor GJ, Ryan D, Bagby M. Toward the development of a new self-report alexithymia scale. *Psychother psychosomatics*. (1985) 44:191–9. doi: 10.1159/000287912

38. Bagby RM, Taylor GJ, Parker JD. The twenty-item Toronto Alexithymia Scale—II. Convergent, discriminant, and concurrent validity. *J psychosomatic Res*. (1994) 38:33–40. doi: 10.1016/0022-3999(94)90006-X

39. Yi J, Yao S, Zhu X. The Chinese version of the TAS-20: reliability and validity. *Chin Ment Health J*. (2003) 11:763–7.

40. Joreskog K, Sorbom D. *Structural equation modelling: Guidelines for determining model fit* Vol. 6. . NY: University Press of America (1993) p. 141–6.

41. Al-Dwaikat TN, Rababah JA, Al-Hammouri MM, Chlebowy DO. Social support, self-efficacy, and psychological wellbeing of adults with type 2 diabetes. *Western J Nurs Res*. (2021) 43:288–97. doi: 10.1177/0193945920921101

42. Wen Q, Zhaoyan D, Zehua W, Haiqing T. Analysis of the current situation of social comparison tendency of diabetic patients and its influencing factors. *Chin Gen Pract Nurs*. (2023) 21:2984–7.

43. Qing L, Wei X, Lu G, Liping J, Mengyun X. The mediating effect of social support on the relationship between diabetes distress and blood glucose levels in diabetic patients. *Chin J Gerontology*. (2022) 42:974–7.

44. Karakaş SA, Karabulutlu EY, Akyil RÇ, Erdem N, Turan GB. An analysis of alexithymia and social support in patients with hypertension and asthma. *J Psychiatr Nurs*. (2016) 7:68–74.

45. Cobb S. Presidential Address-1976. Social support as a moderator of life stress. *Psychosom Med*. (1976) 38:300–14. doi: 10.1097/00006842-197609000-00003

46. Cyranka K, Matejko B, Chrobak A, Dudek D, Kieć-Wilk B, Cyganek K, et al. Assessment of the spectrum of depression and bipolarity in patients with type 1 diabetes. *Diabetes Metab Res Rev*. (2023) 39:e3583. doi: 10.1002/dmrr.3583

47. Wan EY, Yu EY, Chen JY, Wong IC, Chan EW, Lam CL. Associations between usual glycated haemoglobin and cardiovascular disease in patients with type 2 diabetes mellitus: A 10-year diabetes cohort study. *Diabetes Obes Metab*. (2020) 22:2325–34. doi: 10.1111/dom.14157

48. Arnqvist HJ, Westerlund MC, Fredrikson M, Ludvigsson J, Nordwall M. Impact of hbA1c followed 32 years from diagnosis of type 1 diabetes on development of severe retinopathy and nephropathy: the VISS study. *Diabetes Care*. (2022) 45:2675–82. doi: 10.2337/dc22-0239

49. Rawshani A, Rawshani A, Franzén S, Sattar N, Eliasson B, Svensson AM, et al. Risk factors, mortality, and cardiovascular outcomes in patients with type 2 diabetes. *N Engl J Med*. (2018) 379:633–44. doi: 10.1056/NEJMoa1800256

50. Martino G, Caputo A, Vicario CM, Catalano A, Schwarz P, Quattropani MC. The relationship between alexithymia and type 2 diabetes: a systematic review. *Front Psychol*. (2020) 11:2026. doi: 10.3389/fpsyg.2020.02026

51. Hackett RA, Steptoe A. Type 2 diabetes mellitus and psychological stress - a modifiable risk factor. *Nat Rev Endocrinol*. (2017) 13:547–60. doi: 10.1038/nrendo.2017.64

52. Shayeghian Z, Amiri P, Hajati E, Gharibzadeh S. Moderating role of alexithymia in relationship between perceived social support, diabetes-related quality of life, and glycated hemoglobin in patients with type 2 diabetes. *J Res Health*. (2020) 10:27–34. doi: 10.32598/JRH

53. Mnif L, Damak R, Mnif F, Ouanes S, Abid M, Jaoua A, et al. Alexithymia impact on type 1 and type 2 diabetes: A case-control study. *Annales d'Endocrinologie*. (2014) 75:213–9. doi: 10.1016/j.ando.2014.06.001

54. Castillo-Hernandez KG, Laviada-Molina H, Hernandez-Escalante VM, Molina-Segui F, Mena-Macossay L, Caballero AE. Peer support added to diabetes education improves metabolic control and quality of life in mayan adults living with type 2 diabetes: A randomized controlled trial. *Can J Diabetes*. (2021) 45:206–13. doi: 10.1016/j.jcjd.2020.08.107

55. Denham SA, Manoogian MM, Schuster L. Managing family support and dietary routines: Type 2 diabetes in rural Appalachian families. *Families Systems Health*. (2007) 25:36. doi: 10.1037/1091-7527.25.1.36

56. Burns RJ, Deschênes SS, Schmitz N. Associations between depressive symptoms and social support in adults with diabetes: comparing directionality hypotheses with a longitudinal cohort. *Ann Behav Med*. (2016) 50:348–57. doi: 10.1007/s12160-015-9760-x

57. Yan J, Wu C, He C, Lin Y, He S, Du Y, et al. The social support, psychological resilience and quality of life of nurses in infectious disease departments in China: A mediated model. *J Nurs Manag*. (2022) 30:4503–13. doi: 10.1111/jonm.13889

58. Gonzalez HT, González-Ramírez LP, Hernández-Corona DM, Maciel-Hernández EA. Anxious depression in patients with Type 2 Diabetes Mellitus and its relationship with medication adherence and glycemic control. *Glob Public Health*. (2021) 16:460–8. doi: 10.1080/17441692.2020.1810735

59. Golden SH. A review of the evidence for a neuroendocrine link between stress, depression and diabetes mellitus. *Curr Diabetes Rev*. (2007) 3:252–9. doi: 10.2174/157339907782330021

60. Lin EH, Katon W, Von Korff M, Rutter C, Simon GE, Oliver M, et al. Relationship of depression and diabetes self-care, medication adherence, and preventive care. *Diabetes Care*. (2004) 27:2154–60. doi: 10.2337/diacare.27.9.2154

61. Fisher EB, Thorpe CT, Devellis BM, Devellis RF. Healthy coping, negative emotions, and diabetes management: a systematic review and appraisal. *Diabetes Educ*. (2007) 33:1080–103. doi: 10.1177/0145721707309808

62. Lin EH, Rutter CM, Katon W, Heckbert SR, Ciechanowski P, Oliver MM, et al. Depression and advanced complications of diabetes: a prospective cohort study. *Diabetes Care*. (2010) 33:264–9. doi: 10.2337/dc09-1068

frontiers | Frontiers in Endocrinology

TYPE Original Research
PUBLISHED 02 September 2024
DOI 10.3389/fendo.2024.1426175

OPEN ACCESS

EDITED BY
Heidi de Wet,
University of Oxford, United Kingdom

REVIEWED BY
Bryan Bjork,
Midwestern University, United States
Helen Christian,
University of Oxford, United Kingdom

*CORRESPONDENCE
Siresha Bathina
siresha.bathina@bcm.edu

†PRESENT ADDRESS
Georgia Colleluori,
Department of Experimental and Clinical Medicine, Marche Polytechnic University, Ancona, Marche, Italy

RECEIVED 30 April 2024
ACCEPTED 13 August 2024
PUBLISHED 02 September 2024

CITATION
Bathina S, Colleluori G, Villareal DT, Aguirre L, Chen R and Armamento-Villareal R (2024) A PRDM16-driven signal regulates body composition in testosterone-treated hypogonadal men.
Front. Endocrinol. 15:1426175.
doi: 10.3389/fendo.2024.1426175

A PRDM16-driven signal regulates body composition in testosterone-treated hypogonadal men

Siresha Bathina[1,2]*, Georgia Colleluori[1†], Dennis T. Villareal[1,2], Lina Aguirre[3,4], Rui Chen[1,2] and Reina Armamento-Villareal[1,2]

[1]Division of Endocrinology Diabetes and Metabolism at Baylor College of Medicine, Houston, TX, United States, [2]Department of Medicine, Michael E. DeBakey Veterans Affairs (VA) Medical Center, Houston, TX, United States, [3]Department of Medicine, University of New Mexico School of Medicine, Albuquerque, NM, United States, [4]Department of Medicine, New Mexico VA Health Care System, Albuquerque, NM, United States

Background: Testosterone (T) therapy increases lean mass and reduces total body and truncal fat mass in hypogonadal men. However, the underlying molecular mechanisms for the reciprocal changes in fat and lean mass in humans are not entirely clear.

Methods: Secondary analysis of specimens obtained from a single-arm, open-label clinical trial on pharmacogenetics of response to T therapy in men with late-onset hypogonadism, conducted between 2011 and 2016 involving 105 men (40-74 years old), who were given intramuscular T cypionate 200 mg every 2 weeks for 18 months. Subcutaneous fat (SCF), peripheral blood mononuclear cells (PBMC) and serum were obtained from the participants at different time points of the study. We measured transcription factors for adipogenesis and myogenesis in the SCF, and PBMC, respectively, by real-time quantitative PCR at baseline and 6 months. Serum levels of FOLLISTATIN, PAX7, MYOSTATIN, ADIPSIN, and PRDM16 were measured by ELISA.

Results: As expected, there was a significant increase in T and estradiol levels after 6 months of T therapy. There was also a reduction in fat mass and an increase in lean mass after 6 months of T therapy. Gene-protein studies showed a significant reduction in the expression of the adipogenic markers *PPARγ* in SCF and ADIPSIN levels in the serum, together with a concomitant significant increase in the expression of myogenic markers, *MYOD* in PBMC and PAX7 and FOLLISTATIN levels in the serum after 6 months of T therapy compared to baseline. Interestingly, there was a significant increase in the adipo-myogenic switch, *PRDM16*, expression in SCF and PBMC, and in circulating protein levels in the serum after 6 months of T therapy, which is likely from increased estradiol.

10.3389/fendo.2024.1426175

Conclusion: Our study supports that molecular shift from the adipogenic to the myogenic pathway in men with hypogonadism treated with T could be mediated directly or indirectly by enhanced PRDM16 activity, in turn a result from increased estradiol level. This might have led to the reduction in body fat and increase in lean mass commonly seen in hypogonadal men treated with T.

KEYWORDS

adipogenesis, myogenesis, PRDM16, estrogen, testosterone

1 Introduction

Age-related reduction in gonadal steroids is associated with changes in body composition, i.e., increase in fat mass and decrease in lean mass (1) These body composition changes, result not only from the lack of androgens, but also from the reduced amount of the androgen-derived estrogen (2). In these subjects, testosterone (T) therapy results in improvement in the body composition (3) possibly due to the combined action of T and that of estradiol (E2) deriving from T. Previous studies from our lab demonstrated the improvement in body composition with T therapy (4, 5). The mechanism underlying the effect of T in enhancing myogenesis and ablating adipogenesis has been explored *in vitro* (6), and in pre-clinical models (7) however, data in humans are scarce. Myocytes, and adipocytes originate from a common mesenchymal stem cell (MSCs) (8). How MSCs differentiate into distinct lineages under the influence of T in hypogonadal men needs to be explored. The commitment of MSCs to a particular lineage always rely on interaction among transcriptional regulators with crucial genes. One such gene is positive regulatory domain zinc finger region protein 16 (PRDM16),a highly conserved 140kDa zinc finger transcriptional co-regulator (9) which has important function in cell fate determination and function of brown and beige adipocytes, in maintenance of hematopoietic and neural stem cells, and proliferation of cardiomyocytes (10, 11). Though PRDM16 is a nuclear bound transcription factor, Pinheiro et al, identified Prdm16 and Prdm3 as redundant H3K9ME1-speciifc methyl transferases in the cytoplasm directing methylation via anchoring to nuclear periphery to maintain integrity of mammalian heterochromatin (12). Evidence suggests that Prdm16, transcriptional factor involved in brown fat adipogenesis (13), interacts with peroxisome proliferator-activated receptor γ (PPARγ) (14) and CCAAT-enhancer binding protein-alpha (CEBPα) (15) resulting in the trans-differentiation of myoblasts to brown adipocytes (16). When it comes to interaction between these genes and sex steroids, Zhao et al. found that androgen receptor (AR) directly binds the *Prdm16* locus and inhibit white adipose tissue (WAT) browning via suppression of *Prdm16*. These investigators also reported higher PRDM16 levels in WAT of women (17). Moreover, the administration of E2 resulted in WAT browning from an increase in the browning genes *UCP*-1, *PGC-1α*, and *Prdm16* and decreased body weight and visceral fat in ovariectomized (OVX) mice (18). Altogether, the above studies imply the crucial role of PRDM16 in adipose tissue biology. Furthermore, though the above findings are consistent with the regulatory role of both T and E2 in adipose tissue deposition and browning, the specific factors involved are still to be identified.

Aside from prior study showing that T administration in eugonadal men resulted in an increase in PAX7 (Paired box 7), a transcription factor which regulates the regeneration and proliferation of myogenic precursors (19) most of the information available comes from *in-vitro* or pre-clinical models with limited scope. In this study, we aim to evaluate the *in-vivo* gene-protein machinery involved in adipogenesis and myogenesis in hypogonadal men given T therapy. We hypothesize that PRDM16 plays a crucial role in the observed reduction in fat mass and increase in lean mass with T therapy in hypogonadal men. Results from this study may provide a consolidated mechanistic insight on how T improves the body composition in hypogonadal men.

2 Materials and methods

2.1 Study design, study participants, and intervention

This study is an analysis of the longitudinal data and samples obtained from a prior open-label clinical trial (NCT01378299) investigating the pharmacogenetics of CYP19A1 gene on the response to testosterone therapy in men with hypogonadism. A total of 342 male veterans attending the Endocrine, Urology and Primary Care Clinics of the New Mexico Veterans Administration Health Care System (NMVAHCS) and Michael E. DeBakey Veterans Affairs Medical Center (MEDVAMC) were screened for the study. Recruitment was accomplished either through flyers or letters to physicians about patients who may qualify for the study. Written informed consent was obtained from each subject. The protocol was approved by the Institutional Review Board of the University of New Mexico School of Medicine and the Baylor College of Medicine; and study was conducted in accordance with guidelines in the Declaration of Helsinki for the ethical treatment of human subjects.

2.2 Inclusion, and exclusion criteria

Information regarding study design, inclusion, and exclusion criteria of the subjects, as well as details of T therapy have been published elsewhere (4), Briefly, participants in this study included men, between 40 and 75 years of age with an average fasting, morning (between 8 to 11AM) total T level taken twice, at least 30 minutes apart, of <300 ng/dl, with no medical problems that may prevent them from finishing the study. Exclusion criteria included treatment with bone-acting drugs (e.g., bisphosphonates, teriparatide, denosumab, glucocorticoids, sex steroid compounds, selective estrogen receptor modulators, androgen deprivation therapy, and anticonvulsants) and finasteride. Additional exclusion criteria included osteoporosis and history of fragility fractures or diseases known to affect bone metabolism, such as hyperparathyroidism, chronic liver disease, uncontrolled or untreated hyperthyroidism, and significant renal impairment (creatinine of >1.5 mg/dl). Those with a history of prostate cancer, breast cancer, and untreated sleep apnea also met the criteria for exclusion.

2.3 Testosterone therapy

Testosterone cypionate was initiated at a dose of 200 mg every 2 weeks by intramuscular injection and adjusted to a target serum testosterone level between 17.3 to 27.2 nmol/L (500–800 ng/dl). However, after the 3rd year of the study upon the direction of the FDA, this target was changed to 17.3–20.8 nmol/L (300–600 ng/dl). This change affected the data in the last 6M of 16 subjects at NMVAHCS and all 15 subjects at MEDVAMC. Comparing testosterone levels at different timepoints showed no significant differences between those who were and those not affected by the change except at 6M where levels are higher for those affected. T therapy was given for 18 months. Fifty-one participants at NMVAHCS did self-injections, 38 received injections from the study team only, while 2 started with the study team and later did self-injections. At MEDVAMC, 5 subjects received injections from the study team while 10 did self-injections. Dosage adjustments were based on serum testosterone and hematocrit levels, and occurrence of symptoms and done by increments or decrements of 50 mg. A decrease in the dose was done for patients who develop a hematocrit of >52%. Repeat testosterone measurement was performed 2 months after a dose change, including a repeat hematocrit for those with elevated hematocrit. Otherwise, testosterone levels were measured at baseline, 3, 6, 12 and 18 months. Safety monitoring included assessment of prostate specific antigen (PSA), hematocrit, lipid profile, liver enzymes at baseline, 3, 6, 12, and 18 months.

2.4 Body mass index (BMI)

Body mass index (BMI) calculated as weight (kg) divided by the square of the height (m2). Height and weight were measured using a standard stadiometer and weighing scale, respectively.

2.5 Body composition

Assessment of body composition was performed by dual-energy X-ray absorptiometry (DXA) (Hologic-Discovery; Enhanced Whole Body 11.2 software version; Hologic Inc, Bedford, MA; USA) at baseline, 6, 12 and 18 months as previously described (4) Fat-free mass was calculated by adding whole body bone mineral content to the lean mass. The CV for lean mass and fat mass in our laboratory is 1.5% (20).

2.6 Subcutaneous fat biopsy

Fat biopsies were performed on patients recruited at the NMVAHCS at baseline and after 6 months of T therapy as previously described (4). Briefly, fat samples were obtained from the abdominal subcutaneous adipose tissue depot. The periumbilical area was disinfected and local anesthesia using 2% lidocaine was applied before proceeding with a small incision. Adipose tissue (~500 mg) was collected using a liposuction needle under sterile conditions. Samples were then washed in isotonic NaCl, snap-frozen in liquid nitrogen and kept at −80°C until utilization for the gene expression studies. A limited number of samples were available to perform longitudinal analysis of gene and protein expression that occur with T therapy in hypogonadal men (N=15 for SAT, N=22 for PBMC and N=38 for serum assessments).

2.7 Gene expression studies

2.7.1 Subcutaneous fat (SCF)

We measured the adipogenic transcription factors (*PPARγ*, *CEBPα*), enzymes (*LPL*, Adipsin) from (SCF) in triplicates using real-time quantitative polymerase chain reaction at BL and 6M respectively. Total RNA was isolated from SCF obtained at baseline and after 6M using RNeasy Plus Universal Mini Kit (QIAGEN, Valencia, CA, USA) and Fast Prep 24–5G homogenizer (MP Biomedicals, Santa Ana, CA, USA) following the manufacturer's instructions. The quality and quantity of total RNA were analyzed by using both, nanodrop and Bioanalyzer 2100 (Agilent Technologies, Santa Clara, CA, USA). RNA was extracted as above and 200ng of RNA were used for retro transcription into cDNA and performed using Superscript VILO Master Mix (Invitrogen, Carlsbad, CA, USA) following protocol instructions. FAM-labeled TaqMan Gene expression assays (Applied Biosystem, College Station, TX, USA) for *PPARγ* (Assay ID: Hs01115513_m1); *CEBPα* (Assay ID: Hs00269972_s1); Lipoprotein Lipase *(LPL)*(Assay ID: Hs00173425_m1), and VIC-labeled TaqMan gene expression assay for housekeeping 18S (Assay ID: Hs03928990_g1) and TaqMan Universal Master Mix in triplicates were used following the manufacturer's protocol. Estrogen receptor (ESRα) and Cytochrome P450 Family 19 Subfamily A member 1 (*CYP19A1*) gene expression from SCF were previously analyzed and reported in a prior publication (20) The gene expression data of both genes in the subset of men who were part of this study are included in the analysis.

10.3389/fendo.2024.1426175

2.7.2 Peripheral blood mononuclear cells (PBMC)

PRDM16, MYF-5, MYO-D and *PAX-7* gene expression from PBMC was performed by real-time quantitative polymerase chain reaction at baseline (BL), 6months (6M). As earlier results from our lab indicated that the effect of T therapy is maximal after 6M, we chose to study the specimens at BL and 6M. RNA was extracted from PBMC using RiboPure Blood (Invitrogen, #AM1928). 200ng of RNA were used for retro transcription into cDNA and performed using Superscript VILO Master Mix (Invitrogen, Carlsbad, CA, USA) in triplicates following protocol instructions. FAM-labeled TaqMan Gene expression assays (Applied Biosystem, College Station, TX, USA) for myoblast determination protein 1 (*MYOD*1) (Assay ID: Hs00159528_m1); Myogenic factor 5 (*MYF5)* (Assay ID: Hs00929416_g1); *PRDM16* (Assay ID: Hs00223161_m1); *PAX7* (Assay ID: Hs00242962_m1); and VIC-labeled TaqMan gene expression assay for housekeeping 18S (Assay ID: Hs03928990_g1) and TaqMan Universal Master Mix were used following the manufacturer's protocol.

2.7.3 Relative quantification

ΔΔCT relative quantification: gene expression of our sample vs gene expression of human control total RNA (Applied Biosystem #4307281) adjusted for housekeeping gene expression. Data analysis was performed using Real Time PCR system QuantStudio5 and Quant Studio Design & Analysis Software 1.3.1, respectively.

2.8 Elisa studies

The following were measured using enzyme linked immunosorbent assay (ELISA)kits: Human ADIPONECTIN kit EZHADP-61K Human Leptin kit, EZHL-805K, Temecula, CA, USA); Human FOLLISTATIN (FST) ELISA kit, DFN00; Human GDF-8/MYOSTATIN Immunoassay DGDF80, (Quantikine; R&D Systems, Minneapolis, MN,USA),; Human CFD Elisa kit (EHCFD) (Invitrogen, Carlsbad, CA, USA), PRDM16 Human Elisa kit (Biomatik, EKN52948, Wilmington, Delaware, USA); PAX7 Immunoassay kit (MBS2606278). The CVs for the above assays in our laboratory are <10%. There were a limited number of patients who had corresponding baseline and 6-month samples available to perform longitudinal analysis of gene and protein expression, i.e., N=15 for SCF, N=22 for PBMC and N=38 for serum assessments. An additional file shows the details of kits, chemicals, and instrumentation details (See Supplementary Table) used in this study.

2.9 Statistical analysis

As earlier results from our lab, effect of T therapy is maximal after 6M, we chose to study the specimens at baseline (BL) and 6months (6M). All data are presented as mean ± SEM in figures and mean ± SD in table, were analyzed by Two-tailed Student's paired or unpaired t test. The association between changes in body composition and changes in PRDM16 were analyzed by simple regression analysis. All analyses were performed using Prism 9.0 (GraphPad, San Diego, CA, USA). A p value of < 0.05 is considered significant.

3 Results

Table 1 shows the body composition, hormonal profile, adipogenic and myogenic markers in the forty men with available baseline (BL) and 6M samples of SCF, PBMC and serum included in the analysis. There were significant increase in T (BL: 258.6 ± 90.34 ng/dl vs 6M:578.3 ± 241.7 ng/dl, p=0.001), E2 (BL: 15.69 ± 6.06 pg/ml vs 6M:39.4 ± 21.2 pg/ml, p=0.001) and estradiol/testosterone ratio (E/T) (BL: 0.70 ± 90.38 vs 6M:71.3 ± 40, p=0.001) (Table 1) at 6 months when compared to baseline. Furthermore, T therapy resulted in a significant decrease in total % body fat (BL:30.71 ± 6.35% vs 6M:27.8 ± 5.2%, p<0.05) along with significant increase in total lean mass (BL: 63201 ± 5894 g vs 6M: 67006 ± 7495 g, p=0.03) (Table 1) There were no significant

TABLE 1 Six months of T therapy improved the body composition in hypogonadal men.

Parameter in Study-	Baseline (BL) characteristics	T Therapy (6M)	P value
Age	59.8 ± 8.5	60.1 ± 8.7	0.86
BMI	32.1 ± 5.1	32.2 ± 4.9	0.90
Testosterone	258.6 ± 90.34	578.3 ± 241.7	**0.001**
Estradiol	15.69 ± 6.06	37.39 ± 21.2	**0.001**
E/T	0.70 ± 0.38	71.3 ± 40.1	**0.001**
Total body fat mass (g)	31505 ± 11391	28222 ± 9629	0.21
Total % body fat	30.71 ± 6.35	27.79 ± 5.2	**<0.05**
Trunk fat mass (g)	16843 ± 7495	14921 ± 6227	0.27
Total lean mass (g)	63201 ± 5894	67006 ± 7495	**0.03**
Appendicular lean mass (g)	29043 ± 4474	30586 ± 4040	0.14
Fat-free mass (g)	67696 ± 7652	69669 ± 7637	0.29
Leptin (ng/ml)	2.7 ± 2.01	2.1 ± 1.5	0.15
Adiponectin (μg/ml)	49.7 ± 27.6	45.37 ± 27.1	0.50
CYP19A1-Fat	2.99 ± 0.90	6.58 ± 2.26	0.26
ESRα-Fat	56.2 ± 17.76	68.96 ± 28.8	0.74
ADIPSIN (ng/ml)	1864 ± 1538	1193 ± 520.5	**0.02**
PRDM16 (ng/ml)	0.30 ± 0.11	0.55 ± 0.72	**<0.05**
PAX7 (ng/ml)	31.2 ± 13.3	42.3 ± 13.9	**0.001**
FOLLISTATIN (pg/ml)	2344 ± 1684	3508 ± 1725	**0.003**
MYOSTATIN (pg/ml)	3437 ± 2029	2882 ± 1800	0.40

The above table explore the Baseline and 6M characteristics of the subset who participated in the study. Six months of Testosterone (T) therapy significantly enhanced T, estradiol, E/T along with serum levels of Myogenic (PRDM16, PAX7, FST) and total lean mass, while decreased total % body fat, adipokine ADIPSIN. BMI, Body mass index; E, estradiol; T, Testosterone; CYP19A1 gene, Cytochrome P450 Family 19 Subfamily A member 1; ESRα gene, Estrogen receptor alpha; PAX7, Paired box7 protein; PRDM16, PR domain containing protein 16; The bolded p values are statistically significant, All values are Mean ± SD.

10.3389/fendo.2024.1426175

differences in the other parameters such appendicular lean mass, trunk fat mass, total body fat mass and fat free mass between BL and 6 months.

We next studied the gene and protein machinery that may be involved in the changes in body composition we observed *in-vivo*.

3.1 Adipogenic

Our results showed that T therapy resulted in the significant reduction in the adipogenic gene mRNA levels of *PPARγ*, in SCF (BL: 2.59 ± 0.57 vs 6M: 1.22 ± 0.26, p=0.03) (Figure 1A) Gene expression of *CEBPα*, displayed a non-significant trend for reduction (1.7-fold from baseline; p=0.10) (Figure 1B) in SCF. Similarly, *LPL*, a key factor in lipid homeostasis, was also non-significantly reduced (BL: 2.81 ± 0.73 vs 6M: 1.74 ± 0.6, p=0.27) (Figure 1C). On the other hand, the levels of serum ADIPSIN, significantly decreased with T therapy (BL:1864 ± 1538 ng/ml vs 6M:1193 ± 520.5 ng/ml p=0.02) (Figure 1D), while levels of serum ADIPONECTIN and LEPTIN did not vary significantly (Table 1).

3.2 Myogenic

Because previous studies have demonstrated that PBMC gene expression is strongly correlated with skeletal muscle transcriptional profile (21) we examined the expression of skeletal muscle gene machinery in PBMC. There was a non-significant trend for increased expression of *PAX7* with T therapy (BL:1.27 ± 0.17 vs 6M: 1.89 ± 0.44, p=0.2) (Figure 2A), in PBMC. However, a significant increase in PAX7 from baseline (BL:31.22 ± 13.3 ng/ml vs 6M: 42.3 ± 13.9 ng/ml, (p=0.001) (Figure 2D) was observed in the serum. Because Pax7 regulates the activation of myogenic regulators (22), we next analyzed the expression of the myogenic lineage gene machinery by RT-qPCR in PBMC. Although T therapy did not result in a significant increase in expression of the myomarker *MYF5* (BL: 6.1 ± 9.7 vs 6M: 14.06 ± 6.14, p=0.18), (Figure 2B), there was a significant increase in the expression of its downstream effector *MYOD1*, (Figure 2C) (BL:1.34 ± 0.35 vs 6M: 8.2 ± 12.7, p=0.02). Also, previous studies found that T-therapy upregulated FST in satellite cells (23), hence we assessed FST serum levels following 6M of T

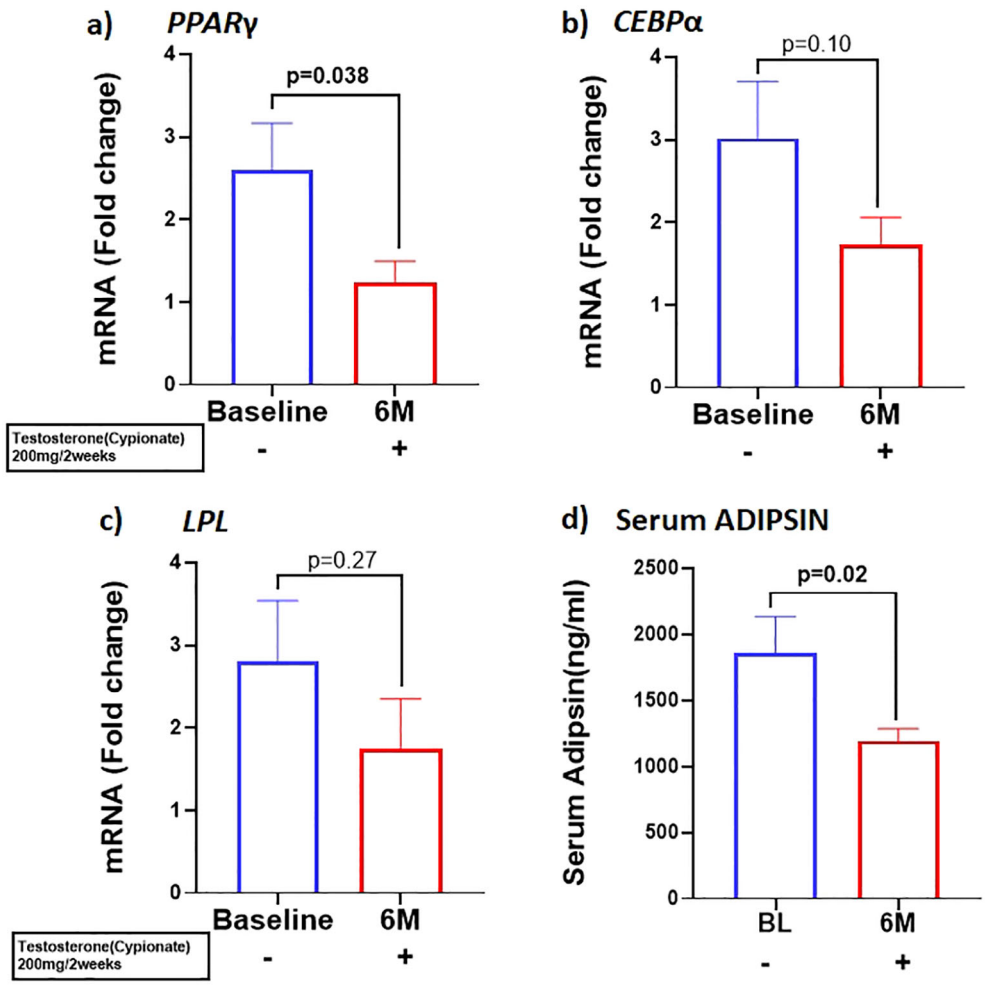

FIGURE 1
T therapy downregulated the adipogenic gene machinery with reduction in mRNA levels of adipogenic markers **(A)** *PPARγ*, **(B)** *CEBPα*, and **(C)** *LPL* in Sub cutaneous fat (SCF), and in **(D)** Adipsin protein levels in the serum after 6 months of T-therapy in hypogonadal men. Data shown as Mean ± SEM. All analyses were done using Two-tailed Student's paired or unpaired t test; bolded p values are significant at 6 months compared to baseline.

10.3389/fendo.2024.1426175

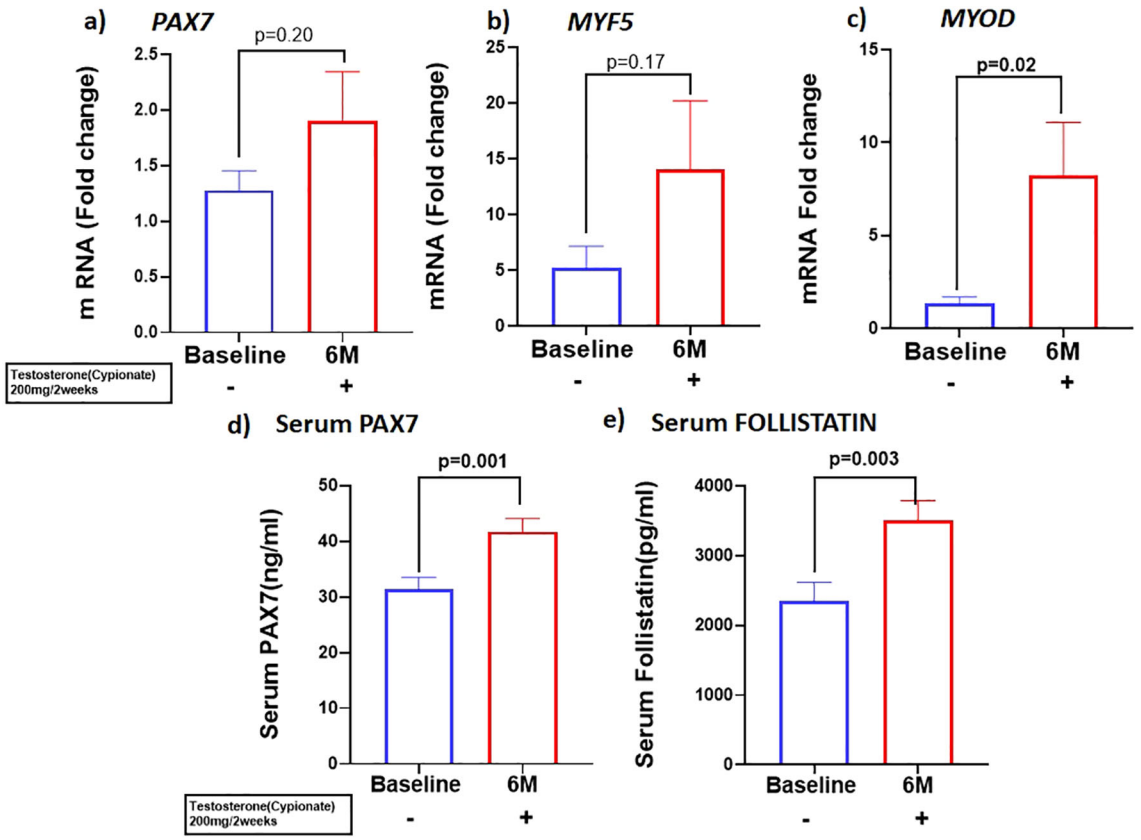

FIGURE 2
T therapy enhanced Myogenic gene machinery. mRNA levels of **(A)** *PAX7* and **(B)** *MYF5* were moderately increased along with significant increase in mRNA levels of myogenic marker **(C)** *MYOD* in peripheral blood mononuclear cells (PBMC); Protein levels of **(D)** Serum PAX7 and **(E)** Serum FOLLISTATIN after 6 months of T-therapy in hypogonadal men. Data shown as Mean ± SEM. All analyses were done using Two-tailed Student's paired or unpaired t test; bolded p values are significant at 6 months compared to baseline.

therapy and observed a significant increase (BL: 2344 ± 1684 pg/ml vs 6M: 3508 ± 1745 pg/ml, p=0.003) (Figure 2E) in levels. However, serum MYOSTATIN levels did not vary following T treatment (BL: 3437 ± 2029 pg/ml vs 6M: 2882 ± 1800pg/ml, p=0.40) (Table 1).

3.3 Adipomyogenic switch

We investigated the expression of the adipo-myogenic switch, PRDM16, and observed a significant upregulation of *PRDM16* expression in the SCF (BL: 2.59 ± 0.56 vs 6M: 1.23 ± 0.26, p=0.03). (Figure 3A) and in the PBMC (BL: 1.8 ± 0.42 vs 6M: 4.5 ± 0.92, p<0.01), (Figure 3B) after 6 months of T therapy. Serum level of PRDM16 was also significantly increased (BL: 0.30 ± 0.11 ng/ml vs 6M: 0.55 ± 0.72 ng/ml, p=0.042) (Figure 3C) following 6M of T therapy.

We examined the correlation between the changes PRDM16 levels in the different tissues and body composition. We found no significant correlations between the changes in PRDM16 in the SCF, PBMC and serum with changes in any parameters of body fat. We also found no correlation between the changes in PRDM16 in the SCF and PBMC with total and appendicular lean and fat-free mass. However, significant correlations were observed between changes in PRDM16 protein levels in the serum with changes in total lean mass (r=0.65, p=0.002), appendicular lean mass (r=0.48, p=0.02) and fat-free mass (r=0.51, p=0.01), see Figure 4.

4 Discussion

Previous studies demonstrated a reduction in total body and truncal fat mass along with an increase in lean mass in T-treated hypogonadal men (4, 5). Although animal and *in-vitro* studies suggest reduced adipogenesis coupled with increased myogenesis as the mechanisms for this observation, occurrence of these changes in humans and which pathways are involved, remain uncertain. The present study confirmed the reduction in the expression of adipogenic and an increase in myogenic modulators occur in human subjects taking T. More importantly, our results also suggest for the first time the potential role of enhanced PRDM16 in regulating these pathways perhaps directly or indirectly by unknown downstream targets which was never explored before, providing insights into a regulatory network that underpins the positive effects of T on body composition in men with hypogonadism.

The anti-adipogenic effect of androgens has been suggested by studies demonstrating that T and its metabolite, dihydroxytestosterone (DHT), downregulate *PPARγ*, a key transcription factor regulating adipogenesis and *CEBPα*, a transcription factor that coordinates

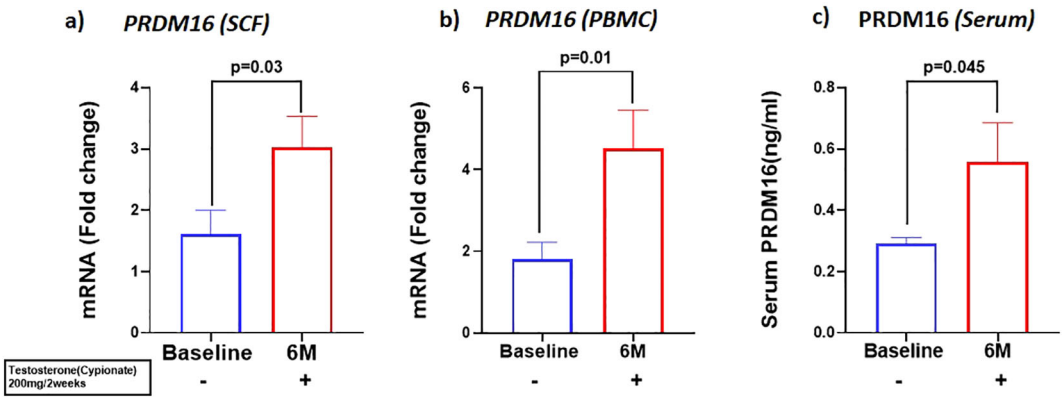

FIGURE 3
Increase in the expression of PRDM16, in mRNA levels of **(A)** *PRDM16* in Sub cutaneous fat (SCF) and **(B)** *PRDM16* in peripheral blood mononuclear cells (PBMCs), and **(C)** Protein levels (Serum PRDM16) after 6 months of T-therapy in hypogonadal men. Data shown as Mean ± SEM. All analyses were done using Two-tailed Student's paired or unpaired t test; bolded p values are significant at 6 months compared to baseline.

proliferation and differentiation of adipocytes (24). This results in inhibition of the commitment of subcutaneous human adipose stem cells obtained from nonobese women to preadipocytes and reduce early-stage adipocyte differentiation Moreover, Singh et al., reported that administration of T (0-300nM) or DHT(0-30nM) to C3H10T1/2 to pluripotent cells not only inhibited adipogenic lineage, but also promoted the commitment of MSCs to the myogenic lineage (6). On the other hand, the CYP19A1 activity present in the adipose tissue results in conversion of T to E2 (See Figure 5). *In vivo* studies in female ovariectomized rats demonstrated downregulation of the adipogenic markers with E2 treatment (25). These studies suggest that both T and E2 are involved in downregulation of adipogenesis. Our results agree with these findings; we observed a significant reduction in adipogenic machinery, primarily *PPARγ*, in SCF following 6M of T therapy. Moreover, even though we did not detect significant changes in circulating LEPTIN and ADIPONECTIN, we found significant decrease in ADIPSIN, another adipokine, linked to increased fat mass and adipose tissue dysfunction in metabolic disorders (26), at 6M of T therapy. Since myocytes and adipocytes are derived from the same MSCs, we sought to elucidate the T-induced signaling that may explain the fat and muscle changes observed in hypogonadal men.

PRDM16 is recognized as the factor involved in the switch from white to brown adipocytes, and possibly also as the interconvertible switch between myocyte to adipocyte lineage differentiation (16).

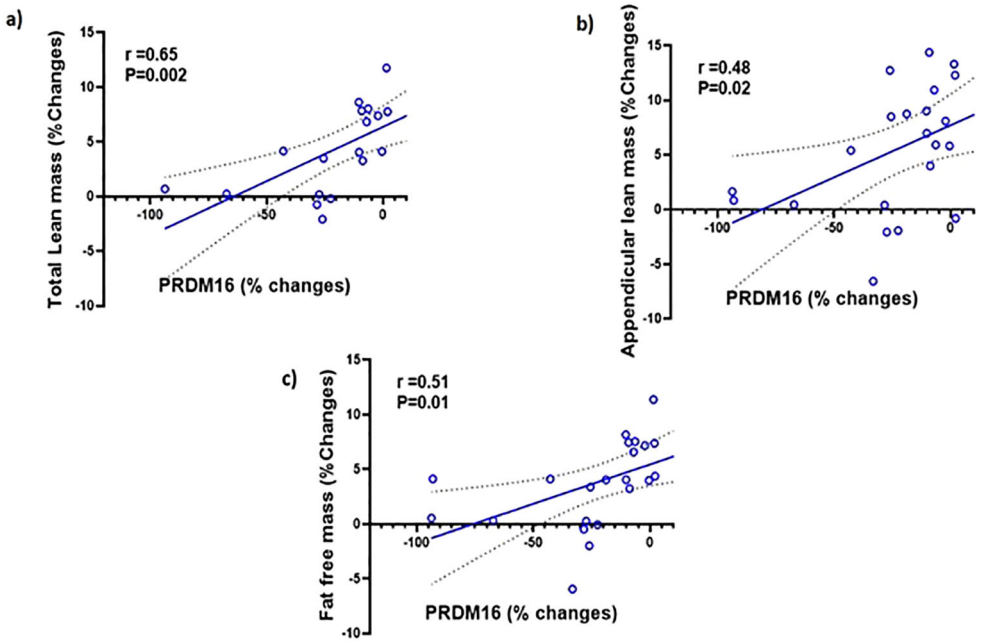

FIGURE 4
Simple regression analysis showing changes (%) in PRDM16 in the serum are significantly positively correlated with changes (%) in: **(A)** total lean mass (r=0.65, P=0.002); **(B)** Appendicular lean mass (r=0.48, P=0.02); **(C)** fat-free mass (r=0.51, P=0.01) with testosterone therapy.

10.3389/fendo.2024.1426175

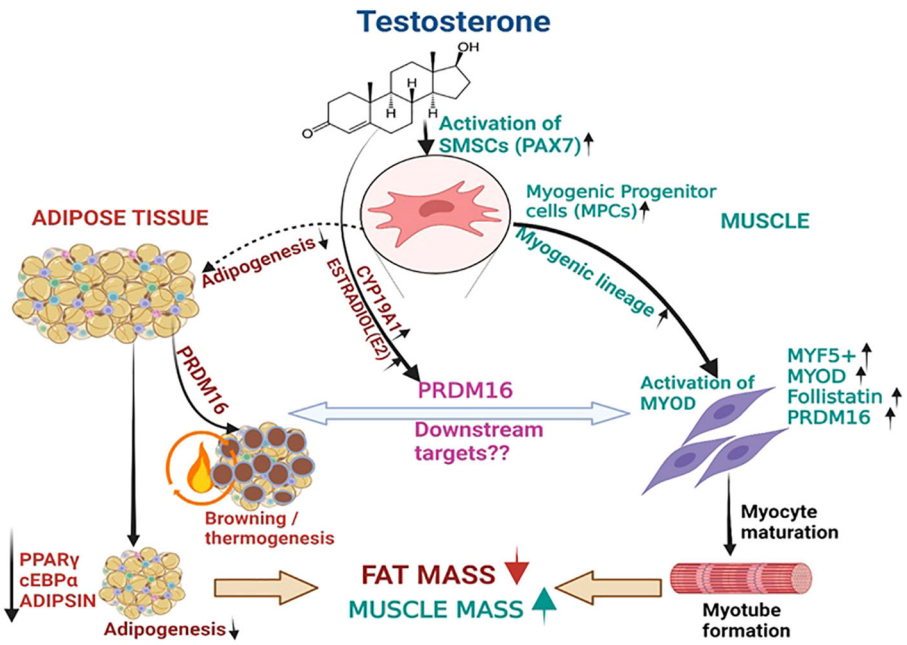

FIGURE 5
T therapy reduced adipogenic machinery and enhanced Myogenic gene machinery. T activate the MSCs via PAX7 to promote the commitment of MSCs to the myogenic lineage and subsequently activate MYF5 a key transcription factor for myogenic stem cells commitment to myoblast lineage. This in turn might increase the expression of its downstream effector myoblast determination protein 1 (*MYOD1)*, a transcription factor promoting myoblast proliferation and FOLLISTATIN leading to myotube formation. On the other hand, Estradiol formed from T by the action of CYP19A1 activates the formation of PRDM16, which not only acts as a bi-directional switch between adipogenesis and myogenesis but also causes thermic browning which along with unknown downstream targets might enhance myogenesis. Thus, adipogenic gene machinery of PPARγ, and ADIPISIN are decreased significantly leading to reduction in fat mass by T therapy.

Interestingly, we found a significant increase in PRDM16 expression in SCF, PBMC, and in serum with T therapy. We believe that this is due to the increase in E2 which likely upregulates PRDM16 in the different tissue compartments. Although Zhao et al. showed a negative regulation of PRDM16 by androgens in animals given a nonaromatizable androgen (17), these authors also reported higher levels of PRDM16 in the omental WAT of women compared to men (17) suggesting that the presence of E2 (which is normally found in humans irrespective of gender), overcomes the suppressive effect of androgens on PRDM16. Moreover, an *in-vitro* study by Sul et al. reported that the adipose tissue browning effect of E2 could be mediated by enhanced levels of PRDM16 (18). Our results showed significantly increased levels of circulating E2 and E/T ratio after 6 months of T therapy, likely from enhanced conversion of exogenously administered T to E2. This could account for the increased expression of PRDM16 not only in the SCF, but also in the PBMC and in the serum of men treated with T. We hypothesize that E2 has stimulatory effect on PRDM16 biosynthesis and is responsible for the increase in PRDM16 in all tissues examined in our subjects. While prior studies have established PRDM16 as the crucial switch between white and brown adipogenesis (13), a study by Jiang et al. suggested that it may also function as a switch between adipogenesis and myogenesis (27). In their study, targeted inhibition of PRDM16 by MIR-499 resulted in inhibition of adipogenic while enhancing myogenic markers. Results from our study seem to support the potential role of PRDM16 on the shift from adipogenesis to myogenesis.

Aside from browning of white adipose tissue, it is possible that PRDM16 could have a significant contribution to other aspects of adipose tissue biology. Overexpression of PRDM16 was found to reduce adipogenesis by inhibiting maturation of pig preadipocytes to mature adipocytes through increased lipolysis (28). In this study, there was a significant reduction on PPARγ expression in the early stages of preadipocyte differentiation. Similarly, we found a significant reduction in PPARγ and increase in PRDM16 in the SCF of our subjects which may account for decreased body fat in our hypogonadal men treated with T.

In the myogenic cascade, *PAX7* is the critical transcription factor which regulates regeneration and proliferation of myogenic precursors (29)**;** *MYF5*, is the key transcription factor for myogenic stem cells commitment to myoblastic lineage while *MYOD* directs progenitor cells to myocyte differentiation (30). In preclinical studies, T (100nM) upregulated Pax7 in satellite cells of 2–3-month-old C57BL/6 male mice (23). Another study also reported an increase in the satellite cells of denervated levator ani muscle of rats given T implants compared to non-treated animals (31). Furthermore, Sihna-Hikim et al. demonstrated that T therapy at doses of 300 and 600mg weekly for 20 weeks caused a significant increase in satellite number of the vastus lateralis muscle compared to baseline resulting in muscle hypertrophy (32). The significant increase in PAX7 in the serum of our patients along with the significant increase in *MYOD* expression in PBMC and levels of FST in the serum seem to support the effect of T in stimulating the commitment of skeletal MSCs into the myogenic lineage (33). FST

has been reported to increase with T therapy and promote myogenesis by inhibiting MYOSTATIN, a negative regulator of myogenic proliferation (23). Although we cannot detect a significant change in *MYF5* or MYOSTATIN in our study, the small sample size in our study may have impaired our ability to observe such change.

Although our results showing upregulation of MYOD with increase in PRDM16 may contradict previous concept about the function of PRDM16 on myogenesis, Li et al, found that deletion of PR domain from PRDM16 protein in C2C12 cells resulted in significant downregulation of myofiber markers, MyoD, MyHC (Myosin heavy chain) and MCK (Muscle creatinine kinase) as compared to cells transfected with intact PRDM16 (34). The PR domain gene family (PRDM) encodes 19 different transcription factors which are the zinc finger motifs to mediate protein-RNA, protein-DNA interactions (35). In general, PRDM16 exist in two isoforms, a full length PRDM16 with PR domain (fPRDM16) and short PRDM16 which lacks the N-terminal PR domain (sPRDM16) Each isoform has opposing effects, at least in malignancies (38) For instance, while the fPRDM16 is crucial for hematopoetic stem cell (HSC) maintenance and functions as leukemia suppressor, sPRDM16 has the ability to maintain the elongated mitochondria in HSCs, induce inflammation and promote the development of leukemic cells (36). In humans, 1p36 chromosomal deletion that includes the terminal 14 exons of PRDM16 (including exons 4 and 5 of the PR domain) and inactivating point mutations in the gene resulting in loss of function have been found among individuals with left ventricular noncompaction cardiomyopathy and dilated cardiomyopathy (37) The cardiac abnormalities in these patients were attributed to findings of impairment in cardiomyocyte proliferative capacity and even apoptosis of these cells (38) Furthermore, mice with conditional PRDM16 knockout in vascular smooth muscle cell showed increased apoptosis, while PRDM16 deficiency has been demonstrated in abdominal aortic aneurysm lesions in humans (39). Although the latter are examples of pathology involving smooth muscles, yet in conjunction with the data from Li et. al., perhaps would altogether suggest a positive role of PRDM16 in myogenesis (skeletal and smooth muscles). On the other hand, it is also possible that *PRDM16* may upregulate the myogenic pathway via unknown downstream factors. As far as our study is concerned, we measured the full-length PRDM16 transcripts in the SCF and PBMC and the full-length protein in the serum. By showing a correlation between changes in PRDM16 protein levels in the serum and changes in lean and fat-free mass, our data suggest that PRDM16 could have a distinct and separate role in promoting myogenesis apart from its well-recognized function as the adipomyogenic switch.

The strengths of our study include: 1) novelty, our study is the first to explore gene and protein machinery involved in the increase in lean mass and reduction in fat mass in men with hypogonadism given T therapy, and 2), this is the first study to evaluate the molecular mechanism behind the positive effects of T-therapy *in-vivo* on body composition in hypogonadal men. However, this study presents several limitations. Firstly, it is a secondary analysis of samples from our prior clinical trial; hence, we have limited number of samples available to perform longitudinal analysis of gene and protein expression that occur with T therapy and this may have resulted in lack of significance in certain adipogenic and myogenic markers. Secondly, PBMC was used as a surrogate of skeletal muscle gene expression. However, gene expression studies in PBMCs can be used as a substitute for muscle gene expression has been suggested by Rudkowska et al. (21). These authors investigated the correlation between transcriptome in PBMCs and skeletal muscle tissues before and after 8-week supplementation with n-3 polyunsaturated fatty acid (PUFAs) in 16 obese and insulin resistant human subjects (7). They found that 88% of the transcripts were co-expressed in both tissues. Moreover, there was a strong correlation ($r = 0.84$, $p < 0.0001$) between transcript expression levels in PBMCs and skeletal muscle tissues after n–3 PUFA supplementation. These led them to conclude that in the interest of cost and practicality, PBMCs can be used as a surrogate model for skeletal muscle gene expression. Furthermore, very recently Banerji et al. (2023) found that expression of PAX7 target genes in the muscle of fascioscapulo humeral muscular dystrophy patients (the so-called FSHD blood-biomarker) was significantly correlated with the levels in PBMCs (P=0.002) and suggested this could be used as a novel muscle-blood biomarker to measure clinical severity of FSHD (40), again suggesting the potential utility of PBMCs as surrogate for muscles. Lastly, both Prdm16 and Pax7 are traditionally considered as nuclear proteins. However, newer data suggests that nuclear contents can be detected outside of the nucleus and inside extracellular vesicles (EVs) (41). EVs carry proteins and can transfer from one tissue to another or enter the circulation allowing tissue to tissue communication (41, 42). The presence of PRDM16 in EVs has been reported by Sun et.al (43). These investigators showed that uptake of PRDM16-containing EVs from hepatic stellate cells by hepatocellular carcinoma cells results activation of NOTCH signaling leading to tumor progression (43). Thus, presence of PRDM16 in EVs may allow its detection in the serum as our study was able to determine. Similarly, for PAX7, it is possible that EVs carrying PAX7 find their way into the circulation allowing measurement of this factor in the serum. Nevertheless, since we are the first to report measurement of both factors in the serum, our findings need confirmation in future studies.

5 Conclusion

In summary, our results suggest that T therapy promoted a shift from the adipogenic to the myogenic gene/protein machinery which may explain the reduction in body fat and increase in lean mass in our subjects of older hypogonadal men. These desirable effects on body composition may be modulated in part by enhanced PRDM16 driven signal resulting from an increase in estradiol levels leading to subsequent changes in downstream target of genes and proteins involved in adipogenesis and myogenesis. Thus, PRDM16 may represent a target for drug development to improve body composition in patients with age-related loss in muscle mass with concomitant increase in fat mass such as those with sarcopenic obesity.

Data availability statement

The original contributions presented in the study are included in the article/supplementary material, further inquiries can be directed to the author RA-V.

Ethics statement

The protocol was approved by the Institutional Review Board of the University of New Mexico School of Medicine and the Baylor College of Medicine. The studies were conducted in accordance with the local legislation and institutional requirements. The participants provided their written informed consent to participate in this study.

Author contributions

SB: Conceptualization, Data curation, Formal analysis, Investigation, Methodology, Software, Writing – original draft, Writing – review & editing. GC: Investigation, Writing – review & editing. DV: Investigation, Writing – review & editing. LA: Investigation, Writing – review & editing. RC: Investigation, Writing – review & editing. RA-V: Conceptualization, Funding acquisition, Investigation, Project administration, Resources, Supervision, Validation, Writing – review & editing.

Funding

The author(s) declare financial support was received for the research, authorship, and/or publication of this article. This study was supported by VA merit Review 101CX000424, 101CX001665, and NIH R01 HD093047 to RA-V. The findings reported in this article are the result of work supported with resources and the use of facilities at the New Mexico VA Health Care System and Michael E. De Bakey VA Medical Center.

Acknowledgments

Preliminary data from the study were presented in the form of abstract at ENDO-2023, the annual scientific meeting of the Endocrine Society (38). We thank the participants for their cooperation.

Conflict of interest

The authors declare that the research was conducted in the absence of any commercial or financial relationships that could be construed as a potential conflict of interest.

The author(s) declared that they were an editorial board member of Frontiers, at the time of submission. This had no impact on the peer review process and the final decision.

Publisher's note

Author disclaimer

The content is solely the responsibility of the authors and does not necessarily represent the official views of the National Institutes of Health and the Department of Veterans Affairs or the United States Government.

Supplementary material

The Supplementary Material for this article can be found online at: https://www.frontiersin.org/articles/10.3389/fendo.2024.1426175/full#supplementary-material

References

1. Chin KY, Soelaiman IN, Naina Mohamed I, Shahar S, Teng NI, Suhana Mohd Ramli E, et al. Testosterone is associated with age-related changes in bone health status, muscle strength and body composition in men. *Aging Male*. (2012) 15:240–5. doi: 10.3109/13685538.2012.724740

2. Stárka L, Hill M, Pospíšilová H, Dušková M. Estradiol, obesity and hypogonadism. *Physiol Res*. (2020) 69:S273–s8. doi: 10.33549/physiolres

3. Bhasin S, Storer TW, Berman N, Yarasheski KE, Clevenger B, Phillips J, et al. Testosterone replacement increases fat-free mass and muscle size in hypogonadal men. *J Clin Endocrinol Metab*. (1997) 82:407–13. doi: 10.1210/jc.82.2.407

4. Aguirre LE, Colleluori G, Robbins D, Dorin R, Shah VO, Chen R, et al. Bone and body composition response to testosterone therapy vary according to polymorphisms in the CYP19A1 gene. *Endocrine*. (2019) 65:692–706. doi: 10.1007/s12020-019-02008-6

5. Deepika F, Ballato E, Colleluori G, Aguirre L, Chen R, Qualls C, et al. Baseline testosterone predicts body composition and metabolic response to testosterone therapy. *Front Endocrinol (Lausanne)*. (2022) 13:915309. doi: 10.3389/fendo.2022.915309

6. Singh R, Artaza JN, Taylor WE, Gonzalez-Cadavid NF, Bhasin S. Androgens stimulate myogenic differentiation and inhibit adipogenesis in C3H 10T1/2 pluripotent cells through an androgen receptor-mediated pathway. *Endocrinology*. (2003) 144:5081–8. doi: 10.1210/en.2003-0741

7. Varlamov O, White AE, Carroll JM, Bethea CL, Reddy A, Slayden O, et al. Androgen effects on adipose tissue architecture and function in nonhuman primates. *Endocrinology*. (2012) 153:3100–10. doi: 10.1210/en.2011-2111

8. Zuk PA, Zhu M, Mizuno H, Huang J, Futrell JW, Katz AJ, et al. Multilineage cells from human adipose tissue: implications for cell-based therapies. *Tissue Eng*. (2001) 7:211–28. doi: 10.1089/107632701300062859

9. Mochizuki N, Shimizu S, Nagasawa T, Tanaka H, Taniwaki M, Yokota J, et al. A novel gene, MEL1, mapped to 1p36.3 is highly homologous to the MDS1/EVI1 gene and is transcriptionally activated in t(1;3)(p36;q21)-positive leukemia cells. *Blood*. (2000) 96:3209–14. doi: 10.1182/blood.V96.9.3209

10. Chi J, Cohen P. The multifaceted roles of PRDM16: Adipose biology and beyond. *Trends Endocrinol Metab*. (2016) 27:11–23. doi: 10.1016/j.tem.2015.11.005

11. Aguilo F, Avagyan S, Labar A, Sevilla A, Lee DF, Kumar P, et al. Prdm16 is a physiologic regulator of hematopoietic stem cells. *Blood*. (2011) 117:5057–66. doi: 10.1182/blood-2010-08-300145

12. Pinheiro I, Margueron R, Shukeir N, Eisold M, Fritzsch C, Richter FM, et al. Prdm3 and Prdm16 are H3K9me1 methyltransferases required for mammalian heterochromatin integrity. *Cell*. (2012) 150:948–60. doi: 10.1016/j.cell.2012.06.048

13. Seale P, Bjork B, Yang W, Kajimura S, Chin S, Kuang S, et al. PRDM16 controls a brown fat/skeletal muscle switch. *Nature*. (2008) 454:961–7. doi: 10.1038/nature07182

14. Ohno H, Shinoda K, Spiegelman BM, Kajimura S. PPARγ agonists induce a white-to-brown fat conversion through stabilization of PRDM16 protein. *Cell Metab*. (2012) 15:395–404. doi: 10.1016/j.cmet.2012.01.019

15. Kajimura S, Seale P, Kubota K, Lunsford E, Frangioni JV, Gygi SP, et al. Initiation of myoblast to brown fat switch by a PRDM16-C/EBP-beta transcriptional complex. *Nature*. (2009) 460:1154–8. doi: 10.1038/nature08262

16. Frühbeck G, Sesma P, Burrell MA. PRDM16: the interconvertible adipo-myocyte switch. *Trends Cell Biol*. (2009) 19:141–6. doi: 10.1016/j.tcb.2009.01.007

17. Zhao S, Nie T, Li L, Long Q, Gu P, Zhang Y, et al. Androgen receptor is a negative regulator of PRDM16 in beige adipocyte. *Adv Sci (Weinh)*. (2023) 10: e2300070. doi: 10.1002/advs.202300070

18. Sul OJ, Hyun HJ, Rajasekaran M, Suh JH, Choi HS. Estrogen enhances browning in adipose tissue by M2 macrophage polarization via heme oxygenase-1. *J Cell Physiol*. (2021) 236:1875–88. doi: 10.1002/jcp.29971

19. Sinha-Hikim I, Taylor WE, Gonzalez-Cadavid NF, Zheng W, Bhasin S. Androgen receptor in human skeletal muscle and cultured muscle satellite cells: up-regulation by androgen treatment. *J Clin Endocrinol Metab*. (2004) 89:5245–55. doi: 10.1210/jc.2004-0084

20. Colleluori G, Aguirre LE, Qualls C, Chen R, Napoli N, Villareal DT, et al. Adipocytes ESR1 expression, body fat and response to testosterone therapy in hypogonadal men vary according to estradiol levels. *Nutrients*. (2018) 10:1226. doi: 10.3390/nu10091226

21. Rudkowska I, Raymond C, Ponton A, Jacques H, Lavigne C, Holub BJ, et al. Validation of the use of peripheral blood mononuclear cells as surrogate model for skeletal muscle tissue in nutrigenomic studies. *Omics*. (2011) 15:1–7. doi: 10.1089/omi.2010.0073

22. McKinnell IW, Ishibashi J, Le Grand F, Punch VG, Addicks GC, Greenblatt JF, et al. Pax7 activates myogenic genes by recruitment of a histone methyltransferase complex. *Nat Cell Biol*. (2008) 10:77–84. doi: 10.1038/ncb1671

23. Braga M, Bhasin S, Jasuja R, Pervin S, Singh R. Testosterone inhibits transforming growth factor-β signaling during myogenic differentiation and proliferation of mouse satellite cells: potential role of follistatin in mediating testosterone action. *Mol Cell Endocrinol*. (2012) 350:39–52. doi: 10.1016/j.mce.2011.11.019

24. Chazenbalk G, Singh P, Irge D, Shah A, Abbott DH, Dumesic DA. Androgens inhibit adipogenesis during human adipose stem cell commitment to preadipocyte formation. *Steroids*. (2013) 78:920–6. doi: 10.1016/j.steroids.2013.05.001

25. Jeong S, Yoon M. 17β-Estradiol inhibition of PPARγ-induced adipogenesis and adipocyte-specific gene expression. *Acta Pharmacol Sin*. (2011) 32:230–8. doi: 10.1038/aps.2010.198

26. Milek M, Moulla Y, Kern M, Stroh C, Dietrich A, Schön MR, et al. Adipsin serum concentrations and adipose tissue expression in people with obesity and type 2 diabetes. *Int J Mol Sci*. (2022) 23:2222. doi: 10.3390/ijms23042222

27. Jiang J, Li P, Ling H, Xu Z, Yi B, Zhu S. MiR-499/PRDM16 axis modulates the adipogenic differentiation of mouse skeletal muscle satellite cells. *Hum Cell*. (2018) 31:282–91. doi: 10.1007/s13577-018-0210-5

28. Gu T, Xu G, Jiang C, Hou L, Wu Z, Wang C. PRDM16 represses the pig white lipogenesis through promoting lipolysis activity. *BioMed Res Int*. (2019) 2019:1969413. doi: 10.1155/2019/1969413

29. Florkowska A, Meszka I, Zawada M, Legutko D, Proszynski TJ, Janczyk-Ilach K, et al. Pax7 as molecular switch regulating early and advanced stages of myogenic mouse ESC differentiation in teratomas. *Stem Cell Res Ther*. (2020) 11:238. doi: 10.1186/s13287-020-01742-3

30. Yamamoto M, Legendre NP, Biswas AA, Lawton A, Yamamoto S, Tajbakhsh S, et al. Loss of myoD and myf5 in skeletal muscle stem cells results in altered myogenic programming and failed regeneration. *Stem Cell Rep*. (2018) 10:956–69. doi: 10.1016/j.stemcr.2018.01.027

31. Nnodim JO. Testosterone mediates satellite cell activation in denervated rat levator ani muscle. *Anat Rec*. (2001) 263:19–24. doi: 10.1002/ar.1072

32. Sinha-Hikim I, Roth SM, Lee MI, Bhasin S. Testosterone-induced muscle hypertrophy is associated with an increase in satellite cell number in healthy, young men. *Am J Physiol Endocrinol Metab*. (2003) 285:E197–205. doi: 10.1152/ajpendo.00370.2002

33. Seale P, Sabourin LA, Girgis-Gabardo A, Mansouri A, Gruss P, Rudnicki MA. Pax7 is required for the specification of myogenic satellite cells. *Cell*. (2000) 102:777–86. doi: 10.1016/S0092-8674(00)00066-0

34. Li X, Wang J, Jiang Z, Guo F, Soloway PD, Zhao R. Role of PRDM16 and its PR domain in the epigenetic regulation of myogenic and adipogenic genes during transdifferentiation of C2C12 cells. *Gene*. (2015) 570:191–8. doi: 10.1016/j.gene.2015.06.017

35. Sorrentino A, Federico A, Rienzo M, Gazzerro P, Bifulco M, Ciccodicola A, et al. PR/SET domain family and cancer: novel insights from the cancer genome atlas. *Int J Mol Sci*. (2018) 19:3250. doi: 10.3390/ijms19103250

36. Corrigan DJ, Luchsinger LL, Justino de Almeida M, Williams LJ, Strikoudis A, Snoeck HW. PRDM16 isoforms differentially regulate normal and leukemic hematopoiesis and inflammatory gene signature. *J Clin Invest*. (2018) 128:3250–64. doi: 10.1172/JCI99862

37. Arndt AK, Schafer S, Drenckhahn JD, Sabeh MK, Plovie ER, Caliebe A, et al. Fine mapping of the 1p36 deletion syndrome identifies mutation of PRDM16 as a cause of cardiomyopathy. *Am J Hum Genet*. (2013) 93:67–77. doi: 10.1016/j.ajhg.2013.05.015

38. Sun B, Rouzbehani OMT, Kramer RJ, Ghosh R, Perelli RM, Atkins S, et al. Nonsense variant PRDM16-Q187X causes impaired myocardial development and TGF-β Signaling resulting in noncompaction cardiomyopathy in humans and mice. *Circ Heart Fail*. (2023) 16:e010351. doi: 10.1161/CIRCHEARTFAILURE.122.010351

39. Wang Z, Zhao X, Zhao G, Guo Y, Lu H, Mu W, et al. PRDM16 deficiency in vascular smooth muscle cells aggravates abdominal aortic aneurysm. *JCI Insight*. (2023) 8:e167041. doi: 10.1172/jci.insight.167041

40. Banerji CRS, Greco A, Joosten LAB, van Engelen BGM, Zammit PS. The FSHD muscle-blood biomarker: a circulating transcriptomic biomarker for clinical severity in facioscapulohumeral muscular dystrophy. *Brain Commun*. (2023) 5:fcad221. doi: 10.1093/braincomms/fcad221

41. Cai J, Wu G, Jose PA, Zeng C. Functional transferred DNA within extracellular vesicles. *Exp Cell Res*. (2016) 349:179–83. doi: 10.1016/j.yexcr.2016.10.012

42. Rome S. Muscle and adipose tissue communicate with extracellular vesicles. *Int J Mol Sci*. (2022) 23:7052. doi: 10.3390/ijms23137052

43. Sun C, Xu W, Xia Y, Wang S. PRDM16 from hepatic stellate cells-derived extracellular vesicles promotes hepatocellular carcinoma progression. *Am J Cancer Res*. (2023) 13:5254–70.

frontiers | Frontiers in Endocrinology

TYPE Original Research
PUBLISHED 11 February 2025
DOI 10.3389/fendo.2025.1424350

OPEN ACCESS

EDITED BY
Heidi de Wet,
University of Oxford, United Kingdom

REVIEWED BY
Hiroya Ohta,
Hokkaido University of Science, Japan
Rodney Bowden,
Baylor University, United States

*CORRESPONDENCE
Chunli Piao
pcl2013@sina.cn

†These authors have contributed equally to this work and share first authorship

RECEIVED 27 April 2024
ACCEPTED 27 January 2025
PUBLISHED 11 February 2025

CITATION
Gong L, Xu J, Zhuang Y, Zeng L, Peng Z, Liu Y, Huang Y, Chen Y, Huang F and Piao C (2025) Association between adult body shape index and serum levels of the anti-aging protein Klotho in adults: a population-based cross-sectional study of the NHANES from 2007 to 2016. *Front. Endocrinol.* 16:1424350. doi: 10.3389/fendo.2025.1424350

Association between adult body shape index and serum levels of the anti-aging protein Klotho in adults: a population-based cross-sectional study of the NHANES from 2007 to 2016

Li Gong[1†], Jinghan Xu[2†], Yiyang Zhuang[3], Liwei Zeng[1], Zhenfei Peng[1], Yuzhou Liu[1], Yinluan Huang[1], Yutian Chen[1], Fengyi Huang[1] and Chunli Piao[2*]

[1]Department of Diabetes, Shenzhen Bao'an District Hospital of Traditional Chinese Medicine, Guangzhou University of Chinese Medicine, Shenzhen, China, [2]Department of Endocrinology, Shenzhen Hospital (Futian) of Guangzhou University of Chinese Medicine, Shenzhen, China, [3]Department of Geriatrics, Shenzhen Bao'an District Hospital of Traditional Chinese Medicine, Guangzhou University of Chinese Medicine, Shenzhen, China

Purpose: Adult body shape index (ABSI) is widely recognized as a reliable indicator for evaluating body fat distribution and dysfunction. However, the relationship between ABSI and Klotho protein, known for its anti-aging biological function, has not yet been investigated. Therefore, the aim of this study was to assess the correlation between ABSI and serum Klotho levels in adults residing in the United States.

Methods: A cross-sectional study of participants was conducted based on the 2007–2016 National Health and Nutrition Examination Survey. Visceral adiposity was determined using the ABSI score, and Klotho protein concentration was measured using an enzyme-linked immunosorbent assay kit. Multiple regression models were used to estimate the association between ABSI and Klotho protein after adjusting for several potential confounding variables. Subgroup analysis of ABSI and Klotho was performed using restricted cubic splines.

Result: A total of 11,070 adults were eligible for participation, with a mean ABSI of 8.28 ± 0.45 and a mean Klotho protein concentration of 853.33 ± 309.80 pg/mL. Multivariate regression analysis showed that participants with high ABSI scores had lower serum Klotho protein concentrations. When ABSI was divided into quartiles, after full adjustment, Klotho protein levels were lower in participants in the fourth fully adjusted ABSI quartile (Q4: -0.352 pg/ml) than in those in the lowest quartile (Q1) (P<0.0001).

Conclusion: There was a negative linear correlation between ABSI score and serum Klotho concentration. Higher ABSI was associated with lower serum Klotho concentrations; however, this association did not seem to be significant in subjects with BMI ≥30 kg/m2.Further study is needed to verify the causality of this association and elucidate the underlying mechanisms.

KEYWORDS

adult body shape index, Klotho protein, national health and nutrition examination survey, obesity, cross-sectional study

1 Introduction

In recent years, obesity has emerged as an independent risk factor for various diseases, significantly impacting life expectancy worldwide (1). Body mass index (BMI) and waist circumference (WC) are the commonly used indicators of body size; however, they have certain limitations. Adult body shape index (ABSI) is a novel anthropometric index that considers abdominal circumference, height, and weight to better reflect individual fat distribution and visceral fat proportion, compared with BMI (2). ABSI proves to be a superior predictor of cardiovascular disease risk when compared with WC (3–6), as well as mortality associated with central obesity. Studies on nutrition have demonstrated that ABSI and its changes can independently predict all-cause mortality in the elderly Chinese population (7). Moreover, a strong positive correlation exists between ABSI and directly measured visceral fat content (8, 9), making it a potential surrogate indicator for arterial stiffness in patients with type 2 diabetes mellitus. By replacing WC with ABSI in the diagnostic criteria for metabolic syndrome, one can more effectively identify individuals at risk of renal function decline and arterial stiffness (10). Furthermore, ABSI provides a more accurate description of changes in circulating insulin and lipoproteins than traditional obesity indicators (11). Studies have confirmed consistent exposure-response relationships between ABSI and all-cause/cardiovascular mortality in cohorts of Asian patients with diabetes (12).

In 1997, Kuro-o et al. (13) discovered that mice with deficient Klotho gene expression exhibited premature aging syndromes and a shortened lifespan, confirming the role of Klotho as an aging regulator. The Klotho gene produces α-Klotho, β-Klotho, and γ-Klotho proteins; however, "Klotho" typically refers to α-Klotho (14). Reportedly, α-Klotho binds to the ligand domain of the fibroblast growth factor receptor and then binds to FGF-23 to exert biological effects (15). Both α-Klotho and β-Klotho are crucial components of the endocrine fibroblast growth factor receptor complex. Targeting the FGF-Klotho endocrine axis plays a critical role in the pathophysiology of aging-related diseases, such as diabetes, cancer, arteriosclerosis, and chronic kidney disease (16), some of which are associated with obesity (e.g., arteriosclerosis, diabetes, osteoporosis) (17, 18). Additionally, Klotho protein expression improves vascular calcification by increasing autophagy, which is beneficial for vascular-related diseases (19–21). Furthermore, Klotho appears to be involved in regulating phosphate homeostasis and insulin signaling while also inhibiting oxidative stress, thereby participating in glucose and lipid metabolism (22). Additionally, there is a correlation between serum Klotho concentration and age in humans (23). A study revealed that cerebrospinal fluid levels of Klotho were significantly negatively correlated with body weight/BMI due to the central involvement in obesity's pathological process (24), while soluble Klotho concentration was inversely correlated with abdominal obesity/high triglycerides (14). Recently, a nonlinear relationship between visceral adiposity index (VAI) score and serum concentration of the anti-aging protein Klotho has been reported. This suggests a potential direct involvement between Klotho expression level and obesity/aging relationships (25).

The ABSI index is a new measure used to assess an individual's body size and health risk, which combines data from three dimensions: weight, height, and waist circumference. Previous studies (7, 10) have mainly explored the association between ABSI and metabolic and cardiovascular diseases; However, its relationship with Klotho protein has not been thoroughly examined. Considering that obesity may lead to a reduced metabolic rate and is associated with an increased risk of multiple chronic diseases (12), thereby promoting aging and shortened life expectancy, it seems particularly important to investigate the association between ABSI index and Klotho protein. Therefore, in-depth study of the relationship between ABSI index and Klotho protein will not only help us to more fully understand the possible pathogenesis of aging, but also provide new perspectives and strategies for the prevention of aging. Therefore, we used the National Health and Nutrition Examination Survey (NHANES) data to analyze the association between ABSI and Klotho protein levels, aiming to provide new ideas about its mechanism. We hypothesized that higher ABSI would be associated with lower serum Klotho protein concentrations.

2 Materials and methods

2.1 Study design and population

The information in this study was based on the NHANES data collected from 2007 to 2016. NHANES is a research program designed to investigate the health and nutritional status of

participants in the United States, comprising interviews, examinations, and laboratory components. The data from 2007 to 2016 included five consecutive cycles, totaling 13,766 cases. There were 96,862 ABSI cases initially. Subsequently, 85,792 participants without information on ABSI or Klotho protein data were excluded from this study. After performing sensitivity analysis, 11,070 eligible participants were included for further analysis. Written informed consent was obtained for all study protocols included in this study, and the research was approved by the research ethics review board of the National Center for Health Statistics.

2.2 Outcome and exposure factors

The main exposure factor was ABSI, calculated using the following formula:

$$\text{ABSI} = \frac{WC(\text{cm})}{\sqrt{Height(cm)} \bullet \sqrt[3]{\text{BMI}^2}}$$

Where WC was expressed in cm and BMI in kg/m^2.

The primary outcome was serum Klotho concentration. Serum samples were collected from participants, transferred, and stored at −80°C. Klotho concentrations were determined using a commercially available enzyme-linked immunosorbent assay kit produced by IBL International, Japan. The sensitivity level of the assay was 6 pg/mL. All study samples were run in duplicate, bisected, and measured separately. The mean of the two concentration values was calculated as the result.

2.3 Covariates

Data regarding additional covariates were collected from each cycle of the NHANES. Continuous variables included age and poverty-to-income ratio (PIR). Categorical variables included sex, age, race, education level, marital status, smoking, alcohol consumption, hypertension, and diabetes. Based on previous studies, we adjusted for several possible confounding variables. The variables were divided into different categories: age: 40–59 years and ≥60 years; BMI:<25, 25-30, and ≥30 kg/m^2; PIR: ≤1.3, >1.3 and ≤3.5, >3.5%, or missing; race: Mexican American, other Hispanic, non-Hispanic White, non-Hispanic Black, and other races; marital status: married and other; education level: below high school, grades 9–12, and above high school; smoking status, alcohol consumption status, and self-reported medical conditions, including diabetes and hypertension: yes or no. When the missing covariate value exceeded 2% of the total population, dummy variables were used instead.

2.4 Statistical analysis

Table 1 clearly describes the baseline characteristics of all participants by proportions or means ± standard errors (SE). Categorical variables were analyzed using weighted chi-square analysis, and continuous variables were evaluated using a weighted linear regression model. ABSI was treated not only as a continuous independent variable but also as a categorical variable, divided into quartiles, with the lowest quartile as the reference. To investigate the independent relationship between ABSI and Klotho protein, we performed a multivariate generalized linear regression analysis. Model 1 was not adjusted. Model 2 was adjusted for age, sex, and race. Model 3 was adjusted for sex, age, race, PIR, BMI, education, marital status, smoking, alcohol consumption, diabetes, and hypertension to allow for further subgroup analysis and explore potential nonlinear associations. All statistical analyses were conducted using R version 3.6.3 and EmpowerStats. A P-value<0.05 was considered statistically significant (two-tailed).

3 Results

3.1 Participant characteristics

The baseline characteristics of the participants according to the ABSI category are shown in Table 1. A total of 11,070 US adults were eligible to participate in the study. Among them, 50.94% were female and 49.06% were male. The mean ± SE of ABSI was 8.28 ± 0.45. The mean ± SE of Klotho protein concentration was 853.33 ± 309.80 pg/ml. Participants in the fourth ABSI quartile had the lowest serum Klotho protein concentration (Q4: 822.153 ± 287.954pg/ml), compared with those in the other three quartiles (Q1: 893.589 ± 331.977, Q2: 852.179 ± 313.726, and Q3: 844.986 ± 299.446 pg/ml, p≤ 0.0001).

3.2 Multivariate regression analysis

Table 2 shows that, in the unadjusted model [b (95% confidence interval [CI]) = -0.163 (-0.191, -0.136)], the minimum adjustment model [-0.109 (-0.138, -0.080)], and the fully adjusted model [-0.119 (-0.149, -0.089)], ABSI was negatively correlated with Klotho protein concentration. Multivariate regression analysis showed that participants with higher ABSI scores had lower serum Klotho protein concentrations. When ABSI was categorized into quartiles, Klotho protein levels were lower among fully adjusted ABSI participants in the fourth quartile (Q4: -0.352 pg/ml), compared with the levels in participants in the lowest quartile (Q1) (P<0.0001). Significant associations were found between ABSI and Klotho protein levels for each quartile array in all three models (P<0.0001). Klotho protein levels were also significantly lower in models 1, 2, and 3 for participants with higher ABSI scores in the second, third, and fourth quartiles than for those with lower ABSI scores in the first quartile (6.10-7.96), with P for trend<0.0001 for all three models.

3.3 Subgroup analysis

We performed subgroup analyses, presented as restricted cubic splines, to explore potential nonlinear associations between ABSI and serum Klotho protein concentrations (Figure 1, Table 3). The

10.3389/fendo.2025.1424350

TABLE 1 Characteristics of participants by categories of adult body shape index in NHANES 2007–2016[ab].

Characteristic	All	ABSI quartiles				P-value
		Q1(6.10-7.99)	Q2(7.99-8.28)	Q3(8.28-8.57)	Q4(8.57-11.10)	
No. of participants	11070	2812	2713	2752	2793	
Adult body shape index	8.28 ± 0.45	7.711 ± 0.243	8.141 ± 0.082	8.421 ± 0.084	8.842 ± 0.236	<0.0001
Klotho concentration (pg/ml)	853.33 ± 309.80	893.589 ± 331.977	852.179 ± 313.726	844.986 ± 299.446	822.153 ± 287.954	<0.0001
Age (years)	57.62 ± 10.83	52.862 ± 9.816	55.664 ± 10.238	58.598 ± 10.228	63.343 ± 10.043	<0.0001
40-59 (%)	54.45	18.509	15.393	12.520	8.121	
≥60 (%)	45.55	6.893	9.115	12.340	17.109	
Sex (%)						<0.0001
Female	50.94	16.893	12.285	10.894	10.867	
Male	49.06	8.509	12.222	13.966	14.363	
Race (%)						<0.0001
Mexican American	15.31	3.279	4.146	4.038	3.749	
Other Hispanic	10.87	2.692	2.918	2.773	2.484	
Non-Hispanic white	45.40	9.874	10.136	11.454	13.939	
Non-Hispanic black	19.62	7.218	4.932	4.246	3.225	
Other races	8.80	2.240	2.376	2.349	1.834	
Poverty income ratio	2.65 ± 1.65	2.85 ± 1.67	2.73 ± 1.66	2.63 ± 1.66	2.39 ± 1.57	<0.0001
≤1.3 (%)	29.85	6.531	6.929	7.570	8.817	
>1.3 and ≤3.5 (%)	36.16	8.808	8.835	8.835	9.684	
>3.5 (%)	33.99	10.063	8.744	8.455	6.730	
BMI (kg/m2)						<0.0001
<25 (%)	23.62	6.531	6.929	7.570	8.817	
25-30 (%)	34.94	8.808	8.835	8.835	9.684	
≥30 (%)	41.44	10.063	8.744	8.455	6.730	
Education level (%)						<0.0001
Less than high school	26.41	5.474	5.953	6.902	8.085	
High school	22.32	5.393	5.294	5.574	6.061	
More than high school	51.26	14.535	13.261	12.385	11.084	
Marital Status (%)						<0.0001
Married	60.10	14.824	15.176	15.474	14.625	
Others	39.90	10.578	9.332	9.386	10.605	
Hypertension (%)						<0.0001
Yes	46.01	9.494	10.524	11.689	14.230	
No	53.99	15.908	13.984	13.170	10.930	
Diabetes (%)						<0.0001
Yes	18.11	2.755	3.550	4.878	6.929	
No	81.89	22.647	20.958	19.982	18.302	
Smoking (%)						<0.0001
Yes	49.23	9.874	11.319	12.990	15.050	

(Continued)

TABLE 1 Continued

Characteristic	All	ABSI quartiles				P-value
		Q1(6.10-7.99)	Q2(7.99-8.28)	Q3(8.28-8.57)	Q4(8.57-11.10)	
No	50.77	15.528	13.189	11.870	10.181	
Alcohol consumption (%)						<0.0001
Yes	71.40	17.407	17.552	18.302	18.139	
No	28.60	7.995	6.947	6.558	7.064	

[a]Mean ± SE for continuous variables, and a P-value calculated by weighted t-test.
[b]% for categorical variables, and P-value calculated by weighted Chi-square test.

fully adjusted restricted cubic spline plot (Figure 1) showed no nonlinear relationship between ABSI and Klotho protein levels (P for nonlinearity=0.126). Subgroup analysis showed no significant correlation between Klotho protein level and ABSI when BMI was ≥30 kg/m^2 (95% CI: 0.85-1.02; P=0.148). Additionally, after adjusting for confounding variables including smoking, gender, age, diabetes, alcohol consumption, and other covariates, a significant inverse association was observed between ABSI and Klotho protein levels.

4 Discussion

To the best of our knowledge, this is the first study to assess the association between ABSI and serum concentrations of the anti-aging protein Klotho by analyzing extensive population data from NHANES. However, there was a significant negative correlation between ABSI and Klotho protein concentration after adjusting for confounding factors, such as smoking, sex, age, diabetes, and alcohol consumption.

TABLE 2 Association between adult body shape index and serum anti-aging protein Klotho.

Exposure	Model 1[a]	Model 2[b]	Model 3[c]
	β (95% CI) P-value	β (95% CI) P-value	β (95% CI) P-value
ABSI	-0.163 (-0.191, -0.136)	-0.109 (-0.138, -0.080)	-0.119 (-0.149, -0.089)
	<0.0001	0.0002	<0.0001
ABSI quartile			
Q1	Ref	Ref	Ref
Q2	-0.387 (-0.441, -0.333)	-0.299 (-0.383, -0.215)	-0.313 (-0.398, -0.228)
	<0.0001	0.0004	0.0002
Q3	-0.474 (-0.558, -0.389)	-0.343 ((-0.431, -0.256)	-0.356 ((-0.444, -0.269)
	<0.0001	<0.0001	<0.0001
Q4	-0.481 (-0.566, -0.397)	-0.321 (-0.410, -0.231)	-0.352 (-0.444, -0.260)
	<0.0001	0.0004	0.0001

[a]Model 1: adjusted for no covariates.
[b]Model 2: adjusted for age, sex, and race.
[c]Model 3: adjusted for sex, age, race, poverty income ratio, body mass index, education, marital status, smoking, alcohol use, diabetes, hypertension.

In this study, we investigated the correlation between the ABSI index and Klotho protein. In addition, we used subgroup analyses to explore their associations in different populations. We found an inverse correlation between ABSI index and Klotho protein. Under subgroup analysis, we found no significant association between ABSI index and Klotho protein in participants with BMI ≥ 30 kg/m^2. Previous studies have also explored the association between Klotho protein and several clinicopathological factors (22, 24).The Klotho gene is predominantly expressed in kidney and brain tissues, giving rise to membrane-bound and secreted proteins that function as membrane-bound receptors and humoral regulators, respectively. The biological functions attributed to Klotho can give rise to various physiological effects, as well as diseases, including obesity (18, 19). Several studies have demonstrated an indisputable relationship between increased all-cause mortality and overweight or obesity, as measured by BMI (6). Moreover, ABSI seems to describe changes in circulating insulin and lipoproteins more accurately, compared with BMI (11), and ABSI can help determine the risk of sarcopenia in overweight/obese individuals (26).Previous studies have shown (6) that BMI, as a single quantitative indicator of obesity, cannot distinguish between fat and muscle content and cannot reflect individual fat distribution, while ABSI was selected as an indicator in our study to make up for this deficiency.

Our study found that after adjusting for confounding factors, higher ABSI population was associated with lower Klotho protein concentration. However, this relationship was not evident in individuals with BMI≥30 kg/m 2. This may be based on the difference between BMI and ABSI. Our results show that in the subgroup analysis, ABSI is significantly correlated with Klotho protein in variables such as age, gender, smoking history, drinking history, and diabetes history. Study (26) found a direct and significant association between age and obesity phenotype, with a higher chance of obesity phenotype in women with a history of diabetes and older age; however, it also pointed out that in different models of obesity, current smokers have a lower chance of obesity phenotype than non-smokers. A cross-sectional study (27) proposed that age and smoking are risk factors for cardiovascular and cerebrovascular diseases, while Klotho is a protective factor. Previous studies have shown that there is no significant correlation between serum soluble Klotho and gender, but serum soluble

10.3389/fendo.2025.1424350

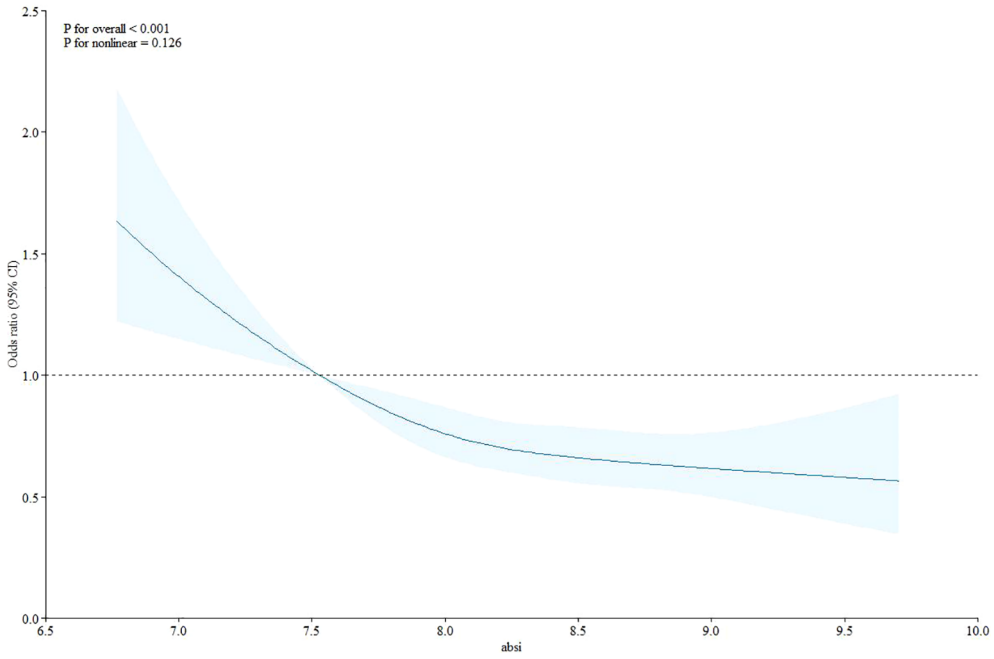

FIGURE 1
Restricted cubic splines for the association of adult body shape index (ABSI) and serum anti-aging protein.

TABLE 3 Subgroup analysis.

	OR	95%CI	P value
BMI (kg/m^2)			
<25	0.83	0.74-0.93	<0.001
25-29	0.87	0.78-0.96	0.007
≥30	0.93	0.85-1.02	0.148
Smoking			
No	0.88	0.81-0.95	<0.001
Yes	0.90	0.82-0.99	0.022
Diabetes			
No	0.89	0.84-0.96	<0.001
Yes	0.86	0.76-0.98	0.024
Alcohol consumption			
No	0.91	0.83-1.00	0.048
Yes	0.87	0.81-0.94	<0.001
Sex			
Female	0.88	0.82-0.95	<0.001
Male	0.87	0.79-0.96	0.005
Age (years)			
40-59	0.88	0.82-0.96	0.002
≥60	0.88	0.81-0.96	0.005

Subgroup analyses were adjusted for sex, age, smoking, alcohol use, and diabetes.

Klotho levels usually decrease with age. These findings prompt us to further raise questions in multiple covariates such as age, gender, smoking history, and diabetes history.

Existing studies have shown that visceral obesity is a risk factor for various metabolic diseases (27). Recent studies have shown that inflammation, both local and systemic, can reduce Klotho expression in the kidneys (28, 29). Therefore, proinflammatory cytokines from adipose tissue may affect serum Klotho protein concentrations. This can explain the possible correlation between ABSI and Klotho protein concentration from the perspective of inflammation.

Recent studies have confirmed that Klotho knockout mice are resistant to obesity induced by a high-fat diet due to a reduction in white adipose tissue, implying an effect of Klotho on adipocyte differentiation and maturation *in vivo* (24). Abnormal expansion of white adipose tissue and abnormal recruitment of adipose precursor cells can not only lead to obesity but also affect glucose metabolism (23). Klotho may affect adipocyte maturation, as well as systemic glucose metabolism. ABSI is not associated with BMI, but it is more likely to reflect central obesity when combined with waist circumference. This is different from previous studies (25) that directly reflect the relationship between visceral fat, and ABSI is more convenient than VAI in terms of measurement methods.

Additionally, previous studies have confirmed a negative correlation between CSF a-Klotho and BMI (24). Similarly, our study revealed a comparable association between serum a-Klotho levels and ABSI. It has been shown that soluble Klotho protein concentration is negatively correlated with the occurrence of metabolic syndrome, as well as abdominal obesity and hypertriglyceridemia (14). Obesity is classified into several types (30), and ABSI is used to quantify the severity of visceral obesity.

Similarly, a recent study revealed a relationship between VAI and Klotho protein levels in different cases, establishing the optimal VAI cut-off value (25). Likewise, the association between serum Klotho levels and ABSI in our study holds, which enriches the study of visceral obesity and Klotho protein.

Our study has some strengths. First, to the best of our knowledge, this is the first report of an association between visceral fat and serum anti-aging protein levels in humans. This provides new and practical insights into resistance or delay in aging, including appropriate weight control, especially visceral fat. Second, Klotho protein has a wide range of biological effects, indicating its important role not only in the mechanism of anti-aging but also in the occurrence and development of many diseases, which our study complements. Moreover, we used a multiethnic and large multiregional population based on the large population analysis from NHANES, which included a relatively large sample size of 11,070 Americans.

This study has some limitations. Due to the characteristics of the cross-sectional study design, the main limitation is the inability to establish a causal relationship between ABSI and Klotho concentration. Within a certain range, lower protein levels were associated with higher ABSI. Additionally, information on ABSI was obtained from the questionnaire. Some participants may have been reluctant to answer relevant questions for various reasons, resulting in missing data, while others may have omitted some information when answering the questionnaire, both of which inevitably lead to bias. Finally, although we attempted to account for confounding factors as much as possible in the adjusted models, there may still be potential confounding factors that have not been adjusted. Whether these factors affect the association between the two variables requires further research for confirmation.

4.1 Conclusion

Based on a nationally representative population, this study shows a negative correlation between ABSI and serum levels of the anti-aging protein Klotho in adults in the United States, with no nonlinear relationship.

Data availability statement

The datasets presented in this study can be found in online repositories. The names of the repository/repositories and accession number(s) can be found in the article/Supplementary Material.

Ethics statement

The studies involving humans were approved by the National Center for Health Statistics. The studies were conducted in accordance with the local legislation and institutional requirements. The participants provided their written informed consent to participate in this study.

Author contributions

LG: Conceptualization, Data curation, Formal analysis, Methodology, Writing – original draft, Writing – review & editing, Investigation, Supervision. JX: Conceptualization, Data curation, Methodology, Supervision, Writing – original draft, Writing – review & editing, Formal analysis. YZ: Data curation, Software, Writing – review & editing, Formal analysis. LZ: Resources, Software, Data curation, Formal analysis, Writing – review & editing. ZP: Data curation, Resources, Software, Writing – review & editing, Formal analysis. YL: Data curation, Resources, Software, Writing – review & editing, Formal analysis. YH: Data curation, Software, Writing – review & editing, Formal analysis, Resources. YC: Data curation, Resources, Software, Writing – review & editing, Formal analysis. FH: Resources, Software, Writing – review & editing, Data curation. CP: Conceptualization, Formal analysis, Methodology, Project administration, Validation, Visualization, Writing – review & editing, Supervision.

Funding

The author(s) declare financial support was received for the research, authorship, and/or publication of this article. This work was supported by the Sanming Project of Medicine in Shenzhen (grant number SZZYSM202202010).

Acknowledgments

We would like to thank Editage (www.editage.cn) for English language editing.

Conflict of interest

The authors declare that the research was conducted in the absence of any commercial or financial relationships that could be construed as a potential conflict of interest.

Publisher's note

Supplementary material

The Supplementary Material for this article can be found online at: https://www.frontiersin.org/articles/10.3389/fendo.2025.1424350/full#supplementary-material

References

1. Jaacks LM, Vandevijvere S, Pan A, McGowan CJ, Wallace C, Imamura F, et al. The obesity transition: stages of the global epidemic. *Lancet Diabetes Endocrinol.* (2019) 7:231–40. doi: 10.1016/S2213-8587(19)30026-9

2. Krakauer NY, Krakauer JC. A new body shape index predicts mortality hazard independently of body mass index. *PloS One*. (2012) 7:e39504. doi: 10.1371/journal.pone.0039504

3. Leone A, Vizzuso S, Brambilla P, Mameli C, Ravella S, De Amicis R, et al. Evaluation of different adiposity indices and association with metabolic syndrome risk in obese children: is there a winner? *Int J Mol Sci.* (2020) 21:4083. doi: 10.3390/ijms21114083

4. Bertoli S, Leone A, Krakauer NY, Bedogni G, Vanzulli A, Redaelli VI, et al. Association of Body Shape Index (ABSI) with cardio-metabolic risk factors: a cross-sectional study of 6081 Caucasian adults. *PloS One*. (2017) 12:e0185013. doi: 10.1371/journal.pone.0185013

5. Geraci G, Zammuto M, Gaetani R, Mattina A, D'Ignoto F, Geraci C, et al. Relationship of a Body Shape Index and Body Roundness Index with carotid atherosclerosis in arterial hypertension. *Nutr Metab Cardiovasc Dis*. (2019) 29:822–9. doi: 10.1016/j.numecd.2019.04.013

6. Chang Y, Guo X, Li T, Li S, Guo J, Sun Y. A Body shape index and body roundness index: two new body indices to identify left ventricular hypertrophy among rural populations in Northeast China. *Heart Lung Circ*. (2016) 25:358–64. doi: 10.1016/j.hlc.2015.08.009

7. Yang N, Zhuo J, Xie S, Qu Z, Li W, Li Z, et al. A body shape index and its changes in relation to all-cause mortality among the Chinese elderly: A retrospective cohort study. *Nutrients*. (2023) 15:2943. doi: 10.3390/nu15132943

8. Bouchi R, Asakawa M, Ohara N, Nakano Y, Takeuchi T, Murakami M, et al. Indirect measure of visceral adiposity "A Body Shape Index" (ABSI) is associated with arterial stiffness in patients with type 2 diabetes. *BMJ Open Diabetes Res Care*. (2016) 4:e000188. doi: 10.1136/bmjdrc-2015-000188

9. Bawadi H, Abouwatfa M, Alsaeed S, Kerkadi A, Shi Z. Body shape index is a stronger predictor of diabetes. *Nutrients*. (2019) 11:1018. doi: 10.3390/nu11051018

10. Nagayama D, Fujishiro K, Tsuda S, Watanabe Y, Yamaguchi T, Suzuki K, et al. Enhanced prediction of renal function decline by replacing waist circumference with "A Body Shape Index (ABSI)" in diagnosing metabolic syndrome: a retrospective cohort study in Japan. *Int J Obes (Lond)*. (2022) 46:564–73. doi: 10.1038/s41366-021-01026-7

11. Malara M, Kęska A, Tkaczyk J, Lutosławska G. Body shape index versus body mass index as correlates of health risk in young healthy sedentary men. *J Transl Med*. (2015) 13:75. doi: 10.1186/s12967-015-0426-z

12. Lu CY, Chen HH, Chi KH, Chen PC. Obesity indices and the risk of total and cardiovascular mortality among people with diabetes: a long-term follow-up study in Taiwan. *Cardiovasc Diabetol*. (2023) 22:345. doi: 10.1186/s12933-023-02072-3

13. Kuro-o M, Matsumura Y, Aizawa H, Kawaguchi H, Suga T, Utsugi T, et al. Mutation of the mouse klotho gene leads to a syndrome resembling ageing. *Nature*. (1997) 390:45–51. doi: 10.1038/36285

14. Cheng YW, Hung CC, Fang WH, Chen WL. Association between soluble α-klotho protein and metabolic syndrome in the adult population. *Biomolecules*. (2022) 12:70. doi: 10.3390/biom12010070

15. Gu H, Jiang W, You N, Huang X, Li Y, Peng X, et al. Soluble klotho improves hepatic glucose and lipid homeostasis in type 2 diabetes. *Mol Ther Methods Clin Dev*. (2020) 18:811–23. doi: 10.1016/j.omtm.2020.08.002

16. Kuro-o M. The klotho proteins in health and disease. *Nat Rev Nephrol*. (2019) 15:27–44. doi: 10.1038/s41581-018-0078-3

17. Para I, Albu A, Porojan MD. Adipokines and arterial stiffness in obesity. *Med (Kaunas)*. (2021) 57:653. doi: 10.3390/medicina57070653

18. Fassio A, Idolazzi L, Rossini M, Gatti D, Adami G, Giollo A, et al. The obesity paradox and osteoporosis. *Eat Weight Disord*. (2018) 23:293–302. doi: 10.1007/s40519-018-0505-2

19. Xu JP, Zeng RX, He MH, Lin SS, Guo LH, Zhang MZ. Associations between serum soluble α-klotho and the prevalence of specific cardiovascular disease. *Front Cardiovasc Med*. (2022) 9:899307. doi: 10.3389/fcvm.2022.899307

20. Chen WY. Soluble alpha-klotho alleviates cardiac fibrosis without altering cardiomyocytes renewal. *Int J Mol Sci*. (2020) 21:2186. doi: 10.3390/ijms21062186

21. Li L, Liu W, Mao Q, Zhou D, Ai K, Zheng W, et al. Klotho ameliorates vascular calcification via promoting autophagy. *Oxid Med Cell Longev*. (2022) 2022:7192507. doi: 10.1155/2022/7192507

22. Xu Y, Sun Z. Molecular basis of klotho: from gene to function in aging. *Endocr Rev*. (2015) 36:174–93. doi: 10.1210/er.2013-1079

23. Pedersen L, Pedersen SM, Brasen CL, Rasmussen LM. Soluble serum klotho levels in healthy subjects. Comparison of two different immunoassays. *Clin Biochem*. (2013) 46:1079–83. doi: 10.1016/j.clinbiochem.2013.05.046

24. Landry T, Li P, Shookster D, Jiang Z, Li H, Laing BT, et al. Centrally circulating α-klotho inversely correlates with human obesity and modulates arcuate cell populations in mice. *Mol Metab*. (2021) 44:101136. doi: 10.1016/j.molmet.2020.101136

25. Cui J, Yang Z, Wang J, Yin S, Xiao Y, Bai Y, et al. A cross-sectional analysis of association between visceral adiposity index and serum anti-aging protein klotho in adults. *Front Endocrinol (Lausanne)*. (2023) 14:1082504. doi: 10.3389/fendo.2023.1082504

26. Sedaghat Z, Khodakarim S, Sabour S, Valizadeh M, Barzin M, Nejadghaderi SA, et al. The effect of obesity phenotype changes on cardiovascular outcomes in adults older than 40 years in the prospective cohort of the Tehran lipids and glucose study (TLGS): joint model of longitudinal and time-to-event data. *BMC Public Health*. (2024) 24:1126. doi: 10.1186/s12889-024-18577-9

27. Martín-Núñez E, Donate-Correa J, Ferri C, López-Castillo Á, Delgado-Molinos A, Hernández-Carballo C, et al. Association between serum levels of Klotho and inflammatory cytokines in cardiovascular disease: a case-control study. *Aging (Albany NY)*. (2020) 12:1952–64. doi: 10.18632/aging.102734

28. Jayawardena R, Sooriyaarachchi P, Misra A. Abdominal obesity and metabolic syndrome in South Asians: prevention and management. *Expert Rev Endocrinol Metab*. (2021) 16:339–49. doi: 10.1080/17446651.2021.1982381

29. Li SS, Sheng MJ, Sun ZY, Liang Y, Yu LX, Liu QF. Upstream and downstream regulators of klotho expression in chronic kidney disease. *Metabolism*. (2023) 142:155530. doi: 10.1016/j.metabol.2023.155530

30. Typiak M, Piwkowska A. Antiinflammatory actions of klotho: implications for therapy of diabetic nephropathy. *Int J Mol Sci*. (2021) 22:956. doi: 10.3390/ijms22020956

Frontiers in Endocrinology

Explores the endocrine system to find new therapies for key health issues

The second most-cited endocrinology and metabolism journal, which advances our understanding of the endocrine system. It uncovers new therapies for prevalent health issues such as obesity, diabetes, reproduction, and aging.

Discover the latest Research Topics

See more →

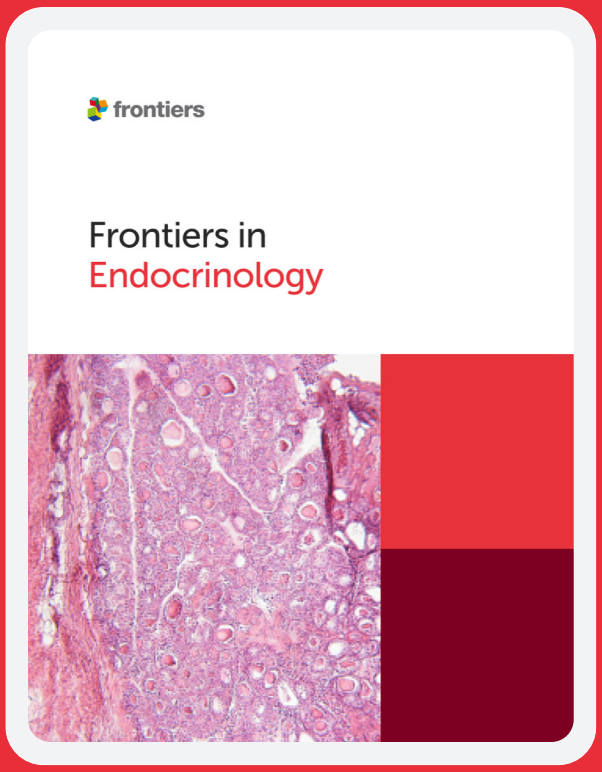

Frontiers

Avenue du Tribunal-Fédéral 34
1005 Lausanne, Switzerland
frontiersin.org

Contact us

+41 (0)21 510 17 00
frontiersin.org/about/contact